

UNIT PROCESSES IN EXTRACTIVE METALLURGY
HYDROMETALLURGY

TN
688
US
1970

STUDENT INFORMATION

This is a two-semester-hour credit course. It is divided into seven units called modules. Each module is divided into an appropriate number of learning activities, i.e., each learning activity is approximately equivalent to one hour of conventional lecture material. This means you will be studying about thirty hours of prepared materials. As is true of any course, study time beyond the time spend in class is required. You should allow at least one-two hours of study for each hour of material covered.

It is, therefore, obvious that when taking a self-paced tutorial course that you must develop study habits that carry you through the material at a uniform pace. In fact, your instructor may force you to complete each module by some predesignated time or you will be dropped from the course or your grade may be appropriately lowered.

Tutorial assistance will be arranged and announced at the first class meeting. An instructor will be available at a designated time and place at least two hours a week. In most cases, the instructor will be available more often.

Each module and each learning activity will have a short list of objectives, i.e., you will know what you are expected to learn from each set of material.

After you have completed your study of each learning activity, you should take the self-assessment test. This is for your use as a tool to assess whether you have properly studied the material.

After completing all the learning activities in a module, you should see your instructor. He will give you a test covering that module.

Remember to study carefully the materials presented to you. They have been selected and arranged in an order to lead you through the subject material. The self-paced concept, with tutorial help, will be one you will use throughout your career, i.e., you will collect materials pertinent to your job, study those materials, discuss the subject matter with experts, consultants, co-workers, etc., form your conclusions and make decisions. You will have to, in many cases, defend your decisions (in a sense be tested on these decisions).

The preparation of this course material has been partially supported by Higher Education Directorate of the National Science Foundation (NSF-HES-75-04821).

ARTHUR LAKES LIBRARY
COLORADO SCHOOL OF MINES
GOLDEN, CO 80401

UNIT PROCESSES IN EXTRACTIVE METALLURGY-HYDROMETALLURGY

Course Outline

Module 1

FUNDAMENTALS - SOLUTION CHEMISTRY

- 1.1 Introduction *Learning Activity 1*
 - 1. Liquid State
 - 2. Structure and Properties of Aqueous Solutions
 - 3. Stability Relations
 - 4. Reaction Types
- 1.2 Activity - Concentration Relationships *Learning Activity 2*
 - 1. Definition of Standard State
 - 2. Mean Ionic Activity - Individual Ionic Activity
 - 3. Estimating Ionic Activity Coefficients
- 1.3 Complex Equilibria *Learning Activity 3*
 - 1. Complex Ions
 - 2. Stability Constants
 - 3. Distribution of Species
 - 4. Computer Program for Solution Equilibrium Calculations *Learning Activity 4*
- 1.4 Oxidation-Reduction Reactions *Learning Activity 5, 6*
 - 1. Convention
 - 2. Electrochemical Phase Diagrams
 - 3. Appendix

Module 2

FUNDAMENTALS - MASS TRANSFER AND REACTION KINETICS

- 2.1 Introduction *Learning Activity 1*
 - 1. Classification of Reactions
 - 2. Definition of Reaction Rate
- 2.2 Homogeneous Kinetics *Learning Activity 2*
 - 1. Law of Mass Action and Rate Law
 - 2. Theories of Rate Constant
 - 3. Catalysis
 - 4. Reaction Order from Batch Reactor Data
 - 5. Suggested Readings
- 2.3 Heterogeneous Kinetics *Learning Activity 3*
 - 1. Reaction Steps and the Rate Controlling Step
 - 2. Transport Within Phases
 - 3. Kinetics of Adsorption Reactions
 - 4. Reaction of the Interface *Learning Activity 4*

5. Electrochemical Reaction on an Electrode Surface
 6. Rate Equation for Heterogeneous Reaction - Flat Plate Geometry *Learning Activity 5*
 7. Fluid-Particle Reaction - Spherical Geometry *Learning Activity 6*
 8. Suggested Readings
- 2.4 Rate Phenomenon in Hydrometallurgical Processes *Learning Activity 7*
1. Dissolution of Metal by Spinning Disc Technique
 2. Dissolution of Oxides
- 2.5 References

Module 3

LEACHING SYSTEMS FUNDAMENTALS

- 3.1 Particle Characterization *Learning Activity 1*
1. Particle Size
 2. Particle Shape
 3. Shape Factor
 4. Particle Size Distribution
 5. References
- 3.2 Hydrodynamics and Mass Transfer for a Packed Bed *Learning Activity 2*
1. Flow Through a Packed Bed
 2. Mass Transfer Between Fluid and Solid in a Packed Bed
 3. References
- 3.3 Dump and In Situ Leaching Practice
1. Introduction
 2. Leaching Systems
 1. Conventional Leaching Practice
 2. Solution Mining Systems
 3. Rate Processes
 1. Leaching of Sulfide Ores
 2. Leaching of Oxide Ores
 4. References
- 3.4 Agitation Vessels *Learning Activity 3*
1. Introduction
 2. Air Lift Agitation Mixer
 1. Types of Pachuca Tanks
 2. Selection of Pachuca Tank
 3. Scale-up Parameters
 3. Impeller Agitation Mixer
 1. Impellers
 2. Flow Pattern in Impeller Stirred Tank
 3. Energy Dissipation and Power Characteristic of Stirred Tank

4. Suspension of Solid in a Stirred Tank
 5. Mass Transfer to Particles in Agitation Tanks
 4. References
- 3.5 Reactor Design *Learning Activity 4*
1. Types of Reactors
 2. Design Parameters
 1. Review of the Kinetics of Fluid Particle Reaction
 2. Concentration of the Lixiviant
 3. Modeling and Design for Continuous Leaching Systems - J. A. Herbst
 1. Symbols and Notations
 2. Description of Governing Equations
 3. Results from Computer Simulation
 4. Design Work Sheet and Example
 4. References

Module 4

PHASE SEPARATION

- 4.1 Thickening *Learning Activity 1*
1. Introduction
 2. How a Continuous Thickener Functions
 3. Elements of a Thickener
 4. Some Factors that Size Continuous Thickener Basins
 5. Practical Mill Design Considerations for Thickeners
 6. Major Factors Influencing Thickener Design
- 4.2 Filtering *Learning Activity 2*
1. Introduction
 2. Types of Continuous Filters
 3. Applied Theory of Continuous Filtration
 4. Applied Theory Use in Predicting Full Scale Results

Module 5

LEACHING OF METALS, OXIDES AND SULFIDES

- 5.1 Overview *Learning Activity 1*
1. Introduction
 2. Leaching Methods and Equipment
 3. Thermodynamics of Leaching Reactors
 4. Leaching Kinetics
 5. References

5.2 Leaching of Metals

Learning Activity 2

1. Gold Cyanidation
 1. Chemistry and Mechanism of Cyanide Leaching of Gold
 2. Gold Cyanidation Practice
 3. Conventional Gold Cyanidation
 4. Carbon Adsorption and Desorption Process
 5. Electrowinning
 6. Cyanide Heap Leaching of Gold Ore
 7. Cortez Heap Leach Cyanidation
2. Leaching of Metallic Copper
 1. Chemistry
 2. Practice
3. References

5.3 Leaching of Oxides

Learning Activity 3, 4

1. Thermodynamics and Kinetics
2. Leaching of Uranium Oxides
 1. Hydrometallurgical Process for Uranium Oxides
 2. Acid Leaching of Uranium Oxides
 3. Carbonate Leaching of Uranium Oxides
3. Leaching of Bauxite--Bayer Process
4. Leaching of Nickel Oxides
 1. General Considerations
 2. Direct Sulfuric Acid Leach
 3. Reductive Roasting/Ammoniacal Leaching
 4. Sulfidization Process
5. Leaching of Ocean Manganese Nodules
 1. General Considerations
 2. Kennecott Cuprion Process
6. Leaching of Copper Oxide
 1. Leaching Methods
 2. In-situ Leaching
 3. Dump Leaching
 4. Heap Leaching
 5. Vat Leaching
 6. Agitation Leaching
7. References

5.4 Leaching of Sulfides

Learning Activity 5

1. Introduction
 1. Thermodynamics
 2. Kinetics
2. Leaching of Nickel and Cobalt Sulfide Minerals
 1. Ammonia Oxidation Leaching of Ni-Co Sulfides
 2. Acid Leaching of Nickel and Cobalt Sulfides
 3. Leaching of Copper-Nickel Matte

3. Leaching of Copper Sulfides-Fundamental Studies *Learning Activity 6*
 1. Sulfuric Acid Leach
 2. Ammonia-Oxygen Leach
 3. Ferric Chloride Leach
 4. Nitric Acid Leach
 5. Cyanide Leach
 6. Microbiological Leach *Learning Activity 7*
 7. Electrochemical
4. Leaching of Copper Sulfide-Processes *Learning Activity 8*
 1. Roast-Leach-Electrowin Process
 2. Ammonia Leach Processes
 3. Ferric Chloride Leach Processes
 4. Acid Leach Processes
5. Leaching of Other Sulfides
 1. Roast Leach Process for Zinc Sulfide
 2. Direct Leaching of Zinc Sulfide
6. References

Module 6

SOLUTION CONCENTRATION AND PURIFICATION

- 6.1 Solvent Extraction *Learning Activity 1*
 1. Introduction
 2. Characterization of Extraction Reaction
 3. Extraction Chemistry *Learning Activity 2*
 4. Solvent Extraction Systems *Learning Activity 3*
- 6.2 Ion Exchange *Learning Activity 4*
 1. Introduction
 2. General Principles
 1. Chemical Composition and Structure of Resins
 2. Selectivity of Ion Exchanger
 3. Kinetics of Ion Exchange Reaction
 3. Hydrometallurgical Applications *Learning Activity 5*
 1. Uranium Extraction--Chemistry of Adsorption and Elution
 2. Uranium Ion Exchange--Processes and Equipment
 3. Extraction of Other Metals
 4. Separation of Metal Ions

Module 7

METAL RECOVERY

- 7.1 Gaseous Reduction in Aqueous Solution *Learning Activity 1*
 1. Hydrogen Gas Reduction
 2. Other Gases
- 7.2 Cementation *Learning Activity 2*

1. Introduction
2. Theory
3. Initial Concentration
4. Temperature
5. Summary

7.3 Electrolysis

Learning Activity 3

1. Introduction
2. Sample Calculations

3. Electrowinning of Copper

Learning Activity 4

1. Electrowinning Reactions
2. Cell Voltage and Energy Consumption
3. Cathode Current Efficiency: Interfering Iron Reactions
4. Purity of Cathode: Behavior of Electrolyte Impurities
5. Electrowinning Tankhouse Practice
6. Special Problems of Solvent Extraction Electrolytes
7. Recent Improvement in Electrowinning Procedure
8. Summary

7.4 Electrowinning Plant Practice

Learning Activity 5

1. Purpose of Process
2. The Cathodic Process
3. The Anodic Process
4. Solution Mixing
5. Control of Acid Mist
6. Problems of Heat Generation
7. Metal Recovery and Size of Operations
8. Chemistry and Electrochemistry of the Zinc Cell
9. Cathode Materials
10. Anode Materials
11. Cell Design Considerations

COURSE INTRODUCTION

In the broadest sense, the field of hydrometallurgy involves the recovery of valuable components from both primary and secondary raw materials by relatively low temperature reactions accomplished in an aqueous phase. In this regard, the term is a bit misleading since it can include the processing of non-metallic particulate materials as well as metallic particulate materials.

Generally, three distinct operations can be identified in any hydrometallurgical flowsheet:

- leaching
- solution concentration and/or purification
- product recovery

Conceptually, any process can be thought of in terms of the flowsheet presented in Figure 1. Common to all hydrometallurgical flowsheets is the solid-liquid separation. Generally, the separation is accomplished by thickening and/or filtration. This particular aspect can turn out to be one of the most critical steps in the processing sequence and always requires careful evaluation in the analysis of any proposed or operating system.

Leaching: The various leaching processes that are encountered can be classified with respect to reaction chemistry which will be discussed in this course. Generally, the particular lixiviant selected for a given raw material is one which results in good selectivity for the valuable components to be recovered. If many components of the raw material are dissolved, then the subsequent leach liquor concentration and purification step will become more difficult. However, with respect to process engineering, it probably is of more significance to classify the leaching operation with respect to the extent of raw material preprocessing rather than with respect to reaction chemistry. Leaching systems extend from the leaching of marginal low grade ore in which there is no materials handling to the leaching of high grade concentrates produced from physical and physico-chemical separations by mineral processing technology, see Figure 2.

Leach Liquor (treatment) Concentration and Purification: Impurity removal is accomplished by a number of techniques in order to prepare the leach solution for product recovery. These techniques are most conveniently classified according to reaction chemistry and include the following categories:

- precipitation
- cementation
- solvent extraction
- ion exchange

Figure 1. Components of Hydrometallurgical Flowsheets.

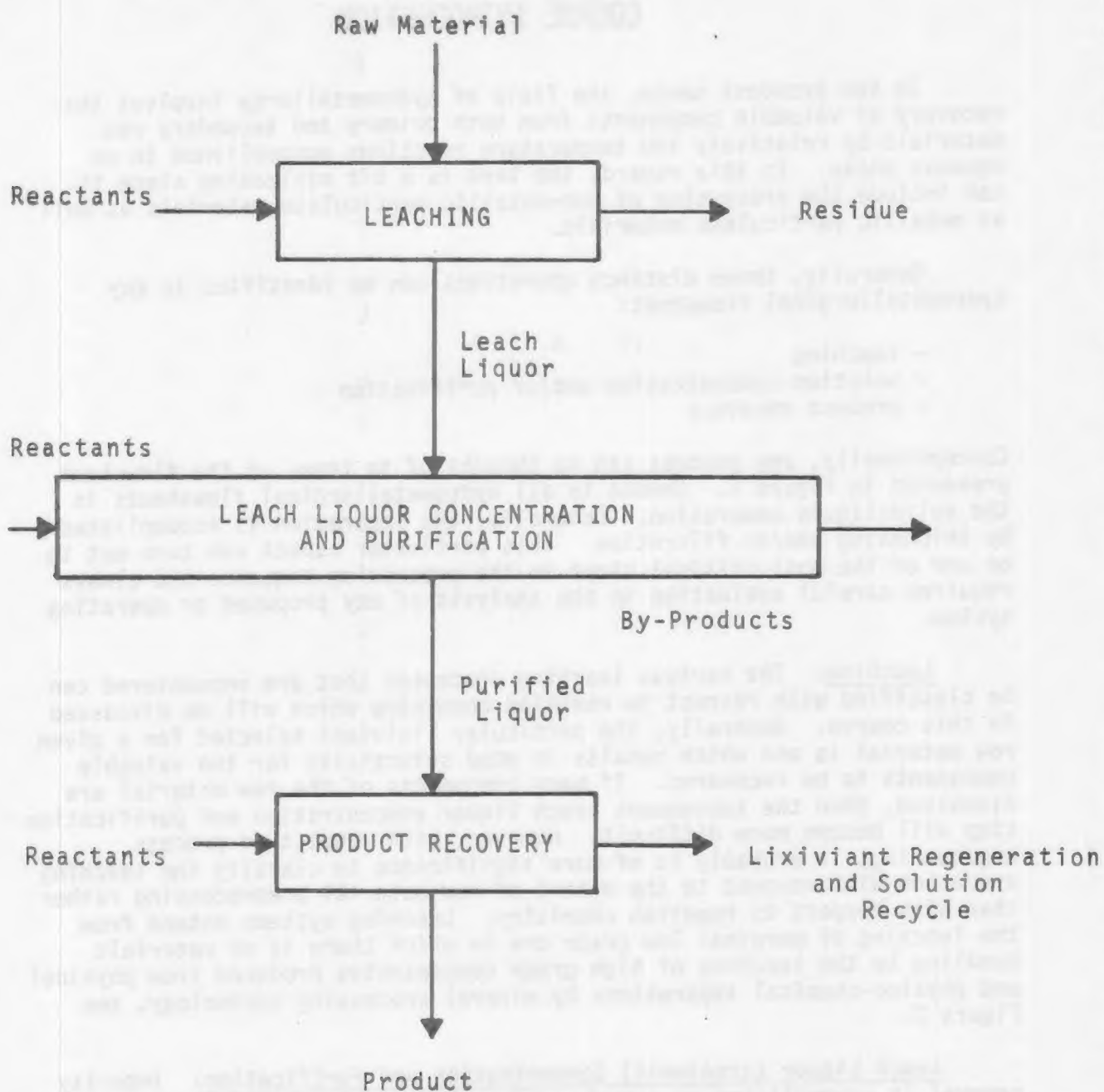


Figure 2. Leaching Systems.

LOW GRADE MATERIAL

In-situ Mining
(No Transportation or Mineral Processing)

Dump Leaching
(Transportation and Size Reduction)

Vat Leaching
Agitation Leaching
(Transportation, Size Reduction and Classification)

HIGH GRADE MATERIAL

Concentrate Leaching
(Transportation, Size Reduction and Classification) and Separation of Mineral Concentrate

Secondary Materials Leaching
(Scrap)

The application of any one of these processes depends mainly on the impurities to be removed and the component to be recovered. In some instances this intermediate stage of processing will involve the selective recovery of a solid phase containing the valuable component, e.g., copper cementation from dump leach liquors. In other instances, impurities may be removed (either in the solid stage or in aqueous stream) with the valuable component to be recovered from a concentrated, purified solution, e.g., rejection of impurity components in raffinate during solvent extraction of uranium, copper and other metals.

Product Recovery: The valuable component is then converted into a marketable product with associated quality specifications. This product recovery phase of hydrometallurgy may involve purification of a solid phase or recovery from a concentrated purified aqueous solution. Common techniques employed for product recovery include:

electrolysis
gaseous reduction
precipitation

To appreciate the concepts that have been mentioned, it is worthwhile to consider the flowsheets for two common examples of hydrometallurgical processes. The first is a typical flowsheet, Figure 3, for the processing of uranium ore by agitation leaching with sulfuric acid. In this case there is an intermediate level of preprocessing. Solution concentration and purification is accomplished by ion exchange, and product recovery is achieved by precipitation of yellow cake, sodium diuranate ($\text{Na}_2\text{U}_2\text{O}_7$).

The flowsheet for uranium should be compared to that for dump leaching of copper presented in Figure 4. Note that the three distinct steps of any hydrometallurgical process can be identified in each case. Dump leaching of copper requires considerably less preprocessing than the agitation leaching of uranium. Significant differences also are seen in the other steps. In the case of copper dump leaching, solution concentration and purification is accomplished by solvent extraction and product recovery is achieved by electrolysis.

Probably the unique feature of hydrometallurgical processes which distinguishes these systems from other process engineering systems is that hydrometallurgical processes specifically involve heterogeneous reactions of particulate matter in an aqueous phase. As a result, accurate particle characterization ultimately is required in order to quantitatively describe the accompanying unit operations. Particle characterization includes determination of particle size distribution, particle shape, density, specific surface area and porosity.

Aside from the unique feature of processing particulate assemblies, the principles of solution chemistry and the analysis of heterogeneous reaction rates provide the fundamental basis for treating these systems quantitatively. In this regard, the fundamental principles underlying

Figure 3. Uranium Ore Processing.

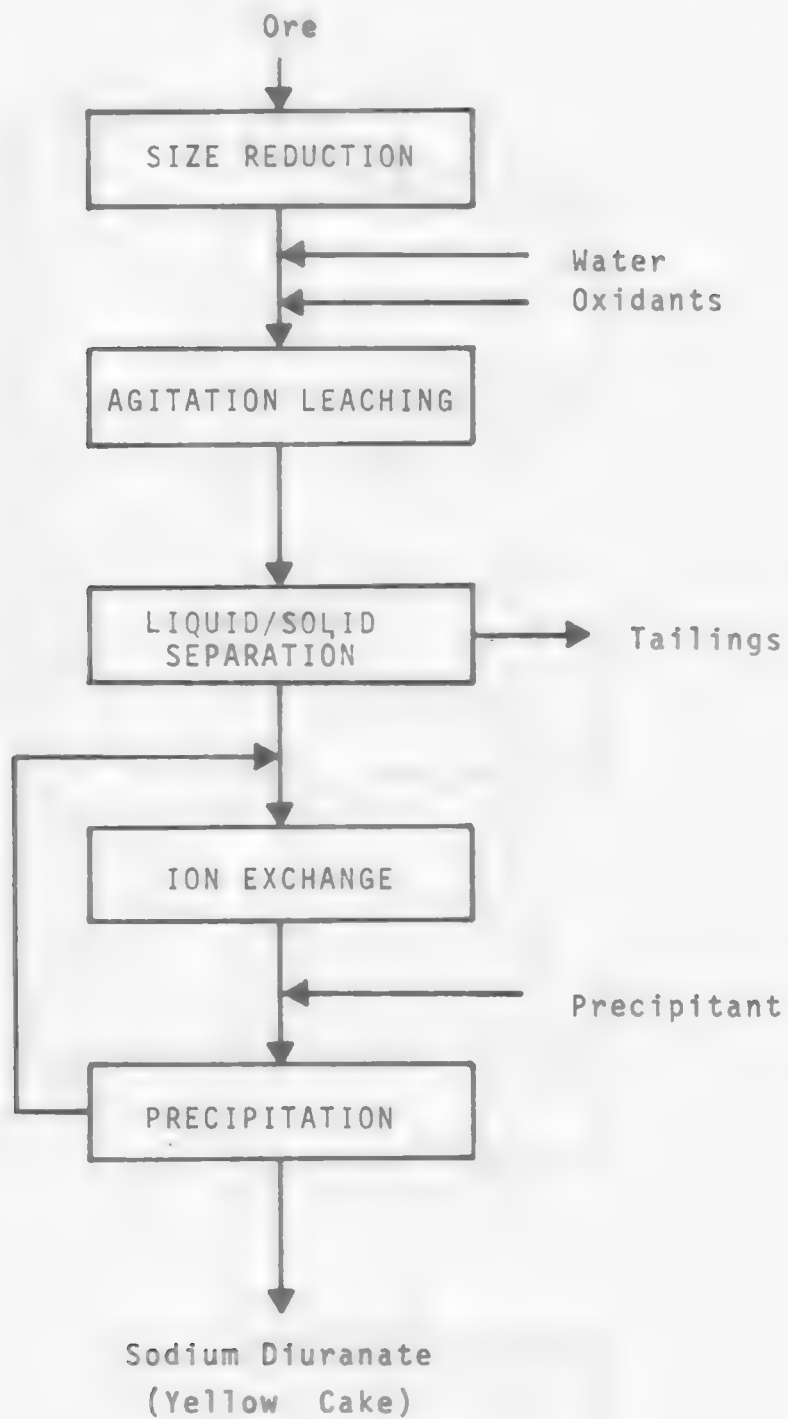
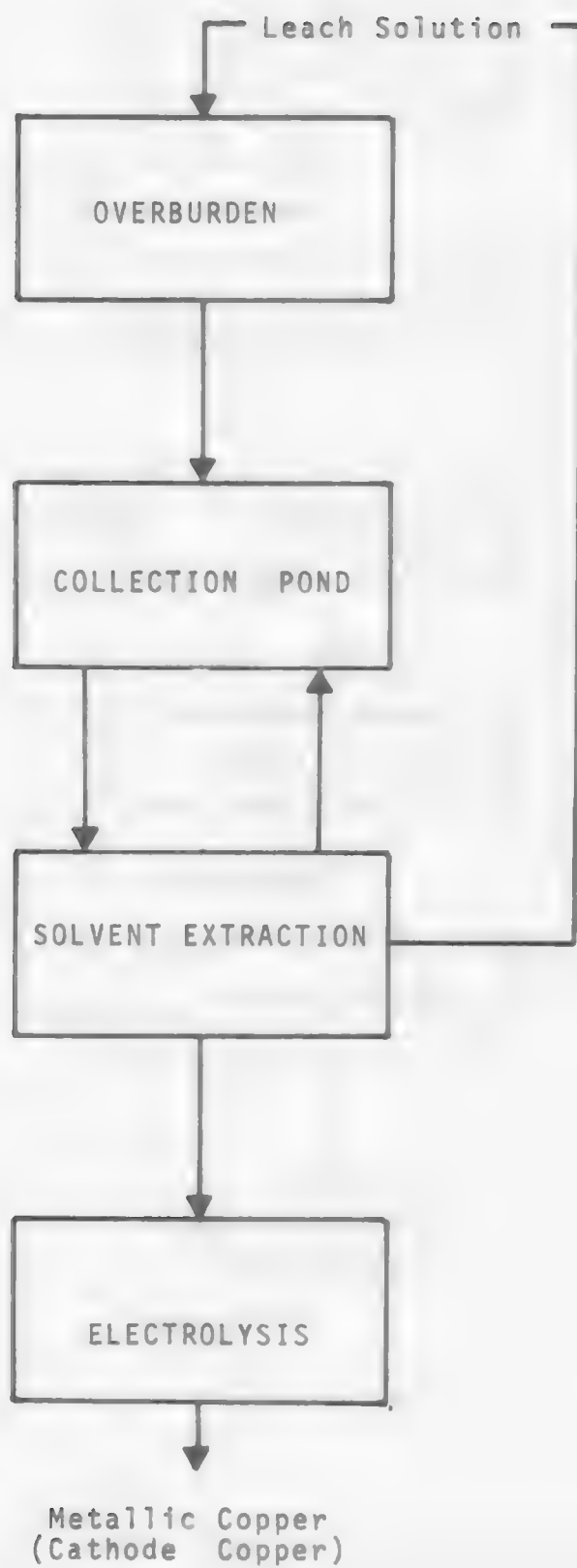


Figure 4. Dump Leaching.



the hydrometallurgical operations will be examined during the first part of the course, while the application of these principles to leaching, solution concentration and/or purification, and product recovery will be considered during the later part of this course.

UNIT PROCESSES IN EXTRACTIVE METALLURGY

HYDROMETALLURGY

Module 1

Fundamentals - Solution Chemistry

SIX LEARNING ACTIVITIES

Module Coordinator: Dr. J. D. Miller
Professor of Metallurgical Engineering
Department of Metallurgy and Metallurgical
Engineering
University of Utah

Module 1 Contents

Fundamentals - Solution Chemistry

- | | | |
|-----|--|-------------------------------|
| 1.1 | Introduction | <i>Learning Activity 1</i> |
| 1. | Liquid State | |
| 2. | Structure and Properties of Aqueous Solutions | |
| 3. | Stability Relations | |
| 4. | Reaction Types | |
| 1.2 | Activity - Concentration Relationships | <i>Learning Activity 2</i> |
| 1. | Definition of Standard State | |
| 2. | Mean Ionic Activity - Individual Ionic Activity | |
| 3. | Estimating Ionic Activity Coefficients | |
| 1.3 | Complex Equilibria | <i>Learning Activity 3</i> |
| 1. | Complex Ions | |
| 2. | Stability Constants | |
| 3. | Distribution of Species | |
| 4. | Computer Program for Solution Equilibrium Calculations | <i>Learning Activity 4</i> |
| 1.4 | Oxidation-Reduction Reactions | <i>Learning Activity 5, 6</i> |
| 1. | Convention | |
| 2. | Electrochemical Phase Diagrams | |
| 3. | Appendix | |

LEARNING ACTIVITY 1

1.1 IntroductionLearning Activity Objective

After completing your study of this material you should be able to qualitatively describe the fundamental properties of liquid solutions. In addition, you should be able to recognize reaction types and make elementary free energy calculations to predict the stability of various compounds and species in the aqueous phase.

1.1.1 Liquid State

Liquids are intermediate in their properties between solids and gases. They are characterized by the fact that they:

- (1) Display a considerable degree of local order reflected in the tendency for groups of neighboring molecules to arrange themselves in a definite geometric pattern (in this sense similar to the solid state).
- (2) On the other hand, the high fluidity of liquids--inability to withstand shear forces--results in the virtual absence of any long-range order (in this sense similar to the gaseous state).

What attractive forces are operative in the liquid state that account for its behavior? The term "le Van der Waals forces" has long been used to designate the inter-molecular attractions which give rise to deviations from ideality in the behavior of real gases and which account for the cohesion of molecular liquids. These forces can be considered to arise from three effects:

Orientation effect	}	
Induction effect	}	le Van der Waal's Forces
Dispersion effect	}	

Orientation Effect - Applies to molecules which possess a permanent dipole moment resulting in a preferred orientation. A dipole exists when an unequal charge distribution exists between atoms in a molecule.

A:B

 $\overset{-}{A}:\overset{+}{B}$

like atoms share
charge equally

unlike atoms result in unsymmetrical
charge distribution and a dipole (A is
more electro-negative than B)

The magnitude of this charge difference is expressed in terms of the dipole moment, μ , which is the product of the charge and the separation distance. Dipole moments are on the order of

$$10^{-18} \text{ esu-cm} \left[\begin{array}{l} \text{molecular distances} = 10^{-8} \text{ cm} \\ \text{electronic charge} = 4.8 \times 10^{-10} \text{ esu credits} \end{array} \right]$$

The dipole moments for the molecule is the vector sum of constituent moments. A perfectly symmetrical molecule will, therefore, be nonpolar although it may contain polar linkages, e.g., CCl_4 , CO_2 are symmetrical molecules--no moment. On the other hand, HI which has an interatomic distance 1.87Å might be expected to have a maximum dipole moment of $(4.8 \times 10^{-10} \text{ esu})(1.87 \times 10^{-8} \text{ cm}) = 9 \times 10^{-18}$. The measured moment, 0.38×10^{-18} , is rather low and indicates the predominately covalent nature of the bond.

The existence of dipoles permit apparently neutral molecules to attract ions (charged species) or other molecules which results in molecular aggregates which are not compounds in the sense that there is no classical chemical bond formation either via electron (e^-) sharing or transfer. Dipole moments for some common molecules are presented in Table 1.1.1.

TABLE 1.1.1. Dipole Moments for Various Molecules in a Vacuum.

Molecule	$\mu \times 10^{18}$, esu-cm
Water (H_2O)	1.86
Methanol (CH_3OH)	1.68
Ethanol ($\text{C}_2\text{H}_5\text{OH}$)	1.70
Ammonia (NH_3)	1.49
Isopropanol ($\text{C}_3\text{H}_7\text{OH}$)	1.70
Carbon Disulfide (CS_2)	0
Hydrogen Chloride (HCl)	1.03

Induction Effect - A molecule possessing a permanent dipole will affect the charge distribution of neighboring molecules by inducing opposing dipoles in them. This results in an induced attractive force, e.g., inert gas--hydrates which form at high pressures.

Dispersion Effect - Finally there are attractive forces which act between nonpolar molecules such as atoms of the inert gases. The nature of these forces was first suggested by London in 1930. These forces apparently have their origin in the continuous variation in the intensity of charge concentration in the electron atmosphere.

Examples of relative molecular interaction effects are presented in Table 1.1.2.

TABLE 1.1.2. Relative Magnitude of Molecular Interaction Effects, ($\frac{\text{kcal}}{\text{mole}}$).

Substance	Dipole Moment	Orienta- tion	Induction	Dispersion
A	0	0	0	57
CO	0.12	0.003	0.057	67
HCl	1.03	18.6	5.4	105
H ₂ O	1.8	190.	10.	47

- (1) Only dispersion forces contribute to the cohesion of nonpolar molecules such as argon.
- (2) With fairly polar molecules such as HCl (D.M.=1.0), these dispersion forces still predominate over those due to orientation and induction.
- (3) Only with very polar molecules such as H₂O which have large dipole moments does the orientation forces make the major contribution to the overall attractive force.

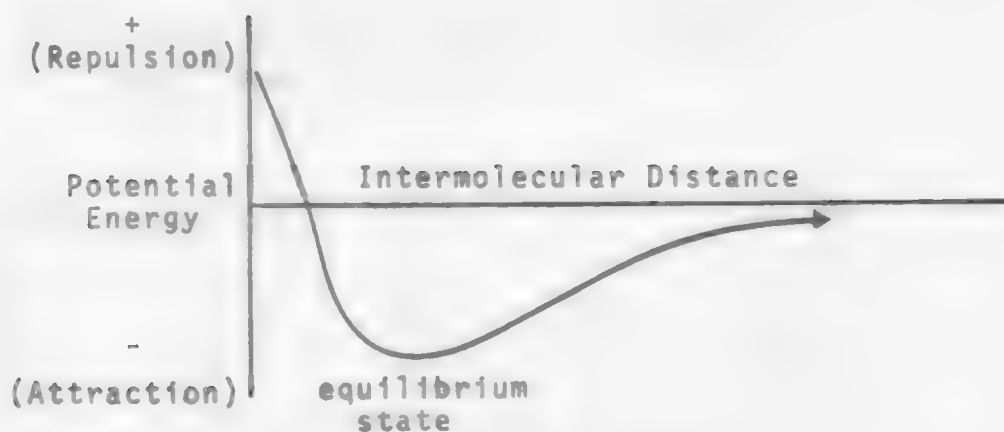
Attractive forces give rise to energies of molecular attraction which generally have an inverse dependence on the sixth power of the separation distance, r , i.e.,

$$\begin{array}{l} \text{molecular} \\ \text{attraction} \\ \text{energy} \end{array} = -\text{constant} \cdot r^{-6} \quad [1.1.1]$$

Repulsive Forces - An intermolecular repulsive potential due to coulombic interaction of overlapping electron shells results in repulsion energies. These energies can be represented by

$$\begin{array}{l} \text{molecular} \\ \text{repulsion} \\ \text{energy} \end{array} = +\text{constant} \cdot r^{-12} \quad [1.1.2]$$

Consequently, when molecules are brought in close proximity the potential energy of interaction can be represented schematically in the following manner,



As molecules approach each other they are attracted to one another, the energy of attraction reaching a minimum at the equilibrium position. If the separation distance is less, then repulsion forces become more predominant.

Hydrogen Bond - The molecular interaction of dipoles (orientation effect) which involves a hydrogen atom are especially strong due to the high charge density on the hydrogen atom. This interaction effect is called hydrogen bonding and is particularly prevalent in the case of water accounting for its unusual physical properties.

Hydrogen-linked atoms must be strongly electronegative due to the electrostatic nature of the bond. In general, the strength of the bond increases with increasing electronegativity of the atoms that are bridged by hydrogen. Hydrogen bonding is not limited to water but is prevalent for inorganic and organic compounds--solids, liquids, and gases. The most common atoms which participate in hydrogen bonding are oxygen, nitrogen and fluorine. In certain instances hydrogen bonds are formed between carbon and oxygen and between carbon and nitrogen--but only when the carbon is attached to a strongly electronegative atom.

Although chlorine has approximately the same electronegativity as nitrogen, it is only infrequently involved in hydrogen bond formation--apparently as a result of the fact that chlorine has a less intense electric field due to its size. However, chlorine and even sulfur are sometimes involved in a hydrogen bond--but they must be attached to a more strongly electronegative atom such as oxygen or nitrogen.

Bond energy for the hydrogen bond is about 5 kcal/mole (as compared to about 90 kcal for valence bonds). A rather weak bond with respect to chemical bonds, but the significance of the hydrogen bond is revealed by a comparison of the physical properties of H_2O (O forms H bond) and H_2S (S does not form H bond).

	<u>Molecular Weight</u>	<u>Freezing Point</u>	<u>Boiling Point</u>	<u>Dielectric Constant</u>
H ₂ O	18	0	100	80
H ₂ S	34	-83	-62	6

Hydrogen bond formation leads to molecular associations in both solid and liquid states for hydrogen fluoride, water and ammonia. In hydrogen fluoride the hydrogen bond is reported to persist even in the gaseous state.

1.1.2 Structure and Properties of Aqueous Solutions

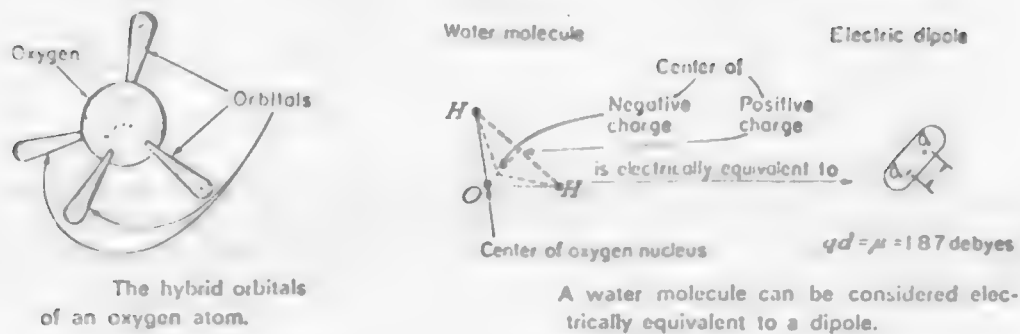
It is evident from the magnitude of the orientation force and the dipole moment for the water molecule, that the hydrogen atoms are bonded asymmetrically to the oxygen atom. Instead of being a linear molecule the molecule is bent and the two hydrogen atoms form an angle of 105° with respect to the oxygen atom. The smaller hydrogen atoms are imbedded in the electron cloud of the molecule. Two of the hybrid orbitals (sp³) are occupied by the hydrogen atoms and the remaining two orbitals contain free electron pairs. Because the center of gravity of negative charge is not coincident with the center of gravity of positive charge there is charge separation within the electrically neutral water molecule and it can be considered to be an electric dipole as shown in Figure 1.1.1.

In the case of the solid phase, ice, the oxygen atoms lie in layers with each layer consisting of a network of open puckered hexagonal rings, Figure 1.1.2. Each oxygen atom is tetrahedrally surrounded by four other oxygen atoms, in between each pair of oxygen atoms is a hydrogen atom which provides for the H-bonding, Figure 1.1.3. At any instance, the hydrogen atoms are not situated exactly half-way between the two oxygens. The H-bond is on the order of 1.75 Å, whereas, if we could assign hydrogen atoms to oxygen atoms, the interatomic distance would be 1.0 Å. The resulting network structure for the solid state contains interstitial regions which are larger than the dimensions of a water molecule--hence a free non-associated water molecule can enter the interstitial regions with little disruption of the structure.

In the case of liquid water the structure is broken-down somewhat and the liquid water can be thought of as an expanded form of the ice lattice, preserving short-range order. We can think of a short-range structured network of water (establishment) and interstitial water molecules (free) which are in dynamic equilibrium with each other.

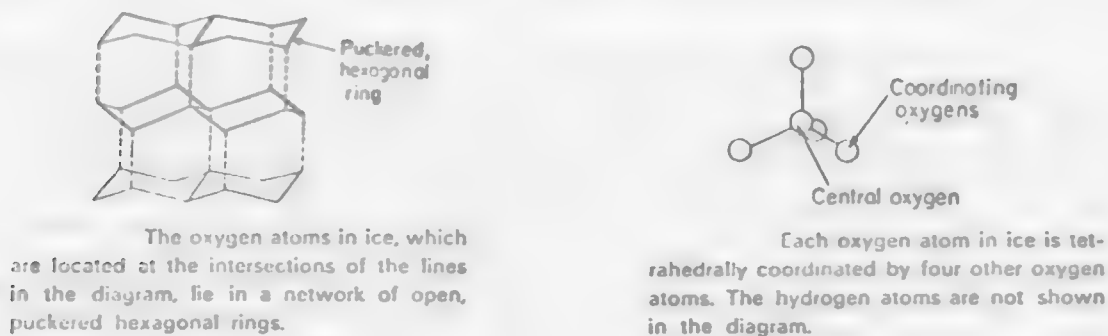
The tetrahedral arrangement persists in small regions of the liquid state and has four nearest neighbors. The association is, of course, due to hydrogen bonds. The small value for the enthalpy of fusion of ice (1.44 kcal/mole) compared to the estimate of 10 kcal/mole H if all hydrogen bonds were broken suggests that only a small fraction (15%) of the hydrogen bonds break on melting. On the other hand, the heat of vaporization very nearly approximates the hydrogen bond energy

Figure 1.1.1. Water Molecule.



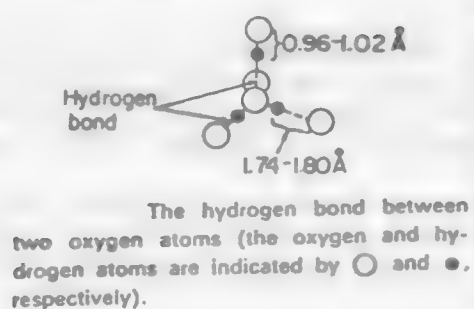
Source: Bockris and Reddy, Modern Electrochemistry, Plenum, 1, p. 74 (1970).

Figure 1.1.2. Ice Structure.

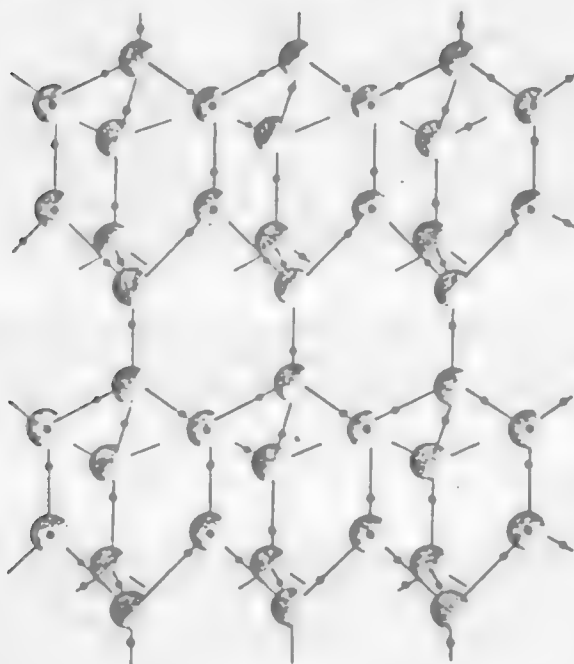


Source: Bockris and Reddy, Modern Electrochemistry, Plenum, 1, p. 74 (1970).

Figure 1.1.3. Hydrogen Bonding in Ice.



Source: Bockris and Reddy, Modern Electrochemistry, Plenum, 1, p. 75 (1970).



The arrangement of molecules in the ice crystal.

Source: J. D. Hunt, Metal Ions in Aqueous Solution, Benjamin, p. 20, (1965).

of 10 kcal/mole of water which presumably would have two hydrogen bonds per molecule. These considerations suggest that short-range structure and well defined molecular interactions persist in the liquid state but significant molecular association is absent in the gaseous state.

The hydrogen bonding and short-range order leads to the situation that water is not a uniform dielectric. This is especially true when one considers the properties of water at interfaces.

Interfaces induce pronounced structural change in vicinal water which may extend over considerable distances. For example, see reference 1.

Ion-Dipole Interactions

The term, ion, refers to either a monoatomic or polyatomic charged species. The origin of the word is from the Greek and has the meaning wanderer. Ions orient dipoles and these forces are the basis for explaining the behavior of aqueous solutions. Water molecules in the vicinity of an ion are trapped and oriented in its electric field. These water molecules no longer participate in the short-range structure of water and in essence, can be considered to be immobilized, relatively speaking. They move with the ion and are considered to constitute the primary hydration sheath--a sheath of oriented, immobilized water molecules.

Further from the ion the forces are inoperative and the normal bulk structure of water persists. At intermediate positions, the water molecules are caught between the two types of influence as shown in Figure 1.1.4.

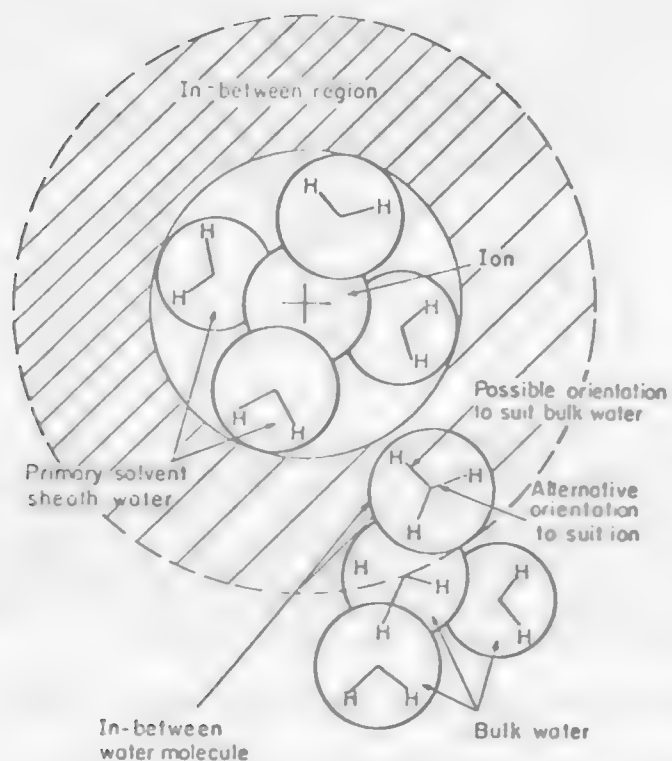
Solvation (Hydration) Number

The number of water molecules coordinated in the primary hydration sheath is referred to as the solvation, hydration or coordination number. Beyond the distance of 10 Å, the water molecules are unaware of the ions presence. Experimental results show varied hydration numbers, e.g., for the sodium ion, hydration numbers from 1 to 71 have been reported. The results appear to be sensitive to the experimental technique, i.e., what type of ion-solvent interactions are detected. See Table 1.1.3.

TABLE 1.1.3. Comparison of Hydration Numbers
Determined by Various Techniques.

<u>Ion</u>	<u>Compressibility</u>	<u>Mobility</u>	<u>Entropy</u>	<u>Theoretical</u>
Li ⁺	5-6	6	5	6
Zn ⁺⁺		10-12.5	12	
Cd ⁺⁺		10-12.5	11	
Fe ⁺⁺		10-12.5	12	
Cu ⁺⁺		10-12.5	12	

Figure 1.1.4. Solvated Ion in Bulk Water.



Schematic diagram to indicate that, in the (hatched) region between the primary solvated ion and bulk water, the in-between water molecules must compromise between an orientation which suits the ion (oxygen-facing ion) and an orientation which suits the bulk water (hydrogen-facing ion).

Source: Bockris and Reddy, p. 78.

For this reason, the primary hydration number is defined as the number of molecules which surrender their own translation freedom and remain with the ion relative to the surrounding solvent, i.e., the number of molecules which remain aligned in the ion's force field and move with the ion. On the other hand in the strictest sense, the coordination number establishes the number of molecules that should be in contact with the ion according to the geometrical considerations. Therefore, the hydration number and the coordination number are not necessarily equivalent. The hydration number is a dynamic quantity and can be greater or less than the coordination number. Generally, hydration numbers decrease with increasing ionic size.

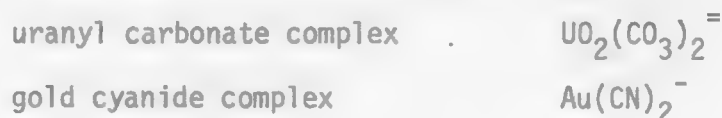
	<u>Mobility</u>	<u>Entropy</u>
Cl^-	0.9	3
Br^-	.6	2
I^-	.2	1

As should be apparent from this discussion, the ionic size of a species in an aqueous solution is not that of the ionic crystal radius but rather is the size of the hydrated ion, the ion plus immobilized water molecules in the primary hydration sheath. Measurement of this effective radius is difficult. Generalizations regarding effective ionic radii in aqueous solutions have been made which involve the addition of an empirical term to the crystal radius.

$$\text{Effective radius} = \text{Ionic crystal radius} + \text{Empirical term} \quad [1.1.3]$$

In one correlation, it is suggested that a value of 0.1 Å be used for anions and 0.85 Å be used for cations. In another analysis the empirical term, which takes into consideration the contribution of hydrated water molecules to the ionic site, is assigned a value of 1.0 Å for anions and 2.0 Å for cations.

Of course, the composition of aqueous solutions is generally more complex than has been indicated. In addition to simple monoatomic ions, there are polyatomic complex ions; such as the oxyanions; nitrate (NO_3^-), sulfate (SO_4^{2-}), and phosphate (PO_4^{3-}). Frequently, multi-component complexes form in solution in which specific chemical interactions occur to form these charged species. Hydrometallurgical examples of this type of important interaction include:

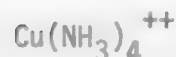


In most instances the formation of the complex can be easily identified as the displacement of coordinated water molecules by another ligand which frequently is accompanied by a change in coordination number,

tetrachloro cobaltous complex



tetramine cupric complex



Finally, neutral molecular species also are found in aqueous systems. Because these species are not charged, their interaction with water molecules differs significantly from that of charged species. Examples of interest in hydrometallurgy are: H_2CO_3^0 (carbonic acid or hydrated carbon dioxide) and $\text{UO}_2(\text{NO}_3)_2^0$ (aq). Other neutral species in aqueous systems that are of interest are gases such as oxygen (O_2), hydrogen (H_2), and ammonia (NH_3).

1.1.3 Stability Relations

The cornerstone for stability relations is the Law of Mass Action, which provides a measure of the extent to which the system is displaced from an equilibrium position. This differential is a measure of the driving force for a reaction to occur and is determined by the activities of reactants and products. The state of the system is expressed by the product of the activities* of reaction products, each raised to the power of its numerical coefficient as dictated by the stoichiometry of the reaction, divided by the product of the activities of the reactants each raised to the appropriate power. This parameter is referred to as the reaction quotient and for the following reaction,



the reaction quotient (Q) is:

$$Q = \frac{a_D^d \cdot a_E^e}{a_B^b \cdot a_C^c} \quad [1.1.4]$$

where a_i^i represents the activity of component I raised to the power, i, the numerical coefficient of component I in the balanced reaction.

For systems at equilibrium, the reaction quotient takes on a value unique to the system being investigated--the equilibrium constant (K).

Any system not at equilibrium will change spontaneously with release of energy. Since generally we deal with systems neither of constant entropy nor of constant energy, the appropriate energy term to be considered is the free energy of the system. The free energy for constant total pressure is defined as:

*Activity (unitless) can be thought of as a thermodynamic concentration referenced to a specified standard state, representing the effective concentration from a chemical thermodynamic standpoint.

$$\Delta G = \Delta H - T\Delta S \quad [1.1.5]$$

where: ΔG is the free energy, cal/mole
 ΔH is the enthalpy, cal/mole
 ΔT is the temperature, °K
 ΔS is the entropy, cal/°K mole

For a chemical reaction the free energy change of the system is expressed as the difference in energy of the two states:

$$\Delta G_r = \Sigma \text{free energy products} - \Sigma \text{free energy reactants.}$$

The basis on which the free energy of different states can be compared is the Standard Free Energy of Formation (ΔG_f°). The standard free energy of formation of a compound is the free energy change which accompanies the formation of one mole of the compound from the stable elements under standard conditions. An important convention that you should remember is

"The standard free energy of formation of the stable configuration of an element in its standard state is taken as zero."

This is similar to the convention in which the hydrogen half cell is taken as zero potential in developing the electromotive series.

The standard free energy of a reaction is the sum of the free energies of formation of the products in their standard states, minus the free energies of formation of the reactants in their standard states:

$$\Delta G_r^\circ = \Sigma \Delta G_f^\circ \text{ products} - \Sigma \Delta G_f^\circ \text{ reactants} \quad [1.1.6]$$

In general, the free energy of the system at some non-standard state condition can be calculated from the following relationship:

$$\Delta G_r = \Delta G_r^\circ + RT \ln Q \quad [1.1.7]$$

Note the free energy expression for the reaction consists of two components: the standard free energy of reaction and the reaction quotient term. At equilibrium the system is not changing its composition, there is no driving force ($\Delta G_r = 0$), and the reaction quotient must be equal to the equilibrium constant, hence the standard free energy of reaction is related to the equilibrium constant in the following way

$$\Delta G_r^\circ = -RT \ln K \quad [1.1.8]$$

at 25° C

$$\Delta G_r^\circ = -0.001987 \text{ kcal/deg} \times 298.23 \text{ deg} \times 2.303 \log K \quad [1.1.9]$$

$$\Delta G_r^\circ = -1.364 \log K \quad (\Delta G_r^\circ \text{ in kcal/mole}) \quad [1.1.10]$$

Several important consequences arise from these considerations which should be recognized by the student:

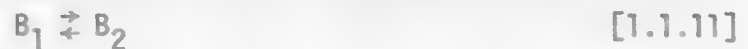
- (1) The equilibrium state of the system is defined for $\Delta G_r = 0$
- (2) Reaction is spontaneous from left to right when $\Delta G_r = \text{negative value}$ (by convention)
- (3) When components of the system are in their standard state, $\Delta G_r = \Delta G_r^\circ$.

To test your knowledge of these concepts, consider the following question:

Can ΔG_r° be equal to zero? If that is possible, does it necessarily mean that the system is at equilibrium?

1.1.4 Reaction Types

If the reaction system involves the transformation of a pure solid from one crystal structure to another at a given temperature and a 1 atm total pressure,



$$\Delta G_r = \Delta G_r^\circ + RT \ln \frac{a_{B_2}}{a_{B_1}} \quad [1.1.12]$$

Since the components are pure solids they are in their standard state and the activities of each solid are equal to unity and

$$\Delta G_r = \Delta G_r^\circ \quad [1.1.13]$$

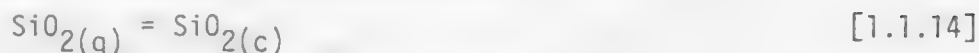
The standard free energies of formation for some of the common compounds and species of interest in hydrometallurgy systems can be found from Garrels and Christ, Solutions, Minerals and Equilibria, Appendix 2.

Example (1): Solid Transformations

Consider silicon dioxide which can exist in the following forms:

	ΔG_f° (298°K), kcal/mole
Quartz	192.4
Cristobalite	192.1
Tridymite	191.9
Vitreous	190.9

For the reaction of quartz to cristobalite:



$$\Delta G_r = \Delta G_r^\circ = \Delta G_f^\circ, \text{ cristobalite} - \Delta G_f^\circ, \text{ quartz} \quad [1.1.15]$$

$$\Delta G_r = \Delta G_r^\circ = -192.1 - (-192.4) = +0.3 \text{ kcal} \quad [1.1.16]$$

The reaction free energy change is positive and, therefore, the reaction does not occur, i.e., quartz is the stable form of silica at 298°K.

Example (2): Reactions of Solids in Nearly Pure Water



Assuming that the water is sufficiently pure to be considered to be in its standard state,

$$\Delta G_r = \Delta G_r^\circ$$

$$\Delta G_r = \Delta G_f^\circ, \text{ Ni(OH)}_2 - \Delta G_f^\circ, \text{ H}_2\text{O} - \Delta G_f^\circ, \text{ NiO} \quad [1.1.18]$$

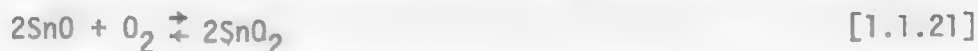
$$= -108.3 - (-56.7) - (-51.3) \quad [1.1.19]$$

$$= -0.3 \text{ kcal} \quad [1.1.20]$$

The free energy is negative, therefore, the nickel oxide should hydrate in water forming nickel hydroxide.

Example (3): Reactions Involving a Gas Phase. At nominal pressures the activity of a gas is very well approximated by its partial pressure.

Consider the oxidation of pure stannous oxide to pure stannic oxide



$$\Delta G_r^\circ = 2\Delta G_f^\circ, \text{ SnO}_2 - (2\Delta G_f^\circ, \text{ SnO} + \Delta G_f^\circ, \text{ O}_2) \quad [1.1.22]$$

$$= 2(-134.2) - [2(-61.5) + 0] \quad [1.1.23]$$

$$= -123.4 \text{ kcal} \quad [1.1.24]$$

However, unlike the previous examples, whether or not the reaction occurs spontaneously is dependent on the P_{O_2} since oxygen was not specified as being "pure", that is in its standard state.

$$\Delta G_r = -123.4 + RT \ln \frac{1}{P_{O_2}} \quad [1.1.25]$$

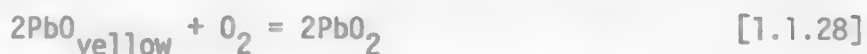
The oxygen pressure required for equilibrium between SnO and SnO₂ at 25° C is found by setting $\Delta G_r = 0$. Then,

$$123.4 = 1.364 \log \frac{1}{P_{O_2}} \quad [1.1.26]$$

$$\log \frac{1}{P_{O_2}} = 90.47$$

$$P_{O_2} = 10^{-90.47} \text{ atm.} \quad [1.1.27]$$

This low oxygen pressure indicates the SnO is rather unstable. Only for oxygen pressures less than 10^{-90} , would SnO be produced. Compare the tin system with the lead system,

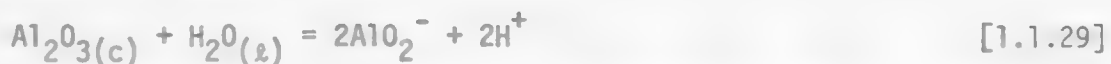


A similar calculation shows that the oxygen pressure necessary for equilibrium between the two solid lead oxide phases is $10^{10.7}$ atm.

Example (4): Reactions Involving Dissolved Species

Again the condition of spontaneity is determined by the activities of the dissolved species.

Consider as an example



$$\Delta G_r = \Delta G_r^\circ + RT \ln (a^2_{(\text{AlO}_2^-)})(a^2_{(\text{H}^+)}) \quad \text{(assuming pure Al}_2\text{O}_3(\text{c}) \text{ and pure H}_2\text{O}(\text{l})) \quad [1.1.30]$$

$$\Delta G_r^\circ = (2\Delta G_{\text{H}^+}^\circ + 2\Delta G_{\text{AlO}_2^-}^\circ) - (\Delta G_{\text{Al}_2\text{O}_3}^\circ + \Delta G_{\text{H}_2\text{O}}^\circ) \quad [1.1.31]$$

$$= 0 + 2(-200.7) - [-376.66 + (-56.7)] \quad [1.1.32]$$

$$= -401.4 + 463.5$$

$$= +62.1 \text{ kcal} \quad [1.1.33]$$

At equilibrium,

$$\Delta G_r^\circ = -RT \ln K \quad [1.1.34]$$

and

$$\log K = \frac{62.1}{1.364} = -45.5 \quad [1.1.35]$$

under equilibrium conditions

$$\log(a_{\text{AlO}_2^-}^2)(a_{\text{H}^+}^2) = -45.5 \quad [1.1.36]$$

$$2 \log a_{\text{AlO}_2^-} = -45.5 - 2 \log (\text{H}^+)$$

$$\log a_{\text{AlO}_2^-} = -22.75 + \text{pH} \quad [1.1.37]$$

This illustrates a useful relationship, i.e., the activity (concentration) of dissolved species may be represented in equation form as a function of pH.

LEARNING ACTIVITY 2

1.2 Activity - Concentration RelationshipsLearning Activity Objective

After completing your study of the material in this learning activity you should be able to define standard state, activity, mean ionic activities and activity coefficients, and individual ionic activities and activity coefficients. You should be able to calculate mean ionic activities and be able to estimate individual ionic activity coefficients.

1.2.1 Definition of Standard State and Electrolyte Activity

Activity in the thermodynamic sense is a term used to indicate how reactive a substance is, indeed the chemical potential of a substance is defined in terms of its activity. Since we cannot measure absolute energies or potentials we must always evaluate or compare the material in a given state to some other state. In this regard, we use the term "standard state" to designate the reference state at which we are making the comparison, that is, how active is species i (what is the activity of species i) compared to the same material in its standard state.

The chosen standard state is quite arbitrary, but by convention, the following general guidelines are used extensively in the science and engineering community.

<u>Material's State</u>	<u>Standard State</u>
solid	pure solid
gas	pure gas at a fugacity of one atmosphere
liquid (as solvent)	pure liquid
dissolved component (solute)	a number of standard states are used depending on the system. <ol style="list-style-type: none"> 1) pure material as reference 2) an arbitrary level of solution such as 1 wt. % 3) a hypothetical standard state of 1 molar determined by the behavior of the solution at infinite dilution (used extensively for aqueous systems).

Physically, what is the difference between activity and concentration? We measure concentration in a variety of ways: mole fraction, pressure, weight percent, moles/liter, etc. The law of mass action can be used with just concentration terms; but the tendency for components to react with one another depends on more than just their mass density. This tendency is what distinguishes activity from concentration.

Our consideration in this module will be limited to activity-concentration relationships for solutes in the aqueous phase. Relationships for other systems are given elsewhere, reference 2. The behavior of ionic species in the aqueous phase are determined in part by their interaction with water molecules (discussed in the last learning activity) and in part by ion-ion interactions.

The extent to which these interactions affect the physical and chemical properties of the electrolytic solution is dependent on the ionic density of the solution and the mean distance of charge separation. The interionic fields are distant dependent.

A description of an assemblage of ions in terms of the energetics (free energy), or the chemical potential change, can be attempted by evaluation of the spatial distribution of charges with regard to a reference point. If the distribution can be determined, the potential at that point can be determined from the fact that the potential at a point due to an assemblage of charges is the sum of the potentials due to each of the charges in the assembly. Debye and Huckel in 1923 describe the distribution of charges around an ion, leading today to what is referred to as the Debye Huckel theory.

The Debye-Huckel approach is to consider a central ion standing alone in a continuum. Water, the solvent, enters the analysis in the guise of a dielectric constant and the remaining ions of the assembly are expressed in terms of the excess charge density, i.e., $\rho \neq 0$. The electrostatic forces try to order the charges operating through the dielectric constant of the solvent whereas the thermal forces cause ionic motion which tend to drive $\rho = 0$. The overall solution, of course, is electrically neutral and a time averaged spatial distribution of ionic charge is calculated.

As should be evident from this discussion, the potential field which influences the behavior of an ion and its activity is determined by the number of charges with which the reference ion can interact. A useful term which characterizes solutions in this respect is the ionic strength of the solution, I , first defined by Lewis and Randall;

$$I = \frac{1}{2} \sum_i m_i z_i^2 \quad [1.2.1]$$

where

- I = ionic strength
- m_i = molality of species i
- z_i = valence of species i

The ionic strength term provides a convenient measure of the number of charge carriers and provides a basis for the comparison of electrostatic interaction. In the absence of complexation reactions, activity coefficients for a given strong electrolyte are the same in all solutions of the same ionic strength.

The normal standard state of salts in aqueous solution is the hypothetical one molar solution; hypothetical in the sense that the standard state is established by the behavior of the system at infinite dilution. This approach to defining standard state is known as Henry's Law - in this case applied to aqueous solutions. When a salt dissociates into 2 moles of ions, the relationship between activity and molality is a square function:

$$CA = C^+ + A^- \quad [1.2.2]$$

$$a_{CA} = km_{CA}^2 \quad [1.2.3]$$

more generally

$$C_{v_+} A_{v_-} = v_+ C + v_- A \quad [1.2.4]$$

$$v = v_+ + v_- \quad [1.2.5]$$

and

$$a_{CA} = km_{CA}^v \quad [1.2.6]$$

or

$$a_{C_{v_+} A_{v_-}} = km_{C_{v_+} A_{v_-}}^v$$

The standard state concept is depicted in Figure 1.2.1. At infinite dilution $a = km^v$ and a linear relationship is established, whereas for more concentrated solutions the behavior deviates considerably from linearity. A projection of the linear relationship to a concentration of one molal fixes the activity scale and identifies the hypothetical 1 molar standard state.

1.2.2 Mean Ionic Activity - Individual Ionic Activity

Although individual ionic activities cannot be measured in an absolute sense, by analogy with the behavior of the salt, the activity of the constituent ions are defined as being equal to their respective molalities at infinite dilution.

$$\begin{aligned} a_+ &= m_+ \\ a_- &= m_- \end{aligned} \quad \text{as } m \rightarrow 0$$

From this definition it follows for a symmetrical electrolyte that;

1.2.3

$$a = a_+ a_- \quad [1.2.7]$$

and in the most general case,

$$a = a_+^{v_+} a_-^{v_-} \quad [1.2.8]$$

which is taken to hold at all concentrations.

The mean ionic activity of a symmetrical electrolyte a_{\pm} is defined as

$$a_{\pm} = (a_+ a_-)^{1/2} = a^{1/2} \quad [1.2.9]$$

On the basis of these identities, individual ionic activity coefficients are defined;

$$\gamma_+ = \frac{a_+}{m_+} \quad [1.2.10]$$

$$\gamma_- = \frac{a_-}{m_-} \quad [1.2.11]$$

and in line with previous statements, γ_+ and γ_- approach unity at infinite dilution. Similarly then, the mean ionic activity coefficient is defined

$$\gamma_{\pm} = (\gamma_+ \gamma_-)^{1/2} \quad [1.2.12]$$

For unsymmetrical electrolytes, the following more general expressions can be written for the mean ionic activity,

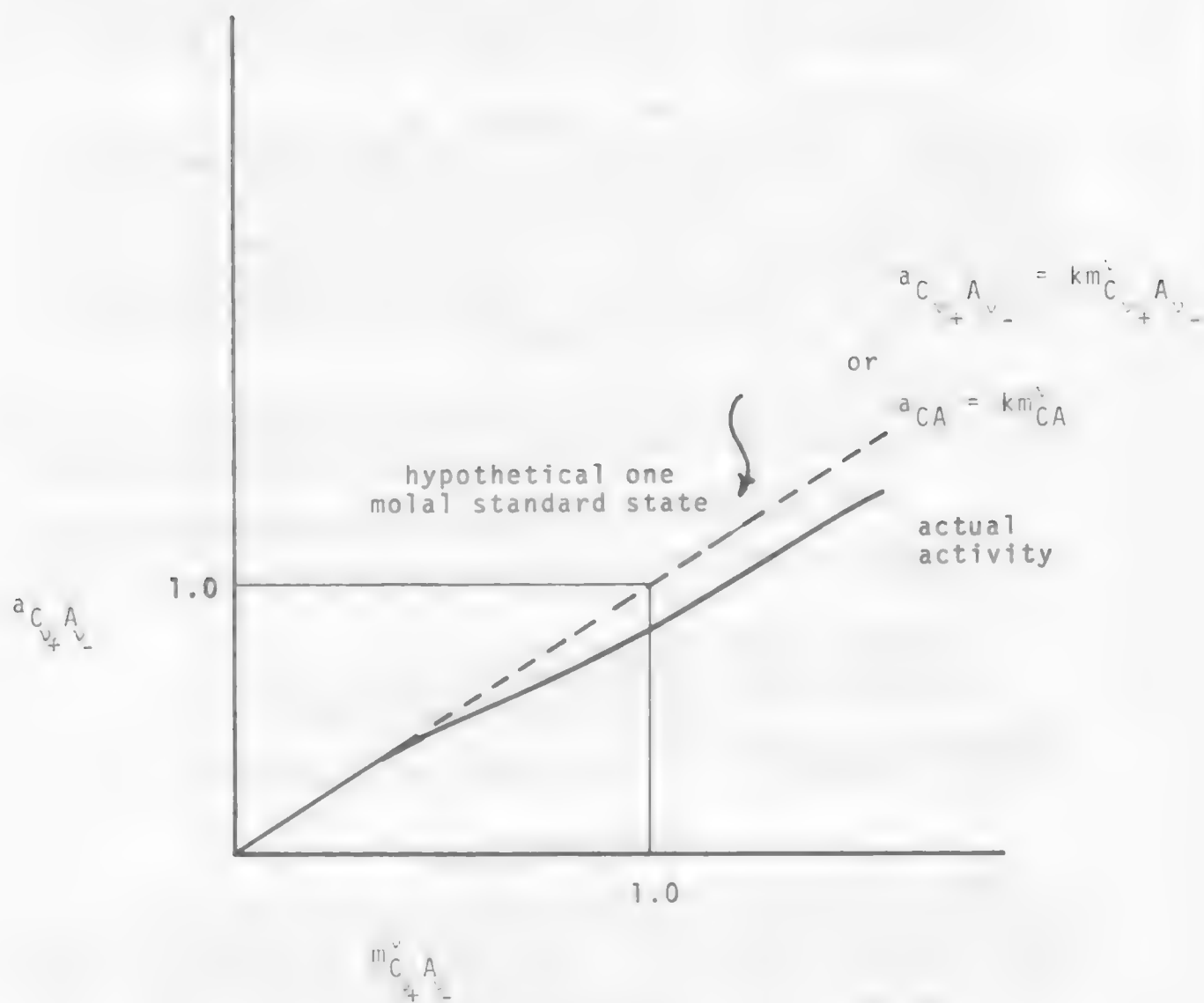
$$a_{\pm} = [(a_+^{v_+})(a_-^{v_-})]^{1/v} \quad [1.2.13]$$

Also, in a more general sense the mean ionic activity coefficient should be,

$$\gamma_{\pm} = [\gamma_+^{v_+} \gamma_-^{v_-}]^{1/v} \quad [1.2.14]$$

Experimentally determined mean activity coefficients for strong electrolytes taken from Oxidation Potentials by Latimer are tabulated in Appendix A. Frequently experimental values are not available at the desired ionic strength. In such cases, the correlations developed by Meissner and his students may be of considerable value (Meissner and Kusik, 1972). The correlations are based on a reduced activity coefficient γ° and the ionic strength of the system. The reduced activity coefficient is defined in the following manner:

Figure 1.2.1. Standard State for Solutes.



$$\gamma^{\circ} = (\gamma_{\pm})^{1/z_1 z_2}$$

The correlations at 25° for strong electrolytes are shown by the family of curves presented in Figure 1.2.2. Each curve represents the behavior of a given electrolyte, so that when one value of γ° for a strong electrolyte is known at a given concentration, the entire curve for this salt can be estimated from Figure 1.2.2.

For example, if we want to determine the mean activity coefficient of KOH at a concentration of 9 molal, first the activity coefficient at some other molality must be found. From the literature, it is found that when $I = 2$, $\gamma_{\pm} = 0.863$ which corresponds to $\log \gamma^{\circ} = 0.064$. If this point is located on the correlation plot, the appropriate curve can be used to determine $\log \gamma^{\circ}$ at $I = 9$. Following this procedure, $\log \gamma^{\circ}$ is found to be 0.66 which corresponds to a mean activity coefficient of $\gamma_{\pm} = 4.57$. Location of the proper curve requires knowledge of at least one value of $\log \gamma^{\circ}$ at a given ionic strength.

In addition to this correlation, relationships have been established which allow calculation of the reduced activity coefficient for a given salt at temperatures other than 25°C and for mixed electrolyte systems.

1.2.3 Determination of Individual Ionic Activity Coefficients

Individual ionic activity coefficients can be determined by a number of techniques:

- experimental data (mean salt method)
- theoretical relationships (Debye-Huckle equation)
- empirical extension of theoretical relationships

Each technique has its own limitations which must be considered for a particular application.

Experimental Data

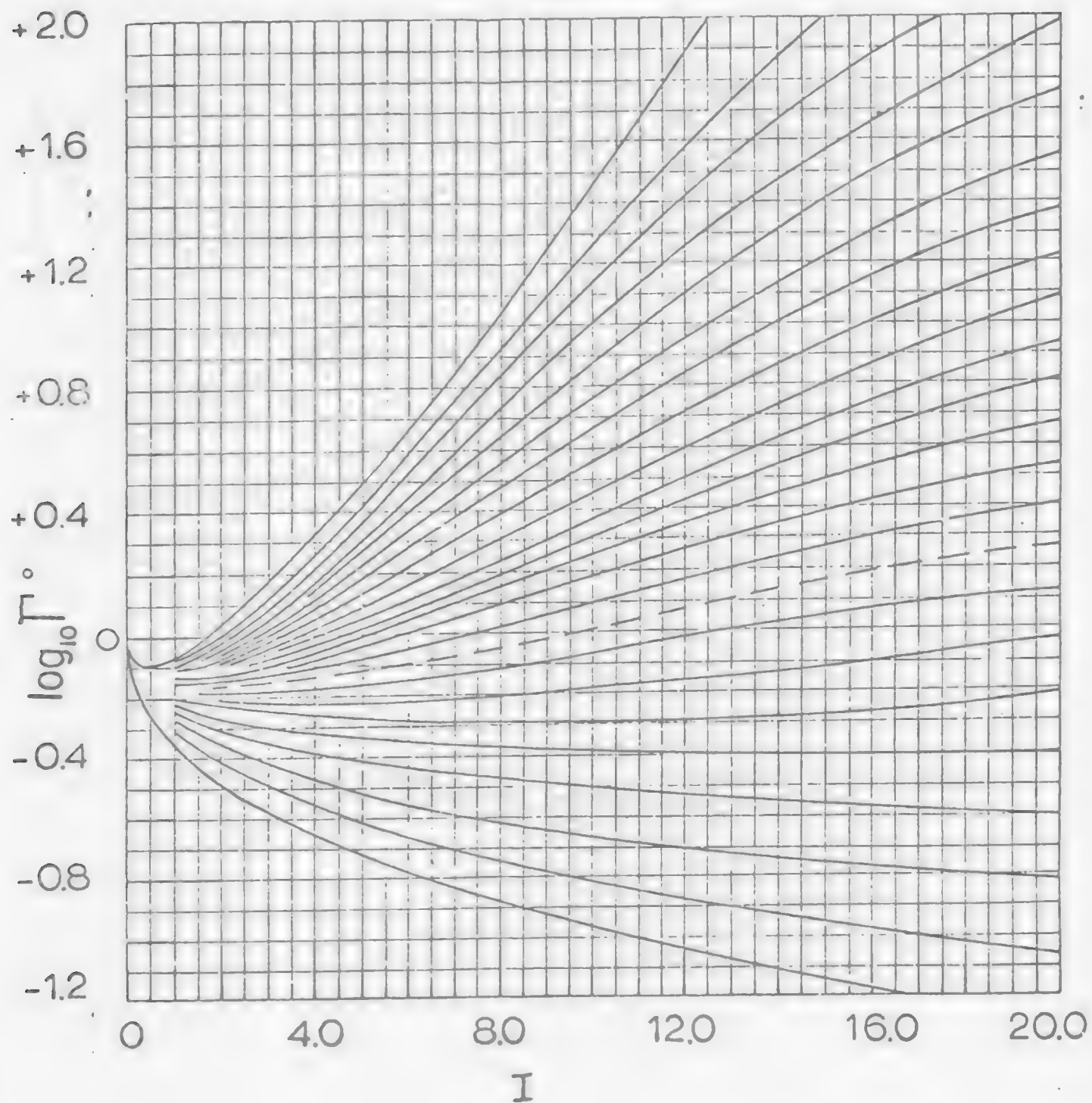
Experimental activity coefficient data is usually tabulated (Appendix A) or presented graphically with the mean activity coefficient as a function of ionic strength (Figure 1.2.3). Using this data to calculate individual ionic activity coefficients is accomplished by the *mean salt method*. The mean salt method is based on the MacInnes assumption that

$$\gamma_{\pm KCl} = (\gamma_K + \gamma_{Cl^-})^{1/2} = \gamma_K^+ = \gamma_{Cl^-} \quad [1.2.15]$$

From this relationship individual ionic activity coefficients can be calculated from experimental mean activity coefficient data at a specified ionic strength.

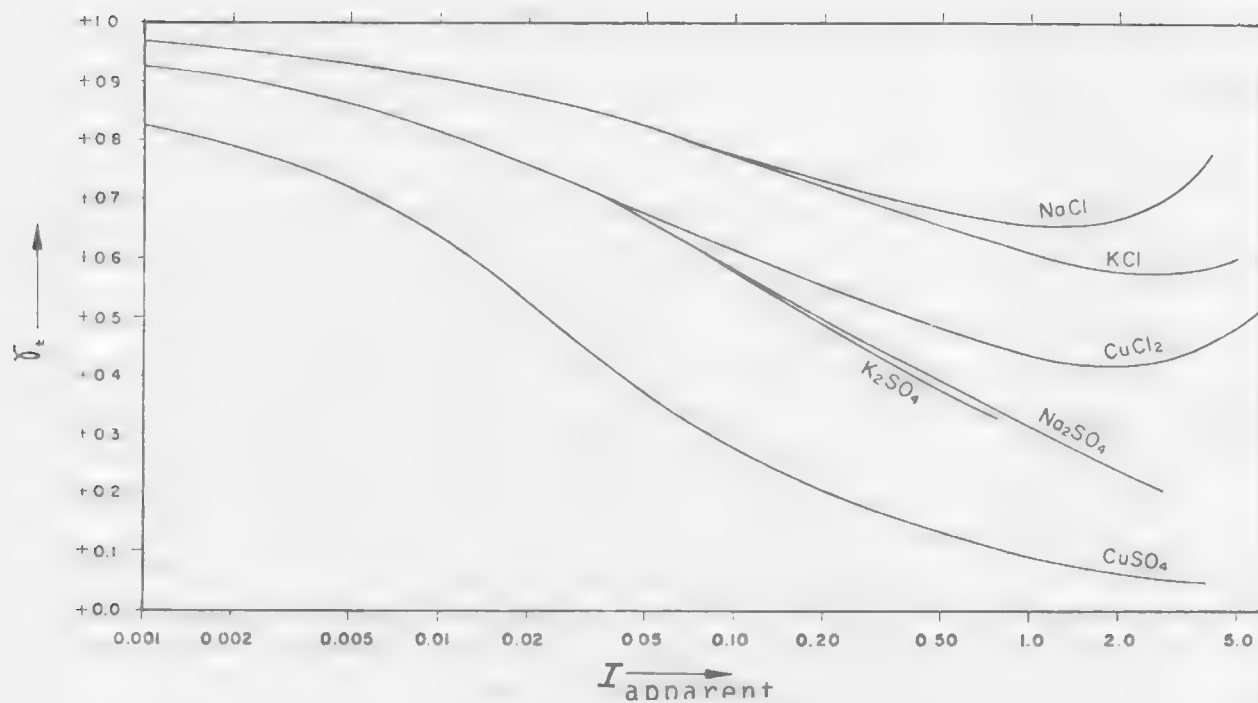
For example, the activity coefficient for cupric ion in 0.05 M copper sulfate solution assuming complete disassociation would be calculated in the following way:

Figure 1.2.2. Generalized Plot of the Reduced Activity Coefficient γ Versus Ionic Strength I Over the Ionic Strength Range of 1.0 to 20.



Source: Meissner and Tester, "Activity Coefficients of Strong Electrolytes in Aqueous Solutions," I&EC Process Design & Dev., II, p. 128 (1972).

Figure 1.2.3. Mean Activity Coefficient as a Function of Ionic Strength.



Source: R. M. Garrels and C. L. Christ, Solutions, Minerals, and Equilibria, Harper and Row, New York, p. 59.

$$I = \frac{1}{2} \sum_i m_i z_i^2 = 0.2 \text{ M} \quad [1.2.16]$$

The mean ionic activity coefficients for this ionic strength are:

$\gamma_{\pm} \text{ @ } I = 0.2 \text{ M}$	
KCl	.72
CuSO ₄	.21
K ₂ SO ₄	.49

$$\gamma_{\pm \text{KCl}} = \gamma_{\text{K}} = \gamma_{\text{Cl}} = 0.72 \quad [1.2.17]$$

$$\gamma_{\pm \text{K}_2\text{SO}_4} = (\gamma_{\text{K}}^2 \gamma_{\text{Cl}})^{1/3} \quad [1.2.18]$$

Solving for the activity coefficient of sulfate ion and substitution of the activity coefficient values for potassium sulfate and potassium ion,

$$\gamma_{\text{SO}_4} = \frac{\gamma_{\text{K}_2\text{SO}_4}}{\gamma_{\text{K}}^2} = \frac{(.49)^3}{(0.72)^2} = 0.23 \quad [1.2.19]$$

$$\gamma_{\text{CuSO}_4} = (\gamma_{\text{Cu}} \gamma_{\text{SO}_4})^{1/2} \quad [1.2.20]$$

Solving for the activity coefficient of cupric ion and substitution of the activity coefficient values for copper sulfate and sulfate ion,

$$\gamma_{\text{Cu}} = \frac{\gamma_{\text{CuSO}_4}^2}{\gamma_{\text{SO}_4}} = \frac{(0.21)^2 (0.72)^2}{(0.49)^3} = 0.19 \quad [1.2.21]$$

Of course this technique is limited to systems for which mean ionic activity coefficients have been measured at the ionic strength of interest. A situation which is not always the case.

Debye-Huckel Theory

(From R. M. Garrels and C. L. Christ, *Solutions Minerals and Equilibria*, pp. 61-62).

"Even in very dilute solutions of electrolytes the charged ions contained in these solutions exert long-range electrostatic forces upon one another with the result that the values of the activity coefficient are lowered. This effect has been evaluated in the Debye-Huckel theory and several very useful equations have been derived on the basis of that theory, which are of great value in handling experimental data.

In dilute solutions, the individual ion activity coefficient is given by the Debye-Huckel expression

$$-\log \gamma_i = \frac{Az_i^2 \sqrt{I}}{1 + a_i^\circ B \sqrt{I}} \quad [1.2.23]$$

Here, z_i and I have the meanings previously ascribed in the definition of ionic strength, and A and B are constants characteristic of the solvent (here considered to be water), at the specified temperature (at 1 atmosphere) are given in Table 1.2.1. The quantity a_i° has a value dependent upon the "effective diameter" of the ion in solution, and is determined largely from experiment; values of a_i° are listed in Table 1.2.2. The physical significance of a_i° , which is commonly related to the diameter of the ion in solution, merits a brief digression.

TABLE 1.2.1. Values of Constants for Use in Debye-Huckel Equation (Aqueous Solution)

Temperature, °C	A	B (x 10 ⁻⁸)
0	0.4883	0.3241
5	0.4921	0.3249
10	0.4960	0.3258
15	0.5000	0.3262
20	0.5042	0.3273
25	0.5085	0.3281
30	0.5130	0.3290
35	0.5175	0.3297
40	0.5221	0.3305
45	0.5271	0.3314
50	0.5319	0.3321
55	0.5371	0.3329
60	0.5425	0.3338

TABLE 1.2.2. Values of a_i^0 for Some Individual Ions in Aqueous Solutions.

$a_i^0 \times 10^8$	Ion
2.5	Rb^+ , Cs^+ , NH_4^+ , Tl^+ , Ag^+
3.0	K^+ , Cl^- , Br^- , I^- , NO_3^-
3.5	OH^- , F^- , HS^- , BrO_3^- , IO_4^- , MnO_4^-
4.0-4.5	Na^+ , HCO_3^- , H_2PO_4^- , HSO_3^- , Hg_2^{++} , SO_4^{--} , SeO_4^{--} , CrO_4^{--} , HPO_4^{--} , PO_4^{3-}
4.5	Pb^{++} , CO_3^{--} , SO_3^{--} , MoO_4^{--}
5.0	Sr^{++} , Ba^{++} , Ra^{++} , Cd^{++} , Hg^{++} , S^{--} , WO_4^{--}
6	Li^+ , Ca^{++} , Cu^{++} , An^{++} , Sn^{++} , Nm^{++} , Fe^{++} , Ni^{++} , Co^{++}
8	Mg^{++} , Be^{++}
9	H^+ , Al^{3+} , Cr^{3+} , trivalent rare earths
11	Th^{4+} , Zr^{4+} , Ce^{4+} , Sn^{4+}

Values of a_i^0 are ordinarily larger than values of ionic diameters given for ions in crystals. This difference presumably stems from the envelope of water molecules that surround the ions in aqueous solution. Some attempts have been made to interpret a_i^0 values structurally, but a clear-cut picture of the coordination of water molecules around the charged ions has not yet emerged. Detailed discussion of the hydration problem is given by Robinson and Stokes" (end quote from Garrels and Christ).

Generally the use of the extended Debye-Huckel equation has been limited to solutions with ionic strengths less than 0.01 M. The good agreement between theory and experimental data for $I < 0.01$ is shown in Figure 1.2.4. However, consideration of complexation reactions and ion pair formation may allow the Debye-Huckel equation to be extended to higher ionic strengths.

With regard to the effectiveness of the Debye-Huckel equation, consider the previous example, 0.05 M CuSO_4 solution ($I = 0.2$). The activity coefficient can be calculated according to equation 1.2.22;

$$-\log \gamma_{\text{Cu}^{++}} = \frac{.509(2)^2 \sqrt{.2}}{1 + .328(6) \sqrt{.2}} \quad [1.2.24]$$

$$\gamma_{\text{Cu}^{++}} = .328$$

As is evident, there is considerable differences between the cupric ion activity coefficient calculated from experimental data by the mean salt method, $\gamma_{\text{Cu}^{++}} = 0.19$, and that calculated from theory according to the extended Debye-Huckel equation.

Empirical Extensions

Finally, the usefulness of the Debye-Huckel equation has been extended by empirical modifications such as the Guntelberg equation, the Guggenheim equation, and the Davies equation. One of the more common modifications is that by Davies;

$$-\log \gamma_i = A z^2 \left(\frac{\sqrt{I}}{1 + \sqrt{I}} - 0.21 \right) \quad [1.2.25]$$

An alignment chart based on the Davies equation is presented in Figure 1.2.5 for graphical estimation of activity coefficients. Note in the case of our 0.05 M copper sulfate example that the value for the activity coefficient of cupric ion is found to be:

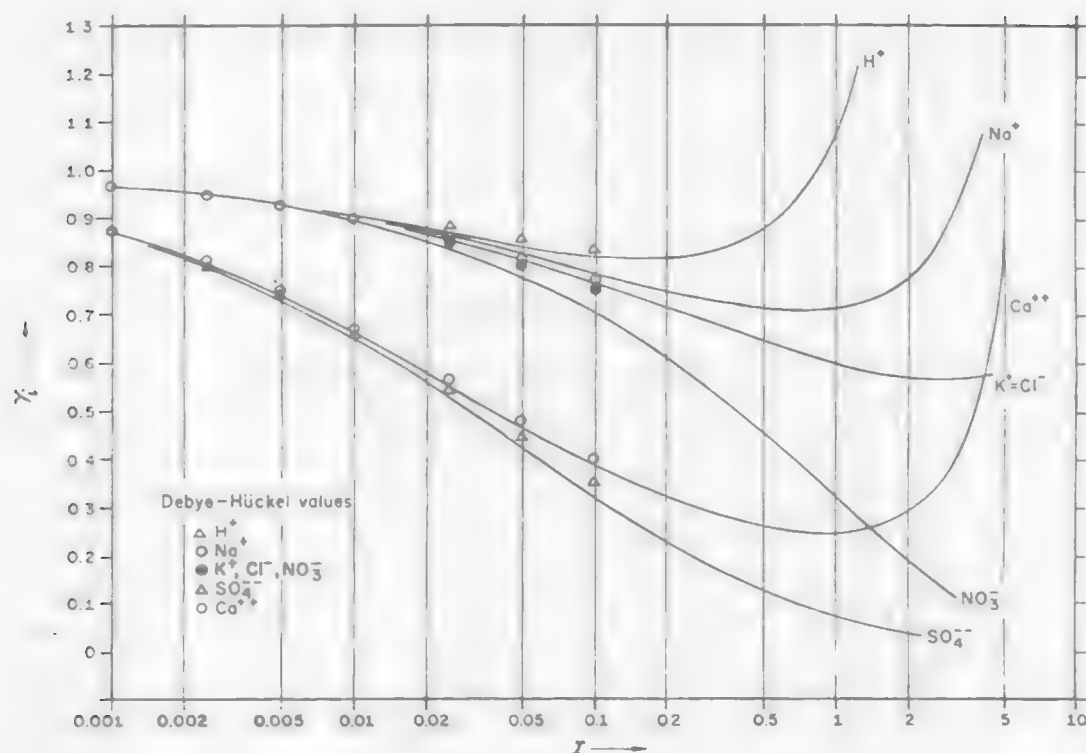
$$\gamma_{\text{Cu}^{++}} = 0.28$$

Although this may be a better estimate of the activity coefficient of the cupric ion, it still deviates significantly from that determined from experimental data by the mean salt method.

A comparison of the cupric ion activity coefficients calculated by the various techniques is presented in Table 1.2.3 for several ionic strengths. These deviations arise because the formation of complex ions has been neglected. Consideration of complex formation shows that the values are much closer and indicates that the Debye-Huckel theory can be used at high apparent ionic strengths.

The comparison presented in Table 1.2.3 is based on the assumption that copper sulfate is completely dissociated, i.e., no interactions occur (no formation of complex ions). A discussion of the nature of complex ions and complexation reactions is presented in the next section.

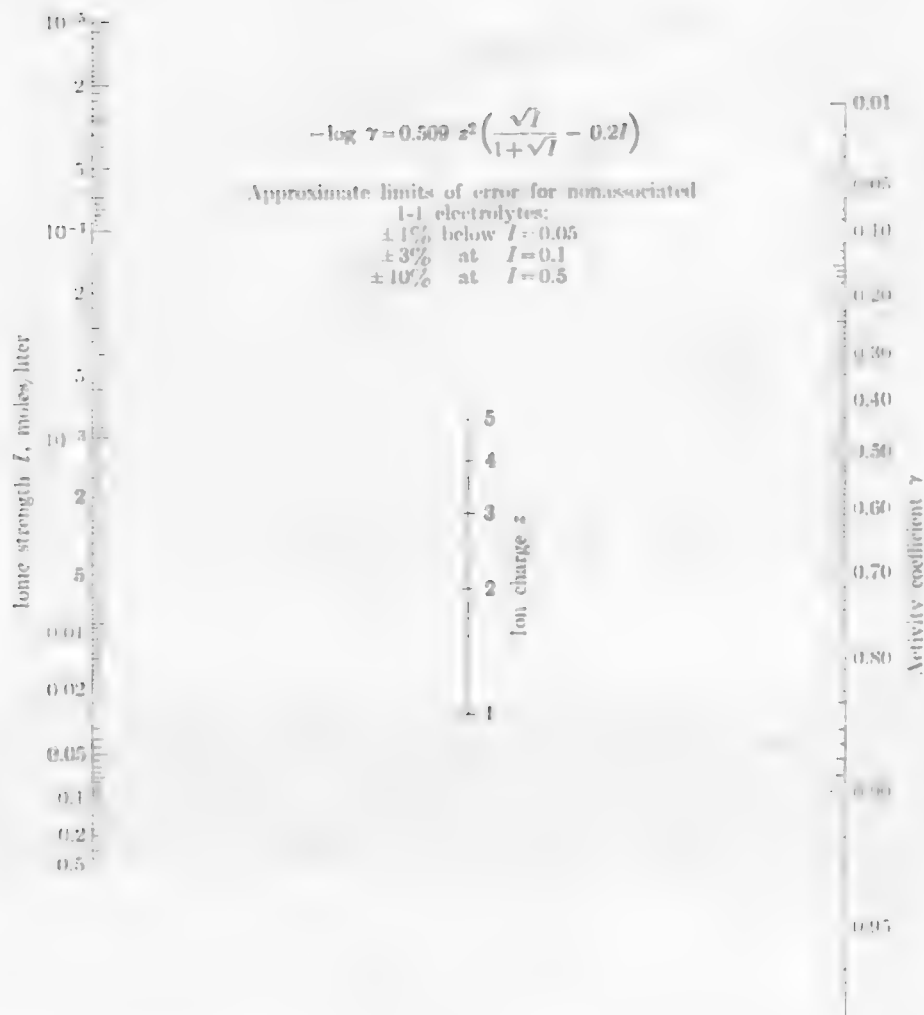
Figure 1.2.4. Individual Ionic Activity Coefficients.*



*Single ion activity coefficients vs. ionic strength for some common ions. Solid lines represent the values calculated by the mean salt method. Debye-Hückel values were calculated using equation 1.2.22, with $108/a_i^\circ = 9$ for H^+ ; 4 for Na^+ ; 3 for K^+ , Cl^- , NO_3^- ; 5 for Ca^{2+} ; and 4 for SO_4^{2-} . The Debye-Hückel γ_i values for the monovalent ions converge, within experimental error, for $I < 0.01$.

Source: R. M. Garrels and C. L. Christ, Solutions, Minerals, and Equilibria, Harper and Row, New York, p. 63.

Figure 1.2.5. Alignment Chart for Calculating Activity Coefficients, Based on the Davies Equation.



Source: Butler, Ionic Equilibrium A Mathematical Approach, Addison-Wesley (1964).

TABLE 1.2.3. Comparison of Activity Coefficients for Cupric Ion in Various Copper Sulfate Solutions Determined by Different Computational Techniques.

Computational Method	Copper Sulfate Molality		
	0.0005	0.005	0.05
Mean Salt (experimental data)	0.77	0.50	0.19
Extended Debye-Huckel equation 1.2.22 (theory)	0.83	0.59	0.33
Davies equation 1.2.25 (semi-theoretical)	0.82	0.57	0.29
Apparent Ionic Strength (assuming no complex formation)	.002	.02	.2

The significance of this phenomenon with respect to the estimation of activity coefficients is that the composition of the aqueous phase may not be as simple as assumed. For example, in the case of copper sulfate system, the cupric ion and sulfate ion associate to form a neutral ion pair species, CuSO_4^0 . As a result, the concentration of both cation and anion is reduced and the effective ionic strength decreases.

Because these interactions can be significant they must be taken into consideration. The definition of the mean ionic activity coefficient for an electrolyte presented in equation 1.2.14 is more accurately represented by;

$$\gamma_{\pm} = \left[\left(\frac{m_+}{m_{T+}} \gamma_+ \right)^{v_+} \left(\frac{m_-}{m_{T-}} \gamma_- \right)^{v_-} \right]^{1/v} \quad [1.2.26]$$

where

m_{T+} , m_{T-} are the total molalities of cation and anion in all forms,

and, m_+ , m_- are the actual molalities of the cation and anion. This formulation takes into consideration the complexation reactions that may occur and accounts for the discrepancies between theory and experiment presented in Table 1.2.4. Reconsideration of the copper sulfate system in light of the following complexation reaction;



results in the following cupric ion activity coefficients presented in Table 1.2.4. The equations necessary to make this calculation are discussed in the next section (1.3.3 Distribution of Species) on page 1.3.3. For this simple system involving a symmetrical electrolyte and the neutral ion pair, CuSO_4° , note that equation 1.2.27 reduces to

$$\gamma_{\pm} = \frac{m}{m_T} (\gamma_+ \gamma_-)^{1/2} \quad [1.2.28]$$

since $m_+ = m$ and $M_{T+} = m_{T-} = m_T$

Under these circumstances, it is observed that much closer agreement between theory and experiment is realized and it appears that the Debye-Huckel equation may be used with some confidence at higher concentrations by consideration of complexation reactions.

TABLE 1.2.4. Comparison of Activity Coefficients for Cupric Ion in Various Copper Sulfate Solutions Taking into Consideration Complexation Reactions.

Computational Method	Copper Sulfate Molality		
	0.0005	0.005	0.05
Mean Salt (experimental data)	0.84	0.70	0.33
Extended Debye-Huckel equation 1.2.22 (theory)	0.83	0.62	0.38
Davies equation 1.2.25 (semi-theoretical)	0.83	0.60	0.33
Ionic Strength Considering Complexation Reaction	0.00190	0.0161	0.128

1.2.4 Activity Coefficients of Neutral Molecular Species

The activity coefficient-ionic strength relationship for neutral molecular aqueous species; such as dissolved gases, ion pairs, and weak acids or bases, generally is of the following form for ionic strengths of less than 5 molal: (Butler, p. 439)

$$\log \gamma_0 = kI$$

The activity coefficients of these species are generally equal to, or greater than, unity (HCN_{aq} is an exception). The constant k is referred to as the salting coefficient due to the fact that an increase in the concentration of dissolved ionic species (increased ionic strength) results in a decrease in solubility of the neutral molecular species, the salting-out-effect. As a first approximation, which should be valid for ionic strengths of less than 0.1 molar, the activity coefficient for neutral molecular species can be taken as being equal to unity.

Appendix A

ACTIVITY COEFFICIENTS OF STRONG ELECTROLYTES

Electrolyte	.001	.002	.005	.01	.02	.05	.1	.2	.5	1.0	2.0	3.0	4.0
HCl	.966	.952	.928	.904	.875	.830	.796	.767	.758	0.809	1.01	1.32	1.76
HBr	.966929	.906	.879	.838	.805	.782	.790	0.871	1.17	1.67	...
HNO ₃	.965	.951	.927	.902	.871	.823	.785	.748	.715	0.720	0.783	0.876	0.982
HClO ₄	0.81	1.04	1.42	2.02
HIO ₄	.96	.94	.91	.86	.80	.69	.58	.46	.29	0.19	0.10	0.073	0.060
H ₂ SO ₄	.830	.757	.630	.544	.453	.340	.265	.209	.154	0.130	0.124	0.141	0.171
NaOH8273	.69	0.68	0.70	0.77	0.89
KOH92	.90	.86	.82	.8073	0.76	0.89	1.08	1.35
CsOH92	.88	.83	.80	.76	.74	0.78
Ba(OH) ₂853	.773	.712	.627	.526	.443	.370
AgNO ₃92	.90	.86	.79	.72	.64	.51	0.40	0.28
Al(NO ₃) ₃20	.16	.14	0.19	0.45	1.0	1.2
BaCl ₂	.8877	.7256	.49	.44	.39	0.39	0.44
Ba(NO ₃) ₂	.88	.84	.77	.71	.63	.52	.43	.34
Ba(IO ₃) ₂	.83	.79	.71	.64	.55
CaCl ₂	.89	.85	.785	.725	.66	.57	.515	.48	.52	0.71
Ca(NO ₃) ₂	.88	.84	.77	.71	.64	.54	.48	.42	.38	0.35	0.35	0.37	0.42
CdCl ₂	.76	.68	.57	.47	.38	.28	.21	.15	.09	0.06
CdI ₂	.76	.65	.49	.38	.28	.17	.11	.068	.038	0.025	0.018
CdSO ₄	.73	.64	.50	.40	.31	.21	.17	.11	.067	0.045	0.035	0.036	...
CsF	.98	.97	.96	.95	.94	.91	.89	.87	.85	0.87
CsCl92	.90	.86	.79	.75	.69	.60	0.54	0.49	0.48	0.47
CsBr93	.90	.86	.79	.75	.69	.60	0.53	0.48	0.46	0.46
CsI75	.69	.60	0.53	0.47	0.43	...
CsNO ₃73	.65	.52	0.42
CaAc79	.77	.76	0.80	0.95	1.15	...
CuCl ₂	.89	.85	.78	.72	.66	.58	.52	.47	.42	0.43	0.51	0.59	...
CuSO ₄	.7453	.41	.31	.21	.16	.11	.068	0.047
FeCl ₂	.89	.86	.80	.75	.70	.62	.58	.55	.59	0.67
Fe ₂ (SO ₄) ₃142	.092	.054	.035	.022
KF96	.95	.93	.92	.88	.85	.81	.74	0.71	0.70
KCl	.965	.952	.927	.901815	.769	.719	.651	0.606	0.576	0.571	0.579
KBr	.965	.952	.927	.903	.872	.822	.777	.728	.665	0.625	0.602	0.603	0.622
KI	.965	.951	.927	.905	.88	.84	.80	.76	.71	0.68	0.69	0.72	0.75
K ₄ Fe(CN) ₆19	.14	.11	.067
KClO ₃	.967	.955	.932	.907	.875	.813	.755
K ₂ O ₈	.89	.86	.81	.74	.68	.58	.50	.43	.36	0.33	0.33	0.39	0.49
K ₂ CO ₃	.965	.951	.924	.895	.857	.788
K ₂ SO ₄	.8978	.71	.64	.52	.43	.36
LaCl ₃38	.32	.28	.27	0.36
La(NO ₃) ₃57	.49	.39	.33	.27
LaCl	.963	.948	.921	.89	.86	.82	.78	.75	.73	0.76	0.91	1.18	1.46
LiBr	.966	.954	.932	.909	.882	.842	.810	.784	.783	0.848	1.06	1.35	...
LiI81	.80	.81	0.89	1.19	1.70	...
LiNO ₃	.966	.953	.930	.904	.878	.834	.798	.765	.743	0.76	0.84	0.97	...
LiClO ₄	.967	.955	.933	.911	.884	.842	.810	.782	.77	0.81
LiClO ₃	.967	.956	.935	.915	.890	.853	.825	.805	.82	0.91
MgCl ₂56	.53	.52	0.62	1.05	2.1	...
Mg(NO ₃) ₂	.88	.84	.77	.71	.64	.55	.51	.46	.44	0.50	0.69	0.93	...
MgSO ₄40	.32	.22	.18	.13	.088	0.064	0.055	0.064	...
MnSO ₄25	.17	.11	0.073	0.058	0.062	0.079

Source: W. M. Latiman, Oxidation Potentials, 2nd ed., Prentice Hall.

Appendix A (continued)

ACTIVITY COEFFICIENTS OF STRONG ELECTROLYTES

<i>m</i>	001	002	005	01	02	05	1	2	5	10	20	30	40
NaSO ₄							.18	.13	.075	0.051	0.041		
NH ₄ Cl	.961	.944	.911	.88	.84	.79	.74	.69	.62	0.57			
NH ₄ Br	.964	.949	.901	.87	.83	.78	.73	.68	.62	0.57			
NH ₄ I	.962	.946	.917	.89	.86	.80	.76	.71	.65	0.60			
NH ₄ NO ₃	.959	.942	.912	.88	.84	.78	.73	.66	.56	0.47			
(NH ₄) ₂ SO ₄	.874	.821	.726	.67	.59	.48	.40	.32	.22	0.16			
NaF			.93	.90	.87	.81	.75	.69	.62				
NaCl	.966	.953	.929	.904	.875	.823	.780	.730	.68	0.66	0.67	0.71	0.78
NaBr	.966	.955	.934	.914	.887	.844	.800	.740	.695	0.686	0.734	0.826	0.934
NaI	.97	.96	.94	.91	.89	.86	.83	.81	.78	0.80	0.95		
NaNO ₃	.966	.953	.93	.90	.87	.82	.77	.70	.62	0.55	0.48	0.44	0.41
Na ₂ SO ₄	.887	.847	.778	.714	.641	.53	.45	.36	.27	0.20			
NaClO ₄	.97	.95	.93	.90	.87	.82	.77	.72	.64	0.58			
PbCl ₂	.86	.80	.70	.61	.50								
Pb(NO ₃) ₂	.88	.84	.76	.69	.60	.46	.37	.27	.17	0.11			
RbCl			.93	.90			.76	.71	.63	0.58	0.54	0.54	0.54
RbBr							.76	.70	.63	0.58	0.53	0.52	0.51
RbI							.76	.70	.63	0.57	0.53	0.52	0.51
RbNO ₃							.73	.65	.53	0.43	0.32	0.25	0.21
RbAc							.73	.65	.52	0.42			
TlCl	.96	.95	.93	.90									
TlNO ₃						.77	.70	.60					
TlClO ₄						.79	.73	.65	.53				
TlAc						.80	.74	.68	.59	0.51	0.44	0.40	0.38
ZnCl ₂	.88	.84	.77	.71	.64	.56	.50	.45	.38	0.33			
ZnSO ₄	.70	.61	.48	.39			.15	.11	.065	0.045	0.036	0.04	

LEARNING ACTIVITY 3

1.3 Complex EquilibriaLearning Activity Objective

After completing your study of this learning material you should be able to list the basic features of complex ions, be able to set-up and solve a set of simultaneous equations to determine the distribution of aqueous species, and be able to use the computer programs for these tedious calculations.

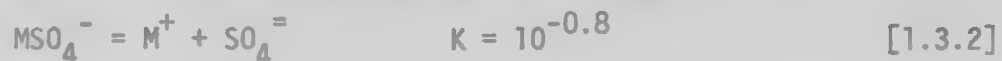
1.3.1 Complex Ions

Ionic interactions may result in the formation of complex ions, a phenomenon which is of primary importance in hydrometallurgical reactions. The stability of various complex ions such as $\text{UO}_2(\text{SO}_4)_2^-$, $\text{Au}(\text{CN})_2^-$ and $\text{Cu}(\text{NH}_3)_4^+$ constitute the basis of many hydrometallurgical processes.

Perhaps the simplest complex ion is that which forms simply by association phenomena. Ions of opposite charge associate into a distinct entity which can be identified by experimental techniques. The bonding is weak and each component generally retains its primary waters of hydration. The best illustration of this type of complex ion is given by the complexes which form between simple divalence cations and the sulfate radical. The stabilities of these complexes are independent of the particular cation involved and all have about the same disassociation constant,



A similar situation exists for monovalent cations for which



The implication is that the complex (an ion pair) is an association between the hydrated cation and the sulfate anion since the hydrated radii of the cations would be similar perhaps resulting in similar bond strengths in the ion pair and as a consequence the same disassociation constant. In other cases the formation of ion pairs appears to involve more specific chemical interaction and the bond strength of the ion pair (unlike the sulfate ion pairs) reflects the electronegativity of the participating ions such as hydroxy complexes (MOH^+) and carbonate ion pairs ($\text{MCO}_3 \text{aq}$).

More specific interactions generally are of greater interest to the hydrometallurgists. Complex formation in this case usually involves displacement of coordinated water molecules by other ligands, the complexing agents. This displacement is frequently accompanied by a change in coordination number.

Ligands can be any negative ion or neutral molecule which are directly attached to a positively charged metal ion. The most common types of ligands are monatomic or polyatomic negative ions and neutral polar molecules. The neutral molecules have one or more pair of unshared electrons, for example NH_3 and H_2O . The charged or polar ligands are oriented so that the excess charge or unshared pair of electrons points directly at the metal ion.

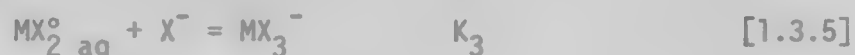
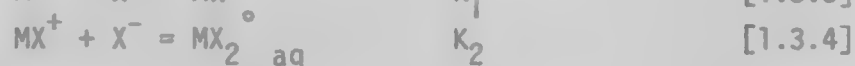
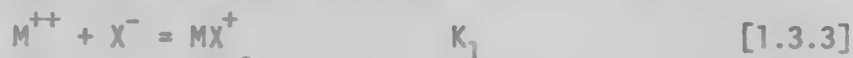
In the case of transition-metal ions the d orbitals are either only partially filled or completely empty. In the absence of a negative field, the d-electrons of the metal ion have orbitals of equal energy, i.e., degenerate orbitals. In presence of the ligand's field, the energies of these orbitals are split into different levels. As a result, the ligands will complex with the ion with specific ligand orientation - such as tetrahedral complexes, octahedral complexes, etc.

Metal-ligand interaction has been described by the Crystal Field Theory as a pure electrostatic force where no orbital overlapping occurs. Alternately, the interaction has been described by the Molecular Orbital Theory as a covalent bond in which ligand and d orbitals are completely overlapping. Note, however, the ligands are not point charges as described by the Crystal Field theory, and they are not pure covalent bonds as described by the Molecular Orbital theory. Later, one Ligand Field theory was adopted which is based on the Crystal Field theory but allows for some electron cloud overlap effects by inserting certain parameters for empirical adjustment of the data.

1.3.2 Stability Constants

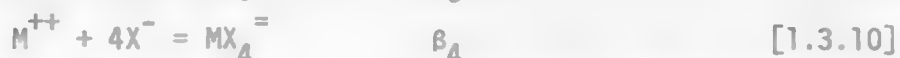
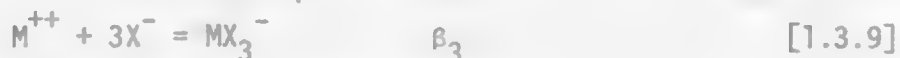
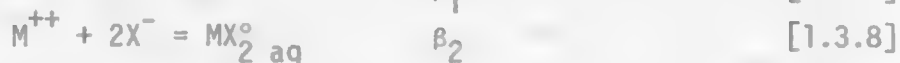
Whatever the bonding may be in these complex ions, from the engineer's standpoint, the concentration of these species must be calculated in order to determine kinetic parameters and equilibrium states for a particular system. The stabilities of various complex ions are generally represented either by stepwise formation constants (K) or overall formation constants (β).

The stepwise formation constants are equilibrium constants which describe the sequential addition of ligands to a particular cation. Consider the hypothetical example of a divalent cation (M^{++}) and the univalent anion (X^-). The following reactions may occur:



K_1 , K_2 , K_3 and K_4 represent the stepwise formation constants for the first, second, and third and fourth ligand additions, respectively.

Overall formation constants (β) differ in that the complexation reaction is written in terms of the uncomplexed cation and the appropriate number of ligands. Using the same notations as previously used;



It should be noted that the stepwise formation constants and the overall formation constants are related by,

$$\beta_n = \prod_{i=1}^n K_i \quad [1.3.11]$$

Both forms of the stability constants will be found reported in the literature. Probably the most exhaustive reference for the stability constants of complex ions is, "Stability Constants. Part III: Inorganic Ligands" by Bjerrum, Schwarzenbach and Sillen, London, The Chemical Society (1958). Care must be taken in using these values to establish whether the reported value is a true thermodynamic equilibrium constant (corrected for $I=0$) or if the constant reported is simply based on the concentration of reactants and products at equilibrium, the ion product for ($I>0$).

1.3.3 Distribution of Species

To determine the concentration of each species present in a particular system, a number of defining equations are used. The equilibrium state of the system may be defined in terms of the following equation types:

mass balance equations

based on the conservation of the mass of a particular component

charge balance equations

based on the electroneutrality that must be maintained in the solution

mass action expressions

based on the chemical interaction between various species and defined in terms of the appropriate equilibrium constant.

The first two equation types are based on the concentration of each species, whereas the last equation type, the mass action expressions, are based on the activity of each of the species involved in a particular equilibrium.

In order to solve the set of simultaneous equations which arises, the activity coefficient for each species must be estimated and this then links the linear equations (mass balance and charge balance) with the non linear equations (mass action expressions). Frequently the estimation of the activity coefficients is accomplished by use of the extended Debye-Huckel equation and if the ionic strength (I) is not known a-priori, then the calculation of the concentration of each species becomes an iterative process which for multicomponent systems is most easily done on the computer. See Section 1.3.4. Regardless, the concept or approach is the same and will be illustrated by manual calculation for some simple systems.

To begin with, consider the copper sulfate example in Section 1.2.3 in which it was stated that consideration of complexation reactions allowed the extended Debye-Huckel equation to be used with good confidence at higher ionic strengths than would normally be recommended. The calculation which shows this probably represents the simplest distribution of species problems that one could design. To restate the problem, consider a 0.05 m CuSO_4 solution and determine the concentration of each species in solution at equilibrium. The stability of the copper sulfate ion pair, CuSO_4° , (a dissolved neutral molecular species) is given by the following dissociation constant,



These species constitute the only aqueous species present in the system. The following defining equations should be recognized:

mass balance on copper,

$$0.05 = (\text{Cu}^{++}) + (\text{CuSO}_4^\circ)_{\text{aq}} \quad [1.3.13]$$

charge balance

$$(\text{H}^+) + 2(\text{Cu}^{++}) = (\text{OH}^-) + 2(\text{SO}_4^{=}) \quad [1.3.14]$$

(Since the solution is at a neutral pH and since the concentrations of (Cu^{++}) and $(\text{SO}_4^{=})$ will greatly exceed the concentrations of (H^+) and (OH^-) , they are insignificant and can be eliminated from the equation.)

$$\frac{a_{\text{Cu}^{++}} \cdot a_{\text{SO}_4^{=}}}{a_{\text{CuSO}_4^\circ \text{ aq}}} = 10^{-2.23} \quad [1.3.15]$$

or

$$\frac{(\gamma_{\text{Cu}^{++}})(\text{Cu}^{++})(\gamma_{\text{SO}_4^{=}})(\text{SO}_4^{=})}{(\text{CuSO}_4^\circ)_{\text{aq}}} = 10^{-2.23} \quad [1.3.16]$$

(recall that $\gamma_{\text{CuSO}_4^{\circ} \text{aq}} = 1.0$, see Section 1.2.4).

Note that if the activity coefficient were known (specified ionic strength), then we have three equations and three unknowns. Combining equations [1.3.13], [1.3.14], and [1.3.16], the following quadratic equation in $(\text{CuSO}_4^{\circ})_{\text{aq}}$ is obtained.

$$\frac{(\gamma_{\text{Cu}^{++}})(\gamma_{\text{SO}_4^{\circ}})[0.05 - (\text{CuSO}_4^{\circ})_{\text{aq}}]^2}{(\text{CuSO}_4^{\circ})_{\text{aq}}} = 10^{-2.23} \quad [1.3.17]$$

or

$$(\text{CuSO}_4^{\circ})_{\text{aq}}^2 - (0.1 + \frac{5.89 \times 10^{-3}}{\gamma_{\text{Cu}^{++}} \gamma_{\text{SO}_4^{\circ}}})(\text{CuSO}_4^{\circ})_{\text{aq}} + 2.5 \times 10^{-3} = 0 \quad [1.3.18]$$

By assuming an ionic strength, the activity coefficients ($\gamma_{\text{Cu}^{++}}$ and $\gamma_{\text{SO}_4^{\circ}}$) can be calculated from the extended Debye-Huckel (DH) equation and the quadratic equation solved for the $(\text{CuSO}_4^{\circ})_{\text{aq}}$; and subsequently for the concentrations of the other species. The ionic strength can then be calculated and compared to that which had been assumed. Iteration on this procedure (each time taking the calculated ionic strength as the new value) until calculated and assumed ionic strengths agree represents the solution to the set of defining equations. In this example the ionic strength would be,

$$I = \frac{1}{2} \sum_i z_i^2 c_i = \frac{1}{2} [2^2 (\text{Cu}^{++}) + 2^2 (\text{SO}_4^{\circ})] \quad [1.3.19]$$

and since $(\text{Cu}^{++}) = (\text{SO}_4^{\circ})$

$$I = 4(\text{Cu}^{++})$$

As an initial guess assume $I = 0.2$ (complete dissociation). Calculating the activity coefficients from the extended DH equation (1.2.22) and solving equation [1.3.18], it is found that $(\text{CuSO}_4^{\circ})_{\text{aq}} = 0.0168$; therefore $(\text{Cu}^{++}) = (\text{SO}_4^{\circ}) = 0.05 - 0.0168 = 0.0332$ and the calculated ionic strength is

$$I = 4(0.0332) = 0.1338$$

which deviates considerably from the value of 0.2 which was assumed.

Now using this value of I to estimate new activity coefficients and solving again for $(\text{CuSO}_4^{\circ})_{\text{aq}}$, it is found that $(\text{CuSO}_4^{\circ})_{\text{aq}} = 0.0192$ and the corresponding calculated ionic strength is,

$$I = 4(0.0308) = 0.1232$$

which is much closer to the assumed value of 0.1338. Further iterations would bring even closer agreement and this exercise is left for the student.

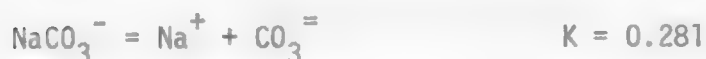
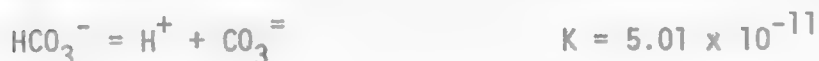
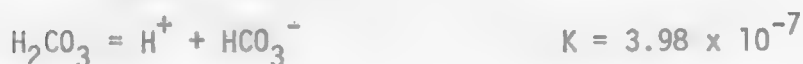
A more complicated system illustrates the usefulness of the computer in solving these complex equilibria problems. Calculate the distribution of species in a closed system containing 0.1 m total sodium and 0.1 m total carbon at pH 8.4 and 25°C.

Species: Na^+ , NaCO_3^- , $\text{NaHCO}_3^\circ_{\text{aq}}$, $\text{CO}_3^{=}$, HCO_3^- , $\text{H}_2\text{CO}_3^\circ_{\text{aq}}$

Sodium Balance: $(\text{Na}^+) + (\text{NaCO}_3^-) + ((\text{NaHCO}_3^\circ)_{\text{aq}}) = 0.1$

Carbon Balance: $(\text{NaCO}_3^-) + (\text{NaHCO}_3^\circ)_{\text{aq}} + (\text{CO}_3^{=}) + (\text{HCO}_3^-) + (\text{H}_2\text{CO}_3) = 0.1$

Mass Action Expressions:



Note that if the activity coefficients (ionic strength) were known, this represents a system of six equations and six unknowns.

LEARNING ACTIVITY 4

Learning Activity Objective

After studying the material presented in this learning activity you should be able to use the computer program to solve for the concentration of solution species in a complex hydrometallurgical solution.

1.3.4 Computer Program for Solution Equilibrium Calculations

These tedious calculations are considerably simplified by the solution equilibrium computer program developed at the University of Utah. The Program Strategy, the User's Manual (including an example calculation) and a Program Listing are presented below.

PROGRAM STRATEGY

Problem Statement: It is desired to determine the concentration and activity of ' n_s ' species in solution. In practice, this reduces to solving a system of ' n_s ' non-linear equations and unknowns.

Method of Solution: The following basic relationships can be established:

1. LINEAR EQUATIONS: (Mass or Charge Balance)

$$\sum_{j=1}^{n_s} a_{ij} c_j = d_i; i = 1, 2, \dots, n_1 \quad [1.4.1]$$

where:

n_s = total number of species in solution

a_{ij} = coefficient of c_j in the i^{th} equation

c_j = concentration of the j^{th} species in solution

d_i = constant

n_1 = total number of linear equations $\leq n_s$

2. NON-LINEAR EQUATIONS: (Mass Action Expressions)

$$\sum_{j=1}^{n_s} b_{ij} \ln(\gamma_j c_j) = \ln K_i; i = n_1 + 1, n_1 + 2, \dots, n_s \quad [1.4.2]$$

where:

- b_{ij} = stoichiometry coefficient of species 'j' in reaction i ($b_{ij} > 0$ for products, $b_{ij} < 0$ for reactants)
- γ_j = activity coefficient of species 'j' (Estimated by the Debye-Huckel relationship)
- $\ln K_i$ = natural logarithm of the equilibrium constant for reaction i

Note that the index i refers to the equation number and the index j refers to the species.

Let's define:

$$x_j = \ln c_j \Leftrightarrow c_j = e^{x_j}, \quad j = 1, 2, \dots, n_s \quad [1.4.3]$$

Then, Equations 1 and 2 become

$$\sum_{j=1}^{n_s} a_{ij} e^{x_j} = d_i, \quad i = 1, 2, \dots, n_1 \quad [1.4.4]$$

$$\sum_{j=1}^{n_s} b_{ij} x_j = \ln K_i - \sum_{j=1}^{n_s} b_{ij} \ln \gamma_j = d_i,$$

$$i = n_1 + 1, n_1 + 2, \dots, n_s \quad [1.4.5]$$

By defining:

$$a_{ij} = 0; \text{ for any } i > n_1$$

$$\text{and: } b_{ij} = 0; \text{ for any } i \leq n_1$$

Equations 1.4.4 and 1.4.5 can be combined to yield the non-linear problem:

Find $\underline{x} = (x_1, x_2, \dots, x_{n_s})$, such that:

$$F_i(x_1, x_2, \dots, x_{n_s}) \equiv \sum_{j=1}^{n_s} a_{ij} e^{x_j} + \sum_{j=1}^{n_s} b_{ij} x_j - d_i = 0, \quad i = 1, \dots, n_s \quad [1.4.6]$$

This problem can be solved numerically by using the Newton - Raphson method. A first order Taylor series expansion of the function $F_i(\underline{x})$ about an initial guess of the solution, $\underline{x}^{(1)}$, is given by:

$$F_i(\underline{x}) \approx F_i(\underline{x}^{(1)}) + \sum_{k=1}^{n_s} \left[\frac{\partial F_i}{\partial x_k} \right]_{\underline{x}^{(1)}} \cdot \Delta x_k^{(1)}; \quad i = 1, \dots, n_s \quad [1.4.7]$$

where: $\underline{\Delta x}^{(1)} = (\Delta x_1^{(1)}, \Delta x_2^{(1)}, \dots, \Delta x_{n_s}^{(1)}) = \underline{x} - \underline{x}^{(1)}$

$$\left[\frac{\partial F_i}{\partial x_k} \right]_{\underline{x}^{(1)}} = a_{ik} e^{x_k^{(1)}} + b_{ik} \quad \begin{matrix} i = 1, 2, \dots, n_s \\ k = 1, 2, \dots, n_s \end{matrix}$$

assuming $(\frac{\partial d_i}{\partial x_k})_{\underline{x}} \rightarrow 0$

A better approximation to the true solution, \underline{x} , is the vector:

$$\underline{x}^{(2)} = \underline{x}^{(1)} + \underline{\Delta x}^{(1)} \quad [1.4.8]$$

such that:

$$F_i(\underline{x}^{(2)}) \approx F_i(\underline{x}^{(1)}) + \sum_{k=1}^{n_s} \left(\frac{\partial F_i}{\partial x_k} \right)_{\underline{x}^{(1)}} \cdot \Delta x_k^{(1)} = 0 \quad [1.4.9]$$

The problem is now reduced to the solution of a linear system of equations, whose solution is the unknown increment vector $\underline{\Delta x}^{(1)}$.

From Equations 1.4.3, 1.4.6, 1.4.9:

$$\sum_{j=1}^{n_s} (a_{ij} c_j^{(1)} + b_{ij}) \Delta x_j^{(1)} = d_i - \sum_{j=1}^{n_s} a_{ij} c_j^{(1)} - \sum_{j=1}^{n_s} b_{ij} x_j^{(1)} \quad [1.4.10]$$

$i = 1, 2, \dots, n_s$

or, in matrix form:

$$(\underline{A} \underline{C}^{(1)} + \underline{B}) \underline{\Delta X}^{(1)} = \underline{D}^{(1)} - \underline{A} \underline{C}^{(1)} \underline{U} - \underline{B} \underline{X}^{(1)} \quad [1.4.11]$$

where:

$$\underline{A} = \begin{bmatrix} a_{11} & a_{12} & \dots & a_{1n_s} \\ \vdots & \vdots & & \vdots \\ a_{n_s 1} & a_{n_s 2} & \dots & a_{n_s n_s} \end{bmatrix}; \underline{C}^{(1)} = \begin{bmatrix} c_1^{(1)} & \bigcirc & \dots & \bigcirc \\ \vdots & \vdots & \ddots & \vdots \\ \bigcirc & \dots & \dots & c_{n_s}^{(1)} \end{bmatrix}$$

$$\underline{B} = \begin{bmatrix} b_{11} & b_{12} & \dots & b_{1n_s} \\ \vdots & \vdots & & \vdots \\ b_{n_s 1} & b_{n_s 2} & \dots & b_{n_s n_s} \end{bmatrix}; \underline{\Delta X}^{(1)} = \begin{bmatrix} \Delta x_1^{(1)} \\ \vdots \\ \Delta x_{n_s}^{(1)} \end{bmatrix}$$

$$\underline{D}^{(1)} = \begin{bmatrix} d_1^{(1)} \\ \vdots \\ d_{n_s}^{(1)} \end{bmatrix}; \underline{U} = \begin{bmatrix} 1 \\ \vdots \\ 1 \end{bmatrix} \text{ and } \underline{X}^{(1)} = \begin{bmatrix} x_1^{(1)} \\ \vdots \\ x_{n_s}^{(1)} \end{bmatrix}$$

In general; after 'r' iterations:

$$\underline{\Delta X}^{(r)} = [\underline{P}^{(r)}]^{-1} \underline{Q}^{(r)} \quad [1.4.12]$$

where:

$$\underline{P}^{(r)} = \underline{A} \underline{C}^{(r)} + \underline{B}$$

$$\underline{Q}^{(r)} = \underline{D}^{(r)} - \underline{A} \underline{C}^{(r)} \underline{U} - \underline{B} \underline{X}^{(r)}$$

and the improved solution is given by:

$$\underline{X}^{(r+1)} = \underline{X}^{(r)} + \underline{\Delta X}^{(r)} \quad [1.4.13]$$

Equations 1.4.12 and 1.4.13 are iterated until:

$$|| \underline{C}^{(r+1)} - \underline{C}^{(r)} || \equiv \max_j \left| \frac{c_j^{(r+1)} - c_j^{(r)}}{c_j^{(r+1)}} \right| \leq 10^{-\delta} \quad [1.4.14]$$

$\delta > 0$

COMPUTER PROGRAM: USER'S MANUAL1. General Information:

The computer program at the University of Utah is written in Fortran \overline{V} , using the UUCS's library subroutine "GJR" for matrix inversion. Any subroutine for matrix inversion may be used by eliminating instructions 139-143 and substituting the appropriate instructions for the new inversion subroutine. The program is in file "SOLE" in the Univac 1108 computer system. A listing of the program is appended.

As written, the program is limited to a maximum of 20 species in solution. This number could be increased over 20 simply by adjusting the DIMENSION statement of the program.

Activity coefficients (γ_j , $j = 1, 2, \dots, n_s$) are evaluated using the Debye-Huckel equation:

$$\log \gamma_j = - \frac{Az_j^2 I^{1/2}}{1 + Ba_j I^{1/2}} + \dot{B}_j I \quad [1.4.15]$$

where: $A = \text{constant} = 1.825 \times 10^6 / (\epsilon T)^{1.5}$

$B = \text{constant} = 50.3 / (\epsilon T)^{0.5}$

$\epsilon = \text{dielectric constant of the solvent } (\epsilon = 78.54 \text{ for } H_2O)$

$T = \text{solution temperature, } ^\circ K$

$z_j = \text{charge of species } j$

$a_j = \text{effective ionic diameter of species } j$

$I = \text{Ionic Strength} = \frac{1}{2} \sum_{k=1}^{n_s} z_k^2 C_k$

$\dot{B}_j = \text{correction factor for species } j$

2. Data Input:

- a. Card: COL 1-5: NS, total number of species (Format I5)
COL 6-10: NL, total number of linear equations (Format I5)

COL 11-15: ITMAX, maximum number of iterations.

(Format I5)

COL 16-20: IFLAG in Format I5.

If IFLAG = 0 => Calculations are not checked

If IFLAG \neq 0 => Calculations are checked
by comparing the specified and calculated
RHS of the non-linear system of equations
(Equations 1 and 2).

- b. Cards^(*): COL 1-10: Species name in Format 2A5
COL 11-20: Z(I), I = 1, NS, charge of species j
in Format E10.4
COL 21-30: a_i , i = 1, n_s , species diameter in
Format E10.4
COL 31-40: \hat{B}_j , correction factor for species j in
Format E10.4

(*) One card like this for each species.

- c. Card: COL 1-10: TEMP, Temperature in $^{\circ}\text{K}$ (Format E10.4)
COL 11-20: EPS, dielectric constant (Format E10.4)
- d. Card(s): Input matrix of coefficients for the linear
equations row by row [a_{ij} , j = 1, . . . , n_s]
i = 1, . . . , n_l] in Format 16I5.
(If $n_s > 16$, two cards will be needed for each
equation).
- e. Card(s): Input matrix of coefficients for the non-linear
equations, row by row [b_{ij} , j = 1, n_s],
i = $n_l + 1$, . . . , n_s] in Format 16A5.
(If $n_s > 16$, two cards will be needed for each
equation).
- f. Card(s): Input right hand side of linear equations
(d_i , i = 1, . . . , n_l) in Format 8E10.4.
- g. Card(s): Input equilibrium constants (K_i , i = $n_l + 1$,
. . . , n_s) in Format 8E10.4.
- h. Card(s) Input initial guess of concentrations
($c_j^{(1)}$, j = 1, . . . , n_s) in Format 8E10.4.

3. Example of Application:

Calculate the distribution of species in an aqueous solution of 0.1 M total Na and 0.1 M total carbon, at pH 8.4 and 25°C.

Species: Na^+ , NaCO_3^- , NaHCO_3 , $\text{CO}_3^{=}$, H_2CO_3 , H^+

Linear Equations: (Mass or Charge Balance)

$$\text{Na Balance: } (m_{\text{Na}^+}) + (m_{\text{NaCO}_3^-}) + (m_{\text{NaHCO}_3}) = 0.1 \quad [1.4.16]$$

$$\begin{aligned} \text{C Balance: } & (m_{\text{NaCO}_3^-}) + (m_{\text{NaHCO}_3}) + (m_{\text{CO}_3^{=}}) + (m_{\text{HCO}_3^-}) + (m_{\text{H}_2\text{CO}_3}) \\ & = 0.1 \end{aligned} \quad [1.4.17]$$

Non-Linear Equations: (Mass Action Expressions)

$$\text{NaHCO}_3 = \text{Na}^+ + \text{HCO}_3^- ; K_3 = 1.77 \quad [1.4.18]$$

$$\text{H}_2\text{CO}_3 = \text{H}^+ + \text{HCO}_3^- ; K_4 = 3.98 \times 10^{-7} \quad [1.4.19]$$

$$\text{NaCO}_3^- = \text{H}^+ + \text{CO}_3^{=} ; K_5 = 5.01 \times 10^{-11} \quad [1.4.20]$$

$$[\text{H}^+] = 10^{-8.4} ; K_6 = 3.98 \times 10^{-9} \quad [1.4.21]$$

$$\text{NaCO}_3^- = \text{Na}^+ + \text{CO}_3^{=} ; K_7 = 0.281 \quad [1.4.22]$$

Note that the hydrogen activity must be included with the non-linear equations which involve activity terms. The data input and computer printouts are presented in the next pages.

4. Computer program

```

1*      C      THIS PROGRAM CALCULATES THE CONCENTRATION AND ACTIVITY OF 'NS'
2*      C      SPECIES IN SOLUTION BY USING THE NEWTON-RAPHSON'S METHOD TO SOLVE
3*      C      A SYSTEM OF 'NS' NON-LINEAR EQUATIONS.
4*
5*      C      A(I,J)  = COEFFICIENT OF THE JTH SPECIES IN THE ITH LINEAR
6*      C                  EQUATION.
7*      C      AD(J)  = EFFECTIVE DIAMETER OF THE JTH SPECIES.
8*      C      AA      = DEBYE-HUCKEL PARAMETER.
9*
10*
11*
12*
13*
14*
15*
16*
17*
18*
19*
20*
21*
22*
23*
24*
25*
26*
27*
28*
29*
30*
31*
32*
33*
34*
35*
36*
37*
38*
39*
40*
41*
42*
43*
44*
45*
46*
47*
48*
49*
50*
51*      C      DATA READING
52*
53*      C      READ TOTAL NUMBER OF SPECIES AND LINEAR EQUATIONS.
54*      READ 100,NS,NL,ITMAX,IFLAG
55*      100 FORMAT(16F5)
56*
57*      C      READ SPECIES NAME (MAX. 10 CHARACTERS),CHARGE,DIAMETER AND RDOT
58*      C      (ONE CARD PER SPECIES)
59*      DO 1 I=1,NS
60*          READ 110,SPEC1(I),SPEC2(I),Z(I),AD(I),RDOT(I)
61*      110 FORMAT(2A5,3E10,4)
62*      1 CONTINUE
63*
64*      C      READ SOLUTION TEMPERATURE (KELVIN) AND DIELECTRIC CONSTANT.
65*      READ 120,TEMP,EPS

```

ACT(J) = ACTIVITY OF SPECIES 'J' IN SOLUTION.
 B(I,J) = STOICHIOMETRIC COEFFICIENT OF THE JTH SPECIES IN THE ITH EQUATION.
 BH = DEBYE-HUCKEL PARAMETER.
 BDOT(J) = DEBYE-HUCKEL PARAMETER FOR SPECIES 'J'.
 CONC(J) = CONCENTRATION OF SPECIES 'J' IN SOLUTION.
 D(I) = RIGHT HAND SIDE OF THE ITH EQUATION (LINEAR OR NON-LINEAR).
 DCAL = CALCULATED VALUE OF D(I) FOR THE LINEAR EQUATION 'I'.
 EPS = DIELECTRIC CONSTANT OF THE SOLVENT.
 GAMMA(J) = ACTIVITY COEFFICIENT OF SPECIES 'J' IN SOLUTION.
 IFLAG = 0 : CALCULATIONS CHECK-OUT IS NOT PERFORMED.
 = 1 : CALCULATIONS CHECK-OUT IS PERFORMED AND PRINTED.
 IONIC = IONIC STRENGTH.
 IT = ITERATION NUMBER.
 ITMAX = MAXIMUM NUMBER OF ITERATIONS.
 JC(.) = DUMMY ARRAY (REQUIRED BY INVERSION SUBROUTINE '6JR').
 K(I) = EQUILIBRIUM CONSTANT FOR THE ITH EQUATION.
 KCAL = CALCULATED VALUE OF K(I), I=NL1,...,NS.
 LOG10(J) = LN(GAMMA(J)).
 NL = TOTAL NUMBER OF LINEAR EQUATIONS.
 NL1 = NL + 1.
 NS = TOTAL NUMBER OF SPECIES (OR EQUATIONS).
 P(I,J) = ELEMENT OF THE MATRIX OF COEFFICIENTS OF THE LINEARIZED SYSTEM OF EQUATIONS.
 PI(I,J) = ELEMENT OF 'P INVERSE'.
 Q(I) = RIGHT HAND SIDE OF THE ITH LINEARIZED EQUATION.
 SPEC1(J) = NAME OF SPECIES 'J' (ALPHANUMERIC).
 SPEC2(J) = SAME AS SPEC1(J).
 TEMP = SOLUTION TEMPERATURE, DEGREES KELVIN.
 V(.) = DUMMY ARRAY (REQUIRED BY INVERSION SUBROUTINE '6JR').
 XNEW(J) = IMPROVED VALUE OF LN(CONC(J)).
 XOLD(J) = PREVIOUS VALUE OF LN(CONC(J)).
 Z(J) = CHARGE OF SPECIES 'J'.

```

45*      DIMENSION AD(20),ACT(20),BDOT(20),CONC(20),D(20),GAMMA(20),
46*      100(20),PI(20,20),P(20,20),Q(20),SPEC1(20),SPEC2(20),V(2),
47*      2AMEW(20),XOLD(20),Z(20)
48*      INTEGER A(20,20),R(20,20)
49*      REAL IO,IC,K(20),KCAL,LOG10(20)
50*
51*      C      DATA READING
52*
53*      C      READ TOTAL NUMBER OF SPECIES AND LINEAR EQUATIONS.
54*      READ 100,NS,NL,ITMAX,IFLAG
55*      100 FORMAT(16F5)
56*
57*      C      READ SPECIES NAME (MAX. 10 CHARACTERS),CHARGE,DIAMETER AND RDOT
58*      C      (ONE CARD PER SPECIES)
59*      DO 1 I=1,NS
60*          READ 110,SPEC1(I),SPEC2(I),Z(I),AD(I),RDOT(I)
61*      110 FORMAT(2A5,3E10,4)
62*      1 CONTINUE
63*
64*      C      READ SOLUTION TEMPERATURE (KELVIN) AND DIELECTRIC CONSTANT.
65*      READ 120,TEMP,EPS

```


Computer program (Continued)

```

670      C      READ MATRIX OF COEFFICIENTS FOR THE LINEAR EQUATIONS.
680      DO 2 I=1,NL
690      READ 120,(C(I,J),J=1,NL)
700      C(I,J)=C(I,J)*10.0
710      C(I,J)=C(I,J)/10.0
720      C(I,J)=C(I,J)/10.0
730      C(I,J)=C(I,J)/10.0
740      C(I,J)=C(I,J)/10.0
750      C(I,J)=C(I,J)/10.0
760      C      READ MATRIX OF COEFFICIENTS FOR THE NON-LINEAR EQUATIONS.
770      DO 4 I=1,NL
780      READ 120,(K(I,J),J=1,NL)
790      K(I,J)=K(I,J)*10.0
800      K(I,J)=K(I,J)/10.0
810      K(I,J)=K(I,J)/10.0
820      K(I,J)=K(I,J)/10.0
830      K(I,J)=K(I,J)/10.0
840      C      READ RIGHT HAND SIDE OF LINEAR EQUATIONS.
850      READ 120,(D(I),I=1,NL)
860      D(I)=D(I)*10.0
870      D(I)=D(I)/10.0
880      C      READ EQUILIBRIUM CONSTANTS.
890      READ 120,(K(I),I=1,NL)
900      K(I)=K(I)*10.0
910      K(I)=K(I)/10.0
920      C      READ INITIAL GUESS OF CONCENTRATIONS.
930      READ 120,(CONC(I),I=1,NL)
940      DO 7 I=1,NL
950      CONC(I)=CONC(I)/10.0
960      CONC(I)=CONC(I)/10.0
970      C      CALCULATIONS.
980      C      COMPUTE DEBYE-HUCKEL COEFFICIENTS AA AND BB.
990      AA= 1.825E6/(TEMP*TEMP)*0.5
1000      BB= 1.825E6/(TEMP*TEMP)*0.5
1010      C      START ITERATIONS.
1020      DO 9 IT=1,ITMAX
1030      C      COMPUTE IONIC STRENGTH AND ACTIVITY COEFFICIENTS.
1040      IONIC = 0.
1050      DO 10 I=1,NL
1060      IONIC=IONIC+ Z(I)*Z(I)*CONC(I)
1070      IONIC = 0.5*IONIC
1080      DO 11 I=1,NL
1090      GAMMA(I)= -AA*Z(I)*Z(I)*IONIC**0.5/(1.0+BB*Z(I)*IONIC**0.5)
1100      GAMMA(I)= GAMMA(I)/10.0
1110      GAMMA(I)= GAMMA(I)/10.0
1120      GAMMA(I)= GAMMA(I)/10.0
1130      GAMMA(I)= GAMMA(I)/10.0
1140      GAMMA(I)= GAMMA(I)/10.0
1150      C      COMPUTE RIGHT HAND SIDE OF NON-LINEAR SYSTEM.
1160      DO 6 I=1,NL
1170      KK = K(I)
1180      KK = KK/10.0
1190      KK = KK/10.0
1200      DO 6 J=1,NL
1210      U(I)=D(I)-C(I,J)*LOG10(J)*2.3026
1220      C      CONTINUE

```

Computer program (continued)

```

123*
124*      C      COMPUTE THE MATRIX OF COEFFICIENTS FOR THE LINEARIZED SYSTEM
125*      C      OF EQUATIONS.
126*      DO 13 I=1,NS
127*      DO 13 J=1,NS
128*      13 P(I,J)=A(I,J)*CONC(J) + F(I,J)
129*
130*      C      COMPUTE THE 'RHS' OF THE LINEARIZED SYSTEM OF EQUATIONS.
131*      DO 14 I=1,NS
132*      Q(I) = Q(I)
133*      DO 14 J=1,NS
134*      14 Q(I) = Q(I) - (A(I,J)*CONC(J) + B(I,J)*XCLD(J))
135*
136*      C      SOLVE THE SYSTEM OF EQUATIONS : PX = Q
137*      C      THE NEXT 5 SENTENCES ARE REQUIRED TO USE SUBROUTINE 'GJPI'
138*      C      FOR MATRIX INVERSION.
139*      DO 15 I=1,NS
140*      DO 15 J=1,NS
141*      15 P(I,J) = P(I,J)
142*      V(I)=1.
143*      CALL GJPIPT,20,20,NS,NS,123,JC,V)
144*      DO 12 I=1,NS
145*      XNER(I)=XOLD(I)
146*      DO 12 J=1,NS
147*      12 XNER(I)=XNER(I) + P(I,J)*Q(J)
148*      DO 15 I=1,NS
149*      15 CONC(I)=EXP(XNER(I))
150*
151*      C      CHECK FOR THE CONVERGENCE OF THE SOLUTION.
152*      DO 16 I=1,NS
153*      DELTA=ABS(1.-EXP(XOLD(I)-XNER(I)))
154*      IF(DELTA.GT.1.0E-6) GO TO 17
155*      16 CONTINUE
156*      GO TO 1P
157*      17 CONTINUE
158*      DO 19 I=1,NS
159*      19 XOLD(I)=XNER(I)
160*      9 CONTINUE
161*
162*      C      PRINT OUT OF RESULTS.
163*
164*      18 PRINT 200
165*      200 FORMAT(1H1,3X,*,* * * SOLUTION EQUILIBRIUM CALCULATIONS * * *,//,
166*      192A,'UNIV. OF UTAH,1978',//)
167*      PRINT 210,TEMP,EPS,NS
168*      210 FORMAT(4X,'1. DATA INPUT :',//,9X,'- SOLUTION TEMPERATURE :',F6.1,
169*      1' KELVIN',//,9X,'- DIELECTRIC CONSTANT :',F6.2,//,9X,
170*      2' - NUMBER OF SPECIES :',I6,/)
171*      PRINT 220
172*      220 FORMAT(9X,'- MATRIX OF COEFFICIENTS (LINEAR EQUATIONS) :',//)
173*      DO 20 I=1,NS
174*      PRINT 230,(A(I,J),J=1,NS)
175*      230 FORMAT(10X,20I5)
176*      20 CONTINUE
177*      PRINT 240
178*      240 FORMAT(//,9X,'- MATRIX OF COEFFICIENTS (NON-LINEAR EQUATIONS) :',//)
179*      DO 21 I=1,NS

```

Computer program (continued)

```

180*      PRINT 230,(N(I,J),J=1,N5)
181*      21 CONTINUE
182*
183*      C      COMPUTE ACTIVITIES.
184*      DO 22 I=1,N5
185*      22 ACT(I)=GAMMA(I)*CONC(I)
186*
187*      PRINT 250
188*      250 FORMAT(10I1,3X,'2. CALCULATIONS :',//,11X,'SPECIES   CHARGE DIAME
189*      1IER   ROOT   ACTIVITY',3X,'MOLAR',7X,'ACTIVITY',//,47X,'COEFFICIENT
190*      1   CONCENTRATION',//)
191*      DO 22 I=1,N5
192*      PRINT 260,(N(I),SPEC1(I),SPEC2(I),Z(I),AD(I),ROOT(I),GAMMA(I),CONC(I),
193*      1 ACT(I))
194*      260 FORMAT(10X,2A5,F7.1,F10.2,F8.2,E12.4,E14.4,E13.4)
195*      22 CONTINUE
196*      PRINT 270,TONIC,II
197*      270 FORMAT(//,11X,'TONIC STRENGTH :',E10.4,//,11X,'ITERATIONS   :',
198*      111,///)
199*      IF(IFLAG.EQ.0) GO TO 28
200*
201*      C      CALCULATIONS CHECK-OUT.
202*      PRINT 280
203*      280 FORMAT(10X,'3. CALCULATIONS CHECK-OUT :',//,9X,'- LINEAR EQUATIONS
204*      1:',//,25X,'SPECIFIED   CALCULATED',//)
205*      DO 24 I=1,NL
206*      DCAL = 0.
207*      DO 25 J=1,N5
208*      25 DCAL = DCAL + A(I,J)*CONC(J)
209*      PRINT 290,I,D(I),DCAL
210*      290 FORMAT(13X,'16',I2,')',F17.4,F16.4)
211*      24 CONTINUE
212*      PRINT 300
213*      300 FORMAT(//,9X,'- NON-LINEAR EQUATIONS :',//,25X,'SPECIFIED   CALC
214*      1ULATED',//)
215*      DO 26 I=NL1,N5
216*      KCAL = 1.0
217*      DO 27 J=1,N5
218*      27 KCAL = KCAL*(GAMMA(J)*CONC(J))**B(I,J)
219*      PRINT 310,I,K(I),KCAL
220*      310 FORMAT(14X,'16',I2,')',F17.4,F16.4)
221*      26 CONTINUE
222*      GO TO 28
223*      23 PRINT 320
224*      320 FORMAT(11I1,5X,'UNDEFINED CHEMICAL SYSTEM . REVIEW PROBLEM STATEMEN
225*      1T')
226*      28 CONTINUE
227*      END

```


Computer Output

• • • SOLUTION EQUILIBRIUM CALCULATIONS • • •

1. DATA INPUT :

- SOLUTION TEMPERATURE : 298.3 KELVIN
- DIELECTRIC CONSTANT : 78.5
- NUMBER OF SPECIES : 7
- MATRIX OF COEFFICIENTS (LINEAR EQUATIONS) :

1	1	1	0	0	0	0
0	1	1	1	1	1	0

- MATRIX OF COEFFICIENTS (NON-LINEAR EQUATIONS) :

1	0	-1	0	1	0	0
0	0	0	0	1	-1	1
0	0	0	1	-1	0	1
0	0	0	0	0	0	1
1	-1	0	1	0	0	0

2. CALCULATIONS :

SPECIES	CHARGE	DIAMETER	ROOT	ACTIVITY COEFFICIENT	MOLAR CONCENTRATION	ACTIVITY
NA+	1.0	4.00	.00	.7776+00	.9720-01	.7565-01
NAC03-	-1.0	4.00	.00	.8303+00	.1028-04	.8532-05
NAHC03	.0	.00	.00	.1000+01	.2702-02	.2702-02
CO3--	-2.0	5.00	.00	.3906+00	.9114-04	.3169-04
HCO3-	-1.0	4.00	.00	.7776+00	.8132-01	.6323-01
H2C03	.0	.00	.00	.1000+01	.1588-01	.1588-01
H+	1.0	9.00	.00	.8303+00	.1204-06	.1000-06

IONIC STRENGTH : .8947-01

ITERATIONS : 11

3. CALCULATIONS CHECK-OUT :

- LINEAR EQUATIONS :

	SPECIFIED	CALCULATED
U(1)	.1000+00	.1000+00
U(2)	.1000+00	.1000+00

- NON-LINEAR EQUATIONS :

	SPECIFIED	CALCULATED
K(3)	.1770+01	.1770+01
K(4)	.3981-06	.3981-06
K(5)	.5012-10	.5012-10
K(6)	.1000-06	.1000-06
K(7)	.2810+00	.2810+00

LEARNING ACTIVITY 5,6

1.4 Oxidation - Reduction ReactionsLearning Activity Objective

After completing your study of the material in this learning activity you should be able to construct electrochemical phase diagrams.

1.4.1 Convention

Oxidation-reduction reactions, particularly electrochemical reactions, are of considerable importance in hydrometallurgy. The electron exchange for one or more elements results in a change of the oxidation state, or valence, of that element. In redox reactions, the loss of electrons by an element (oxidation) must be accompanied by a corresponding gain of electrons by an element (reduction). As a consequence, the reaction can be divided arbitrarily into two parts by writing each part of the reaction in terms of the electrons gained or lost. The oxidation portion of the redox reaction is called the anodic half cell while the reduction portion of the redox reaction is called the cathodic half cell.

Electrochemical reactions are heterogeneous redox reactions, unique in the fact that the electron exchange does not occur at a point in space, but rather the half cells are separated by some finite distance. This requires that the reaction occurs at the surface of an electronic conductor and, as a result, definite anodic and cathodic areas are developed which may be separated by a considerable distance. As a result of these considerations it is seen that the basis for dividing an electrochemical reaction into two parts is really not arbitrary, but has a definite physical significance. Besides providing a realistic way of thinking about redox reactions, the half cell concept provides a convenient method for balancing redox reactions. The procedure consists of the following four basic steps for each half cell:

- 1) Establish the half cell reaction products and balance the elements.
- 2) Balance the oxygen with H_2O .
- 3) Balance the hydrogen with H^+ .
- 4) Balance the charge with electrons.

The balanced half cells then are adjusted and added so that the number of electrons cancel, resulting in the overall redox reaction. This procedure is illustrated below for the redox reaction of thiosulfate to sulfate by oxygen.

Anodic half cell



Aqueous	Manganese Species	$\Delta G_f^\circ, 25^\circ\text{C}$
<u>Ion</u>		
Mn^{++}		-54.5
Mn^{+3}		-19.6
HMnO_2^-		-120.9
MnO_4^-		-107.4
$\text{MnO}_4^{=}$		-120.4

II. Determine unstable solid phases

- a) Reactions involving no change in oxidation state of Mn: stability determined simply by relative free energy values.

	$\Delta G_r^\circ, 25^\circ\text{C}, \text{Kcal}$	
$\text{MnOOH} + \text{H}_2\text{O} \rightarrow \text{Mn}(\text{OH})_3$	+9	[1.5.18]
$2\text{Mn}(\text{OH})_3 \rightleftharpoons \text{Mn}_2\text{O}_3 + 3\text{H}_2\text{O}$	-26.4	[1.5.19]
$\text{Mn}(\text{OH})_2 \rightleftharpoons \text{MnO} + \text{H}_2\text{O}$	+3.8	[1.5.20]
$2\text{MnOOH} \rightleftharpoons \text{Mn}_2\text{O}_3 + \text{H}_2\text{O}$	-2.7	[1.5.21]

- b) Change in oxidation state of Mn: do not consider solid phases which have been eliminated.

$\text{Mn}_3\text{O}_4 + 2\text{H}_2\text{O} + 2\text{H}^+ + 2\text{e}^- \rightleftharpoons 3\text{Mn}(\text{OH})_2$	[1.5.22]
$E = .484 - .059 \text{ pH}$	[1.5.23]
$3\text{Mn}_2\text{O}_3 + 2\text{H}^+ + 2\text{e}^- \rightleftharpoons 2\text{Mn}_3\text{O}_4 + \text{H}_2\text{O}$	[1.5.24]
$E = .697 - .059 \text{ pH}$	[1.5.25]
$2\text{MnO}_2 + 2\text{H}^+ + 2\text{e}^- \rightleftharpoons \text{Mn}_2\text{O}_3 + \text{H}_2\text{O}$	[1.5.26]
$E = 1.016 - .059 \text{ pH}$	[1.5.27]

III. Solid-aqueous species equilibria (aqueous concentration or activity = 10^{-4})

- a) Reactions involving Mn^{++}



$$\text{pH} = 9.5 \quad [1.5.29]$$



$$E = 2.17 - .236 \text{ pH} \quad [1.5.31]$$



$$E = 1.68 - 0.118 \text{ pH} \quad [1.5.33]$$



$$E = 1.35 - 0.118 \text{ pH} \quad [1.5.35]$$

- b) The reaction involving $\text{Mn}^{+2} \rightarrow \text{Mn}^{+3}$ is unstable with respect to Mn^{++} as shown by the following half cell:



$$E = E^\circ = 1.51 \quad [1.5.37]$$

Similarly all reactions between solid phases will be unstable with respect to Mn^{+3} field. This is not to say there will not be small concentrations of Mn^{+3} , indeed there will, but the most significant species is Mn^{+2} .

- c) Reactions involving HMnO_2^-



$$\text{pH} = 15.4 \quad [1.5.39]$$



$$E = -.88 + .0295 \text{ pH} \quad [1.5.41]$$



$$E = -1.18 \quad [1.5.43]$$



$$E = .33 - .0295 \text{ pH} \quad [1.5.45]$$

- d) Reactions involving MnO_4^- - exercise for student.

The completed phase diagram can be drawn from the developed equation, Figure 1.5.2.

The electrochemical phase diagrams become more complex as the number of components is increased. Examples are presented in the appendix for the addition of CO_2 to the manganese-water system. The phase diagrams are presented in Figures 1.5.3, and 1.5.4.

Electrochemical phase diagrams which involve sulfur are of particular interest to hydrometallurgists. Leaching of sulfide minerals is encountered in many instances and these electrochemical reactions can be rather complex. In part, this complexity arises from the fact that sulfur can acquire a multitude of oxidation states ranging from -2 to +6. Even when metastable sulfur species, such as sulfate ($\text{SO}_4^{=}$) and thiou-sulfate ($\text{S}_2\text{O}_3^{=}$) are eliminated, electrochemical phase diagrams are still relatively complex.

To illustrate the rudiments of electrochemical phase diagrams containing sulfur, let's consider the stable aqueous sulfur species which should be considered under equilibrium conditions.

Species	ΔG_f°	Species	ΔG_f°
$\text{H}_2\text{S}_{\text{aq}}$	-6.54	H_2SO_4	-179.94
HS^-	3.01	$\text{SO}_4^{=}$	-177.34
$\text{S}^{=}$	21.96		

The equilibria and half cells necessary to establish the predominance areas for electrochemical phase diagrams containing dissolved sulfur are presented in the Appendix attached to this learning activity. The diagrams are shown in Figures 1.5.5 and 1.5.6.

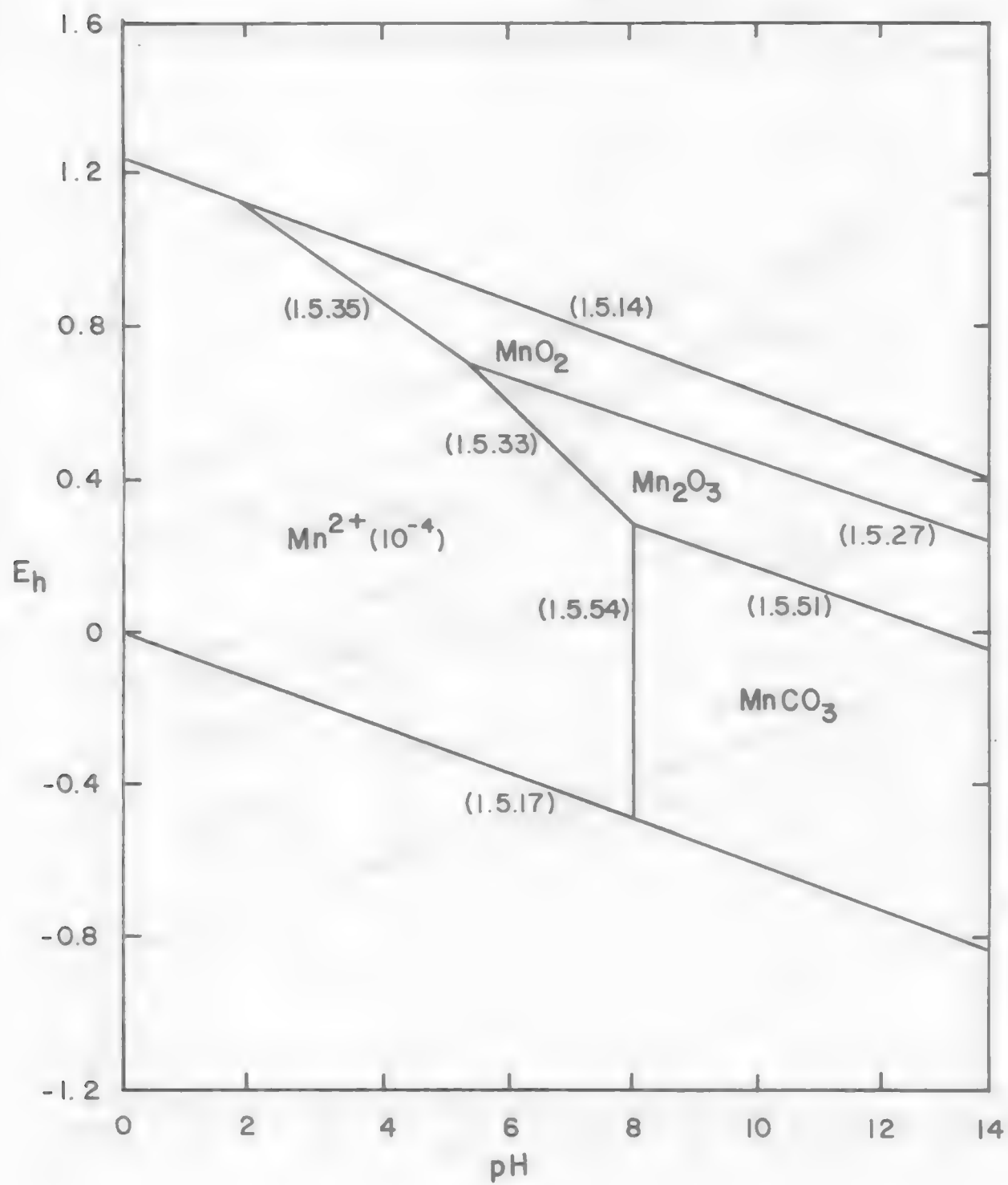
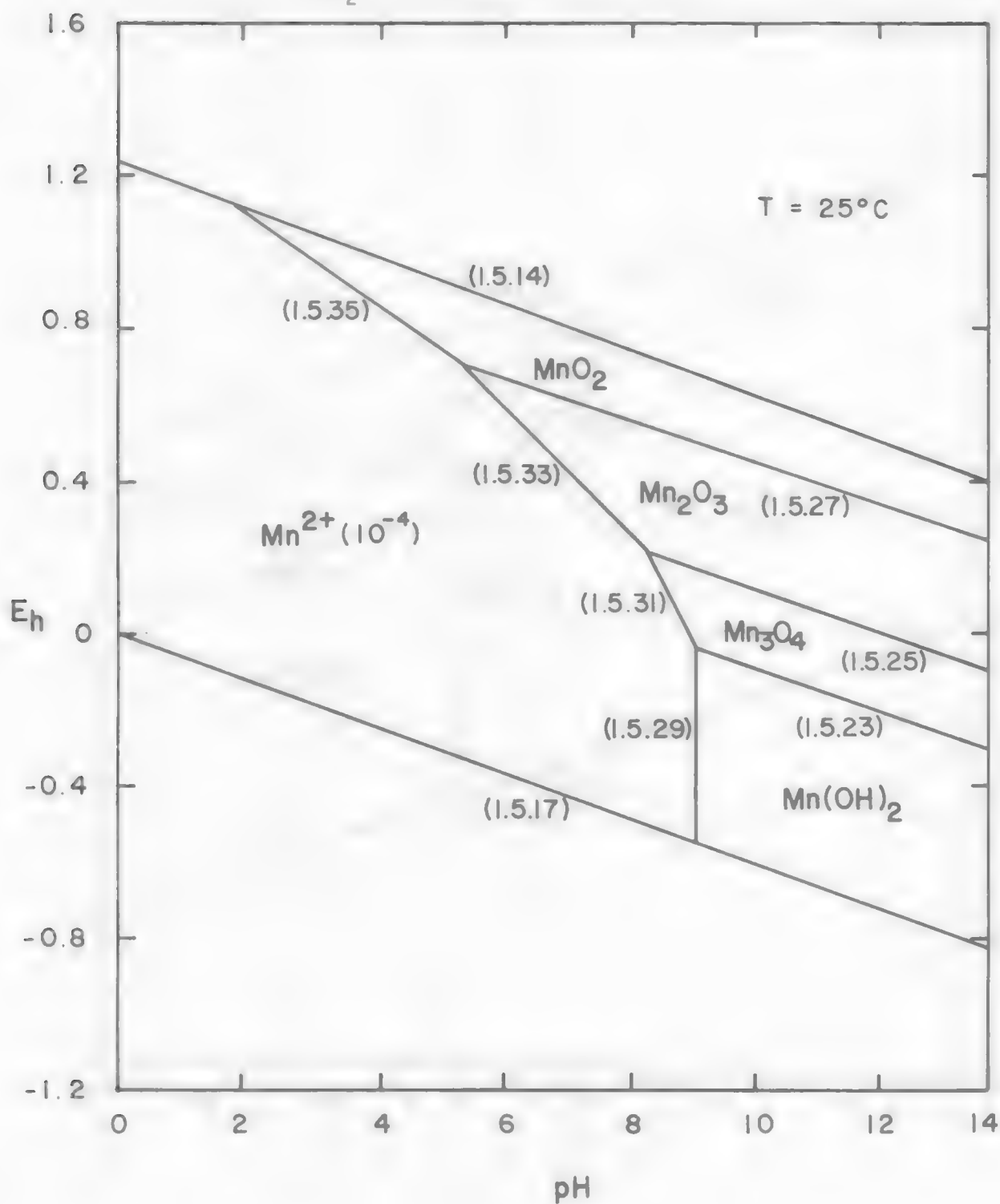
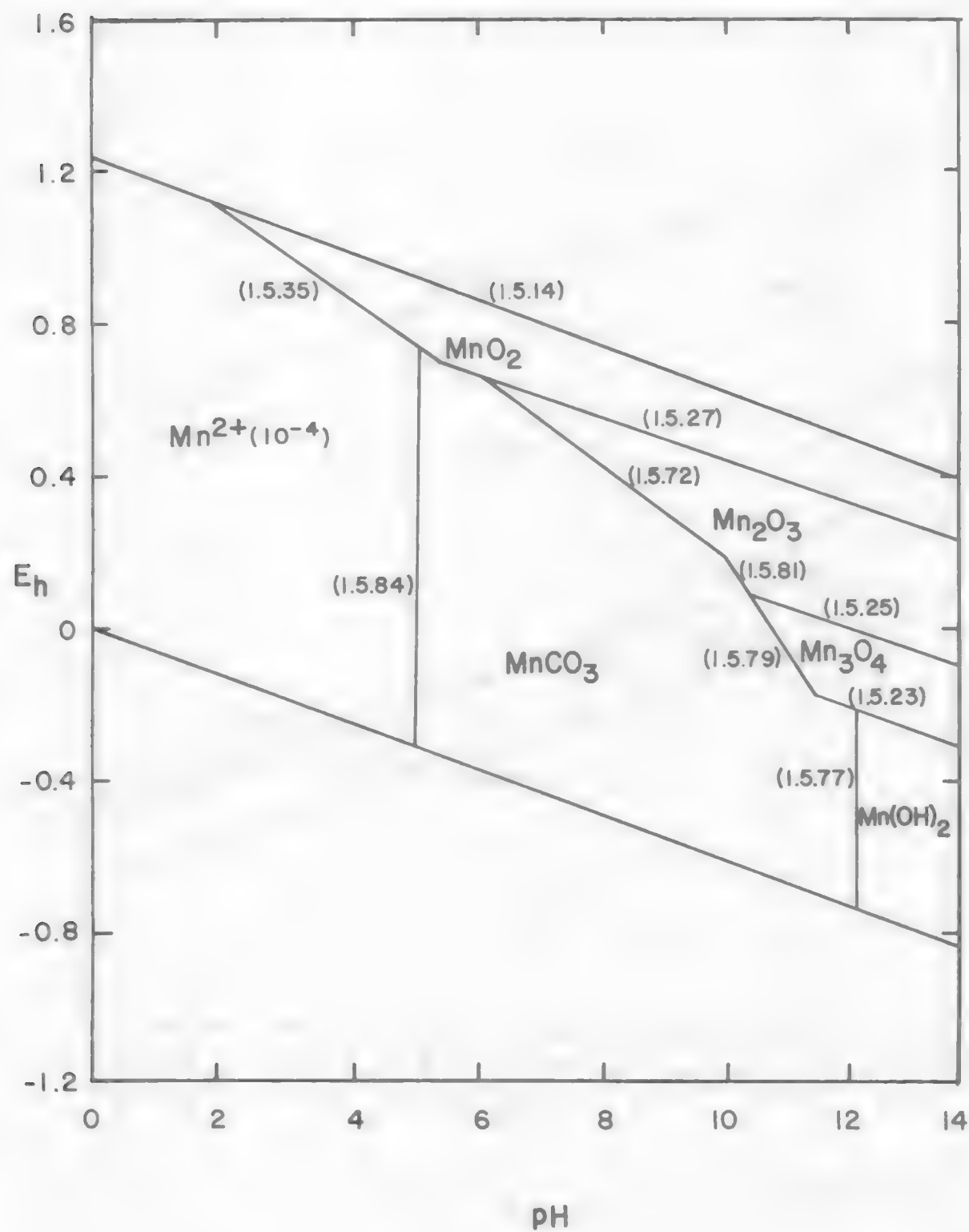
Figure 1.5.2 Mn - H₂O System.

Figure 1.5.3 Mn - H₂O - CO₂ System.* Constant CO₂ Pressure (Open System)
 $P_{\text{CO}_2} = 10^{-3.5} \text{atms}$



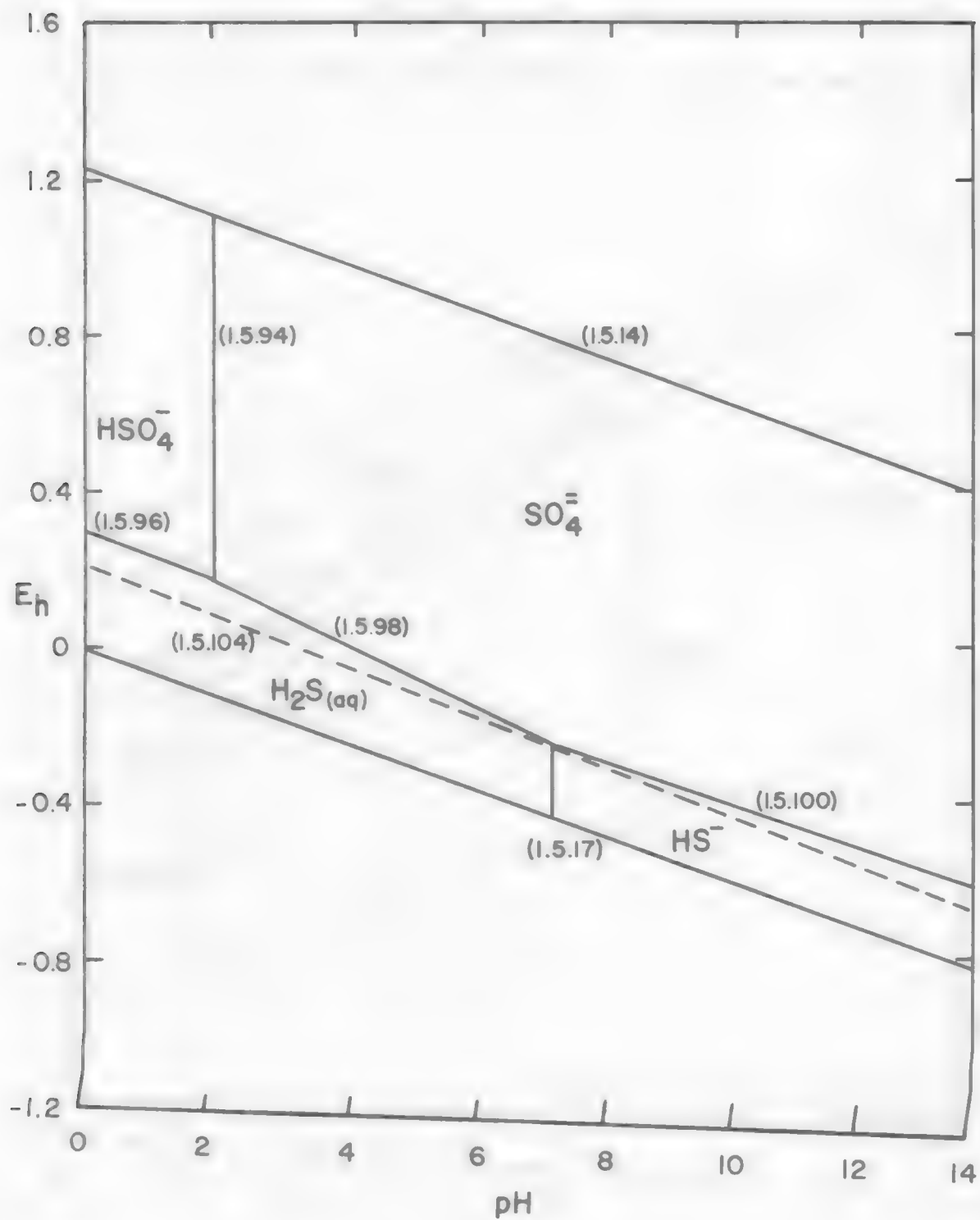
*See Appendix

Figure 1.5.4 Mn - H₂O - CO₂ System.* Constant Dissolved CO₂ Content
(closed system) $\Sigma\text{CO}_2 = 10^{-1.4}\text{M}$



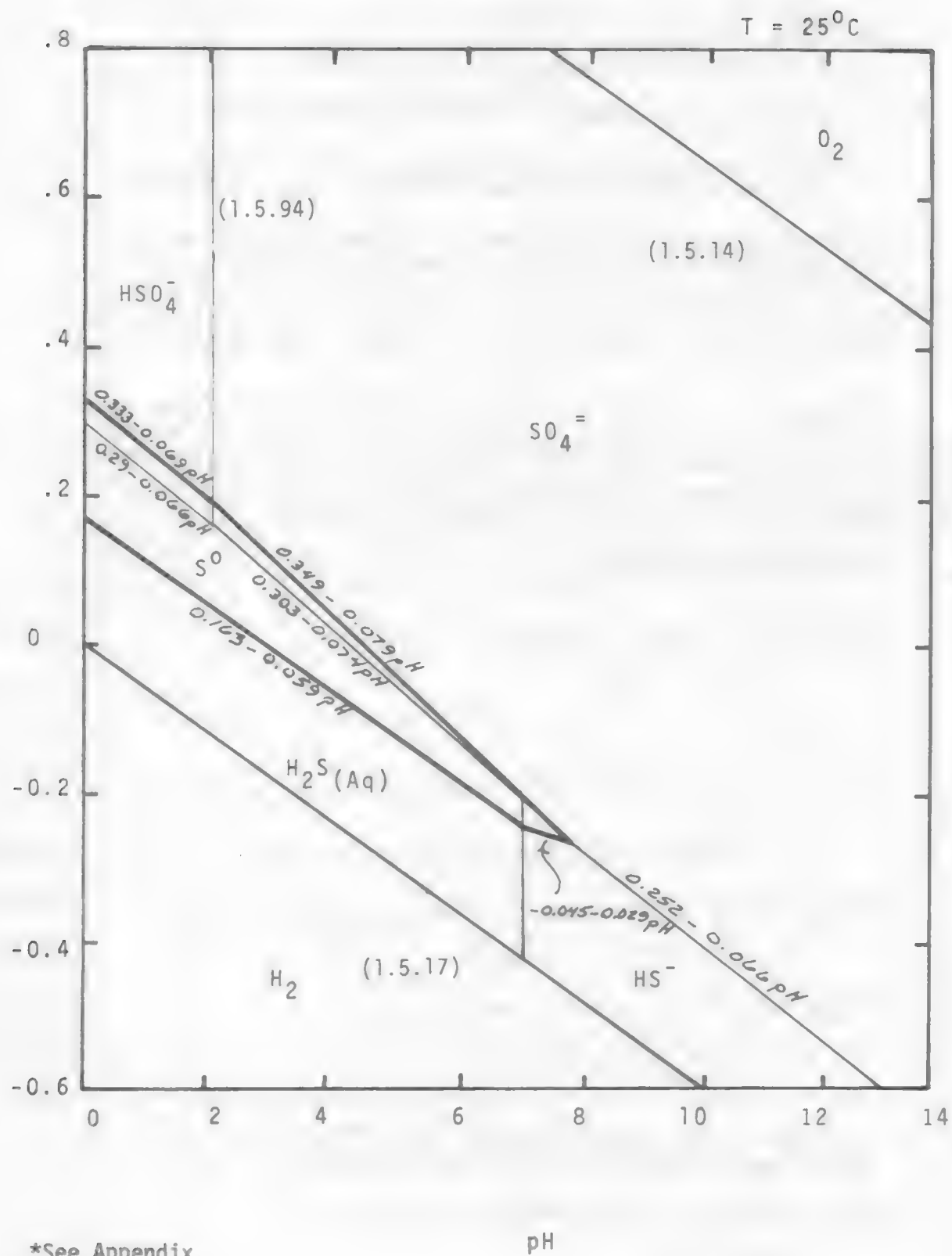
*See Appendix.

Figure 1.5.5. Sulfur Species - Water System.* T = 25°C



*See Appendix.

Figure 1.5.6. Sulfur-Water System.*
 (Total Dissolved Sulfur = $2 \times 10^{-1} \text{M}$)



In the H_2CO_3 predominance area only MnO_2 would have a stability field with respect to MnCO_3 .

b) HCO_3^- Stability field, i.e., $\text{HCO}_3^- = 10^{-1.4}$



$$\Delta G_r = -19.3 + 1.364 \text{ pH} \quad [1.5.68]$$



$$E = 1.74 - .15 \text{ pH} \quad [1.5.70]$$



$$E = 1.40 - .12 \text{ pH} \quad [1.5.72]$$



$$E = 12.0 - .09 \text{ pH} \quad [1.5.74]$$

In the HCO_3^- predominance area both MnO_2 and Mn_2O_3 would have stability fields with respect to MnCO_3 .

c) $\text{CO}_3^{=}$ Stability field, i.e., $\text{CO}_3^{=} = 10^{-1.4}$ [1.5.75]



$$\Delta G_r = -33.3 + 2.73 \text{ pH} \quad [1.5.77]$$

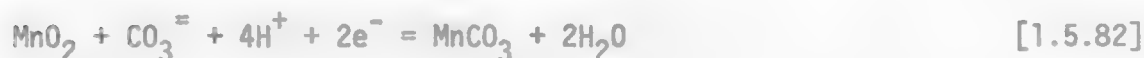
(pH = 12.2)



$$E = 2.65 - .24 \text{ pH} \quad [1.5.79]$$



$$E = 2.0 - .18 \text{ pH} \quad [1.5.81]$$



In the $\text{CO}_3^{=}$ predominance area all of the oxide-hydroxide compounds have stability fields.

d) Mn^{++} Equilibria with MnCO_3 

$$\Delta G_r = -13.45 + 2.73 \text{ pH} \quad [1.5.84]$$

(pH = 4.9)



$$\Delta G_r = -4.75 + 1.364 \text{ pH} \quad [1.5.86]$$



$$\Delta G_r = 22.4 \quad [1.5.88]$$

Sulfur - Water System

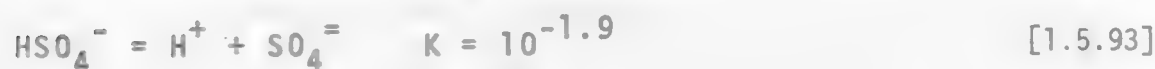
The equilibria and half cell reactions for the construction of Figures 1.5.5 and 1.5.6 are presented.



$$\text{pH} = 7 + \log \left(\frac{\text{H}_2\text{S}_{\text{aq}}}{\text{HS}^-} \right) \quad [1.5.90]$$



$$\text{pH} = 14 + \log \left(\frac{\text{HS}^-}{\text{S}^{--}} \right) \quad [1.5.92]$$



$$\text{pH} = 1.9 + \log \left(\frac{\text{HSO}_4^-}{\text{SO}_4^{--}} \right) \quad [1.5.94]$$



$$= 0.290 - 0.066 \text{ pH} + 0.0074 \log \frac{[\text{HSO}_4^-]}{[\text{H}_2\text{S}]} \quad [1.5.96]$$



$$E = 0.303 - 0.074 \text{ pH} + 0.0074 \log \frac{[\text{SO}_4^{--}]}{[\text{H}_2\text{S}]} \quad [1.5.98]$$



$$E = 0.252 - 0.066 \text{ pH} + 0.0074 \log \frac{[\text{SO}_4^{--}]}{[\text{HS}^-]} \quad [1.5.100]$$



$$E = 0.148 - 0.059 + 0.0074 \log \frac{[\text{SO}_4^{--}]}{[\text{S}^{--}]} \quad [1.5.102]$$

As mentioned previously, the predominance areas are delineated by points of equal activity. Hence the stability regions for two aqueous species is established by setting the activities equal and plotting the respective equation. By using such a procedure for equations 1.5.89 to 1.5.102, the predominance areas for aqueous sulfur species can be constructed as shown in Figure 1.5.5. Note that these predominance areas are independent of the amount of dissolved sulfur in the system.

Only the half cells representing stable equilibria are presented. Metastable equilibria have already been eliminated. For example, the equilibrium for the $\text{HSO}_4^-/\text{HS}^-$ couple is:



$$E = .21 - .059 \text{ pH} \quad [1.5.104]$$

The dashed line on the electrochemical phase diagram is a plot of equation 1.5.104. Note that for pH values less than 7, the equation of the line lies in the H_2S predominance area and HS^- is unstable with respect to $\text{H}_2\text{S}_{\text{aq}}$. For pH values greater than 7, where HS^- is stable, it can be seen that HSO_4^- is unstable with respect to SO_4^{--} . Therefore, the $\text{HSO}_4^-/\text{HS}^-$ couple represents a metastable equilibrium.

When the total dissolved sulfur exceeds 10^{-5}M , a stability region for elemental sulfur forms. This stability region referred to as the "sulfur nose" can be determined by considering the equilibria between S^0 and each of the predominant aqueous sulfur species.

$$E = .142 - \frac{0.059}{2} \log a_{\text{H}_2\text{S}} - .059 \text{ pH}, \text{H}_2\text{S}_{\text{aq}} = \text{S}_{\text{c}} + 2\text{H}_{\text{aq}}^+ + 2e \quad [1.5.105]$$

$$E' = .065 - \frac{0.059}{2} \log a_{\text{HS}^-} - \frac{.059}{2} \text{ pH}, \text{HS}_{\text{aq}}^- = \text{S}_{\text{c}} + \text{H}_{\text{aq}}^+ + 2e \quad [1.5.106]$$

$$E = -.476 - \frac{.059}{2} a_s = S_{aq}^{--} = S_c + 2e \quad [1.5.107]$$

$$E = .34 + .01 \log a_{HSO_4^-} - .068 \text{ pH}, S_c + 4H_2O = HSO_{4aq}^- + 7H_{aq}^+ + 6e \quad [1.5.108]$$

$$E = .357 + .01 \log a_{SO_4} - .079 \text{ pH}, S_c + 4H_2O = SO_{4aq}^{--} + 8H_{aq}^+ + 6e \quad [1.5.109]$$

The positions of these equilibria on the electrochemical phase diagram will be dependent on the amount of dissolved sulfur. For example, if the total dissolved sulfur were $2 \times 10^{-1} M$ then the "sulfur nose" would extend into the bisulfide predominance area as shown in Figure 1.5.6.

Significance of Predominance Area Assumption for Aqueous Species in the Construction of Electrochemical Phase Diagrams

The assumption normally made is that all of a given component exists as a particular aqueous species for a given predominance area. The assumption is only an approximation and rigorously the distribution of species or the coexistence of other species must be considered.

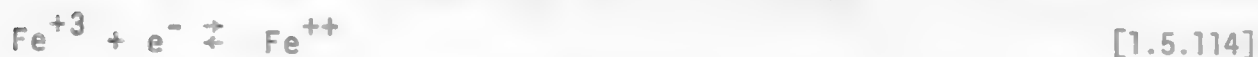
To illustrate the point, consider for example the Fe^{++} , Fe^{+3} Fe_2O_3 equilibria as shown in Figure 1.5.7.



$$\log (Fe^{+3}) = -.72 - 3pH \quad [1.5.111]$$



$$E = 0.728 - .059 \log (Fe^{++}) - .177pH \quad [1.5.113]$$



$$E = 0.77 + .059 \log \frac{Fe^{+3}}{Fe^{++}} \quad [1.5.115]$$

$$Fe^{++} + Fe^{+3} = \Sigma Fe_{aq} \quad [1.5.116]$$

The first equilibrium half cell to be examined is equation 1.5.105, (Fe_2O_3/Fe^{+3}). Using equation 1.5.115 (Fe^{++}/Fe^{+3} couple) and equation 1.5.116 (the mass balance), it is evident that:

$$\frac{Fe^{+3}}{\Sigma Fe - Fe^{+3}} = 10^{(E-.77)/.059} \quad [1.5.117]$$

and

$$\text{Fe}^{+3} + \frac{10^{[x + (E-.77)/.059]}}{1 + 10^{(E-.77)/.059}} \quad \text{where } x = \log \Sigma\text{Fe} \quad [1.5.118]$$

Substitution of this expression for Fe^{+3} into equation 1.5.111 results in

$$\log \frac{10^{[x + (E-.77)/.059]}}{1 + 10^{[(E-.77)/0.59]}} = -.72 - 3\text{pH} \quad [1.5.119]$$

At the potential .77 then

$$\log \frac{10^x}{1+1} = \log \frac{10^x}{2} \quad [1.5.120]$$

For a total iron of 10^{-6} , i.e. $\Sigma\text{Fe}_{\text{aq}} = 10^{-6}$ then $x = -6$
and

$$\log 5 \times 10^{-7} = -.72 - 3 \text{ pH} \quad [1.5.121]$$

$$\text{pH} = 1.86 \quad [1.5.122]$$

Other potentials can be considered for example at $E = 0.8$ again
with $\Sigma\text{Fe} = 10^{-6}$

$$\log \frac{10^{(-6 + .03/.059)}}{1 + 10^{.03/.059}} = -.72 - 3 \text{ pH} \quad [1.5.123]$$

$$- 6.12 + .72 = - 3\text{pH}$$

$$\text{pH} = 1.8 \quad [1.5.124]$$

Consider $E = 0.9$ $\Sigma\text{Fe} = 10^{-6}$

$$\log \frac{10^{(-6 + .13/.059)}}{1 + 10^{.13/.059}} = -.72 - 3 \text{ pH} \quad [1.5.125]$$

$$-6 + .72 = -3\text{pH}$$

$$\text{pH} = 1.76 \quad [1.5.126]$$

The second equilibrium to be considered is that given by equation 1.5.113. Solving equation 1.5.115 and 1.5.116 in terms of Fe^{++} this time yields the expression

$$\frac{\Sigma \text{Fe} - \text{Fe}^{++}}{\text{Fe}^{++}} = 10^{(E-.77)/.059} \quad [1.5.127]$$

$$\text{Fe}^{++} = \frac{\Sigma \text{Fe}}{1 + 10^{(E-.77)/.059}} \quad [1.5.128]$$

Substitution into equation 1.5.113 results in

$$E = 0.728 - .059 (\text{Fe}^{++}) - .177 \text{ pH} \quad [1.5.129]$$

$$E = 0.728 - .059 \log \frac{\Sigma \text{Fe}}{1 + 10^{(E-.77)/.059}} \quad [1.5.130]$$

$$\text{for } \Sigma \text{Fe} = 10^{-6} \quad [1.5.131]$$

$$E - .059 \log [1 + 10^{(E-.77)/.059}] = .728 + .059(6) - .177 \text{ pH} \quad [1.5.132]$$

$$= 1.082 - .177 \text{ pH} \quad [1.5.133]$$

for $E = 0.77$

$$.77 - .059 \log (2) = 1.082 - .177 \text{ pH} \quad [1.5.134]$$

$$\text{pH} = 1.86 \quad [1.5.135]$$

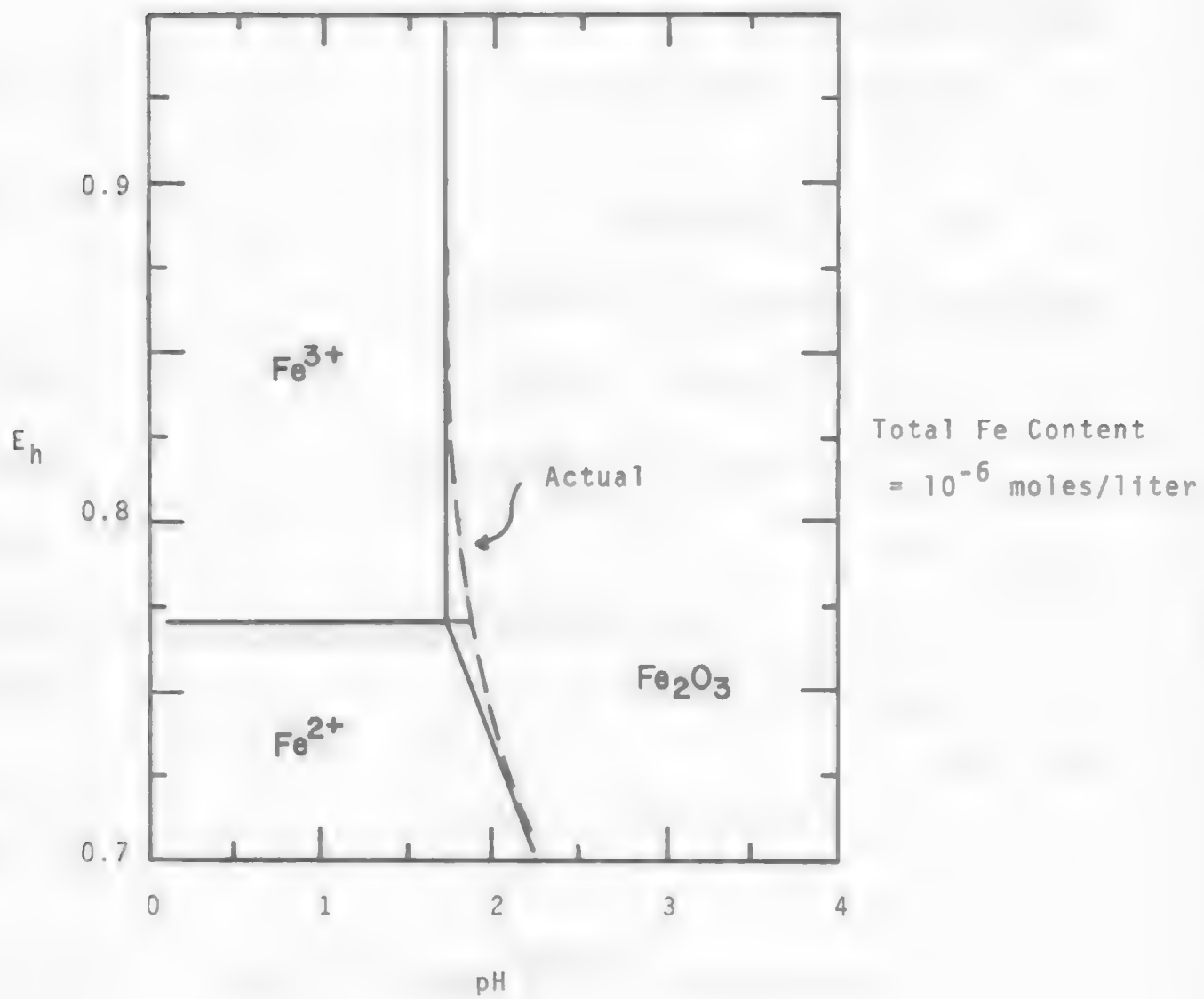
$$E = .75$$

$$.75 - .059 \log [1 + 10^{-.02/.0592}] = 1.082 - .177 \text{ pH} \quad [1.5.136]$$

$$\text{pH} = 1.93 \quad [1.5.137]$$

As can be seen in Figure 1.5.7, only small changes in stability fields are observed when the electrochemical equilibria are treated rigorously. The predominance area assumption normally used can be taken as a good approximation under most circumstances.

Figure 1.5.7. Significance of Predominance Area Assumption.



UNIT PROCESS IN EXTRACTIVE METALLURGY
HYDROMETALLURGY

Module 2

FUNDAMENTALS - MASS TRANSFER AND
REACTION KINETICS

SEVEN LEARNING
ACTIVITIES

Module Coordinator: Dr. H. H. Haung
Assistant Professor of Metallurgical Engineering
Montana College of Mineral Science and Technology

Module 2 Contents

2.1 Introduction

1. Classification of Reactions
2. Definition of Reaction Rate

Learning Activity 1

2.2 Homogeneous Kinetics

1. Law of Mass Action and Rate Law
2. Theories of Rate Constant
3. Catalysis
4. Reaction Order from Batch Reactor Data
5. Suggested Readings

Learning Activity 2

2.3 Heterogeneous Kinetics

1. Reaction Steps and the Rate Controlling Step
2. Transport Within Phases
3. Kinetics of Adsorption Reactions
4. Reaction of the Interface
5. Electrochemical Reaction on an Electrode Surface
6. Rate Equation for Heterogeneous Reaction - Flat Plate Geometry
7. Fluid-Particle Reaction - Spherical Geometry
8. Suggested Readings

Learning Activity 3

Learning Activity 4

Learning Activity 5

Learning Activity 6

2.4 Rate Phenomenon in Hydrometallurgical Processes

1. Dissolution of Metal by Spinning Disc Technique
2. Dissolution of Oxides

Learning Activity 7

2.5 References

LEARNING ACTIVITY 1

Learning Activity Objective

After completing this learning activity you should be able to define a homogeneous reaction and a heterogeneous reaction and their corresponding rate expressions, and be able to relate the rate from one component to the other component by the stoichiometry.

2.1 Introduction

In the preceding module you were introduced to the basic concepts of thermodynamics that apply to the hydrometallurgical processes for predicting the possible direction of reaction, the equilibrium concentrations of reactants and products and the effect of temperature and concentration on reactions. Thermodynamics, however, does not allow us to predict the rate of a possible reaction. The rate at which a reaction proceeds in a hydrometallurgical process is of great concern. Hydrometallurgical reactions normally occur at relatively low temperatures and involve more than one phase. The reactions are, therefore, normally relatively slow processes. The use of thermodynamic principles allows us to anticipate the possible end products. But step-by-step analyses of the reaction sequence and reaction rate provides us with important information, i.e., the mechanism of the reaction and intrinsic kinetic data necessary to design satisfactory equipment for practical commercial application.

2.1.1 Classification of Reactions

The study of rate processes is a field that deals with the rate at which processes occur (change of concentration of reactants per unit time). There are many ways of classifying rate processes. One is to divide them into two main categories, first, the kinetics of physical processes, and second, the kinetics of chemical reactions. The former deals with the study of the rate of processes that do not alter any chemical property of the constituents. The latter, chemical kinetics, is mainly concerned with the rate at which certain chemical reactions proceed. In some cases, however, both chemical and physical processes may be involved simultaneously.

Another classification is needed to describe more complicated systems. A useful classification scheme is to classify the rate processes according to the number and types of phases involved. The major divisions are: homogeneous and heterogeneous systems. A reaction is homogeneous if it takes place in a single phase and reacts uniformly throughout the whole volume of that phase. In this case only the chemical kinetics, not physical kinetics, are important due to the fact that the reactants have been homogeneously distributed throughout the whole system. A reaction is heterogeneous if it involves at least two phases and reacts at a common phase boundary (interface). In this case, physical rate processes may play an important role in determining the overall kinetics, e.g., the transport of reactants from the bulk phase to the reaction interface.

2.1.2 Definition of Reaction Rate

To express the rate of a reaction, it is necessary to select one reacting component i for consideration and to define the rate in terms of that component. The rate expression that describes component i is related to the rest of the components and is based on intensive rather than extensive properties. The rate of change of component i is dN_i/dt , i.e., moles of component i reacted per unit time or some equivalent units. The form of the rate equation depends on whether the reaction is homogeneous or heterogeneous. For a homogeneous reaction, because the reaction takes place uniformly throughout the whole system, the rate expression is defined as moles of component i generated or consumed per unit volume, V , per unit time,

$$r_i = \frac{1}{V} \frac{dN_i}{dt} \quad [2.1.1]$$

But for a heterogeneous reaction where the reaction is taking place only at the interface, the rate is expressed as moles of component i generated or consumed per unit interfacial area, S , per unit time,

$$r_i = \frac{1}{S} \frac{dN_i}{dt} \quad [2.1.2]$$

If the component i is a reaction product the rate, r_i , will be positive, if it is a reactant the rate will be negative.

The relationship between rate expressions for all the components involved in the reaction can be determined from the stoichiometric equation,



ν_i = stoichiometric coefficient for component i , reactant species will have a negative sign and product species will have a positive sign.

An example of the rate relationship between two species A and B is as follows:

$$\frac{r_A}{\nu_A} = \frac{r_B}{\nu_B} \quad [2.1.4]$$

2.2 Homogeneous Kinetics

In homogeneous reactions all reacting materials are found within a single phase. The phase can be a gas, liquid or solid. Although there are a number of ways of defining the rate of reaction, the definition based on unit volume of reacting fluid is used almost exclusively for

homogeneous systems. Thus, the rate of reaction of a reaction product is defined as,

$$r_D = \frac{1}{V} \frac{dN_D}{dt} = \frac{(\text{moles of D produced})}{(\text{unit volume})(\text{unit time})} \quad [2.1.5]$$

or

$$= \frac{dC_D}{dt} = \frac{(\text{concentration of D increased})}{(\text{unit time})} \quad [2.1.6]$$

where C_D is the concentration of D in the system. The rate of reaction of a reactant A consumed is defined as

$$-r_{C_A} = \frac{-1}{V} \frac{dN_A}{dt} = \frac{-dC_A}{dt} \quad [2.1.7]$$

In general, the rate at which the homogeneous chemical reaction proceeds depends upon (a) the nature of the reactants, (b) their concentration, (c) the temperature, and (d) the presence of catalysts.

2.2.1 Law of Mass Action and Rate Law

The Law of Mass Action states that the rate of a chemical reaction is directly proportional to the active mass of the reacting species. The term active mass is described as being dependent upon the number of reacting species per unit volume, i.e., concentration. In harmony with the law of mass action, reaction rates do depend upon some function of the concentration.

Suppose, for example, a reaction is progressing from a general stoichiometric equation,



the rate is described by the rate equation:

$$\frac{-dC_A}{dt} = k(C_A^{n_A})(C_B^{n_B}) \quad [2.1.9]$$

where

$dC_A = C_{A,2} - C_{A,1}$ = concentration difference of species A between times t_2 and t_1 ,

$dt = t_2 - t_1$ = time difference between t_2 and t_1 ,

C_A, C_B = concentration of A and B, respectively,

k = specific rate constant,

n_A, n_B = order of reaction with respect to A and B, respectively.

Note that the reaction orders, n , are not necessarily related to the stoichiometric coefficient, ν .

Those reactions in which the rate equation does correspond to a stoichiometric equation, i.e., reaction order = stoichiometric coefficient, are called elementary reactions. An elementary reaction is a single step reaction that goes from reactants directly to products without forming any intermediates. But when there is no correspondence between stoichiometry and the rate then it is a non-elementary reaction. The classical example of a non-elementary reaction is that between hydrogen and bromine,



which has the experimental rate expression given below,

$$r_{\text{HBr}} = \frac{k_1[\text{H}_2][\text{Br}_2]^{1/2}}{k_2 + [\text{HBr}]/[\text{Br}_2]} \quad [2.1.11]$$

where square brackets represent concentrations.

Non-elementary reactions are explained by assuming that what we represent as a single reaction [2.1.10] is in reality the overall effect of a sequence of elementary reactions. By analyzing the experimental rate data, the reaction mechanism has been proposed to be:



where H^\cdot and Br^\cdot are hydrogen and bromine free radicals.

Chemical reactions are also divided into single and complex reactions. A single reaction is any reaction involving a single stoichiometry and a single rate equation, such as



Complex reactions are any combination of two or more single reactions, e.g.,

series or consecutive	$A \rightarrow B \rightarrow C$	[2.1.14]
opposing or reversible	$A \rightleftharpoons C$	[2.1.15]
and parallel reactions	$A \rightarrow B$ and $A \rightarrow C$	[2.1.16]

2.2.2 Theories of Rate Constant

From the previous discussion, the rate of a chemical reaction will depend not only on the mass action but also on the nature of the reactants and the temperature. The effect of the last two factors has been lumped into an experimental rate constant k presented in the rate equation [1.1.9]. At present it is impossible to predict exactly the velocity of a chemical reaction from the knowledge of the nature of the reactants such as the electronic structure of elements and molecules and their chemical and physical properties. But the effect of temperature on the rate of reaction has been studied quite extensively and several theories have been proposed.

Arrhenius developed a concept for the variation of the rate with temperature based on the thermodynamic argument. He showed that the rate constant increases in an exponential manner with the temperature:

$$k = A \exp[-E_a/RT] \quad [2.1.17]$$

where

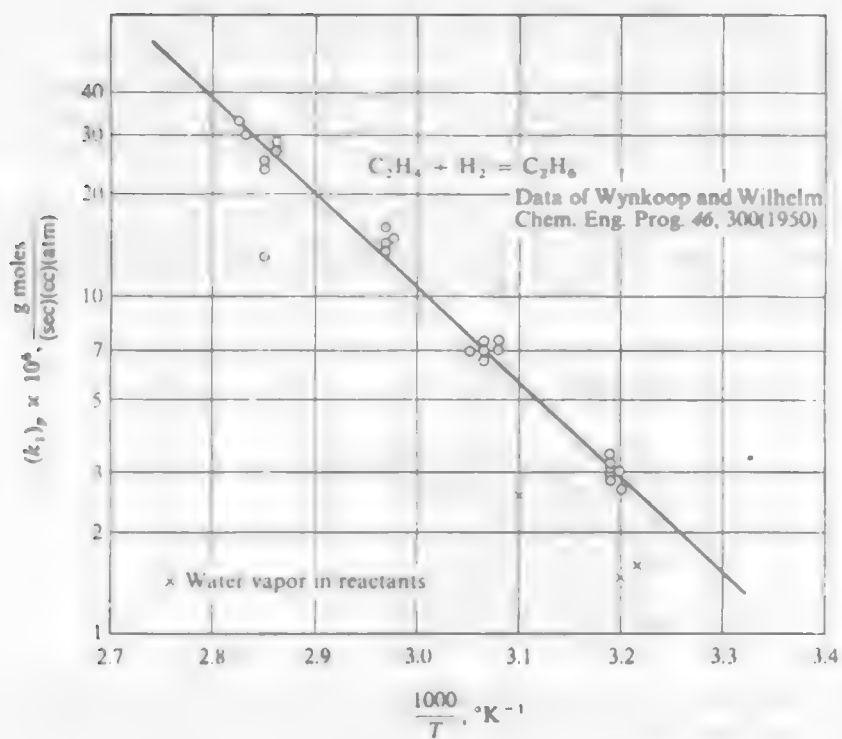
k = specific rate constant,
 A = frequency factor,
 \exp = exponential,
 R = gas constant,
 T = absolute temperature, and
 E_a = activation energy.

The Arrhenius expression fits experimental data over wide temperature ranges and has been an accepted way of presenting kinetic data. The numerical value of the energy of activation can be determined by plotting $\ln k$ against $1/T$, $-E_a/R$ is the slope of the plot. An example plot is given in Figure 2.1.1. The example chosen for illustration is the hydrogenation of ethylene. The activation energy for the reaction is 12.8 kcal/mole⁽¹⁾. The value of the activation energy is usually positive. It has been interpreted to be the quantity of potential energy that must be overcome before a specific chemical reaction can occur regardless of the internal energy of reactants.

The concept of activation energy has been described in terms of two theories, the collision theory and the transition state theory. Only a brief discussion will be given here (more detailed explanation, however, can be found in an advanced physical chemistry text book).

Collision Theory. In a system consisting of molecules or atoms there is a natural tendency for them to take up positions such that the energy of the system is minimum. For the reaction, $A + B \rightarrow C + D$, for example (Figure 2.1.2), molecules A and B are at stable positions having

Figure 2.1.1. Plot of Arrhenius Equation for Hydrogenation of Ethylene.



Source: Data of Wynkoop and Wilhelm, Chem. Eng. Prog. 46, 300(1950).

their minimum energy on the left hand side of the graph and molecules C and D are at their stable position on the right side of the graph. The path that leads from A+B to C+D is obstructed by a certain energy barrier E_a . It is clear that unless the reactants A and B together possess an energy in excess of E_a , they will not be able to overcome the energy barrier, i.e., they will not proceed to the thermodynamically stable level of the products C and D. In other words, at any temperature a collision between molecules which have a combined energy (activated molecules) greater than E_a will lead to a chemical reaction. The concept of activated molecules and activation energy can be explained by the Boltzmann's distribution law based on a statistical approach to the problem. The exponential factor, $\exp[-E_a/RT]$, may be taken to represent the fraction of all the molecules which have an energy of activation at least equal to E_a . From this concept the conclusion is drawn that the rate of a reaction is proportional to $\exp[-E_a/RT]$,

$$\text{reaction rate} \propto \exp[-E_a/RT] \propto k$$

$$k = A \exp[-E_a/RT] \quad [2.1.18]$$

Transition State Theory. The transition state theory assumes that before a reaction takes place, reactants form an unstable intermediate compound called an "activated complex." The "activated complex" instantaneously decomposes into the products. It is further assumed that an equilibrium exists between reactants and the complex.



where $K^* = \text{equilibrium constant,}$
 $AB^* = \text{activated complex.}$

A plot of energy versus a reaction coordinate is presented in Figure 2.1.3.

The concentration of the complex, AB^* can be expressed in terms of the equilibrium constant as,

$$K^* = \frac{C_{AB^*}}{C_A C_B} \quad [2.1.20]$$

$$C_{AB^*} = K^* C_A C_B \quad [2.1.21]$$

Also recall that the equilibrium constant is related to the free energy by the relationship

$$\Delta G^* = -RT \ln K^* \quad [2.1.22]$$

Therefore,

$$C_{AB}^* = C_A C_B \exp[-\Delta G^*/RT] \quad [2.1.23]$$

The rate of the overall reaction at any given time is assumed to be equal to the product of C_{AB}^* times a frequency factor. The frequency factor is proportional to the average velocity of the complex across the energy barrier divided by the length of the barrier, δ , see Figure 2.1.3. The frequency factor is equivalent to RT/hN_{Avogadro} where h is Plank's constant, N_{Avogadro} is Avogadro's Number.

Therefore,

$$r_{AB} = \frac{RT}{hN} C_{AB}^* \quad [2.1.24]$$

$$= \frac{RT}{hN} C_A C_B \exp[-\Delta G^*/RT] \quad [2.1.25]$$

$$= \frac{RT}{hN} C_A C_B \exp[\Delta S^*/R] \exp[-\Delta H^*/RT] \quad [2.1.26]$$

Since,

$$r_{AB}^* = k C_A C_B$$

$$k = T \exp[-\Delta H^*/RT] \quad [2.1.27]$$

If $\Delta H^* \sim E_a^*$, then this equation is equivalent to the Arrhenius equation, 1.1.13, except the proportional constant in the Arrhenius equation is not a function of temperature as is shown by this equation. This difference is, however, only of minor significance in actual reactions.

In summary, collision theory depicts reaction rates to be determined by the number of energetic collisions between reactants. It disregards the existence of the unstable intermediate. Transition state theory, on the other hand, depicts the reaction rate to be governed by the rate of the decomposition of the intermediate, while the formation of the intermediate is assumed to be so rapid that it is always at equilibrium with reactants. The difference can be illustrated as below:



Collision theory views the first step to be slow and rate controlling, whereas transition state theory views the second step to be the rate controlling factor. In a sense, these two theories complement each other.

Figure 2.1.2. Energy Diagram of Simple Reaction $A + B \rightarrow C + D$ According to Collision Theory.

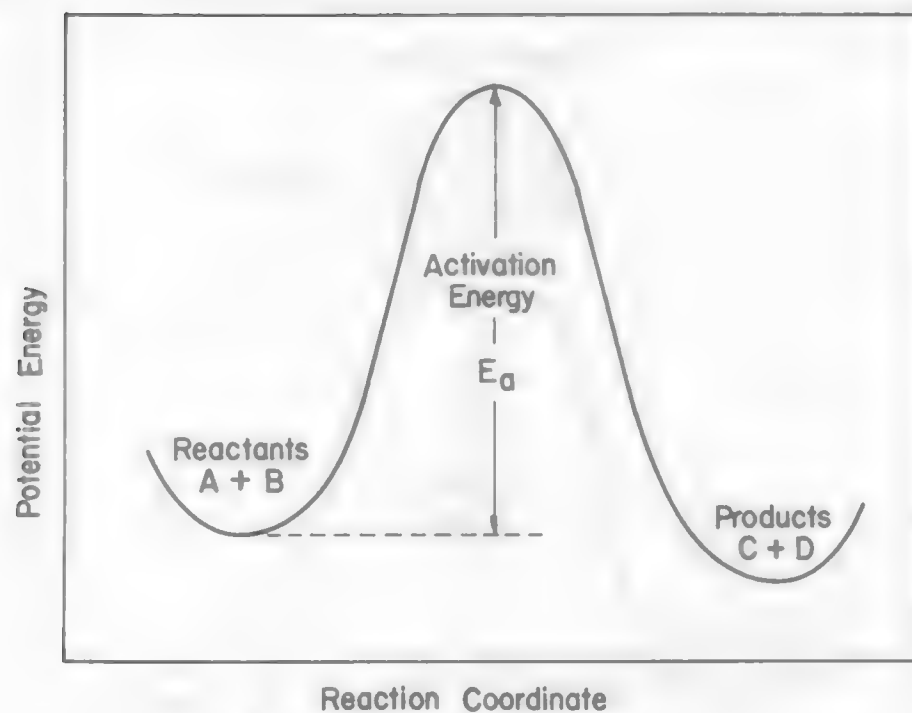
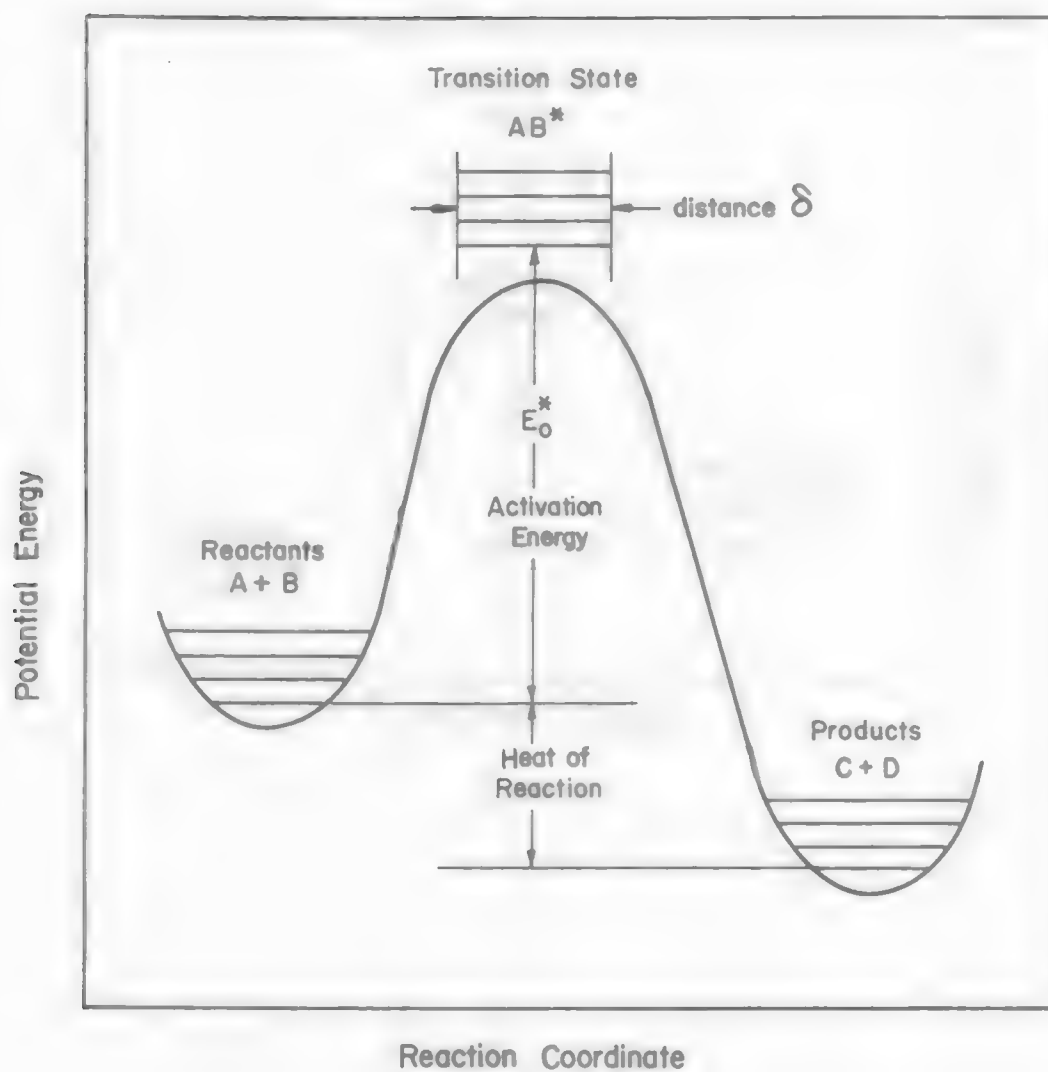


Figure 2.1.3. Diagram Illustrating Potential Energy Relationship Between Reactants, Activated State, and Products According to Transition State Theory.

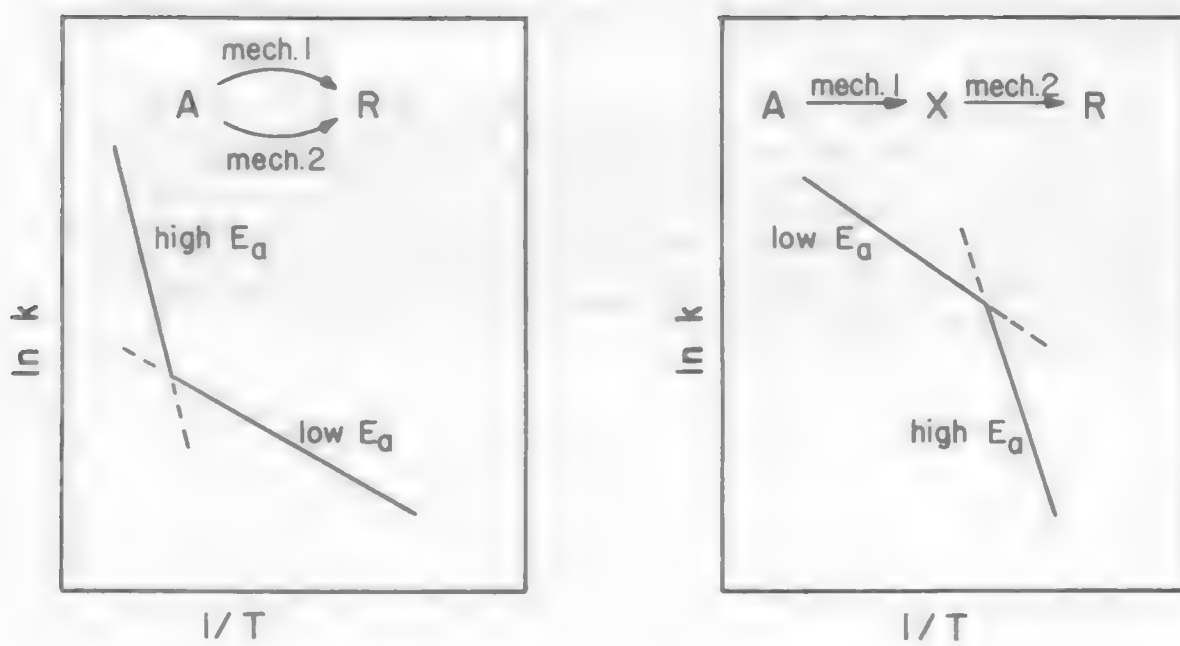


The experimental activation energies are frequently used to distinguish a chemical reaction from a physical process. Physical processes generally have low E_a values, i.e., E_a is generally <5 kcal. Chemical reactions normally have E_a values between 10 and 25 kcal.

The activation energy can sometimes be useful in determining the reaction mechanism. For example, a change in activation energy with temperature will indicate a shift has occurred in the controlling step of a complex reaction. For example, suppose a complex reaction involves two elementary steps and E_a shifts from a low value to a high value with temperature (shown in Figure 2.1.4). These two steps should be in parallel because the rate is controlled by the faster step which has a large k value. On the other hand, if the E_a value decreases with temperature, the two steps should be in series because the rate is controlled by the slower step which has a small k value. This conclusion is illustrated in Figure 2.1.4.

From an engineering point of view, the activation energy provides useful kinetic information over a wide range of temperature. The rate of a reaction at a particular temperature can be calculated from the Arrhenius equation. Furthermore, the values of activation energies (reactions with high activation energies are very temperature sensitive, and vice versa) are important criteria in determining the optimal temperature for an operation, i.e., temperature influences both production rate and economics of the process.

Figure 2.1.4. Rate Constant Versus Reciprocal Temperature.



LEARNING ACTIVITY 2

Learning Activity Objective

After completing your study of this material you should be able to describe the function of a catalysis and be able to determine reaction order from reactor data.

2.2.3 Catalyses

A catalyst can be defined as a substance that influences the velocity of a reaction but is itself not a reagent in the overall chemical reaction. **If the presence of a substance results in an increased reaction rate,** then the substance is called a catalyst. However, if the substance causes a decrease in the reaction rate, then it is known as an inhibitor. The catalytic action can generally be classified as homogeneous catalysis and heterogeneous catalysis.

In a homogeneous catalytic reaction the catalyst is uniformly distributed throughout the system. The function of the catalyst is to decrease the activation energy of a given reaction, and thus to increase its rate, because more molecules will then have the required energy for reaction to occur. The mechanism for catalysis is thought to be achieved by the formation of a compound between the reactants and the catalyst. The compound then decomposes, thereby regenerating the catalyst and forming the reaction products. This process is illustrated below:

For the reaction



In the presence of a catalyst, C, the reaction steps may be



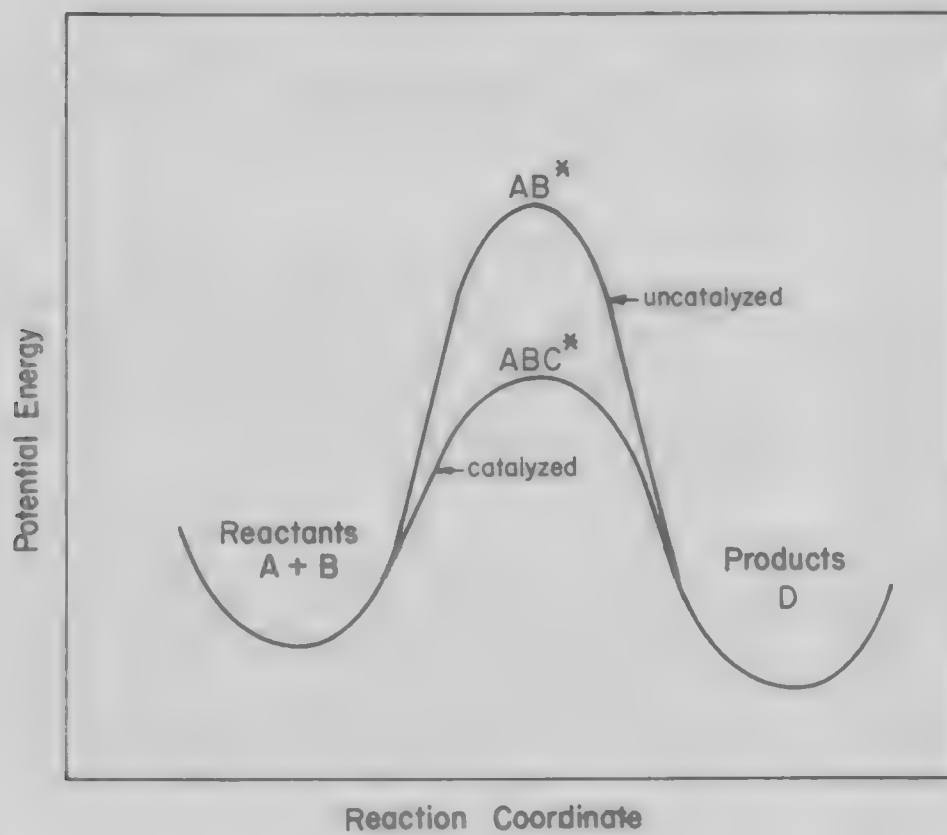
An energy diagram for this sequence is shown in Figure 2.2.1.

In a heterogeneous catalytic reaction the catalyst is not uniformly distributed throughout the system, but is present as a separate phase. The uses of solid catalysts for many gaseous reactions are commonly found. The catalytic effect is explained by a sequence of reactions. First the gaseous reactants are adsorbed on the surface of the catalyst, and then, after passing through a transition state, they form a compound with simultaneous desorption from the surface.

2.2.4 Reaction Order from Batch Reactor Data

Due to the complication of predicting the rate of reaction from theoretical considerations, the rate equation is usually determined from experimental measurements. The procedure normally used is to

Figure 2.2.1. A Schematic Energy Diagram for a Catalyzed Reaction.



measure the yield as a function of concentration and temperature. Experiments can be performed in either a batch or a continuous flow reactor. A batch reactor is simply a container into which the reactants are placed (at zero time) without further addition or removal of significant amount of material, i.e., concentration of a particular component is measured as a function of time. The batch reactor is usually operated isothermally and at constant volume. This makes the interpretation of the data much simpler. For a constant volume system the rate expression for the disappearance of reactant A is:

$$-r_A = -\frac{1}{V} \frac{dN_A}{dt} = -\frac{dC_A}{dt} = f(k, C) \quad [2.2.4]$$

For a reaction $\nu_A A + \nu_B B \rightarrow \text{product}$, the rate equation may be written as,

$$-\frac{dC_A}{dt} = k_1 (C_A)^{n_A} (C_B)^{n_B} \quad [2.2.5]$$

The simplest experimental procedure is to investigate the effects of concentration A and concentration B individually. This can be accomplished by the isolation method, i.e., an excess amount of one of the components, such as component B, is used. Therefore, B will remain almost constant throughout the course of the reaction. The rate equation can then be written as,

$$-\frac{dC_A}{dt} = k C_A^n \quad [2.2.6]$$

because $C_B^{n_B}$ is a constant and becomes a part of the rate constant, k. There are several procedures for analyzing kinetic data, three will be discussed in this course, i.e., the differential method, the half-life time method, and the integral method.

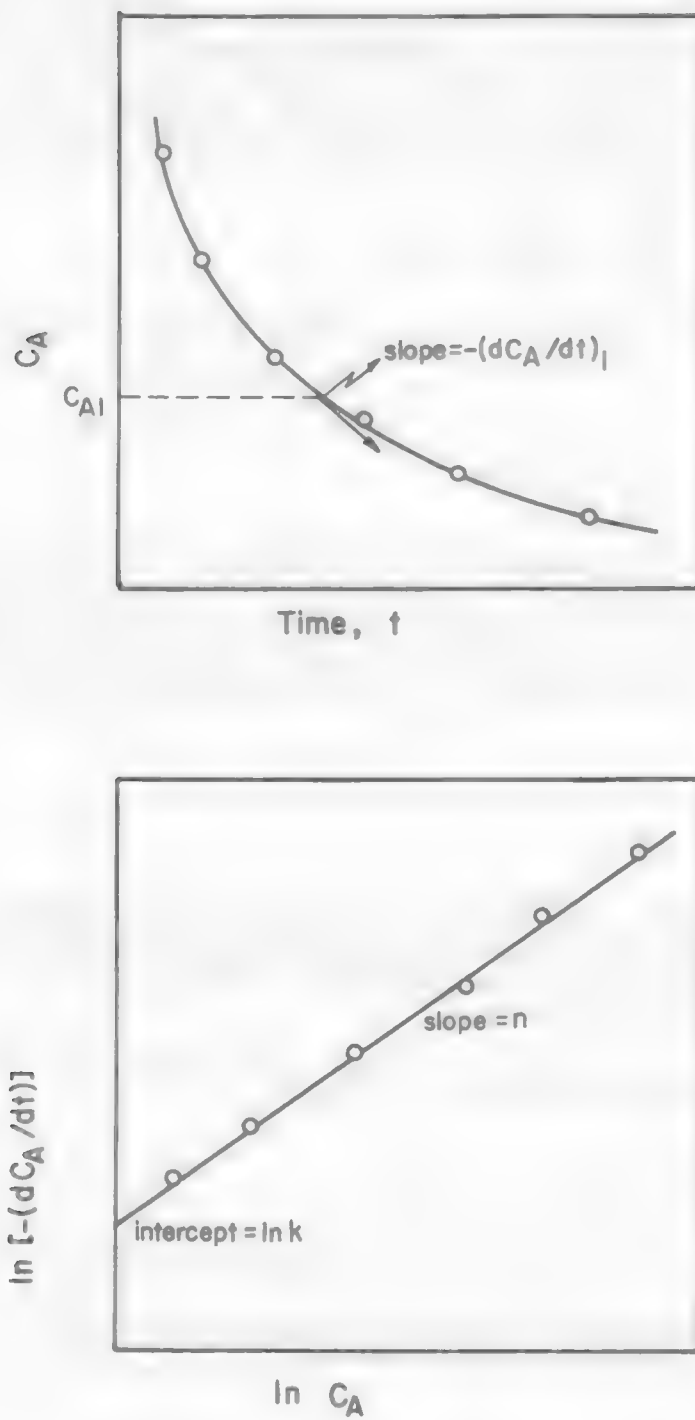
Differential Method of Analysis. We can rewrite equation [2.2.6] in the following form:

$$\ln \left(-\frac{dC_A}{dt} \right) = \ln k + n \ln C_A \quad [2.2.7]$$

The reaction order can be determined by the following simple procedure:

1. Plot the concentration of specie A versus time. Draw in a smooth curve to fit the data. An illustration is given in Figure 2.2.2.
2. Choose several concentrations and determine the slope for each concentration, i.e., the $-\frac{dC_A}{dt}$.

Figure 2.2.2. Procedure for Testing a Rate Equation by the Differential Method of Analysis.



3. Plot the $\ln \left(-\frac{dC_A}{dt}\right)$ versus $\ln (C_A)$. For the simple case chosen for illustration (excess concentration of B) the plot will be a straight line. The slope of the plot will be the reaction order and the intercept will be $\ln k$.

The disadvantage of the differential method is that a large body of experimental data is required and precision can easily be lost when determining slopes from non-linear curves.

Half-Life Time, $t_{1/2}$, Analysis. Half life is defined as the time required for the concentration of reactants to decrease to one-half the original value. This procedure can be illustrated by integrating equation [2.2.6].

$$\int_{C_{A_0}}^{\frac{C_{A_0}}{2}} \frac{dC_A}{C_A^n} = -k \int_0^{t_{1/2}} dt \quad [2.2.8]$$

The result is:

$$t_{1/2} = \frac{2^{n-1}-1}{k(n-1)} C_{A_0}^{1-n}$$

or

$$\ln t_{1/2} = \ln \frac{2^{n-1}-1}{k(n-1)} + (1-n) \ln C_{A_0} \quad [2.2.9]$$

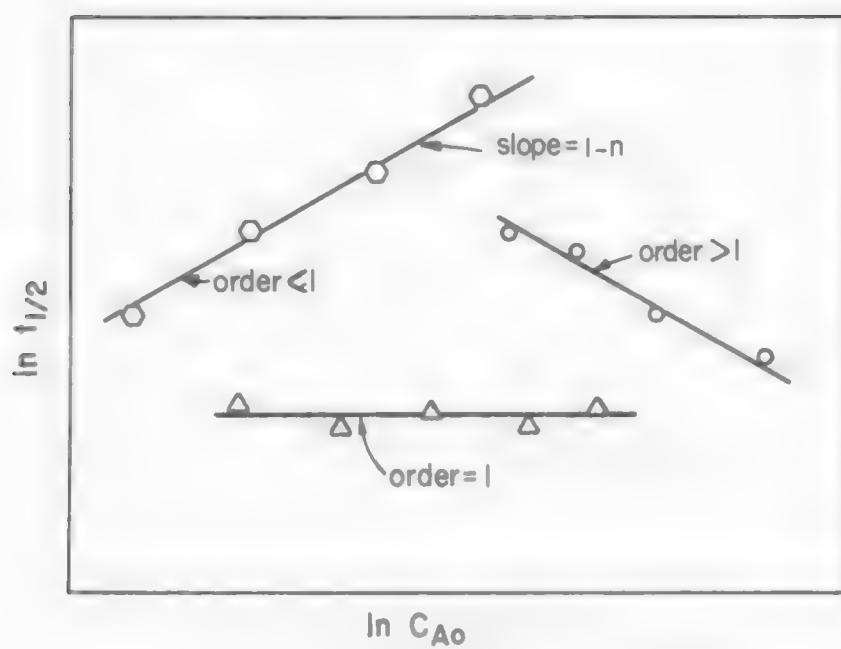
The half life depends on reaction order, n , and initial concentration, C_{A_0} , examples are given below:

$$t_{1/2} = \frac{0.693}{k} \quad (1st \text{ order}) \quad [2.2.10]$$

$$t_{1/2} = \frac{1}{kC_{A_0}} \quad (2nd \text{ order}) \quad [2.2.11]$$

The reaction order can be determined from a set of data by plotting the logarithms of several initial concentrations versus the log of the corresponding half-life. The reaction order can be determined from the slope, i.e., slope = $1-n$, see Figure 2.2.3. You should be aware that this method may give you a problem if the reaction order shifts with concentration.

Figure 2.2.3. Reaction Order from a Series of Half-Life Time Experiments, Each at a Different Initial Concentration of Reactant, (Equation 2.2.9).



Integral Method of Analysis. This method of analysis consists of assuming a particular rate equation applies, then test the data by graphically plotting the integrated form of the equation. If a straight line results, then the order can be determined. If a straight line does not fit the data, then another rate equation must be chosen and tested. Examples are discussed below:

- a. Irreversible zero order reactions. If a reaction,
 $A \rightarrow \text{products}$ [2.2.12]

is presumed to be a zero order reactant, its rate equation can be written as,

$$-\frac{dC_A}{dt} = k \quad [2.2.13]$$

and its integrated rate expression would be as follows,

$$C_A = C_{A0} - kt \quad [2.2.14]$$

The concentration of A at $t = 0$ is C_{A0} .

If a plot of concentration of C_A versus time is a straight line (as shown in Figure 2.2.4), then the slope can be used to determine the rate constant, i.e., slope = $-k$.

- b. First order reactants. If a unimolecular reaction,
 $A \rightarrow \text{product}$ [2.2.15]

is presumed to be a first order reaction, then its rate equation can be written as,

$$-\frac{dC_A}{dt} = k C_A \quad [2.2.16]$$

and its integrated rate equation would be

$$-\ln \frac{C_A}{C_{A0}} = k t \quad [2.2.17]$$

A plot of $-\ln (C_A/C_{A0})$ versus time can be used to test the hypothesis (see Figure 2.2.5).

- c. Second order reactions.
 Case I. If a bimolecular reaction,
 $2A \rightarrow \text{products}$ [2.2.18]

is presumed to be second order, then the rate expression can be written:

$$-\frac{dC_A}{dt} = k C_A^2 \quad [2.2.19]$$

Figure 2.2.4. Graphical Test for a Zero Order Reaction (Equation 2.2.14).

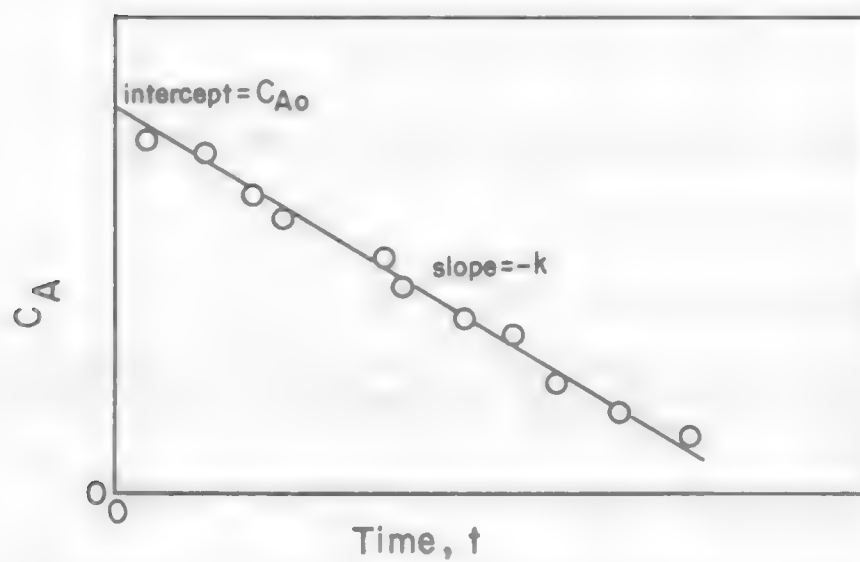
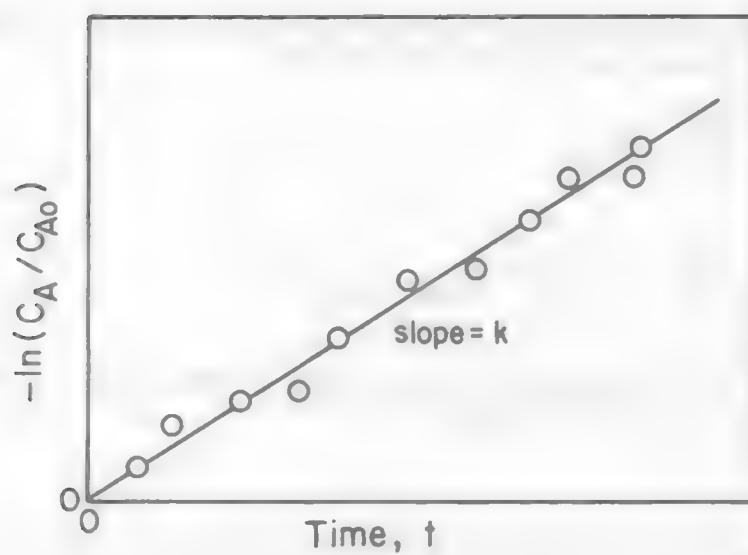


Figure 2.2.5. Graphical Test for a First Order Reaction (Equation 2.2.17).



and its integrated form would be

$$\frac{1}{C_A} = \frac{1}{C_{A0}} + kt \quad [2.2.20]$$

A linear relationship should be found between $1/C_A$ and time as shown in Figure 2.2.6 if the data is satisfied by the assumed rate equation.

Case II. If a bimolecular reaction,
 $A + B \rightarrow \text{products}$ [2.2.21]

is presumed to be a second order overall reaction, then the differential and integral rate equations will be as follows:

$$-\frac{dC_A}{dt} = kC_A C_B \quad [2.2.22]$$

and

$$\ln \frac{C_B}{C_A} = \ln \frac{C_{B0}}{C_{A0}} + (C_{B0} - C_{A0})kt \quad [2.2.23]$$

If the reaction is as presumed, then a straight line will be found for a plot of $\ln \frac{C_B}{C_A}$ versus time (Figure 2.2.7).

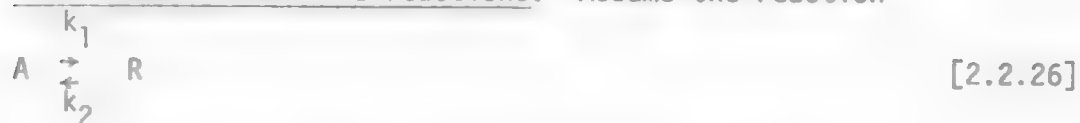
For the special case, when concentration of component B is large and does not change its concentration significantly during the reaction, the following relationships are valid:

$$\frac{C_B}{C_{B0}} \approx 1 \text{ and } C_{B0} - C_{A0} \approx C_{B0} \quad [2.2.24]$$

The reaction rate equation, therefore, is first order dependent on A:

$$\ln \frac{C_{A0}}{C_A} = C_{B0}kt \quad [2.2.25]$$

d. First order reversible reactions. Assume the reaction



is a first order reversible reaction with the equilibrium constant K , the rate equation is written as follows:

Figure 2.2.6. Graphical Test for the Bimolecular Mechanism, $2A \rightarrow \text{Product}$ (Equation 2.2.20).

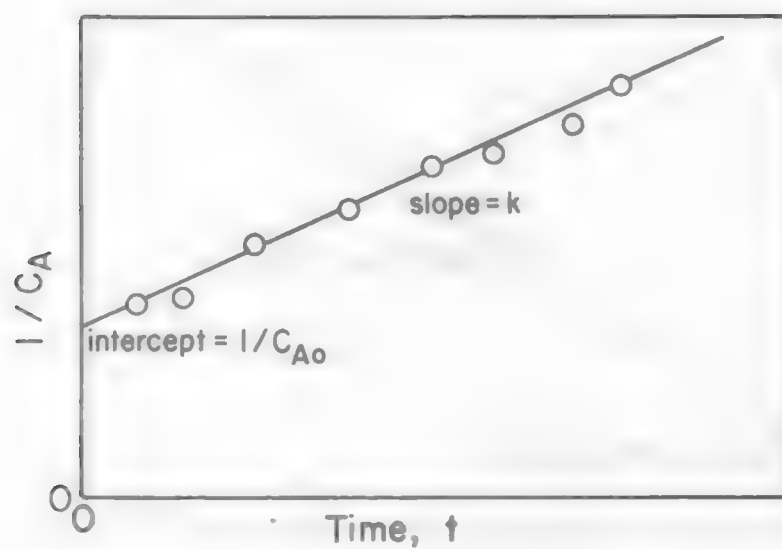
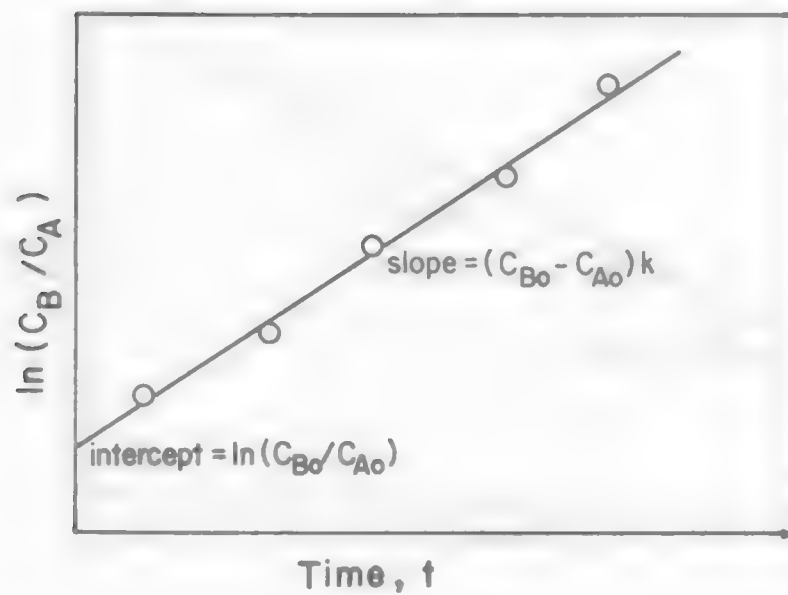


Figure 2.2.7. Test for the Bimolecular Mechanism $A + B \rightarrow \text{Product}$ (Equation 2.2.23).



$$-\frac{dC_A}{dt} = k_1 C_A - k_2 C_R \quad [2.2.27]$$

The first term on the right side of the equation is the rate of disappearance of component A. The second term on the right side of the rate equation is the rate of generation of component A due to the reverse reaction. The integrated rate expression can be derived (see if you can do this derivation. A hint is that the equilibrium constant is

$$K = \frac{k_1}{k_2}):$$

$$-\ln \frac{C_A - C_{Aeq}}{C_{Ao} - C_{Aeq}} = k_1 \left(1 + \frac{1}{K}\right) t \quad [2.2.28]$$

where

C_{Aeq} = equilibrium concentration of component A,

k_1, k_2 = specific rate constant for forward and backward reaction, respectively,

$$K = \text{equilibrium constant} = C_{Req}/C_{Aeq} = k_1/k_2 \quad [2.2.29]$$

A plot of the \ln term versus t will yield a straight line if this rate equation fits the data, see Figure 2.2.8. For the special case when the equilibrium constant is large, i.e., k_2/k_1 is small, the rate equation, Equation [2.2.28], can be simplified to (same as a first order irreversible rate equation):

$$-\ln \frac{C_A}{C_{Ao}} = kt \quad [2.2.30]$$

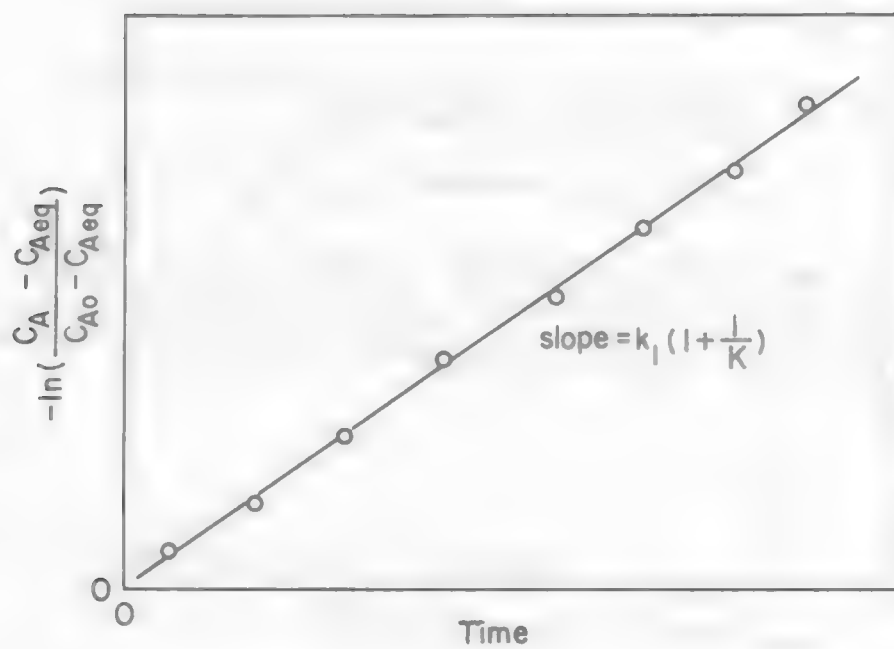
because $1 + \frac{1}{K} \approx 1$ and $C_{Aeq} \approx 0$. Equation 2.2.30 is actually the rate equation for an irreversible first order reaction.

Although the above discussion is only for elementary reactions, it is worth examining reaction reversibility from a thermodynamic point of view. If the reversibility is defined as a ratio of specific rate constants between forward and reverse reactions, k_2/k_1 , a large value will indicate that the reaction is highly reversible. According to Equation 2.2.29 reversibility can be predicted from thermodynamic data,

$$k_2/k_1 = 1/K = \exp[+\Delta G^\circ/RT] \quad [2.2.31]$$

where ΔG° = Gibbs free energy of reaction. In other words, for a highly favorable reaction, $\Delta G^\circ \ll 0$, k_2/k_1 becomes very small, and the reaction may be irreversible. However, the reaction reversibility depends not only on the Gibbs free energy but also on the reaction temperature. A comparison between the reversibility of a pyrometallurgical reaction and that of a hydrometallurgical reaction as a function of Gibbs free energy

Figure 2.2.8. Graphical Test for a First Order Reversible Reaction (Equation 2.2.28).



of reaction is shown in Table 2.2.1; the temperature of the reaction is assumed to be 1500°K for the pyrometallurgical reaction and 300°K for the hydrometallurgical reaction.

TABLE 2.2.1
Reaction Reversibility at 1500 and 300°K

Reversibility k_2/k_1	ΔG° (1500°K) kcal/mole	ΔG° (300°K) kcal/mole
0.1	-6.86	-1.37
0.01	-13.73	-2.75
0.001	-20.56	-4.12

These results indicate that for the hydrometallurgical reaction, the reversible reaction can probably be neglected when the free energy of reaction is less than -3 kcal/mole. This observation suggests that most of the hydrometallurgical processes may be irreversible, exceptions to this are the reversible solvent extraction and ion exchange reactions.

2.2.5 Suggested Reading

1. O. Levenspiel, Chemical Reaction Engineering, 2nd ed., John Wiley and Sons, New York, Cap. 2 (1972).
2. J. M. Smith, Chemical Engineering Kinetics, 2nd ed., McGraw-Hill, Chap. 2 (1970).

LEARNING ACTIVITY 3

2.3 Heterogeneous KineticsLearning Activity Objective

After completing this learning activity you should be able to describe the reaction sequence in a heterogeneous reaction, to describe the concept of rate controlling step, to formulate rate equations for surface chemical reactions and for mass transport reactions, and to interpret the kinetic data for a simple surface geometry.

The term, heterogeneous, is used here in the special sense in which the reactants come from different phases and then meet and react at a common phase boundary. The reaction will continue until the bulk chemical potentials are equalized. The rate of the reaction will not only depend on the chemical reaction but also on the mixing processes within phases. In addition, the rate will also depend on the area of the reactive surface, which may change during the course of reaction. These conditions represent complicating features not found in homogeneous reactions. Unfortunately, most of the hydrometallurgical processes are heterogeneous.

2.3.1 Reaction Steps and the Rate Controlling Step

Heterogeneous reactions always involve the following consecutive processes: (1) mass transport of reactants from a bulk phase to the reaction interface, (2) chemical reaction at the interface, and (3) mass transport of products away from the interface. The types of processes found in each of these stages are listed in Table 2.3.1. The interfacial chemical reaction may proceed by a complex reaction mechanism and be thought of as a homogeneous reaction involving a number of separate steps. While several of the above steps must take place in series, it is possible for one of them to be considerably slower than the others. The rate of the slow step will then be essentially the rate of the whole reaction.

TABLE 2.3.1

Possible Rate Controlling Processes in Heterogeneous Reactions

-
- I. Mass Transport of Reactants to or from the Reaction Interface
 - A. Diffusion through a Solid Reaction Product
 - 1. solid state diffusion
 - 2. fluid diffusion through pores
 - B. Mass Transport in a Fluid Phase Adjacent to the Interface
 - 1. diffusion in stagnant liquid or gas
 - 2. convective diffusion in liquid or gas
 - II. Interfacial Chemical Reactions
 - A. Adsorption Reaction
 - B. Chemical Reaction
 - C. Electrode Reaction
-

It is necessary to consider each reaction step separately and to estimate the maximum possible rate, that is, the rate which would be observed when a maximum concentration or concentration gradient exists in the particular step and all preceding and succeeding steps were in equilibrium. The step with the slowest maximum rate will be the rate limiting step. For instance when a reaction at the interface is the slowest, the chemical potentials, i.e., concentrations are practically uniform throughout each bulk phase, but change sharply at the interface. This analysis, however, does not apply to a mixed-kinetic controlled mechanism. More discussion of this will be presented later in this learning activity.

In order to simplify the discussion, the surface chemical reaction is assumed to be irreversible. This is a reasonable assumption for many hydrometallurgical reactions (discussed in the previous learning activity). If this is the case, the surface equilibrium concentration of reactants will be negligibly small, and step (3), transport of products away from the interface, probably will not be a rate limiting step.

Rate equations for each reaction step will be discussed individually in the following sections.

2.3.2 Transport Within Phases

Transport of reactants from the bulk phase to the phase boundary is accomplished by diffusion in solids and by diffusion and convective transport in fluids. Diffusion is faster in fluids than in solids and convective transport in fluids is far more rapid than diffusion. It is, therefore, to be expected that diffusion in the fluid will not be the controlling step if a solid reactant or product is present in the process.

Diffusion in Solids. The rate of any diffusion process can be described by Fick's first law. This law states that the rate of material transport is proportional to the concentration gradient, i.e.,

$$j_A = -D_A \cdot \frac{dC_A}{dx} \quad [2.3.1]$$

where

j_A = molar flux of species A, usually in moles/cm²·sec;
(+) sign is used to indicate diffusion away from the interface,

C_A = concentration of species A in moles/cm³,

x = distance x away from the interface,

D_A = diffusion coefficient of species A in solid, liquid, or gas phase.

Example values of diffusion coefficients are presented in Tables 2.3.2 and 2.3.3, e.g., molecular diffusion in gases, liquid and solids, and ionic diffusion in water, respectively.

When applying the Fick's law, strictly speaking, the driving force is not a concentration difference but a chemical potential difference. Thus, it may be necessary to correct the concentration by including the activity coefficient.

TABLE 2.3.2. Diffusivities of Some Gases, Liquids and Solids

	<u>System</u>	<u>Temperature, °C</u>	<u>D cm²/sec.</u>
Gases	H ₂ O in N ₂	25	0.26
	H ₂ in CH ₄	25	0.73
	H ₂ in O ₂	25	0.70
	CO ₂ in N ₂	0	0.144
Liquids	Ethanol in water	25	1.13x10 ⁻⁵
	Water in butanol	30	1.24x10 ⁻⁵
	Ag in Silver melt	1060	3.22x10 ⁻⁵
	Cu in Cu ₂ S melt	1160	7.49x10 ⁻⁵
	C in 3.5% iron melt	1550	6.0x10 ⁻⁵
Solids	Bi in Pb	20	1.1x10 ⁻¹⁶
	Hg in Pb	20	2.5x10 ⁻¹⁵
	Al in Cu	20	1.3x10 ⁻³⁰
	Cd in Cu	20	2.7x10 ⁻¹⁵

As illustrated in Tables 2.3.2 and 2.3.3, solid-state diffusion is the slowest type process. Diffusion is achieved by movements of individual atoms, molecules, ions, electrons or vacancies. To apply Fick's first law, a steady-state condition is assumed, that is, the concentration gradient is constant. A steady-state condition can be achieved immediately for a fast diffusion process, such as liquid or gaseous diffusion, but for slow processes, i.e., solid-state diffusion, sometimes steady state conditions may not be established. Fick's second law is used for the nonsteady-state diffusion condition, i.e.,

TABLE 2.3.3. Diffusion Coefficients of Ions in Aqueous Solution

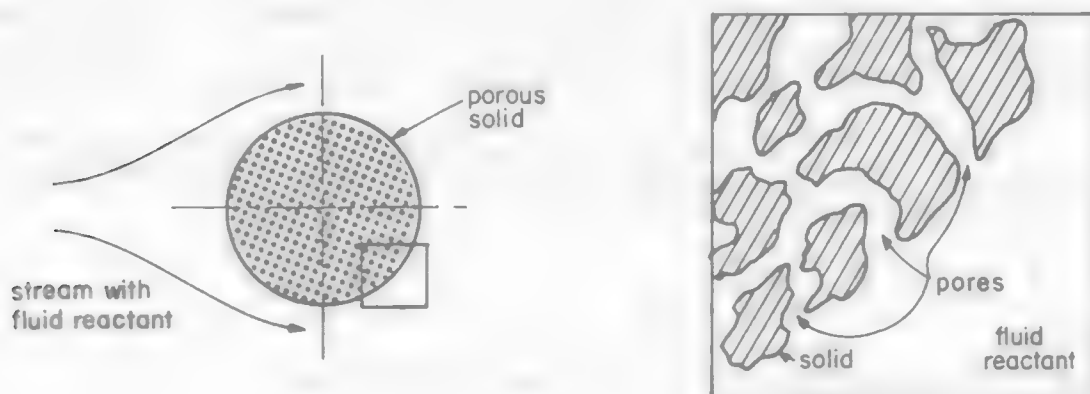
Cation	D_A° ($10^{-6} \text{ cm}^2/\text{sec}$)			Anion	D_A° ($10^{-6} \text{ cm}^2/\text{sec}$)		
	0°C	18°C	25°C		0°C	18°C	25°C
H ⁺	56.1	81.7	93.1	OH ⁻	25.6	44.9	52.7
Li ⁺	4.72	8.09	10.3	F ⁻	----	12.1	14.6
Na ⁺	6.27	11.3	13.3	Cl ⁻	10.1	17.1	20.3
K ⁺	9.86	16.7	19.6	Br ⁻	10.5	17.6	20.1
Rb ⁺	10.6	17.6	20.6	I ⁻	10.3	17.2	20.0
Cs ⁺	10.6	17.7	20.7	IO ₃ ⁻	5.05	8.79	10.6
NH ₄ ⁺	9.80	16.8	19.8	HS ⁻	9.75	14.8	17.3
Ag ⁺	8.50	14.0	16.6	S ²⁻	----	6.95	----
Tl ⁺	10.6	17.0	20.1	HSO ₄ ⁻	----	----	13.3
Cu(OH) ⁺	----	----	8.30	SO ₄ ²⁻	5.00	8.90	10.7
Zn(OH) ⁺	----	----	8.54	SeO ₄ ²⁻	4.14	8.45	9.46
Be ²⁺	----	3.64	5.85	NO ₂ ⁻	----	15.3	19.1
Mg ²⁺	3.56	5.94	7.05	NO ₃ ⁻	9.78	16.1	19.0
Ca ²⁺	3.73	6.73	7.93	HCO ₃ ⁻	----	----	11.8
Sr ²⁺	3.72	6.70	7.94	CO ₃ ²⁻	4.39	7.80	9.55
Ba ²⁺	4.04	7.13	8.48	H ₂ PO ₄ ⁻	----	7.15	8.46
Ra ²⁺	4.02	7.45	8.89	HPO ₄ ²⁻	----	----	7.34
Mn ²⁺	3.05	5.75	6.88	HP ₄ ³⁻	----	----	6.12
Fe ²⁺	3.41	5.82	7.19	H ₂ AsO ₄ ⁻	----	----	9.05
Co ²⁺	3.41	5.72	6.99	H ₂ SbO ₄ ⁻	----	----	8.25
Ni ²⁺	3.11	5.81	6.79	CrO ₄ ²⁻	5.12	9.36	11.2
Cu ²⁺	3.41	5.88	7.33	MoO ₄ ²⁻	----	----	9.91
Zn ²⁺	3.35	6.13	7.15	WO ₄ ²⁻	4.27	7.67	9.23
Cd ²⁺	3.41	6.03	7.17				
Pb ²⁺	4.56	7.95	9.45				
UO ₂ ²⁺	----	----	4.26				
Sc ³⁺	----	----	5.74				
Y ³⁺	2.60	----	5.50				
La ³⁺	2.76	5.14	6.17				
Yb ³⁺	----	----	5.82				
Cr ³⁺	----	3.90	5.94				
Fe ³⁺	----	5.28	6.07				
Al ³⁺	2.36	3.46	5.59				
Th ⁴⁺	----	1.53	----				

$$\frac{\partial C_A}{\partial t} = D_A \frac{\partial^2 C_A}{\partial x^2} \quad [2.3.2]$$

This equation is actually the continuity equation where the term on the left hand side of equation represents the rate of mass accumulation in an elementary volume, while the term on the right represents the difference between the rate of mass diffusion into and out of that elementary volume. The equation is useful only in integrated form, but the integration is dependent on the sample geometry, and the initial and boundary conditions. Several methods can be used for integration, e.g., separation of variables, numerical integration, or by Laplace transformation, etc.⁽²⁾

Another diffusion process in solids is pore diffusion. Pore diffusion is actually a diffusion process within a fluid phase, i.e., that phase present in the tortuous passages in a porous solid. This is illustrated in Figure 2.3.1. Pore diffusion is slower than diffusion in a bulk fluid. It is, however, a much faster process than solid-state diffusion. Pore diffusion has been shown to be important in many fluid-solid reactions, e.g., solid-catalyzed gaseous reactions, direct gaseous reduction of oxide minerals, leaching of porous minerals, etc.

Figure 2.3.1 Spherical Porous Particle.



The magnified version of inset is on the right which indicates the diffusion of fluid reactant through the pores.

Solid porosity may result from the natural porosity of the rock types, e.g., sandstone; from chemical fracturing, e.g., removal of metal values by leaching thereby leaving behind a porous gangue mineral, or from thermal decomposition, e.g., calcination of limestone, etc.

Fick's first and second laws can be applied to the pore diffusion process. However, the diffusion coefficient has to be modified to account for the blockage of the solid and the tortuosity of the path, as

$$D_{\text{eff}} = D_f \epsilon / \tau \quad [2.3.3]$$

where D_{eff} = effective diffusivity of species A in a porous solid,

D_f = diffusivity of diffusion of A in the fluid phase,

ϵ = porosity of solid,

τ = tortuosity, normally having a value of 2.

Diffusion and Convection in Fluid Phases. Diffusion in liquids or gases is essentially the same process as solid-state diffusion and can be described by Fick's law. Diffusion in fluids is much more rapid than in solids; see Tables 2.3.2 and 2.3.3. Convective transport rather than diffusion is usually a more important transfer process in fluids, i.e., since fluids cannot sustain shear forces, bulk movements of macrogroups of molecules become possible. Therefore, a simple stirrer system can produce sufficient shear forces to promote effective mixing of fluids.

The total flux of material in a direction, x , is therefore, obtained by combining the diffusion and convective processes. Mathematically, this is represented as below:

$$j = -D \frac{\partial C}{\partial x} + U_x C \quad [2.3.4]$$

where U_x is the component of fluid velocity in the x direction.

A practical example of a heterogeneous reaction is a fluid-solid reaction in which the fluid is moving past a solid surface. If we assume zero velocity for the fluid moving at the surface of the solid, then mass transfer from the fluid to the solid surface will be governed by the diffusion process:

$$j_A = -D_A \left. \frac{\partial C_A}{\partial x} \right|_{x=0} \quad [2.3.5]$$

It is rather difficult to measure the concentration gradient at the solid-fluid interface. A "film theory" has been used quite successfully on a

wide variety of situations. This model assumes that near the surface of the solid there exists a slowly moving film through which only diffusion occurs. This film is sometimes referred to as stagnant film or mass transfer boundary layer. Outside the film will be a well-mixed fluid in which concentration gradients are negligible. A schematic diagram is presented to illustrate this model in Figure 2.3.2. It is further assumed that the concentration gradient is constant within the film. The mass transfer from the fluid phase to the solid surface, under the above assumed conditions is

$$-j_A = D_A \frac{C_{A(b)} - C_{A(o)}}{\delta} = k_m (C_{A(b)} - C_{A(o)}) \quad [2.3.6]$$

where

$C_{A(b)}, C_{A(o)}$ = concentration of A in the fluid bulk phase and at the solid-fluid interface, respectively (moles/cm³),

δ = thickness of mass transfer boundary layer (cm),

k_m = mass transfer coefficient = D_A/δ (cm/sec),

$-j_A$ = negative sign represents mass transfer rate from bulk phase to the interface.

The thickness of mass transfer boundary layer will depend on the degree of stirring, i.e., the velocity of the fluid. Stirring reduces the film thickness, resulting in a faster mass transfer. However, the thickness can only be reduced to a minimum value (usually in the order of 1×10^{-3} cm).

Several empirical correlations can be used to estimate the mass transfer coefficients, k_m . Some of these correlations are listed on Table 2.3.4.

TABLE 2.3.4. Correlations for Mass Transfer Coefficient

I. Flow over a flat plate.

- A. $k_{m,loc}$ - local mass transfer coefficient at position x away from the leading edge,

$$\frac{k_{m,loc} x}{D_A} = 0.332 \left(\frac{V_x}{\nu} \right)^{1/2} \left(\frac{\nu}{D_A} \right)^{1/3} \quad [2.3.7]$$

B. $k_{m,ave}$ = average k_m from leading edge to distance L

$$\frac{k_{m,ave} L}{D_A} = 0.664 \left(\frac{VL}{\nu}\right)^{1/2} \left(\frac{\nu}{D_A}\right)^{1/3} \quad [2.3.8]$$

II. Flow over a sphere.

$$\frac{k_{m,d}}{D_A} = 2.0 + 0.60 \left(\frac{dV}{\nu}\right)^{1/2} \left(\frac{\nu}{D_A}\right)^{1/3} \quad [2.3.9]$$

III. Mass transfer to a rotating disc-laminar flow.

$$k_m = 0.62 D_A^{2/3} \nu^{-1/6} \omega^{1/2} \quad [2.3.10]$$

Notation:

k_m = mass transfer coefficient (cm/sec),

x = position at a distance x away from the leading edge, (cm),

D_A = diffusion coefficient (cm²/sec),

V = approaching velocity of the fluid (cm/sec),

ν = kinematic viscosity of the fluid (cm²/sec),

L = position at a distance L away from the leading edge, (cm),

d = diameter of the sphere (cm),

ω = stirrer velocity (rad/sec).

Example 1.

The cementation reaction of copper with zinc metal from a dilute sulfate solution can be written as,



The mass transfer coefficient k_m of Cu^{2+} to the Zn rotating disc at 800 rpm at room temperature can be estimated by Equation 2.3.10.

(Levich Equation) as,

Parameters: Viscosity of aqueous solution = 0.89 cp
 Kinematic viscosity of aqueous solution = 0.0089 cm²/sec
 Diffusivity of Cu²⁺ reported in the literature = 7.3×10^{-6} cm²/sec
 Stirrer velocity =

$$800 \frac{\text{rev}}{\text{min}} \times \frac{1 \text{ min}}{60 \text{ sec}} \times 2\pi \frac{\text{rad}}{\text{rev}} = 83.78 \text{ rad/sec.}$$

therefore,

$$k_m = (0.62)(7.3 \times 10^{-6})^{2/3} (0.0089)^{-1/6} (83.78)^{1/2} \\ = 4.69 \times 10^{-3} \text{ cm/sec.}$$

The mass transfer coefficient for the same system was measured to be 5.79×10^{-3} cm/sec which is in the same order of magnitude to what is estimated.

Electrode reactions are important in several hydrometallurgical processes, e.g., electrowinning, cementation. In these processes diffusion may be the rate limiting step. A general treatment of these processes is inappropriate for this course because of their complexity (see reference 3 if you want to do more reading on this subject). In this course, we will consider only the electrowinning of copper as an example system.

Copper is deposited by the following reactions at the cathode.



Mass transport of Cu²⁺ from the electrolyte to the electrode surface and the discharge reaction of the copper ions must occur. The mass flux from the solution to the solid surface in an electrode process is composed of a diffusion term and a migration term:

$$-j_{\text{Cu}^{2+}} = D_{\text{Cu}^{2+}} \frac{\partial C_{\text{Cu}^{2+}}}{\partial x} - \frac{i}{F} \frac{t_{\text{Cu}^{2+}}}{z_{\text{Cu}^{2+}}} \quad [2.3.13]$$

where

$-j_{\text{Cu}^{2+}}$ = mass flux of Cu²⁺ from electrolyte to electrode (mole Cu²⁺/cm²·sec),

i = current density, + sign for anodic reaction and - sign for cathodic reaction, (amp/cm²),

$z_{\text{Cu}^{2+}}$ = charge number of Cu²⁺, i.e., 2,

F = Faraday constant,

x = distance from the electrode surface into the electrolyte (cm),

$t_{\text{Cu}^{2+}}$ = transport number of Cu^{2+} .

The migration term can normally be neglected in a high concentration field of supporting electrolyte. This assumption can be made for most hydrometallurgical processes. Therefore, equation 2.3.13 can be simplified to,

$$-j_{\text{Cu}^{2+}} = D_{\text{Cu}^{2+}} \frac{C_{\text{Cu}^{2+}}(b) - C_{\text{Cu}^{2+}}(o)}{\delta} \quad [2.3.14]$$

where

$C_{\text{Cu}^{2+}}(b), C_{\text{Cu}^{2+}}(o)$ = concentration of Cu^{2+} in bulk electrolyte and at electrode surface, respectively (moles/cm³),

δ = thickness of mass transfer boundary layer (cm).

The molar flux is related to the current density through the Faraday constant. (3) Equation 2.3.14 therefore becomes:

$$-j_{\text{Cu}^{2+}} = D_{\text{Cu}^{2+}} \frac{C_{\text{Cu}^{2+}}(b) - C_{\text{Cu}^{2+}}(o)}{\delta} = \frac{i_{\text{Cu}^{2+}}}{nF} \quad [2.3.15]$$

where

$\nu_{\text{Cu}^{2+}}$ = stoichiometric coefficient of Cu^{2+} from equation 2.3.12, $\nu_{\text{Cu}^{2+}} = -1$,

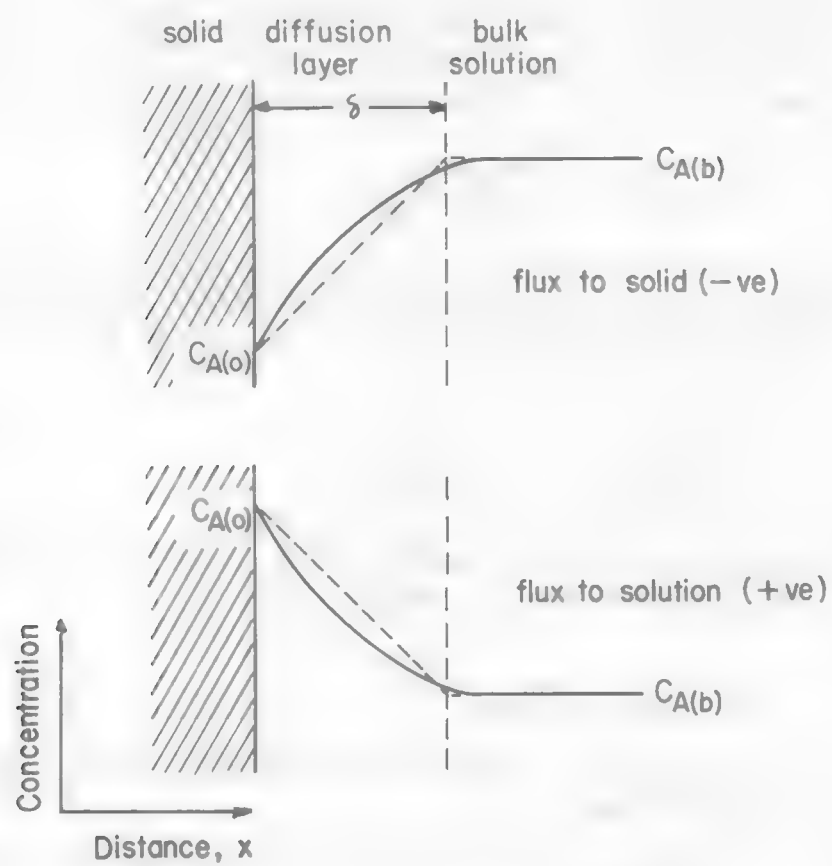
n = number of electrons involved in equation 2.3.12, $n = 2$.

(Note that in equation 2.3.15 the current density must be negative to be consistent with equation 2.3.12, i.e., cathodic reduction of cupric ions to copper metal, [note anodic current density has + sign, cathodic current density has - sign]). Equation 2.3.15 can be rewritten in terms of cathodic current density:

$$-i = \frac{nFD_{\text{Cu}^{2+}}}{\delta} (C_{\text{Cu}^{2+}}(b) - C_{\text{Cu}^{2+}}(o)) \quad [2.3.16]$$

The values of concentration gradient and the surface concentration are determined by the cathodic current density. There is a maximum value for

Figure 2.3.2. Film Model for Mass Transfer.



cathodic current density, $-i_{d,Cu^{2+}}$, at which the cupric ion concentration at electrode surface is completely depleted ($C_{Cu^{2+}(o)} = 0$). This current density is called the limiting diffusion density, i.e., the maximum rate at which a metal ion can be discharged at a cathode (see Figure 2.3.3).

$$-i_{d,Cu^{2+}} = \frac{nFD_{Cu^{2+}}}{\delta} C_{Cu^{2+}(b)} \quad [2.3.17]$$

The reaction will occur no faster than the value determined by this limiting current density, unless another electrode reaction also takes place. By combining Equations 2.3.16 and 2.3.17, we obtain

$$\frac{C_{Cu^{2+}(o)}}{C_{Cu^{2+}(b)}} = 1 - \frac{(-i)}{(-i_{d,Cu^{2+}})} \quad [2.3.18]$$

The potential required to generate the current in the diffusion process is defined as diffusion over voltage

$$\eta_d = E_{(o)} - E_{(b)} \quad [2.3.19]$$

where $E_{(o)}$ = potential in volts at the electrode surface when current flows,

$E_{(b)}$ = potential in volts at the electrode surface when no current flows.

The potential at the electrode surface will depend on the surface concentration, $C_{Cu^{2+}(o)}$, according to Nernst equation. For the copper reaction, $Cu^{2+} + 2e \rightarrow Cu^0$,

$$E_{(o)} = E_o - \frac{RT}{nF} \ln \frac{1}{C_{Cu^{2+}(o)}} \quad [2.3.20]$$

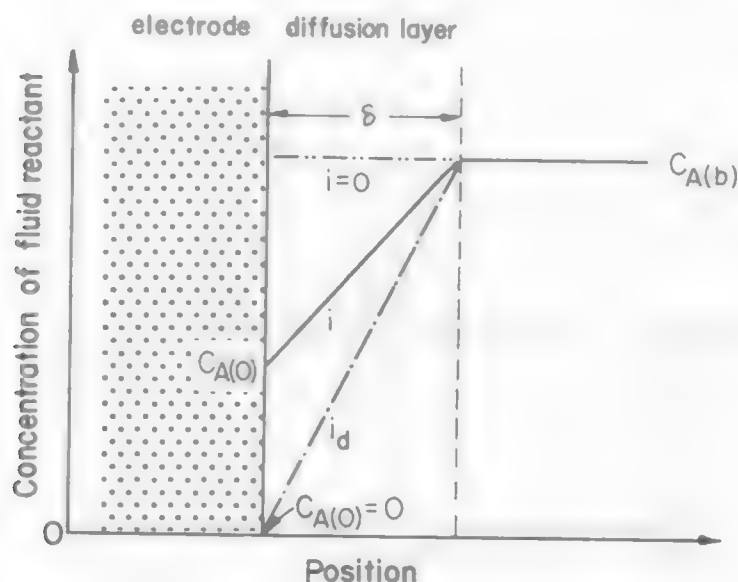
and

$$E_{(b)} = E_o - \frac{RT}{nF} \ln \frac{1}{C_{Cu^{2+}(b)}} \quad [2.3.21]$$

Note that $C_{Cu^{2+}(o)} = C_{Cu^{2+}(b)}$ when there is no current flow. By combining Equations 2.3.20 and 2.3.21, the overvoltage can be written as:

$$\eta_d = \frac{RT}{nF} \ln \frac{C_{Cu^{2+}(o)}}{C_{Cu^{2+}(b)}} \quad [3.2.22]$$

Figure 2.3.3. Concentration Distribution within a Diffusion Layer of Thickness δ (limiting current "dash-dot" line).



If $C_{\text{Cu}^{2+}}(i) < C_{\text{Cu}^{2+}}(b)$, η_d will be negative indicating a cathodic overvoltage. The overvoltage-current relationship can be determined by combining Equations 2.3.18 and 2.3.22,

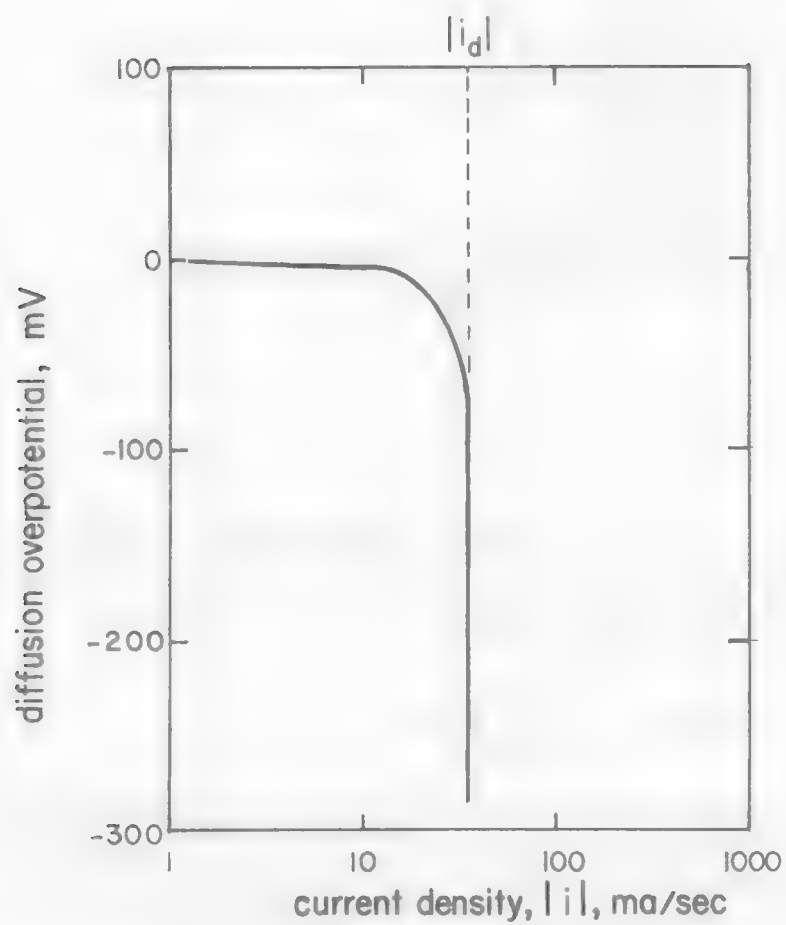
$$\eta_d = \frac{RT}{nF} \ln \left(1 - \frac{(-i)}{(-i_{d,\text{Cu}^{2+}})} \right) \quad [2.3.23]$$

Figure 2.3.4 illustrates a current vs. voltage plot in the cathodic region for a pure diffusion process for the electrode reaction $\text{Cu}^{2+}(\text{aq}) + 2e \rightarrow \text{Cu}^0(\text{s})$. It can be seen clearly that no matter how great an applied voltage, the current (or rate of copper deposition) will not be increased beyond that represented by the limiting current.

Example 2.

Suppose we want to use a conventional electrowinning cell to deposit copper from a solution containing 40 g/l Cu^{2+} with an excess of inert ions. The maximum current density according to Equation 2.3.17 can be calculated as

Figure 2.3.4. Overvoltage-Current Relationship.



(i_d is the limiting current density for Cu^{2+}).

$$i_{d,Cu^{2+}} = - \frac{nFD_{Cu^{2+}}}{\delta} C_{Cu^{2+}}(b) \quad [2.3.17]$$

Parameters:

n = no. of electron involved in Equation 2.3.12 = 2,

F = Faraday constant = 96500 coul/equivalent,

$D_{Cu^{2+}}$ = diffusivity of copper = 7.3×10^{-6} cm²/sec,

$C_{Cu^{2+}}$ = copper concentration in bulk phase = 6.30×10^{-4} mole Cu²⁺/cc,

δ = mass transfer boundary layer thickness = 0.03 cm for a non-agitated conventional electrolytic cell.

Therefore,

$$i_{d,Cu^{2+}} = \text{limiting current density} = -2 \times 96500 \times 7.3 \times 10^{-6} \times 6.30 \times 10^{-4} / 0.03 = -29.6 \text{ mA/cm}^2, \text{ or, } -27.5 \text{ A/sq.ft.}$$

(note: negative sign represents cathodic current density)

In terms of molar flux, according to Equation 2.3.15, we have

$$j = -1.53 \times 10^{-7} \text{ mole Cu}^{2+} \text{ deposited/cm}^2 \cdot \text{sec.}$$

In practice, when the current density is run near the limiting current density, the copper cathode becomes unacceptable rough, powdery, and impure. Also, hydrogen ions are discharged causing a decrease in current efficiency. As a result, in conventional operations, copper is electrowon at current densities ranging from 15 to 25 A/sq.ft. Low current densities usually require large capital investments.

The limiting current for metal ion discharge cannot be increased by increasing the cell potential. However, it can be improved by decreasing the diffusion layer thickness (according to Equation 2.3.17). Several attempts have been made in this direction by agitating or by injecting the inlet fluid in the cell.⁽⁴⁾

2.3.3 Kinetics of Adsorption Reactions

The kinetics of adsorption reactions are unique in heterogeneous reactions. The process applies to the situation when surface blockage occurs due to the adsorption (normally chemisorption) of reactants, products or intermediates on the reaction interface. The rate of adsorption depends on a) the concentration of adsorbate in the bulk phase, b) the activation energy of the adsorption process, and c) the fraction of surface that is occupied. The following relationship applies,

$$r_a = \beta C (1-\theta) \exp (-E_a/RT) \quad [2.3.24]$$

where

C is the concentration of adsorbate,

θ is the fraction of surface site being occupied,

β is a proportionality constant, and

E_a is the activation energy (which depends on the activity of the surface site).

Two postulates have been proposed based on the above equation. If the activity of the surface is uniform, i.e., a constant activation energy; with respect to surface coverage, then the Langmuir equation is valid,

$$r_A = k C (1-\theta) \quad [2.3.25]$$

However, the Langmuir equation does not usually agree with experimental data. Observed rates decrease rapidly with increasing coverage θ . This variation may be caused by surface heterogeneity; that is, the activity of the sites varies, so that different sites possess different values of E_a . The most active sites have the lowest activation energy and would be occupied first. In other words, the activation energy of adsorption varies with the surface coverage. Therefore, E_a in equation 2.3.24 is a function of θ , i.e.,

$$r_A = \beta C (1-\theta) \exp [-E_a(\theta)/RT] \quad [2.3.26]$$

In many cases of chemisorption the variation in the rate with surface coverage is accounted for entirely in the exponential term, i.e., $(1-\theta)$ is a weaker function. This simplification leads to the result (for constant temperature)

$$r_A = \beta C \exp (-\gamma\theta) \quad [2.3.27]$$

commonly known as the Elovich equation. (This equation can be derived from Equation 2.3.24 by assuming E_a is a linear function of θ .)

LEARNING ACTIVITY 4

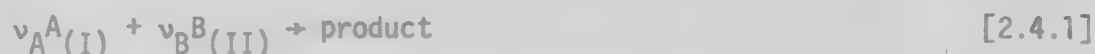
Learning Activity Objective

The material presented as Learning Activity 4 is a continuation of the subject on heterogeneous kinetics. Refer back to Learning Activity 3 for objectives. The topics in this Learning Activity continues the discussion of individual steps in a reaction sequence.

2.3.4 Reaction at the Interface

Mass transport to and from the reaction interface is only part of the overall heterogeneous reaction mechanism. Chemical reaction at the interface is also a necessary part. The process can be simple, e.g., exchanging ions or can also be complicated, e.g., leaching of sulfide minerals. Surface reactions must obey the same principles of homogeneous reactions discussed earlier. The driving force for the reaction is the difference in free energy between the initial and final states. Reactants require sufficient potential energy to overcome the reaction barrier. The rate of the reaction, in moles per unit area per unit time, according to the law of mass action, depends on the reactant concentrations adjacent to the reaction interface.

Assume we have the following heterogeneous reaction occurring between species A in phase I and species B in phase II:



the rate of the irreversible reaction can be written as,

$$-r_A = \beta \exp [-E_a/RT] C_{A(I)}^{n_A} C_{B(II)}^{n_B} \quad [2.4.2]$$

$$\text{or } = k C_{A(I)}^{n_A} C_{B(II)}^{n_B} \quad [2.4.3]$$

where $-r_A$ = rate of disappearance of A; moles/unit area·time

β = frequency factor

E_a = activation energy

k = specific rate constant

$C_{A(I)}$, $C_{B(II)}$ = concentration near the reaction interface of species A in phase I and species B in phase II, respectively.

For a fluid-solid reaction such as,



the rate dependence of the concentration in the solid phase is sometimes lumped into the rate constant,

$$-r_A = k' C_{A(l)}^{n_A} \quad [2.4.4]$$

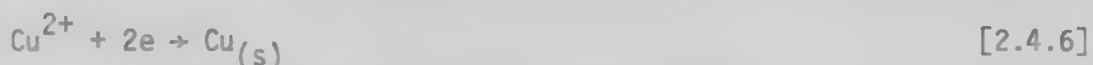
the value of k' contains not only the specific rate constant and necessary conversion factor to keep units consistent but also the concentration of potentially reactive surface sites.⁽⁵⁾ As a result, even with the area of the solid exposed, leaching of a high grade ore should occur at a **faster rate than leaching of a low grade ore.**

2.3.5 Electrode Kinetics⁽³⁾

An electrode process is an electrochemical reaction taking place at an interface of an electrode and an electrolyte. It is often encountered in the hydrometallurgical processes such as leaching, cementation, electro-winning, electrolytic refining, hydrogen reduction, etc. Consider the refining of copper for example. There are two electrode reactions that occur in the electrolytic cell. At the anode surface, copper dissolves in aqueous solution producing cupric ion according to the following reaction,



At the same time, metallic copper is recovered from the solution on the cathode:



A detailed discussion on the kinetics of an electrode reaction can be found in Reference 3, and only a brief summary will be given here.

Consider a simple metal-ion electrode reaction,



The cathodic reaction representing the deposition of metal is the reaction that proceeds to the right. The anodic reaction representing the dissolution of metal proceeds to the left. When there is no net current across the electrode, there exists a dynamic equilibrium between the cathodic current and the anodic current (illustrated in Figure 2.4.1):

$$i_{\text{net}} = i_a + i_c = 0 \quad [2.4.8]$$

$$i_a = |i_c| = i_0 \quad [2.4.9]$$

where i_a , i_c , and i_0 = anodic, cathodic and exchange current density, respectively. The anodic current density and cathodic current density are equal in value but opposite sign. The absolute value of each current density is called the exchange current density (i_0). At equilibrium, the reaction also has an equilibrium potential, E_0 (which is usually represented on the standard hydrogen electrode (SHE) scale). The value of E_0 for a reaction can be calculated directly from thermodynamic data. For instance, the equilibrium potential for $\text{Cu}^{2+}/\text{Cu}^0$ electrode (normal standard state) is 0.34 v (SHE).

When a voltage greater than E_0 is applied to the electrode, the equilibrium will be disturbed. The voltage will enhance the anodic reaction and hinder the cathodic reaction as illustrated in Figure 2.4.1. In Figure 2.4.1 the length of the arrow represents a measure of the magnitude of the current density. The difference between the applied voltage and the equilibrium potential is often called charge transfer overvoltage,

$$\eta = E - E_0 \quad [2.4.10]$$

η = charge transfer overvoltage, +ve for anodic overvoltage, -ve for cathodic overvoltage

E , E_0 = applied and equilibrium potential, respectively.

On the other hand, if the applied voltage is less than the equilibrium potential, i.e., $\eta < 0$, the anodic reaction will be hindered and the cathodic reaction will be accelerated.

From Figure 2.4.1, the rate of an electrode reaction is not only influenced by the activation energy and the reactant concentrations (that usually accounts for an ordinary heterogeneous reaction), but is also dependent on the charge transfer overvoltage. The overvoltage, in terms of potential energy (equals $zF\eta$, where z is the charge of the metal ion, and F is the Faraday constant) will influence the rate of an electrode reaction in an exponential manner as the activation energy does. However, not total but only a fraction of potential energy of $\alpha z\eta F$, will enhance (assume η to be positive) the anodic reaction, and a fraction of potential energy of $(1-\alpha)z\eta F$ will hinder the cathodic reaction. The current densities for cathodic reaction and anodic reaction for Equation 2.4.7 can be represented as:

$$i_a = nFk_a C_{\text{Me}} \exp [\alpha zF\eta/RT] = nFk_a C_{\text{Me}} \exp [\alpha zF(E-E_0)/RT] \quad [2.4.11]$$

$$\text{or } i_c = nFk_a C_{\text{Me}} \exp [\alpha zEF/RT] \quad [2.4.12]$$

and

$$\begin{aligned}
 i_c &= nFk'_c C_{Me}^{z+} \exp [-(1-\alpha)zF\eta/RT] \\
 &= nFk'_c C_{Me}^{z+} \exp [-(1-\alpha)zF(E-E_0)/RT]
 \end{aligned}
 \quad [2.4.13]$$

$$\text{or} \quad = -nFk_c C_{Me} \exp [-(1-\alpha)zFE/RT] \quad [2.4.14]$$

where

α = transfer coefficient, normally between 0.35 and 0.75

n = no. of electron involves in the reaction

k_a, k'_a = rate constants in the anodic reaction

k_c, k'_c = rate constants in the cathodic reaction

C_{Me}, C_{Me}^{z+} = concentration of metal in the electrode and concentration of metal ions in the electrolyte, respectively.

The net current density under a potential of E will be,

$$\begin{aligned}
 i_{net} &= i_a + i_c \\
 &= nF(k_a C_{Me} \exp[\alpha zFE/RT] - k'_c C_{Me}^{z+} \exp[-(1-\alpha)zFE/RT])
 \end{aligned}
 \quad [2.4.15]$$

$$= i_0 (\exp [\alpha zF\eta/RT] - \exp [-(1-\alpha)zF\eta/RT]) \quad [2.4.16]$$

Equation 2.4.15 is known as Bultler-Volmer equation.

For a large anodic overvoltage, i.e., $\eta \gg RT/zF$, the 2nd term of Equation 2.4.16 becomes very small, and the net current density will be solely determined by the anodic current density and anodic overvoltage. As a result, a linear relationship between η and $\log i$ can be found as,

$$\eta = a + b \log i \quad [2.4.17]$$

where

$$a = \frac{-2.303RT}{\alpha zF} \log i_0 \quad [2.4.18]$$

$$b = \frac{2.303RT}{\alpha zF} \quad (\text{anodic Tafel slope}) \quad [2.4.19]$$

And for a large cathodic overvoltage, $\eta \ll -RT/nF$, the first term of Equation 2.4.16 can be neglected, and results in the following equation,

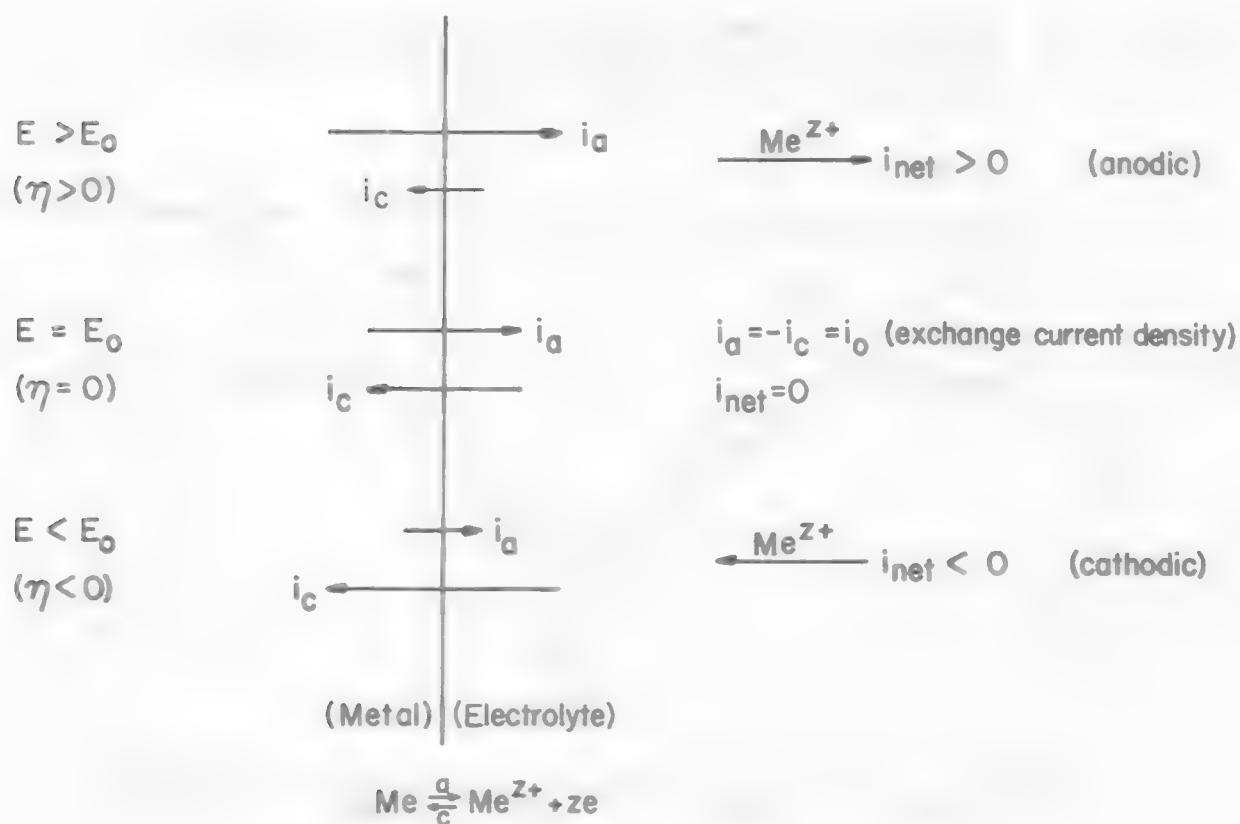
$$\eta = c + d \log i \quad [2.4.20]$$

$$c = \frac{2.303RT}{(1-\alpha)zF} \log i_0 \quad [2.4.21]$$

$$d = \frac{-2.303RT}{(1-\alpha)zF} \quad (\text{cathodic Tafel slope}) \quad [2.4.22]$$

Equations 2.4.17 and 2.4.22 are known as Tafel equations. The straight lines that result from a plot of η vs. $\log i$ are Tafel lines. Extrapolating these two lines to $\eta=0$ yields the current density that is the exchange current density i_0 .

Figure 2.4.1. Charge Transfer Polarization for the Reaction $\text{Me} = \text{Me}^{Z+} + ze$ Under the Condition of Anodic or Cathodic Overvoltage.



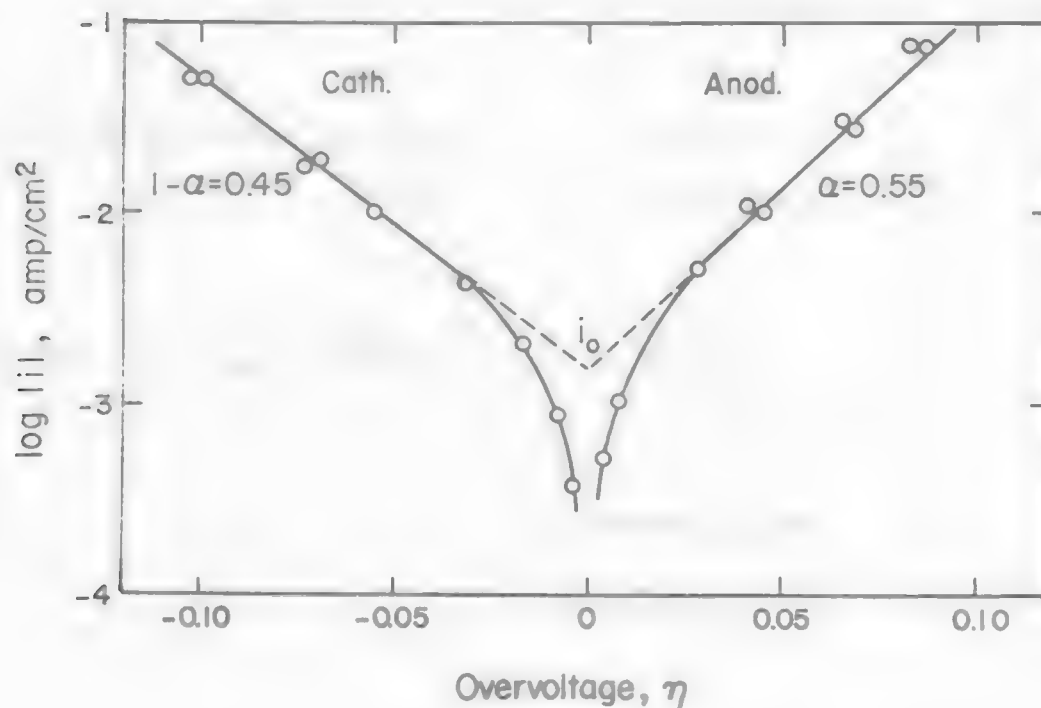
Example 3-3:

W. Lorenz⁽⁶⁾ has studied the charge transfer reaction of a cadmium electrode:



He used the galvanostatic method to determine for the current-dependence of the charge transfer overvoltage. The experiment was designed to measure the overvoltage versus $\log i$ at 20°C. The concentration of cadmium ions in the solution was 0.01 N. The results for both anodic overvoltage and cathodic overvoltage are shown in Figure 2.4.2. A linear Tafel relationship can be found in both regions of high anodic overvoltage and cathodic overvoltage. By extrapolating two Tafel lines to $\eta=0$ leads to the same value of exchange current density of 1.5 ma/cm². The anodic Tafel slope and the cathodic Tafel slope were found to be +0.53 and -0.65 mv/decade, respectively. By substituting these two Tafel slopes into the corresponding equations (Equations 2.4.19 and 2.4.22) yields an α value of 0.55.

Figure 2.4.2. Galvanostatic Measurements of the Charge-Transfer Overvoltage η and Current Density for a Cd Electrode in 0.001 N Cd^{2+} + 0.8 N K_2SO_4 at 20°C.



Gathering all the information, the Butler-Volmer equation for the cadmium deposition and dissolution at 20°C ($C_{Cd^{2+}} = 0.01$ N) can be obtained:

$$i = 1.5 (\exp[0.043\eta] - \exp[-0.043\eta]) \text{ ma/cm}^2 \quad [2.4.24]$$

where overvoltage, η , is in mv unit. This equation allows us to predict the rate of cadmium deposition or dissolution at various overvoltages as long as the reaction is controlled by the charge transfer reaction.

For instance, at 20°C and $C_{Cd^{2+}} = 0.01$, an applied overvoltage to the cadmium electrode of +50 mv will yield a net current density of:

$$\begin{aligned} i &= 1.5 (\exp[0.043 \times 50] - \exp[-0.043 \times 50]) \\ &= 1.5 (8.59 - 0.12) \\ &= 12.88 \text{ ma/cm}^2 \cdot \text{sec.} \end{aligned}$$

The positive sign of current density indicates an anodic current flow. This means that cadmium dissolves. A current density of $12.88 \text{ ma/cm}^2 \cdot \text{sec}$ corresponds to a dissolution rate of 6.67×10^{-8} mole of Cd/sec·cm². See the following calculation:

$$\begin{aligned} j = \frac{i}{nF} &= \frac{2.88 \times 10^{-3} \frac{\text{coul}}{\text{cm}^2 \cdot \text{sec}}}{96500 \times 2 \frac{\text{coul}}{\text{equivalent}} \times \frac{\text{equivalent}}{\text{mole}}} \\ &= 6.67 \times 10^{-8} \text{ mole Cd dissolved/sec} \cdot \text{cm}^2 \end{aligned}$$

If -50 mv of overvoltage is applied to the Cd electrode, the net current density will be:

$$\begin{aligned} i &= 1.5 (\exp[0.043 \times -50] - \exp[0.043 \times 50]) \\ &= -12.88 \text{ ma/cm}^2 \end{aligned}$$

The negative sign on the current density indicates a cathodic current. This means cadmium will be deposited. A current density of $-12.88 \text{ ma/cm}^2 \cdot \text{sec}$ corresponds to a deposition rate of 6.67×10^{-8} mole of Cd/sec·cm².

LEARNING ACTIVITY 5

Learning Activity Objective

The material presented as Learning Activity 5 is a continuation of the subject on heterogeneous kinetics. After you have studied this material you should be able to discuss the overall rate equations that apply to a flat plate geometry.

2.3.6 Rate Equation for Heterogeneous Reaction - Flat Plate Geometry

In previous sections we discussed the rate equation for each of the individual steps that may be encountered in a heterogeneous reaction. However, the overall rate equation for a heterogeneous reaction includes more than one process. If the reaction requires a number of steps that take place in series, then at steady state all these steps should proceed at the same rate, i.e.,

$$r_{\text{overall}} = r_1 = r_2 = \dots = r_n \quad [2.5.1]$$

The rate equation for a reaction step can be regarded as the product of an intensive property and an extensive property. Consider the diffusion process as an example, $r_A = -D \frac{dc}{dx}$, the diffusion coefficient is

intensive which depends only on the nature of the reactant, while the concentration gradient or concentration is extensive and depends on the amount of the material present in the system. The rate equation that has the highest intensive term in it will proceed faster (at the same concentration). However, the rate of a high intensive reaction can be reduced by decreasing the concentration. The strategy of maximizing a heterogeneous reaction is, then, to ration the available reactant concentration to each mechanistic step so that every step will proceed at a same rate. A more detailed discussion will be given in the following example.

Fluid-Solid Reaction without Solid Product-Flat Plate Geometry.

An irreversible reaction,



takes place as shown in Figure 2.5.1(A). Specie A diffuses through a stagnant film onto a plane surface of solid B. There A and B react to yield a fluid product C which diffuses back through the film into the main fluid stream. The diffusion flux of A arriving at the surface is given by,

$$-r_{A(f)} = D_A \frac{C_{A(b)} - C_{A(i)}}{\delta} = k_m (C_{A(b)} - C_{A(i)}) \quad [2.5.3]$$

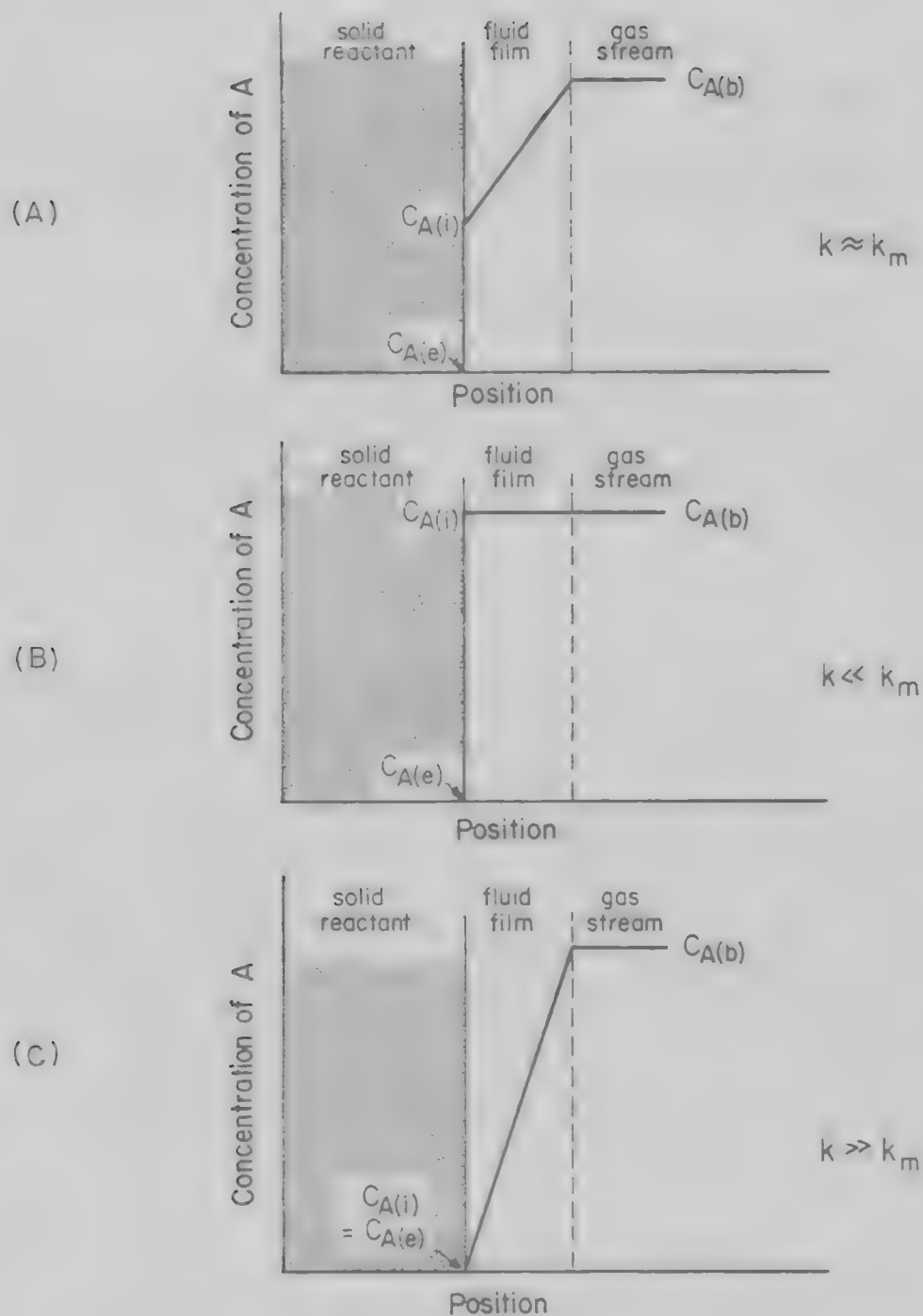


Figure 2.5.1. Schematic diagram of concentration distribution in fluid-solid reactions without the formation of solid product under the following conditions: (A) both chemical reaction and diffusion are controlling $k \approx k_m$, (B) chemical reaction control, i.e., $k \ll k_m$, and (C) diffusion control, i.e., $k \gg k_m$.

And the interfacial reaction is assumed to be first order with respect to A,

$$-r_{A(i)} = kC_{A(i)} \quad [2.5.4]$$

where k is the specific rate constant, and $C_{A(i)}$ is the concentration of A adjacent to the solid surface (which cannot be measured). In this physical picture, the mass transfer step and the chemical reaction step are in series. The rate for each step must be equal at steady state,

$$-r_{A(f)} = -r_{A(i)} \quad [2.5.5]$$

$$\text{or} \quad k_m(C_{A(b)} - C_{A(i)}) = kC_{A(i)} \quad [2.5.6]$$

Solve the equations for surface concentration,

$$C_{A(i)} = \frac{k_m}{k + k_m} C_{A(b)} \quad [2.5.7]$$

Then by placing the surface concentration value in either Equation 2.5.3 or 2.5.4, a general rate equation can be obtained in terms of bulk concentration,

$$-r_{A(\text{overall})} = -r_{A(f)} = -r_{A(i)} = \frac{1}{\frac{1}{k} + \frac{1}{k_m}} C_{A(b)} \quad [2.5.8]$$

Equation 2.5.8 is the mixed kinetic rate expression where the values of the rate constants for each step are included. Very often we find that **one or the other of the two constants will be smaller. In such cases** the slow step is the rate-controlling step and the overall rate will be determined by this step alone. To illustrate the method, assume the above example to be a slow surface reaction process, $k_m \gg k$. Several observations can be made. First, surface concentration can be determined from Equation 2.5.7 to be, $C_{A(i)} \approx C_{A(b)}$. The concentration profile, shown in Figure 2.5.1(B), reveals that almost no concentration gradient exists along the diffusion path. This suggests that the diffusion process is at quasi-equilibrium. Second, the overall rate, according to Equation 2.5.8, $-r_{(\text{overall})} \approx kC_{A(b)}$, is determined solely by the surface reaction, and the concentration that applied to the rate equation is maximum, $C_{A(i)} = C_{A(b)}$.

For a slow diffusion process, $k_m \ll k$. In this case, $C_{A(i)} \approx 0$ and $-r_{(\text{overall})} \approx D_{AB}C_{A(b)}/\delta$. Therefore, the overall rate equation is determined by the diffusion process alone, and the concentration gradient is maximum along the diffusion path, shown also in Figure 2.5.1(C).

It is also of importance to study the rate in terms of the amount of solid material that is reacted. For the above example, assuming the rate is controlled by the slow surface reaction, the rate equation can be written in terms of the moles of fluid A disappearing per unit area per unit time,

$$-r_A = -\frac{1}{S} \frac{dN_A}{dt} = kC_{A(b)} \quad (\text{first order irreversible}) \quad [2.5.9]$$

Also, in terms of the disappearance of solid component B (from stoichiometry) the rate equation can be written,

$$-r_B = -\frac{1}{S} \frac{dN_B}{dt} = \frac{v_B}{v_A} kC_{A(b)} \quad [2.5.10]$$

where N_B is the moles of component B in the solid phase. The value of N_B can be represented by the volume of the solid as,

$$N_B = \frac{Sx}{v} \quad [2.5.11]$$

where S is the area, x is the thickness of the solid (Sx is, therefore, the volume of the solid) and v is the molar volume of solid, i.e., the volume of solid per mole of component B. By differentiating Equation 2.5.11 and then substituting into Equation 2.5.10, we obtain,

$$-\frac{dx}{dt} = \frac{v_B}{v_A} vkC_{A(b)} \quad [2.5.12]$$

This indicates the rate of penetration into solid B is linear kinetics with respect to time if the reaction is controlled by the surface reaction.

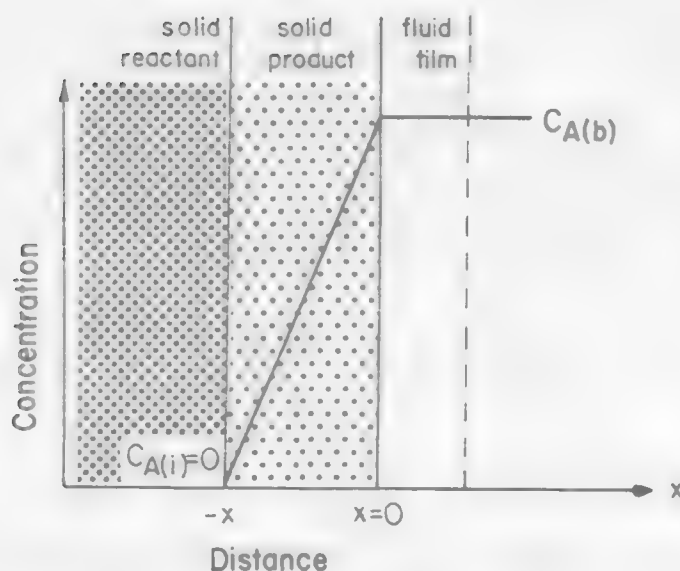
Fluid-Solid Reaction with Solid Product - Flat Plate Geometry.

In the case of an irreversible fluid-solid reaction that produces a solid product, the reaction can be represented by,



As the reaction progresses, a sharp reaction interface advances slowly into the solid leaving behind it a layer of product through which fluid A and C must diffuse. Overall three steps act in series, e.g., film diffusion, product layer diffusion, and interfacial reaction; shown in Figure 2.5.2.

Figure 2.5.2. Schematic diagram of a flat-plate geometry heterogeneous reaction when the diffusion through solid product is the controlling step.



The reaction rate is normally controlled by either chemical reaction or by product layer diffusion. The rate equation for interfacial reaction controlled process is the same regardless whether a solid forms or not,

$$r_{A(i)} = kC_{A(b)}^n \quad (n\text{-th order, irreversible}) \quad [2.5.14]$$

As far as the product layer diffusion control is concerned, the concentration gradient along the solid product should be maximum, shown in Figure 2.5.2. It is also assumed that the reaction product occupies essentially the original volume. Let the original position of the solid-fluid surface be at 0 (see Figure 2.5.2), and the position of the solid product-solid reactant interface (reaction interface) at time t be at position $-x$ (negative sign represents that the interface is actually moving into the bulk solid). The thickness of the product will be equal to x . The rate equation can be formulated as,

$$-r_{A(p)} = \frac{D_{A(\text{eff})}C_{A(b)}}{x} \quad [2.5.15]$$

$$D_{A(\text{eff})} = \text{effective diffusivity of A through the fluid within the porous solid product} = D_{A(f)} \epsilon / \tau$$

x = thickness of the product layer, a function of time.

(Notice that solid state diffusion must be applied to the rate equation if the solid product has no porosity.) Equation 2.5.15 indicates that the rate of a product layer controlled reaction is not constant (as shown in the surface reaction or film diffusion processes), but is rather a function of reaction time, i.e., x changes with t . In order to estimate the instantaneous rate at time t , the corresponding thickness of the product layer has to be determined. This can be determined by the velocity movement of the reaction interface using the same method as previously discussed, i.e., the rate equation for product layer diffusion can be written in terms of the disappearing of solid component B,

$$-r_{B(p)} = -\frac{1}{S} \frac{dN_B}{dt} = -\frac{1}{Sv} \frac{dSx}{dt} = -\frac{1}{v} \frac{dx}{dt} = \frac{D_{A(\text{eff})} C_{A(b)} v_B}{x v_A} \quad [2.5.16]$$

$$\text{or } -\frac{dx^2}{dt} = 2v D_{A(\text{eff})} C_{A(b)} \frac{v_B}{v_A} \quad [2.5.17]$$

The thickness of the product layer, x , can be evaluated by integrating Equation 2.5.17 with the boundary conditions that: $x = 0$ when $t = 0$ and $x = -x$ when $t = t$. The solution is,

$$x = (2v D_{A(\text{eff})} C_{A(b)} \frac{v_B}{v_A} t)^{1/2} \quad [2.5.18]$$

The instantaneous rate equation at time t can then be found by substituting Equation 2.5.18 into 2.5.15,

$$-r_{A(p)} = \left(\frac{D_{A(\text{eff})} C_{A(b)} v_A}{2v t v_B} \right)^{1/2} \quad [2.5.19]$$

The rate decreases as time increases, this is usually called parabolic kinetics and is common for product layer diffusion processes.

In summary, for a flat plate geometry, the reaction rate for a heterogeneous reaction may be controlled by film diffusion, by product layer diffusion or by surface reaction. The surface reaction control can be further divided into surface chemical reaction and charge transfer reaction control. The possible controlling steps and their corresponding rate equations for a flat plate or disc are listed in the following table.

TABLE 2.5.1. Rate Equations for Flat Plate Geometry

Controlling Step	Rate Equation $(-r_A, \text{ moles/area} \cdot \text{time})$	Velocity movement of the reaction interface $-dx/dt$
Product Diffusion	$D_{A(f)} C_{A(b)} / \delta$	$-\frac{dx}{dt} = v_B v D_{A(f)} C_{A(b)} / v_A \delta$
Product Layer Diffusion	$\frac{D_{A(\text{eff})} C_{A(b)} v_A^{1/2}}{(2v v_B t)^{1/2}}$	$-\frac{dx}{dt} = 2v_B v D_{A(\text{eff})} C_{A(b)} / v_A$
Surface Chemical Reaction	$k_A^n C_{A(b)}^n$	$-\frac{dx}{dt} = v_B v k_A^n C_{A(b)}^n / v_A$
Charge Transfer Reaction	$k_a C_{Me} \exp[\alpha z F E / RT]$	
(for $Me \rightarrow Me^{z+} + Ze$)	$-k_c C_{Me}^{z+} \exp[-(1-\alpha) z F E / RT]$	

LEARNING ACTIVITY 6

Learning Activity Objective

The material presented in Learning Activity 6 is a continuation of the subject of heterogeneous kinetics. After you have completed your study of this material you should be able to discuss the overall rate equations that apply to spherical geometry kinetics.

2.3.7 Fluid-Particle Reaction - Spherical Geometry

Fluid-particle reactions are numerous and of great industrial importance. Unlike the flat plate geometry from which the rate of reaction can be considered to be a one dimensional process, a fluid-particle reaction is three dimensional and the reacting area is subjected to change during the reaction. Many particle shapes are possible, such as spheres, cubes, octahedrons, etc., but only the spherical particle will be discussed here.

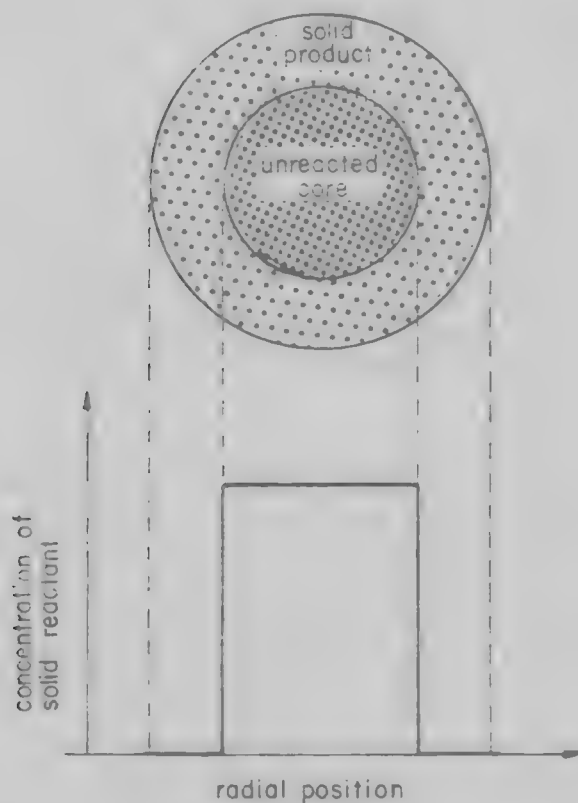
Two simply idealized models have been proposed for the reaction of spherical particles with a surrounding fluid. They are the progressive-conversion model and the shrinking-core model. For particles that have a high porosity and a low reaction rate, the fluid phase enters the particle and reacts throughout the particle as a function of time. Thus, the solid phase is converted continuously and progressively throughout the particle. This is called the progressive-conversion model. The shrinking-core model is used to visualize a reaction of a particle that has only limited porosity, i.e., the particle reaction is primarily at the outer surface of the particle. A sharp reaction interface then moves into the solid. The reaction may leave behind a completely reacted solid material as the product. Thus, reaction occurs only at the solid product-unreacted core interface, and the unreacted core of material shrinks in size during reaction. This is illustrated in Figure 2.6.1. Data from a wide variety of studies shows that, although the unreacted core and reacted product may not always be as sharply defined as the model illustrates, the shrinking core model approximates real systems better in most cases, than does the progressive-conversion model. Therefore, the kinetic equations for the shrinking-core model are developed in the following section.

Fluid-Particle Reaction - Formation of Product Layer. The shrinking-core model assumes that the porous product is generated within the particle as a product layer, and the moving boundary between the product and solid reactant continues towards the center of the particle. The original shape of the particle is maintained in a topochemical manner. Assume a fluid-particle reaction is depicted by the following equation,



One can visualize that five steps occur in succession during the reaction:

Figure 2.6.1. Schematic diagram of shrinking-core model, reaction proceeds at a narrow front which moves into solid particle. Solid reactant is completely converted as the front passes by.



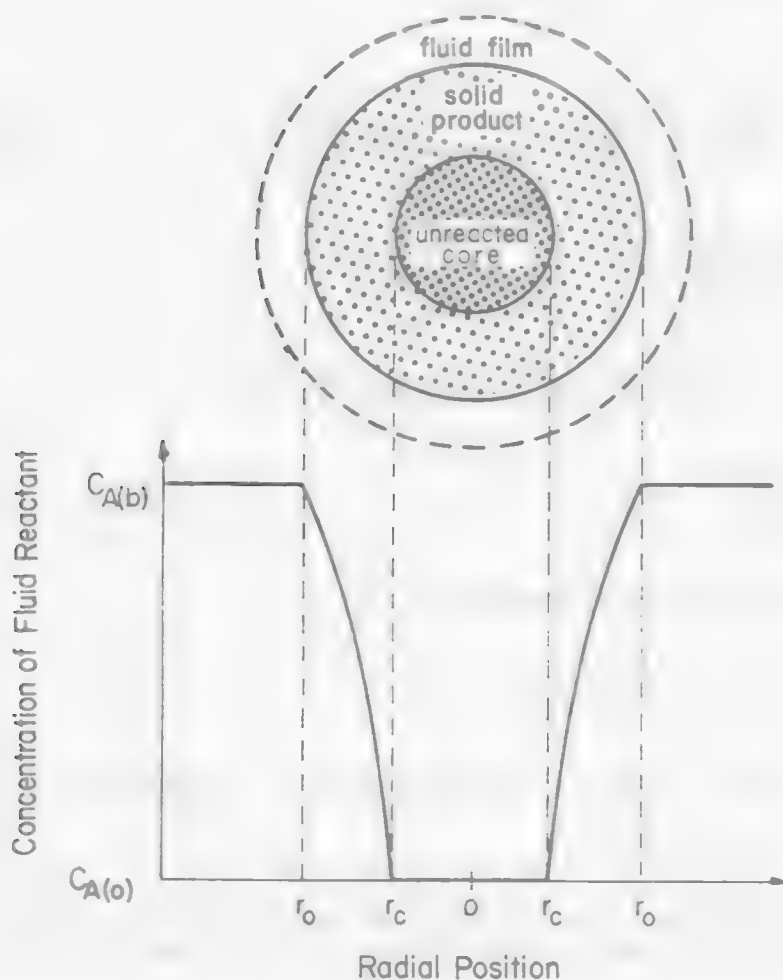
- Step 1, Diffusion of A through the stagnant film to the surface of the particle,
- Step 2, Diffusion of A through the product layer to the unreacted core,
- Step 3, Reaction of A with solid B at this reaction interface,
- Step 4, Diffusion of fluid product C through the product layer to the exterior surface of the solid,
- Step 5, Diffusion of C through stagnant film back to the main fluid stream.

Steps 4 and 5 will not be rate controlling steps if a fluid product is not formed, or if the reaction is irreversible. The reaction is normally controlled by steps 1, 2, or 3. The integrated rate expression for each

controlling step will be given later in this section, but the equation derivation will only be given for product layer diffusion control. However, the same principles and same procedure can be used to derive the rate expressions for other controlling steps.

Diffusion Through Product Layer Control. Figure 2.6.2 illustrates the shrinking-core model in which product layer diffusion controls the rate of the reaction. A maximum concentration gradient can be seen to exist through the product layer. Notice that the concentration gradient is not constant.

Figure 2.6.2. Schematic diagram of a reacting particle follows the shrinking-core model when diffusion through the product layer is the controlling step.



Because the cross section areas are not the same along the diffusion path, the constant molar flux model which applied for rectangular coordinate will not be suitable for spherical coordinate. The constant molar flow (mole/time) model has to be converted to the spherical or cylindrical coordinate system. The molar flow that enters any imaginary spherical area $4\pi r^2$ at any position r within the solid product is,

$$-\frac{dN_A}{dt} = 4\pi r^2 D_{A(\text{eff})} \frac{\partial C_A}{\partial r} \quad [2.6.2]$$

Where area, $4\pi r^2$ is a function of r and the concentration gradient, $\partial C_A / \partial r$, is not constant. The right hand side of Equation 2.6.2 (see Figure 2.6.2) can be integrated for the following boundary conditions,

$$\begin{aligned} C_A &= C_{A(b)} & r &= r_0 \\ C_A &= 0 & r &= r_c \end{aligned}$$

where r_0 and r_c are the radius of the original particle and the unreacted core, respectively. The result of the integration is,

$$-\frac{dN_A}{dt} = \frac{4\pi D_{A(\text{eff})} C_{A(b)}}{\frac{1}{r_c} - \frac{1}{r_0}} \quad [2.6.3]$$

From stoichiometry, the rate of solid component B reacted is,

$$-\frac{dN_B}{dt} = -\frac{v_B}{v_A} \frac{dN_A}{dt} \quad [2.6.4]$$

and the rate of the solid volume reacted is,

$$-\frac{dN_B}{dt} = -\frac{1}{v} \frac{dV}{dt} = \frac{-4\pi r_c^2 dr_c}{v dt} \quad [2.6.5]$$

where v = molar volume = volume of solid per mole of component B,

V = volume of the solid.

By substituting Equations 2.6.5 and 2.6.4 into Equation 2.6.3, a differential equation between time and the radius of the unreacted core results,

$$\left(\frac{r_c^2}{r_0} - r_c\right) dr_c = \frac{v_B}{v_A} v D_{A(\text{eff})} C_{A(b)} dt \quad [2.6.6]$$

This equation can be integrated for the following boundary conditions,

$$r_c = r_o \quad t = 0$$

$$r_c = r_c \quad t = t$$

to give the following results,

$$\frac{r_o^2}{2} \left[1 - \left(\frac{r_c}{r_o} \right)^2 - \frac{2}{3} \left(1 - \left(\frac{r_c}{r_o} \right)^3 \right) \right] = \frac{v_B}{v_A} D_{A(\text{eff})} C_{A(b)} t \quad [2.6.7]$$

By introducing a symbol α as the fraction of solid reacted,

$$\alpha = \left(\frac{4}{3} \pi r_o^3 - \frac{4}{3} \pi r_c^3 \right) / \left(\frac{4}{3} \pi r_o^3 \right) = 1 - \left(\frac{r_c}{r_o} \right)^3 \quad [2.6.8]$$

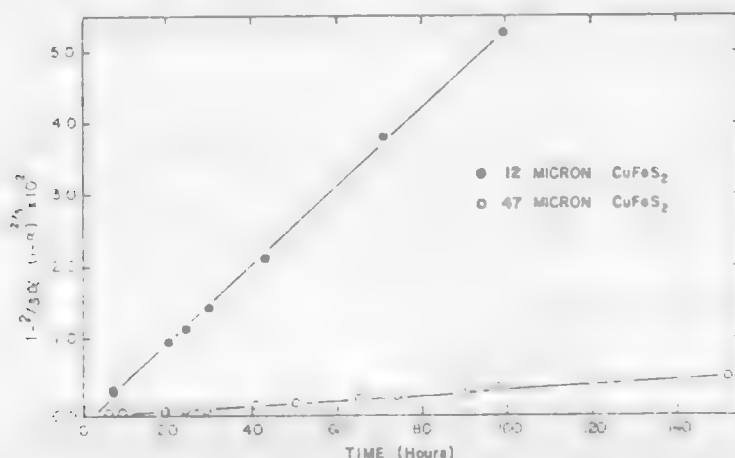
an integrated rate expression in terms of the fraction of solid reacted as a function of time can be found. The resulting equation is,

$$1 - \frac{2}{3} \alpha - (1 - \alpha)^{2/3} = \frac{2 D_{A(\text{eff})} v_B}{r_o^2 v_A} C_{A(b)} t \quad [2.6.9]$$

This equation indicates that for a product layer diffusion controlled process, a plot of $1 - \frac{2}{3} \alpha - (1 - \alpha)^{2/3}$ versus t should yield a straight line

(shown in Figure 2.6.3). The effective diffusivity can be determined from the slope of the plot. Another unique feature for a product layer diffusion controlled reaction is that the modified rate constant k_p , or rate of reaction is sensitive to the particle size, i.e., the rate decreases with an increase in particle size (see Figure 2.6.3).

Figure 2.6.3. A plot of $1 - \frac{2}{3} \alpha - (1 - \alpha)^{2/3}$ for mono-size chalcopyrite particles as a function of time.



The same calculational procedure as above can be used to determine the rate equation for a reaction controlled process. The integrated rate expression in terms of the fraction of solid reacted is shown by the following equation:

$$1-(1-\alpha)^{1/3} = \frac{v_B v k C_{A(b)}^n}{v_A r_o} t \quad [2.6.10]$$

This equation will yield a straight line by plotting $1-(1-\alpha)^{1/3}$ vs. time, and the specific rate constant k can be determined from the slope. The rate equation indicates that the rate is inversely proportional to the particle size.

For film diffusion process, the rate equation can be calculated to be

$$\alpha = \frac{3v_B v k_m C_{A(b)}}{v_A r_o} t \quad [2.6.11]$$

where k_m is the mass transfer coefficient for species A diffusing through a stagnant film.

Fluid-Particle Reaction - Shrinking Spherical Particles. When a fluid-particle reaction does not generate any solid product, the reacting particle shrinks during reaction and finally disappears. The reaction can either be controlled by a film diffusion process or be controlled by a surface reaction. When chemical reaction controls, the behavior is identical to that of particles forming a solid product, i.e., equation 2.6.10. The integrated rate expression for a film diffusion process for a shrinking spherical particle is,

$$1-(1-\alpha)^{2/3} = \frac{2v_B v k_m C_{A(b)}}{v_A r_o^2} t \quad [2.6.12]$$

In summary, for a fluid-particle reaction, the reaction can be controlled by film diffusion, product layer diffusion or chemical reaction. The possible controlling steps and their corresponding rate equation for a spherical particle is listed in the following table. Literature is quoted where experimental systems were studied and found to obey the various model conditions.

TABLE 2.6.2. Rate Equations for Shrinking Core Model

A. Formation of Product Layer: $v_A A(f) + v_B B(s) \rightarrow v_C C(f) + v_D D(s)$

1. Film Diffusion Controls

Equation: $\alpha = \frac{3v_B v k_m C_{A(b)}}{v_A r_o} t$

Table 2.6.2 cont'd.

Example: First stage ferric sulfate leaching of chalcocite to blue-remaining covellite, the rate is controlled by the diffusion of ferric ions to the particle surface (6).

2. Product Layer Controls

$$\text{Equation: } 1 - \frac{2}{3}\alpha - (1-\alpha)^{2/3} = \frac{2v_B v_D A(\text{eff})}{v_A r_0^2} C_{A(b)} t$$

Example: Leaching of chalcopyrite with ferric sulfate, the rate is controlled by the diffusion through elemental sulfur layer (7).

3. Surface Reaction Controls

$$\text{Equation: } 1 - (1-\alpha)^{1/3} = \frac{v_B v k}{v_A r_0} C_{A(b)} t$$

Example: Leaching of chalcopyrite with ferric chloride, the rate is controlled by the surface reaction (8).

4. Mixed Kinetic Controls (surface reaction and product layer diffusion)(9)

$$\text{Equation: } \frac{r_0^2}{2D_{A(\text{eff})}} \left(1 - \frac{2}{3}\alpha - (1-\alpha)^{2/3}\right) + \frac{r_0}{k} (1 - (1-\alpha)^{1/3}) = \frac{v_B v}{v_A} C_{A(b)} t$$

Example: Leaching of chrysocolla with sulfuric acid (10).

B. Shrinking Particle $v_A A(f) + v_B B(s) \rightarrow v_C C(f)$

1. Film Diffusion Controls

$$\text{Equation: } 1 - (1-\alpha)^{2/3} = \frac{2v_B v k_m}{v_A r_0} C_{A(b)} t$$

Example: Leaching of copper shperes with cupric chloride when concentration of cupric chloride is less than 0.02 M (11).

2. Product Layer Diffusion: Not applicable.

Table 2.6.2 cont'd.

3. Surface Reaction Controls

$$\text{Equation: } 1-(1-\alpha)^{1/3} = \frac{v_B v_k}{v_A r_o} C_{A(b)}^n t$$

Example: Chlorination of rutile (12).

Limitations of Shrinking Core Model. The assumption of the shrinking core model is not always precisely applicable. For example, a reaction may occur along a diffusion front rather than along a sharp interface between the product and reactant. A reaction zone model has been proposed by assuming the reaction is taking place within a zone rather than an interface.

Also, the rate equations are derived based on a single particle. Although these equations can be applied directly to a system that has a single particle size, they are not directly applicable to a system that contains a distribution of particle sizes.

2.3.8 Suggested Reading

O. Levinspel, Chemical Reaction Engineering, John Wiley, New York, 2nd ed., Chap. 14, 460 (1972).

M. E. Wadsworth, "Rate Process in Hydrometallurgy," 2nd Tutorial Symposium on Extractive Metallurgy, Denver, Colorado, 1972.

LEARNING ACTIVITY 7

2.4 Rate Phenomenon in Hydrometallurgical ProcessesLearning Activity Objective

After completing this learning activity you should be able to interpret some simple kinetic data and to determine the rate limiting steps that occur in some hydrometallurgical processes.

The previous learning activities provide us with some useful tools to interpret or predict simple kinetics in a heterogeneous reaction system. Examples on hydrometallurgical processes will be discussed in this section. Experimental data are taken directly from the results of a hydrometallurgy laboratory class conducted at the University of Utah under the supervision of Professor M. E. Wadsworth. Acknowledgement is made to both graduate and undergraduate students who participated in the class. Although the laboratory program consisted of 1) leaching of metals, 2) leaching of oxides, 3) leaching of sulfides, 4) cyanidation, and 5) solvent extraction, only the first two topics will be presented in this section.

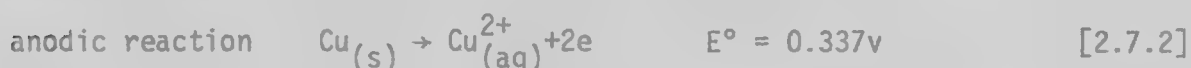
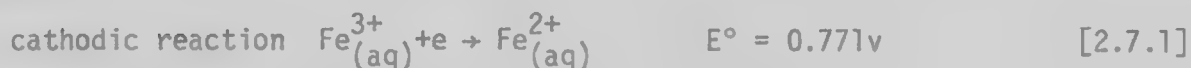
2.4.1 Dissolution of Metal by Spinning Disc Technique

Leaching of metallic copper with a ferric ion reagent was studied in the laboratory by using the spinning disc technique. The technique has been widely used for electrode kinetic studies. The experimental system is well defined with respect to the hydrodynamic behavior and uniform mass transfer boundary layer. The mass transfer coefficient for spinning disc experiments can be calculated from the equation listed in the previous section in Table 2.6.2.

Background. The reaction steps for the dissolution of copper with ferric ions can be visualized as,

1. Diffusion of ferric ions across the stagnant film to the surface of the copper metal, and
2. Charge transfer reactions on the surface of the metal.

These are:



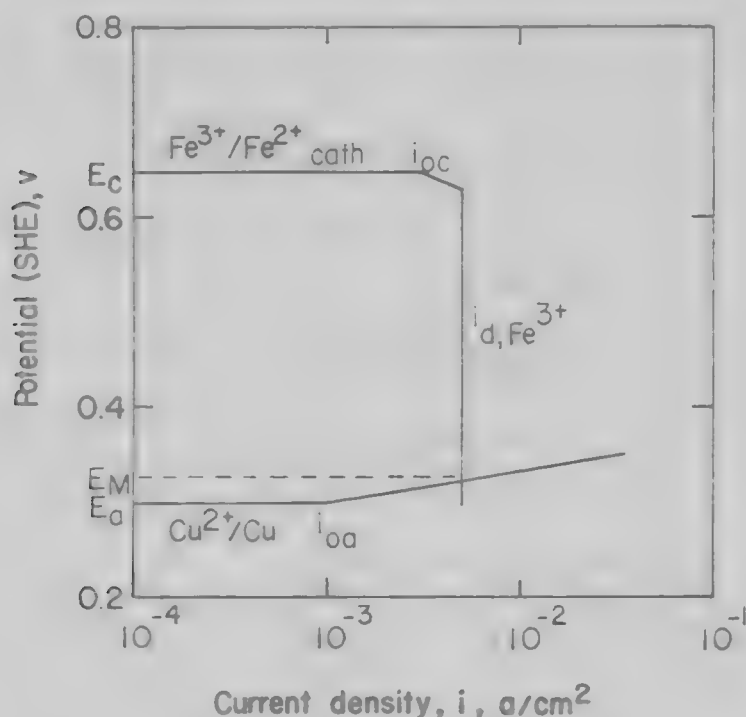
The overall reaction has a standard free energy of reaction of approximately -17 kcal/mole, so that the reaction can be assumed to be irreversible.

Electrode kinetic studies of the reaction $\text{Fe}^{3+} + e \rightarrow \text{Fe}^{2+}$ in a sulfuric acid system has been extensive. In a condition where $C_{\text{Fe}^{3+}} = 8.7 \times 10^{-3} \text{ M}$, and $C_{\text{Fe}^{2+}} = 1.0 \times 10^{-2} \text{ M}$, the equilibrium half cell potential, E_0 , was found to be 0.646 volts on the SHE scale; exchange current density, i_0 , to be 3.2 ma/cm^2 ; and the transfer coefficient, α , to be 0.52. The cathodic limiting current density, $-i_{d,\text{Fe}^{3+}}$, is therefore estimated to be 5.0 ma/cm^2 (the mass transfer boundary layer is assumed to be $1 \times 10^{-3} \text{ cm}$). The Butler-Volmer equation that includes charge transfer and diffusion for the cathodic reaction can be written as,

$$i = -i_0 \left(1 - \frac{i}{i_{d,\text{Fe}^{3+}}} \right) \exp[-(1-\alpha)F(E-E_0)/RT] \quad [2.7.4]$$

The relationship between the cathodic current density and cell potential, E , can be found by substituting numerical values into Equation 2.7.4. The result is presented graphically in Figure 2.7.1. The reaction is controlled by charge transfer at low overvoltage, and controlled by diffusion at high overvoltage.

Figure 2.7.1. Polarization curves for $\text{Fe}^{3+}/\text{Fe}^{2+}$ and $\text{Cu}^{2+}/\text{Cu}^0$ couples. E_M represents the mixed potential when these two couples are connected together.



The charge transfer reaction for $\text{Cu}^0 \rightarrow \text{Cu}^{2+} + 2e$ in a sulfuric acid system has also been studied. For a system where $C_{\text{Cu}^{2+}} = 0.1 \text{ M}$, the equilibrium half cell potential was found to be 0.28 volts (SHE); the exchange current density to be 1 ma/cm^2 ; Tafel slope to be 0.030 volt per decade; and no anodic diffusion limiting current density. The Butler-Volmer equation can be written as,

$$i = i_0 \left(\exp(2F(E-E_0)/RT) - \left(1 - \frac{i}{i_{d,\text{Cu}^{2+}}}\right) \exp(-2F(E-E_0)/RT) \right) \quad [2.7.5]$$

A plot of $\log i$ vs. E is shown in Figure 2.7.1.

When these two half cells occur together, the original equilibrium potentials for each reaction will be disturbed, a new mixed-potential, E_M , between the two equilibrium potentials is established (see Figure 2.7.1). That is, the cathodic current must be equal to the anodic current. The two current densities are equal if the cathodic area is equal to the anodic area. By examining Figure 2.7.1, the mixed-potential is close to the equilibrium potential of Cu/Cu^{2+} half cell potential. This suggests that the anodic reaction is probably at quasi-equilibrium, and the overall rate should be controlled by the cathodic reaction which can be charge transfer or diffusion. Figure 2.7.1 also shows that a large overvoltage exists for the cathodic reaction, which suggests the reaction is probably controlled by the diffusion of ferric ions.

Experiment and Results. The experimental system consisted of a reaction vessel with 750 cc of solution containing 0.1 to 0.5 ml of Fe^{3+} ions, and a copper spinning disc with a diameter of 1.75". The temperature of the reactor was controlled by a temperature controlled oil bath. The spinning disc velocity was 600 rpm, pH=2, and temperature 30°C . The concentration of ferric ion at reaction time, t , was back calculated by measuring the copper concentration in the solution.

If the reaction is indeed controlled by diffusion, the rate equation can be written as,

$$-\frac{1}{S} \frac{dN_{\text{Fe}^{3+}}}{dt} = -\frac{V}{S} \frac{dC_{\text{Fe}^{3+}}}{dt} = k_m C_{\text{Fe}^{3+}} \quad [2.7.6]$$

where V, S = volume of solution and area of the disc, respectively,

k_m = mass transfer coefficient = $D_{\text{Fe}^{3+}}/\delta$,

δ = thickness of mass transfer boundary layer.

The integrated rate equation is a first order reaction,

$$\ln \frac{C_{\text{Fe}^{3+}}^0}{C_{\text{Fe}^{3+}}} = \frac{S}{V} k_m t \quad [2.7.7]$$

where $C_{Fe^{3+}}^0, C_{Fe^{3+}}^t$ = ferric ion concentration at time zero and time t , respectively.

The experimental results justified the above analysis as shown in Figure 2.7.2 for several ferric ion concentrations. The mass transfer coefficient can be calculated to be an average of 4.65×10^{-3} cm/sec. The diffusion coefficient, D , of ferric ion can then be calculated from the Levich Equation,

$$k_m = 0.62 D^{2/3} \nu^{-1/6} \omega^{1/2} \quad [2.7.8]$$

The diffusion coefficient was found to have an average of 9.2×10^{-6} cm²/sec which is comparable to the value reported in the literature of 6.5×10^{-6} cm²/sec at 25°C. The proposed diffusion control step is also supported by the low activation energy of about 3 kcal/mole shown in Figure 2.7.3, a plot of $\ln k_m$ vs. $1/T$. The Levich Equation, Equation 2.7.8, was also tested by varying the spinning velocity. A linear relationship should be found between mass transfer coefficient and the square root of spinning velocity. This relationship should not be found if a surface reaction controls the process. Results justify the Levich equation, shown in Figure 2.7.4.

Figure 2.7.2. First order reaction plot for several ferric ion concentrations (ferric sulfate leaching of metallic copper).

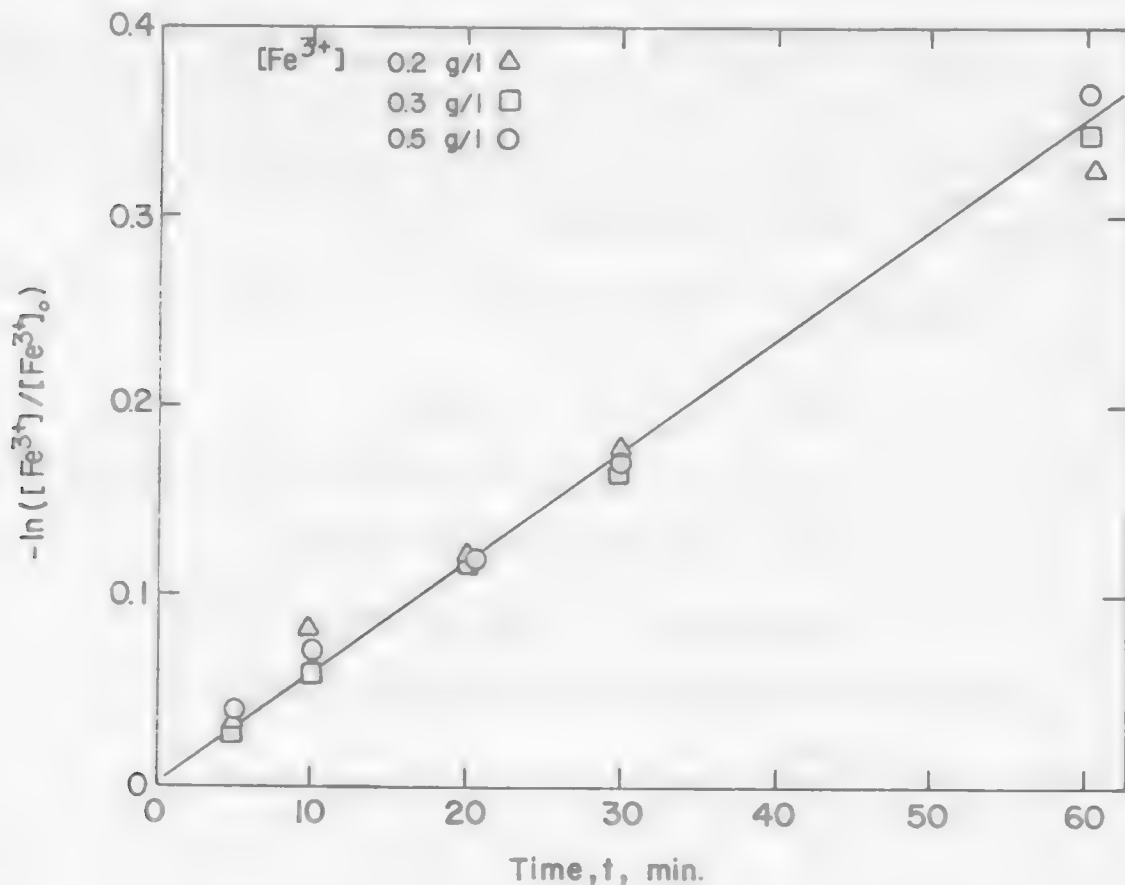


Figure 2.7.3. Arrhenius plot for the dissolution of metallic copper in the presence of ferric ions.

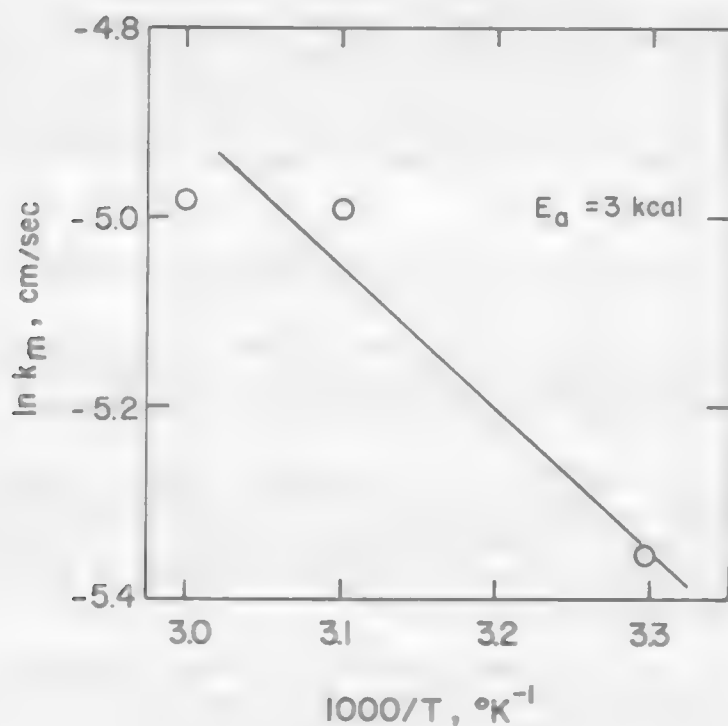
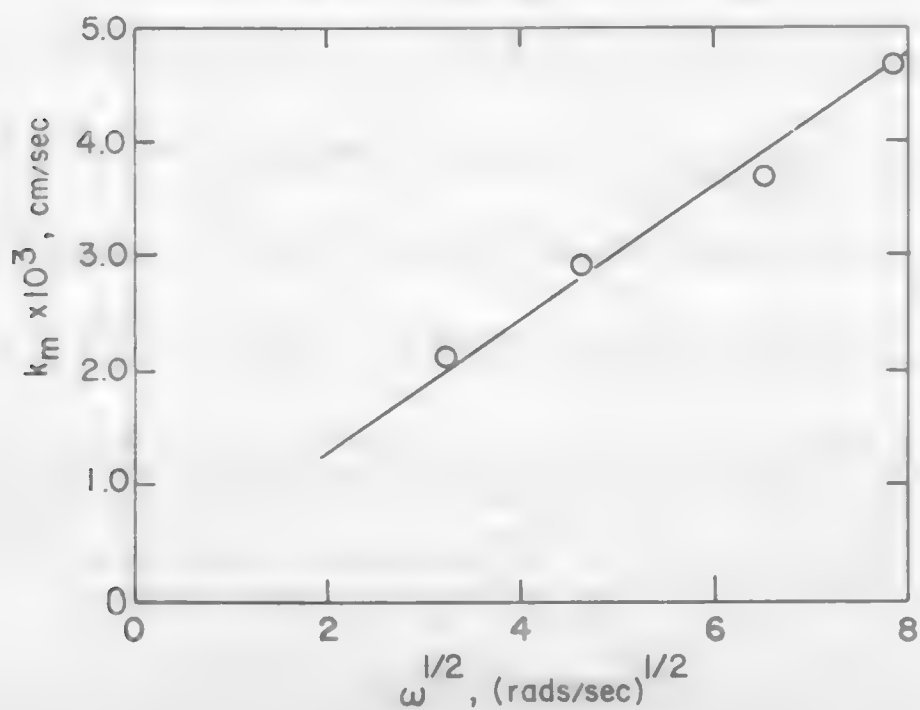
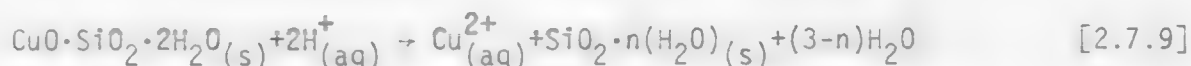


Figure 2.7.4. Test of the Levich equation in which mass transfer coefficient is a linear function of the spinning velocity to the one half power.



2.4.2 Dissolution of Oxides - Leaching of Copper Silicate

Oxide minerals of copper which are often encountered in copper dump leaching are malachite, $\text{CaCO}_3 \cdot \text{Cu}(\text{OH})_2$; azurite, $2\text{CuCO}_3 \cdot \text{Cu}(\text{OH})_2$, and chrysocolla, $\text{CuO} \cdot \text{SiO}_2 \cdot 2\text{H}_2\text{O}$. These minerals are readily leached with acid. Chrysocolla is a hydrated silicate with CuO associated in the lattice. When leached with sulfuric acid, copper oxide will be dissolved and a silicate will be left behind as a porous solid product. The reaction can be written as,



Microprobe analysis on the partially leached particle indicates a product layer of silicate surrounding an unreacted core. The shrinking core model may be applied to interpret the kinetic data for this system.

The experiment was carried out by leaching 1 gram of monosized chrysocolla in a batch reactor containing 750 cc solution (0.03 to 0.10 N of sulfuric acid) using a stirring speed of 500 rpm. The concentration of hydrogen was much greater than is required to dissolve the copper, so that C_{H^+} can be considered to be constant.

The kinetic results for leaching the 100 x 150 mesh monosize material at various acid concentrations are shown in Figure 2.7.5, a plot of fraction of solid reacted versus reaction time. A product layer diffusion controlled model was tested graphically using the equation,

$$1 - \frac{2}{3} \alpha - (1 - \alpha)^{2/3} = \frac{2v D_{\text{H}^+}(\text{eff}) C_{\text{H}^+}(\text{b})}{r_0^2} \frac{v_{\text{Cu}}}{v_{\text{H}^+}} t \quad [2.7.10]$$

where α = fraction of solid reacted,

$$v = \text{molar volume} = \frac{\text{m.w.}}{\text{wt.}\% \text{ B} \times \rho_{\text{solid}}} = 68.2 \text{ cm}^3 \text{ solid/mole of Cu,}$$

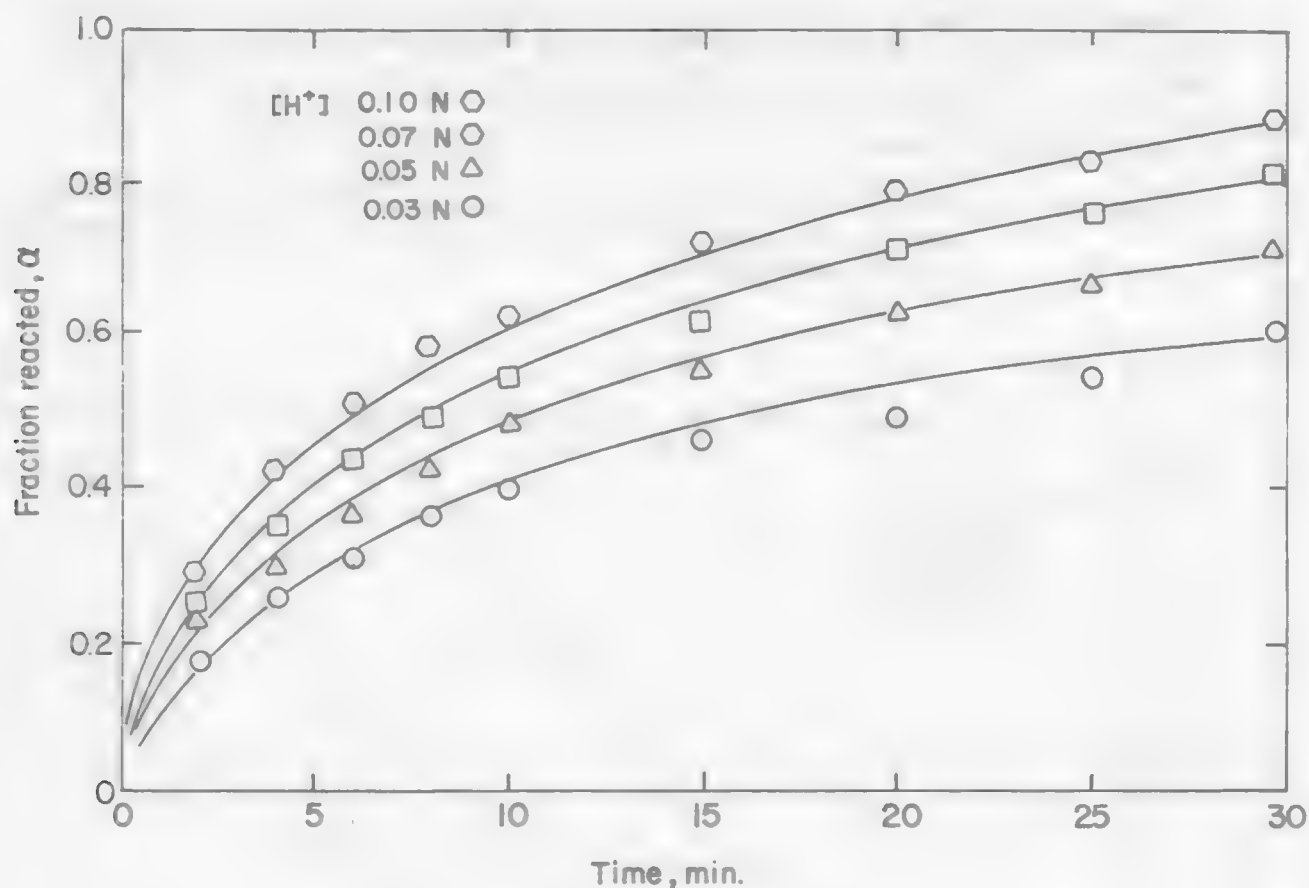
$D_{\text{H}^+}(\text{eff})$ = effective diffusivity of H^+ through the water in porous solid product,

$v_{\text{Cu}}, v_{\text{H}^+}$ = stoichiometric coefficient of CuO and H^+ , respectively,

r_0^2 = original solid particle size = 0.0065 cm for 100 x 150 mesh materials.

Results are shown in Figure 2.7.6. The linear relationship for different hydrogen ion concentrations indicates that the product layer diffusion control mechanism is valid. From the slopes, the effective diffusivity of the hydrogen ion can be estimated, i.e., $6.52 + 0.27 \times 10^{-7} \text{ cm}^2/\text{sec}$. The activation energy for this diffusion controlled process was about 3.3 kcal/mole. This was determined from the plot shown in Figure 2.7.7.

Figure 2.7.5. Fraction of copper in chrysocolla reacted versus time.



However, the initial kinetics cannot be controlled by the product layer. It must be controlled either by diffusion through stagnant film or by surface reaction. For a highly agitated solution, surface reaction is probably the initial rate limiting step. The differential rate equation for a surface reaction control system can be obtained from Equation 2.7.11,

$$\left. \frac{d\alpha}{dt} \right|_{t \rightarrow 0, \alpha \rightarrow 0} = \frac{3k v_B}{r_0 v_A} C_{H^+}^n \quad [2.7.11]$$

where k = surface reaction constant.

By taking the initial slope from the rate curves, it is possible to determine the reaction order and rate constant for this initial stage. First, the reaction order was determined from the equation,

$$\ln \left. \frac{d\alpha}{dt} \right|_{t \rightarrow 0} = \ln \frac{3k v_B}{r_0 v_A} + \ln C_{H^+}^n \quad [2.7.12]$$

By plotting $\ln \frac{d\alpha}{dt} \big|_{t \rightarrow 0}$ vs. $\ln C_{H^+}(b)$ (shown in Figure 2.7.8). The slope of 1 shows the kinetics to be first order. The specific rate constant for various hydrogen ion concentrations can be determined from Equation and have an average value of $4.45 \pm 0.17 (\times 10^{-3})$ cm/sec. The activation energy was estimated to be 6.6 kcal/mole shown in Figure 2.7.9. This high activation energy supports the surface reaction proposal.

Figure 2.7.6. Test of the shrinking-core model for product layer diffusion control for the leaching of chrysocolla at various hydrogen ion concentrations.

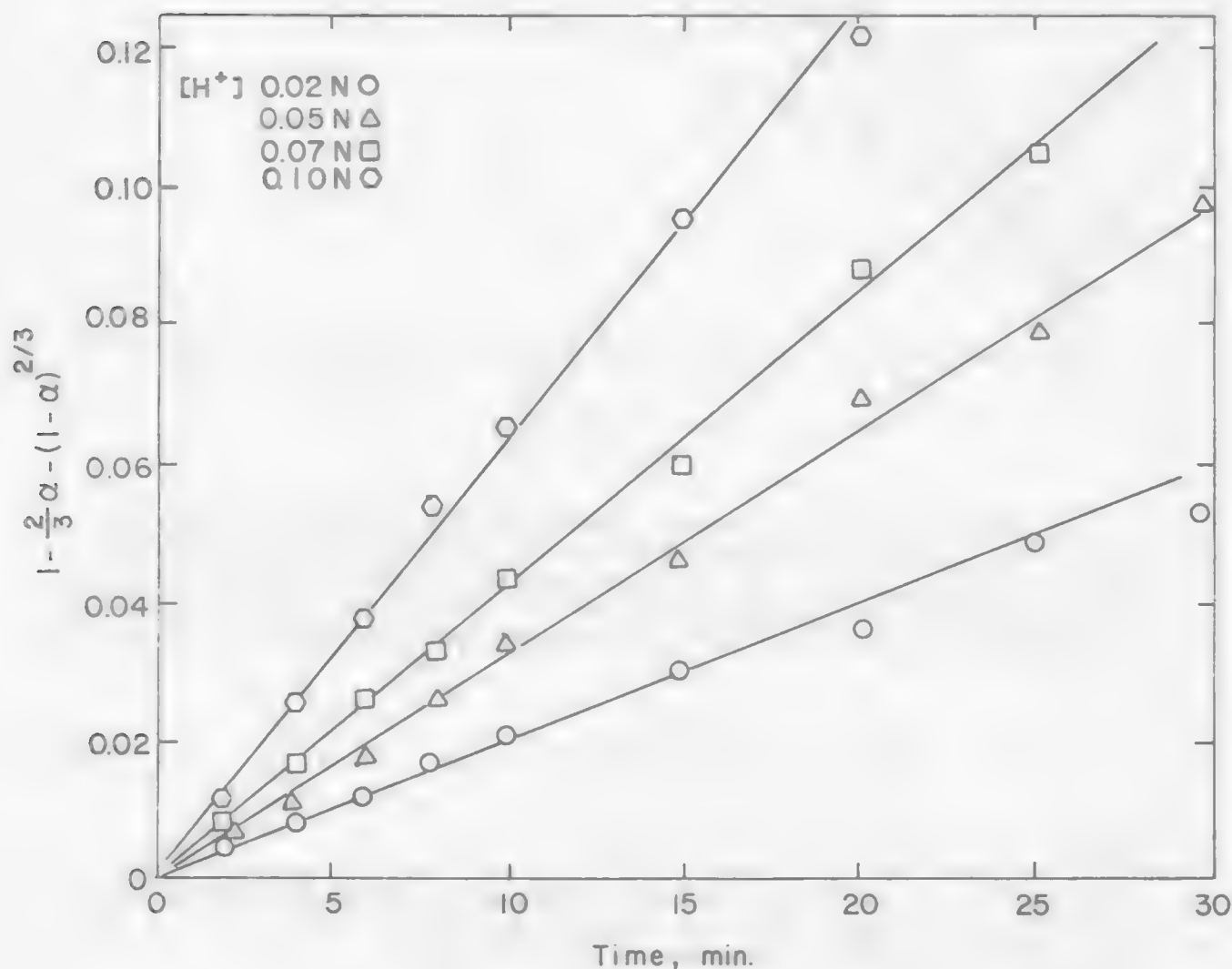


Figure 2.7.7. Arrhenius plot for the diffusion controlled reaction chrysocolla leaching with hydrogen ions.

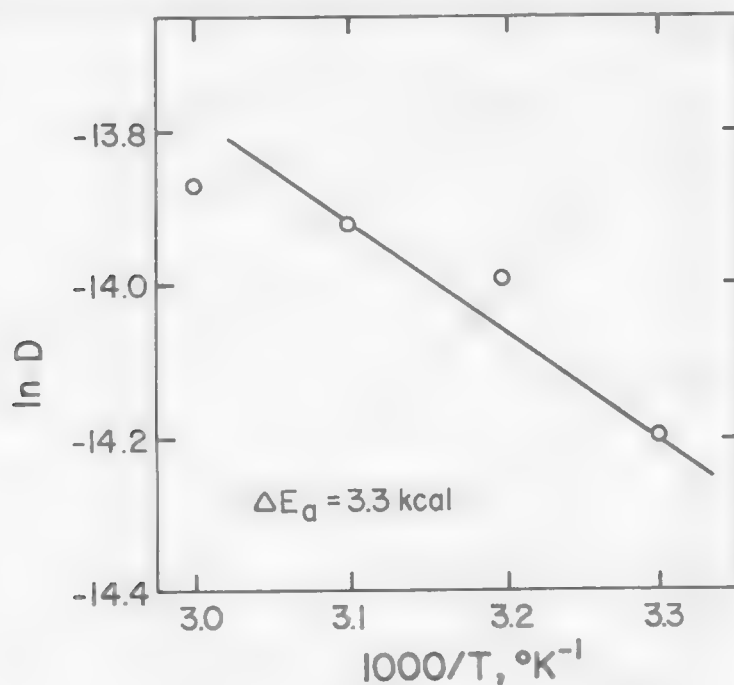


Figure 2.7.8. Determination of reaction order with respect to hydrogen ion concentration from the initial rate of reaction (the shape of 1 indicates the first order reaction).

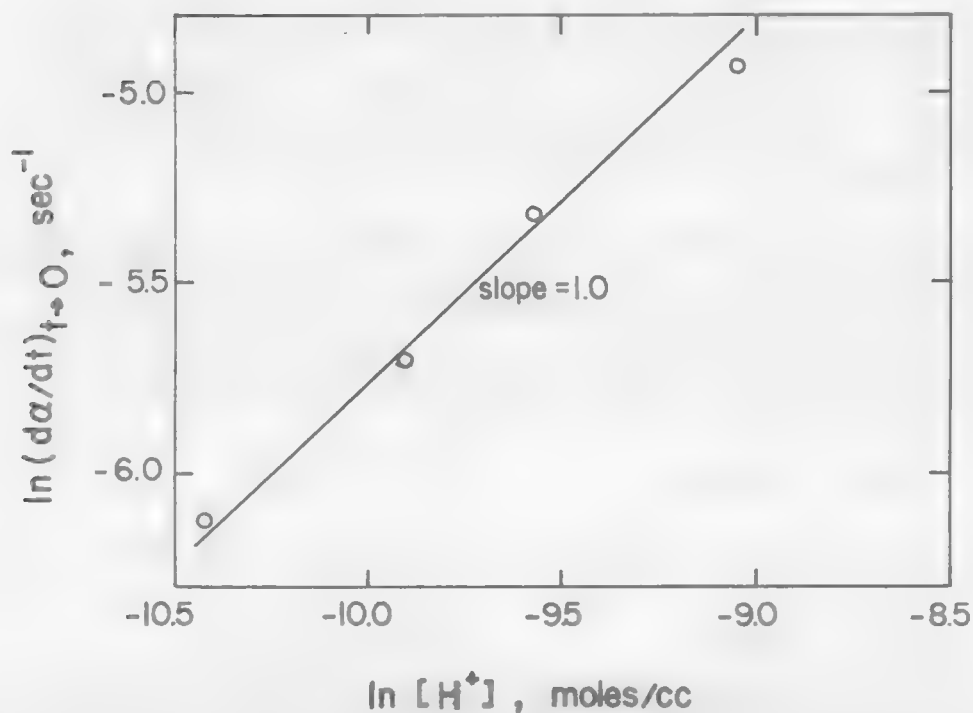
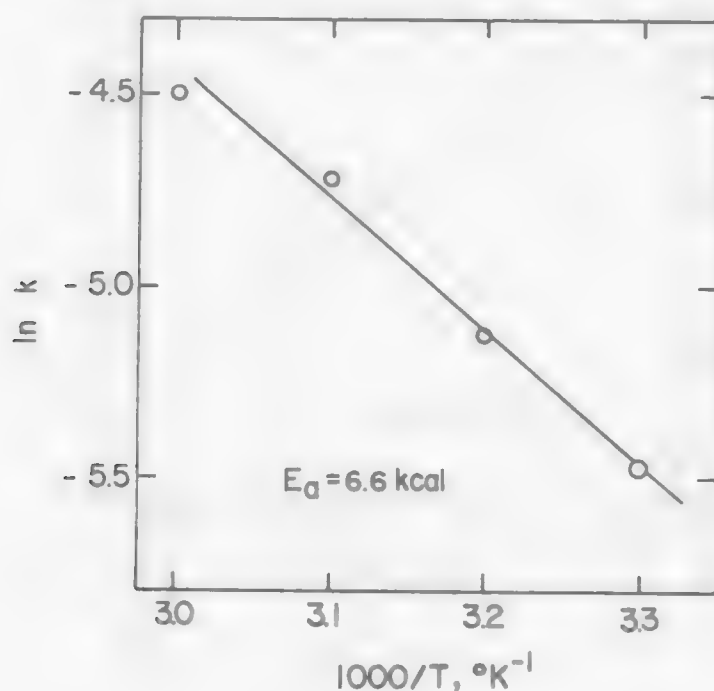


Figure 2.7.9. The Arrhenius plot of the initial rate of chrysocolla leaching.



Additional experiments were also carried out using a larger size material, i.e., 65 x 100 mesh. Results indicate the same controlling step, i.e., product layer diffusion. The effective diffusivity was found to be $5.85 \pm 0.6 (\times 10^{-7}) \text{ cm}^2/\text{sec}$; activation energy for the product layer diffusion to be 3.0 kcal/mole. From initial kinetics, the specific rate constant was found to be $3.44 \pm 0.16 (\times 10^{-3}) \text{ cm/sec}$ with activation energy of 5.75 kcal/mole. These numerical results are in close agreement with those found from the experiment using 100 x 150 mesh material.

It is of interest to compare the rate of individual steps that occur in the leaching of chrysocolla. If we assume the thickness of the stagnant film to be $2 \times 10^{-3} \text{ cm}$, and the diffusivity of hydrogen ion to be $9.3 \times 10^{-5} \text{ cm}^2/\text{sec}$, the mass transfer coefficient, k_m , for film diffusion can be calculated to be about $4.65 \times 10^{-2} \text{ cm/sec}$. This value is large compared to experimental values of product layer diffusion and surface reaction, i.e.,

$k_m = 4.65 \times 10^{-2} \text{ cm/sec}$	film diffusion
$D_{H^+}(\text{eff}) = 6.58 \times 10^{-7} \text{ cm}^2/\text{sec}$	product layer diffusion
$k = 4.45 \times 10^{-3} \text{ cm/sec}$	surface reaction

Film diffusion has the highest value which eliminates that step as a possible rate limiting step. A rough comparison between product layer diffusion and surface reaction can be made by assuming the thickness of the product layer at the early leaching stage to be a flat slab. In such a case, the specific rate constant, k , can be compared directly with the effective diffusivity in the form, $D_{H^+}(eff)/\Delta x$, where Δx is the thickness of the product layer. By substituting numerical values for k and $D_{H^+}(eff)$ in the rate expression (Equations 2.5.9 and 2.5.14 where flat plate geometry is assumed), the rate of product layer diffusion will be equal to the rate of surface reaction at a thickness of 1.5×10^{-4} cm. At the initial stage of leaching, $\Delta x < 1.5 \times 10^{-4}$ cm, the rate should be controlled by surface reaction. The reaction will be controlled by diffusion when $\Delta x > 1.5 \times 10^{-4}$ cm. In this experiment the average particle size was about 7.3×10^{-3} cm in radius, a thickness of 1.5×10^{-4} cm of product represented only about 6% of solid. We can probably state that the reaction is predominantly controlled by the diffusion through the product layer without introducing a large error. A mixed kinetic model that includes product layer and surface reaction reported in the literature can be used for more precise analysis.

2.5 References

1. J. Crank, The Mathematics of Diffusion, Clarendon Press, Oxford, 2nd ed. (1975).
2. K. J. Vetter, Electrochemical Kinetics: Theoretical and Experimental Aspects, English Translation, Academic Press (1967).
3. W. W. Harvey and L. Hsueh, "Copper Electrowinning from Vat Leach Electrolyte," CIM Bulletin, April, 109 (1976).
4. M. E. Wadsworth, "Rate Processes in Hydrometallurgy," 2nd Tutorial Symposium on Extractive Metallurgy, Denver, Colorado, 1972.
5. W. Lorenz, Z. Electrochem. 58, 912(1954), or Reference 2, p. 666.
6. P. Marcantonio, "Chalcocite Dissolution in Acidic Ferric Sulfate Solutions," Ph.D. Thesis, Univ. of Utah, 1976.
7. J. W. Beckstead, et al., "Acid Ferric Sulfate Leaching of Attritor-Ground Chalcopyrite," Extractive Metallurgy of Copper, Vol. II, TMS/AIME, Chap. 31, 611(1976).
8. D. L. Jones and E. Peters, "The Leaching of Chalcopyrite with Ferric Sulfate and Ferric Chloride," Ibid., Chap. 32, 633(1976).
9. R. H. Spitzer, et al., "Mixed-Control Reaction Kinetics in the Gaseous Reduction of Hematite," AIME, 236, 726(1966).
10. S. L. Pohlman and F. A. Olson, "A Kinetic Study of Acid Leaching of Chrysocolla Using a Weight Loss Technique," Solution Mining Symposium, Dallas, Texas, 446(1974).

11. W. K. Tolley, "Reaction Kinetics Involved in Cupric Chloride Leaching of Metallic Copper Spheres in a Stirred Reactor," Master Thesis, Univ. of Utah, 1975.
12. A. J. Morris and R. F. Jensen, "Fluidized Bed Chlorination Rates of Australian Rutile," TMS/AIME, 7B, 89(1976).

UNIT PROCESSES IN EXTRACTIVE METALLURGY
HYDROMETALLURGY

Module 8

LEARNING OBJECTIVES

FOUR LEARNING
ACTIVITIES

Module Coordinator: Dr. H. H. Haug
Assistant Professor of Metallurgical Engineering
Montana College of Mineral Science and Technology

Leaching, Agitation and Filtration

Module 3: Leaching

3.1 Particle Characterization

Learning Activity 1

1. Particle Size
2. Particle Shape
3. Shape Factor
4. Particle Size Distribution
5. References

3.2 Hydrodynamics and Mass Transfer For a Packed Bed

Learning Activity 2

1. Flow Through a Packed Bed
2. Mass Transfer Between Fluid and Solid in a Packed Bed
3. References

3.3 Dump and In Situ Leaching Practice

1. Introduction
2. Leaching Systems
 1. Conventional Leaching Practice
 2. Solution Mining Systems
3. Rate Processes
 1. Leaching of Sulfide Ores
 2. Leaching of Oxide Ores
4. References

3.4 Agitation Vessels

Learning Activity 3

1. Introduction
2. Air Lift Agitation Mixer
 1. Types of Pacnuda Tanks
 2. Selection of Pacnuda Tank
 3. Design Parameters
3. Impeller Agitation Mixer
 1. Impellers
 2. Flow Pattern in Impeller Stirred Tank
 3. Energy Dissipation and Power Characteristic of Stirred Tank
 4. Suspension of Solid in a Stirred Tank
 5. Mass Transfer to Particles in Agitation Tanks
4. References

3.5 Reactor Design

Learning Activity 4

1. Types of Reactors
2. Design Parameters
 1. Review of the Kinetics of Fluid Particle Reaction
 2. Concentration of the Lixiviant

Module 3 Contents

3. Modeling and Design for Continuous Leaching Systems - J. A. Herbst
 1. Symbols and Notations
 2. Description of Governing Equations
 3. Results from Computer Simulation
 4. Design Work Sheet and Example
4. References

LEARNING ACTIVITY 1(*)

Learning Activity Objective

After completing your study of this learning activity you should be able to characterize and describe particles which either occur in nature or are produced from processing operations; to express a group particle distribution in terms of one or several physical properties.

3.1 Particle Characterization

Hydrometallurgical leaching processes involve an aqueous solvent to dissolve metal values from an ore that is being pretreated for the purpose of leaching or from a run of mine ore. The leaching is normally conducted in a confined vessel or a restricted area, called the reactor. Since leaching is one of the main unit operations in metal value recovery, the success achieved in the reactors directly influences the throughput of the entire hydrometallurgy operation.

In general, depending on the flow pattern of the aqueous phase, the leaching practice can be broadly classified as percolation systems and agitation systems. The percolation systems include the in-situ leach, heap leach, percolation leach and vat leach. During the percolation leach process, the solid particles are stationary while the aqueous solutions move through the packed bed by either hydraulic pressure or simply by gravity. The agitation process however, requires a mechanical agitator to maintain the solid particles in suspension. The success of either operation, i.e., either percolation leaching or agitation leaching depends on understanding the hydrodynamic behavior, the mass transfer occurring in the system, the intrinsic kinetics of the leaching reaction, and the physical properties of the solid particles.

In this module, the hydrodynamic behavior and mass transfer for each type of leach system, the solid properties that influence the rate of leaching, the kinetics and the design of each leaching system will be discussed.

The physical character of the solid particles not only influence the rate of the reaction but also influence directly the hydrodynamic behavior of the reaction system. Table 3.1.1 lists several particle properties which are often important in mineral processing and chemical metallurgy systems. The identification of the necessary properties to describe the behavior of a system requires a thorough understanding of the meaning and means of measuring each individual property.

3.1.1 Particle Size

The size of the particle is the best way to describe the dimension of a particulate. Particles, however, are generally irregular in shape

*Coordinator Comment: The following material was partially contributed by Dr. John Herbst, Professor of Metallurgical Engineering, University of Utah. A portion is directly quoted from reference 1.

so that it is difficult to define rigorously what is meant by particle size.

Table 3.1.1 Particle Characteristics and Their Measurement

Property	Method
Size	Microscopic, sedimentation, sieving
Shape	Size (linear dimension), volume, and area measurement
Mineralogical composition	Microscopic, X-ray diffraction
Density	Pycnometer
Surface area	
external	Permeametry
external and internal	Gas adsorption, chromatography
Porosity and pore size	Porosimetry
Surface charge	Electrophoresis, streaming potential
Magnetic susceptibility,	
electrical conductivity	Standard methods of physics
Wettability	Contact angle, microcalorimetry
Strength	Compression, drop weight, grindability tests, etc.

The size of a spherical particle is uniquely defined by its diameter. For a cube, the length along one edge is usually characterized. However, no one can deny that the size of the cube can be regarded as the length of the diagonal, or the diameter of the sphere whose volume is equal to that of the cube. For irregular particles, it is desirable to quote the size of a particle in terms of a single quantity. And the expression most often used is the equivalent diameter. This refers to the diameter of a sphere that would behave in the same manner as the particle when submitted to some specified operation. The assigned equivalent diameter usually depends on the method of measurement, hence the particle-sizing technique should, wherever possible, duplicate the one that one wishes to control.

Several equivalent diameters are commonly encountered. For example, the Stokes' diameter is measured by sedimentation and elutriation techniques; the projected area diameter is measured microscopically and the sieve-aperture diameter is measured by means of sieving. The last refers to the diameter of a sphere equal to the width of the aperture through which the particle just passes. If the particles under test are not true spheres, and they rarely are in practice, this equivalent diameter refers only to their second largest dimension. More detailed description of the particle size for different measurement is presented in Table 3.1.2.

Table 3.1.2 Definitions of particle size

Symbol	Name	Definition
d_s	Surface diameter	The diameter of a sphere having the same surface area as the particle
d_v	Volume diameter	The diameter of a sphere having the same volume as the particle
d_d	Drag diameter	The diameter of a sphere having the same resistance to motion as the particle in a fluid of the same viscosity and at the same velocity
d_a	Projected area diameter	The diameter of a sphere having the same projected area as the particle when viewed in a direction perpendicular to a plane of stability
d_f	Free-falling diameter	The diameter of a sphere having the same density and the same free-falling speed as the particle in a fluid of the same density and viscosity
d_{st}	Stokes' diameter $d_{st} = \sqrt{(d_v^3/d_d)}$	The free-falling diameter in the laminar flow region ($Re < 0.2$)
d_A	Sieve diameter	The width of the minimum square aperture through which the particle will pass
d_{vs}	Specific surfac diameter $d_{vs} = d_v^3/d_s^2$	The diameter of a sphere having the same ratio of surface area to volume as the particle.

A condensed list of some of the more common methods used to determine a analysis, together with their effective size ranges is presented in Table 3.1.3.

Table 3.1.3 Some Methods of Particle-Size Analysis

Method	Approximate Useful Range (microns)
Test Sieving	100,000 - 10
Elutriation	50 - 5
Microscopy (Optical)	50 - 0.25
Sedimentation (gravity)	20 - 1
Sedimentation (Centrifugal)	5 - 0.05
Electron Microscopy	1 - 0.005
Coulter Counter	400 - 0.5
Light-Scattering method	0.1 - 4.0

Test sieving is the most widely used method for particle-size analysis. It covers a very wide range of particle size; i.e., the range of most industrial importance. The standard size scale for sieving screen opening is listed in Table 3.1.4.

Detailed theory, measurement procedure and its application for each method listed on Table 3.1.3 can be found in Reference 2.

3.1.2 Particle shape

Particle shape influences such properties as the hydrodynamics of the fluid, the flowability of the particle, the interaction with the fluid and the packing of the solid. The description of the particle shape is usually in a qualitative manner such as angular, flaky etc. Some of these terms with their description are given in Table 3.1.5.

A more quantitative description of the particle shape is to measure the thickness, the breadth and the length of a particle. These three are mutually perpendicular to each other. The thickness, T , is defined as the minimum distance between two parallel planes which are tangential to the opposite surface of the particle, one plane being the plane of maximum stability. The breadth, B , is referred to the minimum distance between two parallel planes which are perpendicular to the planes defining the thickness and tangential to opposite sides of the particle. And the length, L , is defined as the distance between two parallel planes which are perpendicular to the planes defining thickness and breadth and are tangential to opposite sides of the particle. Heywood⁽²⁾ has proposed two ratios to describe the shape of a particle.

$$\begin{aligned} \text{elongation ratio } n &= L/B \\ \text{flakiness ration } m &= B/T \end{aligned}$$

$$\begin{aligned} [3.1.1] \\ [3.1.2] \end{aligned}$$

Table 3.1.4 A Standard Sizing Scale Based on the Standard 200-Mesh Screen

Size		Mesh	Sizing method	Example
Milli-meters	Microns			
26.67			Screening	River gravel
18.85				
13.33				
9.423				
6.680	3		
4.699	4		Pea gravel
3.327	6		
2.362	8		
1.651	10		
1.168	14		
0.833	20	Classification (elutriation and sedimentation)	Beach sand
0.589	28		
0.417	35		
0.295	48		
0.208	65		
0.147	100		Fine silt
0.104	150		
0.074	200		
0.052	52	270		
0.037	37	400		
	26		Microscope	Blood cells
	18.5	(800)		
	13			
	9.25	(1,600)		
	6.5			
	4.62	(3,200)		Many germs
	3.25			
	2.32			
	1.62			
	1.16			
	0.81		Centrifuge	Wave length of visible light
	0.58			
	0.41			
	0.29			
	0.20			
	0.14			Thinnest iridescent films visible by light interference
	0.10			
	0.07			
	0.05			
	0.035			
	0.025			Very large molecules
	0.017			
	0.012			
	0.008			
	0.006			
	0.004			
	0.003			

Table 3.1.4 (Continued)

Size		Mesh	Sizing Method	Example
Milli-meters	Microns			
	0.002			Average unit crystal
	0.0015			
	0.001			
	0.0007			
	0.0005			

Table 3.1.5 Description of particle shape

Acicular	needle shaped.
Angular	sharp edged or having roughly polyhedral shape.
Crystalline	freely developed in a fluid medium of geometric shape.
Dendritic	having a branched crystalline shape.
Fibrous	regularly or irregularly thread-like.
Flaky	plate-like.
Granular	having approximately an equidimensional irregular shape.
Irregular	lacking any symmetry.
Modular	having rounded, irregular shape.
Spherical	global shape.

3.1.3 Shape factors

Similar to the "size" of the particle, the shape factor is also a unique description of a particle shape which requires a common description of particle topology. Commonly used measures of shape include: the volume shape factor,

$$C_3 = \text{volume of the particle divided by the particle diameter cubed,} \quad [3.1.3]$$

and area-shape factor

$$C_2 = \text{external area of the particle divided by the particle diameter squared.} \quad [3.1.4]$$

These quantities can be related to regular geometrical shapes, e.g., spheres, cubes, tetrahedra, disks, etc. One of the most commonly used

measures of a particle's shape is its sphericity,

ϕ = surface area of a sphere with the same volume as the particle divided by the actual surface area of the particle.

For a sphere, $\phi = 1$, and for all other particle shapes $0 < \phi < 1$. For broken solids ϕ is usually about 0.63. Calculated sphericities of different solids are presented in Table 3.1.6. In terms of C_2 and C_3 , particle sphericity is given by

$$\phi = 4.84 C_3^{2/3} / C_2 \quad [3.1.5]$$

It is apparent from this expression that an "infinite" number of combinations of the shape factors C_2 and C_3 can yield the same value of ϕ .

Table 3.1.6 Data on Sphericity ϕ . (3)

Material	ϕ
Sand	0.600, 0.861
Iron catalyst	0.578
Bituminous coal	0.625
Celite cylinders	0.861
Broken solids	0.63
Sand	0.534-0.628
Silica	0.554-0.628
Pulverized coal	0.696

3.1.4 Particle size distribution

The solid particles encountered in nature or produced in processing operations seldom conform to one size. It is of importance to describe the amount of particle quantitatively distributed among the various sizes. In other words, it is necessary to find the amount of solid in terms of the fraction of particles in a given size or size interval in order to present or to predict the overall assembly behavior. This is usually termed particle size distribution which represents the fraction (usually in volume, weight or number) of particle in a specified size range. However, other properties such as surface area of a particle size distribution may be readily calculated from the particle size analysis.

The particle size distribution is similar in form to the probability distribution but it may also be represented by fractional analysis (density function) and by cumulative analysis (distribution function).

The two functions are shown graphically in Figure 3.1.1 a and b. (The following is directly quoted from Herbst⁽¹⁾).

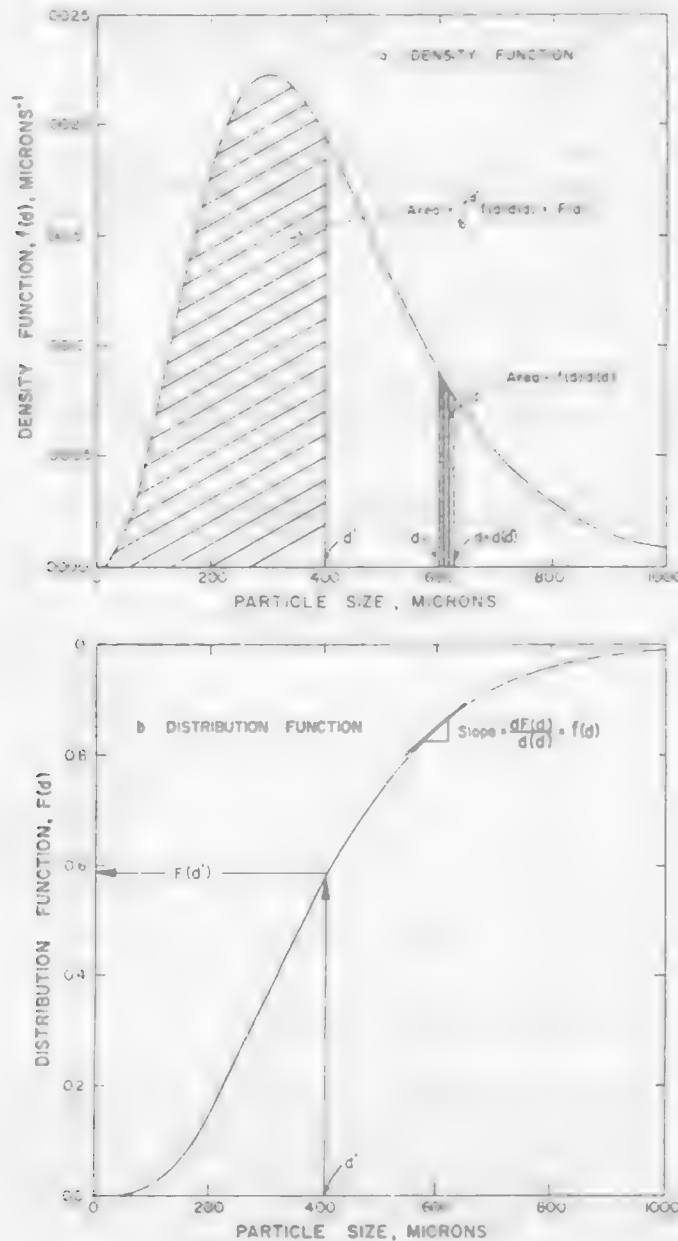


Figure 3.1.1. Plot of a typical density function (a) and distribution function (b) for particle size in an assembly of particles. The equivalence of the distribution function and the area under the density function curve and the density function and the slope of the distribution function curve are illustrated.

"The quantity $f(d)$ is termed the particle-size density function for the assembly. Physically $f(d) d(d)$ is equal to the fraction of the particles in a population that lie in a differential size interval d to $d + d(d)$. Geometrically this fraction can be represented by the shaded area under the density function between the differential limits d to $d + d(d)$ shown in Figure 3.1.1a. In order to find the fraction of particles smaller than some size d' , one must add the fractions of particles $f(d) d(d)$ from the minimum size in the population, d_{\min} , to the size of interest, d' . This summation is accomplished by integration of the density function, i.e.,

$$F(d') = \sum_{\substack{d_{\min} \\ \text{all } d(d)}}^{d'} f(d) d(d) = \int_{d_{\min}}^{d'} f(d) d(d) \quad [3.1.6]$$

The function $F(d')$, termed the *distribution function*, gives the fraction of the population with size less than d' . It is apparent from equation [3.1.6] that $F(d')$, depicted in Figure 3.1.1b, equals the area under the density function curve between d_{\min} and d' (cross-hatched area in Figure 3.1.1a). It is easily shown that the fraction of particles between any two sizes d_a and d_b ($d_b > d_a$) is given by $F(d_b) - F(d_a)$, that $F(d_{\max}) = 1.0$, and that $f(d_a) = [dF(d)/d(d)]_{d=d_a}$. It is important to recognize that if one $f(d)$ or $F(d)$ is known, everything about the distribution of particle sizes in the assembly is known.

In many instances it is not necessary, nor is it possible experimentally, to determine the complete density function or distribution function for a certain property. In such instances it may suffice to determine *selected characteristics* of the distribution. One such set of characteristics is the fraction of particles in a series of discrete property intervals. If, for example, the entire size range of particles d_{\min} to d_{\max} is broken up into a series of n discrete subintervals, then the fraction in the i th interval (bounded by d_i above and $d_i + \Delta$ below) is given by

$$f_i = \int_{d_{i+1}}^{d_i} f(d) d(d) = F(d_i) - F(d_{i+1}), \quad i=1,2,3,\dots,n \quad [3.1.7]$$

Information of this type might be generated experimentally by sizing an assembly using a series of n sieves. The set of f_i values determined in this manner does not completely characterize the distribution (since no information is contained in f_i concerning the distribution within the interval d_{i+1} to d_i), but approximations to the complete density function and distribution function can be obtained from these data. It is apparent from equation [3.1.7] that the following equality holds for the distribution function at the discrete points d_i , $i=1,2,\dots,n$:

$$F(d_i) = \sum_{i=1}^n f_i \quad [3.1.8]$$

From the mean-value theorems of calculus the density function can be approximated by

$$f(d_i^*) = \frac{F(d_i) - F(d_{i+1})}{d_i - d_{i+1}} = \frac{f_i}{d_i - d_{i+1}} \quad [3.1.9]$$

where d_i^* is an average value of d in the interval d_i to d_{i+1} . Commonly used values for d_i^* include the arithmetic average $(d_i + d_{i+1})/2$, the geometric average $(d_i d_{i+1})^{1/2}$, and the harmonic average $2d_i d_{i+1}/(d_i + d_{i+1})$. Figure 3.1.2 shows the density and distribution functions of Figures 3.1.1a and b along with the discrete approximations obtained for ten equispaced size intervals, $d_i^* = (d_i + d_{i+1})/2$. The discrete approximations are seen to reproduce the essential characteristics of the continuous functions; such approximations become even better as the number of size intervals is increased.

In certain instances, only one or two parameters are used to characterize a distribution. The mean and variance of the distribution are often used in such instances. The mean or average size of a population is determined from the density function using the defining equation

$$\mu = \int_{d_{min}}^{d_{max}} df(d) d(d) \quad [3.1.10]$$

Its corresponding approximation obtained from a set of f_i values is

$$\hat{\mu} = \sum_{i=1}^n d_i^* f(d_i^*) \Delta d_i = \sum_{i=1}^n d_i^* f_i \quad [3.1.11]$$

The variance or spread of sizes (around the mean) is given by

$$\sigma^2 = \int_{d_{min}}^{d_{max}} (d - \mu)^2 f(d) d(d) \quad [3.1.12]$$

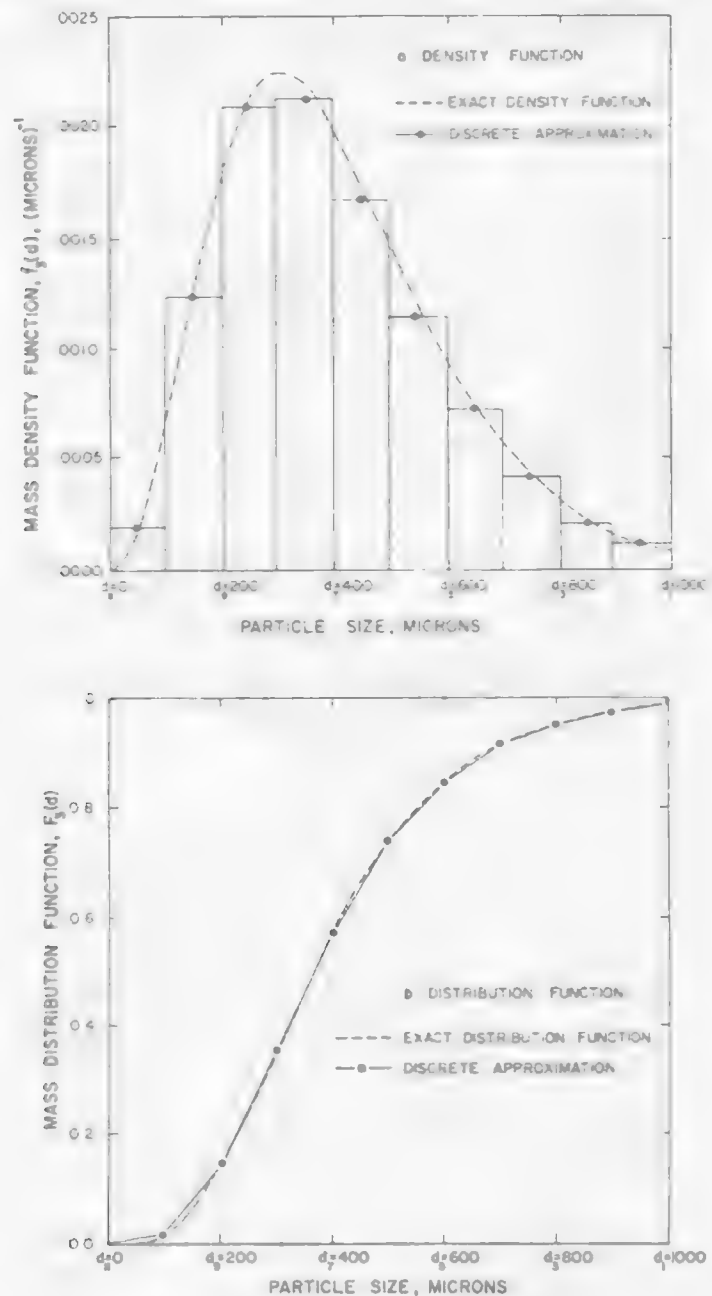
or approximated by

$$\hat{\sigma}^2 = \sum_{i=1}^n (d_i^* - \hat{\mu})^2 f_i \quad [3.1.13]$$

The normalized spread of sizes is characterized by the coefficient of variation

$$CV = \sigma/\mu \quad [3.1.14]$$

Figure 3.1.2. Plot illustrating ten size fraction discrete approximations to a density function (a) and distribution function (b).



Source: Reference 1

Figures 3.1.3a and b illustrate the way in which these characteristics change with changes in the density function, $f(d)$. Figure 3.1.3a shows distributions with the same coefficient of variation but different mean sizes and Figure 3.1.3b shows distributions with the same mean size but different CV values.

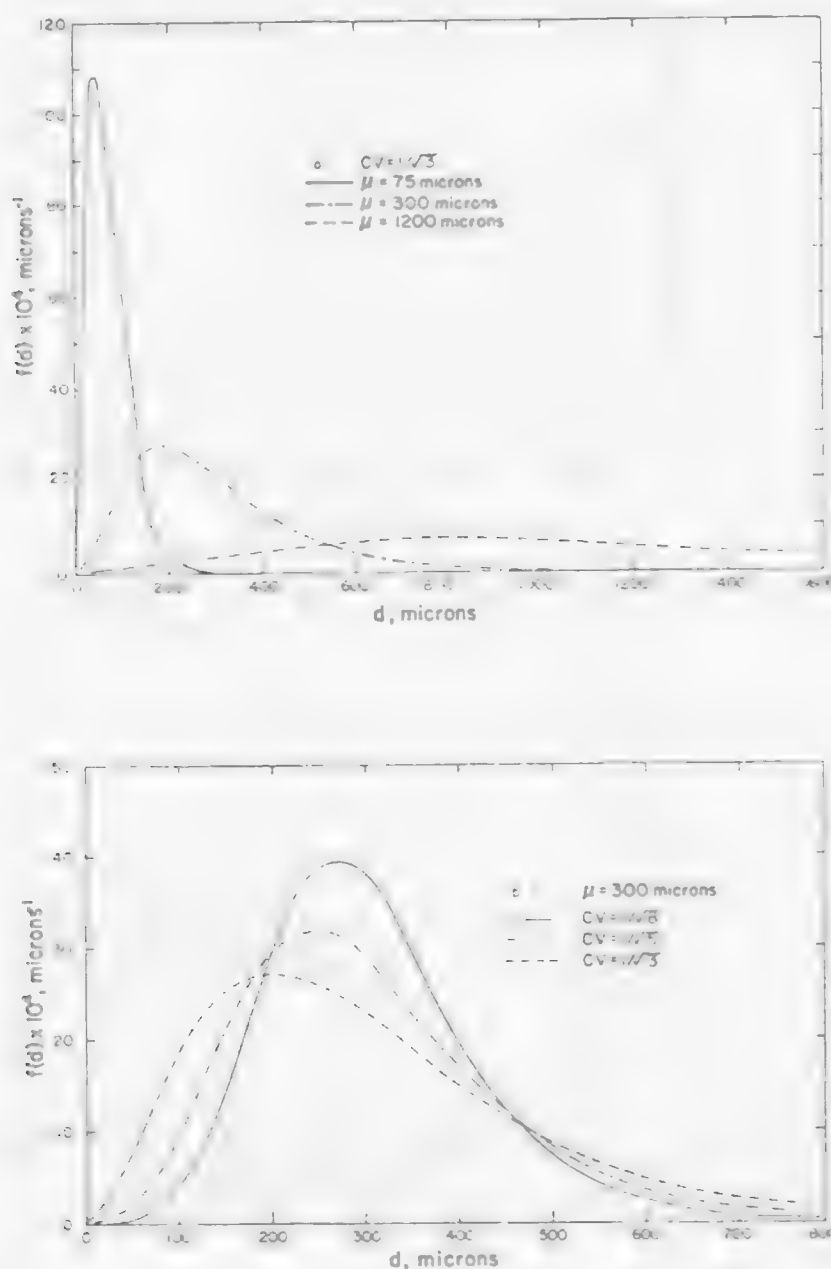


Figure 3.1.3. Illustration of density function changes resulting from changes in the mean for a fixed coefficient of variation (a) and changes in the coefficient of variation for a fixed mean (b).

Several commonly used empirical size distributions are listed in Table 3.1.7 along with the corresponding mean sizes, variances, and coefficients of variation. These two parameter distributions can be fitted to experimental-size distribution data by plotting or moment matching. The best fit values of the adjustable parameters for each of the distributions can be determined directly from plots or from computed values of the mean and variance." Insert by module author: Figure 3.1.4 shows the fitting of the ball mill grinding output by using normal distribution, log-normal distribution and by gamma distribution with a particle mean of 0.4120 mm, and a variance of 0.1467.

Table 3.1.7. Commonly Used Empirical Size Distributions⁽¹⁾

Name	Gaudin-Schuhmann	Rosin-Rammler	Log-Normal	Gamma ^a
Adjustable parameters	m, d_{max}	m, l	$\log \sigma, l'$	b, p
Density function, $f(d)$	$m \frac{d_{max}^m}{d^{m+1}}$	$\frac{m}{l^m} d^{m-1} \exp \left[-\left(\frac{d}{l} \right)^m \right]$	$\frac{1}{(2\pi)^{1/2} d \log \sigma} \exp \left[-\frac{\log^2 (d/l')}{2 \log^2 \sigma} \right]$	$\frac{b^p d^{p-1}}{\Gamma(p)} e^{-bd}$
Distribution function, $F(d)$	$\left(\frac{d}{d_{max}} \right)^m$	$1 - \exp \left[-\left(\frac{d}{l} \right)^m \right]$	numerical integration of density function or standard tabulations	
Range, $[d_{min}, d_{max}]$	$[0, d_{max}]$	$[0, \infty]$	$[0, \infty]$	$[0, \infty]$
Mean, μ	$\frac{m}{m+1} d_{max}$	$l \Gamma \left(\frac{m+1}{m} \right)$	$l' \exp \left(\frac{1}{2} \log^2 \sigma \right)$	$\frac{p}{b}$
Variance, σ^2	$\left[\frac{m}{(m+2)} - \left(\frac{m}{m+1} \right)^2 \right] d_{max}^2$	$l^2 \left[\Gamma \left(\frac{m+2}{m} \right) - \Gamma^2 \left(\frac{m+1}{m} \right) \right]$	$l'^2 [\exp(\log^2 \sigma) - \exp(\frac{1}{2} \log^2 \sigma)]$	$\frac{p}{b^2}$
Coefficient of variation, CV	$\frac{m}{m+2} - \left(\frac{m}{m+1} \right)^2$	$\frac{\left[\Gamma \left(\frac{m+2}{m} \right) - \Gamma^2 \left(\frac{m+1}{m} \right) \right]}{\Gamma^2 \left(\frac{m+1}{m} \right)}$	$\frac{[\exp(2 \log^2 \sigma) - \exp(\log^2 \sigma)]^{1/2}}{\exp(\frac{1}{2} \log^2 \sigma)}$	$\frac{1}{p^{1/2}}$

^a The distribution function of the gamma distribution is given by $\Gamma(p) = \int_0^\infty x^{p-1} e^{-x} dx$, $\Gamma(p+1) = p\Gamma(p)$. For p an integer, the incomplete gamma function is given by $\Gamma(p, x) = \int_x^\infty t^{p-1} e^{-t} dt = (p-1)! e^{-x} \sum_{k=0}^{p-1} \frac{x^k}{k!}$.

Source: Sohn and Wadsworth, Rate Processes of Extractive Metallurgy, Plenum, Chap. 2, (1979).

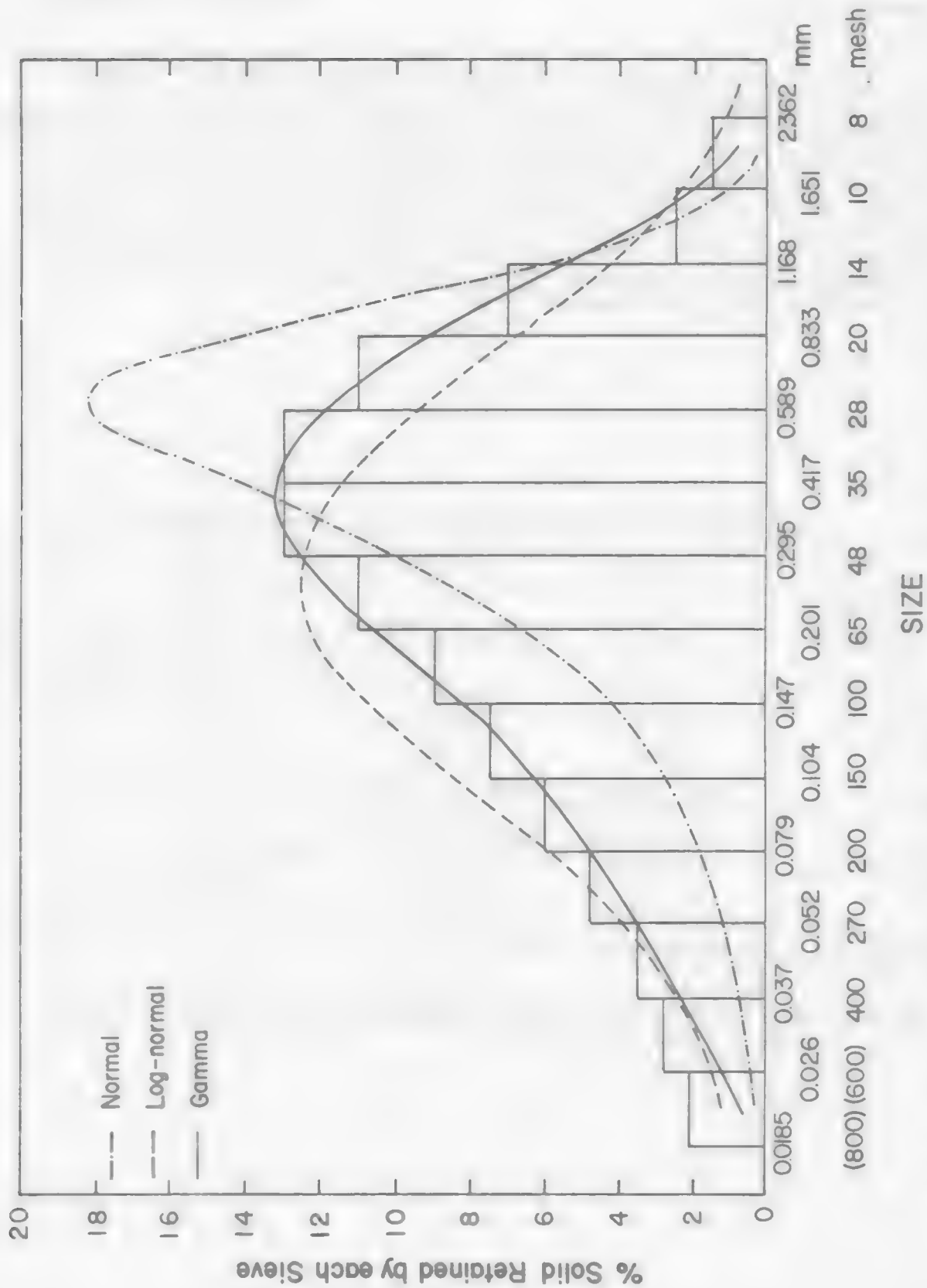


Figure 3.1.4. The particle size distribution from a ball mill product by empirical distribution functions.

"In the preceding discussion of $f(d)$ and $F(d)$, it was not specified whether these quantities referred to fractions of the total number of particles or fractions of the total mass or volume of particles in population. This is an important distinction and the ability to convert from one type of size distribution (e.g., fraction by number) to another (e.g., fraction by volume or mass) is required in many applications. Number distributions, denoted by $f_o(d)$ and $F_o(d)$, are generally considered to be the most fundamental form of distribution. On the other hand, we often determine distributions experimentally on the basis of mass (e.g., sieving and weighing). Hence the mass distribution, denoted by $f_3(d)$ and $F_3(d)$, is important in many instances. Figure 3.1.5 shows a comparison of a typical number distribution and the associated mass distribution for a particle assembly. The general relationship between a number distribution and a mass distribution can be obtained from the following equality for particles of size d to $d + d(d)$ in any assembly:

$$\left[\begin{array}{c} \text{mass of particles of} \\ \text{size } d \end{array} \right] = \left[\begin{array}{c} \text{mass of particles of} \\ \text{size } d \end{array} \right]$$

$$\left[\begin{array}{c} \text{total mass of} \\ \text{particles} \end{array} \right] \left[\begin{array}{c} \text{mass fraction} \\ \text{of particles} \\ \text{of size } d \end{array} \right] = \left[\begin{array}{c} \text{mass of a} \\ \text{particle} \\ \text{of size } d \end{array} \right] \left[\begin{array}{c} \text{number of} \\ \text{particles} \\ \text{of size } d \end{array} \right]$$

$$W f_3(d) d(d) = \rho C_3 d^3 N f_o(d) d(d) \quad [3.1.15]$$

where N is the total number of particles in the population, $f_o(d) d(d)$ is the number fraction of the particles with size d to $d + d(d)$, W is the total mass of particles in the population, $f_3(d) d(d)$ is the mass fraction of particles with size d to $d + d(d)$, ρ is the solid density, and C_3 is the volume-shape factor. If the solid density and volume-shape factor are independent of size, then equation [3.1.15] can be used in conjunction with the equations $\int_{d_{min}}^{d_{max}} f_o(d) d(d) = 1$ and $\int_{d_{min}}^{d_{max}} f_3(d) d(d) = 1$ for integration over all values of d to show that

$$f_3(d) = \frac{d^3 f_o(d)}{\int_{d_{min}}^{d_{max}} d^3 f_o(d) d(d)} \quad [3.1.16a]$$

$$f_o(d) = \frac{d^{-3} f_3(d)}{\int_{d_{min}}^{d_{max}} d^{-3} f_3(d) d(d)} \quad [3.1.16b]$$

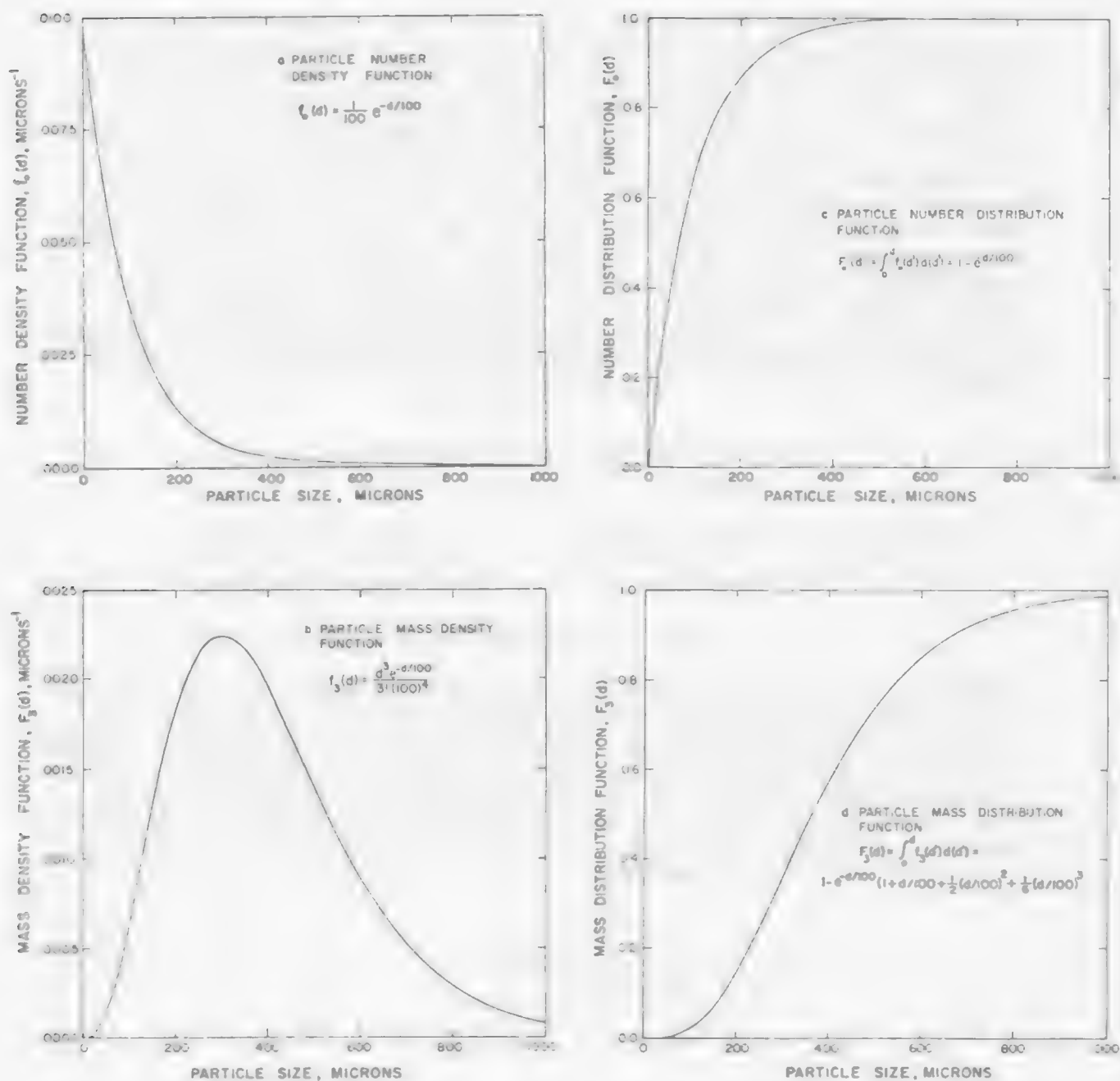


Figure 3.1.5 Illustration of the transformation of a size distribution from a number to a mass basis.

The last two equations permit the transformation from one type of size distribution to the other. The reader should use the above expressions to confirm the transformation $f_O(d) \rightarrow f_Z(d)$ depicted in Figure 3.1.5. It is also instructive to compute the mean and variance of particle size for the number and mass distributions shown in the figure using equations [3.1.10] and [3.1.12]. Note that, in general, the mean and variance are different for the number size distribution and the mass size distribution.

The preceding discussion of single property distributions has centered around particle size distributions. Clearly, the same type of treatment can be made for any property of interest in a particle assembly. Thus for a general property Z , (e.g., composition, strength, etc.) we can define $f(\xi) d\xi$ = the fraction of particles in the assembly with property Z between ξ and $\xi + d\xi$, and $F(\xi)$ = the fraction of particles with property $Z \leq \xi$. From these definitions we can find the fractions in a set of discrete property intervals $[\xi_i \text{ to } \xi_{i+1}]$ and can compute means and variances of the distribution in an analogous fashion to equations [3.1.7]–[3.1.14]. In the general case, transformations from number to mass distributions can only be made if information is available concerning the relationship between the number and mass of particles in a given property interval.

Up to this point we have treated the case in which only one property of the assembly is of interest. The representation of the distribution of two or more properties simultaneously is a logical extension of what has been done above. Let us say, for example, that we are interested in the distribution of size, d and the mass of some valuable constituent, m_A , in a particle assembly. In this case we can denote the number density function by $f_O(d, m_A)$. This joint density function may look something like that shown in Figure 3.1.6. From the joint density function $f_O(d, m_A)$ we can find the number fraction of particles with size between d and $d + d(d)$ and mass of valuable between m_A and $m_A + d(m_A)$ from the expression

$$f_O(d, m_A) d(d) d(m_A) \quad [3.1.17]$$

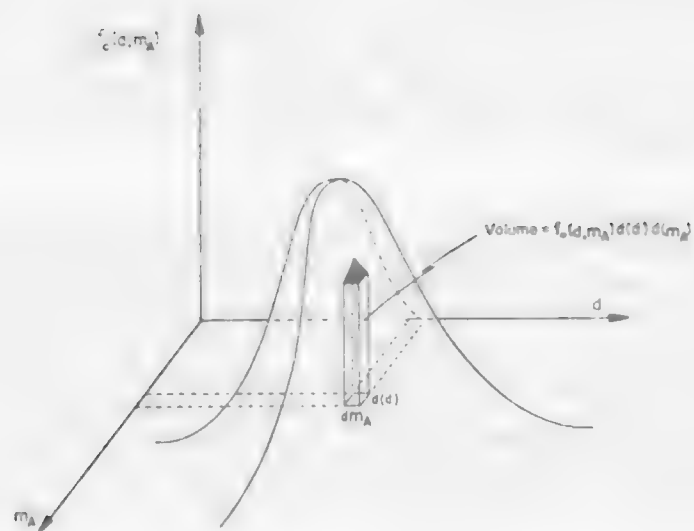
Geometrically this fraction can be represented by the volume under the density function curve between the differential limits shown in the figure. The distribution function is given by

$$F_O(d', m'_A) = \int_{m_{Amin}}^{m'_A} \int_{dmin}^{d'} f_O(d, m_A) d(d) d(m_A) \quad [3.1.18]$$

which gives the number fraction of particles with size less than d' and mass of valuable less than m'_A . Clearly, $F_O(d_{max}, m_{Amax}) = 1.0$ (the sum of all fractions in the population).

The number size distribution (irrespective of the mass of valuable) can be recovered from $f_O(d, m_A)$ by summing over all m_A values:

Figure 3.1.6. Graphical representation of a two-property (size and mass of valuable) density function.



$$f_O(d) = \int_{m_{Amin}}^{m_{Amax}} f_O(d, m_A) d(m_A) \quad [3.1.19]$$

and similarly the distribution of valuable (irrespective of particle size) can be found by summing over all sizes:

$$f_O(m_A) = \int_{dmin}^{dmax} f_O(d, m_A) d(d) \quad [3.1.20]$$

The two latter quantities are termed the *marginal* density functions for d and m_A , respectively. The mean, variance, and coefficient of variation for size and mass of valuable can be computed using equations [3.1.19] and [3.1.20] in defining equations [3.1.10], [3.1.12], and [3.1.13]. The transformation from number to mass distribution can be obtained from equation [3.1.15] written for particles of size d with mass of valuable m_A .

The above procedure for representing property distributions can be extended to any number of properties of interest ($\xi_1, \xi_2, \dots, \xi_j$), using the general joint density function $f(\xi_1, \xi_2, \dots, \xi_j)$.² However, in practice it is rare to consider more than two properties simultaneously because of the complexity of the distributions." (End of quotation from Herbst).

3.1.5 References

1. J.A. Herbst, 'Rate Processes in Multiparticle Metallurgical Systems,' from Rate Processes of Extractive Metallurgy, ed. by H.Y. Sohn and M. E. Wadsworth, Plenum, 1979.
2. T. Allen, Particle Size Measurement, Chapman and Hall, London, 1968.
3. D. Kunii and O. Levenspiel, Fluidization Engineering, R. Krieger (1977).

LEARNING ACTIVITY 2

Learning Activity Objective

After completing the first section of this learning activity you should be able to describe the basic aspects of flow through a packed bed, and the associated mass transfer. After completing the second section of this material you should be able to describe fundamental concepts for the leach systems encountered in hydrometallurgical operations.

3.2 Hydrodynamics and Mass Transfer For A Packed Bed

3.2.1 Flow Through A Packed Bed

Percolation leach systems include: in-situ, heap, dump and vat processes. They all appear to be a bed of solid particles with an aqueous phase flowing through the pores between particles. Flow patterns through a bed of solids are complex. It is, therefore, difficult to derive the velocity or any other transport properties from first principles. Usually empirical correlations are experimentally obtained and are relied upon for design purposes. A major parameter of interest in all these systems is the pressure drop required to achieve a certain volume flow rate.

If the flow occurs under low pressure conditions, that is, it is slow enough, the rate of flow is essentially proportional to the pressure drop per unit length of packing, $\Delta P/L$

$$Q = \frac{k_d A \Delta P}{L} \quad [3.2.1]$$

Where Q = volume of fluid flowing per unit time, cm^3/sec ;

A = cross-sectional area, cm^2 ,

k_d = permeability coefficient, a constant depending on the fluid, temperature and the packing characteristics, $\text{cm}^4/\text{dyne-sec}$ (Equation 3.2.1, known as D'Arcy's law, has been applied to the problem of the filtration of water through a filter cake). The k_d term in Equation 3.2.1 is often called the permeability, which is satisfactory as long as we carry out the test with the same fluid at the same temperature, but in general, it is more common and more desirable to define a specific permeability P :

$$k_d = \frac{P}{\eta} \quad [3.2.2]$$

where η is the viscosity of the fluid.

This allows \bar{P} to be specific to the packing only and, therefore, allows the flow of other fluids, or the same fluid at other temperatures, to be predicted. The units of specific permeability \bar{P} cm^2 , where the unit of specific permeability, the D'Arcy, is now defined as

$$1 \text{ D'Arcy} = 1 \times 10^{-8} \text{ cm}^2.$$

A semi-empirical approach for the flow through a packed bed regards the packed bed as a bundle of tangled tubes of unusual cross section. The theory is then developed by applying the results for single straight tubes to the collection of crooked tubes, extremely irregular tortuous channels.

The friction factor and Reynolds number for the packed bed is defined as

$$\frac{\Delta P}{\frac{1}{2} \rho u_0^2} = \frac{L}{d} 4f \quad \text{Friction factor} \quad [3.2.3]$$

$$\frac{dG}{\mu} \frac{1}{1-\epsilon} \quad \text{Reynolds number} \quad [3.2.4]$$

where ΔP = pressure drop between the inlet and outlet of the flow
(gravitational force is included, i.e., $\Delta P = \Delta p + \rho g L$)

ρ = density of the fluid

u_0 = superficial velocity (this is the average linear velocity of the fluid would it would have if no packing were present).

L = length of the packed column

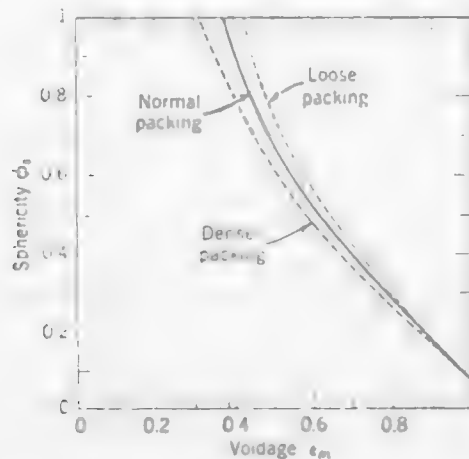
a_v = total particle surface/volume of the particle

ϵ = void fraction of the packed bed

$G = \rho u_0$ = mass flow rate.

According to Brown et al(1), the fraction of voids in a uniformly sized packed bed is related to the sphericity of the particles, as shown in Figure 3.2.1. Since reliable voidage predictions are scarce and since this quantity is easy to measure, it is suggested that ϵ be defined experimentally.

Figure 3.2.1. Voidage in uniformly sized, randomly packed beds (from Brown et al. [1]).



The pressure drop through packed beds of uniformly sized solid particles has been correlated by Ergun using the equation⁽²⁾

$$\frac{\Delta P}{L} g_c = 150 \frac{(1-\epsilon)^2}{\epsilon^3} \frac{\mu u_0}{d^2} + \frac{1.75 \rho u_0^2}{d} \frac{(1-\epsilon)}{\epsilon^3} \quad [3.2.5]$$

The Ergun equation can be applied both in laminar and in turbulent flow regions. The Ergun equation may be written in terms of dimensionless groups:

$$\left(\frac{\Delta P \rho}{G^2} \right) \left(\frac{d}{L} \right) \left(\frac{\epsilon^3}{1-\epsilon^2} \right) = 150 \frac{(1-\epsilon)}{(dG/\mu)} + 1.75 \quad [3.2.6]$$

The graphical presentation of Equation [3.2.6] is presented in Figure 3.2.2.

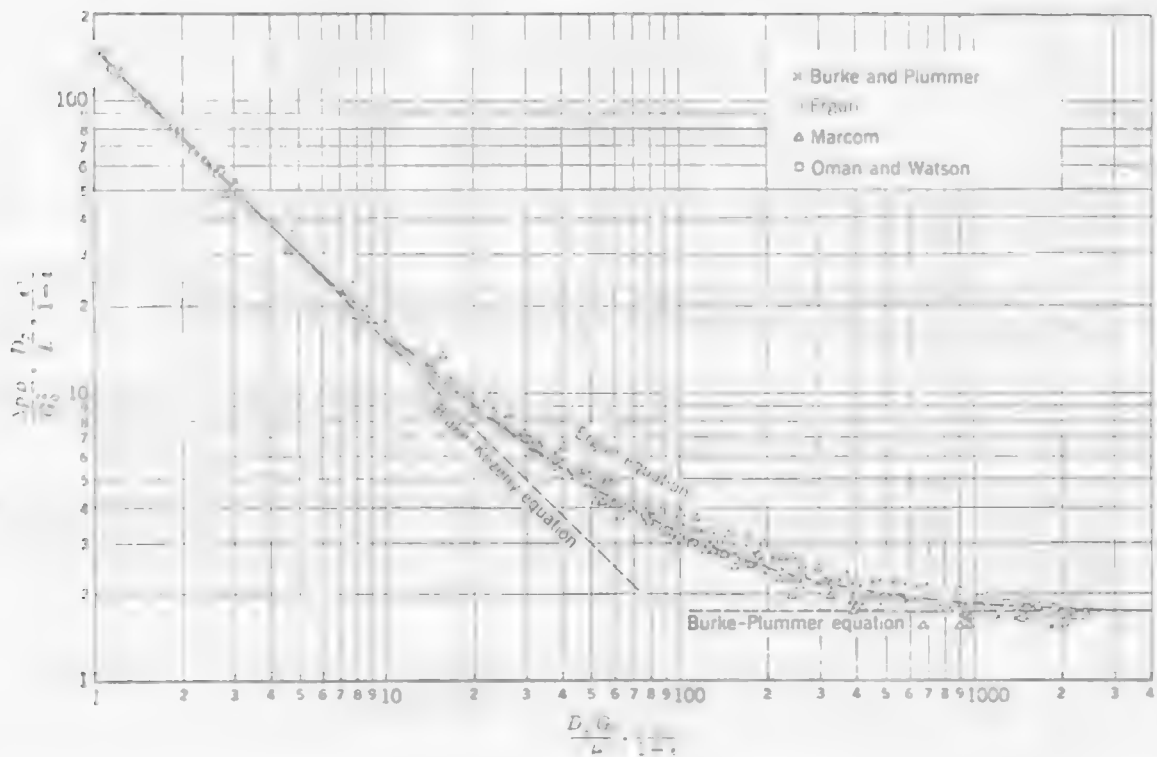
The pressure drop in Equation [3.2.6] represents two factors, the viscous energy and the kinetic energy losses. At low Reynolds numbers the viscous losses predominate and Equation [3.2.5] simplifies to as Blake-Kozeny equation

$$\frac{\Delta P}{L} g_c = 150 \frac{(1-\epsilon)^3}{\epsilon^3} \left(\frac{\mu u_0}{d^2} \right) \quad \text{Re} \leq 20 \quad [3.2.7]$$

At high Reynolds numbers only the kinetic energy losses need be considered. This is called the Burke-Plummer equation.

$$\frac{\Delta P}{L} g_c = 1.75 \frac{1-\epsilon}{\epsilon^3} \frac{\rho u_0^2}{d} \quad \text{Re} > 1000 \quad [3.2.8]$$

Figure 3.2.2. Sketch showing the general behavior of the Ergun equation on a log-log plot. (S. Ergun, Chem. Eng. Prog., 48, 93 1952).



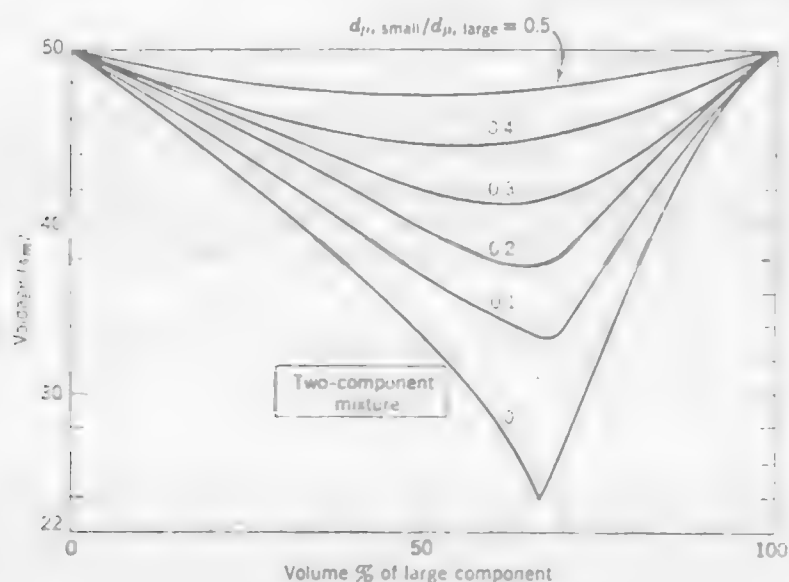
Source: Reference (2)

Pressure drop in beds containing a wide range of size distribution follows the Ergun equation for single size particles. The "d" value is replaced by the average particle size, \bar{d} . Thus equation 3.1.3 becomes

$$\frac{\Delta P}{L} g_c \approx 150 \frac{(1-\epsilon)^2}{\epsilon^3} \frac{u u_0}{\bar{d}} + 1.75 \frac{1-\epsilon}{\epsilon^3} \frac{\rho u_0^2}{\bar{d}} \quad [3.2.9]$$

The voidage for a mixture of sizes cannot be estimated reliably. The factors that must be considered include: how solids are introduced into the vessel, their size, and also the shape of the size distribution curve. For example, if the size variation is large, the fine particles can fit into the void between the large particles, thus greatly decreasing voidage. Figure 3.2.3 illustrates this phenomenon when two size particles are mixed, the voidage of the packing depends on the volume ratio and the size ratio. Actually, since voidage is a relatively simple matter to determine experimentally, there is no need to present equations and predictive procedure for finding it.

Figure 3.2.3. Measured voidage in fixed beds of two sizes of spheres (by Furnas, from Zenz and Othmer [2]).



3.2.2 Mass Transfer Between Fluid And Solid In A Packed Bed

Studies on mass transfer between fluid and solid phases in a packed bed show reasonable agreement for both flowing liquids and gasses. Representative data on mass transfer in packed beds for liquids are shown in Figure 3.2.4 as a graph of j_D vs. Re .

$$Re = \frac{d\bar{u}\rho}{\mu} \quad [3.2.10]$$

where d = diameter of a sphere having the same surface as the particle

ρ, μ = density and viscosity of the fluid

\bar{u} = average fluid velocity,

$$j_D = \frac{k}{\bar{u}} Sc^{2/3} \quad [3.2.11]$$

where j_D = mass transfer j factor

k_m = mass transfer coefficient

Sc = Schmidt number = $\frac{\mu}{\rho D}$

D = diffusivity

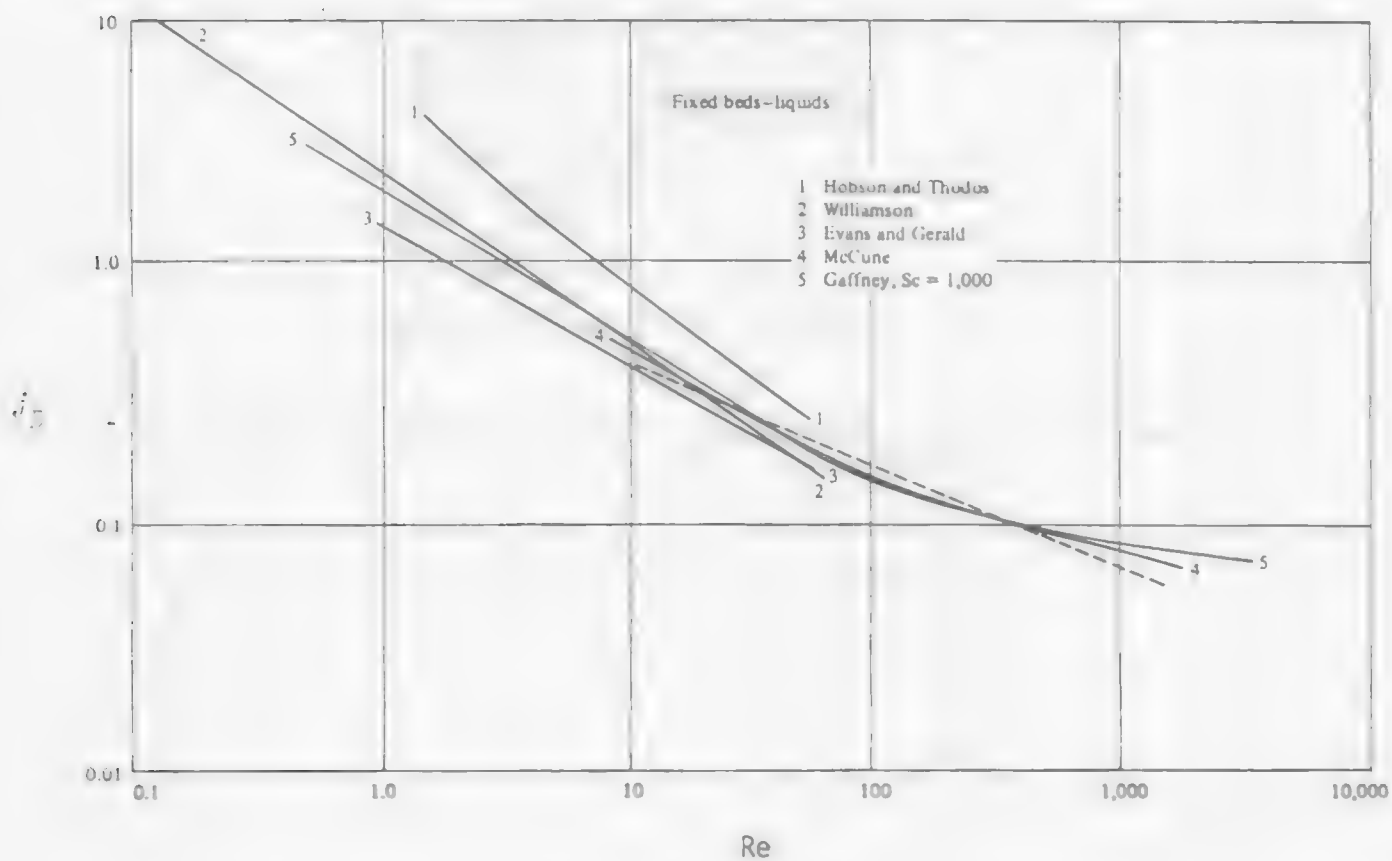
The agreement in the data shown in Figure 3.2.4 between the several investigators is poor. The difference may be due to the difficulty in conducting the experiments. Sherwood⁽³⁾ et al. have summerized the data and proposed a correlation shown as a single straight dashed line on Figure 3.2.4. The correlation which may be employed for engineering estimates is:

$$j_D = \frac{k}{\bar{u}} Sc^{2/3} = 1.17 \left(\frac{d\bar{u}\rho}{\mu} \right)^{-0.415} \quad 10 < Re < 2,500 \quad [3.2.12]$$

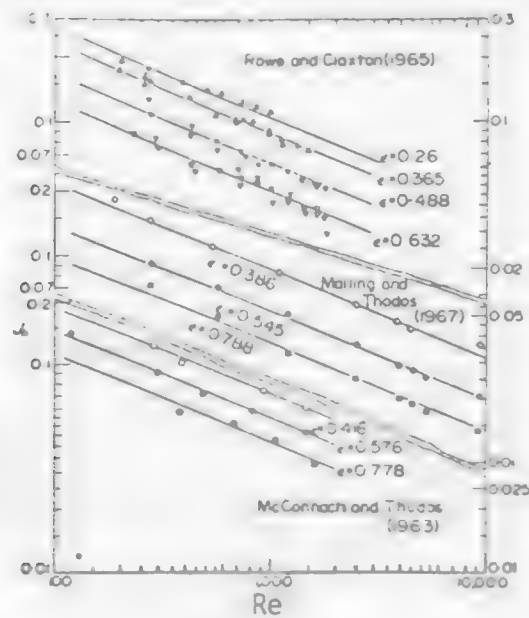
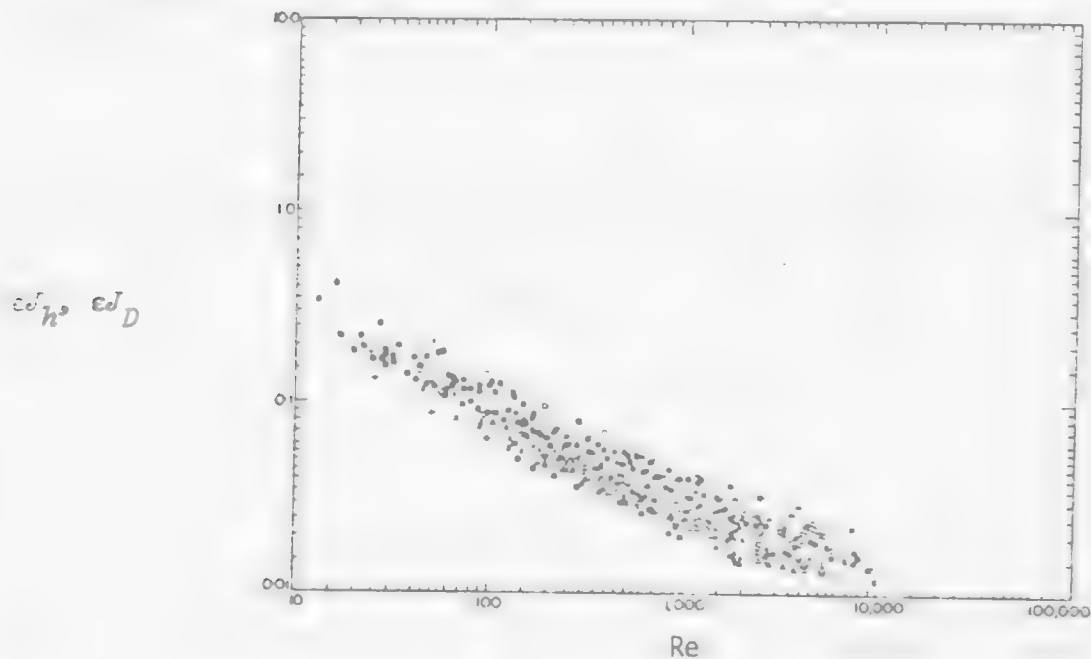
Correlations of the type shown in Figure 3.2.5 fails to allow for variations in the void fraction ϵ , which in fixed beds of spheres and pellets is typically 0.4 to 0.44 but may range from 0.3 to 0.5. Gupta⁽⁴⁾ et al. suggested there is an appropriate way to estimate the correlation by plotting ϵj_D vs Re (see Figure 3.2.6). Ranz⁽¹⁾ summarized the correlation as

$$Sh = 2.0 + 1.8 Sc^{1/3} Re^{1/2} \quad Re > 80 \quad [3.2.13]$$

Figure 3.2.4. Mass transfer between flowing liquids and particles in packed beds.



Source: Reference (3)

Figure 3.2.5. Relationship between J_h vs J_D/μ -effect of void fraction.Figure 3.2.6. Fluid-particle heat and mass transfer in fixed and fluidized beds- ϵJ_h , ϵJ_D .

Source: Reference (4).

3.2.3 References

1. D. Kunii and O. Levenspiel, Fluidization Engineering, R. Kreiger Chapter 3 (1977).
2. R. B. Bird, W. E. Stewart and E. N. Lightfoot, Transport Phenomenon, John Wiley, Chap. 6 (1960).
3. T. K. Sherwood, R. L. Pigford and C. R. Wilke, Mass Transfer, McGraw-Hill, Chap. 6 (1975).
4. S. N. Gupta, R. B. Chaube and S. N. Uphadhyay, Chem. Eng. Sci., 29, 839 (1974).

3.3 Dump and In Situ Leaching Practices*

3.3.1 Introduction

In recent years the general field of hydrometallurgy has received renewed attention, initiated by two major developments. First, consideration of the environment has focused strongly on the minerals producers because of localized emission and earth disturbance. Though small in the total of environmental damage, the minerals and metals industry is making a concerted effort to find and develop new technology. Second, scarcity of materials, particularly raw material sources within the United States, has resulted in renewed exploration activity.

CRUST The direct dissolution of metal values from an ore deposit is an intriguing concept considering the vast mineral wealth of the earth's crust which cannot be mined economically by normal techniques. Detailed rate studies of such systems are few, but significant progress is being made. Scale-up from laboratory to field is a monumental extrapolation requiring knowledge of mineral and ore fragment kinetics, hydrology, gas-flow characteristics, and complex solution chemistry.

Bartlett⁽¹⁾ has developed the basis for a pore-diffusion, mineral kinetics model under non-steady-state conditions. In its general application, this model has greatest potential in providing a fundamental first approximation of extraction kinetics from known porosity data, individual mineral kinetics, and solution chemistry. Useful steady-state models have been employed by Brayn *et al.*⁽²⁾ for deep solution mining of copper sulfides, by Roman *et al.*⁽³⁾ for leaching of oxide ores, and by Madsen *et al.*⁽⁴⁾ for leaching of Cu_2S under dump-leaching conditions. The steady-state solution is based upon a shrinking core model and is valid for the case in which mineral kinetics are relatively rapid compared to the effective diffusion rates in an ore fragment. Cathles and Apps⁽⁵⁾ have extended the shrinking-core model to include thermal effects as predicted from the chemical kinetics. The thermal gradients in turn influence air convection within the deposit.

3.3.2. Leaching Systems

3.3.2.1 Conventional Leaching Practice

The leaching of low-grade ores, as in copper dump leaching, represents an area in which significant advancement has been made in recent years. The leaching of low-grade materials is one of the oldest metallurgical operations known, but its physics and chemistry have been little understood. Heap leaching and vat (percolation) leaching are usually carried out on oxide ores somewhat higher in value than ores considered for dump leaching. Figure 3.2.7 illustrates each type of leaching operation.

*Coordinator comment: The following material (Section 3.3) is quoted directly from Dr. Wadsworth's presentation in the text "Rate Processes of Extractive Metallurgy." It is reproduced here by written permission.

Figure 3.2.7. Various Types of Leaching

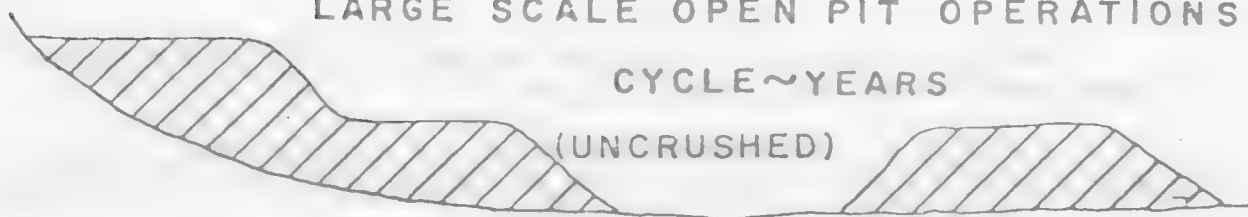
COPPER LEACHING PRACTICE

DUMP LEACHING

LOW GRADE OXIDES AND SULFIDES FROM
LARGE SCALE OPEN PIT OPERATIONS

CYCLE ~ YEARS

(UNCRUSHED)



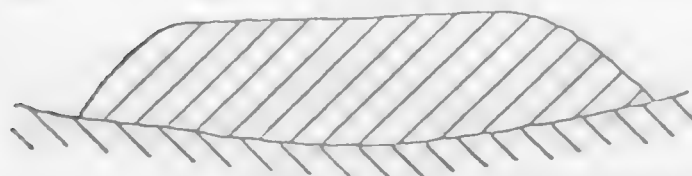
EST. + 20 b. lbs. Cu in Western U.S.

HEAP LEACHING

USUALLY POROUS OXIDIZED ORES

CYCLE ~ MONTHS

(CRUSHED OR UNCRUSHED)



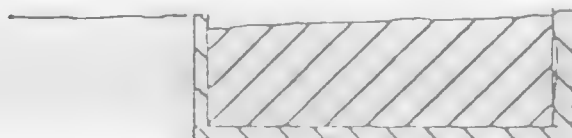
SPECIALLY PREPARED

PAD

VAT LEACHING

CRUSHED COPPER OXIDE ORE

CYCLE ~ DAYS



ABOVE OR
BELOW GROUND
LEVEL

3.3.2.2 Solution Mining Systems

Recently, in-place (*in situ*) leaching of ore deposits has received increased emphasis and appears to be an area in which significant advances will be made in the near future. This type of hydrometallurgical operation is often referred to as *solution mining*. It is useful to consider dump leaching as part of solution mining since the physical and chemical features are similar to the leaching of fragmented or rubblized deposits in place. Much of what is to be expected from *in situ* extraction can be derived from current experience and practice in dump leaching.

Deposits amenable to *in situ* leaching may be classified into the three general groupings shown in Figure 3.2.8.

I. Surface dumps or deposits having one or more sides exposed, and deposits within the earth's crust but above the natural water table.

II. Deposits located below the natural water table but accessible by conventional mining or well-flooding techniques.

III. Deposits below the natural water table and too deep for economic mining by conventional methods.

Dump leaching is placed in the first classification. Type II is characteristic of what is to be expected in the near future. Type III is expected to develop more slowly.

Type I would be the leaching of a fractured ore body near the surface above the natural water table in the surrounding area. This would apply to mined out regions of old mines such as a block-caved portion of a copper mine, or regions which have been fractured by hydrofracturing or by the use of explosives. The chemistry and physical requirements would be essentially the same as in dump leaching.

Type II refers to the leaching of deposits which exist at relatively shallow depths, less than approximately 500 ft, and which are under the water table. Such deposits will have to be fractured in place and dewatered so they may be subjected to alternate oxidation and leach cycles or percolation leaching, although the use of special oxidants may eliminate the drainage cycle. This is a special problem requiring a complete knowledge of the hydrology of the region. Water in the deposit, if removed during the oxidation cycle, must be processed, stored, and returned under carefully controlled conditions. An alternate method of leaching would be by flooding as described for Type III below. An important, rapidly developing example of Type II is the application of flooding using wells distributed on a grid such as is currently under field test for uranium extraction. (6)

SOLUTION MINING

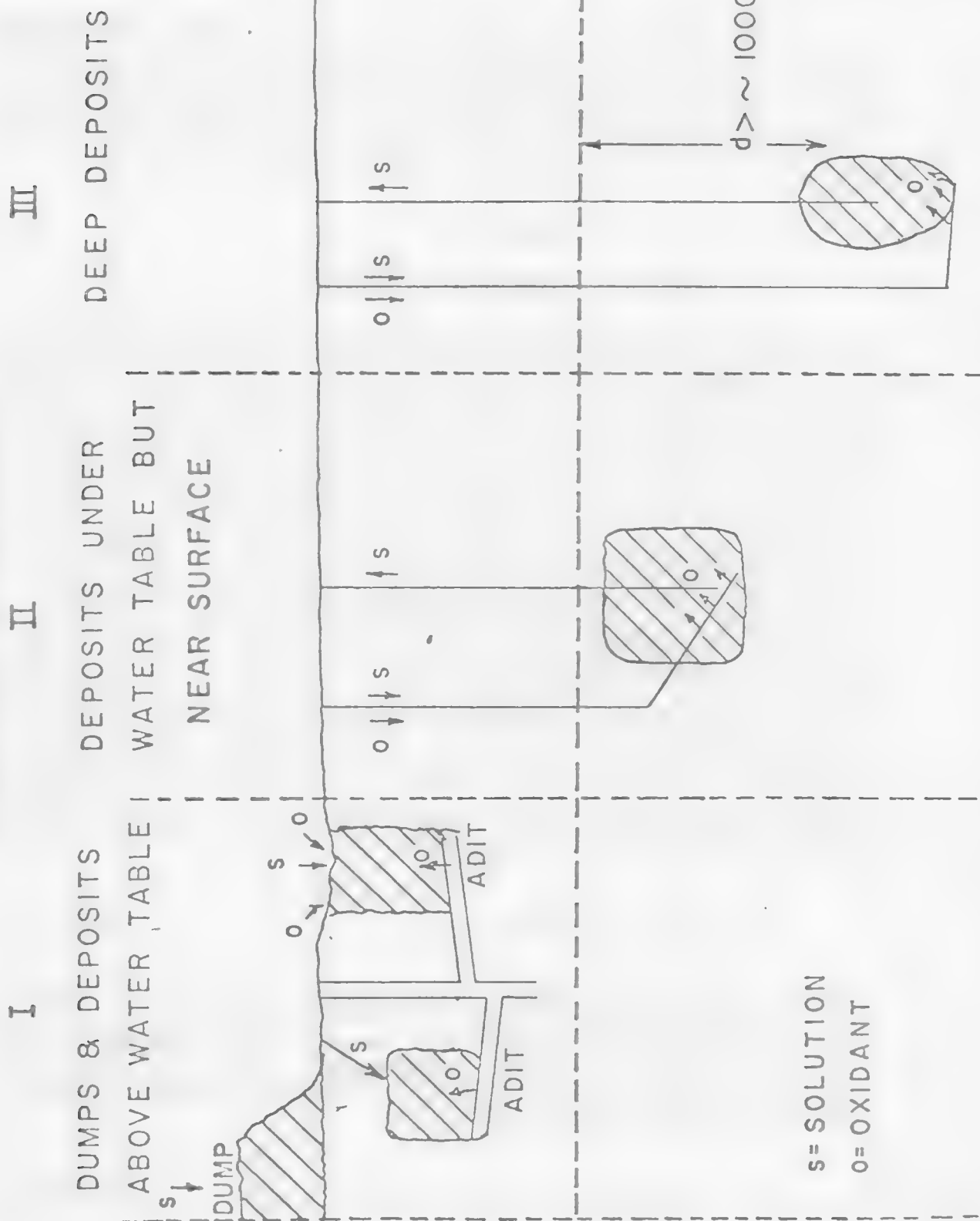


Figure 3.2.8. Three sets of conditions for solution mining

The third general type (Type III) of solution mining is represented by deep deposits below the water table and below approximately 500 ft in depth. The ore body is shattered by conventional or nuclear devices. Again, the hydrology of the region must be well known for proper containment of solutions. This represents a unique situation in that the direct oxygen oxidation of sulfide minerals becomes possible.

3.3.3 Rate Processes

3.3.3.1 Leaching of Sulfide Ores

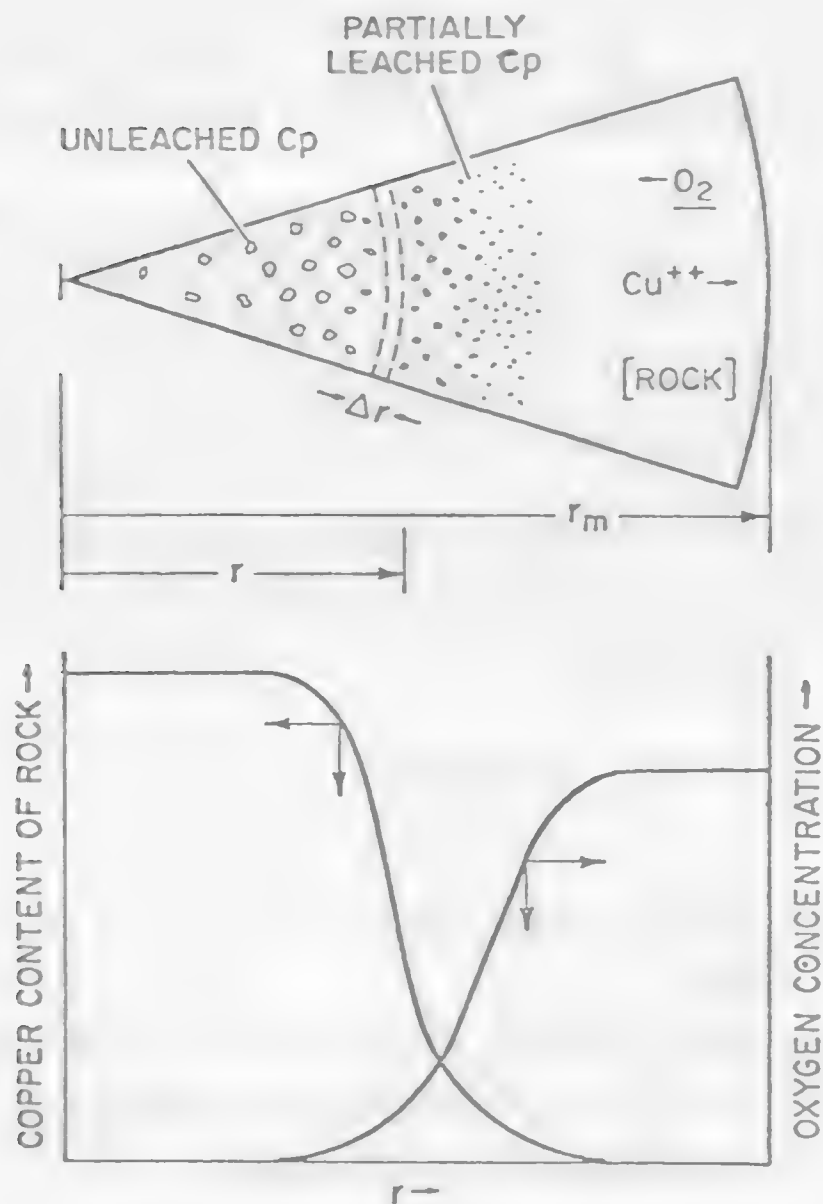
General Leaching Model. Virtually all researchers agree that the leaching of ore fragments involves penetration of solution into the rock pore structure. The kinetics thus involve diffusion of lixiviant into the rock where reaction with individual mineral particles occurs. The kinetics are thus complicated by changing porosity, pH, and solution concentration. Bartlett⁽¹⁾ applied the continuity equation to a system as described by Type III. The system is one in which a copper porphyry ore containing chalcopyrite as the major copper sulfide mineral, is subjected to oxidation under conditions proposed by researchers at the Lawrence Livermore Laboratory (LLL) for deep solution mining.⁽²⁾ Diffusion of oxygen and subsequent reaction with mineral particles combine to give a non-steady-state concentration gradient within the ore fragment. This treatment provides a basis for modeling of all similar leaching systems. The shrinking core concept used by several researchers is a special case of this general treatment. Figure 3.2.9 illustrates the mineral fragment showing different regions at some time, t . Oxygen and copper gradients vary markedly over a broad zone in which chalcopyrite (Cp) particles extend from partly to totally reacted. The fragment, considered as spherical, may be viewed in cross section, as divided into annular rings of thickness Δr . If J is the flux of dissolved reactant diffusing into and out of this incremental volume the continuity equation for an individual ore fragments is

$$\epsilon \frac{\partial C}{\partial t} = -R + \frac{1}{A} \frac{\partial J}{\partial r} \quad [3.2.12]$$

Where A is the area at radius r , and R is the rate of loss of reactant per unit volume because of reaction with mineral particles. Actually, this is a summation of rate processes for all mineral types and sizes, within the incremental volume. The porosity must be included since only the solution volume is involved. Combining equation (3.2.12) with Fick's laws gives for spheres

$$-\epsilon \frac{\partial C}{\partial t} = R + D' \left(\frac{\partial^2 C}{\partial r^2} + \frac{2}{r} \frac{\partial C}{\partial r} \right) \quad [3.2.13]$$

Figure 3.2.9. Schematic Drawing Illustrating the Leaching of a Rock Containing Disseminated Chalcopyrite (Cp).



The evaluation of R requires a knowledge of the kinetics of dissolution of individual mineral processes. Bartlett⁽¹⁾ assumes these particles follow a log-normal size-distribution law. The evaluation of diffusion terms is accomplished by finite difference procedures for each rock fragment size. Using this method a matrix is developed from which the oxygen concentration profile may be determined for any given time, t . Knowing the oxidant concentration for each incremental volume makes it possible to calculate the rate of reaction within each volume for finite time Δt . The summation of metal release values for each incremental volume in turn summed over each finite time interval results in an evaluation of metal recovery versus time. Figure 3.2.10 illustrates percent extraction versus time ⁽¹⁾ for a variety of porosities using this method.

Reaction Zone Model. If the rate of reaction of individual mineral particles is fast enough, the region of partially leached minerals, Figure 3.2.7, is fairly narrow. Such a condition is illustrated in Figure 3.2.11 where a reaction zone of thickness δ moves topochemically inward during the course of the reaction. According to the reaction zone model steady-state diffusion occurs through the reacted outer region and is equal to the rate of reaction within the reaction zone itself. This model was developed by Braun et al.⁽²⁾ for the same ore as considered by Bartlett.⁽¹⁾ The effective area of mineral particles within the moving reaction zone is assumed to be essentially constant and independent of the mineral-particle-size distribution since new particles in each size fraction will begin to leach at the leading edge of the reaction zone just as similar particles are completely leached at the tail of the reaction zone. The rate of reaction within the reaction zone may be expressed by the equation

$$\frac{dn}{dt} = - \frac{4\pi r^2 \delta n_p A_p C_s k_s}{\phi} \quad [3.2.14]$$

where

n = moles of leachable mineral,

t = time,

n_p = number of mineral particles per unit volume of rock,

A_p = average area per particle in the reaction zone,

k_s = rate constant of mineral particle,

C_s = average concentration in the reaction zone, and

N = Avogadro's number.

Figure 3.2.10. Computed and experimental (3) extractions for the LLL San Manuel test to 1 year.

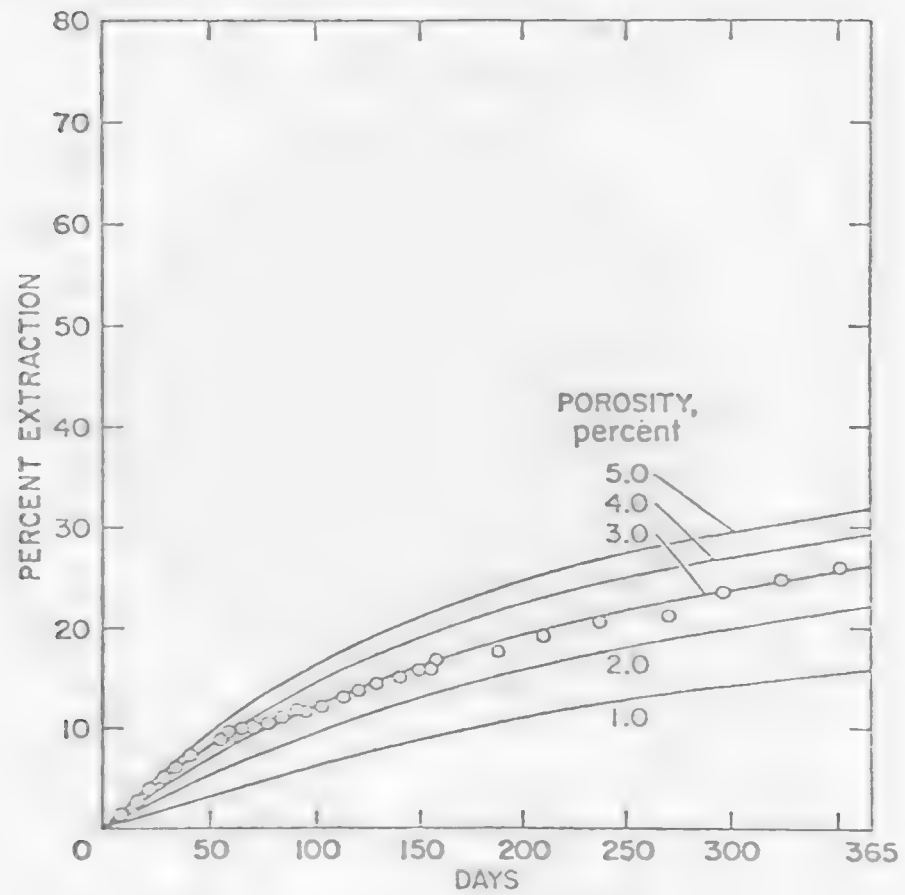
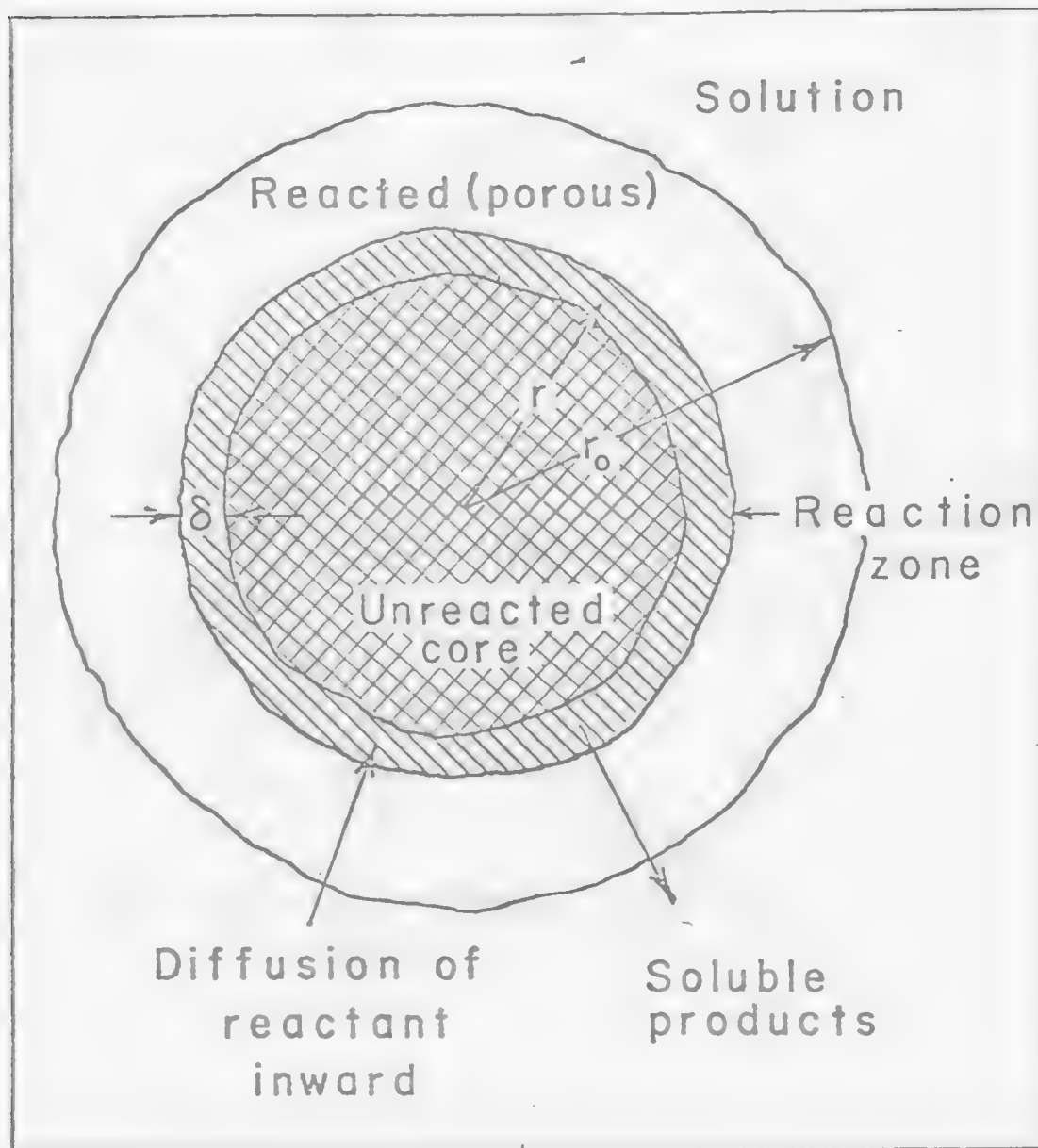


Figure 3.2.11. Reaction zone model with reaction zone thickness δ at concentration C_s .



Diffusion through pores to the reaction zone may be expressed by the equation

$$\frac{dn}{dt} = \frac{4\pi r^2 D' K_h}{\phi \sigma} \frac{dC}{dr} \quad [3.2.15]$$

where

D' = effective coefficient of diffusion,

K_h = Henry constant,

C = bulk solution concentration,

ϕ = geometric factor to account for deviation in sphericity, and

σ = stoichiometry factor (number of moles of reactant required per mole of metal released).

Equation (3.2.15) may be integrated for steady-state transport where for a given geometrical configuration the reaction dn/dt is constant for all values of r and r_o . The result is

$$\frac{dn}{dt} = - \frac{4\pi D r r_o K_h}{\phi (r_o - r) \sigma} (C - C_s) \quad [3.2.16]$$

Equations (3.2.14) and (3.2.16) are mixed diffusion plus surface reaction when a sharp reaction interface results. As before, these equations may be combined under the steady-state approximation giving for ore fragment of radius, r_i ,

$$\frac{dn}{dt} = - \frac{4\pi r_i^2}{\phi \sigma} \left[\frac{1}{G\beta} + \left(\frac{\sigma}{D'} \right) \left(\frac{r_i}{r_{io}} \right) (r_{io} - r_i) \right]^{-1} \quad [3.2.17]$$

where G is the grade (weight fraction of copper sulfide mineral),

$$G = \frac{\delta_A r_p \rho_p}{3\rho_r}; \quad \beta = \frac{3\rho_r k_s \delta}{r_p \rho_p} \quad [3.2.18]$$

where

r_p = average mineral particle radius,

ρ_p = mineral particle density, and

ρ_r = bulk rock density.

Equation (3.2.17) may be integrated numerically and summed over all ore fragment sizes, equation (3.2.19).

$$\alpha = \sum_i w_i \alpha_i \quad [3.2.19]$$

where α_i refers to the fraction reacted in weight fraction w_i , and α is the total size distribution. Weathering of large ore fragments roughened the surface. This was compensated by a correction term giving a variation of ϕ_{oi} with time. Figure 3.2.12 illustrates the copper extraction curve calculated according to equation (3.2.17) using numerical integration. The sample weighed 5.8×10^6 g and varied in particle size from 0.01 to 16 cm.

Madsen *et al.* (4) applied the reaction zone model to the leaching of Butte ore for particles up to 6 in. in diameter. Columns, 5 ft in diameter, containing 5 tons of ore were used. The principal copper mineral was Cu_2S . Equation (3.2.17) in integrated form was used. Integration leads to the equation

$$1 - \frac{2\alpha_i}{3} - (1-\alpha_i)^{2/3} + \frac{\beta'}{\text{Gr}_{oi}} [1 - (1-\alpha_i)^{1/3}] = \frac{\gamma' t}{\text{Gr}_{io}^2} \quad [3.2.20]$$

where α_i is the fraction reacted for the i th particle size. Also

$$\beta' = \frac{2D'}{\sigma B} \quad [3.2.21]$$

$$\gamma' = \frac{2MD'C}{\rho_p \phi_{io}} \quad [3.2.22]$$

where M is the molecular weight of the copper sulfide mineral. Figures 3.2.13a and 3.2.13b illustrate the calculated curves according to equation (3.2.20) for two types of ore.

3.2.3.2 Leaching of Oxide Ores

Roman *et al.* (3) have provided a model for the leaching of copper oxide ores using the shrinking-core model. They found that the surface reaction is fast so that only the diffusion term need be considered. Figure 3.2.14 illustrates a leach heap with a separate column of unit cross-sectional area, "unit heap", removed. Figure 3.2.15 illustrates the variation in acid concentration, copper concentration, and recovery

Figure 3.2.12. Extraction of copper from coarse-size primary sulfide ore at 90°C and 400 psia.

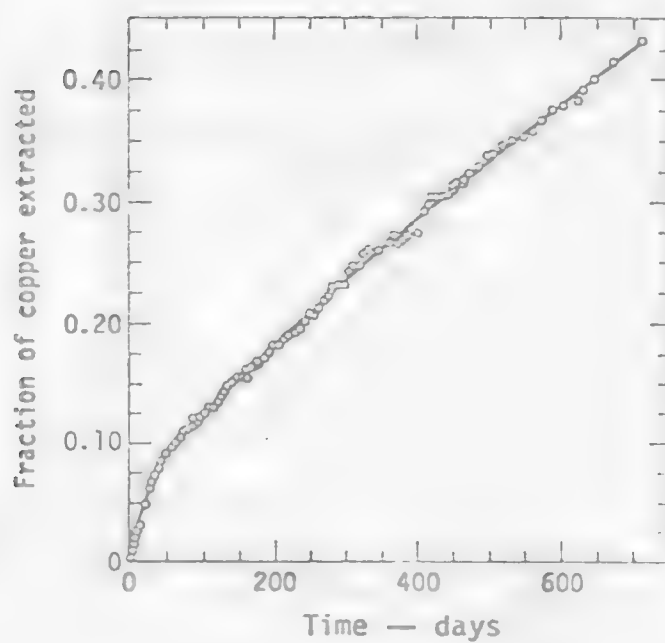
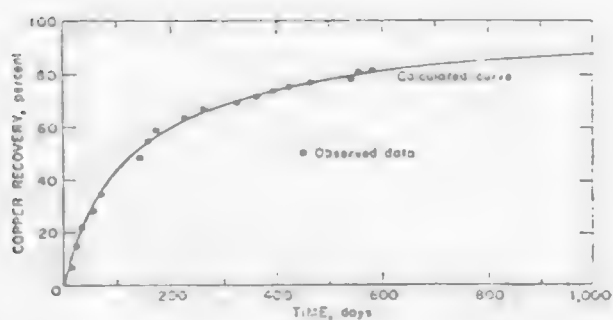
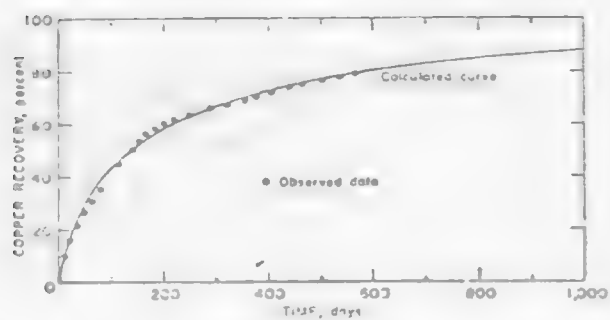


Figure 3.2.13. Modeling of dump leaching kinetics.



(a) Copper recovery from sized monzonite ore
(-6 in., + 1/2 in.).



(b) Copper recovery from sized quartz monzonite ore
(-6 in., + 1/2 in.).

Figure 3.2.14. Schematic diagram of a leach heap.

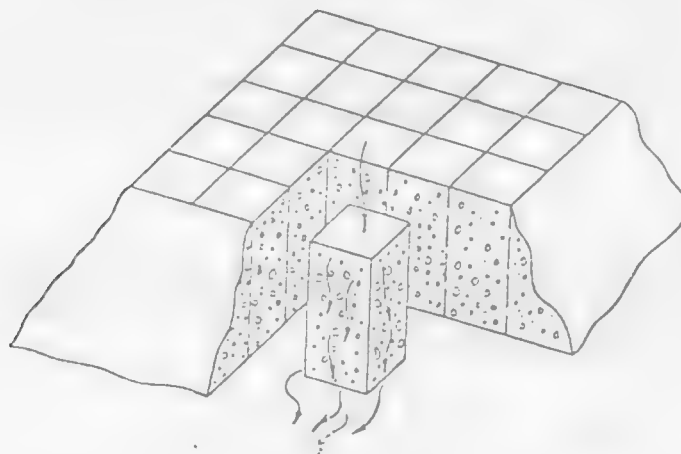
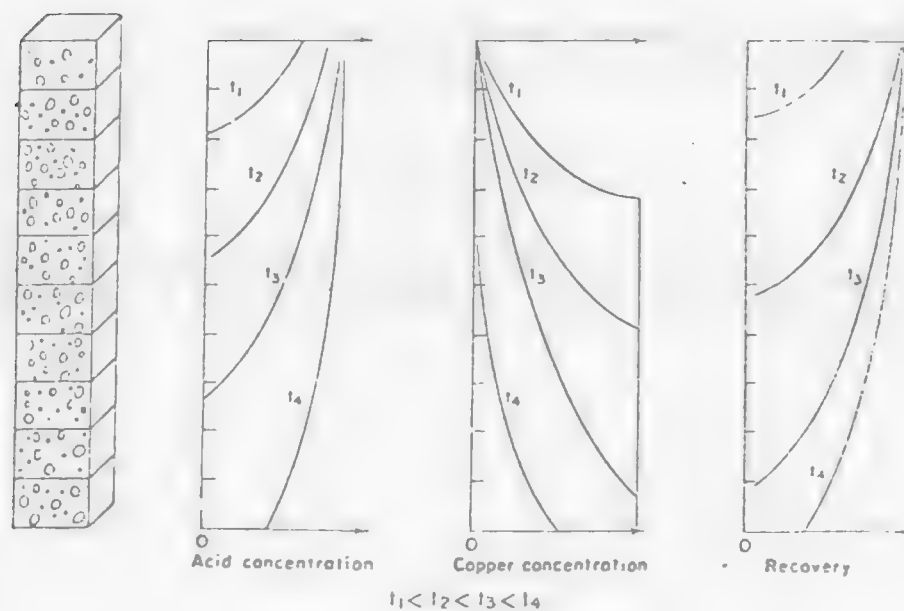


Figure 3. .15. Schematic diagram of a "unit heap" and the acid concentration, copper concentration, and recovery as a function of time and position in the heap.



for various times, t . Since acid is continually consumed the situation is very different from the case of dump leaching where ferric ion is the principal lixiviant and is generated continuously by bacterial oxidation of ferrous iron in solution. The "unit heap" may be divided into reaction volume sections, shown in Figure 3.2.16. For $j=n$, the concentration entering the reaction volume is C_{n-1}^0 and that leaving is C_n^0 . The consumption of acid is related to the copper recovery by the expression

$$-\frac{dA}{dt} = \alpha \frac{dCu}{dt} \quad [3.2.23]$$

where $\alpha = (\text{wt acid})/(\text{wt Cu})$ consumed in the reaction. The value of α may be determined experimentally. The diffusion equation, according to the Roman model becomes

$$\frac{d\alpha_{ij}}{dt} = \frac{3D'G_j^0 (1-\alpha_{ij})^{1/3}}{r_{oi}^2 \rho_r \alpha \phi [1-(1-\alpha_{ij})^{1/3}]} \quad [3.2.24]$$

where α_{ij} refers to the fraction recovered from the i th particle size in volume increment j , G is the grade, ρ_r is the ore density, ϕ is a geometry factor, and D' is the effective diffusivity. Equation (3.2.24) may be evaluated numerically and summed over all unit volumes of the "unit heap." Within one incremental volume

$$\alpha_{ij} = \sum_i \alpha_{ij} w_i \quad [3.2.25]$$

where w_i is the weight fraction of particle size i . Summing over all values gives the total fraction recovered

$$\alpha = \sum_j \alpha_j = \sum_j \sum_i \alpha_{ij} w_i \quad [3.2.26]$$

Figure 3.2.17 illustrates calculated and experimental data for two column leach tests using a computer evaluation of equations (3.2.24) and (3.2.26).

Figure 3.2.16. Volume increments in vertical section of oxide ore. Each increment is assumed to have the same initial size distribution.

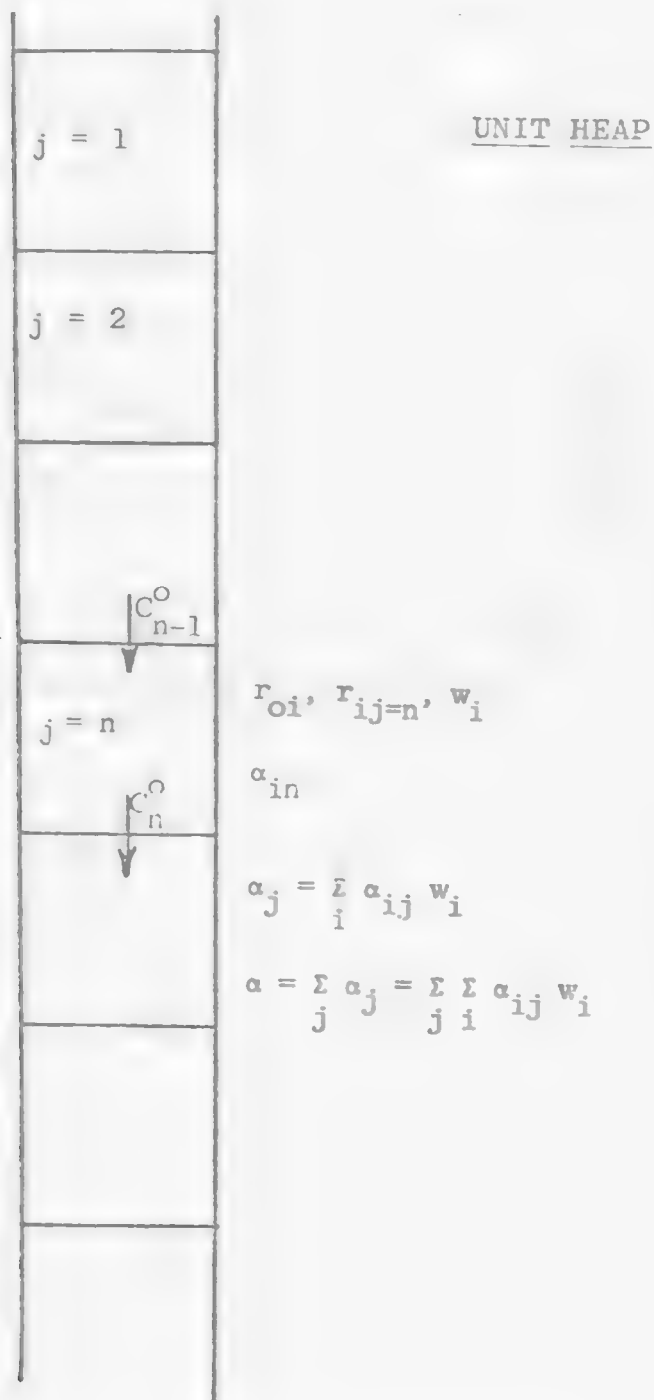
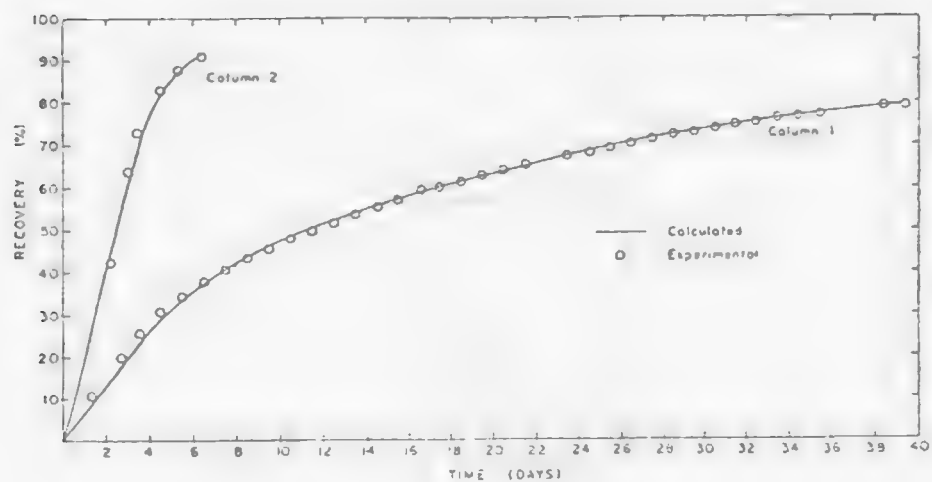


Figure 3.2.17. Recovery vs. time for two experimental columns.



3.3.4 References

1. Bartlett, R. W., Met. Trans., 3, p. 913 (1972).
2. Braun, R. L., Lewis, A. E. and Wadsworth, M. E., Met. Trans., 5, p. 1717 (1974).
3. Roman, R. J., Benner, B. R., and Becker, G. W., Trans. Soc. Min. Eng., 256, p. 247, (1974).
4. Madsen, B. W., Wadsworth, M. E. and Groves, R. D., Trans. Soc. Min. Eng., 258, pp. 69-74 (1974).
5. Cathles, L.M., and Apps. J. "A Model of the Dump Leaching Process that Incorporates by Physics and Chemistry," Kennecott Copper Corporation, presented AIChE Symposium on Modeling and Analysis of Dump and In-Situ Leaching Operations, Salt Lake City, Utah, August 19, 1974.
6. "In-Situ Leaching opens new uranium reserves in Texas," Ed. L. White, Engineering and Mining Journal, p. 7382, July (1975).

LEARNING ACTIVITY 3

Learning Activity Objective

After completing your study of the material in this learning activity you should be able to describe the types and the flow patterns for air lift pacnuda tanks; you should be able to describe the basic differences between various types of impellers, their flow pattern, and you should be able to estimate the mass transfer rate in stirred reactors.

3.4 Agitation Vessels

3.4.1 Introduction

A variety of unit processes in hydrometallurgy are carried out in stirred vessels where vigorous mixing action is required to achieve a uniform suspension of a solid phase (or a liquid phase) in an aqueous phase. Examples of stirred reactor systems are:

- (a) Leaching- the purpose of the reactor is to suspend and disperse the solid particles in an aqueous solvent to provide sufficient contact between the solvent and the mineral to promote fast mass transfer.
- (b) Solvent Extraction- the purpose of the reaction is to create contact by dispersion of two immiscible liquid phases; again to increase the rate of mass transfer.
- (c) Crystallization- the purpose of the reactor is to provide a suspension of the solid so that deposition may occur.
- (d) Other systems involve the dispersion of the gaseous reagents in an aqueous phase.

The commonly used agitation vessels in hydrometallurgy operations can be divided into (1) impeller agitation mixers and (2) air lift agitation mixers. The selection and the design of the type of reactor for each individual process depends not only on the physicochemical properties of solid, liquid and slurry but also on the mechanical behavior of the particles in the reactor itself. The physical character of the mixing action, the behavior of the fluid and the solid, the power requirement, the related mass transfer, the reactor design and the scale up problem for each type of reactor will be discussed in this section.

3.4.2 Air Lift Agitation Mixer⁽¹⁾

Gas (e.g. air, steam) can be used to accomplish the mixing in solid-liquid systems. Gas is not, however, effective for suspending rapidly settling solids but it can be used in high-density slurries having slow settling rates. A common technique is to inject air in

the center of a draft tube so that the pulp rises through the tube to overflow and return downward in an outer annular space. Vessels employing this principle are called Pachuca tanks.

A Pachuca tank (shown on Figure 3.3.1) is normally about 22 ft in diameter and 45 ft in height. It is usually equipped with a center column about 18 inches in diameter. The vessel has a conical bottom (usually with a 60° inclined angle). Air is introduced at the apex of the cone. The conical bottom is intended to direct settled solids into a region from which they may be returned to the top of the tank through the center column by the fluid currents developed by the gas pressure. Air requirements for Pachuca tanks are shown in Table 3.3.1. The power required for air compression varies from 2 to 4 horsepower per 1,000 cubic feet of pulp. Air pressure will depend on the tank height and pulp density. For instance, an air pressure of 40 psig is required for a pulp density of 1.65 and tanks 45 feet high. This high hydraulic pressure assists in dissolving gaseous oxygen which can be very useful for those reactions requiring oxygen.

Table 3.3.1 Air Requirements for Pachuca Tanks

Free air volume (standard cu ft/min)	Measurement basis
0.5 to 0.85	per ton solids (density 60-65% solids)
0.5 to 0.6	per sq ft surface area
15 to 20	per 1,000 cu ft of pulp

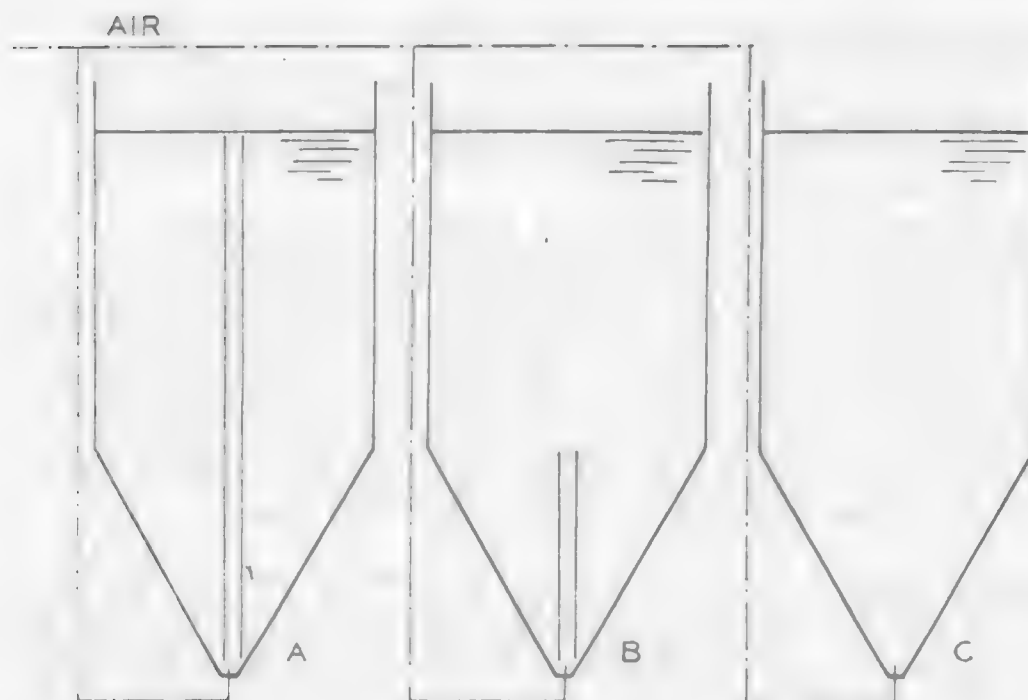
Source: Merritt, extractive metallurgy of uranium, Colorado School of Mines.

All of the South African uranium plants and many of the Canadian and US plants use air-agitated Pachuca Tanks for treating uranium ore in preference to mechanically agitated tanks. This preference is partly based on the concept that Pachuca's are less costly to operate and have fewer operating and maintenance problems in comparison with tanks employing mechanical agitation.

3.4.2.1 Types of Pachuca Tanks

The first requirement of a Pachuca tank is that it maintain a suspension of solids in liquid, that it not allow solid to settle cumulatively. The second requirement is that it aerate the pulp contained in it. Finally, it may be required to scrub films off the solid particles present to increase the mass transfer.

Figure 3.3.1. Sketch showing types of a pachuca tank discussed.



- A. Full-center-column tank
- B. Stub-column tank
- C. Free-airlift tank

Source: Reference 1.

Depending on the length and the position of the center tube, Pachuca tanks can be classified into the types; full-center-column tank; stub-column tank; and free-airlift tank. A brief discussion of the vessels and the flow pattern for each type are given as follows: (a more detailed description can be found in Reference 1).

Full-center-column Tank. The original pachuca tank had a central tube for almost the full tank length (flow as a function of tank height is shown in Figure 3.3.1). Air is introduced at the bottom of the tube. This causes pulp to rise in the tube and circulation is developed in the tank. This type of Pachuca tank yields a high velocity of the pulp but results in a low circulation rate.

Stub-column tank. The second type of Pachuca tank evolved by experimentation in cyanide practice, is recorded by Von Bernwitz, when the upper sections of the full-length air-lift tube were successively raised slightly and then removed. This discovery resulted in the development of tank having the center tube extending as a stub only to the top of the conical section (Figure 3.3.1). The rate pulp circulation varied with the position of the pulp in the column shown in line B Figure 3.3.2. Below the top of the center tube the rate of circulation behaves as the tank with a full length of the tube. Above the top of the center tube free air-lift exists and the pulp circulation rate increases.

Free-air-lift Tank. The third type of the tank is used universally in South African uranium plants. In it, the center tube has been completely removed (Figure 3.3.1). The velocity of the pulp is low, but the rate of the pulp circulation is usually higher (C. Figure 3.3.2) due to the cross-flow pulp in addition to the up-flow pulp. A schematic diagram of the flow pattern of the air-free-lift Pachuca tank is presented in Figure 3.3.3.

3.4.2.2 Selection of Pachuca Tank

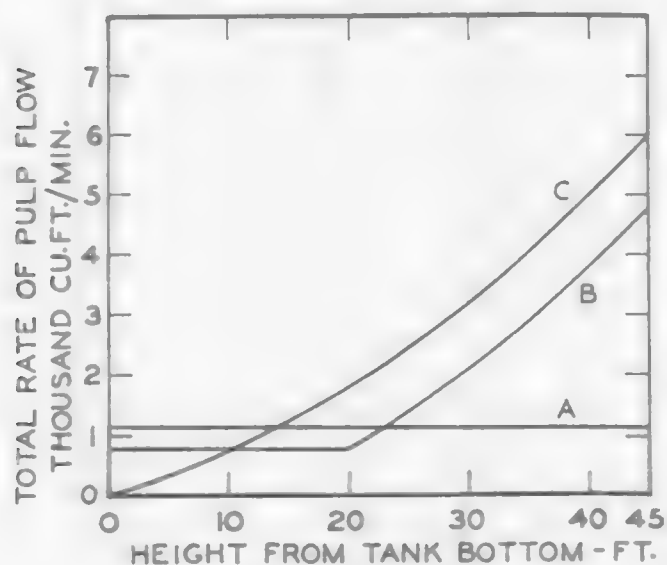
In the metallurgical industry, there is not sufficient data to allow quantitative matching of the characteristics of the various Pachuca tanks with the needs of a particular ore leaching operation. A qualitative assessment of the characteristics of each type of tank will, however, assist in general considerations of their applicability and perhaps in attaching meaning to comparative leaching tests in the various kinds of vessels.

For applications requiring particle scrubbing, the mechanical agitator should be expected to be superior to any air agitated tank. Scrubbing is related to the amount of shear, which in turn, is a function of relative velocities and of energy transfer rates. Of the pachuca tanks, the full-center-tube vessel develops the highest relative velocities. This tank may be better than the other Pachuca tanks.

Aeration is obviously best in the free-airlift and stub-column tanks. The improved gold extraction reported by Von Bernwitz⁽¹⁾ in the progressive conversion of a full-center-tube tank to a stub-column tank was probably caused by improved aeration.

For solid suspension, the full-center-column tanks would appear to be superior to the free airlift tank. Figure 3.3.4 shows that the pumping rate in the free airlift does not equal that in a stub column until a

Figure 3.3.2. Pumping rates in various types of pachuca tank.



Line A--Full-Center-column tank, 18 in. X 45 ft. column.

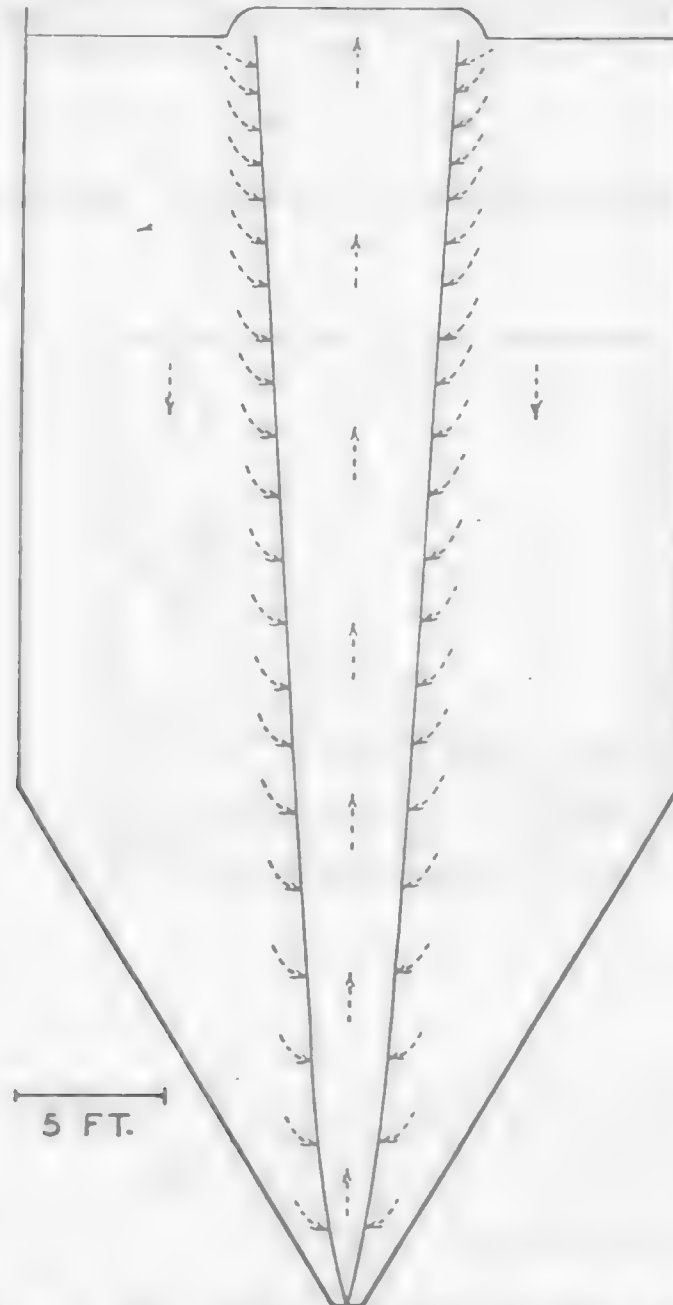
Line B--Stub-column tank, 18 in. X 20 ft. column.

Line C--Free-airlift tank, no column.

Notes--Air rate 300 cu.ft./min. Specific gravity 1.6. Pulp depth 45 ft.

Source: Reference 1.

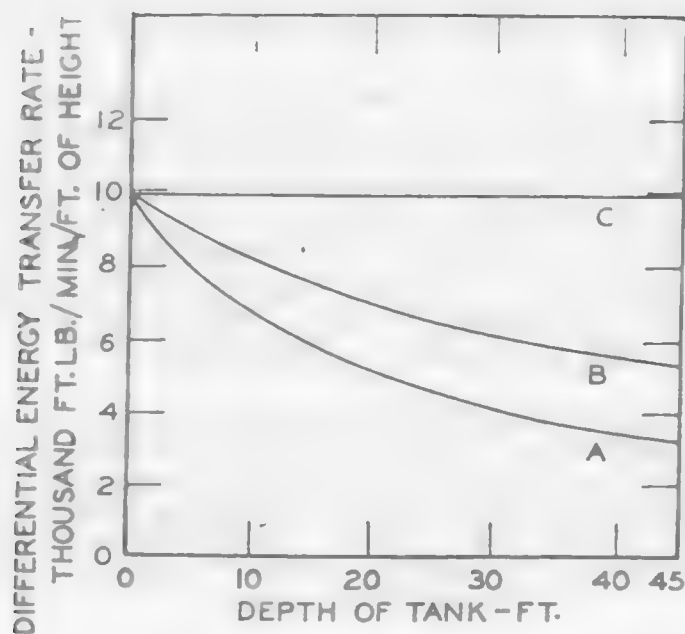
Figure 3.3.3. Representation of flow in a free-airlift pachuca tank.



Tank size 22 ft. 6 in. X 45 ft. of pulp. Air rate 300 cu.ft./min.
Specific gravity 1.6. Solution vapour pressure zero. Number of flow lines
shown entering the rising pulp stream per foot of height is proportional
to the volume rate of flow developed from each level.

Source: Reference 1

Figure 3.3.4. Variation of energy transfer rates with tank depth.



Line A-- Differential transfer rate at the bottom of the tank.

Line B--Overall average transfer rate

Line C--Differential transfer rate at the top of the tank.

Notes--Air rate is 100 cu.ft./min. in each case. Specific gravity 1.6. Solution vapour pressure zero.

Source: Reference 1.

height of about 10 feet above the bottom is reached. The free airlift tank, therefore, will have a tendency to accumulate solids at the bottom to a greater extent than the tanks having center columns.

3.4.2.3 Scale-up Parameters

Pachuca tanks are usually used in the leaching processes where highly intensive agitation is not the main concern. It is fortunate that at least in most uranium and gold cyanidation operations, the process is not particularly sensitive to mixing intensity.

In comparing Pachuca tank operations from place to place, and in designing new installations, two different dimensional factors are commonly used. One refers to air consumption in terms of cu. ft./min. per ton of solids contained in the tank. This is equivalent, for standardized pulp and solid density conditions, to cu. ft./min. of air per cu. ft. of tank volume. The other basis refers to air in terms of cu. ft./min. per sq. ft. of tank top area. The first dimensional factor implies that the air requirements vary with the area and the depth, the second implies that tank depth is unimportant.

Since air-agitated tanks in metallurgical industries are usually used primarily for solid suspension, bottom conditions are most important. Perfect scale-up and analogy in that case exists where the cu. ft./min. per sq. ft. per ft. absolute static pressure at the tank bottom is maintained equal from tank to tank. Small scale testing of Pachuca tanks can be made with confidence on such a basis.

3.4.3 Impeller Agitation Mixer^(2,3,4)

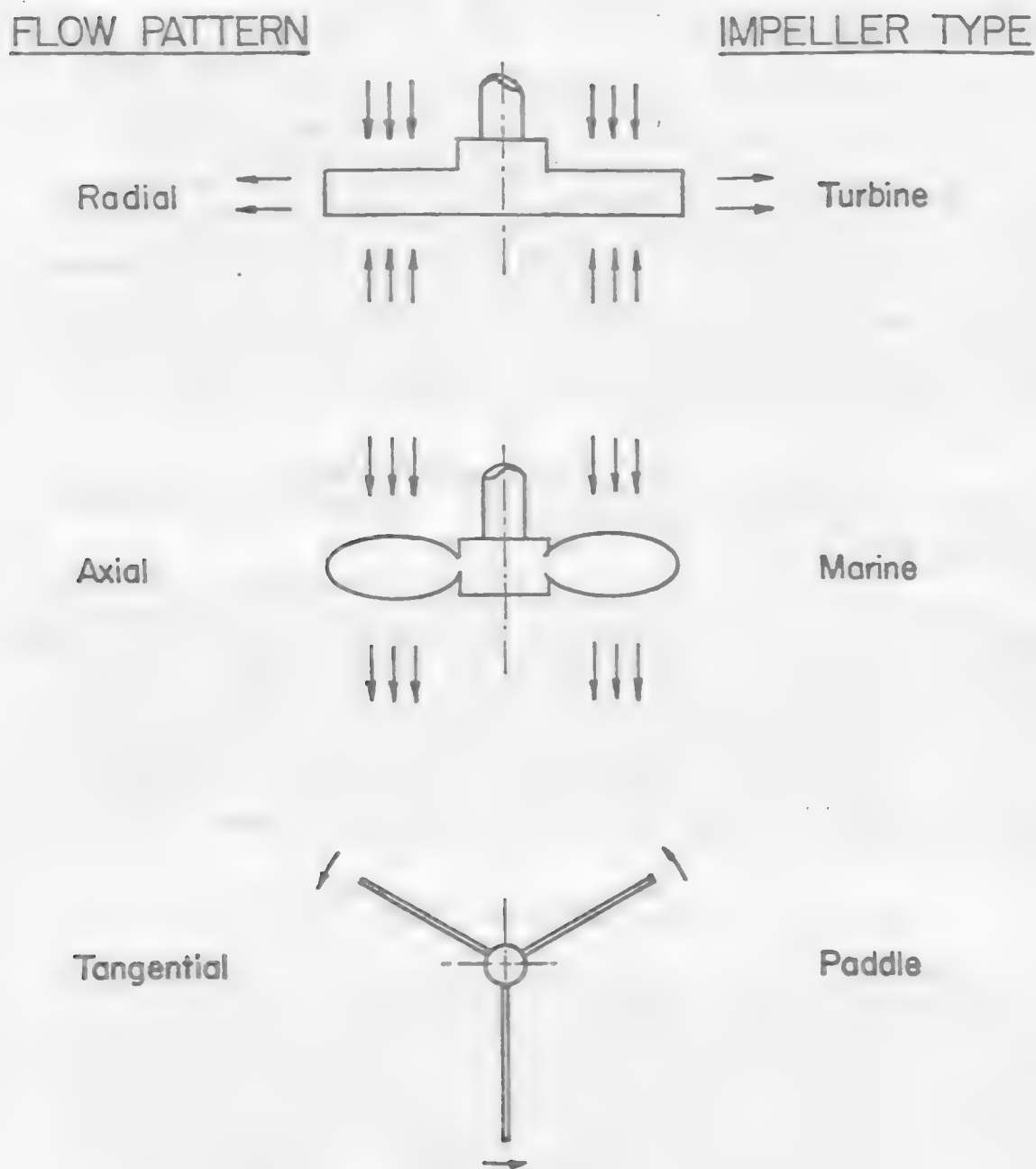
3.4.3.1 Impellers

When high intensive agitation is required for a hydrometallurgical process, the mechanical agitation vessel may be necessary. Normally the mechanical agitation is provided by means of an impeller. Impellers can be included in many types of tanks.

Normally the impellers have been classified according to their physical form, i.e., propeller, paddle and turbine. The first type creates axial flow, the paddle creates tangential flow and the turbine creates both axial and radial flow. The type of flow created by an impeller depends on the angle the blade makes with the shaft. Turbine and paddles have an angle less than 90 degrees. Schematic diagrams of a propeller, turbine and paddle and their flow patterns are shown in Figure 3.4.5.

Propellers are essentially high-speed impellers of the axial-flow type (discharge flow parallel to the agitation shaft). Propellers may be used in low viscosity liquids almost without restriction as to the size and shape of the vessel.

Figure 3.3.5. Classification of Impellers by their flow pattern.



Source: Reference 2.

An often used propeller is the marine type which usually has three blades. The ratio between the total blade area (projected area) and the disk area ranges from 0.45 to 0.55. And the driving face of a blade is flat or concave while the back side is convex.

Turbines are impellers with essentially constant blade angle with respect to a vertical plane having blades either vertical or set at an angle less than 90° with the vertical shaft. Blades may be curved or flat. There are two basic physical forms of the turbine, the flat-blade radial discharge style and the pitched blade axial thrust type. The flat blade discharges radially, creating suction from both top and bottom. Customary operation is in a peripheral speed range from 600 to 900 ft/min. Blade widths are generally $1/5$ to $1/8$ of the vessel diameter. The pitch blade impeller has a constant blade angle over its entire blade length. Its flow characteristic is primarily axial but a radial component exists and can predominate if the impeller is located close to the tank bottom. The blade slope can be anywhere from 0° to 90° , but 45° is the commercial standard.

There are other modifications of the turbine impeller, but the performance is affected in only a minor way. Figure 3.3.6 illustrates the conventional turbines.

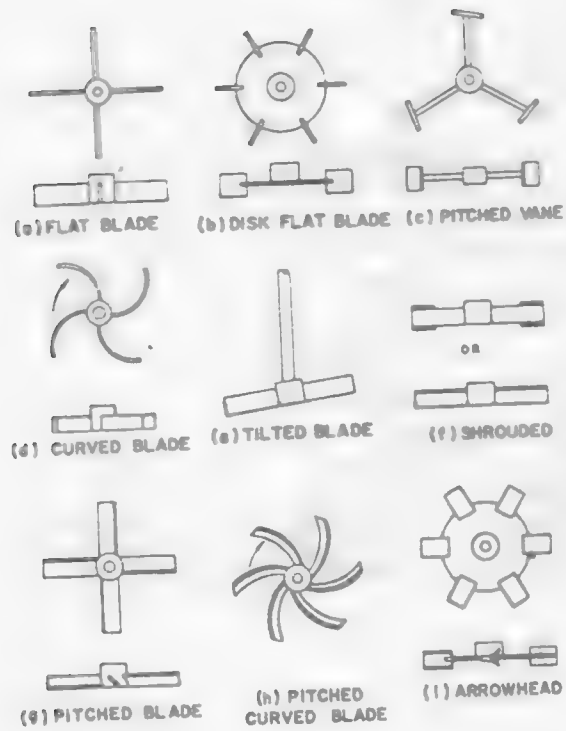
The physical form and the power correlation for the basic form of paddles is similar to the turbine type impeller. But it is worthwhile to retain the distinction for several reasons: the basic paddle is operated in a laminar range, or in the transition and turbulent range without baffles. Turbines are usually run at higher speeds. Paddles usually have large D/T ratio (D= diameter of the impeller, and T= diameter of the tank). And the basic paddle design is not particularly effective for many process operations involving high viscosities. A schematic diagram of the basic paddle and its modifications are shown in Figure 3.3.7.

3.4.3.2. Flow Pattern In Impeller Stirred Tank

Unbaffled tank: If a low-viscosity liquid is stirred in an unbaffled tank by an axially mounted agitator, there is a tendency for a swirling flow pattern to develop, regardless of the type of impeller. Figure 3.3.8 shows a typical flow pattern. The fluid moves in a circular pattern and the vertical velocity is low relative to the circumferential velocity. A vortex is produced because of the centrifugal force acting on the rotating fluid. This type of agitation, in fact, often results in separation rather than mixing. Increased vertical circulation rates may be obtained by mounting the impeller off center as illustrated in Figure 3.3.9.

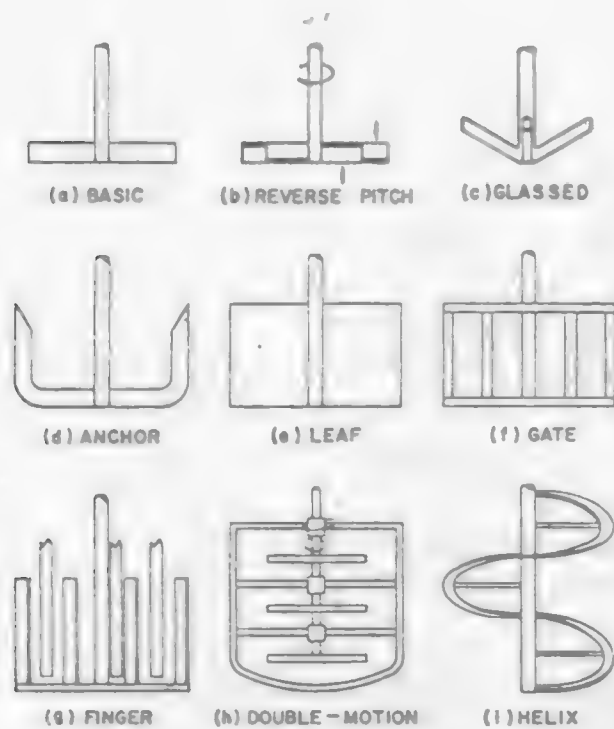
Baffled tank: For vigorous agitation of thin suspensions, a tank is provided with baffles which are flat vertical strips set radially

Figure 3.3.6. Turbine impeller designs.



Source: Reference 2.

Figure 3.3.7. Paddle impeller designs.



Source: Reference 2.

Figure 3.3.8. Typical flow pattern for either axial-or radial- flow impellers in unbaffled tank.

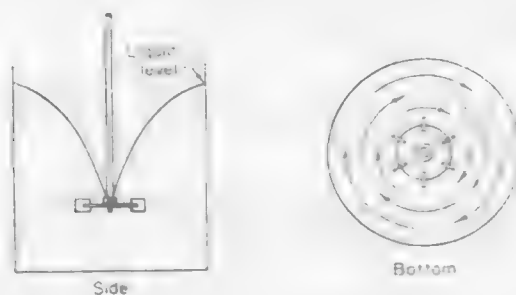
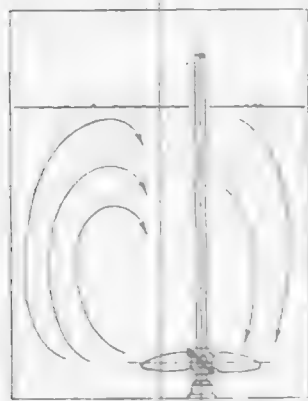


Figure 3.3.9. Flow pattern with paper-stock propeller, unbaffled vertical off-center position.



Source: Perry, Chem. Engr. Handbook, McGraw Hill

along the tank wall (illustrated in Figures 3.3.10 and 3.3.11). Four baffles are almost always adequate. A common baffle width is one-tenth to one-twelfth of the tank diameter. For agitating slurries, the baffles are located one half their width from the bottom of the vessel wall to minimize accumulation of solid on or behind them.

3.4.3.3 Energy Dissipation and Power Characteristic of Stirred Tanks

In a stirred tank the impeller continuously dissipates energy into the fluid by creating circulation and eddies in the fluid phase.

The motion of a single fluid phase is affected by first, the linear dimensions which fully define the geometrical boundary conditions such as the shape for the tank and impeller; second, the fluid properties such as density and viscosity, and third, the kinematic and dynamic characteristics of flow such as velocity, power input or resisting force and the forces of gravity.

Dimensional analysis gives the general equation for the relationship of these variables for stirred vessels:

$$f \left(\frac{D^2 N \rho}{\mu}, \frac{DN^2}{g}, \frac{Pg_c}{\rho N^3 D^5}, \frac{D}{T}, \frac{D}{Z}, \frac{D}{C}, \frac{D}{P}, \frac{D}{W}, \frac{D}{L}, \frac{n_2}{n_1} \right) = 0$$

[3.3.1]

where D = impeller diameter,
 T = tank diameter,
 Z = liquid depth,
 C = clearance of impeller of vessel bottom,
 W = blade width
 P = pitch of blades,
 n = number of blades
 L = blade length
 ρ = density
 μ = viscosity
 P = Power
 N = impeller rotational speed
 g = gravitational acceleration
 g_c = Newton's law conversion factor.

For two agitation systems to be similar, all groups in Equation 3.3.1 have to be equal in the compared systems. The last seven terms in Equation 3.3.1 represent the condition of geometric similarity which requires that all corresponding dimensions in systems of different sizes bear the same ratio to each other.

Given geometric similarity, two systems are dynamically similar when the ratios of all corresponding forces are equal. Kinematic

Figure 3.3.10. Typical flow pattern in baffled tank with propeller or axial-flow turbine positioned on center.

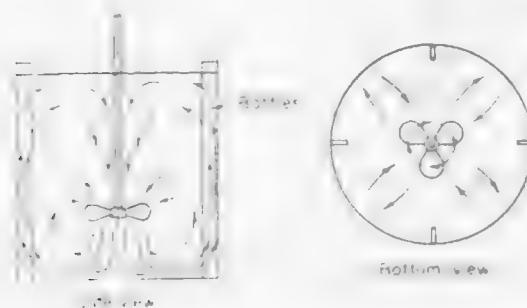
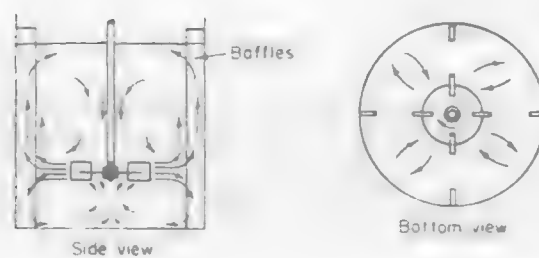


Figure 3.3.11. Typical flow pattern in baffled tank with turbine positioned on center.



Source: Perry, Chem. Eng. Handbook, McGraw-Hill

similarity requires that velocities at corresponding points be in the same ratio. Equation 3.3.1 can be reduced to:

$$f\left(\frac{D^2 N \rho}{\mu}, \frac{DN^2}{g} \frac{Pg_c}{D^5 N^3 \rho}\right) = 0 \quad [3.3.2]$$

where $\frac{D^2 N \rho}{\mu} = Re$, Reynolds number

$\frac{DN^2}{g} = Fr$, Froude number

$\frac{Pg_c}{D^5 N^3 \rho} = Pw$, Power number, equivalent to friction factor

Equation 3.3.2 can be rearranged to yield:

$$Pw = K_1 (Re)^a (Fr)^b \quad [3.3.3]$$

In presenting data graphically, the usual technique in fluid flow is to plot the Reynolds number on the abscissa in a logarithmic plot. To facilitate this, Equation 3.3.3 can be rewritten:

$$\phi = \frac{Pw}{(Fr)^b} = K_1 (Re)^a \quad [3.3.4]$$

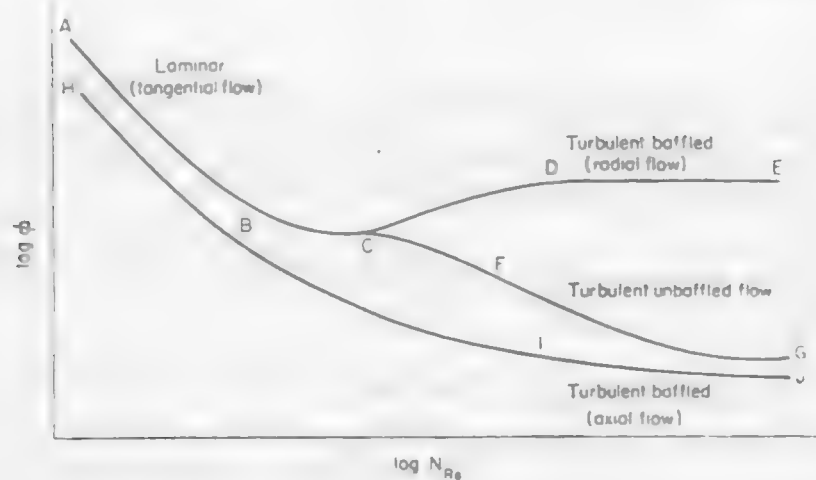
For a fully baffled tank, the Froude number is generally important. The exponent b is equal to zero, and $\phi = Pw$. Typical curves of ϕ vs Re are shown in Figure 3.3.12 for configurations often used in practice. For fully baffled conditions, and in the laminar range ϕ can be assumed to be Pw .

The value of ϕ as a function of Reynolds number for propeller impellers is shown on Figure 3.3.13 under various conditions listed in Table 3.3.2. The correlation for turbine impellers in baffled vessels is shown in Figure 3.3.14. And the correlation for paddle impellers is shown in Figure 3.3.15. A detailed discussion on power data for stirred tank can be found in Reference 2.

The above discussion on the power correlation is necessary for a Newtonian fluid. The correlations still apply for non-Newtonian fluid, however, the viscosity of the fluid has to be determined under the condition of the operation. The viscosity is defined as

$$\mu = \frac{\tau_{3c}}{du/dr} \quad [3.3.5]$$

Figure 3.3.12. Characteristic impeller power curves.



Source: Reference 2.

Figure 3.3.13. Propeller power correlation.

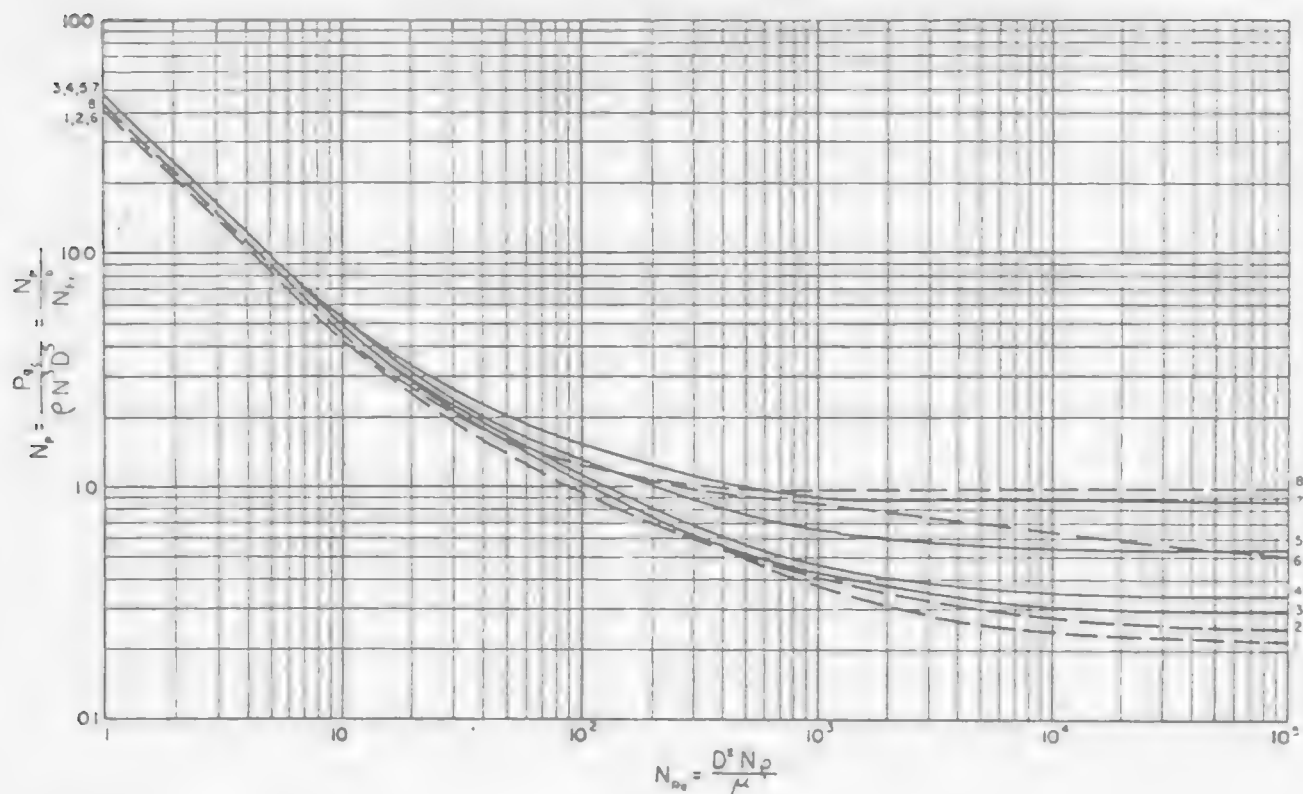
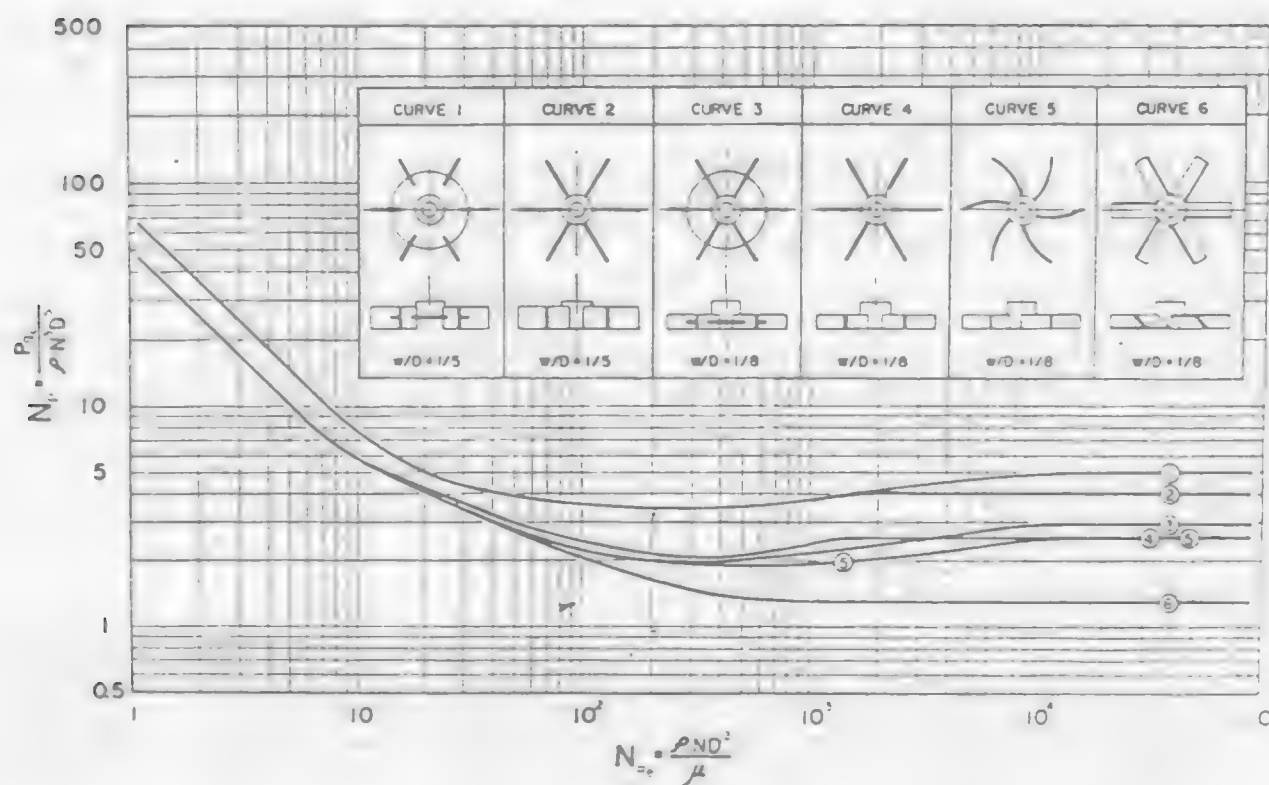
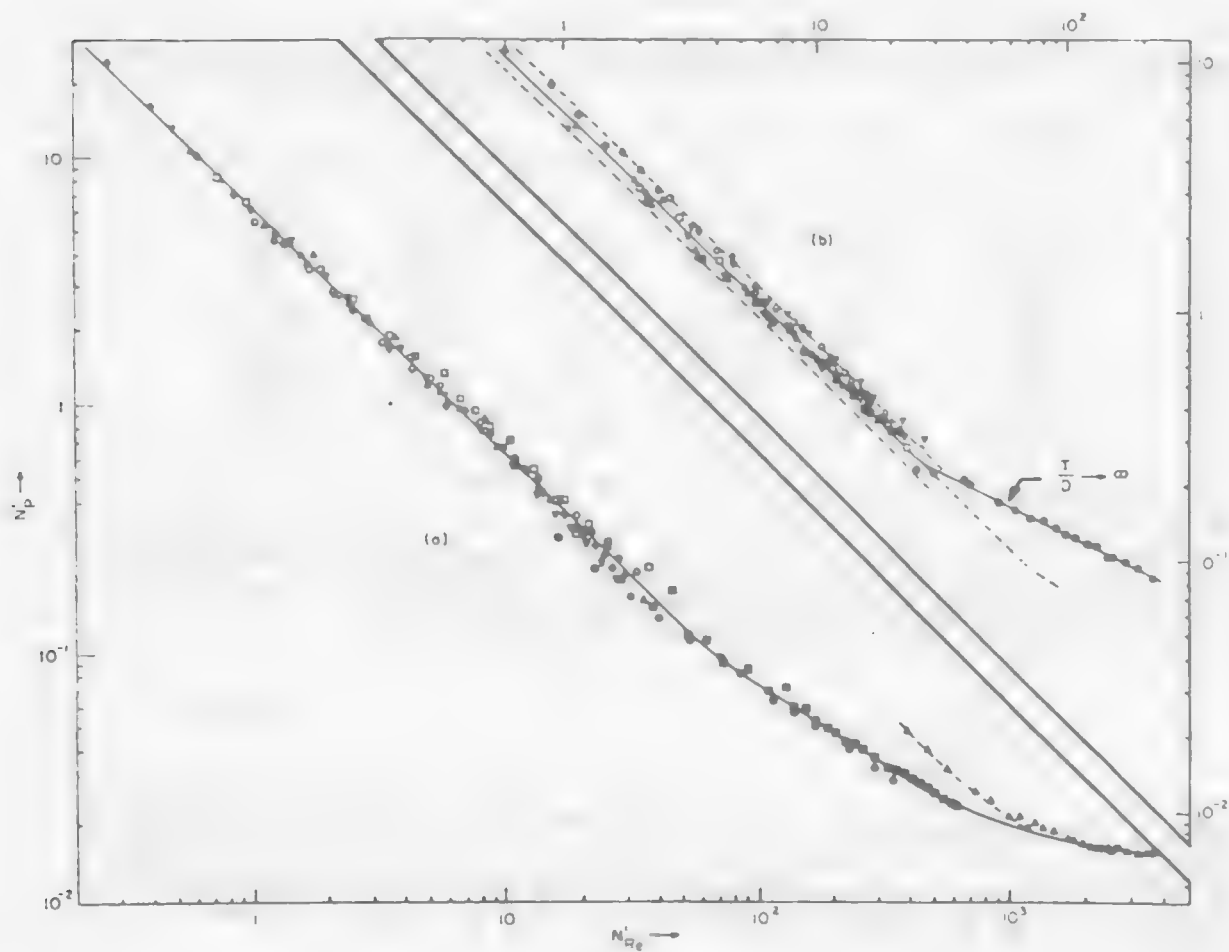


Figure 3.3.14. Turbine Power Correlation.



Source: Reference 2.

Figure 3.3.15. Power characteristics of peddles in Newtonian fluids:
(a) T and L, fixed; (b) T and L, varied.



Source: Reference 2.

where μ = viscosity
 τ = shear stress of the impeller
 du/dr = shear rate of the impeller
 u = velocity of the impeller blade.

Table 3.3.2. Values of ϕ for Three-Blade Propellers

Curve	Source	p/D	D/T	ϕ at Reynolds No. of		
				5	300	105
1 ^a	(R5)	1.02	0.33	8.3	0.60	0.22
2 ^a	(R5)	1.0	0.31	8.3	0.60	0.25
3	(B5)	1.0	0.40	9.7	0.75	0.30
4	(B5)	1.0	0.33	9.7	0.82	0.35
5	(B5)	1.4	0.33	9.7	1.04	0.54
6 ^a	(R5)	2.0	0.31	8.7	1.00	0.52
7	(R5)	1.8	0.30	9.7	1.27	0.86
8	(R5)	2.0	0.31	8.7	1.10	1.0

^aNo baffles

Figure 3.3.16 shows the fluid behavior for various models: Newtonian fluid Bingham plastic, pseudoplastic and dilatant fluid. The shear rate to the impeller speed is characterized by the equation:

$$\left(\frac{du}{dr}\right)_{av} = KN \quad [3.3.6]$$

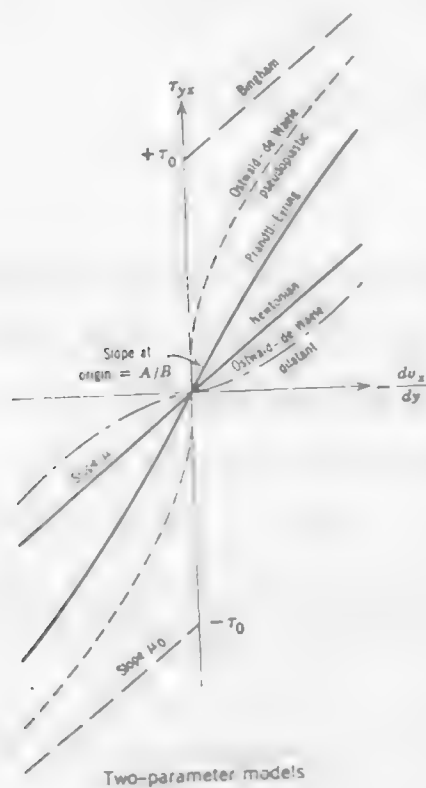
where K is a constant and N is the impeller speed. Once the viscometric curve (shear stress vs shear rate, Figure 3.3.16) for the fluid under study is obtained, then the viscosity can be calculated. And the power requirement can be predicted from a $Pw-Re$ plot by using a suitable Re number.

3.4.3.4 Suspension of Solid In A Stirred Tank

Slurry characteristics. Suspension of a solid in a liquid medium will be obtained when the rising velocity of the liquid phase equals or exceeds the settling velocity of the particles. The fluid flow pattern is a function of impeller and tank selection as previously mentioned. Particle settling velocity is a function of the gravitational force, fluid drag, and other hindering factors referred to below.

Settling velocity of particles may be calculated from empirical correlations of drag coefficient and particle Reynolds number:

Figure 3.3.16. Summary of steady-state non-Newtonian models (the Newtonian model is shown for reference).



$$\gamma^{\circ} = (\gamma_{\pm})^{1/z_1 z_2}$$

The correlations at 25° for strong electrolytes are shown by the family of curves presented in Figure 1.2.2. Each curve represents the behavior of a given electrolyte, so that when one value of γ° for a strong electrolyte is known at a given concentration, the entire curve for this salt can be estimated from Figure 1.2.2.

For example, if we want to determine the mean activity coefficient of KOH at a concentration of 9 molal, first the activity coefficient at some other molality must be found. From the literature, it is found that when $I = 2$, $\gamma_{\pm} = 0.863$ which corresponds to $\log \gamma^{\circ} = 0.064$. If this point is located on the correlation plot, the appropriate curve can be used to determine $\log \gamma^{\circ}$ at $I = 9$. Following this procedure, $\log \gamma^{\circ}$ is found to be 0.66 which corresponds to a mean activity coefficient of $\gamma_{\pm} = 4.57$. Location of the proper curve requires knowledge of at least one value of $\log \gamma^{\circ}$ at a given ionic strength.

In addition to this correlation, relationships have been established which allow calculation of the reduced activity coefficient for a given salt at temperatures other than 25°C and for mixed electrolyte systems.

1.2.3 Determination of Individual Ionic Activity Coefficients

Individual ionic activity coefficients can be determined by a number of techniques:

- experimental data (mean salt method)
- theoretical relationships (Debye-Huckle equation)
- empirical extension of theoretical relationships

Each technique has its own limitations which must be considered for a particular application.

Experimental Data

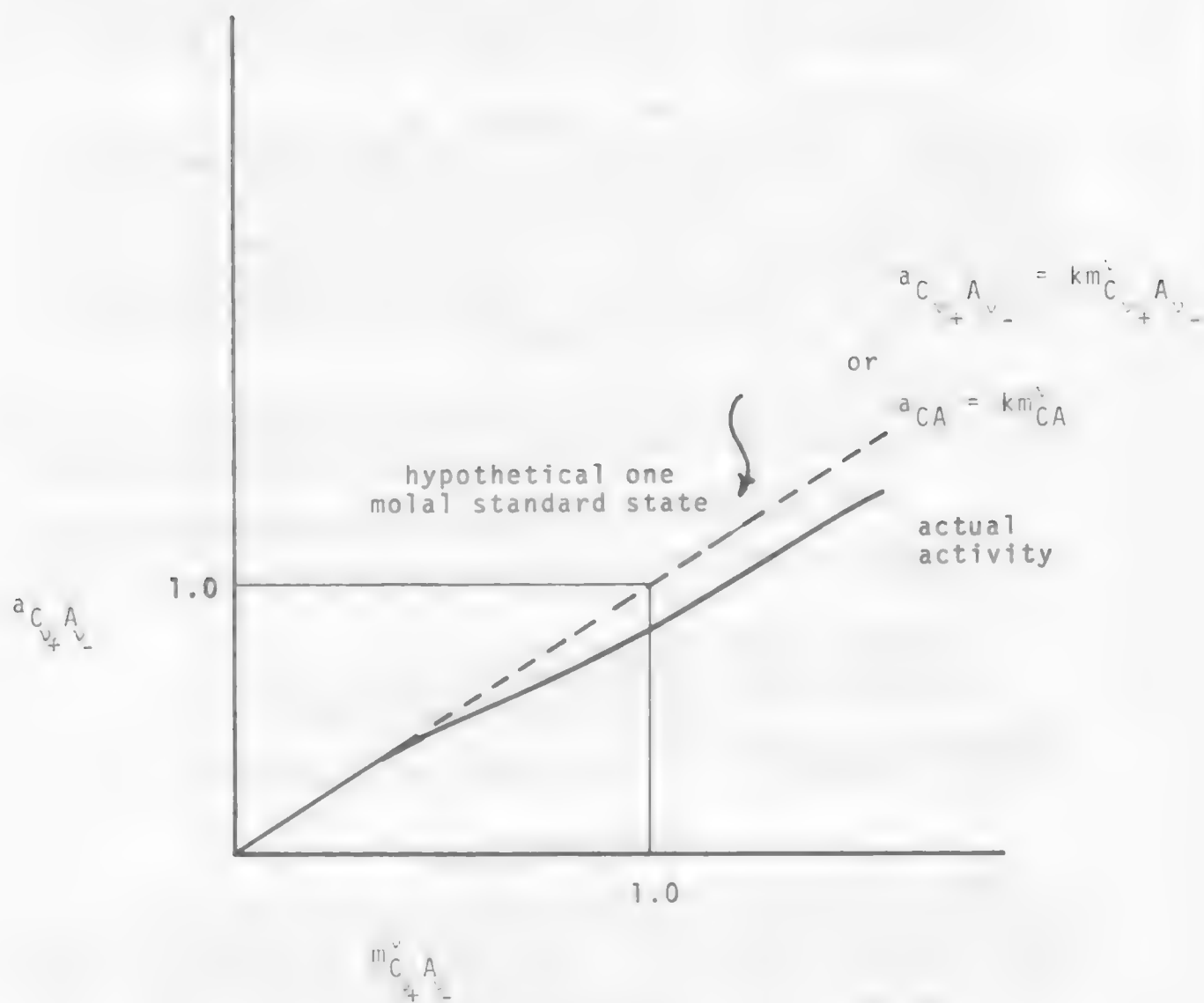
Experimental activity coefficient data is usually tabulated (Appendix A) or presented graphically with the mean activity coefficient as a function of ionic strength (Figure 1.2.3). Using this data to calculate individual ionic activity coefficients is accomplished by the *mean salt method*. The mean salt method is based on the MacInnes assumption that

$$\gamma_{\pm KCl} = (\gamma_K + \gamma_{Cl^-})^{1/2} = \gamma_K^+ = \gamma_{Cl^-} \quad [1.2.15]$$

From this relationship individual ionic activity coefficients can be calculated from experimental mean activity coefficient data at a specified ionic strength.

For example, the activity coefficient for cupric ion in 0.05 M copper sulfate solution assuming complete disassociation would be calculated in the following way:

Figure 1.2.1. Standard State for Solutes.



Drag coefficient

$$C_D = \frac{m_p(\rho_p - \rho)}{\rho_p A_p u^2} = \frac{4gd(\rho_p - \rho)}{3\rho u^2} \quad [3.3.7]$$

and particle Reynolds number

$$Re_p = \frac{d\rho u}{\mu} \quad [3.3.8]$$

where ρ and ρ_p = densities of the fluid and the particle, respectively

A_p = cross-section area of the particle

m_p = mass of the particle

d = diameter of the particle.

The empirical correlation between C_D and Re is shown in Figure 3.3.17.

The important parameters influencing the settling velocity are density difference between liquid and solid, size and shape of solid, and other factors summarized as follows⁽⁴⁾

1. Terminal velocity increases with an increase in
 - a. density of the discrete particle, and
 - b. mass of the discrete particle.
2. Terminal velocity decreases with a increase in
 - a. cross-sectional area of the particle
 - b. irregularity or roughness of the particle surface,
 - c. spread in size spectrum of the particles,
 - d. concentration of solids in the slurry
 - e. free space between particles, and
 - f. viscosity of the fluid medium.

Conditions 2c, d, and e lead to a state commonly termed "hindered settling." As a rule of thumb, the hindered settling can be assumed to exist with solids concentrations starting at about 40% by volume and higher. The settling rate is reduced by non-Newtonian behavior of the slurry.

Slurry Suspension in Stirred Tanks. Zwietering⁽⁵⁾ studied the slurry suspensions by using various type of impellers and liquids in baffled agitation tanks. He defined a critical speed N_c at which no

Figure 3.3.16. Summary of steady-state non-Newtonian models (the Newtonian model is shown for reference).

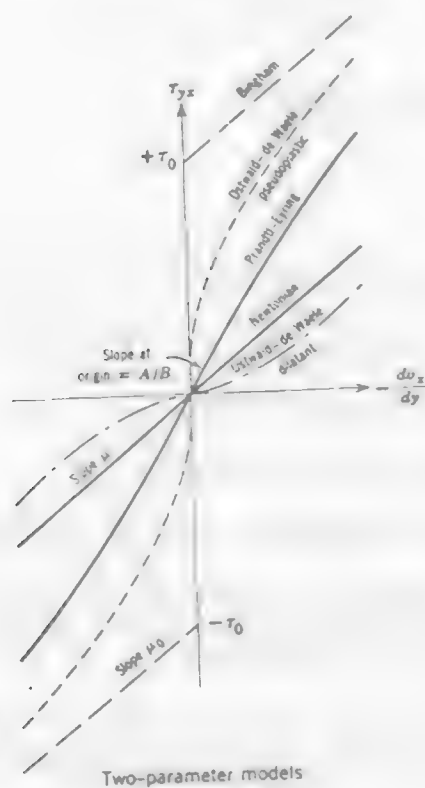
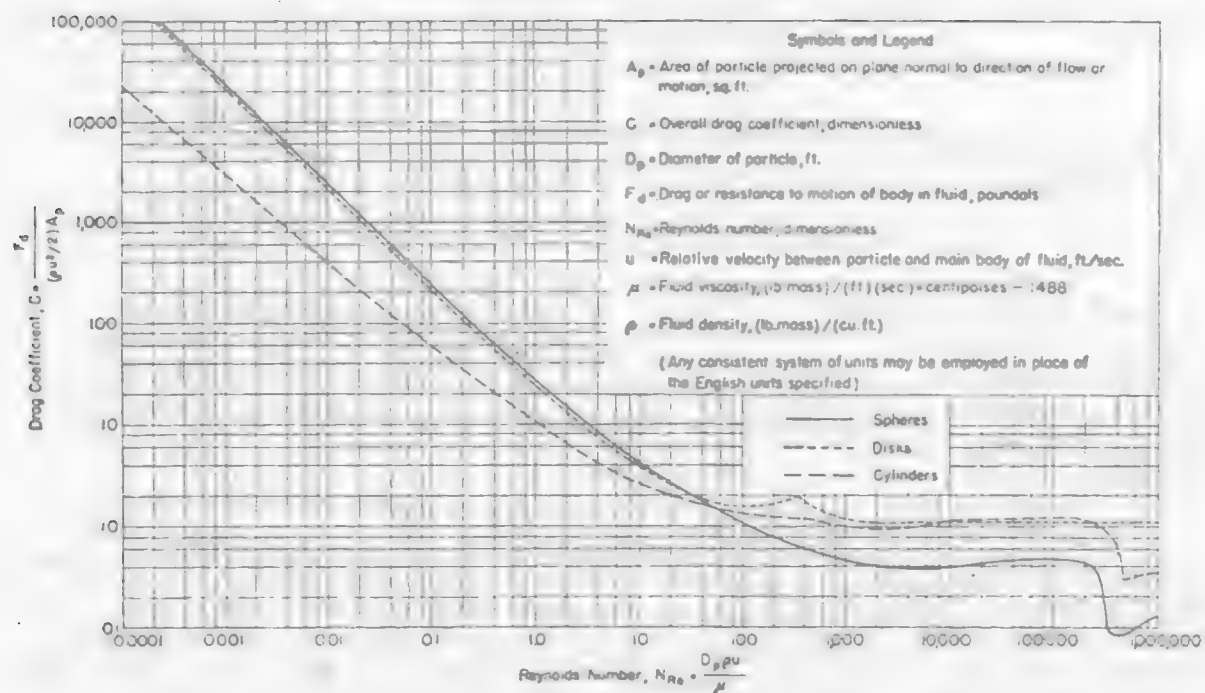


Figure 3.3.17. Drag coefficient for spheres, disks, and cylinders.



Source: Perry, Chemical Engineering Handbook, McGraw Hill

solids remained on the vessel bottom, as

$$N_c = \frac{\psi \left(\frac{T}{D}\right)^t g^{0.45} (\rho_p - \rho)^{0.1} d(100) R^{0.13}}{D^{0.85} \rho^{0.55}} \quad [3.3.9]$$

where R is the weight ratio of solid to liquid, and ϕ ranges from 1.0 to 2.0 (averaging 1.5) and the exponent, t , is approximately 1.4.

3.4.3.5 Mass Transfer To Particles In Agitation Tanks

Mass transfer between a fluid and small suspended particles is important in many industrial situations. The mass transfer from solid particles suspended in a liquid in an agitated vessel will be discussed briefly. The vessel is usually a cylinder with several vertical baffles fixed to the walls. The agitation is provided by a turbine or propeller impeller.

There are many variables involved in mass transfer to and from particles in agitation tanks, e.g., geometry of the vessel, nature of the baffles, type of impeller, speed of rotation, power input, and slurry density all vary with the vessel design and the type of operation. Physical variables include liquid density, viscosity, and molecular diffusivity of the fluid phase. The size distribution, shape, and density of the suspended particles may also be important. The diffusion into a porous particle and the rate of chemical reaction may complicate the reaction. It is not surprising that there is no reliable general correlation of mass transfer coefficients for such systems.

Herriott⁽⁶⁾ has recommended a method of predicting the mass transfer coefficient for particles suspended in baffled tanks. The procedure is summarized here:

Step 1. Calculate the terminal velocity and the corresponding Reynolds number based on the particle diameter. Use a density difference of 0.3 g/cc rather than the true value for very light particles. Depending on the Reynolds number of the particles, the terminal velocity can be calculated by Newton's law, intermediate law, or Stoke's law, which are listed on Table 3.3.3.

Table 3.3.3. Drag coefficient and terminal velocity for spheres

Law of settling	Settling Velocity	Drag Coefficient	Reynolds Number	Critical Particle diameter above which law will not apply
Stoke's law (laminar settling)	$u = \frac{gd^2(\rho_s - \rho)}{18\mu}$	$C = 24/(Re)_p$	$0.0001 < Re < 20$	$K_{cr} = 3.3$
Intermediate	$u = \frac{0.153g^{0.71}d^{1.14}(\rho_s - \rho)^{0.71}}{\rho^{0.29}\mu^{0.43}}$	$C = 18.5/(Re)_p^{0.6}$	$2.0 < Re < 500$	$K_{cr} = 43.5$
Newton's law (turbulent settling)	$u = 1.74 \sqrt{\frac{gd(\rho_s - \rho)}{\rho}}$	$C = 0.44$	$500 < Re < 200,000$	$K_{cr} = 2,360$

The critical particle diameter is defined as

$$d_{cr} = K_{cr} \left[\frac{\mu^2}{g(\rho_p - \rho)} \right]^{1/3} \quad [3.3.10]$$

The Reynolds number of a particle is defined as

$$Re = \frac{du\rho}{\mu} \quad [3.3.11]$$

Step 2. Calculate the mass transfer coefficient, k_c^* for a particle falling at its terminal velocity from the equation,

$$Sh = 2 + 0.6 Re^{0.5} Sc^{0.33}$$

where Sh = Sherwood number = $k_c^* d/D_r$

D_r = diffusivity of diffuse species

Sc = Schmidt number = $\mu/\rho D$

Step 3. Calculate the ratio of mass transfer coefficient, k , for a agitation system from the ratio k_c/k_c^* from Figure 3.3.18.

$$ND^{2/3}(D/T) (T/Z)^{1/3} = 200 \text{ in}^{2/3} \text{min}^{-1}$$

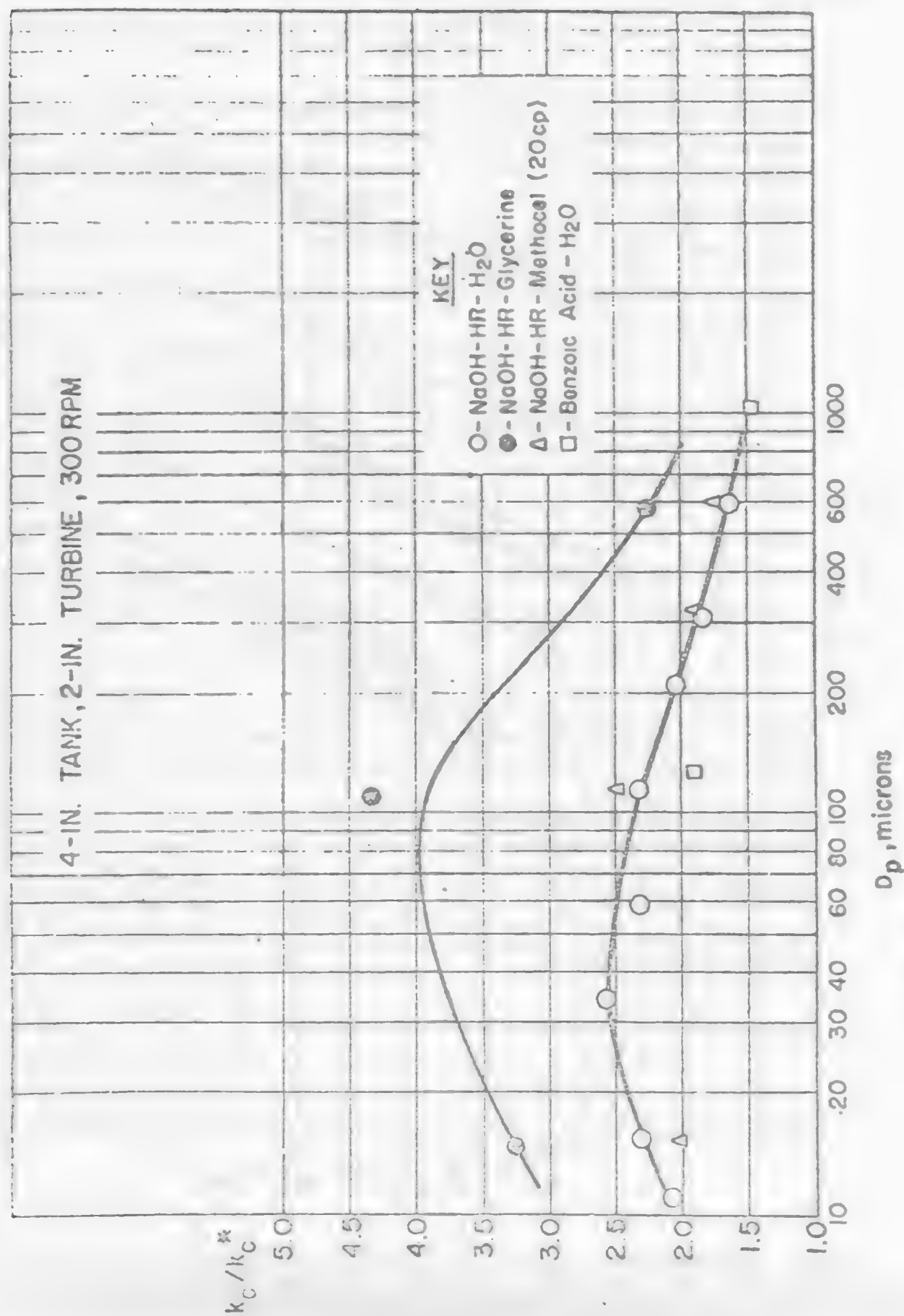
The symbols have been defined previously (Equation 3.3.1) and $D/T=0.5$.

In Figure 3.3.18, use the lower curve for $D \geq 10^{-5}$ cm²/sec and the upper curve for $D = 10^{-6}$ cm²/sec.

Step 4. Extrapolate to the given stirrer speed with the slopes of the line in Figure 3.3.10 (0.5 for particles larger than 100 μ and 0.3 for 15 μ particles). A slight correction can be made for low values of D/T .

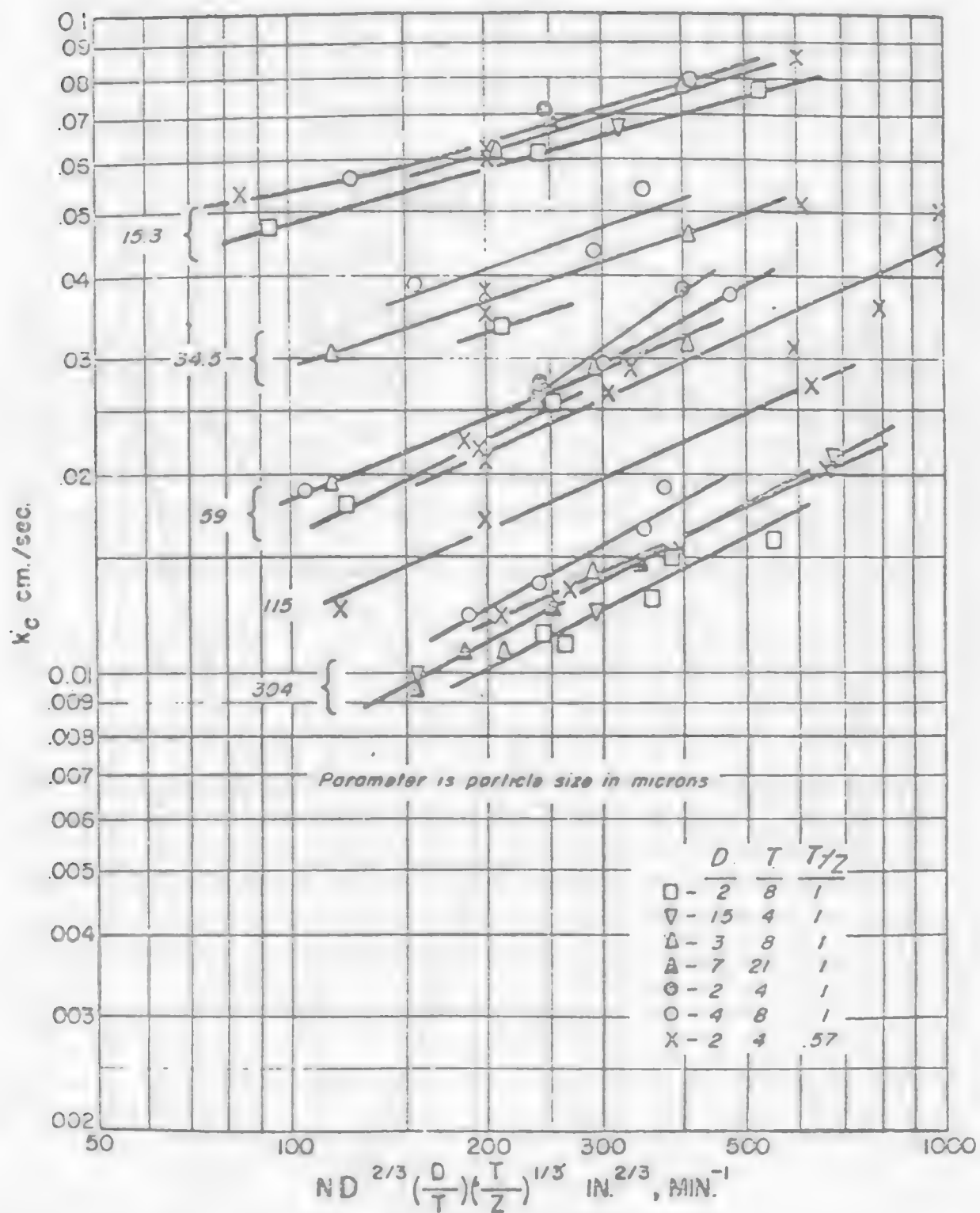
For impellers other than turbines the coefficients are probably between the values predicted for a turbine operating and at the same speed and operating at the same power consumption. For vessels where there is no impeller (mixing done by recirculating the liquid) or only intermittent stirring, the coefficient is probably 1.2 to 1.5 k_c^* .

Figure 3.3.18. Relation between standard mass transfer coefficient, k_c and minimum mass transfer coefficient, k_c^* .



Source: Reference 6.

Figure 3.3.19. Relation between mass transfer coefficient and agitation intensity, $ND^{2/3} \left(\frac{D}{T}\right) \left(\frac{T}{Z}\right)^{1/3}$, for various particle sizes.



Source: Reference 6.

3.4.4 References

1. A. G. W. Lamont, "Air Agitation and Pachuca Tanks," Canadian J. of Chem. Engr., August, 153 (1958).
2. R. L. Bates, P.L. Fondy and J. G. Fenic, "Impeller Characteristic and Power" Mixing, ed. by V.W. Uhl and J. B Gray, Vol I, Chap. 3 Academic Press (1967).
3. R. H. Perry and C. H. Chilton, Chemical Engineers Handbook, Chap. 19. 5th edition (1973).
4. E. J. Lyons, "Suspension of Solids", Mixing, ed. by V.W.Uhl and J.B Gray, Vol II, Chap. 9, Academic Press (1967).
5. T. N. Zwietering, Chem. Eng. Sci, 8, 244 (1958).
6. P. Harriott, "Mass Transfer to Particles: Part 1. Suspended in Agitated Tanks", AIChE. J. 8, No. 1, 93 (1962).

LEARNING ACTIVITY 4

Learning Activity Objective

After completing your study of this learning activity material you should be able to describe the fundamental features of three basic chemical reactors; you should be able to list the important parameters that govern the design of a reactor; and you should be able to complete a design work sheet.

3.5 Reactor Design

3.5.1 Types of Reactors⁽¹⁾

In reactor design we are asked to determine the size and type of reactor and method of operation which are best to accomplish a given task. There are many factors involved in predicting the performance of a reactor, such as time, rate of production, concentrations, temperature, rate of reaction, geometry of the reactor, flow pattern and mixing in the reactor.

Broadly, the reactors encountered in chemical production can be categorized into three general types: the batch, the plug flow, and the mixed flow (continuous agitation) reactors. The basic features and the ideal application of these reactors are discussed in this section.

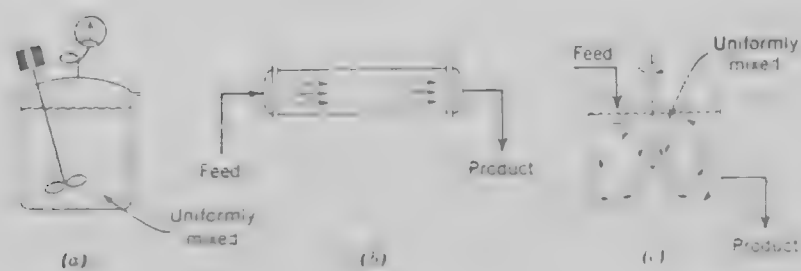
In the ideal batch reactor shown in Figure 3.4.1a the reactants are initially charged into a container, are well mixed and are left to react for a certain period of time. The resultant mixture is then discharged. This is an unsteady state operation where the composition changes with time, however, at any instant the composition throughout the reactor is uniform. The resident time of the reactant in the reactor is simply the time of operation.

The batch reactor is simple, easy to control, needs little supporting equipment, and is, therefore, ideal for small-scale experimental studies on reaction kinetics. Industrially it is used when relatively small amounts of material are to be treated.

The plug flow and mixed flow reactors are operated under steady-state conditions. The reactants are continuously charged to the reactor and the reaction products are simultaneously discharged from the reactor. The steady-state flow reactor is ideal for industrial purposes when large quantities of material are to be processed and when the rate of reaction is fairly rapid. These reactors require a large amount of supporting equipment; however, extremely good product equality can be obtained.

The plug flow reactor is also known as a piston, tubular or unmixed flow reactor. Ideally, the flow of the fluid through the reactor is orderly with no element of fluid overtaking or mixing with any other

Figure 3.4.1. The three types of ideal reactors: (a) batch reactor, (b) plug flow reactor, and (c) mixed flow reactor.



Source: O. Levenspiel, Chemical Reaction Engineering, John Wiley

fluid element ahead of it or behind it. There may be lateral mixing of fluid in a plug flow reactor; however, there must be no mixing or diffusion along the flow path. The necessary and sufficient condition for plug flow is for the residence time in the reactor to be the same for all elements of fluid. The results of a impulse response tracer test⁽¹⁾ for an ideal plug flow reactor is shown in Figure 3.4.2a, which indicated that all the tracer elements injected into the reactor are retained in the reactor for the same time.

The resident time of a packed bed reactor can be calculated by the equation:

$$\bar{t} = \frac{V\epsilon}{v_0} \quad (\text{time}) \quad [3.4.1]$$

where \bar{t} = resident time

V = volume of the reactor

v_0 = volume flow rate of the fluid

ϵ = voidage of the packed-bed.

For homogeneous reaction, the resident time will simply be

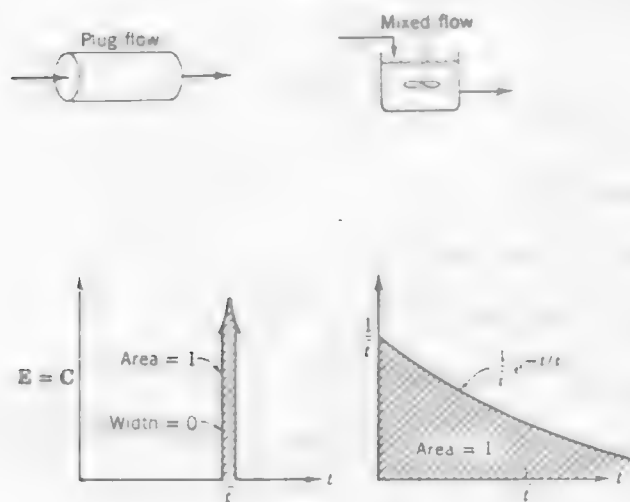
$$\bar{t} = \frac{V}{v_0} \quad [3.4.2]$$

The other ideal steady-state flow reactor is called the mixed reactor, the backmix reactor, the ideal stirring tank reactor or continuous agitation reactor. It is a reactor in which the contents are well stirred and uniform through. Thus the exit stream from this reactor has the same composition as the mixer within the reactor.

Unlike a plug flow reactor in which all the elements of the fluid stay the same amount of time in the reactor, in the mixed flow reactor the element of the fluid or slurry takes different routes through the reactor which may require different lengths of time to pass through the vessel. The distribution of the times of the stream of fluid or slurry leaving the vessel is called the resident time distribution. The response of impulse tracer test for an ideal mixed flow is shown in Figure 3.4.2b. The resident time distribution for a ideal mixed flow can be derived mathematically, and the results are

$$E(t) = \frac{1}{\bar{t}} e^{-t/\bar{t}} \quad [3.4.3]$$

Figure 3.4.2. Properties of the E curve for various flows. Curves are drawn in terms of ordinary time units.



Source: O. Levenspiel, Chemical Reaction Engineering, John Wiley

where E is the resident time distribution

$E dt$ is the fraction of exist stream having a resident time between t and $t + dt$,

\bar{t} is the average retention time which is equal to V/v_0

where V , v_0 are volume of the reactor, and the volume flow rate of the reactant, (Note: for fluid-particle reactions, the volume can be taken as the particle-free volume or volume of particles plus fluid as long as volume flow rates and kinetic terms are defined in a consistent fashion).

3.5.2 Design Parameters

3.5.2.1 Review of the Kinetics Of Fluid Particle Reaction

This topic has been discussed in detail previously in Module 2, Learning Activity 6.

Recall that fluid-particle reactions can be ideally described by two models: the progressive-conversion model and the shrinking-core model. Due to physical characteristics of most particles, the shrinking core model approximates real leaching systems better, in most cases, than does the progressive-conversion model.

Because of the irreversible character of most leaching reactions, the rate of the leaching reaction (when the shrinking core model controls the rate) can be controlled by any one of the following steps:

1. transfer of mobile species in the fluid phase across the the fluid film by diffusion and convective mass transfer
2. transfer of mobile species in the fluid phase across the solid product layer by pore diffusion or solid state diffusion to the reaction interface
3. chemical reaction at the unreacted core/product layer interface (involves solid species and mobile species).

The rate equations for each controlling step are usually expressed in terms of the fraction of solid reacted, α , which primarily depends on the rate constant, the diffusivity of the mobile species, the stoichiometry, the concentrations of the mobile species and the solid, particle size etc. The integrated rate equations are summerized in Table 3.4.1 for the case of the formation of a product layer and for the case of a

shrinking particle (without the formation of product layer).

Table 3.4.1 Rate Equations for Shrinking Core Model

A. Formation of Product Layer $aA_{(s)} + bB_{(f)} \rightarrow cC_{(s)} + dD_{(f)}$ [3.4.4]

1. Film Diffusion Controls

$$\text{Equation: } \alpha = \frac{6 a k_m C_{B(b)} t}{b \rho_A d} \quad [3.4.5]$$

2. Product Layer Controls

$$\text{Equation: } 1 - \frac{2}{3} \alpha - (1 - \alpha)^{2/3} = \frac{8 a D_{B(\text{eff})} C_{B(b)} t}{b \rho_A d^2} \quad [3.4.6]$$

$$\text{or } \alpha = 1 - \left[\frac{1}{2} + \cos\left(\frac{3\theta_1 + 4\pi}{3}\right) \right]^3 \quad [3.4.7]$$

$$\text{where } 3\theta_1 = \cos^{-1}\left(\frac{2t}{L} - 1\right)$$

$$L = \frac{b \rho_A d^2}{8 a D_{B(\text{eff})} C_{B(b)}}$$

3. Surface Reaction Controls

$$\text{Equation: } 1 - (1 - \alpha)^{1/3} = \frac{4 a k_s C_{B(b)}^n t}{b \rho_A d} \quad [3.4.8]$$

$$\alpha = 1 - \left(1 - \frac{4 a k_s C_{B(b)}^n t}{b \rho_A d}\right)^3 \quad [3.4.9]$$

B. Shrinking Particle $aA_{(s)} + bB_{(f)} \rightarrow dD_{(f)}$ [3.4.10]

1. Film Diffusion Controls

$$\text{Equation: } 1 - (1 - \alpha)^{2/3} = \frac{8 a k_m C_{B(b)} t}{b \rho_A d^2} \quad [3.4.11]$$

$$\text{or } \alpha = 1 - \left(1 - \frac{8 a k_m C_{B(b)} t}{b \rho_A d^2}\right)^{3/2} \quad [3.4.12]$$

Table 3.4.1. (Continued)

2. Product Layer Diffusion: Not applicable
3. Surface Reaction Controls: Same as surface reaction controls formation of product layer

Symbols: a, b = stoichiometric coefficients of solid species A, and liquid species B, respectively

$k_m, k_s, D_{B(\text{eff})}$ = mass transfer coefficient of mobile species B, rate constant of chemical reaction, and effective diffusivity of mobile species B through the product layer, respectively

ρ_A = molar density of solid A = mole of A/cc of solid

$C_{B(b)}$ = concentration of B in bulk phase

n = reaction order

d = initial diameter of the solid.

α = fraction of solid reacted.

Normally in each leaching system, the $\rho_A, k_m, k_s, D_{B(\text{eff})}, a$, and b are constant. As a result, the fraction of solid reacted, α , varies with, time, t , concentration of reactant, $C_{B(b)}$ and the initial particle size, d , e.g. $\alpha = f(t, d, C_B)$.

The parameters in each equation can be estimated empirically from batch tests where mono-size particles are usually used. (see Module 2 for details).

3.5.2.2 Concentration Of The Lixiviant

The concentration of the lixiviant in most leaching systems is depleted as the reaction proceeds. The amount of depletion corresponds to the amount of the metal value dissolved according to each stoichiometric equation. For example, the change in concentration of the lixiviant for reactions [3.4.4] and [3.4.10] is :

$$C_{B(o)} - C_{B(t)} = \frac{b}{a} \alpha(t) M_I \quad [3.4.13]$$

where $C_{B(o)}, C_{B(t)}$ = concentrations of lixiviant at time zero or before charging to the reactor, and at time t , respectively.

M_I = total moles of solid A/unit volume of the liquid in the feed, which is = $f_v \rho_A / (1 - f_v)$

f_v = volume fraction of solids in the inlet

$\alpha(t)$ = fraction of solid reacted at time, t .

Another important parameter that governs the design of a reactor is the particle size distribution which has been briefly discussed in Learning Activity 1 of this module.

3.5.3 Modeling and Design for Continuous Leaching System*

3.5.3.1 Symbols and Notations

Most of the symbols used in this section are listed in Table 3.4.2. The unlisted symbols have been defined previously.

Table 3.4.2. Symbols and Notations for Designing A Continuous Leach Vessel

A. Notations: PLD = Product Layer Diffusion

SR = Surface Reaction

MK = Product Layer Diffusion and Surface Reaction Mixed Kinetic Control

MT = Mass Transfer

B. Dimension Quantities for Continuous Leaching

$\bar{\alpha}(t)$ = total fraction of solid reacted for a given average retention time and particle size distribution

$\alpha(C_B, d, t)$ = fraction of solid reacted for a given concentration of lixiviant, initial particle size and retention time

d_{\max}, d_{\min} = maximum and minimum size of a given size distribution

d = initial size

$C_{B(o)}, C_B$ = concentration of lixiviant in inlet and outlet of a continuous leach vessel

$f_3(d)$ = particle size distribution in weight

$E(t)$ = resident (retention) time distribution

\bar{t} = average resident time = V/Q

V = volume of the reaction vessel

Q = volume flow rate to the leaching vessel

*Coordinator Comment: The following material was provided by Dr. J.A. Herbst, professor of Metallurgical Engineering, University of Utah.

Table 3.4.2. (continued)

a, b, c = stoichiometry coefficients in the general leaching reaction:



D_B = effective diffusivity of lixiviant species B across the semiporous product layer, (Area/time). (If PLD does not influence the overall rate of reaction, set $D_B = \infty$)

k_S = surface reaction rate constant (length/time). (If SR does not influence the overall rate of reaction, assume $k_S = \infty$)

k_m = mass transfer coefficient (length²/time, if unknown, assume $k_m = \infty$)

ρ_A = molar density of the valuable A (moles/vol solid)

ρ_C = molar density of the solid product layer (moles/vol solid)
(If unknown, set equal to $(c/a)\rho_A$)

μ = mean particle size of the solids in the inlet, (length)

σ^2 = variance of the inlet size distribution, (length²)

f_V = volume fraction of solids in the inlet

C. Dimensionless Quantities for Continuous Leaching

Particle Size $d^* = d/\mu$

Unreacted Core Size $d_c^* = d_c/\mu$

Lixiviant Concentration $C^* = C_B/C_{B0}$

2. Dimensionless Parameters:

Variance $\sigma^{*2} = \sigma^2/\mu^2$

Product Volume $z^* = c\rho_A/a\rho_C$

Reaction Times $t_{SR}^* = t_{SR}(\mu)/t_c(\mu)$

$t_{PLD}^* = t_{PLD}(\mu)/t_c(\mu)$

$t_{FD}^* = t_{FD}(\mu)/t_c(\mu)$

Stoichiometry Number $\eta^* = \frac{(a/b)(1-f_V)C_{B0}}{f_V\rho_A}$

Mean Residence Time $\tau^* = \tau/t_c(\mu)$

3.5.3.2 Description of Governing Equations

The agitation leaching vessel plays an important role in modern hydrometallurgy. The selection of an appropriate size of vessel (s) for continuous leaching and the optimization of operating conditions for these vessels can be greatly facilitated by developing accurate mathematical models (abstractions) of these unit operations.

This section considers the modeling, simulation and design of a single stage, perfectly mixed leaching vessel (see Figure 3.4.3) in which a topochemical shrinking core leaching reaction occurs.

In designing the size of the reactor, two rate equations have to be solved simultaneously. These equations are the rate at which solid A dissolves, and the rate at which lixiviant is consumed. The amount of solid A that is dissolved can be expressed as 1-fraction of the solid (unreacted) will be the sum of unreacted portion of each particle at a given retention time, that is

Solid conversion

fraction of 1-(total solid A reacted at a given average retention time) =	$\sum_{d_{\min}}^{d_{\max}}$	$\sum_{d_{\min}}^{d_{\max}}$	(1 - fraction of solid reacted at a given particle size, concentration of lixiviant and retention time)	(density function of particle size distribution)	(retention time distribution)
--	------------------------------	------------------------------	---	--	-------------------------------

$$\therefore 1-\bar{\alpha}(t) = \int_0^{\infty} \int_{d_{\min}}^{d_{\max}} (1-\alpha(d, C_B, t)) f_3(d) E(t) d(d) d(t) \quad [3.4.14]$$

where $E(t)$ = retention time distribution = $\frac{1}{\bar{t}} e^{-t/\bar{t}}$

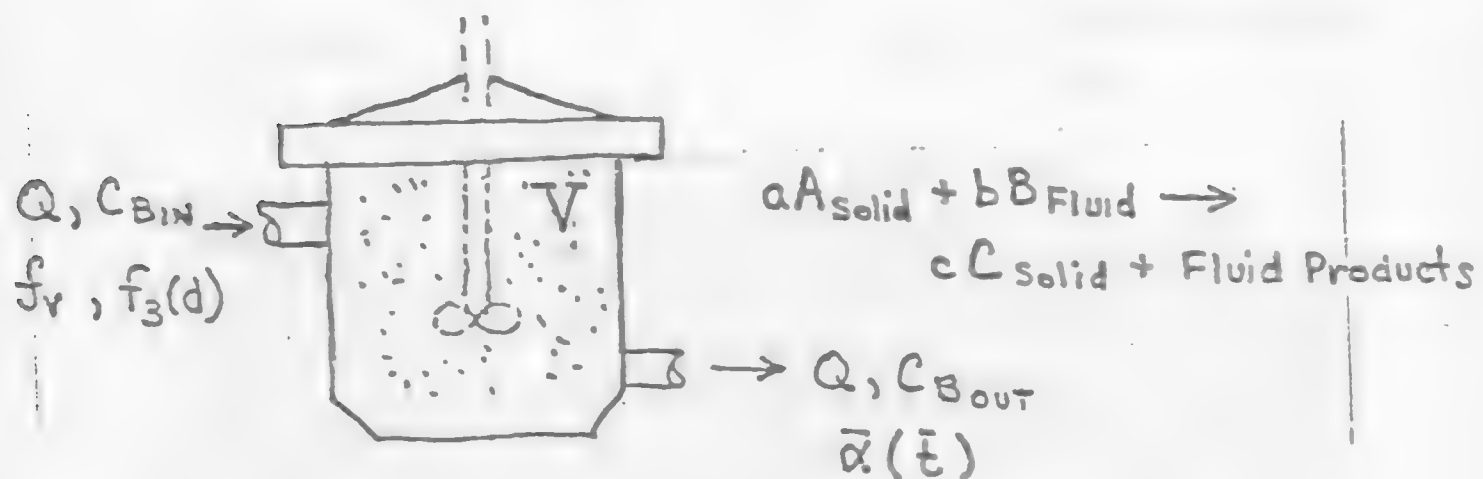
The overall mass balance for the lixiviant yields equations [3.4.13] and [3.4.14].

Lixiviant consumption

$$C_B = C_{B(o)} - \alpha \left(\frac{b}{a} \right) M_I \quad [3.4.13]$$

Equations 3.4.13 and 3.4.14 have to be solved simultaneously. For a given overall fraction reacted the average retention time can be determined, consequently the size of the reactor vessel can be estimated

Figure 3.4.3. Ideal continuous mixed flow reactor for fluid solid reaction.



by knowing the volume feed rate.

The governing equations, 3.4.13 and 3.4.14, for the reactor design can be combined into a dimensionless form:

Solid conversion:

$$\alpha(\tau^*) = 1 - \int_0^{\infty} \int_{d_{\max}^*}^{\infty} (1 - \alpha(d^*, C_B^*, t^*)) f(d^*) E(t^*) d(d) d(t) \quad [3.4.15]$$

Lixiviant consumption:

$$C_B^* (\tau^*) = 1 - \frac{\alpha}{\eta^*} \quad [3.4.16]$$

3.5.3.3 Results from Computer Simulation

Figure 3.4.4 illustrates the simulation results for the total fraction of solid reacted as the function of dimensionless time, τ^* , for a product layer diffusion controlled reaction and the distribution of particle size having a variance of 0.5 for a dimensionless stoichiometry number η^* from 1.0 to ∞ . Notice that η^* is proportional to the lixiviant concentration. As can be seen the rate increases as the η^* value increases. Figure 3.4.5 illustrates the effect of the size distribution on the rate of the extraction in which the dimensionless variance σ^* increases from 0.15 to 1.50. As can be seen in Figure 3.4.5 (same condition except for difference in variance of the size distribution), the rate of the reaction is faster initially for a larger distribution variance. However, for longer reaction times, the rate of reaction for the larger variance case becomes slower. This is reasonable because a particle size distribution with a larger variance contains a larger portion of small particle sizes. This will result in a faster initial rate of reaction. However, a larger variance also contains a greater portion of large particles which will require longer times for complete reaction. Consequently the rate of reaction is reduced as the reaction proceeds.

3.5.3.4 Design Worksheet and Example

The following is a design worksheet and calculation which will lead to the desired size of the agitation vessel required.

Example: Suppose you are a process engineer asked to design the continuous agitation reactor to leach metal value A by using lixiviant B. The concentrate A has a concentration ρ_A of 7×10^{-4} mole A/cc of solid, and the particle size distribution is as listed in Table 3.4.4. The fraction of the solid in the slurry is 0.204 and the slurry contains a lixiviant concentration of 5.1×10^{-4} mole/cc. You would like the reactor to be able to handle the slurry at 20 gal/min and to leach 90% of metal value.

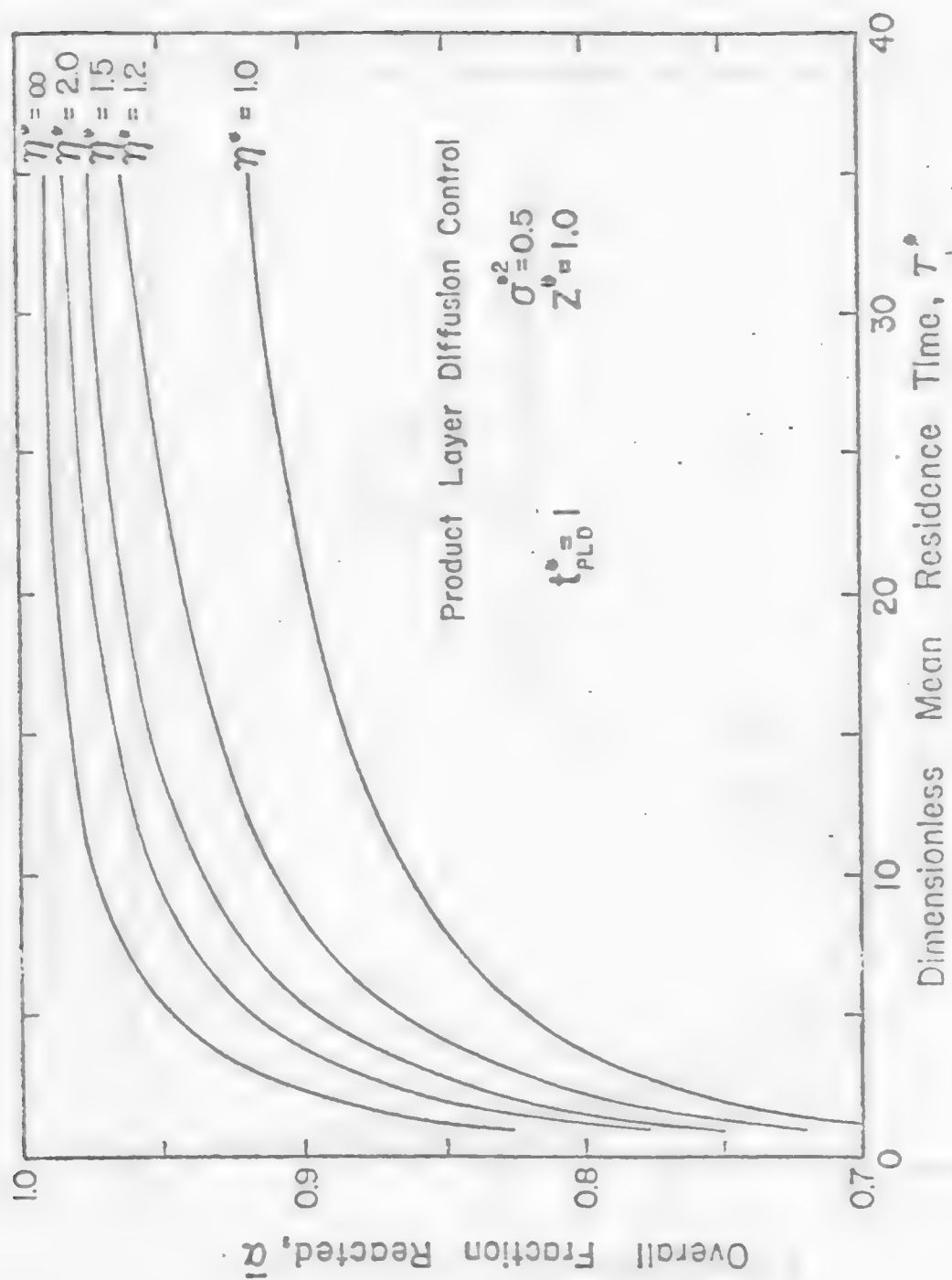


Figure 3.4.4. Computer simulation of the effect dimensionless retention time on conversion for product layer diffusion control ($t_{PLD}^* = 1$, $T^* = 1$).

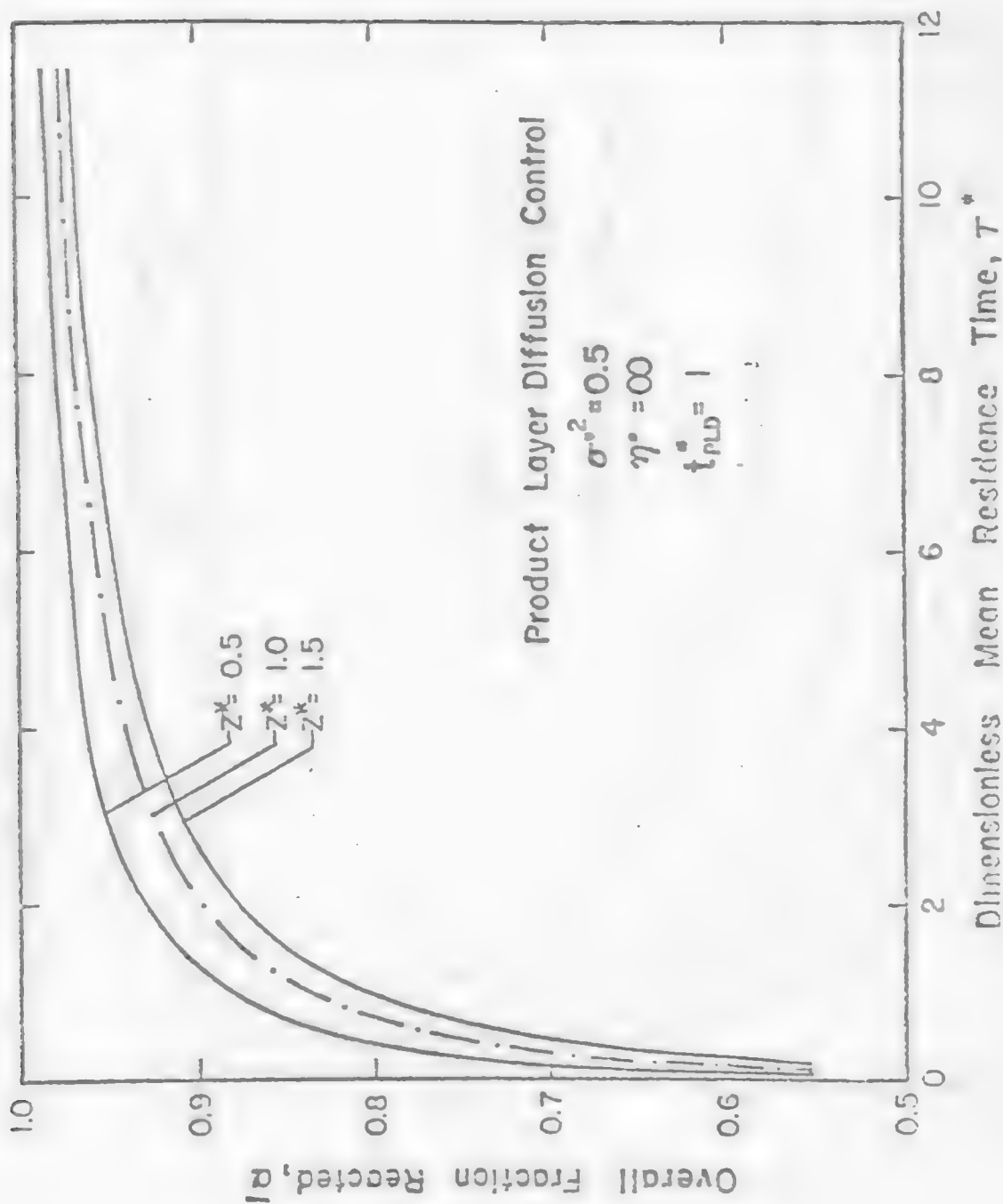


Figure 3.4.5. Computer simulation of the effect of Pilling Bedworth ratio on conversion versus retention time plot.

Laboratory tests indicate that the leaching reaction is topochemical in nature, and the rate is controlled by product layer diffusion having an effective diffusivity of $3.07 \times 10^{-6} \text{ cm}^2/\text{min}$.

Table 3.4.4. Size Distribution of Solid A

Wt fraction	Size (mesh)	Size (cm)	Geometric mean size
0.37	14-20	0.1168-0.0833	0.0986
0.123	20-28	0.0833-0.0589	0.0700
0.052	28-35	0.0589-0.0417	0.0494
0.173	35-48	0.0417-0.0295	0.035
0.0407	48-65	0.0295-0.0208	0.0248
0.0317	65-100	0.0208-0.0147	0.0175
0.0559	100-150	0.0147-0.0104	0.0124
0.0141	150-200	0.0104-0.0074	0.0088
0.0396	200-	0.0074-	0.0037
$\mu=0.0562 \text{ cm}, \sigma^2 = 0.0011 \text{ cm}^2, \sigma = 0.0332 \text{ cm}, \sigma^{\star 2} = 0.349$			

By inputting the data in the accompanying design worksheet step by step, the stoichiometry number is found to be 1.25; and the dimensionless mean residence time is 2.11. After correcting for $\eta^* \neq \infty$, the dimensionless residence time is changed to 7.54 which corresponds to a dimensional residence time of 1010 min. The volume of the reactor can then be estimated from the equation

$$V = Q\bar{t}$$

to be 20,200 gal.

INSTRUCTIONS FOR DESIGN WORKSHEET

(Single Stage Systems)

* NOTATION: PLD = Product Layer Diffusion

SR = Surface Reaction

MK = Mixed Kinetics

I. INPUT DATA:• Stoichiometry Coefficients:

1. a, b, c = stoichiometry coefficients in the general leaching reaction:

• Intrinsic Kinetic Parameters:

2. D_B = effective diffusivity of lixiviant species B across the semi-porous product layer, (Area/time). (If PLD does not influence the overall rate of reaction, set $D_B = \infty$.) $= 3.07 \times 10^{-6} \text{ cm}^2/\text{min.}$
3. k_s = surface reaction rate constant (length/time). (If SR does not influence the overall rate of reaction, assume $k_s = \infty$.) $= \infty$
4. z^* = Pilling-Bedworth ratio $= (\rho_A/a)/(\rho_C/c)$. (If unknown, assume $z^* = 1$.) $= 1$

• Feed Characterization:

5. ρ_A = molar density of the valuable A (moles/vol. solid) $= 7 \times 10^{-4} \text{ mole/cc}$
 ρ_C = molar density of the solid product layer (moles/vol. solid).
 (If unknown, set equal to $(c/a)\rho_A$.) $= -$
6. μ = mean particle size of the solids in the inlet, (length) $= 0.0562 \text{ cm}$
7. σ^2 = variance of the inlet size distribution, (length²) $= 0.0011 \text{ cm}^2$
8. σ^{*2} = dimensionless variance $= \sigma^2/\mu^2 = 0.349$

• Design Specifications:

9. Q = volume flowrate of pulp, (vol. pulp/time) $= 20 \text{ gal/min}$
10. f_v = volume fraction of solids in the inlet $= 0.204$
11. C_{B0} = lixiviant concentration in the inlet, (moles B/vol. sol'n) $= 5.14 \times 10^{-4} \text{ mole/l.}$

12. η^* = stoichiometry number

$$= \frac{(a/b)(1-f_v)C_{Bo}}{f_v \rho_A} = 1.05$$

13. α_0 = nominal (design) overall conversion

I) CALCULATIONS:

14a. $\tau_{\infty}^*(\alpha_0/\text{PLD})$ = dimensionless mean residence time required for an overall conversion $\alpha = \alpha_0$ when $\eta^* = \infty$ and PLD is rate controlling

$$\tau_{\infty}^*(\alpha_0/\text{PLD}) = 1.838(z^*)^{2/3} \left[\frac{0.159 \alpha_0^3}{1-\alpha_0} \right]^{0.835+0.283 \sigma^{*2}} = \underline{2.11}$$

14b. $\tau_{\infty}^*(\alpha_0/\text{SR})$ = dimensionless mean residence time required for an overall conversion $\alpha = \alpha_0$ when $\eta^* = \infty$ and SR is rate controlling

$$\tau_{\infty}^*(\alpha_0/\text{SR}) = 6.285(z^*)^{2/3} \left[\frac{0.039 \alpha_0^{3/2}}{1-\alpha_0} \right]^{0.893+0.109 \sigma^{*2}}$$

$$15a. t_{\text{PLD}}(\mu) = \frac{\mu^2 \rho_A}{24(a/b)C_{Bo} D_B} \text{ (time)} = \frac{(0.002)^2 (7 \times 10^4)}{(24)(0.44)(5.1 \times 10^{-4})(3.07 \times 10^{-6})} = \underline{134 \text{ min}}$$

$$15b. t_{\text{SR}}(\mu) = \frac{\mu \rho_A}{2(a/b)C_{Bo} k_s} \text{ (time)} \approx 0$$

$$16. t_c(\mu) = t_{\text{PLD}}(\mu) + t_{\text{SR}}(\mu) \text{ (time)} = 134 \text{ min}$$

$$17a. t_{\text{PLD}}^* = t_{\text{PLD}}(\mu)/t_c(\mu) = 1$$

$$17b. t_{\text{SR}}^* = t_{\text{SR}}(\mu)/t_c(\mu) \approx 0$$

18. $\tau_{\infty}^*(\alpha_0/\text{MK})$ = dimensionless mean residence time required for an overall conversion $\alpha = \alpha_0$ when $\eta^* = \infty$ and MK is rate controlling

$$\tau_{\infty}^*(\alpha_0/\text{MK}) = t_{\text{PLD}}^* \tau_{\infty}^*(\alpha_0/\text{PLD}) + t_{\text{SR}}^* \tau_{\infty}^*(\alpha_0/\text{SR}) = \underline{2.11}$$

19. Correction for $\eta^* \neq \infty$:

$$\tau_{\eta^*}^* (\alpha_0/MK) = \tau_{\infty}^* (\alpha_0/MK) / (1 - \alpha_0/\eta^*) = 2.11 / (1 - 0.9/1.25) = 7.54$$

20. $\tau_{\eta^*} (\alpha_0/MK)$ = dimensional mean residence time

$$\tau_{\eta^*} (\alpha_0/MK) = t_c(\mu) \cdot \tau_{\eta^*}^* (\alpha_0/MK)(\text{time}) = 134 \times 7.54 = 1010 \text{ min}$$

21. V = reactor volume

$$V = Q \cdot \tau_{\eta^*} (\alpha_0/MK)(\text{vol.}) = 20 \text{ gal/min} \times 1010 \text{ min} = 20,200 \text{ gal.}$$

DESIGN WORKSHEET

SINGLE STAGE
SYSTEMS

I. INPUT DATA

STOICHIOMETRY COEFF.		FEED CHARACTERIZATION		DESIGN SPECIFICATIONS	
1	a,b,c $a/b = 0.44$	5a	P_A 7×10^{-4} moles/cc	9	Q 20 gal/min
KINETIC PARAMETERS		5b	P_C —	10	f_V 0.204
2	D_B 3.07×10^{-6} cm ² /m	6	μ 0.0562 cm	11	C_{B_0} 5.1×10^{-4} mo/p/cc
3	k_s ∞	7	σ^2 0.0011 cm ²	12	η^* 1.25
4	Z^* 1	8	σ^{*2} 0.0349	13	α_0 0.90

II. CALCULATIONS

A. EVALUATE τ_{∞}^* (α_0 IMK)

PRODUCT LAYER DIFFUSION		SURFACE REACTION	
14a	τ_{∞}^* (α_0 PLD) 2.11	14b	τ_{∞}^* (α_0 SR) —
15a	$t_{PLD}(\mu)$ 134	15b	$t_{SR}(\mu)$ —
	16	$t_C(\mu)$ 134 m.s.	
17a	t_{PLD}^* /	17b	t_{SR}^* 0
	18	τ_{∞}^* (α_0 IMK) 2.11	

B. CORRECT FOR $\eta \neq \infty$ 19 τ_{η}^* (α_0 IMK) 2.54

C. MEAN RESIDENCE TIME

20 τ_{η}^* (α_0 IMK) 1010 m.s.

D. REACTOR VOLUME

21 V 20,200 gal

Approximately 5000 gal for 5 vessels
in series.

INSTRUCTIONS FOR DESIGN WORKSHEET

(Single Stage Systems)

* NOTATION: PLD = Product Layer Diffusion

SR = Surface Reaction

MK = Mixed Kinetics

I. INPUT DATA:• Stoichiometry Coefficients:

1. a, b, c = stoichiometry coefficients in the general leaching reaction:

• Intrinsic Kinetic Parameters:

2. D_B = effective diffusivity of lixiviant species B across the semi-porous product layer, (Area/time). (If PLD does not influence the overall rate of reaction, set $D_B = \infty$.)
3. k_s = surface reaction rate constant (length/time). (If SR does not influence the overall rate of reaction, assume $k_s = \infty$.)
4. z^* = Pilling-Bedworth ratio = $(\rho_A/a)/(\rho_C/c)$. (If unknown, assume $z^* = 1$.)

• Feed Characterization:

5. ρ_A = molar density of the valuable A (moles/vol. solid)
 ρ_C = molar density of the solid product layer (moles/vol. solid).
 (If unknown, set equal to $(c/a)\rho_A$.)
6. μ = mean particle size of the solids in the inlet, (length)
7. σ^2 = variance of the inlet size distribution, (length²)
8. σ^{*2} = dimensionless variance = σ^2/μ^2

• Design Specifications:

9. Q = volume flowrate of pulp, (vol. pulp/time)
10. f_v = volume fraction of solids in the inlet
11. C_{B0} = lixiviant concentration in the inlet, (moles B/vol. sol'n)

12. η^* = stoichiometry number

$$= \frac{(a/b)(1-f_v)C_{Bo}}{f_v \rho_A}$$

13. α_0 = nominal (design) overall conversion

CALCULATIONS:

14a. $\tau_{\infty}^*(\alpha_0/\text{PLD})$ = dimensionless mean residence time required for an overall conversion $\alpha = \alpha_0$ when $\eta^* = \infty$ and PLD is rate controlling

$$\tau_{\infty}^*(\alpha_0/\text{PLD}) \approx 1.838(z^*)^{2/3} \left[\frac{0.159 \alpha_0^3}{1-\alpha_0} \right]^{0.835+0.283 \sigma^{*2}}$$

14b. $\tau_{\infty}^*(\alpha_0/\text{SR})$ = dimensionless mean residence time required for an overall conversion $\alpha = \alpha_0$ when $\eta^* = \infty$ and SR is rate controlling

$$\tau_{\infty}^*(\alpha_0/\text{SR}) \approx 6.285(z^*)^{2/3} \left[\frac{0.039 \alpha_0^{3/2}}{1-\alpha_0} \right]^{0.893+0.109 \sigma^{*2}}$$

15a. $t_{\text{PLD}}(\mu) = \frac{\mu^2 \rho_A}{24(a/b)C_{Bo}D_B} \text{ (time)}$

15b. $t_{\text{SR}}(\mu) = \frac{\mu \rho_A}{2(a/b)C_{Bo}k_s} \text{ (time)}$

16. $t_c(\mu) = t_{\text{PLD}}(\mu) + t_{\text{SR}}(\mu) \text{ (time)}$

17a. $t_{\text{PLD}}^* = t_{\text{PLD}}(\mu)/t_c(\mu)$

17b. $t_{\text{SR}}^* = t_{\text{SR}}(\mu)/t_c(\mu)$

18. $\tau_{\infty}^*(\alpha_0/\text{MK})$ = dimensionless mean residence time required for an overall conversion $\alpha = \alpha_0$ when $\eta^* = \infty$ and MK is rate controlling

$$\tau_{\infty}^*(\alpha_0/\text{MK}) = t_{\text{PLD}}^* \tau_{\infty}^*(\alpha_0/\text{PLD}) + t_{\text{SR}}^* \tau_{\infty}^*(\alpha_0/\text{SR})$$

19. Correction for $\eta^* \neq \infty$:

$$\tau_{\eta^*}^* (\alpha_0/MK) = \tau_{\infty}^* (\alpha_0/MK) / (1 - \alpha_0/\eta^*)$$

20. $\tau_{\eta^*} (\alpha_0/MK)$ = dimensional mean residence time

$$\tau_{\eta^*} (\alpha_0/MK) = t_c(\mu) \cdot \tau_{\eta^*}^* (\alpha_0/MK) (\text{time})$$

21. V = reactor volume

$$V = Q \cdot \tau_{\eta^*} (\alpha_0/MK) (\text{vol.})$$

DESIGN WORKSHEET

SINGLE STAGE
SYSTEMS

I. INPUT DATA

STOICHIOMETRY COEFF.		FEED CHARACTERIZATION		DESIGN SPECIFICATIONS	
1	a,b,c	5a	ρ_A	9	Q
KINETIC PARAMETERS		5b	ρ_C	10	f_V
2	D_B	6	μ	11	C_{B_0}
3	k_S	7	σ^2	12	η^*
4	Z^*	8	σ^{*2}	13	α_0

II. CALCULATIONS

A. EVALUATE τ_{∞}^* (α_0 IMK)					
PRODUCT LAYER DIFFUSION			SURFACE REACTION		
14a	τ_{∞}^* (α_0 PLD)		14b	τ_{∞}^* (α_0 SR)	
15a	$t_{PLD}(\mu)$		15b	$t_{SR}(\mu)$	
	16	$t_C(\mu)$			
17a	t_{PLD}^*		17b	t_{SR}^*	
	18	τ_{∞}^* (α IMK)			
B. CORRECT FOR $\eta \neq \infty$			19	τ_{η}^* (α_0 IMK)	
C. MEAN RESIDENCE TIME			20	τ_{η}^* (α_0 IMK)	
D. REACTOR VOLUME			21	V	

3.5.4 Reference

1. O. Levenspiel, Chemical Reaction Engineering, John Wiley, Chap. 5, (1972).

UNIT PROCESSES IN EXTRACTIVE METALLURGY

HYDROMETALLURGY

Module 4

PHASE SEPARATION

TWO LEARNING
ACTIVITIES

Module 4 Contents

Phase Separation

4.1 Thickening

Learning Activity 1

1. Introduction
2. How a Continuous Thickener Functions
3. Elements of a Thickener
4. Some Factors That Size Continuous Thickener Basins
5. Practical Mill Design Considerations for Thickeners
6. Major Factors Influencing Thickener Design

4.2 Filtering

Learning Activity 2

1. Introduction
2. Types of Continuous Filters
3. Applied Theory of Continuous Filtration
4. Applied Theory Use in Predicting Full Scale Results

LEARNING ACTIVITY 1

(Donald L. King, Manager, Development Engineering, Envirotech Corp.)

4.1 Thickening

Learning Activity Objective

After completing your study of this material you should be able to describe a continuous thickener, how it functions and what are the important factors in its design.

4.1.1 Introduction*

This paper has been prepared with the objective of providing basic information on thickening equipment as applied to mineral processing plant design.

THICKENING DEFINITION

Continuous thickening and clarification - by an operation called Sedimentation - is the separation of suspended solid particles from a liquid stream by gravity settling. The primary purpose of thickening is to increase the solids concentration of the feed stream, while that of clarification is to remove solids from the feed stream. Thus, there is no precise distinction between thickening and clarification other than the principal result desired.

The inlet stream going to a thickener generally is called "feed" or "influent". Overflow from the unit may be called "overflow", "effluent" or "supernatant". Underflow may be called "pulp", "sludge", "slurry", "mud", etc.. The terminology will depend upon the industry and application.

HISTORY OF THICKENER DEVELOPMENT

Modern Sedimentation technology was developed in the mining industry. Prior to development of the continuous thickener, batch gravitational settling was employed. In such batch operations, dilute feed was pumped into a tank continuously until a clear overflow was no longer obtained. The feed was then discontinued and the tank left undisturbed until the solids had settled. After a suitable retention time, clear supernatant liquor was decanted and the thickened sludge removed.

* Coordinator's note: This learning activity is a shortened version of a paper prepared for the textbook "Mineral Processing Plant Design", A.I.M.E. copyright, published by Society of Mining Engineers, Chapter 27, pp. 541-577. Figures have been renumbered to conform to our modular format. Further details on the operation of thickeners are given in the original paper. This material is reproduced here by written permission.

Following batch settling operations, cone settlers were developed. These could be operated continuously by delivering a continuous feed stream to the settling cone; removing the settled solids underflow continuously from the bottom of the cone; and the overflow continuously over weirs into launders at the surface and on the periphery of the cone. To maintain a uniform underflow from the cone, and to insure proper removal of the solids, the slope of the cone often had to be fairly steep. A steep cone slope limited the size of the cone settler.

Since the effectiveness of gravitational settling is largely a function of area, it soon was recognized that the basic cone design had serious limitations. As the technology developed it became obvious that continuous movement of the solids deposited over a large area toward a common withdrawal point was necessary. Adopting this general principle, the continuous thickener - with its many modifications - was developed about 1905.

From the mining industry, the continuous thickener was applied to the chemical, water, and waste water treatment industries. However, with minor exceptions the heaviest duty machines are required in the metallurgical industry, while machines of lighter duty are used for water and waste water treatment in other process industries. It is obvious that a higher specific gravity of the solids, and/or larger amounts of solids to be handled by a thickener of given size, requires heavier construction of the thickener mechanism. Many metallurgical pulps have specific gravities of 2.6 or more, and settle to concentrations up to 60-75%, and these machines must be much heavier in design than for water and waste water treatment, where the specific gravity of the solids often are 1.1-1.3 and rarely settle to a concentration of greater than 10%. In some applications, even though the solids in the feed are finely divided and the unit acts as a clarifier, underflow concentrations can be relatively high, thereby requiring a semi heavy duty clarifier mechanism.

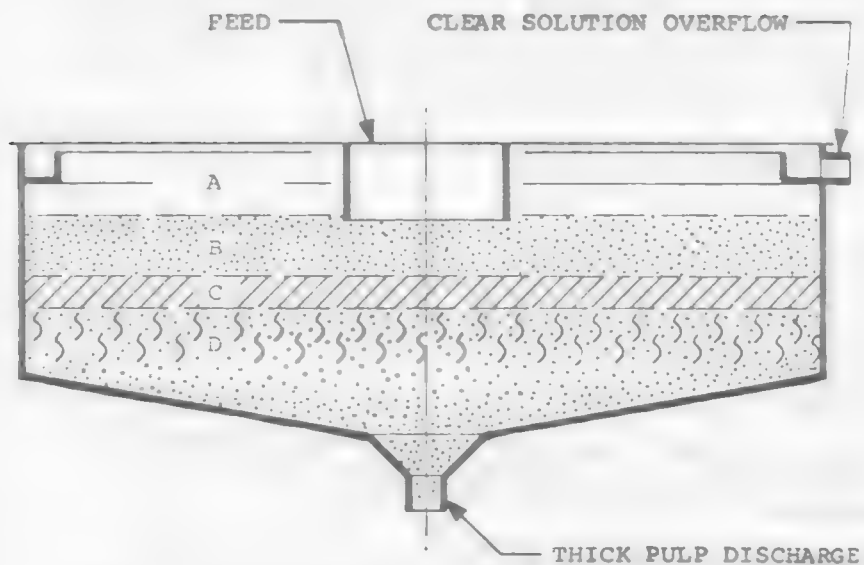
4.1.2 How a Continuous Thickener Functions





As a feed stream enters the thickener, the solids settle to the bottom. Clarified liquor overflows the top and the settled solids underflow is removed from the bottom.

Figure 1 shows a cross-section, schematically illustrating the operation of a continuous thickener. Zone A, which is the clear overflow liquor, is essentially free of solids in most applications. Zone B consists of a pulp of fairly uniform consistency which is nearly the same solids concentration as the feed stream. Zone C is an intermediate state in which the pulp is in a condition of transition between free unhindered settling and compression. Zone D shows the pulp in compression, where dewatering occurs by compression of the solids forcing the liquids out of the interstices.

In actual practice, special characteristics which distinguish zones B, C, and D are not readily discernible, except for an increasing solids concentration, and the description is more academic than realistic.

Figure 4.1.1 Section Through a Continuous Thickener Illustrating Position of Four Zones of Settling Pulp.



- | | |
|---|--|
|  | ZONE A: CLEAR WATER OR SOLUTION |
|  | ZONE B: PULP OF FEED CONSISTENCY |
|  | ZONE C: PULP IN TRANSITION FROM B TO D CONSISTENCY |
|  | ZONE D: PULP IN COMPRESSION |

FOUR ZONES OF SETTLING PULP, ILLUSTRATING
CONTINUOUS THICKENING

Figure 2 presents an illustration of that which actually occurs in a continuous thickener. Feed slurry becomes very diluted on entering the feedwell (unless the feedwell is submerged in a moderately concentrated pulp zone as illustrated in Figure 1), and leaves the feedwell as a dilute suspension from which particulate settling, rather than "zone" or "line" settling must occur. Considerable lateral movement occurs in the floc bed zone as liquid into the feedwell to sustain this dilution action. The floc particles agglomerate and settle to the surface of the thickening pulp, and continue to concentrate in this zone until underflow density is reached.

4.1.3 Elements of a Continuous Thickener and Their Function.

Refer to figure 3 for schematic representations of two basic thickener configurations. The elements are identified by name:

- The Feedwell function is to dissipate energy of movement in the feed stream so as to cause the feed to enter the tank in a relatively quiescent condition and to provide a means of introducing the slurry at an appropriate depth in the thickener.
- The Tank provides holding time to produce settled solids and clarified liquor. The sloped bottom assists movement of the concentrated solids toward the discharge point.
- The Rake Arms serve three functions:
 - (1). Move the settled solids toward the discharge point;
 - (2). Maintain a degree of fluidity in the thickener to ensure hydraulic removal, and
 - (3). Increase underflow solids concentration by providing for channels for water to escape from the thickening solids in the compression zone.
- Cone, or Trench, Scrapers perform an action similar to the Rake Arms so that underflow solids can be discharged.
- The Overflow Launder collects clarified liquor for transport to an outlet. Best design practice is for a uniform rate of overflow around the tank periphery.
- The Rake Drive provides driving force (torque) to move the Rake Arms and Blades against resistance of the thickened solids.
- The Rake Lift provides a means of lifting the Rake Arms out of contact with the more concentrated solids so as to reduce the driving force demand from the rake drive. The lift will operate while the rake arms are rotating.

4.1.4 Some Factors That Size Continuous Thickener Basins

Sizing the Thickener

Detailed sizing techniques are not discussed in this article, but certain basic considerations are covered.

Area: The area of a thickener must provide sufficient detention time to allow the slowest settling particle to reach the bottom of the unit. Thickener size is often expressed in area per unit weight of dry solids per day. (Meter squared/ton of dry solids/day).

Figure 4.1.2 Section Through a Continuous Thickener Illustrating Thickening Action.

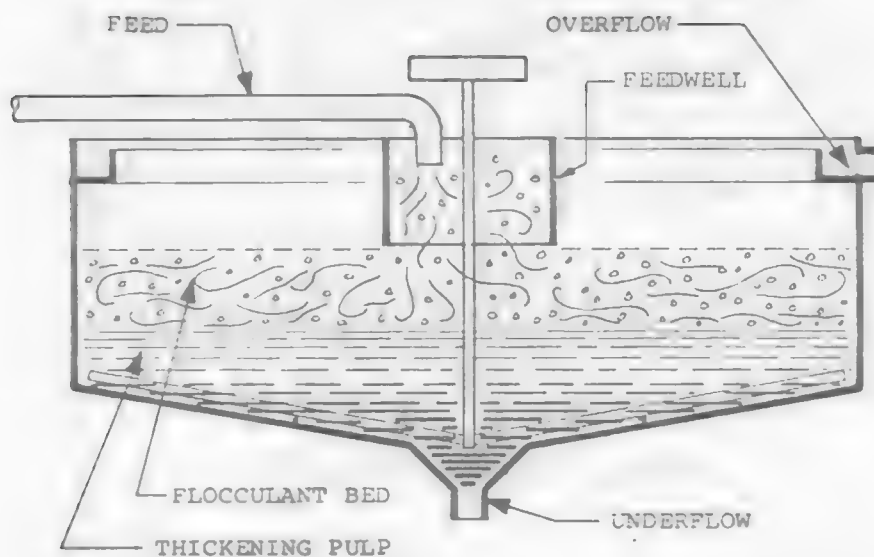
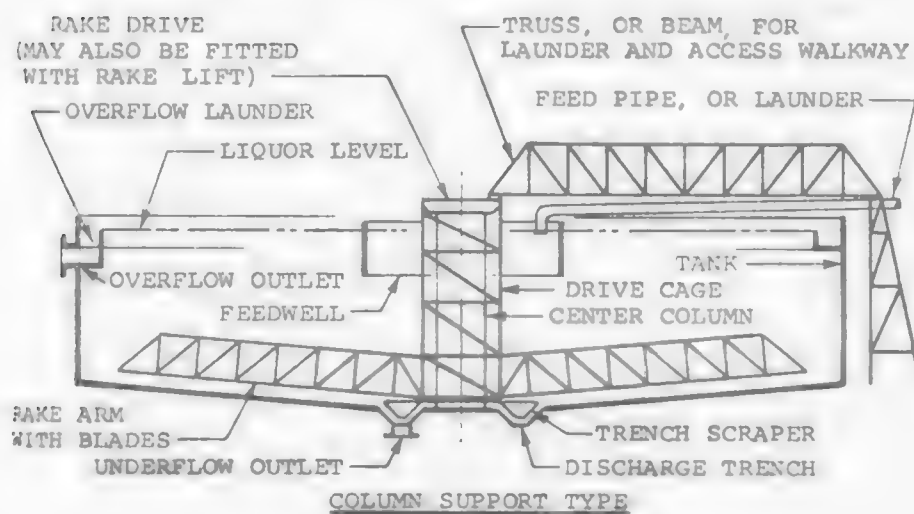
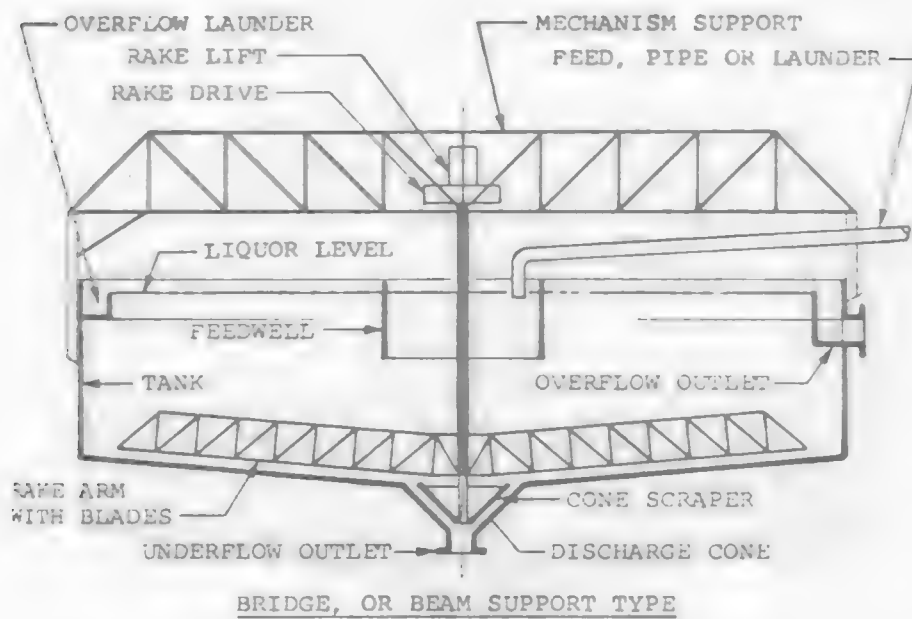


Figure 4.1.3 Elements of a Continuous Thickener.



Overflow Rate: The overflow, or upflow rate, of the unit must be low enough so that excessive turbulence does not prevent separation of the solids from the liquid and not greater than the settling rate of the slowest settling particle or flocculi. Thus, in thickeners which are essentially clarifiers (that is, are used to remove very finely divided material from a dilute suspension) the overflow rate expressed as volume per day per unit area (meter cubed/day/meter squared) becomes a critical design factor. For materials which apparently settle very fast in laboratory tests, it is good practice to design the area and volume of the unit so that the overflow rate does not exceed values established by experience.

Detention Time: In addition to providing sufficient detention time to allow separation of the slow settling particles from the overflow, special consideration must be given to the compression zone. The volume of the compression zone, or for practical purposes the entire volume beneath the pulp level, will have a direct bearing on the final underflow solids concentration as long as the particles within this zone are in a state of subsidence, that is, not at rest.

In an ideal thickener operation the solids in the feed to be withdrawn in the underflow must move continuously toward the withdrawal point at the same rate as they enter the compression zone. The solids do not merely settle on the bottom and then are pushed by the rakes toward the discharge point. The pulp is retained in the compression zone, which must provide adequate time for thickening to final density, but too long a retention time can result in overload to the thickener mechanism. The underflow rate must be controlled so that pulp density, as withdrawn, will be the maximum practical at a given feed rate with the minimum pulp level in the thickener.

PRACTICAL MILL DESIGN CONSIDERATIONS FOR THICKENERS

- A. Utilize the expertise of established equipment manufacturers or consultants experienced in this field to insure the best selection for the requirement. The early stages of a project invariably require some form of economic justification. This, in turn, means that someone must establish a preliminary flowsheet and size the equipment involved. If the Design Engineer is familiar with the particular flowsheet, he can probably complete this preliminary phase without outside help. However, if the flowsheet, or parts of it, are outside the realm of his experience, he must look to others for assistance. Suitable help may be found within his company's files or the general technical literature, or it may be necessary to contact equipment manufacturers or consultants. Equipment manufacturers have dealt with a wide range of flowsheets and applications and, with a reasonable description of the materials involved and process requirements, can quickly estimate equipment size and performance with sufficient accuracy for most preliminary feasibility studies. Many engineers make use of this source of knowledge. Others may spend an unnecessarily large amount of time searching the literature without developing accurate information that could be obtained by consulting a reputable equipment supplier.
- B. Define the requirements for the thickener. In addition to process requirements, upset, or unusual operational conditions, must be anticipated.

- C. Verify the thickener requirements. Pilot plant, or laboratory cylinder tests, are very desirable, but the slurry sample must be representative of the actual slurry. Many fail to recognize the importance of a truly representative slurry sample. The emphasis here is in reference to simulated slurries or slurries produced in small quantities in a bench scale apparatus. These samples must be carefully characterized and their properties, such as size distribution, suspended solids concentration, pH and temperature, can have very pronounced effects on equipment capacity and product quality.

Once it has been determined that the slurry in question is reasonably representative, it is necessary to perform meaningful sizing tests. Although required test procedures and equipment have been prescribed in literature in some detail, if experience is lacking in running these tests, it would be well to consult a recognized authority in this field. There remains a significant degree of "art" in performing solid-liquid separation tests and interpreting the results. Proper thickener selection depends as much upon the recording of significant test observations as upon the routine recording of required test data.

- D. Pilot Plant design and operation is important. As the plant design project progresses, it is frequently necessary to confirm the equipment sizing and performance. This may mean simulating the complete operation including continuous pilot plant equipment. It is at this point that many miss one of the prime opportunities to obtain meaningful design data. When a continuous pilot plant is designed, it is important that all of the various operating units have sufficient capacity to enable the process to operate at or near capacity. It is unfortunate, from equipment sizing basis, that the liquid-solid steps usually have the greatest degree of uncertainty and that the pilot plant equipment is almost always oversized, so that the process may operate continuously regardless of the characteristics of the slurries.

When pilot plant equipment is oversized, it is extremely difficult to get meaningful sizing information. The data obtained is important, but for the results to be interpreted correctly, this must usually be done in conjunction with a good bench scale testing program. Operating conditions in a bench scale test can be varied in a controlled manner that enables one to determine the effect of many variables and to arrive at a reasonable design operating condition. Since conditions in a pilot plant operation are a great deal more difficult to control, pilot plant operation should be used only to confirm design operating conditions, such as how the feed quality varies with time, and to obtain confidence that the type of unit chosen is capable of giving consistent long term results. The observation of feed variations and the confirmation of long term operating reliability are the most important functions of a solid-liquid pilot plant operation.

- E. The thickener feed velocity should be as low as practical. Thickener operation starts with a system that introduces the feed slurry. The feed velocity must be high enough to prevent solid material "sand out" in the feed launder, but not so high as to cause excess turbulence in the thickener feedwell and tank. Most feed arrangements are such that the feed launder is above liquor level, and for those slurries, that contain solids of specific gravity 2, a feed launder slurry velocity of 2.5 to 3 meter/second will usually be sufficient. As a general rule a launder slope of 1 to 1 1/2% will provide the necessary velocity.

- F. Thickener feed entrance into the feedwell should be such as to provide feed stream energy dissipation. Some ways to accomplish this are:

- Minimize elevation difference between feed launder and liquor level. Often the available elevation difference is much greater than a minimum required, and the feedwell of the thickener is used to dissipate the kinetic energy resulting from this elevation difference. This practice can, and usually does, have detrimental effects on thickener operation. Most feedwells are not designed to accept excessive entrance velocities, and there is always a danger that the slurry will enter the feedwell with a significant downward component of velocity that will cause it to stir up the settling pulp. The result can be both decreased underflow solids concentration and increased turbidity in the clarified overflow. Also, there is always a certain amount of air entrainment in any overhead feeding arrangement that requires a vertical drop. If the thickener feed has come from a flotation step, or if it has natural foaming tendencies, excessive feed entrance velocities will aggravate already undesirable conditions by producing froth which floats on the liquor surface causing loss of solids in the overflow.
- The launder should terminate its horizontal run as near the liquor level as possible, and feed should be introduced below liquor level. A good scheme is to introduce feed such that it exits the launder with flow divided into two equal, opposite directions, and nearly horizontal. The opposite, horizontal feed streams are usually introduced at slightly different elevations to create feed stream shear rather than impingement. Feedwells usually have a bottom shelf to help prevent feed stream "short circuit" to the overflow. If the launder is enclosed, provide air release at its feedwell termination.

- G. Make the provision to remove oversize material from the feed. Remember, a thickener is designed to operate within specified limits, and exceeding those limits can cause operation problems. As a general rule the feed to a thickener should contain very little material larger than 250 micron (+60 mesh). There are a number of applications where this rule is violated, but special features are designed into such applications to accommodate larger material.

Oversize tramp material cannot be tolerated, and it must be removed by screening. It is preferable to remove such prior to the feed entering the launder.

- H. Flocculation of the feed must be controlled and must be complete. There are many instances where flocculation control has been incomplete, and in nearly all such instances, thickener results were less than expected. It must be remembered that a sedimentation device is usually designed to provide both clarification and solids concentration. Emphasis is often on one or the other only, and there is a tendency to consider that clarification depends only upon providing an area equivalent to an upflow rate less than the settling rate of the finest particle removed. While this is certainly one of the mechanisms involved, it is seldom that this is the rate controlling mechanism. Most clarification problems involve time dependent functions of coagulation, or flocculation, or a combination of both. Unless the material is naturally flocculent, some type of chemical must be added to force or promote formation of settleable flocs from the dispersed fine particles.

The chemicals which are added must be uniformly dispersed if they are to function properly. When the feed slurry requires only the addition of multi-valent cations, such as alum, the time required to accomplish the dispersion is of a minor consequence, so long as it is possible to provide the necessary mixing in a conveniently sized vessel. However, when synthetic polymers are used, it is usually necessary to provide an efficient and rapid mix. In this case, the main problem is that of getting the polymers dispersed among the suspended solids before their active sites are all used up by particles in their immediate vicinity. Inefficient mixing means that unnecessarily high polymer dosages will be required. Once the required chemicals have been added to the feed slurry, it is frequently necessary to provide a period of mechanical contact time to allow the flocs to grow to a size that will settle rapidly. If the suspended solids concentration in the original feed is too dilute, it may not be possible to grow flocs of useful size and good floc growth could require that additional solids be recirculated to the feed stream to increase the solids concentration. This may be done either by external recirculation or by internal recirculation of thickened solids in a suitably designed unit. Regardless of the design of the particular unit, it is essential that the engineer make certain that the unit does provide that environment that is necessary to produce an agglomeration with a usable settling rate. Since final clarification is almost always a time function, the clarification zone of the unit must not only provide an equivalent upflow rate low enough to prevent particles from being swept out in the effluent, but enough retention time to allow the additional flocculation which does occur within the clarification zone.

- I. Underflow handling. When designing thickener underflow piping for metallurgical and other similar slurries, it is essential to remember that the piping must be designed so that operators can, if necessary, purge or "blow back" with either high pressure water or air. The question is not "What to do if the underflow plugs?" but rather, "What must be possible to do when the underflow plugs?" There are a number of suitable underflow piping and pumping arrangements. The correct one for a particular installation is a function of the solid-liquid system to be handled, tank size, pumped or gravity flow, economics of tunnel versus center pump room, etc.. These considerations may, in turn, be modified by local site conditions such as high ground water, hard rock formation, etc..
- J. Servicing. Oil change, condensate drain, location of lubrication fittings, walkway access, enclosures, location of instrumentation, night lighting, local electrical plugs for tools, etc., all need to be considered for ease of routine maintenance and for more extensive maintenance.
- K. Operator control requires certain observations and measurements. Many are now made by instrumentation. The need exists for periodic verification, and this requires design to minimize the chance of foreign objects falling into the tank. Hard hats for example, make excellent underflow outlet plugs. Tools and other objects, which can get into the underflow outlet, cause pump damage or stoppage. Some installations are provided with protection nets to catch falling objects.
- L. Emergency bypass, or shut-off, of feed and underflow recirculation, are must features. Standby underflow pumps are common.

4.1.6 Major Factors Influencing Thickener Design.

- A. The quantity of solids to be handled. Usually expressed as area per unit weight of dry solids per day. The smaller the number the greater the chance of an upset. This usually requires a combination of a stronger thickener mechanism and a lifting device.
- B. The amount of material larger than 250 micron (+60 mesh) in the feed. This affects tank bottom slope, drive and strength of mechanism. It may also require a mechanism lifting device.
- C. Specific gravity of the solids. The greater the specific gravity the more likely a stronger drive and mechanism will be required.
- D. Overflow launders and feedwell capable of handling additional material when other thickeners are out of service.
- E. Feed and underflow material settling characteristics that may require special rake construction such as blades located a distance below the rake arms on posts or spikes on the blades to cut into packed solids.
- F. Scale build up tendency of feed slurry may require special arms and drive.
- G. An operating requirement to accumulate solids for defined periods of time will require a special mechanism design, as it is not a normal operating procedure.
- H. Froth control or removal.
- I. Slurry temperature, vapors, gases, etc. may require covered and/or insulated tanks with attendant seals.
- J. Soil conditions and ground water elevation affect foundation design and may determine mechanism type.
- K. Climatic conditions may require special considerations, such as enclosures around the drive and instrumentation.
- L. Measurement and control methods and control room location.
- M. An operating requirement to use a powered lift for purposes other than occasional corrective action. Refer to the section on "Thickener Operation and Operator Control."

LEARNING ACTIVITY 2

(Donald A. Dahlstrom, Vice President and Director, Research and Development, Envirotech Corporation)

4.2 Filtering*

Learning Activity Objective

After completing your study of this learning activity you should be able to discuss the factors of importance in selecting and sizing continuous filtering systems.

4.2.1 Introduction

The selection and sizing of filters depends on the characteristics of the type of filter and the feed slurry. In addition, the rate functions of cake formation, cake washing and cake dewatering must be determined in order to design the filter station on the basis of desired performance. This chapter discusses the applied theory used to determine the rate functions and illustrates how to incorporate these into the filter cycle to obtain the required objectives. This also permits the sizing of the filter and auxiliaries as well as the selection of the proper type of filter.

With the growth in technology and size of the mineral processing industry, together with a greater emphasis on hydrometallurgy, most filter applications now employ continuous filtration. This chapter will develop the methods utilized to select and size these units.

4.2.2 Types of Continuous Filters

Types of continuous filters must first be considered as their characteristics will influence data interpretation and sizing. The percent of the filter cycle that can be devoted to cake formation, cake washing and cake dewatering will vary with the basic units. Cake discharge methods can vary within a basic type, whether cake washing can be practiced and even if two or more counter-current washes can be employed.

Table I lists the ranges of the filter cycles that can be devoted to cake formation, cake dewatering and cake washing, as well as the minimum cake thickness that is required for efficient discharge. The Table has been divided into two groups -- those forming their cake against gravity (bottom feed) and those forming cake with gravity (top feed).

* Coordinator's note: This learning activity material was prepared by D. A. Dahlstrom for the text "Mineral Processing Plant Design", S.M.E., A.I.M.E., Chapter 28, pp. 578-600, 1978. It is reproduced here by written permission. Numbering of the sections and figures have been changed to coincide with our modular format.

Table 4.2.1 Characteristics of Basic Types of Continuous Filters.

Basic Type of Filter With Options Indicated	Range of Filter Cycle Percent Deviated to Cake Formation			Number of Washing Slaggs Possible	Maximum Cake Thickness mm
	Cake Washing	Cake Dewatering	Cake Formation Against Gravity		
Disc Filter With and Without Agitation	5 - 40%	Not Recommended	5 - 45%	.	8
Drum Filter Seepage Discharge Roller Discharge String Discharge Continuous Belt Discharge Pneumatic	5 - 50%	0 - 10%*	0 - 60%	1	6 1 6 3 20
Top Feed Drum Filter	5 - 15	0 - 20	25 - 70	1	12
Horizontal Belt Filter	5 - 90	0 - 90	5 - 90	As Many as Possible	3
Horizontal Table or Tilting Pan	5 - 70	0 - 80	5 - 75	2-3	20

* With horizontal belt filter, only active area is considered in cycle. All others include total area including dead time in cycle.

** Can go to 50% if drum is flood washed -- not common.

The factors given in Table I definitely influence the filter selection as well as optimization. For example, as will be shown later, if a filter can discharge a thinner cake, productive capacity per unit area can be greater because of the shorter cycle time. In addition, with apparent submergences greater than 40%, stuffing boxes on the filter trunnions will be required for disc and drum type filters which may not be desirable for the type of feed slurry involved.

The filters forming their cake with gravity are generally applied to relatively fast filtering material and particularly if the solids cannot be left in suspension by reasonable agitation of the type applied in a filter tank. The exception to this is the horizontal belt filter where very thin cakes (as thin as 3 mm) can be discharged and advantage can be taken of counter-current washing while minimizing wash fluid addition. Installation of 5 stages of counter-current wash have been used on the horizontal belt filter.

4.2.3 Applied Theory of Continuous Filtration.

The continuous filter cycle can be divided into three rate functions which can be analyzed separately. These are (1) cake formation rate (2) cake dewatering rate and (3) cake washing rate.⁽²⁾ While one of these will usually be controlling, all of them must be considered in order to incorporate them into the filter cycle. This is another reason why the percentage of filter cycle time that can be devoted to the various three functions for each type filter must be considered.

Cake Formation Rate

As indicated in earlier publications^(1&2) this rate function can be defined by the following equation:

$$\text{Form Filtration Rate} = Z = \quad (1)$$

$$= \left[\frac{Kw\Delta P}{\mu\alpha\theta_f} \right]^{1/2}$$

Where Z = form filtration rate expressed as weight of dry solids per unit area per unit time of cake formation

K = proportionality constant

w = weight of dry cake solids per unit volume of filtrate

ΔP = pressure drop across the cake

μ = viscosity of liquid, centipoises

θ_f = cake formation time per cycle

α = specific resistance of the cake

Z is normally expressed either as kilograms of dry solids per square meter per hour of form time or pounds of dry solids per square foot per hour of form time.

It is stressed that the cake formation rate Z does not take into account the remainder of the filter cycle (cake wash time, cake dewatering time, dead time for discharge, and percentage of apparent submergence required by the specific type of filter). However, once the other rate functions are known, this rate formation can be worked into the total cycle by multiplying by the fraction of the cycle that will be employed for cake formation.

The form filtration rate can be converted to the volumetric rate of filtrate by dividing both sides of the equation by w to obtain:

$$Y = \left[\frac{K \Delta P}{w \theta_f} \right]^{1/2} \quad (2)$$

Where Y = form filtration rate, volume of filtrate per unit area per unit time of cake formation

Equations 1 and 2 are ideal equations and do not consider such things as the resistance of the filter cloth or the internal drainage network of the filter. The former is generally negligible in comparison to the specific resistance of the cake. However, it will be noticed that varying form filtration rates will be experienced with different filter media. This is not generally due to the resistance of the cloth but instead the nature of the cake formed next to the filter cloth. As a tighter filter cloth is employed, the pores of the media bridge over with finer particles yielding a higher specific resistance at this critical layer. After that layer of formation, the cake itself becomes the filter media and the filtrate becomes practically clear in most cases. Therefore, the most open filter media that gives reasonable filtrate clarity for process requirements consistent with good cake discharge and life should be employed.

Specific resistance α is influenced by particle size, particle size distribution and shape. If colloidal solids are present, flocculation may significantly reduce specific resistance. In addition, feed solids concentration can also influence specific resistance. As it will generally decrease to some extent as solids concentration is increased, this further emphasizes the importance of maintaining high filter feed solids concentrations.

Cake Dewatering Rate

The cake dewatering rate is a very complex phenomenon which can be reduced to its simplest form by the following equation: (3)

$$\%M = f(Fa, d, \%M_r) \quad (3)$$

Where $\%M$ = weight % moisture of the discharged cake

$\%M_r$ = Wt.% residual moisture which is the moisture at equilibrium if 100% saturated gas is pulled through the cake at the pressure drop ΔP

F_a = approach factor which depicts the approach to $\%M_r$.

d = particle size, particle size distribution and shape factor

The term d is normally employed as a parameter as specific surface area alone does not give the total influence, although it is undoubtedly a major factor. All of the surface area is wetted by a film of liquid and as this increases, moisture will increase. However, a particle size distribution parameter is normally used such as $\% -200$ mesh, $\% -10$ microns, etc.

$\%M_r$ very seldom needs to be measured because of the correlation methods that will be indicated. However, it should be realized that it is influenced not only by d , but also by ΔP , viscosity of the liquid, sometimes by cake thickness, and can be a function of the filter cloth employed primarily by the phenomenon indicated earlier. Surfactants can also influence $\%M_r$ by decreasing surface tension or interfacial tension. Flocculants generally have little effect on $\%M_r$ because the specific surface area is not changed.

The term F_a is the major factor that is employed to determine optimum moisture content that can be achieved and the requirements to obtain it for a specific feed. From basic theory, it can be shown that F_a can be described by the following equation: (4)

$$a = F_a \left[\frac{\Delta P}{W} \right] \left[\frac{CFM}{Ft^2} \right]_d \theta_d \quad (4)$$

Where W = cake weight of dry solids per unit area per cycle

$\left[\frac{CFM}{Ft^2} \right]_d$ = gas pulled through the cake measured at down stream pressure as cubic feet per minute per square foot during the dewatering portion of the cycle

θ_d = dewatering time during the cycle normally measured in minutes

A plot of $\%M$ versus F_a will yield a descending curve becoming asymptotic to some minimum value ($\%M_r$) as F_a is increased. It should be noted that the term ΔP may still have to be used as a parameter as it can affect $\%M_r$.

The term F_a is valuable from two standpoints. Not only does it predict moisture content as a function of primary variables which can be optimized, but it also yields energy requirements. The two terms ΔP and $\left(\frac{CFM}{Ft^2} \right)_d$ will give the requirements for the vacuum pump or compressor which is used as the driving force for filtration.

From experience, it has been observed that the term F_a can be simplified to the following equation as long as $\left(\frac{CFM}{Ft^2} \right)_d$ is less than 20 CFM/Ft^2 : (5)

$$Pa = f \left[\frac{\theta_d}{W} \right] \quad (5)$$

The same type of curve is experienced but parameters of ΔP must be employed. The $(CFM/Ft^2)_d$ is still measured in order to determine energy requirements.

It should also be noted that as the correlating factor is increased either by increasing θ_d or decreasing W , productivity per unit area of filtration will also decrease. Thus, it is obvious that economics of capital and operating costs are involved to optimize moisture content.

Cake Washing Rate

This rate function has two rate equations that must be considered. These are the rate of flow of the wash fluid through the cake and the efficiency of displacement of the mother liquor by the washing fluid. The first has been shown to follow the expression: (6)

$$\theta_w = K' \theta_f n \quad (6)$$

Where θ_w = wash time during the filter cycle,
normally measured in minutes

K' = proportionality constant

n = volume of wash fluid/volume of
cake liquor

Thus, a coordinate plot of wash time θ_w as a function of wash ratio n should yield a family of straight lines whose separation is proportional to θ_f and will pass through the origin. Another way of plotting to obtain a single line is to plot θ_w/θ_f versus n .

It should be noted that Equation 6 assumes that the mother liquor and wash fluid are miscible and of relatively the same viscosity. If the viscosity of the wash fluid is less than the mother liquor the plot will show a faster penetration rate (less slope) after about a 0.7 wash ratio is achieved.

While the wash flow rate can be determined, this does not yield the efficiency of removal of the soluble solids by the washing fluid. This removal can occur both by displacement and diffusion. The ideal would be plug flow whereby one wash ratio applied would remove all the mother liquor from the cake. However, because of the zero velocity of the liquid film next to the particle surface, some of the mother liquor can only be removed by diffusion. The removal efficiency has been shown to best agree with the following semi-log function: (6)

$$\frac{R}{100} = \left[1 - \frac{E}{100} \right]^n \quad (7)$$

Where R = % of soluble solids remaining
in the cake after washing with
100% being that in the cake
prior to wash

E = wash efficiency % or $100-R$
at $n=1.0$

Thus, a plot of the log of the % remaining R as a function of the wash ratio n should yield a straight line. Experience has shown that the agreement is good until a wash ratio of 1.5 to 2.5 is reached where a curved relationship begins and becomes asymptotic to some minimum value. This is believed due to blocked capillaries which can only be removed by diffusion or reorientation of the cake.

Wash efficiency E has ranged from a low of about 45% to a high of 86% for various applications investigated. Most values will range between 60 and 80%. However, some reduction in wash efficiency is almost always experienced in going from the first stage of wash to the second and so on. This will usually range from 3 to 5 percentage points per stage. Wash efficiencies will, in practically all cases, be higher than simply mixing the unwashed cake and refiltering and at the same time will require less wash fluid.

4.2.4 Applied Theory Use in Predicting Full Scale Results.

The applied theory is very useful in prediction of full scale results from representative samples. In most cases, only a small quantity of feed slurry is available and performance requirements of the filtration step must be determined. Such things as obtainable removal of soluble solids, final moisture content, or dilution of the mother liquor by washing fluid are important economic factors and must be predictable. In addition, filtration rate, and thus capital costs, will be influenced by these same factors.

Normally a 0.1 square foot filter leaf is employed for developing data due to the small amount of sample available. At the same time, a much broader investigation can be made with the test filter leaf if proper correlation methods are used. In this way, all rate functions can be determined, the optimum type of filter can be selected, the rate functions can be combined into the filter cycle to obtain desired performance and the resultant filtration rate can be calculated on the basis of performance.

In performing the filtration step, various items are relatively easily measured.

- Feed solids concentration
- Solids size distribution
- Vacuum level or pressure drop
- Cake weight (wet) and thickness
- Cake moisture content
- Volume of filtrate
- Filtrate solids concentration
- Volume of wash fluid
- Soluble solids content of the cake and mother liquor
- Cake formation time
- Cake washing time
- Cake dewatering time
- Rate and volume of gas pulled through the cake
- Observations are also made on ease of cake discharge and required type of discharge.

From these data, all the rate functions can be determined. It is stressed that every effort should be made to simulate probable full scale conditions such as feeding method, agitation, temperature, etc.

Sizing Based on Cake Formation Rate

To obtain the cake formation rate, form filtration rates are first determined by dividing the dry weight of the cake collected by the area employed (usually $0.1 \text{ ft}^2 = 0.0093 \text{ M}^2$) and by the time of cake formation in minutes and multiplying by 60 to obtain kilograms per square meter per hour of cake formation time.

According to Equation 1, a log-log plot of form filtration rate as a function of cake formation time should yield a straight line with parameters of feed solids concentration, pressure drop and temperature. In addition, because of the importance of cake thickness and its influence on cake discharge for the various types of filters, it is desirable to indicate cake thickness.

Ideally, the line should have a slope of -0.50 . However, if there is migration of solids after cake deposition or there is a shape factor effect, the slope can be more negative. With one exception, the slope should always lie between the limits of -1.0 and -0.50 . Any other values indicate erroneous data. The one exception is the precoat filter where the resistance of the precoat bed can be greater than the deposited cake which can occur generally with feed solids concentration of 300 ppm or less. In these instances, the slope can be between zero and -0.50 .

As the slope becomes more negative, this will generally result in shorter full scale filter cycles to obtain economic filtration rates. However, sufficient cake thickness must be obtained for proper discharge with the type of filter employed.

Figure 1 is a typical plot of the log of form filtration rate as a function of the log of form time. Parameters of feed solids concentration are indicated. Also, the influence of flocculation is also indicated for the particular material. When applicable, a sizeable increase in filtration rate is experienced with flocculation.

Normally, about 5 tests at different form times are sufficient to determine the straight line relationship spread over a 5:1 to 10:1 cake formation time range. Validity of the data can be further checked by back-calculating the feed solids concentration and comparing with the measured value. The back-calculation will normally be slightly lower because the solids must be accelerated to the cake; whereas, the liquid does not. If the back-calculated values are less than about 95% of the measured, solids must be stratifying or settling such that the coarser ones are not being pulled to the cake. Thus, erroneous results will be predicted and corrective action should be taken.

To obtain a full scale rate, the form filtration rate at the desired cake thickness is multiplied by the fraction of the filter cycle time that will be devoted to cake formation and by a scale-up factor. The latter is normally 0.8, but will depend on the type of filter.⁽⁷⁾ The scale-up factor should also take into account such things as reasonable fluctuations in feed quality, filter media blinding with time and other operating factors.

As an example of scale-up based on cake formation rate only, Figure 1 can be employed. It will be assumed that this is of disc type feed and flocculation is required. Furthermore, the feed solids size distribution contains some coarse material that must be kept in suspension so that the Agidisc Filter must be employed. A 35% effective submergence (% of cycle exposed to vacuum under slurry) will be used. Also, a 12 mm cake thickness for good discharge is selected. From Figure 1 at 40% feed solids concentration and with flocculation, the form filtration rate is 500 Kg dry solids/M²/hour of cake formation time. With the disc filter, an 0.8 scale-up factor should be used. Accordingly,

$$\begin{aligned}\text{Full scale design rate} &= 500 \times \frac{35}{100} \times 0.8 \\ &= 140 \text{ Kg dry solids/M}^2/\text{hour} \\ &= 28.7 \text{ lbs.dry solids/F}^2/\text{hour}\end{aligned}$$

It should be emphasized that the scale-up factor takes into account % of cake discharge, and reasonable changes in filterability and solids concentration of the feed. A higher value of cake thickness greater than minimum (8 mm) has been selected so that increased capacity is available for higher production rates when needed.

Scale-up Based on Cake Dewatering Rate

Cake dewatering rate is determined by a coordinate plot of discharged moisture content as a function of the correlating factor θ_d/W . Parameters of vacuum level may also be included. Figure 2 illustrates a typical plot with two vacuum levels. It should be noted that if the $(\text{cfm/ft}^2)_d$ is above 20 during the dewatering step, the correlating factor $\left(\frac{\Delta P}{W}\right)\left(\frac{\text{CFM}}{\text{Ft}^2}\right)_d \theta_d$ should be employed.

A sufficient spread of the correlating factor should be tested to determine the knee of the curve and about 100% beyond that point. This will usually entail a 10:1 range in θ_d/W .

To convert this to a production rate, the desired moisture content should be selected and accordingly a value of θ_d/W . As a scale-up factor this value should normally be multiplied by 1.2 to take into account off-quality feeds and other factors. The cake weight per unit area per cycle is selected that yields a dischargeable cake so that the required cake dewatering time can be calculated. If dewatering time is measured in minutes, the filter cycle time can be calculated in minutes per revolution (MPR) by dividing the cake dewatering time by the fraction of the filter cycle that can be devoted to cake dewatering. Finally, the filtration rate is determined by multiplying W by 60/MPR. Thus

$$\text{Filtration Rate} = \frac{60 \times W}{1.2 (\theta_d/W)_1} \quad (8)$$

Figure 4.2.1 Typical Plot of Form Filtration Rate vs. Form Time.

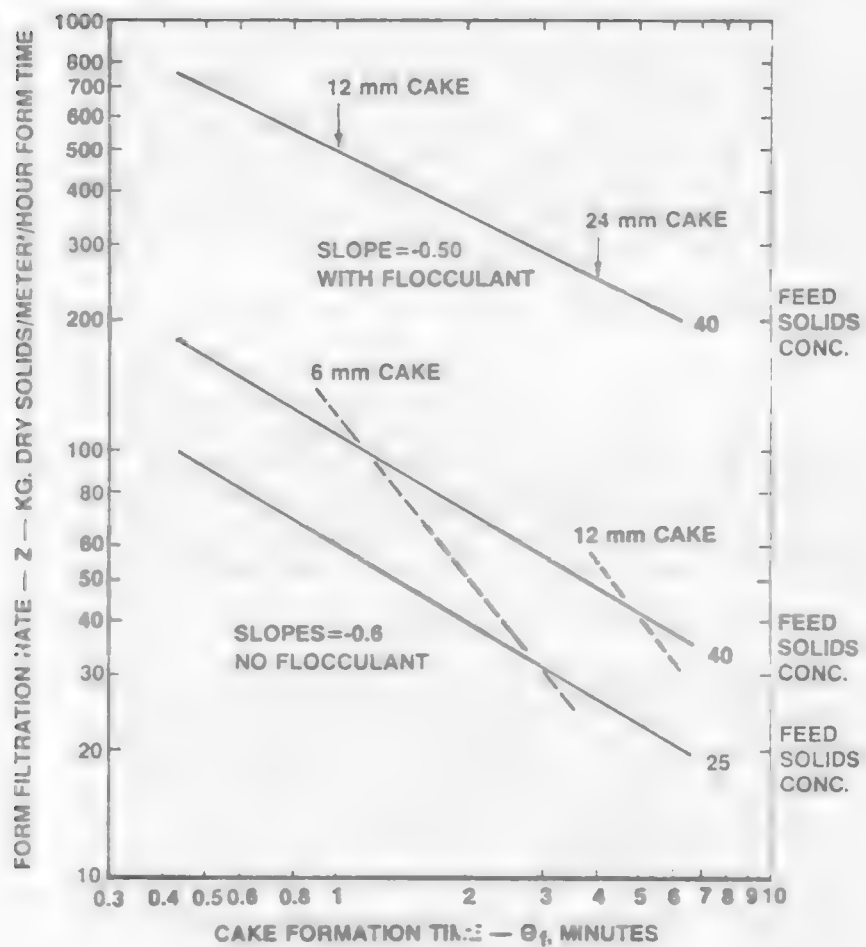
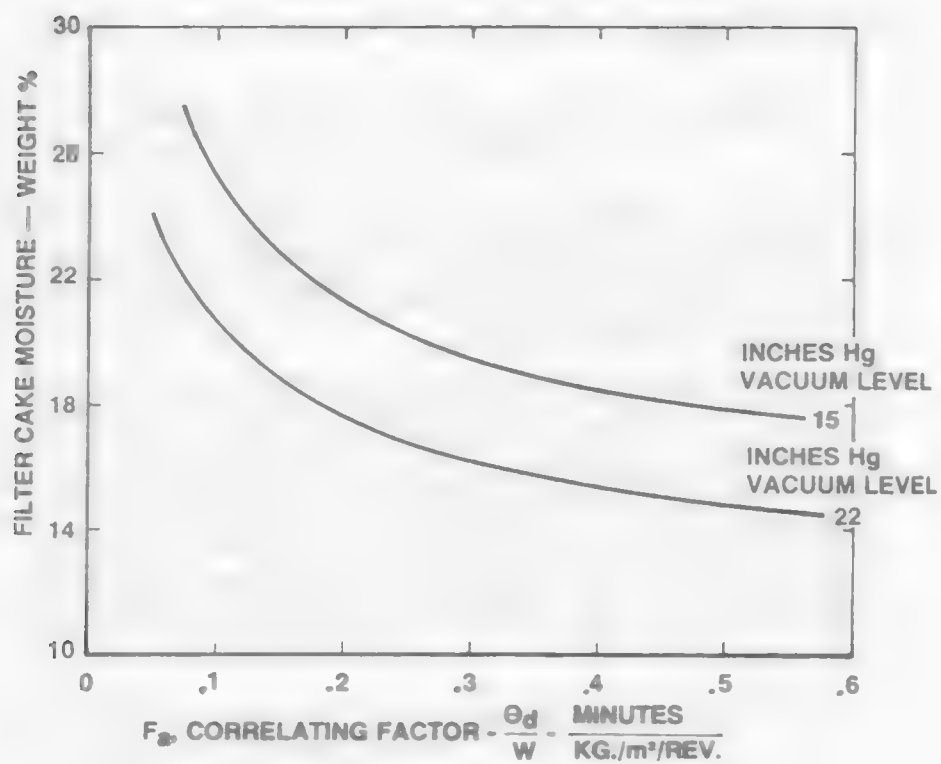


Figure 4.2.2 Typical Plot of Moisture Content vs. The Correlating Factor, F_a .

Where Filtration Rate = weight of dry solids
per unit area per
hour

x = Fraction of cycle time
devoted to dewatering

$\frac{\theta_d}{W}_1$ = required value to achieve
desired moisture

$$\text{MPR} = \frac{1.2(\theta_d)_1}{x} \quad (9)$$

Where $(\theta_d)_1$ = cake dewatering time obtained from
 $(\theta_d/W)_1$ at proper cake thickness

It should be noted that the value of θ_d/W should normally be selected at or beyond the lower portion of the "knee" of the curve as the sharply descending portion is relatively unstable. Furthermore, if moisture content is critical to later processing, it may be desirable to increase the scale-up factor.

As an illustration, if 18% moisture were desired for the material of Figure 2, undoubtedly 22 inches of mercury vacuum would be employed as it could easily be justified. It will also be assumed that a drum filter should be employed as thin cakes are involved. Accordingly, from Figure 2, θ_d/W at 18% moisture = 0.18 minutes per Kg dry solids per meter² per revolution. The solids involved have a specific gravity of 2.7 and a dry solids filter cake density of 101.1 pounds per cubic foot (1609 Kg/M³). With 60% dewatering time on the drum filter and from Equation 8,

$$\begin{aligned} \text{Filtration rate} &= \frac{60(0.6)}{1.2(0.18)} = 166.7 \text{ Kg. dry solids/hr/M}^2 \\ &= 34.2 \text{ lbs.dry solids/hr/ft}^2 \end{aligned}$$

The filter cycle time can also be determined assuming an 8 mm cake thickness.

$$\frac{\theta_d}{W} = 0.18(1.2) = \frac{\theta_d}{1609 (6/1000)}$$

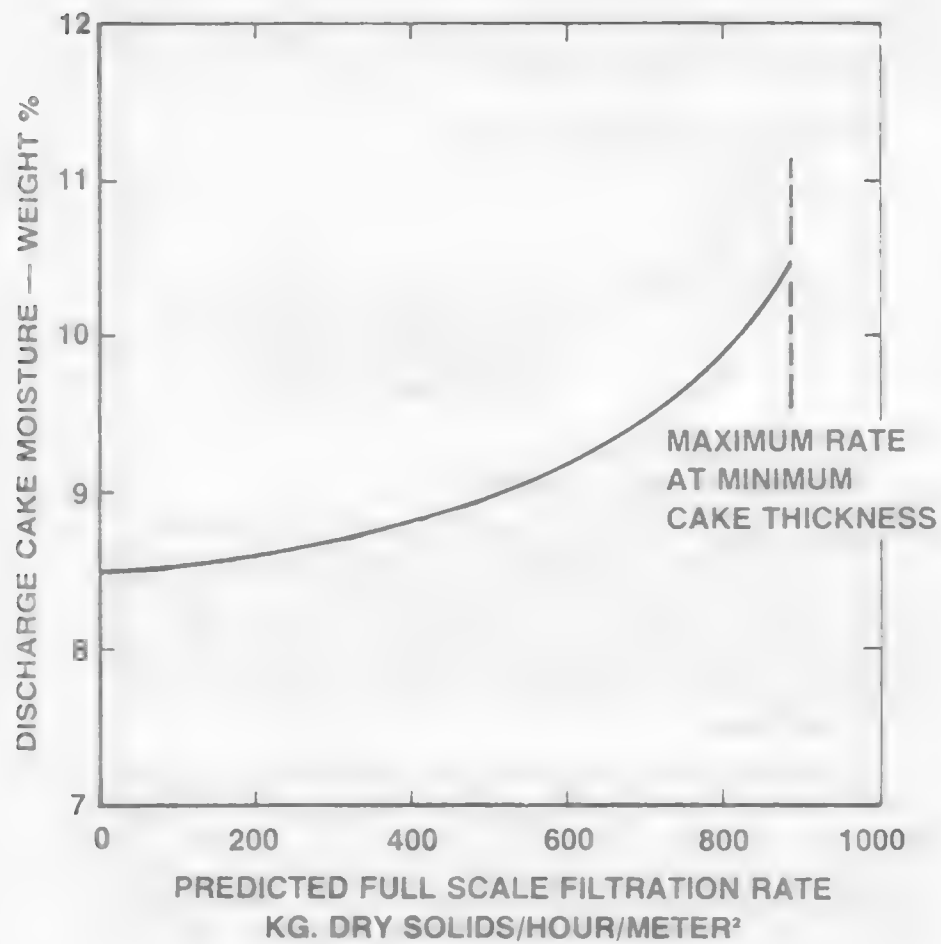
$$\theta_d = 2.09 \text{ minutes}$$

$$\text{MPR} = \frac{2.09}{0.6} = 3.48 \text{ minutes/revolution}$$

By the same method, it is possible to determine moisture content as a function of filtration rate by selecting various θ_d/W values from a plot similar to Figure 2. There will be an upper limit at which cake thickness is too thin to permit effective discharge. Such a plot is shown in Figure 3 which would be typical for some iron ore concentrates. This permits selection of the filter station on the basis of desired performance.

A plot can now be made of moisture content as a function of predicted filtration rate. There will be an upper limit at which cake thickness is too thin to permit effective discharge. A typical plot is shown in Figure 3.

Figure 4.2.3 Typical Curve of Cake Moisture Content as a Function of Filtration Rate.



To determine energy requirements (vacuum pump or compressor), a measurement of gas rate through the cake as a function of dewatering time is made. This should be taken at the desired cake thickness. A typical plot is shown on Figure 4. It will be noted that the instantaneous gas rate increased rapidly and levels off to some maximum value as the capillaries become dewatered. Generally, the maximum rate is employed as the desired value to ensure proper vacuum operation. As the filter internal drainage network must also be evacuated prior to filtration, a scale-up factor of 1.1 is usually employed. As vacuum or compressor requirements are usually based on total area, the following equation permits calculation:

$$\begin{aligned} &\text{Required compressor or vacuum} \\ &\quad \text{pump capacity} = \\ &= 1.1 \left(\frac{\text{CFM}}{\text{Ft}^2} \right)_{d2} \times \end{aligned} \quad (10)$$

Where $(\text{CFM}/\text{Ft}^2)_{d2}$ = maximum gas rate during dewatering expressed as cubic feet per minute per square foot measured at downstream pressure

Scale-up Based on Cake Washing Rate

To determine the cake washing rate functions two plots are required. The first is a plot of θ_w as a function of wash ratio n with parameters of θ_f . A typical plot is shown in Figure 5. To check validity, the ratio of cake washing time at any one wash ratio should be approximately equal to the cake formation time. However, this will generally "fan out" slightly more because of certain phenomenon.

The second is a plot of R as a function of wash ratio n on semi-log paper. A typical plot is shown in Figure 6. Another convenient plot is % soluble solids in the washed cake as a function of the wash ratio on semi-log paper. Figure 6 permits the calculation of the wash efficiency term E at a wash ratio of 1.0. As a scale-up factor, the calculated value of E is usually lowered by 5 percentage points to account for uneven distribution of wash fluid and reasonable off-quality of feed.

Full scale filtration rate for cake washing can now be calculated. From Figure 5, a wash time is selected at a form time that yields a sufficient cake thickness for discharge and at a specific wash ratio. This value divided by the fraction of time during the filter cycle devoted to cake washing yields the cycle time. A scale-up factor of 1.2 is normally employed. Multiplying the cake weight selected by 60/MPR yields the full scale filtration rate. Thus

$$\text{Filtration Rate} = W \frac{60}{1.2 \theta_w} S \quad (11)$$

Figure 4.2.4 Typical Plot of Gas Rate Through the Cake as a Function of Dewatering Time.

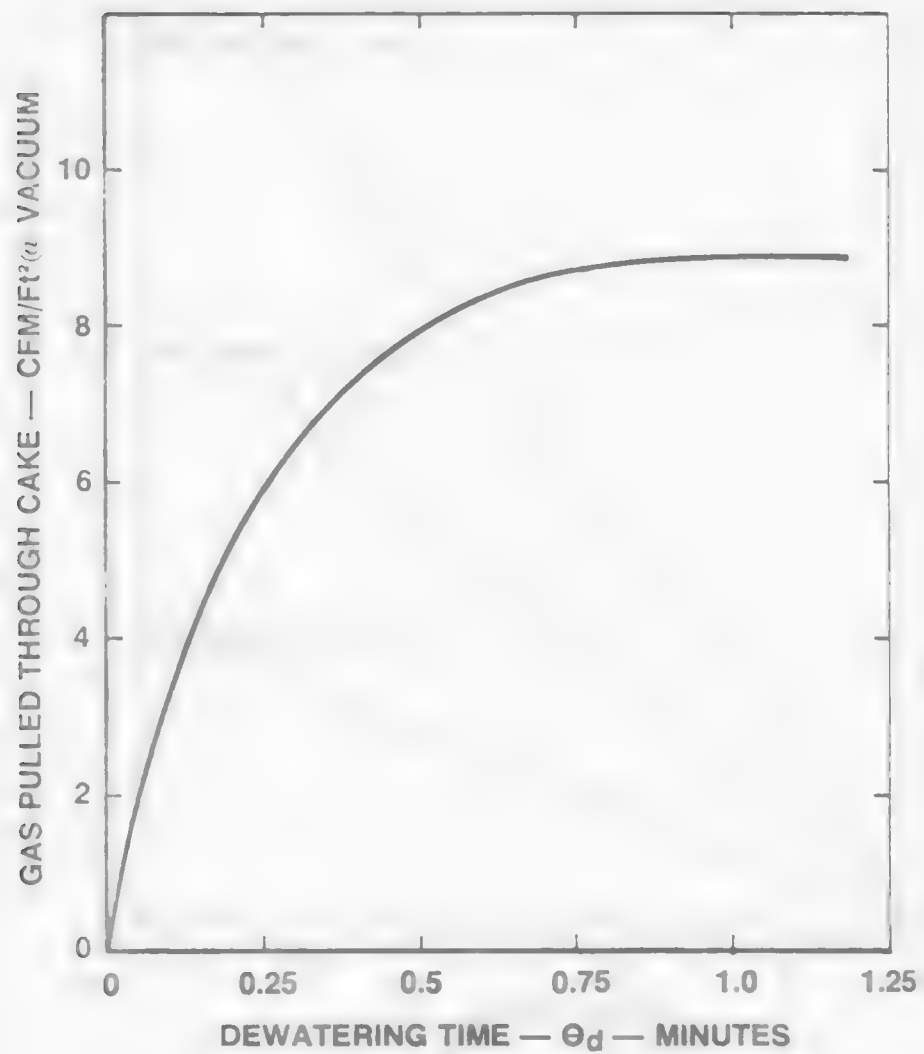


Figure 4.2.5 Typical Plot of Cake Wash Time as a Function of Wash Ratio Parameters of Cake Formation Time.

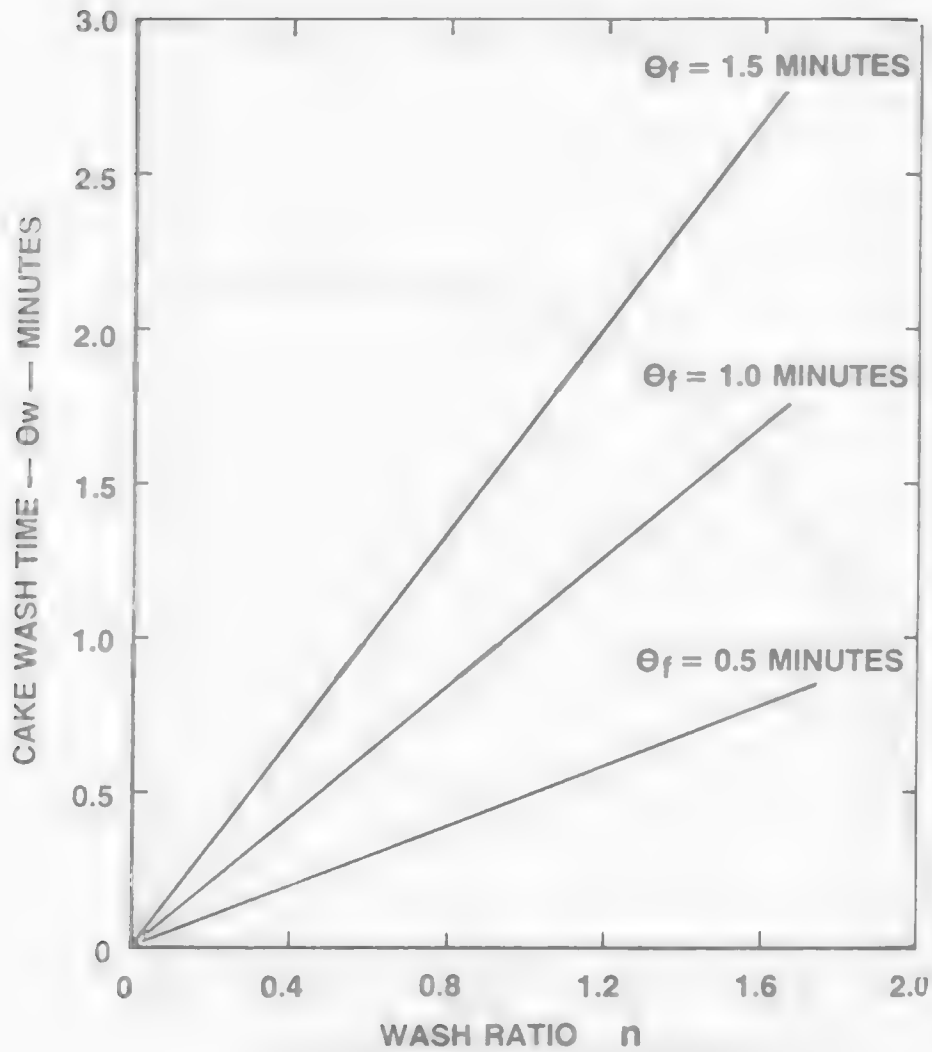
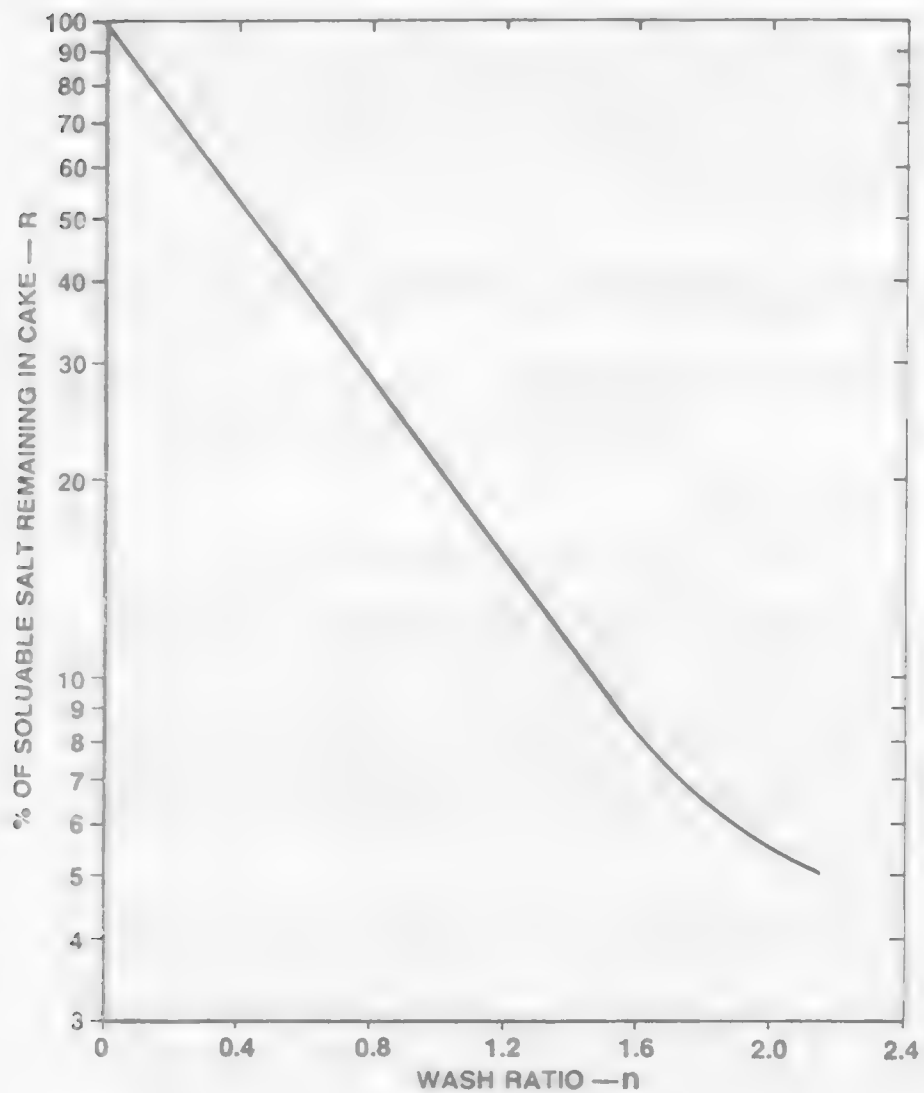


Figure 4.2.6 Typical Plot of % Remaining of Soluble Salt in the Filter Cake as a Function of Wash Ratio.



Where filtration rate is measured in weight of dry solids per hour per total unit area W and θ_w are selected values with θ_w measured in minutes

S = Fraction of filter cycle devoted to cake washing

From the full scale filtration rates calculated, it is now possible to draw plots of rates as a function of filter cycle time with parameters of wash ratio n . A drum filter selection will be assumed for the data of Figure 5. Cake weight at 8 mm cake thickness obtained at a 1.0 cake formation time will also be assumed. Cake weight is 2.48 pounds dry solids/Ft²/Rev. (12.08 Kg. dry solids/M²/Rev.)

As the drum filter has 30% of the cycle available for cake washing, from Equation 11 and Figure 5 at a wash ratio n of 1.2,

$$\begin{aligned}\text{Filtration rate} &= \frac{12.08(60)0.30}{1.2(1.25)} = 145 \text{ Kg. dry Solids/M}^2\text{/Hr.} \\ &= 29.7 \text{ pounds dry solids/hour/foot}^2\end{aligned}$$

Also, from Figure 5

$$\text{MPR} = \frac{1.25}{0.3} = 4.17 \text{ minutes/revolution}$$

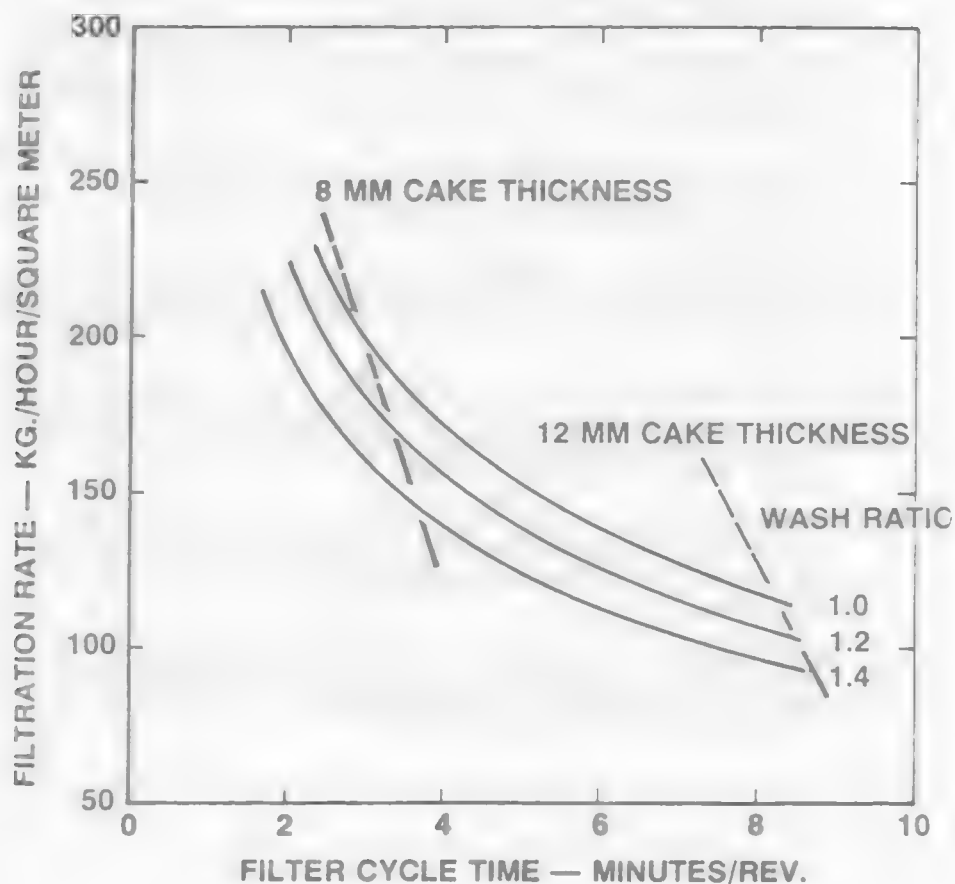
Figure 7 gives the complete plot calculated by the same method. Included on the graph are lines of cake thickness so that proper discharge can be obtained.

To calculate soluble solids recovery in the filtrate or elimination from the cake, the determined value of wash efficiency E is employed with the suitable scale-up factor. This can be done by material balance determinations permitting both soluble solids recovery and concentration of the filtrates in soluble salts.

Normally, one of the rate functions will be controlling with respect to filter cycle time and filtration rate. For example, if high soluble salt recovery or moisture content is critical, these respective rate functions will usually control. However, the others must be calculated to properly incorporate them into the filter cycle. It is also emphasized that in these two cases, the appropriate amount of cake weight per cycle must be applied if desired results are to be achieved. This usually results, for example, that for a drum or disc filter, a lesser amount of the cycle will be devoted to cake formation than is possible with the apparent submergence.

From the previous development, it is possible to design the filter station to achieve desired performance for the respective feed, to optimize the filtration step with respect to economics and to determine energy requirements for any condition. It is emphasized that this stems from applied theory, all of which was developed from the fundamental theory.

Figure 4.2.7 Typical Plot of Full Scale Filtration Rate as a Function of Filter Cycle Time Parameters of Wash Ratio and Cake Thickness.



REFERENCES

1. Dahlstrom, D.A., "Practical Use of Applied Theory of Continuous Filtration", The Second Pacific Chemical Engineering Congress, American Institute of Chemical Engineers, Denver, Colorado, August 28-31, 1977.
2. Dahlstrom, D.A., "Applications of Continuous Filtration in the Metallurgical Flowsheet", The Canadian Institute of Mining & Metallurgy, February, 1959.
3. Nelson, P.A. and Dahlstrom, D.A., "Correlation of Rotary Vacuum Filter Cake Moisture Contents", Chemical Engineering Progress, July, 1957.
4. Henderson, A.A., Cornell, C.F., Dunyon, A.F. and Dahlstrom, D.A., "Filtration and Control of Moisture Content on Taconite Concentrates", Mining Engineering, March, 1957.
5. Silverblatt, C.E. and Dahlstrom, D.A., "Production of Low Moisture Content Fine Coal Without Thermal Drying", International Congress on Coal Preparation Proceedings, Paris, France, 1973.
6. Choudhury, A.P.A. and Dahlstrom, D.A., "Prediction of Cake Washing Results With Continuous Filtration Equipment", Chemical Engineering Journal, December, December, 1957.
7. Dahlstrom, D.A., "Scale-up Methods for Continuous Filtration Equipment", International Symposium on Chemical Processing, Proceedings, London, May, 1959.

UNIT PROCESSES IN EXTRACTIVE METALLURGY
HYDROMETALLURGY

Module 8

Leaching of Metals, Solids and Solphides

EIGHT LEARNING ACTIVITIES

Module Coordinator: Dr. H. H. Haung
Assistant Professor of Metallurgical Engineering
Montana College of Mineral Science and Technology

Module 5 Contents

Leaching of Metals, Oxides and Sulfides

5.1 Overview

Learning Activity 1

1. Introduction
2. Leaching Methods and Equipment
3. Thermodynamics of Leaching Reactors
4. Leaching Kinetics
5. References

5.2 Leaching of Metals

Learning Activity 2

1. Gold Cyanidation
 1. Chemistry and Mechanism of Cyanide Leaching of Gold
 2. Gold Cyanidation Practice
 3. Conventional Gold Cyanidation
 4. Carbon Adsorption and Desorption Process
 5. Electrowinning
 6. Cyanide Heap Leaching of Gold Ore
 7. Cortez Heap Leach Cyanidation
2. Leaching of Metallic Copper
 1. Chemistry
 2. Practice
3. References

5.3 Leaching of Oxides

Learning Activity 3,4

1. Thermodynamics and Kinetics
2. Leaching of Uranium Oxides
 1. Hydrometallurgical Process for Uranium Oxides
 2. Acid Leaching of Uranium Oxides
 3. Carbonate Leaching of Uranium Oxides
3. Leaching of Bauxite--Bayer Process
4. Leaching of Nickel Oxides
 1. General Considerations
 2. Direct Sulfuric Acid Leach
 3. Reductive Roasting/Ammoniacal Leaching
 4. Sulfidization Process
5. Leaching of Ocean Manganese Nodules
 1. General Considerations
 2. Kennecott Cuprion Process
6. Leaching of Copper Oxide
 1. Leaching Methods
 2. In-situ Leaching
 3. Dump Leaching
 4. Heap Leaching
 5. Vat Leaching
 6. Agitation Leaching
7. References

5.4 Leaching of Sulfides

1. Introduction
 1. Thermodynamics
 2. Kinetics
2. Leaching of Nickel and Cobalt Sulfide Minerals
 1. Ammonia Oxidation Leaching of Ni-Co Sulfides
 2. Acid Leaching of Nickel and Cobalt Sulfides
 3. Leaching of Copper-Nickel Matte
3. Leaching of Copper Sulfides--Fundamental Studies
 1. Sulfuric Acid Leach
 2. Ammonia-Oxygen Leach
 3. Ferric Chloride Leach
 4. Nitric Acid Leach
 5. Cyanide Leach
 6. Microbiological Leach
 7. Electrochemical
4. Leaching of Copper Sulfide--Processes
 1. Roast-Leach-Electrowin Process
 2. Ammonia Leach Processes
 3. Ferric Chloride Leach Processes
 4. Acid Leach Processes
5. Leaching of Other Sulfides
 1. Roast Leach Process for Zinc Sulfide
 2. Direct Leaching of Zinc Sulfide
6. References

Learning Activity 5

Learning Activity 6

Learning Activity 7

Learning Activity 8

LEARNING ACTIVITY 1

5.1 Overview

Learning Activity Objective

After completing your study of the material presented in this learning activity you should be able to briefly describe leaching methods, types of leaching equipment, types of leaching reactions, and types of leaching reagents.

5.1.1 Introduction.

Hydrometallurgical processes are playing an increasingly important role in the extractive metallurgy of both base and rare metals. There are several reasons for this growing interest: hydrometallurgical processes are relatively pollution free, especially with respect to air pollution; hydrometallurgical processes allow treatment of low grade ores or mining waste materials that can not be economically upgraded by conventional milling, smelting and refining; hydrometallurgical processes allow the mining and treatment of relatively small ore deposits; hydrometallurgical processes are usually lower in capital cost than smelters; and hydrometallurgical operations are relatively easy to control.

A hydrometallurgical process can generally be divided into three main unit operations; namely, leaching of the desired metal into solution, concentration and purification of the pregnant solution, and, finally, recovery of the metal. The leaching process involves dissolution of metal value from a raw material into an aqueous solution with suitable chemical agents in a confined space. A general review of the raw materials, leaching agents, and leaching methods is presented in the following discussion, and a summary is given in Table 5.1.1.

Raw Materials

Raw materials that may be treated by leaching processes are primary ores and secondary metals. The former is obtained directly from ore deposits and the latter is obtained from recycled scrap and wastes. Secondary metals are further divided into the following categories:⁽¹⁾

- (1) Process waste - saw offcuts, grinding dusts, slags, flue dust, catalysts, sludges, etc.
- (2) Capital waste - discarded plant machinery, automobiles, electrical cables, etc.
- (3) Domestic waste - municipal waste contains large amounts of iron and aluminum, and a fairly large amount of copper and zinc. (The compositions of municipal waste and incinerator residue are listed in Table 5.1.2.)
- (4) Plant and Mine effluent

Most secondary metals are recovered via pyrometallurgical processes. However, several hydrometallurgical processes have been proposed.^(2,3)

The primary source of raw materials are naturally occurring ores. These ores may be native ores, oxide ores, or sulfide ores.

Table 5.1.1 Summary of Leach Process.

Raw Materials

- | | |
|----------|--|
| Metals | a. Native metal
b. Scrap metals
c. Cementation products |
| Oxides | a. Oxide ores
b. Refractorial oxide ores
c. Roasted calcines
d. Sea Nodules |
| Sulfides | a. Sulfide ores
b. Matte sulfides
c. Sulfidized products |

Methods

- | |
|---|
| a. In-situ leach
b. Dump and heap leach
c. Percolation and Vat leach
d. Agitation leach (atmospheric and pressure) |
|---|

Reagents

- | | |
|-------------------|---|
| Acids | a. Sulfuric acid
b. Hydrochloric acid |
| Bases | a. Lime
b. Sodium hydroxide
c. Ammonium hydroxide |
| Complexing Agents | a. Free ammonia
b. Cyanide salts
c. Chloride salts
d. Carbonate salts |
| Oxidation Agents | a. Oxygen
b. Ferric salts
c. Sodium or hydrogen peroxide
d. Permanganate
e. Manganese dioxide |
| Reducing Agents | a. CO gas
b. SO ₂ gas
c. H ₂ gas |

Table 5.1.2 Average Composition of Raw Refuse and Municipal Incinerator Residues. (1)

<u>Material</u>	<u>Raw Refuse, %</u>	<u>Incinerator Residue, %</u>
Glass	9.7	30.0
Aluminum	0.6	1.4
Copper-Zinc	0.3	0.6
Ferrous Metals	8.5	20.0
Ash and Slag	-	48.0
Paper	31.3	-
Food Waste	17.6	-
Yard Waste	19.3	-
Plastic	3.4	-
Leather, Rubber	2.6	-
Wood	3.7	-
Textiles	1.5	-
Dirt, Ceramic, etc.	1.5	-

Native Ores--The metals that commonly occur in the native form are noble metals, such as gold, silver, platinum, and copper, etc. One of the main sources of native copper is located in upper Michigan. Today, high grade ores have been mined out. In-situ leaching has been proposed as a means of recovering copper from the remaining low grade copper deposits.

Oxide Ores--This class includes oxides, carbonate and silicates of common metals. Some hydrometallurgically treated oxide minerals are listed in Table 5.1.3. Copper, nickel, zinc and other oxides usually occur close to the surface of the earth due to the decomposition and alteration of primary sulfide ores. Most of the metal oxides are readily soluble either in acid or in alkaline media. However, they usually occur as finely dispersed substances in a gangue matrix. This makes the physical concentration difficult. Successful hydrometallurgical processing of these types of ore require treatment of large amounts of materials to recover a small amount of metal values.

Sulfide Ores--This class includes copper, zinc, nickel, cobalt, lead, antimony, arsenic and molybdenum sulfides. Treatment of sulfide ores is usually performed by pyrometallurgical operations. However, due to air pollution regulations, hydrometallurgical processing has gained great attention. Also due to the development of dump leaching techniques, several open pit mine operations use dump leaching to recover metal from cutoff grade sulfide ores. Common sulfide minerals and their chemical formula are listed in Table 5.1.4.

Leach Reagents

The choice of a leach reagent depends on its availability, cost, stability, selectivity, ease of producing and regenerating and the ease of recovering the metal value from the leach reagent.

Table 5.1.3 Oxide Minerals.

<u>Material</u>	<u>Mineralogical Form</u>	<u>Chemical Formula</u>
Aluminum	Gibbsite	$\text{Al}(\text{OH})_3$
	Boehmite, Diaspore	AlOOH
Copper	Azurite	$2\text{CuCO}_3 \cdot \text{Cu}(\text{OH})_2$
	Malachite	$\text{CuCO}_3 \cdot \text{Cu}(\text{OH})_2$
	Chrysocolla	CuSiO_3
	Cuprite	Cu_2O
	Tenorite	CuO
Tin	Cassiterite	SnO_2
Uranium	Pitchblende	$\text{UO}_2 + \text{UO}_3$
	Uraninite	$\text{UO}_2 + \text{UO}_3$
Zinc	Zincite	ZnO
	Hydrozincite	$\text{ZnCO}_3 \cdot 2\text{Zn}(\text{OH})_2$
Nickel	Nickeliferous limonite	$(\text{Fe}, \text{Ni})\text{O}(\text{OH}) \cdot n\text{H}_2\text{O}$

Table 5.1.4 Sulfide Minerals.

<u>Material</u>	<u>Mineralogical Form</u>	<u>Chemical Formula</u>
Copper	Chalcopyrite	CuFeS_2
	Chalcocite	Cu_2S
	Covellite	CuS
	Bornite	Cu_5FeS_4
Iron	Pyrite	FeS_2
	Pyrrholite	FeS
Lead	Galena	PbS
Zinc	Sphalerite	ZnS
Nickel	Pendlandite	$(\text{Fe}, \text{Ni})_9\text{S}_8$
Cobalt	Mellerite	NiS
	Linnaeite	Co_3S_4
Molybdenum	Molybdenite	MoS_2
Silver	Argentite	Ag_2S
Antimony	Stibnite	Sb_2S_3
Arsenic	Realgar	As_4S_4

Acids--Sulfuric acid is the most widely used leaching agent, especially in the copper industry. One reason for this is that it is readily available. Sulfuric acid is a by-product at most smelter locations. Hydrochloric acid is sometimes used due to its formation of stable metal-chloride complexes.

Bases--Alkaline leaching shows some advantages over acid leaching. These are: more selective, less corrosive, less reagent consumption for carbonate gangue. Sodium hydroxide, lime and ammonium hydroxide are among the commonly used alkaline reagents. Ammonium hydroxide is commonly used in cobalt, nickel and copper industries due to the formation of stable metal-ammine complexes. Sodium hydroxide may sometimes be generated in-situ in the reactor by combining slaked lime with sodium carbonate:



Oxidizing Agents--Air and oxygen are the most economical and commonly employed oxidizing agents. However, due to the low solubility of oxygen in aqueous solutions, ferric ion and cupric ion are sometimes used as an autocatalyst in leaching processes, i.e., ferric or cupric ion is used to dissolve metal value. The reduced ferrous or cuprous ions are reoxidized by oxygen. Some chemical oxidizing agents such as hydrogen peroxide, potassium permanganate, manganese dioxide, sodium chlorate have been used, but the application has not been widely adopted.

Complexing Agents--Several metal ions, transition metals especially, form stable metal-complex ions with complexing agents, such as the copper (II) tetraammine complex. The commonly used complexing agents are cyanide salts, ammonia, chloride salts, carbonate salts, etc.

5.1.2 Leaching Methods and Equipment.

The principle methods of leaching are in-situ, dump, heap, vat and agitation. The choice of leaching method depends upon the chemical and physical characteristics of the ore and the associated minerals to be treated. The grade of the ore, the solubility of the metal value, the kinetics of the dissolution, the reagent consumption, the size of the operation, the type of the minerals, etc., are all important factors.

In-situ Leach--In-situ leaching involves leaching of the broken ore in the ground as it occurs. The ore can be the shattered rock residue left in the mine after it has been mined out or the rubbleized orebody which can not be economically treated by conventional mining methods. In-situ leaching eliminates mining and handling large tonnages of materials, and depositing of the final waste products.

In-situ leaching involves injecting a water solvent through inflow wells to an ore body. After passing through the ore body and dissolving some metal value, the pregnant solution is pumped out through one or more product wells.

Dump Leach--Dump leaching is used to extract metal values from run-of-mine materials containing metal values less than the cutoff grade. The raw material is usually the waste generated during large scale open pit mining. This material is dumped on an impervious pad, and the aqueous solvent is

sprinkled on the surface of the dump and percolates through the dump by gravity. A pregnant solution is collected at the bottom of the dump and given further treatment. After completing the leaching cycle, the metal free solid residue is left on the pad.

Heap Leach--The basic principle of the heap leaching operation is similar to dump leaching. However, heap leaching is used to extract metal values from run-of-mine ore instead of mining waste. The ore is usually porous and readily soluble in the aqueous solvent.

Vat Leach--Vat leaching is used to extract metal values from higher grade crushed ore in a confined container. This method is preferred to heap leaching if the ore material is not porous and crushing is necessary to permit adequate contact between the aqueous solvent and the metal value in the ore. The crushed ore is usually 3/8-inch to 3/4-inch in size. If the particle size is too fine serious loss of permeability results and the solution cannot percolate through the solids.

A vat leaching plant consists of a number of vats. Each is 60 to 175 ft on each side and 10 to 20 ft deep, and equipped with special solution filters built around outlets at the base of the vat. The vats are usually constructed of reinforced concrete with a lining such as reinforced plastic.

Agitation Leach--Agitation leaching is used to extract metal values from finely ground ore in a well mixed container. The method of agitation can be accomplished either by mechanical agitation or by airlift agitation. The mechanical agitation vessel, about 24 ft in diameter by 14 ft high, is usually baffled and equipped with turbine type propellers. The airlift agitation vessel, normally known as a Pachuca tank, is a cylindrical tank about 23 ft in diameter and 45 ft high, with a 60° conical bottom. Air is injected through the bottom of the cone. The air serves to both lift and aerate the pulp.

Pressure Agitation Leach--The advantages of pressure leaching over leaching at atmospheric pressure is that higher pressure permits operation at higher temperatures. This increases the solubility of the gaseous reagent, resulting in an increase in the leaching rate. Disadvantages, however, are the higher capital cost for the pressure vessels, greater instrumentation is required, and in general, the use of more complicated equipment requires greater operator training.

Agitation in pressure vessels can be accomplished by mechanical agitation or by airlift. The former is known as an autoclave; the latter is a pressure Pachuca tank. A horizontal autoclave is used in most pressure leaching. They are about 10 to 15 ft in diameter and 25 to 50 ft in length. They are divided into three sections by baffle plates. Pulp enters at one end of the autoclave and is discharged at the opposite end after passing through each section. Each compartment is equipped with a turbine-type agitator.

A pressure Pachuca tank is basically the same as a regular Pachuca tank except the top part of the tank is sealed in order to accommodate the higher pressure.

Acids--Sulfuric acid is the most widely used leaching agent, especially in the copper industry. One reason for this is that it is readily available. Sulfuric acid is a by-product at most smelter locations. Hydrochloric acid is sometimes used due to its formation of stable metal-chloride complexes.

Bases--Alkaline leaching shows some advantages over acid leaching. These are: more selective, less corrosive, less reagent consumption for carbonate gangue. Sodium hydroxide, lime and ammonium hydroxide are among the commonly used alkaline reagents. Ammonium hydroxide is commonly used in cobalt, nickel and copper industries due to the formation of stable metal-ammine complexes. Sodium hydroxide may sometimes be generated in-situ in the reactor by combining slaked lime with sodium carbonate:



Oxidizing Agents--Air and oxygen are the most economical and commonly employed oxidizing agents. However, due to the low solubility of oxygen in aqueous solutions, ferric ion and cupric ion are sometimes used as an autocatalyst in leaching processes, i.e., ferric or cupric ion is used to dissolve metal value. The reduced ferrous or cuprous ions are reoxidized by oxygen. Some chemical oxidizing agents such as hydrogen peroxide, potassium permanganate, manganese dioxide, sodium chlorate have been used, but the application has not been widely adopted.

Complexing Agents--Several metal ions, transition metals especially, form stable metal-complex ions with complexing agents, such as the copper (II) tetraammine complex. The commonly used complexing agents are cyanide salts, ammonia, chloride salts, carbonate salts, etc.

5.1.2 Leaching Methods and Equipment.

The principle methods of leaching are in-situ, dump, heap, vat and agitation. The choice of leaching method depends upon the chemical and physical characteristics of the ore and the associated minerals to be treated. The grade of the ore, the solubility of the metal value, the kinetics of the dissolution, the reagent consumption, the size of the operation, the type of the minerals, etc., are all important factors.

In-situ Leach--In-situ leaching involves leaching of the broken ore in the ground as it occurs. The ore can be the shattered rock residue left in the mine after it has been mined out or the rubbleized orebody which can not be economically treated by conventional mining methods. In-situ leaching eliminates mining and handling large tonnages of materials, and depositing of the final waste products.

In-situ leaching involves injecting a water solvent through inflow wells to an ore body. After passing through the ore body and dissolving some metal value, the pregnant solution is pumped out through one or more product wells.

Dump Leach--Dump leaching is used to extract metal values from run-of-mine materials containing metal values less than the cutoff grade. The raw material is usually the waste generated during large scale open pit mining. This material is dumped on an impervious pad, and the aqueous solvent is

The leaching vessel can be constructed from a wide variety of materials. The selection of the material depends on the temperature, the type and the strength of the leaching agent, the pressure of the operation, etc. An approximate guide for the selection of materials for common reagents under oxidizing conditions is listed in Table 5.1.5.(4)

Table 5.1.5 Examples of Containment Materials.

H ₂ SO ₄	HCl	NaOH	NH ₄ OH
Materials of Construction			
Wood	Rubber Lined	Mild Steel	Stainless Steel
F.R.P.	Mild Steel		
Lead	Rubber Lined		
Lead & Acid Brick	Mild Steel &		
Stainless Steel	Acid Brick		
Titanium	Glass		
	Titanium		

5.1.3 Thermodynamics of Leaching Reactions.

The thermodynamics of leaching reactions are best illustrated by the use of Eh-pH diagrams, known as Pourbaix diagrams (Pourbaix diagrams have been presented in detail in an earlier module). Refer to the Eh-pH diagram for the Cu-S-H₂O system (figure 5.1.1) for example. First of all, the dissolved species must exist between the two limits of water stability, e.g., the upper limit of water stability is described by the following reaction:



$$E = 1.228 - 0.0591\text{pH} + 0.0147 \log P_{\text{O}_2} \quad [5.1.2]$$

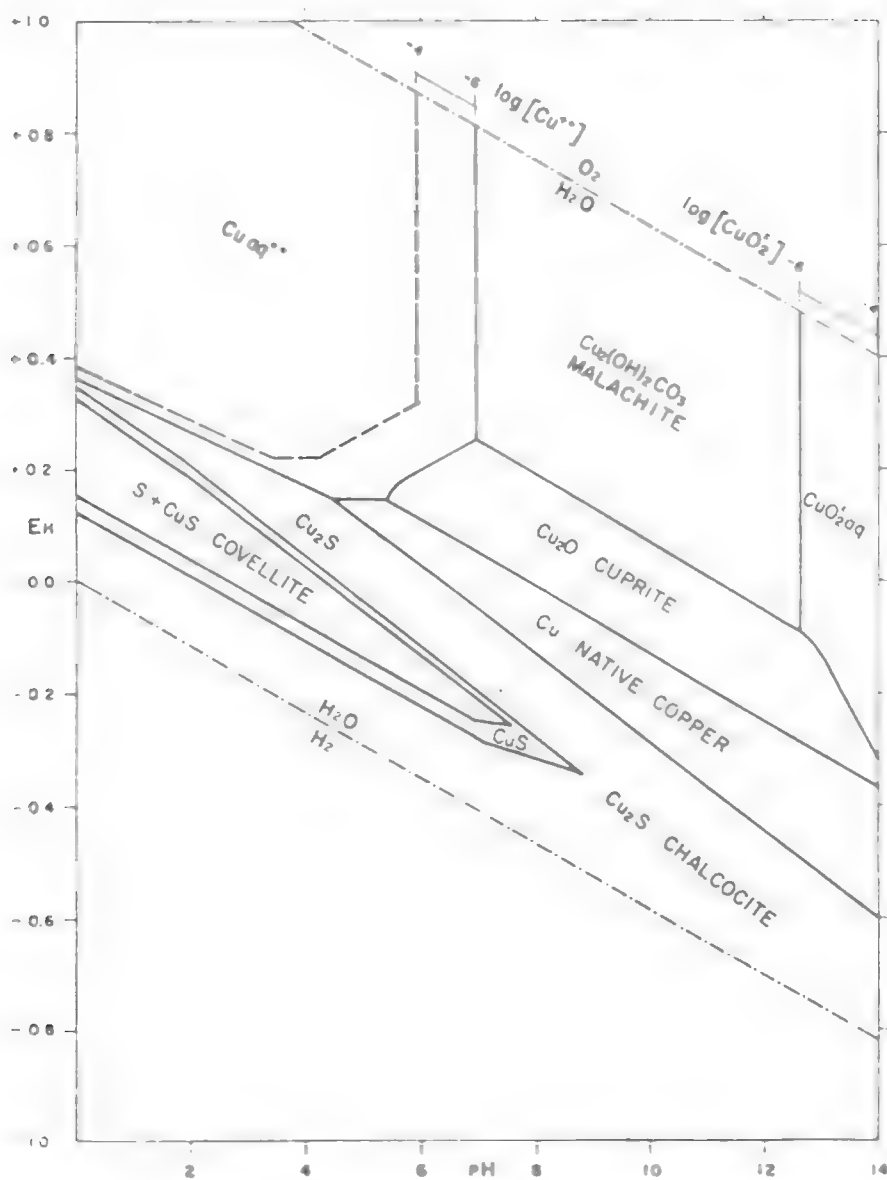
The lower limit of water stability is described by the hydrogen evolution reaction:



$$E = -0.0591 \text{ pH} - 0.0295 \log P_{\text{H}_2} \quad [5.1.4]$$

To stabilize a dissolved species close to the upper limit of water stability, an oxidizing environment is required; on the other hand, to stabilize a dissolved species close to the lower limit of water stability, a reducing environment is required.

Judging from the Eh-pH diagram (figure 5.1.1), cupric ion, Cu²⁺, and cuprite ion, Cu₂O²⁻, are stable ions in acid media and strong alkaline media, respectively. Copper (II) oxide which is stable in a neutral pH is readily soluble in acid or in strong alkaline solutions. Metallic copper, copper sulfides and copper (I) oxide require not only an acid or strong alkaline but also an oxidizing agent, for example

Figure 5.1.1 The Cu-S-H₂O System.

Stability relations among some copper compounds in the system Cu-H₂O-O₂-S-CO₂ at 25 °C and 1 atmosphere total pressure. $P_{\text{CO}_2} = 10^{-1.5}$, total dissolved sulfur species = 10^{-1} . [Courtesy J. Anderson.]

Source: R. M. Garrels, et.al., Solution, Minerals and Equilibria, Freeman, Cooper & Co.



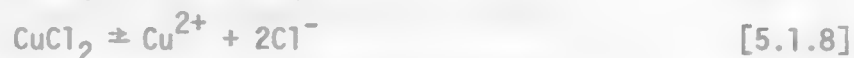
Although the Eh-pH diagram for each metal assemblage is unique, it can be generally stated that: Most base metal oxides when in their highest oxidation state are readily soluble in acid or strong alkaline media; and most metals, metal oxides in their lowest oxidation states, and metal sulfides require not only acid or strong alkaline reagents but also oxidizing agents for dissolution.

You should be cautious about using Pourbaix diagrams when treating metal ions. It is a reasonable assumption to consider the species present to be simple ions only for alkaline or alkaline earth elements. A number of base metals, transition metals especially, tend to react with complexing agents to form stable metal complex ions. The most dramatic example is the dissolution of gold with cyanide salt. Complexing agents play an important role in the leaching process. Another example is cupric oxide, CuO , which is a stable solid in neutral or slightly alkaline media but is readily soluble in an ammoniacal solution, e.g.,



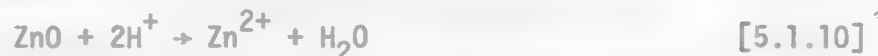
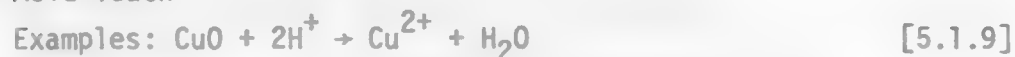
The dissolution of a mineral in an aqueous solution may be described by one of the following reaction types:

(1) Water leach



The minerals may be naturally occurring or may be produced by some other pyrometallurgical unit operation such as pretreatment, e.g., sulfating or chloridizing roast.

(2) Acid leach



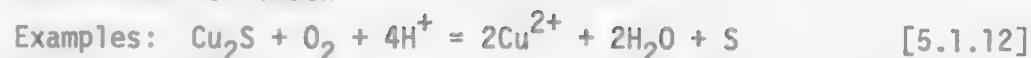
The minerals may be naturally occurring or may be produced by some other unit operation.

(3) Alkaline leach



This example, representative of the Bayer process, demonstrates the effect of changing from acid to alkaline conditions to achieve leaching selectivity. Iron oxide is normally associated with the alumina but is not soluble in normal alkaline solutions and is, thereby, rejected from the system.

(4) Acid Oxidation leach

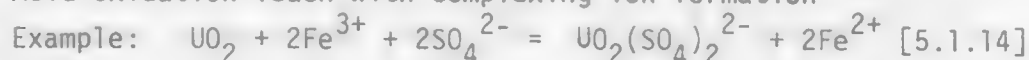


Ferric ion can only serve as an oxidizing agent. In an acid media it precipitates as iron oxide in neutral and alkaline conditions.

(5) Alkaline Oxidation leach

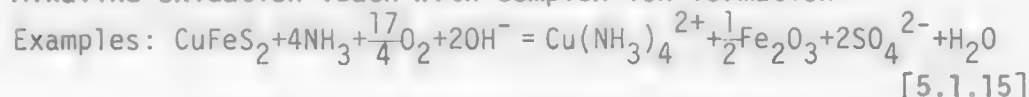


(6) Acid Oxidation leach with complexing ion formation



This complexing reaction demonstrates the changing of the uranyl cation to an uranyl anion by controlling the complexing agent. The anion complex can be selectively extracted by the unit operations of ion exchange or solvent extraction.

(7) Alkaline oxidation leach with complex ion formation



Again, alkaline leach may be more selective than an acid leach.

(8) Reduction leach



There are only a few examples that fit this category: MnO_2 , Fe_2O_3 and SnO_2 etc. The lower oxidation state species are more soluble than the higher oxidation state species.

5.1.4 Leaching Kinetics

Leaching kinetics play an important role in hydrometallurgical processes. The kinetics are usually slow and heterogeneous. A detailed discussion on this topic has been presented in an earlier module, Hydrometallurgical Kinetics.

Leaching reactions usually involve consecutive processes:

1. Dissolution of gaseous reactants into the aqueous solution.
2. Mass transfer of reactants through a liquid film to the solid/liquid interface. The reactants include acid or base, oxidizing or reducing agents, and complexing agents.
3. Mass transfer of reactants through solid product or gangue material to the mineral surface. The process can be carried out by pore diffusion or by solid state diffusion depending upon the porosity of the solid product.
4. Interfacial reaction of the reactants with the mineral. The reactions involve adsorption reactions, chemical reactions and electrochemical reactions.

5.1.5 References

1. M. J. Spendlove, "Recycling Trends in the United States--A Review", U.S.B.M., IC 8711 (1976).
2. M. J. Spendlove, "Bureau of Mines Research on Resource Recovery", U.S.B.M., IC 8750 (1977).
3. A. W. Fletch, "Solvent Extraction in Processes for Metal Recovery from Scrap and Waste", Chemistry and Industry, May 5, 414(1973).
4. E. Peters and H. Veltman, Hydrometallurgy: Theory and Practice, First Tutorial Symposium on Hydrometallurgy, Lecutre note, III-5 (1972).

LEARNING ACTIVITY 2

5.2 Leaching of Metals

Learning Activity Objective

After completing this learning activity you should be able to describe the theory and practice of gold cyanidation and ammonia leaching of metallic copper.

5.2.1 Gold Cyanidation.

5.2.1.1 Chemistry and Mechanism of Cyanide Leaching of Gold.

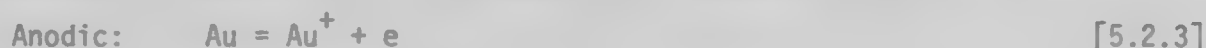
It is well known and thermodynamically proven that oxygen does not oxidize gold in a normal environment,



In the presence of cyanide ions, however, gold is readily soluble. A stable gold cyanide complex forms,



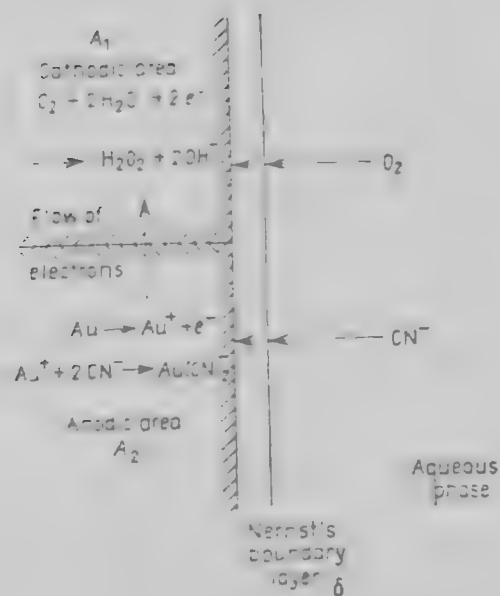
The dissolution of gold in cyanide solution is electrochemical in nature. Thompson⁽¹⁾ has proposed an electrochemical model in which gold is dissolved at anodic sites while oxygen is reduced at cathodic sites. The anode and the cathode form a corrosion couple in which electrons transfer from anodic site to cathodic site through solid gold. The schematic diagram of gold cyanidation is presented in figure 5.2.1. The anodic and cathodic reactions are:



The charge transfer reaction of H_2O_2 , i.e., Equation [5.2.6], is slow resulting in a build up of H_2O_2 intermediate in the solution.

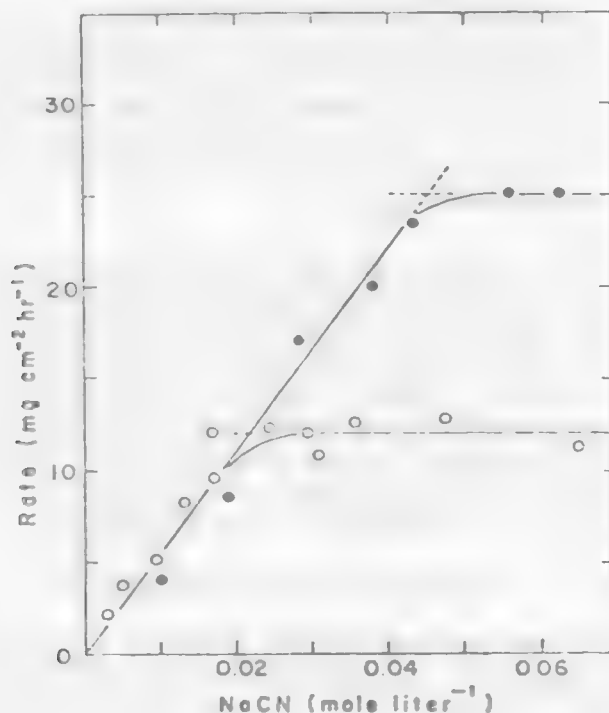
Several investigators^(2,3) have shown that the kinetics of gold and silver cyanidation are diffusion controlled. For high concentrations of oxygen, the rate of the reaction depends on the diffusion of the cyanide ions through a liquid film layer, and for high cyanide concentrations, the rate is controlled by the diffusion of the oxygen through the film layer. For a fixed oxygen partial pressure, the rate increases with increasing cyanide concentration, finally approaching a plateau value at which the rate is proportional to the oxygen partial pressure (figure 5.2.2), indicating a shift from cyanide ion diffusion control to oxygen diffusion control.

Figure 5.2.1 Electrochemical Model for Gold Cyanidization.



Source: F. Habashi, Principles of Extractive Metallurgy, Vol. 2, Hydrometallurgy.

Figure 5.2.2 Effect of Cyanide Concentration and Oxygen Pressure (3.40; 7.40 atm) on the Rate of Dissolution of Silver at 24°C.



Source: M. E. Wadsworth, Principle of Leaching in Rate Processes for Extractive Metallurgy, ed. H. Y. Sohn and M. E. Wadsworth.

5.2.1.2 Gold Cyanidation Practice.

The conventional gold cyanidation process involves an agitation leach, subsequent precipitation with zinc, and finally fire refining. A recent trend, however, is to eliminate the precipitation step by using activated carbon for gold adsorption, with subsequent desorption, and electrowinning. The exhausted carbon can be reactivated for recycling. The carbon-in-pulp process, similar to the resin-in-pulp technique employed in the uranium industry, has been used to treat the slimy leach pulp.⁽⁴⁾

Cyanide heap leaching of low grade gold ores or mine waste materials has been given close attention. It has been practiced commercially in several gold mines in Nevada.⁽⁵⁾

The chemistry involved in the dissolution of gold either in agitation cyanidation or in heap leach cyanidation is essentially the same. Oxygen

is necessary for the dissolution. Chemical oxidants such as sodium peroxide, permanganate, potassium ferricyanide and ozone have been employed but their use has not been widely adopted.

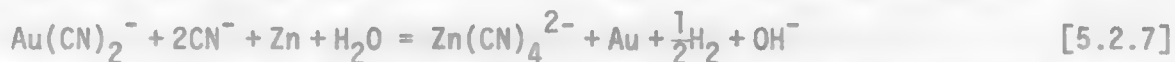
The strength of solution is usually about one lb of cyanide (NaCN equivalent) per ton of solution (water) for most of gold ores. Silver ores may require strength up to 6 lbs of NaCN per ton of solution. Gold-bearing concentrate, obtained by gravitational concentration or flotation, are frequently treated by higher strength solutions. It is essential to use an alkaline solution to provide "protective alkalinity" in the cyanide solution, i.e., a pH range of 9 to 11 is maintained.

Certain constituents known as cyanicides in the ore react with cyanide causing abnormal cyanide consumption and frequently influences dissolution or precipitation of gold and silver. Copper minerals are cyanicides, contents as little as 0.1% copper in the ore will create excessive cyanide consumption due to the formation of copper cyanogen complexes. Iron sulfide minerals if present in the ore are oxidized to some extent during a cyanide leach, thus resulting in the consumption of oxygen and cyanide. Acid neutralizes lime causing a high acid consumption. Arsenic and antimony-bearing minerals inhibit the dissolution of gold and silver to a certain extent.

5.2.1.3 Conventional Gold Cyanidation.

A conventional plant for processing gold ore consists of fine grinding, leaching in cyanide solution, countercurrent decantation for liquid-solid separation and residue washing, clarification of the pregnant solution by filtering, precipitation of the gold with zinc powder, and finally gold refining to produce doré bullion. The simplified flow sheet of a conventional gold cyanidation plant is shown in figure 5.2.3. Before the 1970's gold amalgamation was sometimes used in combination with cyanidation.⁽⁶⁾ However, amalgamation processing has been discontinued due to government restrictions on the discharge of waters containing mercury.

Precipitation of gold on zinc is an important step in the conventional process. The reaction may be represented by the following reaction:



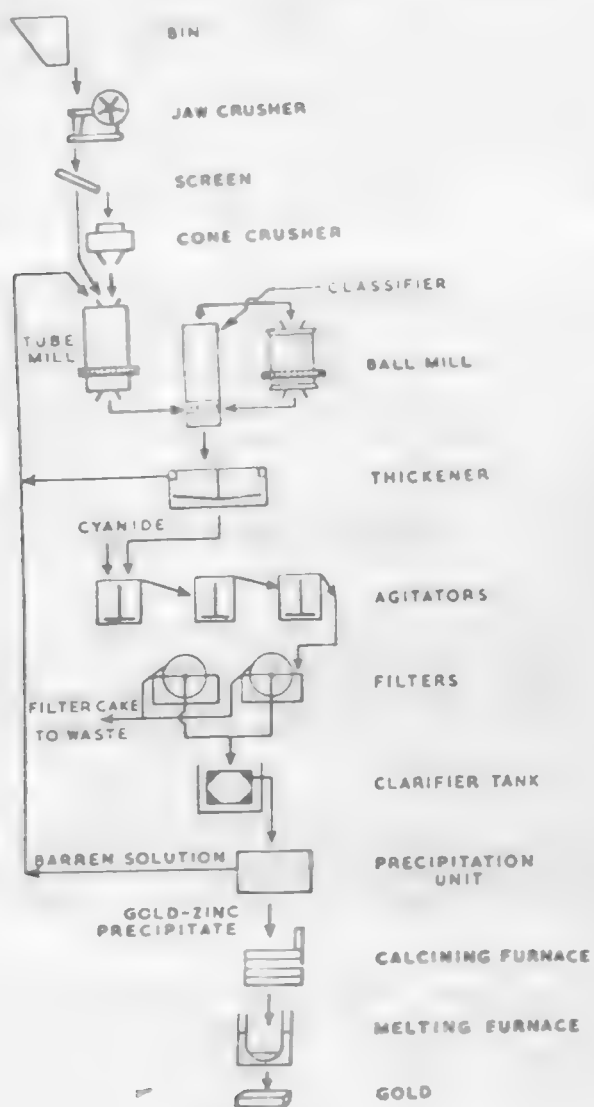
The clarification of the pregnant solution prior to the precipitation is essential. It eliminates the suspended clay constituents that coat the zinc particles and retard the precipitation reaction. Elimination of dissolved oxygen from the pregnant solution is also important to prevent the redissolution of the precipitated gold. Oxygen removal is usually accomplished by a de-aeration process based on spraying or otherwise distributing the solution in a vacuum chamber. Excessive amounts of cyanide ions in the solution will result in an excessive consumption of zinc,



Soluble lead salts such as lead acetate or lead nitrate are often added to the pregnant solutions to form a zinc-lead couple which exhibits a greater activity as a precipitant than does zinc alone.

Hydrometallurgy

Figure 5.2.3 Gold Cyanidation Flow Sheet.



Source: W. H. Dennis, Extractive Metallurgy, Philosophical Library, Inc., New York, 1965, p. 251.

Several gold cyanidation plants separate the ore into sand and slime portions, and subsequently the sand and the slime are leached separated so that the operation procedure can be optimized for each treatment.⁽⁶⁾

A new plant operation employing conventional cyanidation and zinc dust precipitation is located at De Lamar, Idaho.⁽⁷⁾ The plant is designed to treat 1,400 tpd of pit ore and produces 2.2 million oz of silver and 13,400 oz of gold a year. The run-of-mine ore is crushed by 36 x 40-in jaw crushers followed by semi-autogenous grinding in a 18 x 9-ft mill. Lime for protective alkalinity purpose is added to the slurry before the grinding. Cyclones split the slurry from the mills into oversize for regrinding and an overflow for leaching. Dry cyanide is fed to the pulp just before the leaching step.

Leaching is performed in four 40-ft high by 50-ft diameter mechanically agitated tanks. Air is sparged to each tank. The leach pulp advances in series to a counter current decantation (CCD) circuit composed of five 125-ft thickeners. The tailings are transferred to a tailing pond, and the clarified pregnant solution is processed in a standard precipitation and filtering system. The filter cake of gold is converted to gold doré bullion in a gas-fired furnace.

5.2.1.4 Carbon Adsorption and Desorption Process.

Carbon Adsorption--Activated carbon has the capacity of adsorbing the gold cyanide complex from unclarified cyanidation effluents, therefore, eliminating the liquid-solid separation, clarification, and deaeration processing steps that are employed in all zinc precipitation plants. *The mechanism of gold adsorption on activated carbon is still not fully understood. A recent study⁽⁶⁾ indicated that the gold adsorbed as the gold cyanide complex, $\text{Au}(\text{CN})_2^-$, which is either calcium aurocyanide or hydrogen aurocyanide depending on the pH of the cyanide solution and the concentration of the other cations. The adsorption reaction is reversible so that the adsorbed gold can be desorbed or displaced with hot alkaline solution.*

The amount of gold and silver that can be loaded on the carbon may vary widely depending on the tenor of the cyanide leach solution and the characteristics of the activated carbon.⁽⁵⁾ Typical loadings obtained commercially range from 200 to 800 oz of gold, or combination of gold and silver, per ton of carbon. Activated carbon is also capable of adsorbing a large variety of organic substances and inorganic constituents, thus reducing the capacity of carbon adsorption of precious metals. The pH value of the solution for gold and silver adsorption is preferred to be between 9 to 11. The activated carbon manufactured from coconut shells shows a higher capacity for gold adsorption than that of carbons prepared from petroleum coke, wood, or coal.

Carbon Desorption--Activated carbon that is loaded with gold can be burned to recover the gold, but it is preferably stripped, reactivated and returned to the loading circuit. The stripping of gold (and silver) known as the Zadra process⁽⁸⁾ employs a 1.0% NaOH - 0.1% NaCN strip solution at 93°C and atmospheric pressure to remove the gold and silver from the carbon. Current industrial application of the Zadra process requires 50 hours to strip

the gold from a loading of 300 oz of gold to 5 oz of gold per ton of carbon.

The U.S. Bureau of Mines has modified the Zadra process to use hot caustic pressure stripping (figure 5.2.4).⁽⁹⁾ This change greatly reduces process time and reagent consumption. The process provides for stripping with 0.4% NaOH at about 150°C and 52 psi. Cyanide is not ordinarily required. Currently the Gortez gold mine⁽¹⁰⁾ has adopted hot caustic pressure stripping to desorb gold from loaded carbon. Under the condition of 1% NaOH, 116°C and 60 psi, the retention time has been reduced to 12-20 hours.

5.2.1.5 Electrowinning.

The precious metal values contained in the strip solution can be electrowon from the solution, and the spent electrolyte recycled for stripping. The electrolytic cell can be cylindrical⁽⁴⁾ or rectangular⁽¹⁰⁾. The anodes are made of perforated, electrolytic grade carbon or stainless steel screen. The cathodes are usually steel wool confined in perforated containers which are made of polypropylene sheet or stainless steel.

5.2.1.6 Cyanide Heap Leaching of Gold Ore.⁽⁵⁾

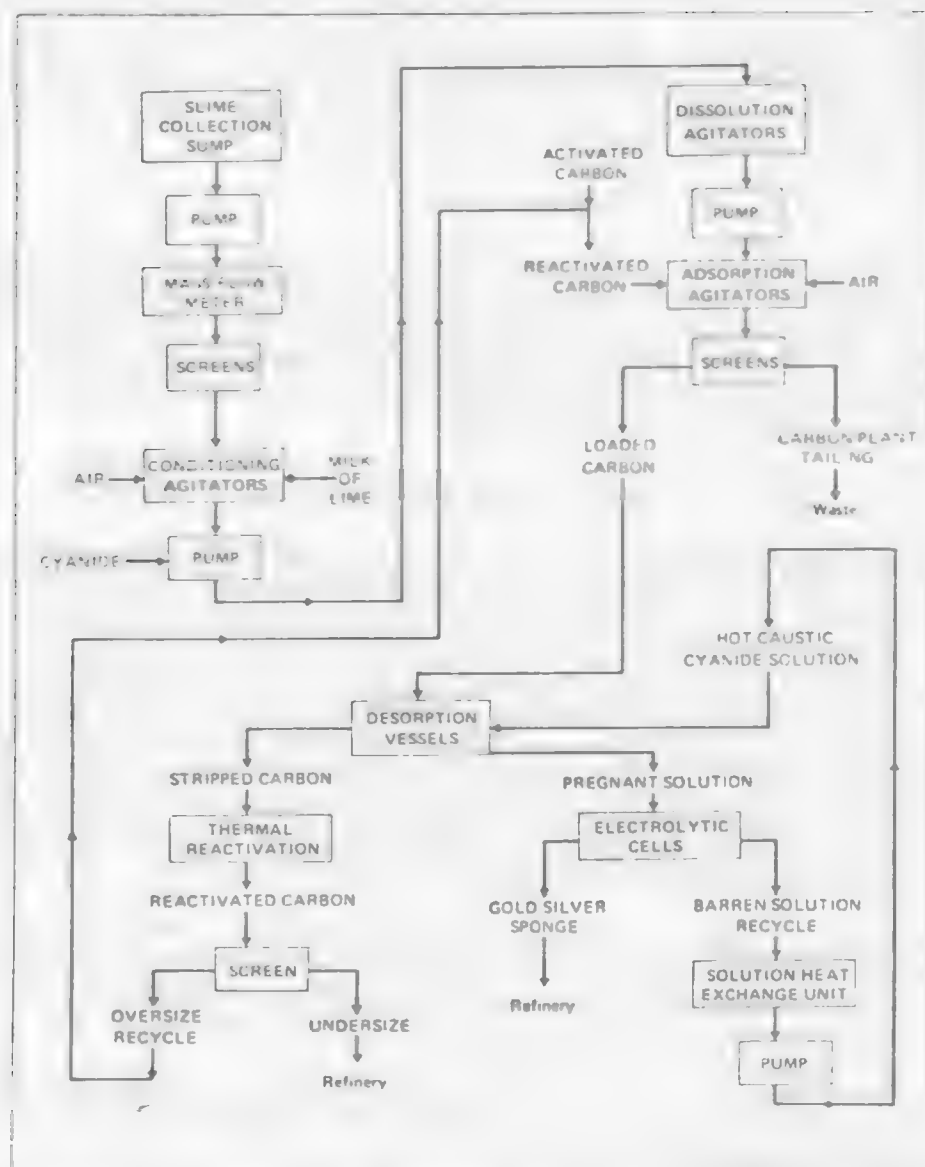
Cyanide heap leaching of gold ores is a comparatively recent hydrometallurgical development for exploiting low-grade ores, mine waste materials or deposits too small to justify construction of milling facilities. The heap leaching process consists of piling coarse, treatable ore on an impervious pad and percolating it with small amounts of dilute lime-cyanide solution. The gold will be recovered from the pregnant solution either by conventional clarification, i.e., the zinc precipitation method such as used by the Carlin Gold Mine Operation⁽¹¹⁾ or by carbon adsorption and desorption followed by electrowinning such as used by the Smoke Valley Mine⁽¹²⁾ and Cortez Gold Mine⁽¹⁰⁾ operations. A schematic diagram of heap leaching followed by carbon adsorption-electrowinning operation is presented in figure 5.2.5.

The types of materials used for constructing the impervious pads include (1) compacted tailings mixed with bentonite, (2) asphalt or lignin sulfonate mix placed on compacted gravel and covered with an asphalt sealer, (3) reinforced concrete pads, and (4) plastic or rubber sheeting.

Heinen et.al. have classified the heap-leach cyanidation operations into two main categories--short-term leaching of crushed ore and long-term leaching of run-of-mine materials.

In practicing short term heap leach cyanidation, the ore is crushed to minus 3/4 inch, stacked 4 to 8 feet high on permanent pads, each with a capacity ranging from 1,000 to 10,000 tons, and leached by sprinkling the top of the heap with dilute cyanide solution. Cyanide solution percolates through the heap dissolving the gold and silver values. It is subsequently collected on the water tight pad and transferred to a storage pond or tank. The leach cycle is generally from 7 to 30 days. After completing one leach cycle, the solid waste is removed from the pad and a new batch of crushed ore is applied. The Carlin Gold Mine⁽¹¹⁾ and Smoke Valley Mine⁽¹²⁾ are operating using this short-term method.

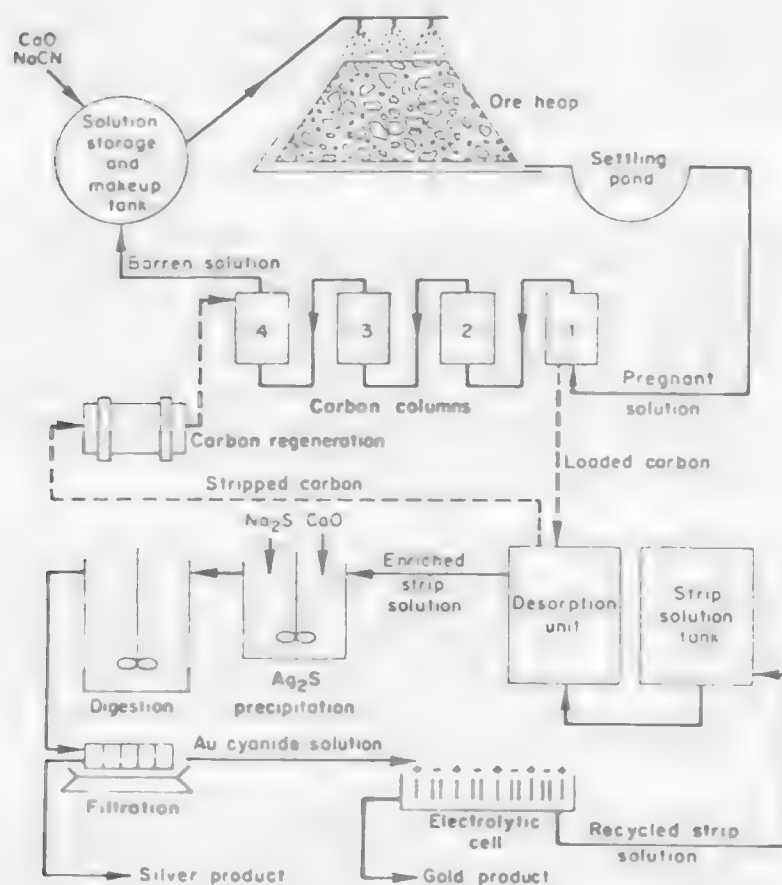
Figure 5.2.4 Modified Zadra Process.



FLWSHEET for Homestake Mining Company's Carbon-in-Pulp plant for gold recovery at Lead, South Dakota, United States. Homestake is America's largest gold mine.

Source: "Homestake Uses Carbon-in Pulp to Recover Gold from Slimes", *World Mining*, Nov. 44(1974).

Figure 5.2.5 Schematic Diagram of Gold Heap Leaching.



Source: Heinen, H. J., D. G. Peterson and R. E. Lindstrom, "Processing Gold Ores Using Heap Leach-Carbon Adsorption Methods", USBM, IC 8770.

Long-term leaching is designed primarily to extract gold from uncrushed, porous, sub-mill-grade material from open pit operations. The ore charges are run-of-mine material about 6 inches in size. The size of the heap ranges from 10,000 to 2,000,000 tons. The height of the heap is about 20 feet. The leach cycle is measured in months or years. After completing the leaching cycle, the waste is left on the pad. Cortez Gold Mines has completed heap leaching approximately 5 million tons of run-of-mine cutoff material.⁽¹⁰⁾ Cortez operated the first known integrated heap-leach cyanidation-carbon adsorption-electrowinning plant at its Gold Acres property. A brief review of its operation is given as follows.

5.2.1.7 Cortez's Heap-Leach Cyanidation.

Heap-Leach--Cortez Gold Mines have been operating heap leaching circuits for low grade gold ore in conjunction with a conventional milling operation at its Nevada mine sites. At the Gold Acres mine the cutoff grade was 0.040 oz per ton. The high grade ore was sent to the cyanidation mill. At a leach cutoff grade of 0.015 oz per ton, the leach ore was trucked to leach pads prepared on a 5% graded terrain. The impervious pads were made of local clay-silt or slime tailings (to a depth of about 15 inches) covered with a 4-inch layer of coarse gravel. Each heap, 20 ft high and 350 ft wide x 450 ft long at the base, contained about 17,000 tons of ore.

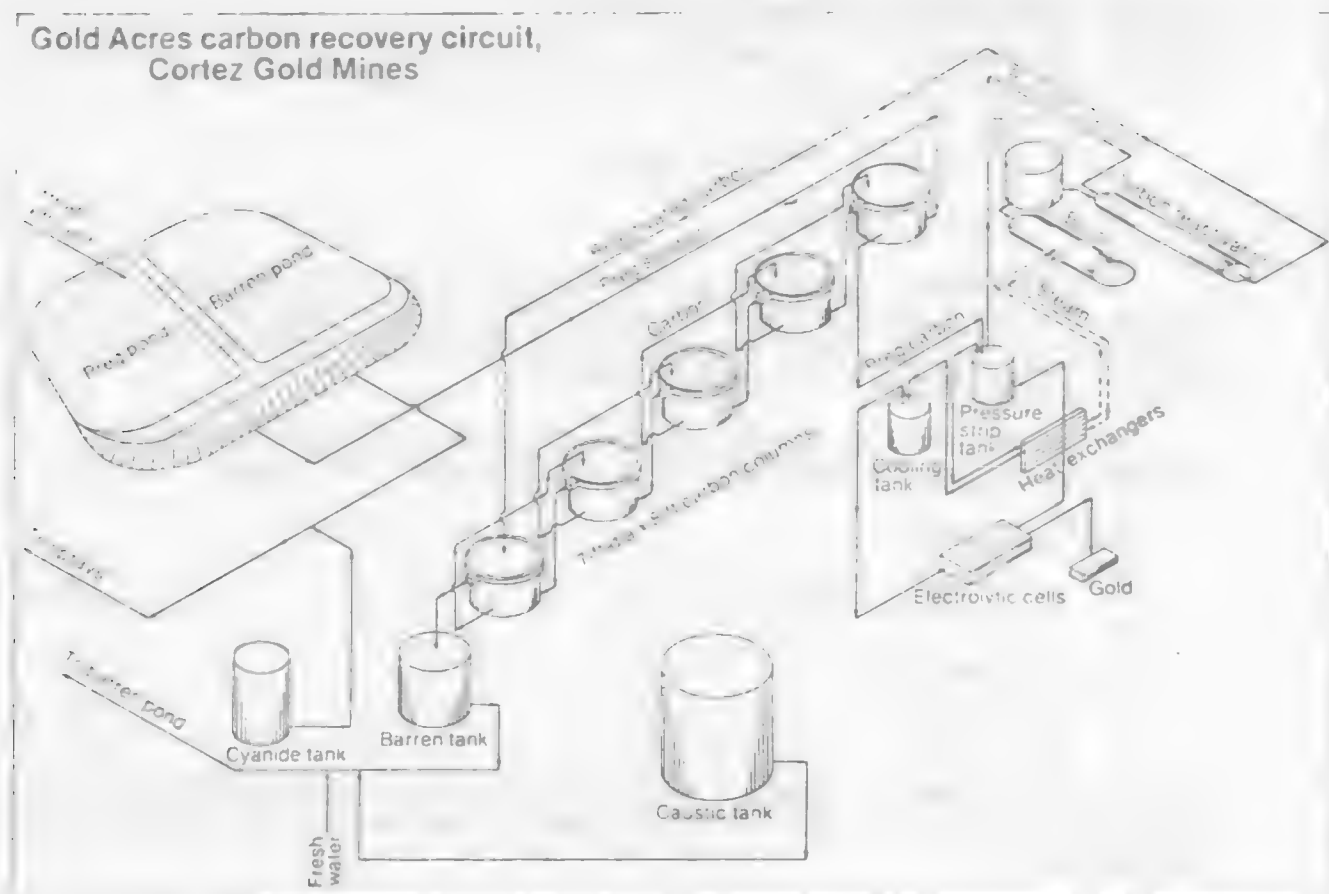
A dilute lime-cyanide solution was sprayed by plastic sprinklers, spaced on 50-ft centers. Solution flow was about 0.0025 gpm per sq.ft. With the addition of NaOH, the pH of the leach solution was maintained at 10.5 and sodium cyanide concentration at 0.030%. Reagent consumption averaged 0.45 lb NaCN and 0.41 lb NaOH per ton of ore. The average extraction of gold averaged 50% for about 3 to 4 months. The pregnant solutions from the heaps were transferred to a pond for further treatment.

Carbon Adsorption--A schematic diagram of Gold Acres carbon recovery circuit is shown in figure 5.2.6. The gold-bearing pregnant solution from the pregnant solution pond was pumped through five carbon columns at a flow rate of 550 gpm. The tanks each held 3,000 lb of 12 x 30-mesh coconut shell activated carbon. The barren solution and the leach solution were run counter current. Normally, the pregnant solution contained 0.021 oz Au per ton of solution, and the barren solution after carbon adsorption contained 0.0005 oz per ton. The loaded carbon contained about 485.4 oz of gold per ton.

Carbon Stripping--At Gold Acres pressurized hot caustic stripping was used to remove the gold cyanide complex from the loaded carbon in a 42-inch diameter, 10-ft high pressure vessel. A 1% NaOH solution was used for stripping, at a pressure of 60 psi and a temperature of 116°C. After a retention time of about 12-20 hours, the carbon was stripped to 0.5 - 2.0 oz of gold per ton, then washed, reactivated and recycled back to the carbon columns.

Electrowinning--Gold was electrowon from the strip solution in two rectangular electrolytic tanks, each measuring 3½ ft long x 3 ft wide x 3 ft deep. Each tank could hold six cathodes and seven anodes. Anodes were made of perforated, electrolytic grade carbon, while cathodes were constructed of perforated polypropylene sheet and fabricated to hold 2 lb of carbon steel wool.

Figure 5.2.6 Gold Acres Carbon Recovery Circuit.



Source: Duncan, D. M. and T. J. Smolik, "How Cortez Gold Mines Heap-Leached Low Grade Gold Ores at Two Nevada Properties", E/MJ, July 65 (1977).

The polypropylene sheet served as an insulating medium between anodes and cathodes. The normal operation conditions were potential difference across anode and cathode of 2.5 v, and current of 22.5 amp per cathode.

The electrowinning operation was performed in a batch system. After 23 hours of electrowinning, the concentration of gold in the solution was reduced from over 24.7 oz per ton to 0.001 oz per ton. The gold containing cathodes were removed from the tanks, and the plated steel wool was treated in the refinery for recovery of gold as doré bullion.

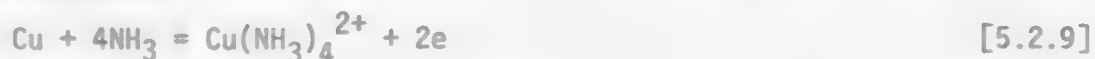
5.2.2 Leaching of Metallic Copper.

5.2.2.1 Chemistry.

Metallic copper heated by hydrometallurgical processing comes from several sources: mainly native copper,^(13,14) cement copper,^(15,16) and copper scrap.⁽¹⁷⁾ The most acceptable method for the leaching of metallic copper is the ammoniacal oxidation leach.

In the presence of oxygen, copper dissolves readily in ammoniacal solution according to the following electrochemical reactions:

Anodic reaction,



Cathodic reaction,

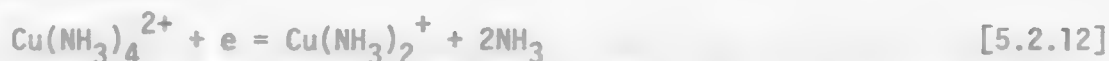


The cupric tetraammine complex, $\text{Cu}(\text{NH}_3)_4^{2+}$, formed from Reaction [5.2.9] can also oxidize metallic copper. The following electrochemical reactions describe the process:

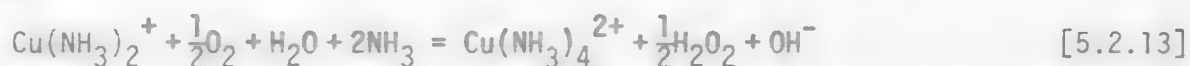
Anodic reaction,



Cathodic reaction,



The cuprous ammine complex produced [5.2.12] will be rapidly oxidized by oxygen



In the latter electrochemical model, the cupric ammine complex behaves as an autocatalyst conducting the dissolution of the metal and the reduction of the oxygen. Nicol⁽¹⁸⁾ has indicated that the rate of dissolution is normally controlled by the diffusion of the oxidants, $\text{Cu}(\text{NH}_3)_4^{2+}$ and O_2 , through the liquid film to the metal surface. Because the diffusions of $\text{Cu}(\text{NH}_3)_4^{2+}$ and O_2 are in parallel, the overall rate will be determined by the larger value of the

diffusion flux either of $\text{Cu}(\text{NH}_3)_4^{2+}$ or of O_2 . Nicol has shown that the mass transfer of $\text{Cu}(\text{NH}_3)_4^{2+}$ will predominate as soon as the cupric ion concentration is greater than $4 \times 10^{-3} \text{ M}$ under an aerated condition at room temperature. Grove et.al.⁽¹⁴⁾ have indicated that the leach solution usually contains enough cupric ion and the metallic copper is usually partially oxidized, so that the leaching reaction normally reveals the catalytic effect without the additional charge of the cupric ion.

5.2.2.2 Leaching of Metallic Copper--Practice.⁽¹⁵⁾

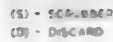
Universal Minerals and Metals Inc. uses the ammonia-ammonium carbonate leach to dissolve metallic copper, followed by hydrogen reduction to produce copper powder. The flow sheet of this plant operation is shown in figure 5.2.8.

The feed for this plant, originally scrap copper, is now cement copper. The high grade copper is charged into large agitation tanks through which leach solution is circulated.

The leaching proceeds at 50 to 60°C at atmospheric pressure and dissolves the copper as ammine complexes. The final leach solution contains 140-160 gpl copper, of which about 100 gpl is Cu^+ and 50 gpl is Cu^{++} . The filtered leach solution contains some lead and tin and these are removed by the addition of ground natural celestite which adsorbs the lead and tin from the solution. After filtration, the clear solution passes to the reduction section, where it is reduced at 200°C in horizontally stirred autoclaves under a total pressure of 900 psig. No nucleation catalyst is required for copper reduction.

The reduced end solution contains about 1.5 gpl Cu^+ and 10 gpl Zn. Some of this solution is boiled to recover NH_3 and CO_2 , which is recycled to the leach section. This boiling also precipitates zinc carbonate, which is filtered off, washed, dried and sold.

The copper powder produced is washed and dried. The powder is then sintered in hydrogen at 600-700°C. The sintered cake is pulverized and screened to produce copper powder.



5.2.3 References

1. Thomson, P.F., "The Dissolution of Gold in Cyanide Solution", *Trans. Electrochem. Soc.*, **91**, 41 (1947).
2. Kudryk, V. and H. H. Kellogg, "Mechanism and Rate-Controlling Factors in the Dissolution of Gold in Cyanide Solutions", *J. Metals*, **6**, 541 (1954).
3. Deitz, G. A. and J. Halpern, "Reaction of Silver with Aqueous Solutions of Cyanide and Oxygen", *J. Metals*, **5**, 1109(1953).
4. "Homestake Uses Carbon-in-Pulp to Recover Gold from Slimes", *World Mining*, Nov. **44**(1974).
5. Heinen, H. J., D. G. Peterson and R. E. Lindstrom, "Processing Gold Ores Using Heap Leach-Carbon Adsorption Methods", USBM, IC 8770(1977).
6. Schmidt, C. E. and F. M. Howell, "Recent Trends in Milling Costs at Homestake", *Unit Processes in Hydrometallurgy*, M. E. Wadsworth and F. T. Davis ed., AIME, Gordon and Breach Science Pub., New York 860(1964).
7. "Gold and Silver: A Mix of Old and New Technology", *E/MJ*, June 142 (1974).
8. Zadra, J. B., A. L. Engel and H. J. Heinen, "Process for Recovering Gold and Silver from Activated Carbon by Leaching and Electrolysis", USBM, RI 4843(1952).
9. Potter, G. M. and H. P. Salisbury, "Innovations in Gold Metallurgy", *Mining Congress Journal*, July **54**(1974).
10. Duncan, D. M. and T. J. Smolik, "How Cortez Gold Mines Heap-Leached Low Grade Gold Ores at Two Nevada Properties", *E/MJ*, July 65(1977).
11. Pizarro, R., J. D. McBeth and G. M. Potter, "Heap Leaching Practice at the Carlin Gold Mining Co., Carlin, Nev.", *Solution Mining Symposium*, F. F. Aplan, W. A. McKinney and A. D. Pernicelli ed., Dallas, 1974. Published by TMS and SME/AIME, Chap. **19**, 253(1974).
12. White, L., "Heap Leaching will Produce 85,000 oz/year of Doré Bullion for Smoky Valley Mining", *E/MJ*, July 70 (1977).
13. Kaczynski, D. A., G. W. Lower and W. A. Hockings, "Kinetics of Leaching Metallic Copper in Aqueous Cupric Ammonium Nitrate Solution", *Solution Mining Symposium*, F. F. Aplan, W. A. McKinney and A. D. Pernicelli ed., Dallas, 1974, SME and TMS of AIME, Chap. **27**.
14. Groves, R. D., T. H. Jeffers and G. M. Potter, "Leaching Coarse Native Copper Ore with Dilute Ammonium Carbonate Solution", *Ibid*, Chap. **26**.
15. Evans, D. J. I., "Production of Metals by Gaseous Reduction from Solution--Processes and Chemistry", *Advances in Extractive Metallurgy*, IMM. **831**(1967).
16. Yorko, W. J., "Refining Copper by Acid Leaching and Hydrometallurgy", *Chem. Eng.*, **73**, August 29, 64-6(1966).
17. Staker, W. L., C. J. Chindgren, and K. C. Dean, "Improved Cupric Ammonium Carbonate Leaching of Copper Scrap", USBM, RI 7554(1971).
18. Nicol, M. J., "An Electrochemical Investigation of the Dissolution of Copper, Nickel, and Copper-Nickel Alloys in Ammonium Carbonate Solutions", *South African Inst. of Mining and Metallurgy*.



LEARNING ACTIVITY 3,4

5.3 Leaching of Oxides

Learning Activity Objective

After completing your study of this learning activity material you should be able to describe the fundamental principles and basic operations of leaching oxide minerals.

5.3.1 Thermodynamics and Kinetics.

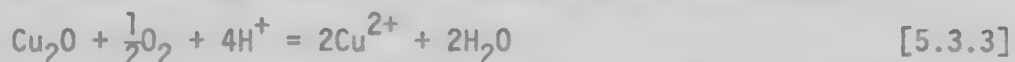
The thermodynamics of leaching of oxides is best explained by the use of Eh-pH diagrams. Figure 5.3.1 shows the Eh-pH diagram for the Cu-O₂-H₂O system at 25°C. This diagram illustrates that copper oxide in its highest oxidation state, CuO, is readily soluble in acid to produce cupric ion.



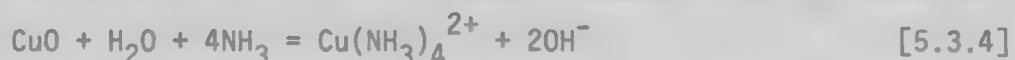
Also, cupric oxide has an amphoteric character, and can be dissolved in a strong alkaline solution as cuprite ion, CuO₂²⁻,



Figure 5.3.1 also illustrates the need for the presence of an oxidizing reagent to dissolve copper oxide in its lower oxidation state, Cu₂O,



Although it isn't shown on the Eh-pH diagram, CuO is soluble in neutral or basic media in the presence of a suitable complexing agent such as ammonia,



The Eh-pH diagram for each metal oxide is unique. However, it can be generally stated that leaching of oxides can be accomplished by one of the following methods.

1. A metal oxide in its highest oxidation state may be soluble in a strong acid; e.g., leaching of zinc calcine,



2. A metal oxide in its highest oxidation state may be soluble in a strong basic solution; e.g., leaching of aluminum hydroxide,



3. A metal oxide in its lowest oxidation state may require a strong oxidizing agent for its dissolution; e.g., leaching of uraninite,

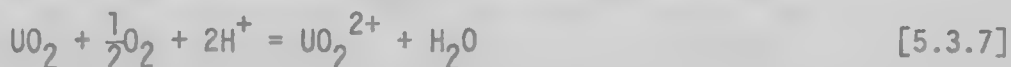
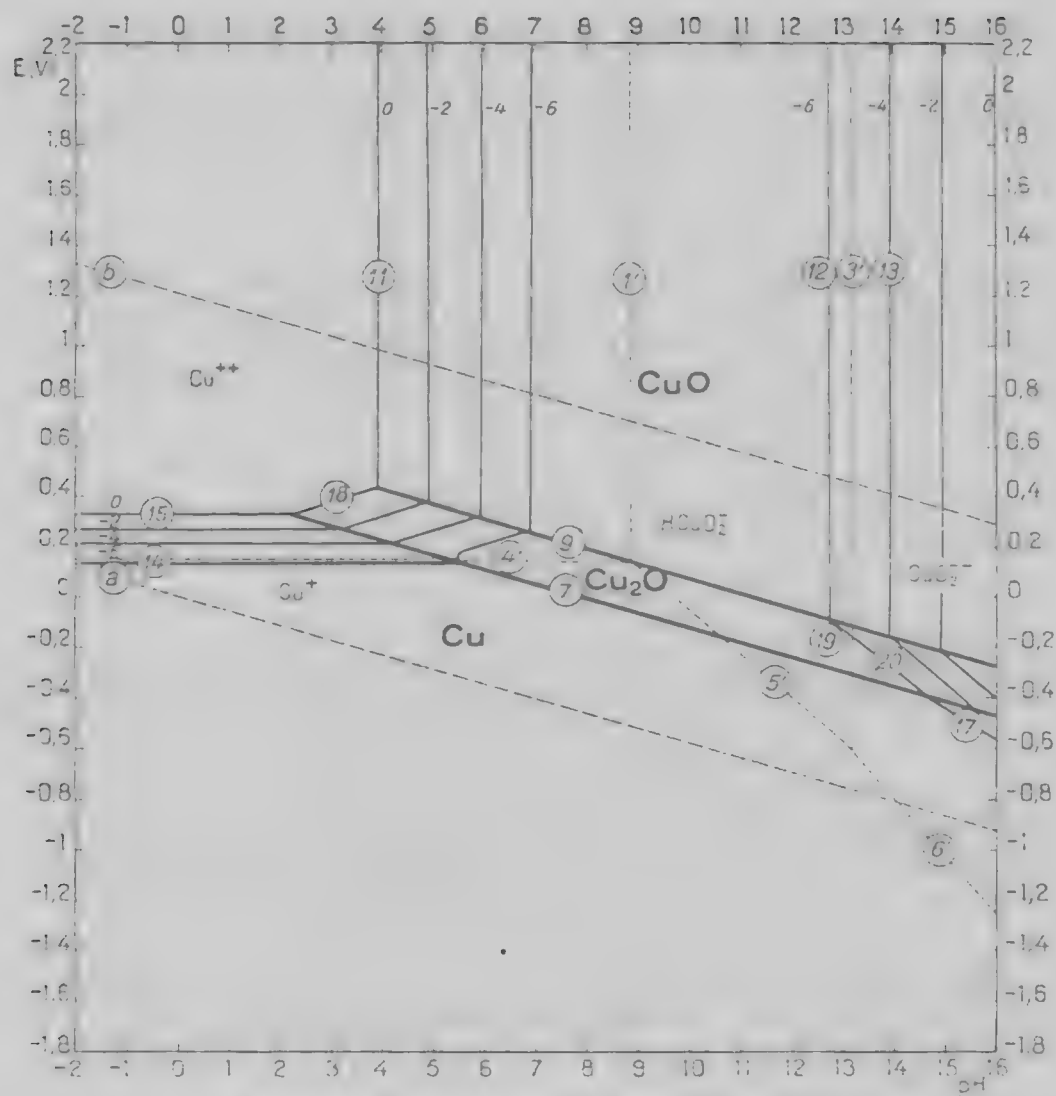


Figure 5.3.1 The Cu-O₂-H₂O System.

Potential-pH equilibrium diagram for the system copper-water, at 25°C
 [Considering the solid substances Cu, Cu₂O and CuO. Cu(OH)₂ is not considered.]

Source: M. Pourbaix, Atlas of Electrochemical Equilibria in Aqueous Solutions.

However, several metal oxides are soluble in their lowest oxidation state; e.g., MnO_2 . In this case a reducing agent is required,



The rate of leaching of oxides is normally faster than the rate of leaching of sulfide minerals. Especially for those readily soluble oxides in which the rate is controlled by the diffusion of reagent to the metal oxide surface. However, several oxide minerals tend to occur in a finely disseminated form within a refractory type matrix, for instance, nickeliferous laterite. The solid state diffusion through those matrixes can be very slow. In addition, these type ores are usually not susceptible to physical concentration. As a result, it is necessary to treat a large quantity of ore in order to recover a small amount of metal values.

5.3.2 Leaching of Uranium Oxides.⁽¹⁾

5.3.2.1 Hydrometallurgical Process for Uranium Oxides.

Uranium can be considered for commercial recovery if it contains about 0.2% U_3O_8 . The uranium is often finely disseminated so that a significantly higher grade concentrate can not be made by physical separation of U_3O_8 from the gangue mineral phases. However, because uranium in its oxidized state is readily soluble in either acid or alkaline media, a hydrometallurgical process can be used to produce high grade U_3O_8 . The process often involves leaching, solution concentration and purification, and U_3O_8 precipitation.

The common uranium minerals are listed in Table 5.3.1. Two of the most common minerals are uraninite and pitchblende. Both are a mixture of UO_2 and UO_3 . The Eh-pH diagram for uranium-oxygen-water is presented in figure 5.3.2. This diagram indicates that UO_2 is relatively insoluble in acid media, while UO_3 is readily soluble.

Table 5.3.1 Common Uranium Minerals.⁽¹⁾

oxide	uraninite	$(\text{U}_{1-x}^{4+}; \text{U}_x^{6+})\text{O}_2$
	pitchblende	variety of uraninite
complex oxide	brannerite	$(\text{U}, \text{Ca}, \text{Fe}, \text{Th}, \text{Y})(\text{Ti}, \text{Fe})_2\text{O}_6$
	bavidite	Ideally FeTiO_7
carbonaceous	asphaltite	U-organic complex
phosphate	autunite	$\text{Ca}(\text{UO}_2)_2(\text{PO}_4)_2 \cdot 10-12\text{H}_2\text{O}$
vanadates	carnotite	$\text{K}_2(\text{UO}_2)_2(\text{VO}_4)_2 \cdot 1-3\text{H}_2\text{O}$

The leaching step is the key operation in treating the uranium ore. The choice of acid or alkaline leach reagents influence the entire flow sheet arrangement shown in figure 5.3.3. Acid is used in a majority of mills. Acid leaching is more effective for most ores. The carbonate alkaline leach, however, is more selective than acid leaching and is especially useful for a high-time ore that would consume excessive amounts of acid. If the uranium

Figure 5.3.2 Eh-pH Diagram of U-O₂-H₂O System, Total Concentration of Soluble Uranium Species is Equal to 1×10^{-6} M.

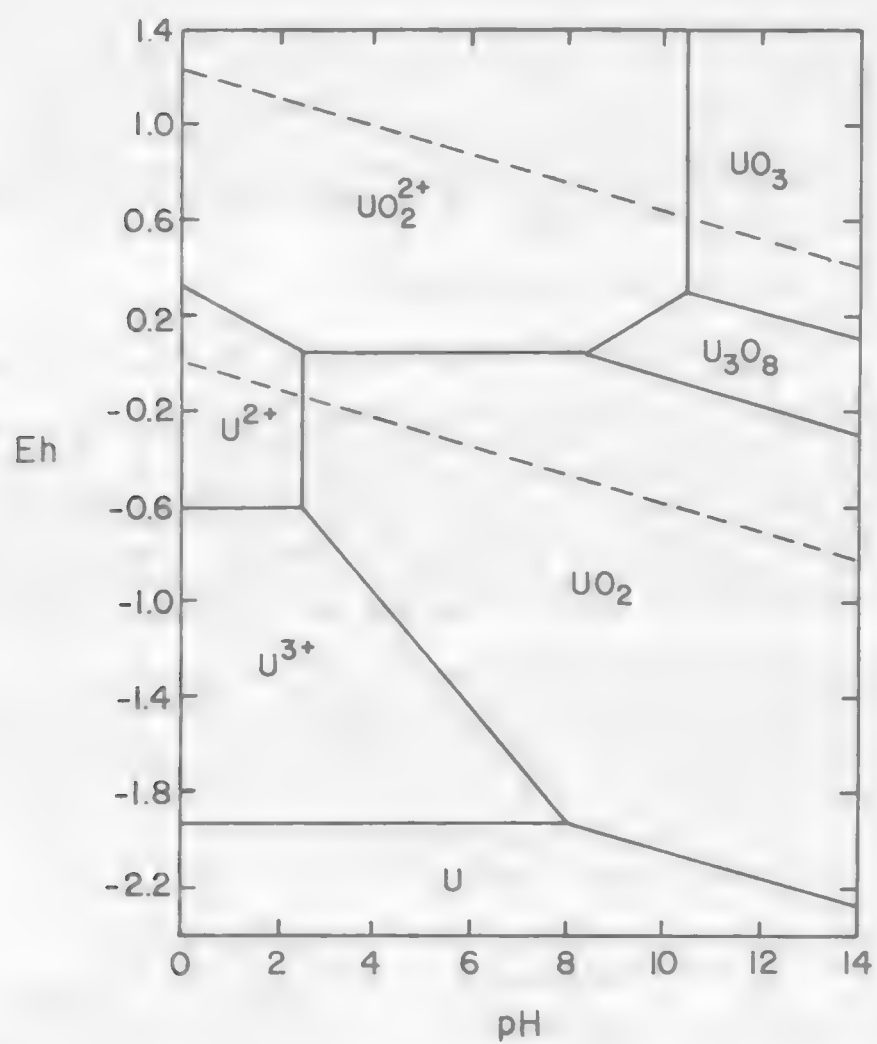
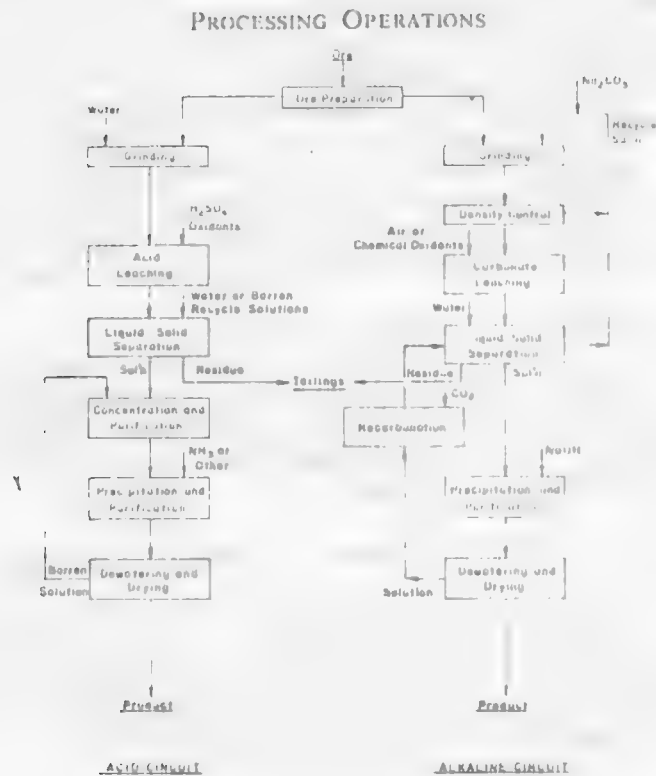


Figure 5.3.3 Comparison of Acid and Alkaline Leach Processing Circuits.



Source: Merritt, R. C., The Extractive Metallurgy of Uranium, Colorado School of Mines Research Institute, Chap. 5.

is in the reduced state (UO_2), an oxidant is required during the leaching. Reagent strength, leaching time, oxidation potential, and temperature are among the controlled variables. The leaching operation can be carried out in an agitation leach, a vat leach, a percolation leach or an in-situ leach depending upon the grade of the ore.

Concentration and purification of uranium from the dilute and impure acid leach solutions are a prerequisite to the production of final high grade U_3O_8 . Alkaline leaching operations may, however, be sufficiently selective to permit elimination of the purification step. The two major techniques used for concentration and purification are ion exchange and solvent extraction, used either individually or in a combination. The ion exchange process is applicable to the treatment of both slurry and clarified acid or alkaline solution. Solvent extraction is presently used to treat only the clarified solution. Solvent extraction has been successfully applied as a second stage of purification following ion exchange. This combination is referred to in the United States as the Eluex process. The product is of high purity.

Final recovery of uranium from the solution is achieved by chemical precipitation. In the alkaline process, the operation usually involves the addition of caustic to increase the pH to nearly 12. At this point uranium precipitates as a sodium uranate. In the acid process, the uranium is precipitated from the solution by neutralization with a base such as lime, magnesia, ammonia, or hydrogen peroxide.

5.3.2.2 Acid Leaching of Uranium Oxides.

Sulfuric acid is the most common lixiviant used in commercial practice. Uranium is present in the mineral as the tetravalent ion and must be oxidized before dissolution can occur. The common oxidant used for the acid leach is MnO_2 , NaClO_3 or O_2 . It is commonly believed that ferric iron is the specie in solution responsible for the oxidation reaction:



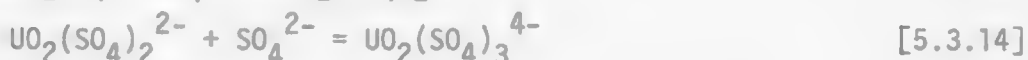
Ferrous iron is reoxidized by the oxidant O_2 , MnO_2 or NaClO_3 to ferric iron for further oxidation,



Acid reaction with hexavalent uranium will also produce UO_2^{2+} ,



The uranyl cation, UO_2^{2+} , further reacts with sulfate ion to produce uranyl sulfate and the complex uranyl sulfate anions as follows:



The dissolved uranium may be present in any of the above forms, depending upon acid and uranium concentration, temperature, and other complex variables in the system.

The uranium content in sandstone-type ore is usually in the form of hexavalent minerals; typically carnotite, tyuyamunite, autunite, torbernite, and uranophane. These minerals are soluble in acid solutions, and oxidants are added only to insure against reduction by other ore constituents. Tetravalent uranium is principally found in the minerals uraninite and amorphous pitchblende which are present in many of the world's deposits. Oxidants are required when leaching these minerals in order to obtain high extraction. Leaching conditions may otherwise be moderate, employing ambient temperature and only enough acid to maintain a pH between 0.5 and 2.0. Some of the more difficult uranium ores to leach are refractory uranium minerals, e.g., most commonly found as brannerite and davidite. Strong acid and concentrated oxidant, high temperature, and long retention times are normally required for effective extraction.

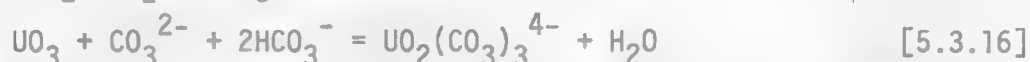
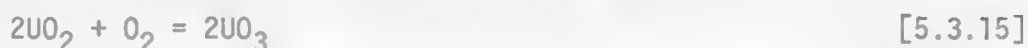
General operation variables used in practice are summarized below:

1. Sufficient liberation of uranium minerals can be obtained by grinding to 30-40% minus 200-mesh.
2. Acid consumption is normally 40-120 lb sulfuric acid/ton ore.
3. The principle oxidants are MnO_2 , NaClO_3 . Air oxidation is feasible but a pressure vessel may be required.
4. Leaching time varies from 4 to 24 hours and temperature from ambient to 80°C .

5.3.2.3 Carbonate Leaching of Uranium Oxides.

Alkaline or ammonium carbonate leaching is possible. The solubilized anion is $\text{UO}_2(\text{CO}_3)_3^{4-}$. Selective dissolution of uranium can be made from suitable ores. Hexavalent uranium minerals are readily soluble in carbonate solution. But minerals containing tetravalent uranium are insoluble until they are oxidized to the hexavalent state. The method usually requires intensive leaching with a strong oxidant and long retention times at high temperatures. Often autoclaves or similar types of pressure vessels are required to achieve a satisfactory extraction of tetravalent uranium minerals.

The basic reactions for carbonate leaching of UO_2 and UO_3 are:



Carbonate leaching is particularly advantageous in the treatment of ores that contain carbonate minerals, such as calcium and magnesium carbonates. The carbonate leach solution does not attack the carbonate compounds of iron, aluminum, titanium, etc., and only slightly dissolves the compounds of molybdates, silicates, phosphates, aluminates, and other complex metal carbonates.

Air, chemical oxidants or catalysts can be used as oxidants for the carbonate leach. The recent trend, however, is toward the use of air aeration in either Pachuca tanks or agitated pressure vessels (autoclaves). A Pachuca

tank is a tall vertical circular tank, about 45-ft high and 10-ft in diameter, with a conical bottom. The ore slurry is agitated by a jet of air entering at the bottom of the cone. A schematic diagram of a pilot-plant scale Pachuca tank is shown in figure 5.3.4. A 45-ft height slurry will create a pressure of approximately 30 psig at the bottom of the tank. The provision for operating under a pressure of up to 20 psig at the top will result in a total pressure of 50 psig at the bottom. This improves the dissolution of oxygen.

Autoclaves are usually divided into three compartments by baffle plates. Pulp enters at one end and discharges at the other after passing through each compartment. Each compartment is agitated by a mechanically driven turbine or propeller agitator. A schematic diagram of a pilot-plant scale autoclave is shown in figure 5.3.5.

The responses of uranium ores to carbonate leaching in Pachuca tanks and autoclaves are shown in figure 5.3.6. A fast leaching rate can be achieved by using high temperature high pressure autoclaves.

Some generalities can be made for uranium carbonate leaching:

1. Fine grinding is usually required; e.g., 70-80% minus 200-mesh.
2. The leach slurry normally contains 50-60% solid.
3. The rate increases with increased carbonate and bicarbonate reagent concentrations. A minimum of 4.2 g/l of bicarbonate is necessary for leaching at a reasonable rate.
4. Operation conditions for autoclaves range in temperature from 95 to 120°C and in total pressures from 30 to 90 psig. Air consumption ranges from 1.3 to 3.0 standard cubic feet per minute per ton ore. The retention time may vary from 4 to 20 hours.
5. Operation temperatures for Pachuca tank leaching range from 75 to 80°C with total air consumption between 0.4 and 1.0 standard cubic feet per minute per ton ore. The retention time is about 3-6 hours.

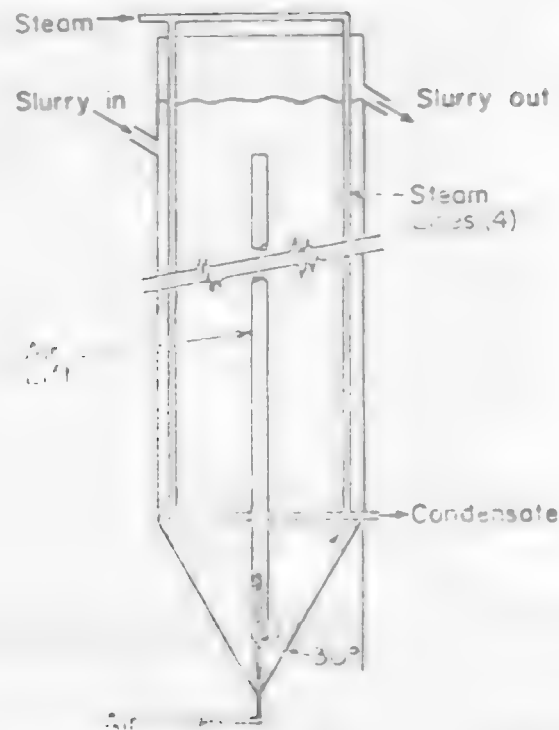
5.3.3 Leaching of Bauxite--Bayer Process.

Bauxite is not a mineral. The name has been applied to various types of aluminum hydroxides; e.g., gibbsite, boehmite and diasporite. Gibbsite is alumina trihydrate. Boehmite and diasporite are alumina monohydrates. A summary of the physical properties of these three minerals is listed in Table 5.3.2.

Table 5.3.2 Types of Bauxite Ores.⁽²⁾

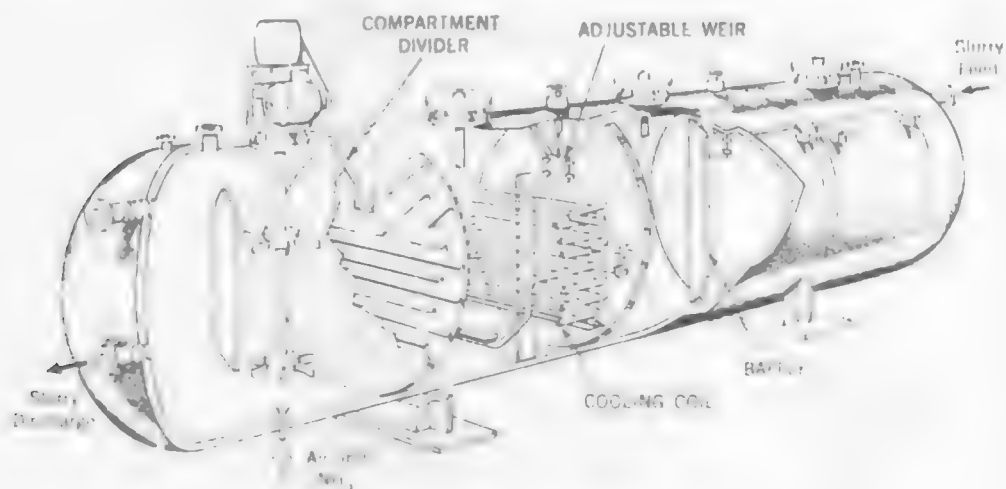
Property	Gibbsite	Boehmite	Diasporite
Formula	Al(OH) ₃	AlOOH	AlOOH
Crystal structure	monoclinic	orthorhombic	orthorhombic
Density	2.42	3.01	3.44
Hardness (Moh)	2.5-3.5	3.5-4	6.5-7
Solubility in 100 g/l NaOH at 125°C, g/l Al ₂ O ₃	128	54	insoluble

Figure 5.3.4 Pachuca Tank.



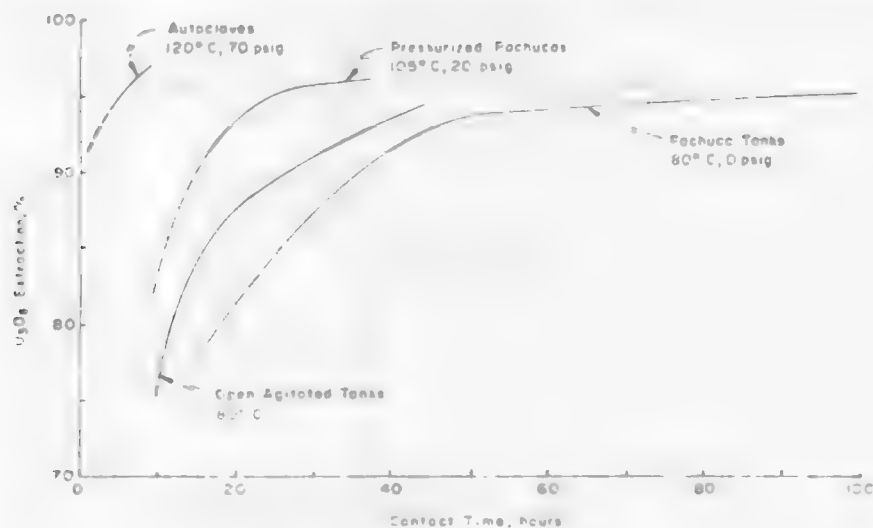
Source: E. Peters, et.al., Hydrometallurgy: Theory and Practice, First Symposium, 1972.

Figure 5.3.5 Pilot Plant Scale Autoclave.



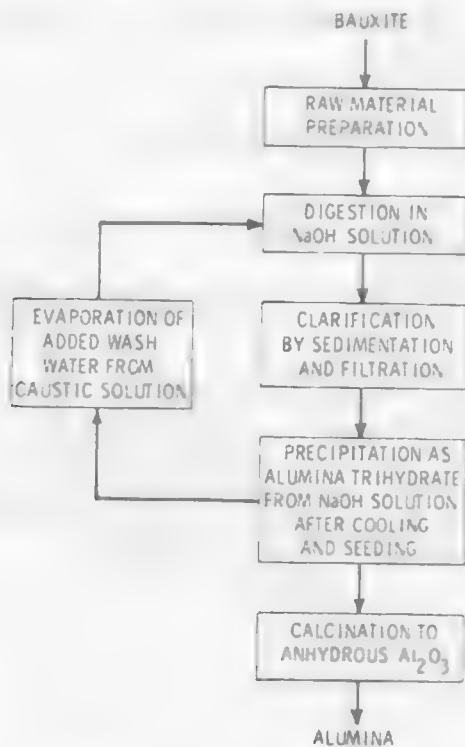
Source: Boldt, J. R., Winning of Nickel.

Figure 5.3.6 Results of Carbonate Solution Leaching of Uranium Ores.



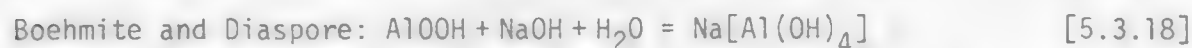
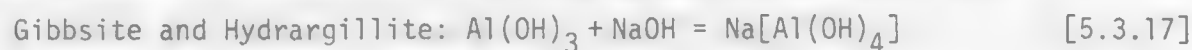
Source: Merritt, R. C., The Extractive Metallurgy of Uranium.

Figure 5.3.7 Flow Sheet of the Bayer Process.



Source: Pehlke, R. D., Unit Processes of Extractive Metallurgy, 1973.

Bauxite is readily dissolved by sulfuric acid and by a caustic solution. Commercial processes are based on a caustic leach because it provides a means for rejecting iron from the alumina product. The process is called the Bayer process. In this process (figure 5.3.7 shows a simplified flow sheet of Bayer process) aluminum hydroxide is extracted by leaching with a caustic soda solution in steam-heated autoclaves. The main leach reactions are:



The temperature of operation depends on the degree of hydration of the bauxite. Gibbsite, presented as the trihydrate, can be successfully leached at a caustic soda concentration of 130 to 200 g/l NaOH, at 120 to 140°C with an average retention time of one hour. Whereas monohydrate bauxite, containing boehmite, requires caustic soda concentrations of 260 to 450 g/l NaOH at temperatures of 180 to 250°C with retention times ranging from 2 to 4 hours. Diaspore requires temperatures above 250°C.

The reagent caustic soda, NaOH, can be prepared separately and charged to the autoclave, or it can be formed inside the autoclave by adding sodium carbonate and lime water,



After solid-liquid separation, pure aluminum hydroxide (trihydrate-hydrargillite) is recovered from the leach liquor by cooling to 50°C in the presence of seed crystals of trihydrate hydrargillite. Alumina trihydrate is filtered, washed and calcined to anhydrous alumina.

Hematite is not attacked by the alkaline leach. It, therefore, reports to the solid residue (red mud). Clay minerals react with caustic to form sodium silicate and sodium aluminate. These two compounds in turn react to form an insoluble sodium aluminum silicate, resulting in a low-silica leach liquor. A typical composition of bauxite, red mud, and calcined alumina product is presented in Table 5.3.3.

Table 5.3.3 Composition of Bauxite and Products

	Bauxite	Red Mud	Calcined Al ₂ O ₃
Al ₂ O ₃	57.8	14.0	99.55
SiO ₂	3.5	7.6	0.05
Fe ₂ O ₃	24.3	57.6	0.04
TiO ₂	2.5	5.7	-

5.3.4 Leaching of Nickel Oxides.

5.3.4.1 General Considerations.

The world's largest known reserves of nickel occur as nickel lateritic oxide ores. The chemistry of laterization started with weathering of parent

rock, peridotite which contains about 0.2% Ni. This weathering slowly separated nickel from the parent rock by dissolution into a liquid phase, and redeposited it at a greater depth, producing zones of high nickel content. Although nickel-bearing laterites vary in composition chemically and mineralogically, lateritic oxide ores are of two types.⁽³⁾ A limonite type, also called nickeliferrous iron ore, occurs in the upper zone of the lateritic deposit in which ferric oxide minerals dominate. And a silicate type, also called nickeliferrous silicate ore or serpentite ore is formed at deeper levels during the laterization.

In nickeliferrous limonites, $(\text{Fe,Ni})\text{O}(\text{OH}) \cdot n\text{H}_2\text{O}$, the nickel oxide is mainly in solid solution with the iron oxide. In nickeliferrous silicates, however, nickel, iron, and cobalt oxides are formed in various proportions replacing part of the magnesium oxide--notably in the mineral serpentinite, $\text{Mg}_6\text{Si}_4\text{O}_{10}(\text{OH})_8$. The limonitic type of ores contain up to 1.5% Ni, whereas the serpentinitic ores contain up to 3.0% Ni. An idealized section of a lateritic nickel orebody showing composition as a function of depth is presented in figure 5.3.8.⁽⁴⁾

The metallurgical processing of nickel oxides is more difficult than for nickel sulfides. Sulfide ores can be upgraded by physical processes such as flotation and magnetic separation. The nickel in oxide ores, however, is uniformly disseminated. This prevents physical separation from gangue minerals. It is therefore necessary to treat large tonages of a relatively low grade nickel oxide to recover nickel. Since oxide ore often contains substantial quantities of high melting point refractory components, pyrometallurgical fusion of the ore requires a large amount of energy. Hydrometallurgical treatment is an alternative means of treating these ores.

Roorda and Queneau⁽²⁾ have suggested that the choice between hydrometallurgy and pyrometallurgy is largely dependent on the composition of the ore, (represented in figure 5.3.8). A serpentite ore that has a high magnesia/iron ratio can be processed by pyrometallurgy if the grade is high enough. For limonite ores that have a low magnesia content, hydrometallurgy is probably the best approach.

Large scale nickel extraction from lateritic nickel ore utilizes either a direct sulfuric acid pressure leach or a reductive-roast followed by an ammoniacal leach or by a sulfuric acid leach.

5.3.4.2 Direct Sulfuric Acid Leach.

Sulfuric acid leaching of nickeliferrous laterite has been practiced in Moa Bay, Cuba.⁽⁵⁾ The laterite in Moa Bay is mainly limonite--low in magnesia. The project started during the late 1950's in Moa Bay. It included ore preparation, leaching, nickel and cobalt recovery. As far as is known, the Moa Bay plant is still in operation.⁽⁶⁾

The key to the sulfuric acid leach at Moa Bay was to selectively leach nickel and cobalt from the iron-rich ore. The composition averaged 1.36% Ni, 0.13% Co, 0.7% MgO and 67.9% iron oxide. If the ore were treated with sulfuric acid at ambient temperature, most of the iron would dissolve along with the nickel and cobalt. However, under autoclave conditions, i.e., 230° to 260°C,

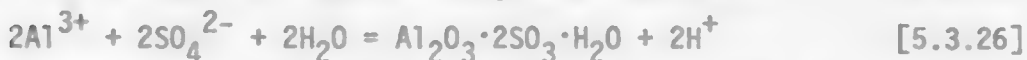
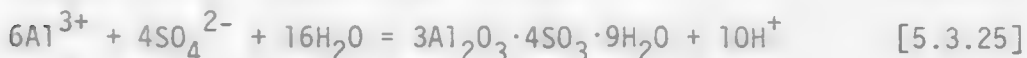
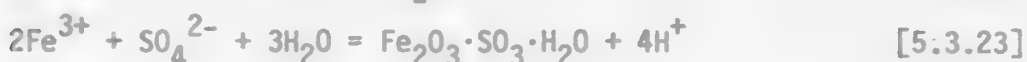
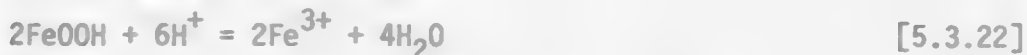
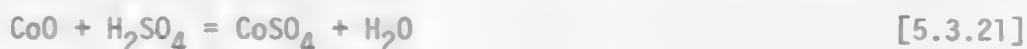
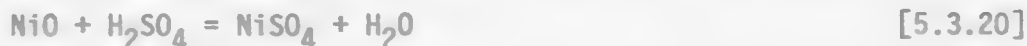
Figure 5.3.8 Idealized Section Through a Lateritic Nickel Orebody Indicating Composition as a Function of Depth, and Proposed Type of Treatment.

IDEALIZED LATERITE	APPROXIMATE ANALYSIS - %					EXTRACTIVE PROCEDURE
	Ni	Co	Fe	Cr ₂ O ₃	MnO	
Hematitic Cap	<0.8	<0.1	>50	>1	<0.5	Overburden to Stockpile
Altered Laterite	0.8 to 1.5	0.1 to 0.2	40 to 50	2 to 5	0.5 to 5	Hydrometallurgy
Altered Peridotite	1.5 to 1.8	0.02 to	25 to 40	1 to	5 to 15	Hydrometallurgy or Pyrometallurgy
	1.8 to 3	0.1	10 to 25	2	15 to 35	Pyrometallurgy
Unaltered Peridotite	0.25	0.01 to 0.02	5	0.2 to 1	35 to 45	Left in situ

Source: Canterford, J. H., "The Treatment of Nickeliferous Laterites", Min. Sci. Eng., 7, No. 1.

95% of nickel and cobalt was dissolved but only a small amount of iron.

At Moa Bay, the ore was ground to 85% minus 325-mesh. The slurry containing 45% solid was leached with concentrated sulfuric acid at 230°C in large vertical autoclaves (600 psi) which were lined with brick and lead. The flow sheet is presented in Figure 5.3.9. Under these conditions nickel and cobalt were solubilized as aqueous sulfate. The iron and aluminum were converted to insoluble hematite and aluminum sulfate.⁽⁵⁾



Acid consumption was via one-third to free acid, one-third to tailings, and one-third to soluble salts. The required retention time was 1 to 2 hours depending on the temperature, acid concentration, ore composition, and particle size.

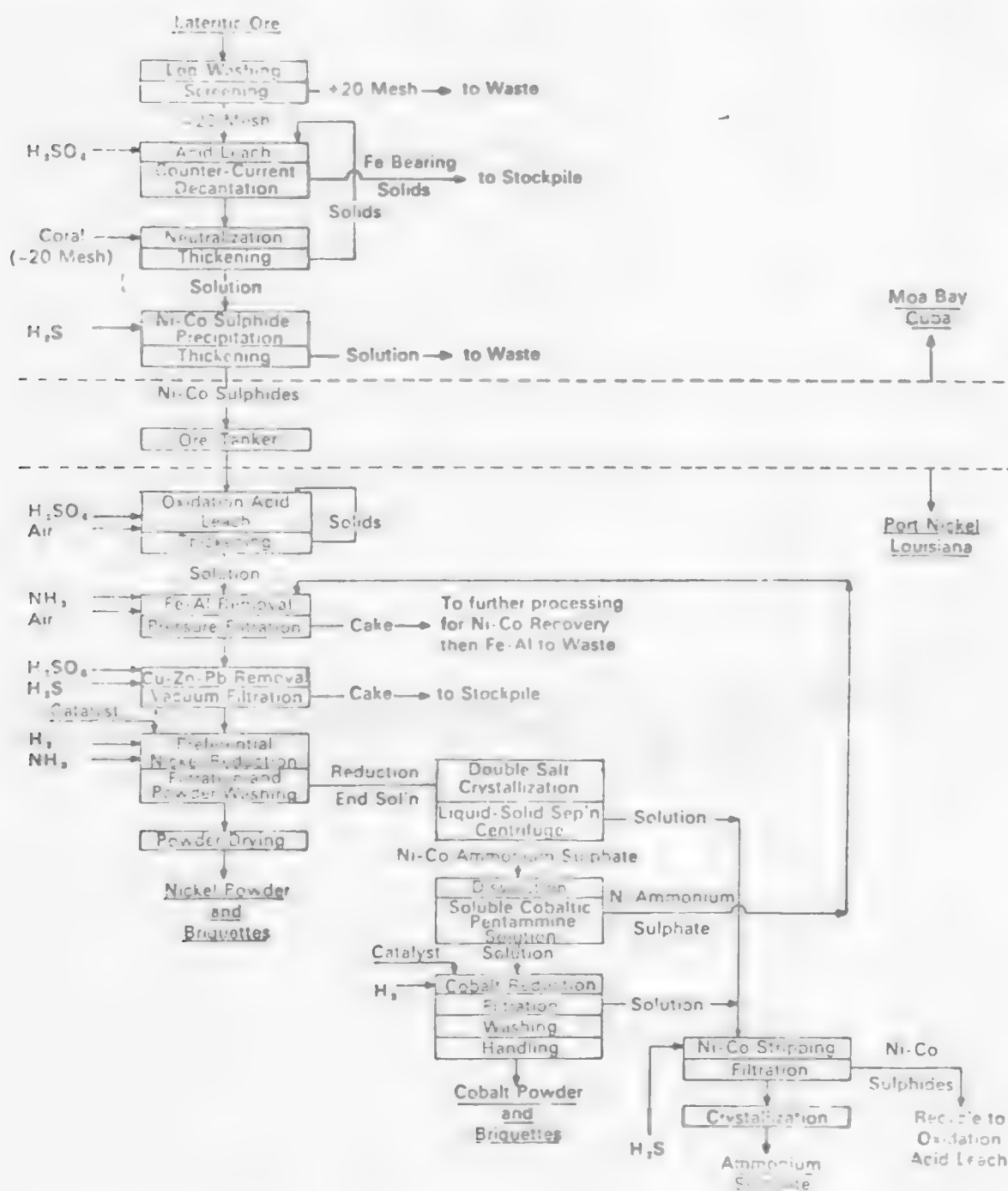
After a solid-liquid separation, the pH value of the solution was raised to 2.5, and the nickel and cobalt were precipitated as sulfides by using hydrogen sulfide gas,



Detailed kinetic and chemistry studies on the direct sulfuric acid leaching of limonite was performed by Chou et.al.⁽⁷⁾ They have indicated that nickel extraction is independent of agitation after a brief initial mixing period. This suggests that film diffusion is not the controlling step. The optimal temperature was found to be between 250 to 270°C (shown in figure 5.3.10) with an activation energy of 30 kcal/mole during the first 30 minutes of leaching. Low temperature leaching apparently does not provide the driving force needed for rapid nickel extraction; and very high temperature apparently results in co-precipitation of nickel with other solid wastes. Another important variable is the weight of acid to a given weight of ore, i.e., acid/ore ratio. Increasing the acid/ore ratio results in an increasing extraction rate. However, short leaching time at high acid/ore ratio will also result in high concentrations of iron, aluminum and sulfate in the pregnant solution.

Based on the Moa Bay operation, several techniques have been proposed to improve the process:

Figure 5.3.9 Freeport Nickel Co. Simplified Flow Diagram for Production of Nickel and Cobalt Powders from Laterites.



Source: Advances in Extractive Metallurgy 1967 I.M.M.

Figure 5.3.10 Nickel Extraction as a Function of Leaching Time and Temperature.



Source: Chou, E. C., P. B. Queneau, and R. S. Rickard, "Sulfuric Acid Pressure Leaching of Nickeliferous Limonites", Met. Trans. 80.

1. The use of the jarosite process or goethite process to remove excess iron from the solution.
2. The use of nickel cementation by iron.
3. The use of pyrite as the source of sulfuric acid, that is, instead of adding sulfuric acid directly, pyrite can be added to the slurry of the ore and will be oxidized to generate sulfuric acid within the autoclave,



5.3.4.3 Reductive Roasting / Ammoniacal Leaching.

Reductive roasting followed by ammonia leaching of lateritic nickel ores has been in operation at Nicaro, Cuba, since the 1940's. Unlike the ore at Moa Bay where the major lateritic ores are limonitic, the deposits at Nicaro are of the silicate type--high in acid soluble magnesia. The process includes the following stages: reductive roasting of the ore, followed by cooling under non-oxidized conditions, leaching in an ammoniacal ammonium carbonate solution, and then heating the pregnant solution to recover nickel and cobalt as a precipitate. The key step to this process was the reductive roasting to reduce the nickel oxide to metal. Nickel then could be leached in an ammoniacal solution. The roast converts most of the iron in the limonitic ore fraction of the ore to magnetite but does not attack most of the iron in the serpentine fraction. Iron compounds were, therefore, not soluble in the ammoniacal leach solution. A brief discussion of the Nicara operation is given below:⁽⁸⁾

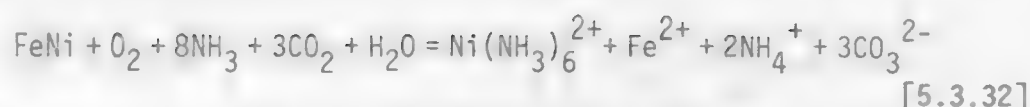
1. Reduction roasting--The roasting was performed in multiple-hearth reduction furnaces. Hot reducing gas was supplied by gas producers using anthracite coal. To control the selective reduction in the furnace, the ratios of hydrogen to water vapor and carbon monoxide to carbon dioxide were held as close to one-to-one as possible at the bottom of the hearth. The roasting temperature was approximately 760°C, and the retention time was about 90 minutes. Under these conditions nickel oxide was reduced to metal, and ferric iron was reduced mainly to magnetite. The reduction reactions are idealized in the following equations:



However, since nickel oxide in the ore was mainly in solid solution, the end product was an iron-nickel alloy.

It was of importance to make sure that the ore was not exposed to the air during cooling. If this happened, the microscopically fine and disseminated nickel metal would rapidly re-oxidize. Thus, making it insoluble in the leaching solution.

2. Ammoniacal oxidative leach--The reduced ore was leached in a series of aerated agitation tanks. The nickel-iron alloy was oxidized and dissolved in the ammonia-ammonium carbonate solution. Nickel combined with ammonia in the solution to form the stable hexamine complex, and iron dissolved as ferrous iron,



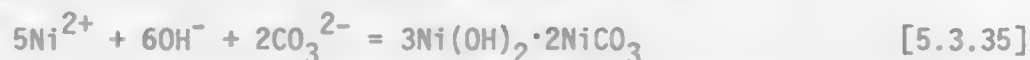
Ferrous iron was further oxidized to the ferric state and precipitated as iron hydroxide:



3. Ammonia stripping and nickel precipitation--The clarified pregnant liquor was steam heated to vaporize ammonia and carbon dioxide for recycle. As the total concentration of ammonia was depleted to 2%, the nickel hexammine was converted to the diammine complex. When further heated, the loss of ammonia led to the reaction:



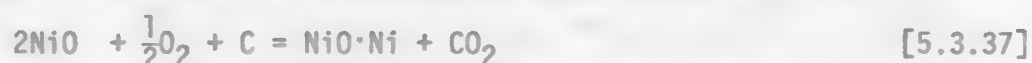
The nickel ions combined with hydroxyl and carbonate ions in the solution to form the insoluble basic nickel carbonate:



4. Calcining--After a solid/liquid separation, the nickel basic carbonate precipitate was dried and calcined in a rotary kiln at 1100°C to drive off water and carbon dioxide, and nickel oxide powder was obtained according to the following reaction:



5. Sintering--The above product was combined with coal and pelletized, then sintered at 980°C to produce a mixture of metal oxide and metal:



The sintered cake contained an average of 88% Ni, 0.7% Co, 0.3% Fe, and 1.7% silica.

Based on the Nicaro operation, several new processes have been proposed to improve the purity of nickel and the recovery of cobalt.⁽⁸⁾

Sherritt-Gordon⁽⁹⁾ has presented a reductive roast/ammoniacal leach/hydrogen reduction process for the treatment of laterite. The process has been tested in a pilot plant at Fort Saskatchewan, and will be used in the new nickel refinery by the Marinduque Mining and Industrial Corporation in the Philippines.

The Sherritt process reduces lateritic ore at 650°C prior to leaching with ammonia carbonate solution at atmospheric pressure (which resembles the process used at Nicaro). But in the Sherritt process, cobalt together with some of the nickel, is removed from the pregnant leach solution by hydrogen sulfide precipitation. The cobalt-free solution is steam heated to strip off ammonia and carbon dioxide for recycle, while nickel basic carbonate is precipitated. The nickel carbonate is redissolved in ammoniacal carbonate solution at a higher nickel concentration. The nickel solution is then partially precipitated by steaming. The resultant nickel carbonate is pressure reduced with hydrogen gas

at 165°C to recover the nickel as metal nickel. A simplified flow sheet diagram is shown in figure 5.3.11.

Sherritt Gordon has also developed a reductive roast/sulfuric acid leach/hydrogen reduction process to treat a calcined cobalt and nickel concentrate. The calcine is a by product from a lead-zinc operation and contains about 14% cobalt and 20% nickel. This material, in the form of refractory ferrites, was found to resist direct pressure leaching. The developed process consists of converting nickel and cobalt to an acid-soluble form by hydrogen reductive roasting at 1350°F, oxidative sulfuric acid leaching at 210°F under oxygen partial pressure of 20 psi, copper removal by hydrogen sulfide precipitation, and iron removal by raising the pH to 5.2 with NH₃ under oxidizing conditions. The purified cobalt nickel solution is then treated in the existing cobalt plant.⁽¹¹⁾ The nickel is separated as nickel ammonium sulfate and the cobalt is recovered as a metal powder by reduction of the solution with hydrogen.

5.3.4.4 Sulfidization Process.

Republic Steel Corp. and the Colorado School of Mines Institute have developed a process to treat lateritic nickel ore from both limonitic and serpentinitic ores. The process, known as the HSO-HTCP process (hydrothermal sulfidization oxidation-high temperature cementation-in-pulp) involves aqueous sulfidization of nickel, followed by oxidation to water-soluble sulfate and recovery of nickel by cementation with iron.^(12,13) The simplified flow sheet diagram of the process is presented in figure 5.3.12, and a brief process description follows:

1. Sulfidization--The lateritic ore, 85% minus 200-mesh, is sulfidized by reacting it with sulfur under hydrothermal conditions at 230 to 240°C under a steam pressure of 455 to 580 psig. The sulfidization reactions for Ni, Co, and Fe are:



The sulfuric acid generated due to the sulfidization reactions immediately reacts with acid consuming constituents of the ores, resulting in a final pH of about 5.0,



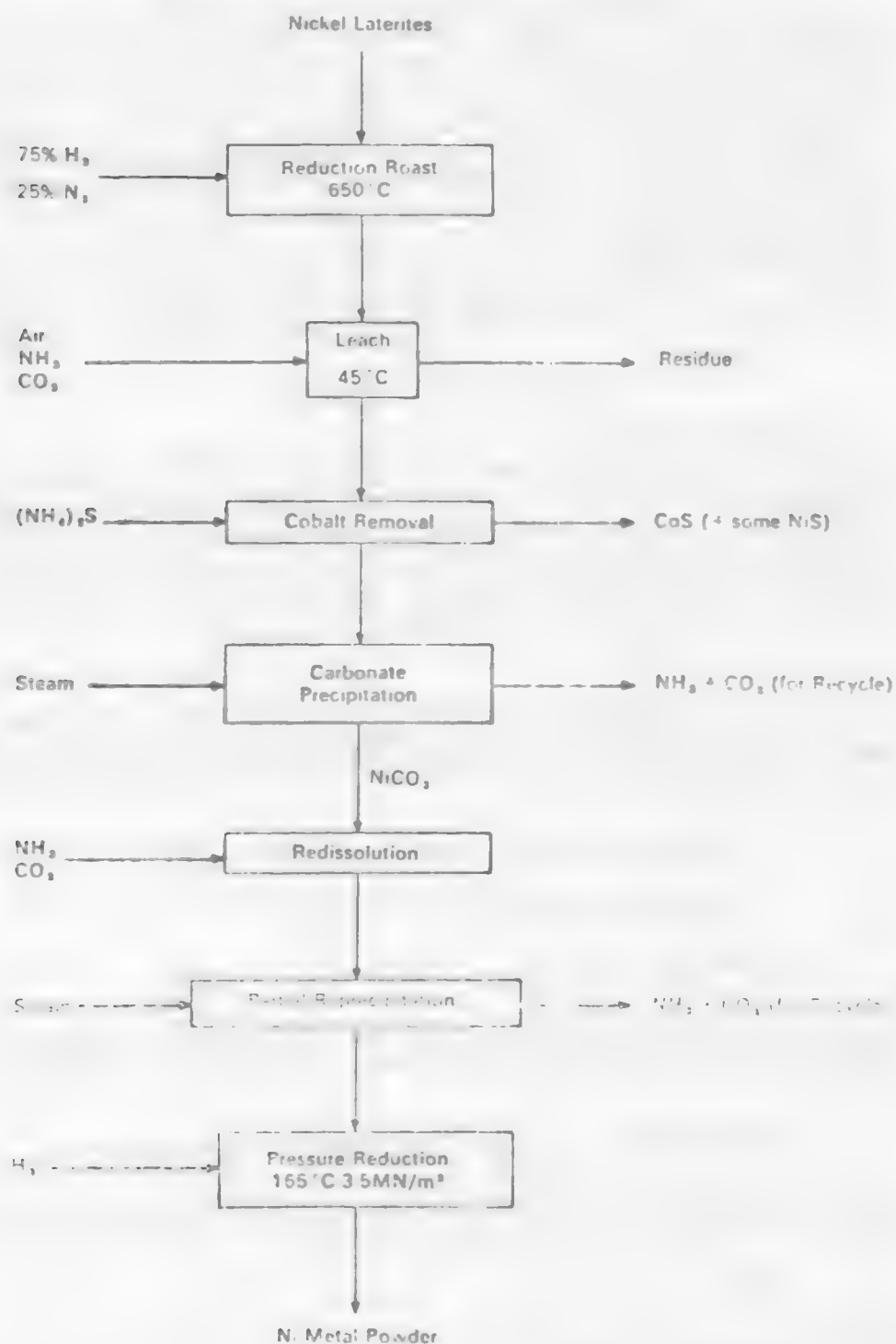
2. Oxidation--The sulfidized pulp is then oxidized at 200°C with air at 200 psig to produce soluble nickel sulfate,



Under the above conditions, iron sulfides are first oxidized to ferrous sulfate and then further oxidized to ferric sulfate and precipitated as ferric oxide.

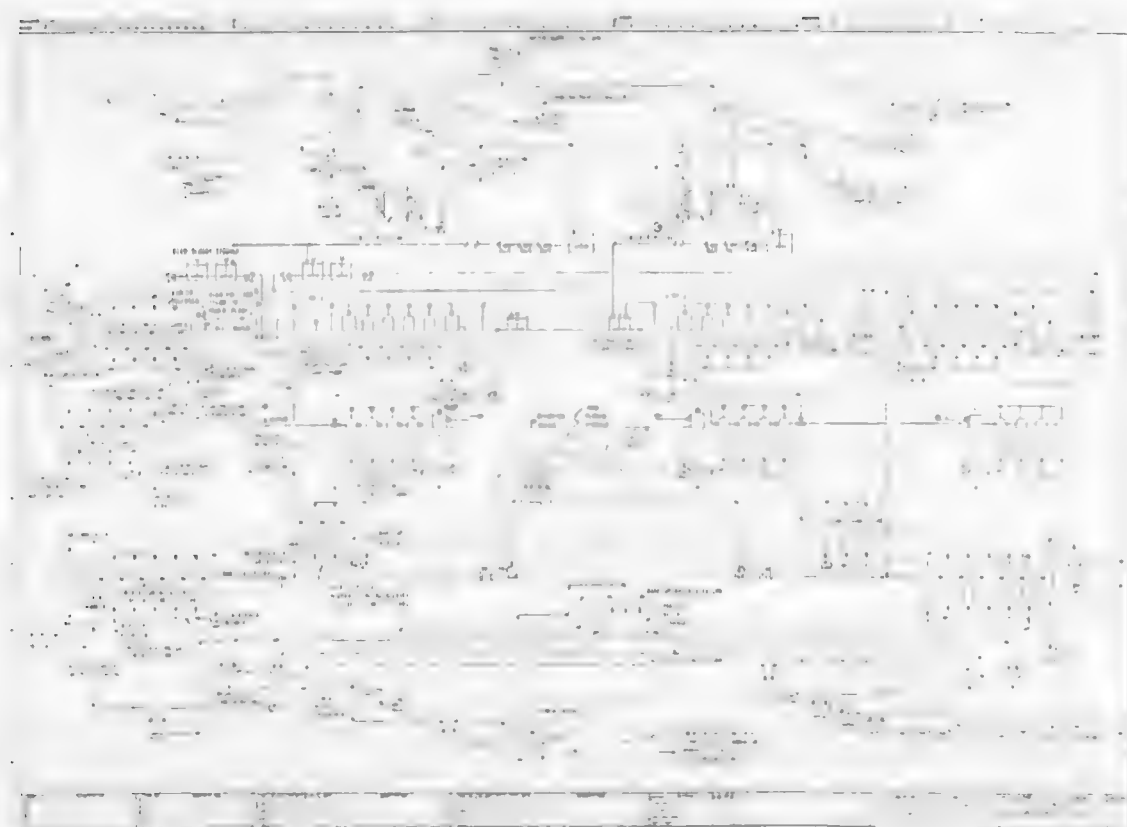


Figure 5.3.11 Reduction Roast--Ammonium Carbonate Leach--Pressure Reduction Process for Treating Nickel Laterite.



Source: R. Derry, Mineral Sci. Engng., Vol. 4., No. 3(1972).

Figure 5.3.12 Flow Sheet of HSO-HTCP.



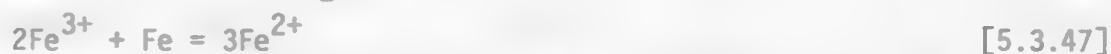
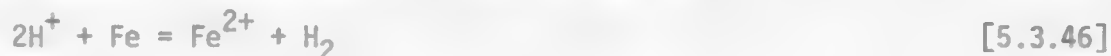
Source: Bush, P.D., et.al., International Symposium on Hydrometallurgy, Chicago, 1973.



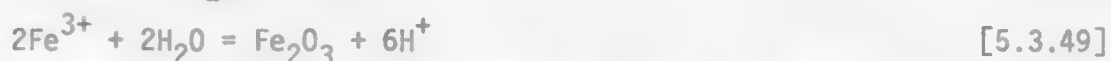
The acid produced reacts with any remaining nickel magnesium silicates,



3. Neutralizing hydrolysis--The oxidation leach pulp usually contains fairly large amounts of acid and ferric iron. These can result in an excessive use of iron powder in the subsequent cementation step:



A neutralizing hydrolysis is used to control this problem, i.e., the removal of excess acid and ferric iron is accomplished by adding acid-consuming material such as high-magnesium lateritic ore to adjust the pH of the pulp to about 2.0,



4. Cementation--The recovery of dissolved nickel and cobalt values from the solution is achieved by cementation with iron at 135 to 150°C.

5.3.5 Leaching of Ocean Manganese Nodules

Extensive deposits of manganese nodules occurring on the ocean floor represent substantial reserves of manganese, nickel, copper and cobalt. Manganese ocean nodules are lumpy black-brown concretions averaging 2 to 4 cm in diameter. The majority of the nodules lie on the surface of the ocean. The average growth rate of the nodule is extremely slow, e.g., a few millimeters every million years.

The principle constituent of sea nodules is manganese, but they also contain the more important metal values nickel, copper and cobalt. A typical analysis of principle metal values for Pacific and Atlantic manganese nodules is presented in Table 5.3.4.

5.3.5.1 General Consideration.

Manganese nodules are composed primarily of manganese and iron oxides and hydroxides with smaller amounts of nearly every known element. Agarwal(15) et.al. have analyzed the market and revenue potential for manganese and iron, and found that their recovery from sea nodules would not be competitive with the existing market. The economic interest in nodules is focused primarily on copper, nickel and cobalt, and several other valuable metals such as molybdenum, titanium and zinc.

The metal values, Ni, Co, and Cu, are finely and chemically disseminated in a manganese oxide matrix of the ore. The ore is not suitable for physical separation. Also, the nodule is very porous; i.e., 50 to 60% porosity. Even when drained, the nodules still contain 30 to 40% free moisture, and another

Table 5.3.4 Average Composition of Air-dry Manganese Nodules (% by weight).⁽¹⁴⁾

	Pacific	Atlantic
Mn	29.8	15.7
Fe	4.8	15.5
Co	0.2	0.41
Ni	1.36	0.59
Cu	1.20	0.14
Zn	0.12	0.05
Pb	0.05	0.15
Al ₂ O ₃	5.70	4.90
SiO ₂	13.0	2.90
Ca	1.47	17.32
Mg	1.70	1.70
Si	0.07	0.19
Ba	0.61	0.52
K	0.79	0.31
Na	2.6	2.3
P	0.05	0.15
Ti	0.44	0.34
Mo	0.05	0.05
V	0.05	0.07
H ₂ O	16.2	15.6
L.O.I.	22.0	23.8

10 to 15% chemical combined water.⁽¹⁶⁾ Based on the above characteristics, the pyrometallurgical processes for smelting this refractory type of nodule requires a large amount of energy to recover only about 3% valuable metals. Even the roasting process requires excessive energy to remove large quantities of water. Pyrometallurgical approaches, suggested by Agarwal et.al.⁽¹⁶⁾, are not well suited to nodule processing.

Several hydrometallurgical processes⁽¹⁷⁾ proposed to recover metal values have been either the selective removal of metal values without disturbing the manganese oxide matrix, or the extraction of metal values while destroying the entire matrix. The former, such as a sulfuric acid leach, requires high temperature, high pressure and high reagent concentrations to overcome the slow diffusion process.⁽¹⁸⁾ In a sulfuric acid leach circuit, it has been reported that acid consumption is usually high.

Manganese exists in the nodule in the tetravalent state which is insoluble in aqueous solution. In order to destroy the manganese matrix a reduction process is required, e.g., the Caron process,⁽¹⁹⁾ gaseous reductive roasting of lateritic nickel oxide (described earlier as applied to the Nicaro Plant). An aqueous reducing leach process for the treatment of nodules has been used, e.g., sulfur dioxide, SO₂, was the reducing agent.⁽²⁰⁾ It was reported that at 25°C equilibrium was reached in less than 5 minutes with 95% dissolution of both Ni and Co, 85% of the copper, 45% of the manganese, and 60% of the iron. The presence of high concentrations of manganese and iron in solution make the recovery of nickel, cobalt and copper difficult.

The Kennecott Copper Corp. has developed a process known as the Kennecott Cuprion process. The process uses aqueous reduction to selectively extract

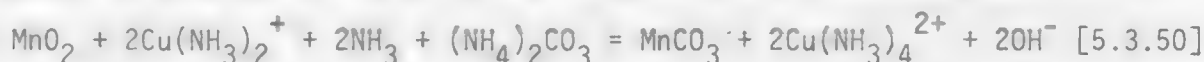
the metal values and leave behind the solid products of manganese and iron. A brief discussion is as follows.

5.3.5.2 Kennecott Cuprion Process.

An ammoniacal ammonium carbonate solution is used to dissolve nickel, cobalt, copper and molybdenum. Carbon monoxide is the aqueous reducing agent. Manganese is reduced, dissolved, and subsequently precipitated by the carbonate ion as a solid product. Although carbon monoxide is a powerful reducing agent, it is kinetically inert at ambient temperature. The key of the process was to utilize cuprous copper ion as a catalyst. The cuprous ion readily reduced manganese dioxide while it was oxidized to the cupric form. The cupric ion, as an intermediate, is reduced back to the cuprous ion by carbon monoxide. Both Cupric and cuprous ions are soluble in ammonia-ammonium carbonate solution. Reagent copper is derived from the ore, no additional charge of copper for this process is necessary.

The process flow sheet is rather simple, i.e., size reduction, reduction leaching, and clarification steps. The nodules (containing 40% sea water) are wet ground with recycle reduction liquor to minus 60-mesh.

The minus 60 mesh ammoniacal nodule slurry is reduced in a series of stirred tank reactors at about 50°C. Twenty minute retention times are required for each tank. The leach slurry contains 3 to 4% solid; a total ammonia concentration of about 100 g/l and carbon dioxide of about 20 g/l. The carbon monoxide is sparged into each reactor. During the leaching, cuprous ions reduce the manganese in the nodule and produce a manganese (II) carbonate precipitate:



Carbon monoxide regenerates the cuprous ion:



At the same time, copper, nickel and cobalt are dissolved as metal ammine complexes, and iron oxide is not attacked by the ammonia. Under these conditions, reduction of the manganese is typically 98% complete, and 98.4% of Ni and 96% Cu are dissolved.

The reduced product enters a clarifier, the overflow is recycled. The underflow carries the dissolved nickel, copper and cobalt and contains approximately 40% solids. It is oxidized with air to convert the cuprous ion to cupric ion to facilitate copper recovery by solvent extraction. The oxidized slurry is washed and decanted. The pregnant liquor contains nickel and copper concentration in the range of 4 to 10 g/l. The tailings retain only a small fraction of the metal values but all of the iron and manganese.

The pregnant liquor includes various metal values, especially copper, nickel, cobalt and molybdenum. Kennecott Copper Corp.⁽²¹⁾ has also developed a fluid ionic exchange (FIX) technology to extract both copper and nickel with LIX reagent while the raffinate may be treated by chemical means to recover cobalt and molybdenum. The residual liquor is recycled. Copper and nickel in the loaded organic is separated by selective stripping. Nickel is first removed

with weak sulfuric acid solution controlled to a pH of 3.0. Copper is then stripped with a stronger sulfuric acid solution. The production of nickel and copper metal is accomplished by electrowinning. The quality of copper and nickel cathode is comparable to electrorefined cathode.

5.3.6 Leaching of Copper Oxide.

Although most research efforts have been directed to the leaching of copper sulfide minerals, commercially the leaching of oxide ores is very important. Copper oxide is usually finely disseminated in an ore. It is the degradation product of an original sulfide deposit. This type of ore is usually low grade and not suitable for physical concentration. The pyrometallurgical processes for the treatment of copper oxide ores may not justify the cost of the operation.

Copper in the form of oxide is readily soluble in acid or alkaline solution. The sources of copper oxide ore are: sulfide flotation tailings,^(22,23) low grade mined ore,⁽²⁴⁾ mining waste,⁽²⁴⁾ and oxide flotation concentrates.⁽²⁵⁾ The principal copper oxide minerals are azurite, chrysocolla, and malachite. Varying amounts of cuprite and tenorite are known to be contained in some ores.

Although ammoniacal solution and other leaching reagents can be used for the leaching of copper oxide, sulfuric acid is used in almost all leaching operations; i.e., H₂SO₄ acid is readily available at a relatively low cost.

An advantage of using sulfuric acid leach technique is the ease of recovering metallic copper from solution. Ferric sulfate usually exists in the sulfuric acid leach solution and is often the oxidizing agent. Sulfuric acid may be generated by the oxidation of pyritic minerals. The leaching reactions for each specific oxide minerals are:

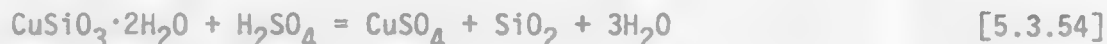
Azurite,



Malachite,



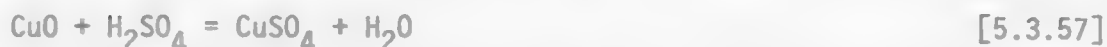
Chrysocolla,



Cuprite,

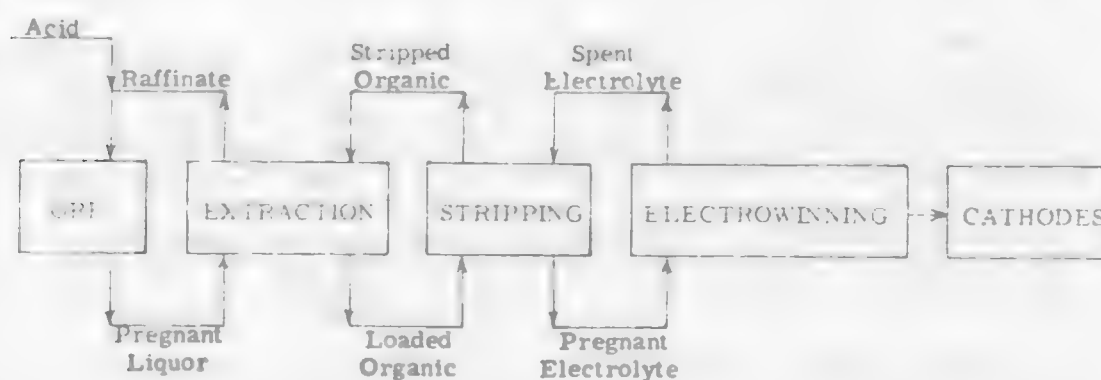


Tenorite,



The recovery of copper from leach liquors is almost entirely by means of either cementation or electrowinning. The cement copper produced by iron metal has a porosity of only about 70%, and an additional refining step is necessary. On the other hand, electrowinning in conjunction with solvent extraction will produce cathodic copper which is comparable to conventional refined copper. A simplified leaching-SX-electrowinning flow sheet is shown in Figure 5.3.13. Leaching acid, organic solvent and stripping acid are regenerated from extraction, stripping and electrowinning steps respectively.

Figure 5.3.13 Copper Leach-SX-EX Circuit.



Source: Power, K. L., "Copper Dump Leaching at Asarco's Silver Bell Unit, Arizona", Unit Processes in Hydrometallurgy.

5.3.6.1 Leaching Methods.

The principal methods of leaching copper oxide ores are (a) in-situ leaching, (b) dump leaching, (c) heap leaching, (d) vat leaching, and (e) agitation leaching. These methods are interrelated, and many items considered necessary for effective leaching by one method are also applicable to the other methods. Typical operating conditions for these types of plants are given in Table 5.3.5.

The choice of leaching method depends upon the chemical and physical characteristics of the ore: the grade of the ore, the solubility of the copper minerals, the amount of acid-consuming associated gangue materials, the size of the operation, and the mode of occurrence of the copper-bearing minerals. (28)

In-situ, dump and heap leaching are essentially the same technique. The ore is broken to expose the copper minerals; and sulfuric acid solution is

Table 5.3.5 Leaching Methods for Hydrometallurgical Treatment of Copper Oxide. (35)

Leach Method	Mineralogy	% Cu in Ore	Leach Time	Size of Operation	Copper Leached tons/day	References
In situ	oxide/sulfide	0.5	2-25 y	4x10 ⁶ tonnes of ore	20	(30,31,32)
Dump	oxide/sulfide	0.5	3-20 y	5x10 ⁶ tons of waste	100	(28)
Heap	oxide	0.5-1	4-6 m	3x10 ⁵ tons of ore	20	(24,25)
Vat	oxide	1-2	5-10 d	6-12 vats	10-120	(34,36)
Agitation						
(a) flotation tailing	oxide	0.1-0.5	2-5 h	10-15 tanks		(22,23)
(b) oxide ore	oxide	1-2	2-5 h	3-10 tanks		(27)
(c) oxide conc.	oxide	20-30	2-5 h	45 tanks		(26)

trickled by gravity over the rocks. The basic requirements for these methods are an impervious base (natural or artificial) to collect the pregnant leach solution. For dump and in-situ leaching, the copper oxide and sulfide minerals are considered as leachable, since the leaching cycle is measured in year. Heap leaching is designed mainly for the extraction of copper from oxide.

Vat and agitation leaching processes are designed to dissolve copper oxide in a confined vessel. When applying these methods, an additional size reduction may be necessary, but rapid extraction and high concentration of copper in the pregnant liquor can be obtained.

5.3.6.2 In-Situ Leaching.

Although there is a great potential for using the in-situ leaching technique to extract copper from deep sulfide deposits, most actual operations have been applied to leaching copper oxide and sulfide minerals from surface or near-surface deposits. The source is either low grade deposits or worked-out mines. First the rock has to be rubblized in place by blasting, block caving or hydrofracturing. Sulfuric acid solution is trickled over the ore pile. Copper is dissolved. The pregnant solution is collected at the bottom of the ore body (a solution collection well may be necessary).

Applications of in-situ copper leaching have been practiced at Miami, Arizona⁽²⁹⁾, the Old Reliable mine near Mammoth, Arizona⁽³⁰⁾, the Big Mike mine near Winnemucca, Nevada⁽³¹⁾, and the Mountain City mine in Mt. City, Nevada⁽³²⁾, and other mines.

A schematic diagram of Big Mike in-situ leach operation is shown in figure 5.3.14.

5.3.6.3 Dump Leaching.

Dump leaching is used for low-grade and mine waste material stripped from open pit operations. The rock is piled into large dumps and the sulfuric acid solution is distributed over the surface and allowed to trickle through the dump. The pregnant solution is collected at the bottom of the dump, and copper is normally recovered by cementation methods.

A schematic diagram of dump leaching operation is shown in figure 5.3.15.

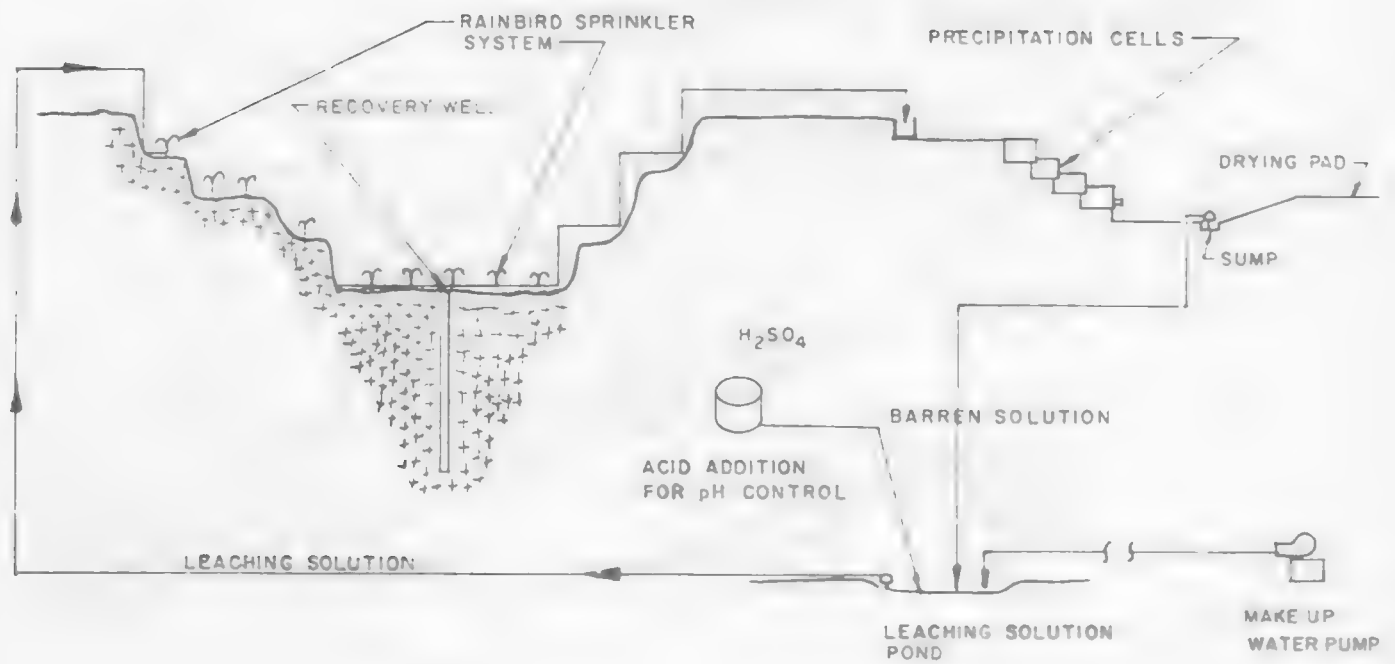
5.3.6.4 Heap Leaching.

Heap leaching is employed to dissolve copper from porous oxide ore that has been placed on a prepared surface. Heap leaching contrasts with dump leaching principally in that oxide ore material is leached instead of mining waste material. A typical example of a heap leaching operation is the Ranchers Exploration and Development Corp. at the Bluebird mine near Miami, Arizona (which is the first operation that utilized solvent extraction-electrowinning technique to recover copper).

5.3.6.5 Vat Leaching.

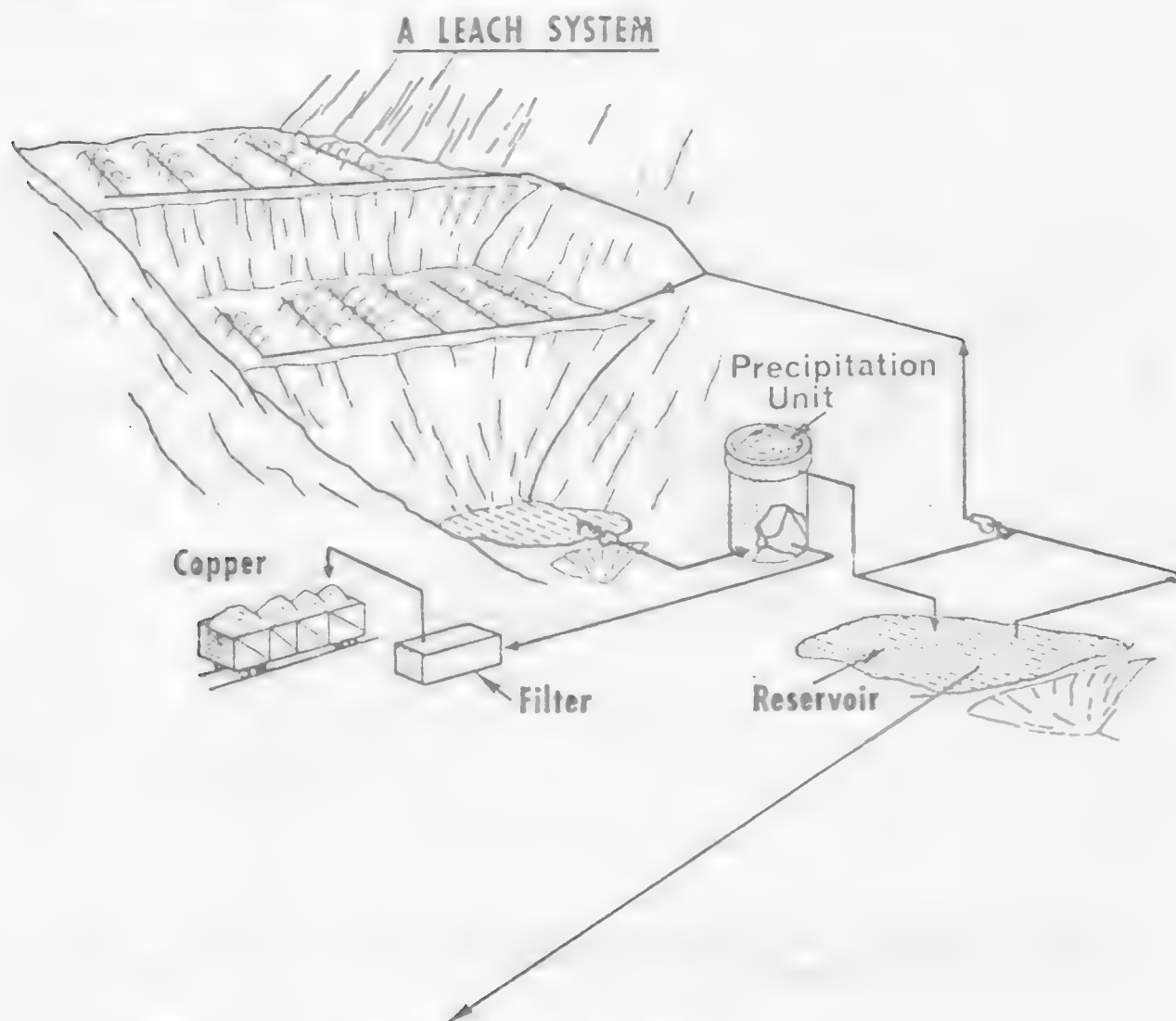
Vat leaching is employed to extract copper from oxide or mixed oxide-sulfide ores containing more than 0.5 percent acid-soluble copper. This method

Figure 5.3.14 Schematic Diagram of Big Mike Copper In-Situ Leach.

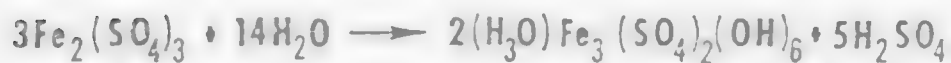
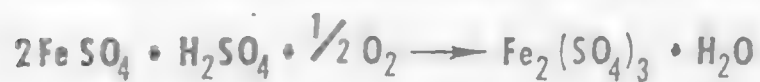


Source: "Ranchers Development Sets Off Blast: Will Leach at Big Mike", Mining Engineering, 25, No. 8.

Figure 5.3.15 Copper Dump Leach Operation.



IRON SULFATE OXIDATION AND HYDROLYSIS



Amorphous Basic Iron Sulfate

Source: E. E. Malouf, Univ. of Utah.

is used in preference to heap leaching if the ore material is not porous and crushing is necessary to permit adequate contact between the leach solution and the copper minerals. Despite increased costs necessary for crushing and screening, numerous advantages exist for vat leaching: high copper recovery in short periods, low pregnant solution loss, and high copper content in pregnant solution (about 30-50 g/l Cu).

A description and illustration of the vat leaching operation at ASARCO's San Xavier⁽³⁶⁾ Cu leach-precipitate plant is given below. An isometric diagram of the ASARCO San Xavier plant is presented in figure 5.3.16. The plant is designed to treat 4,000 tons per day of ore (1% copper). The primary oxide mineral is chrysocolla, with some azurite and malachite. Prior to vat leaching the ore is crushed and screened to minus-3/8-inch. The leaching is carried out in 9 vats. Each vat has a capacity of 4,000 tons. The leaching cycle for each vat requires 9 days; e.g., this includes 5 days of leaching, 1 day of washing and 3 days excavation, cleaning and refilling. Copper is recovered from the leach solution by cementation. The cement copper is shipped to ASARCO's Hayden and El Paso smelters for direct charging into converters.

5.3.6.6 Agitation Leaching.

Agitation leaching involves the rapid leaching of copper oxide minerals from fine particles (usually minus 48 mesh). Sulfide minerals are not leached during the short contact periods. The leaching usually takes place continuously in a series of Pachuca reactors.

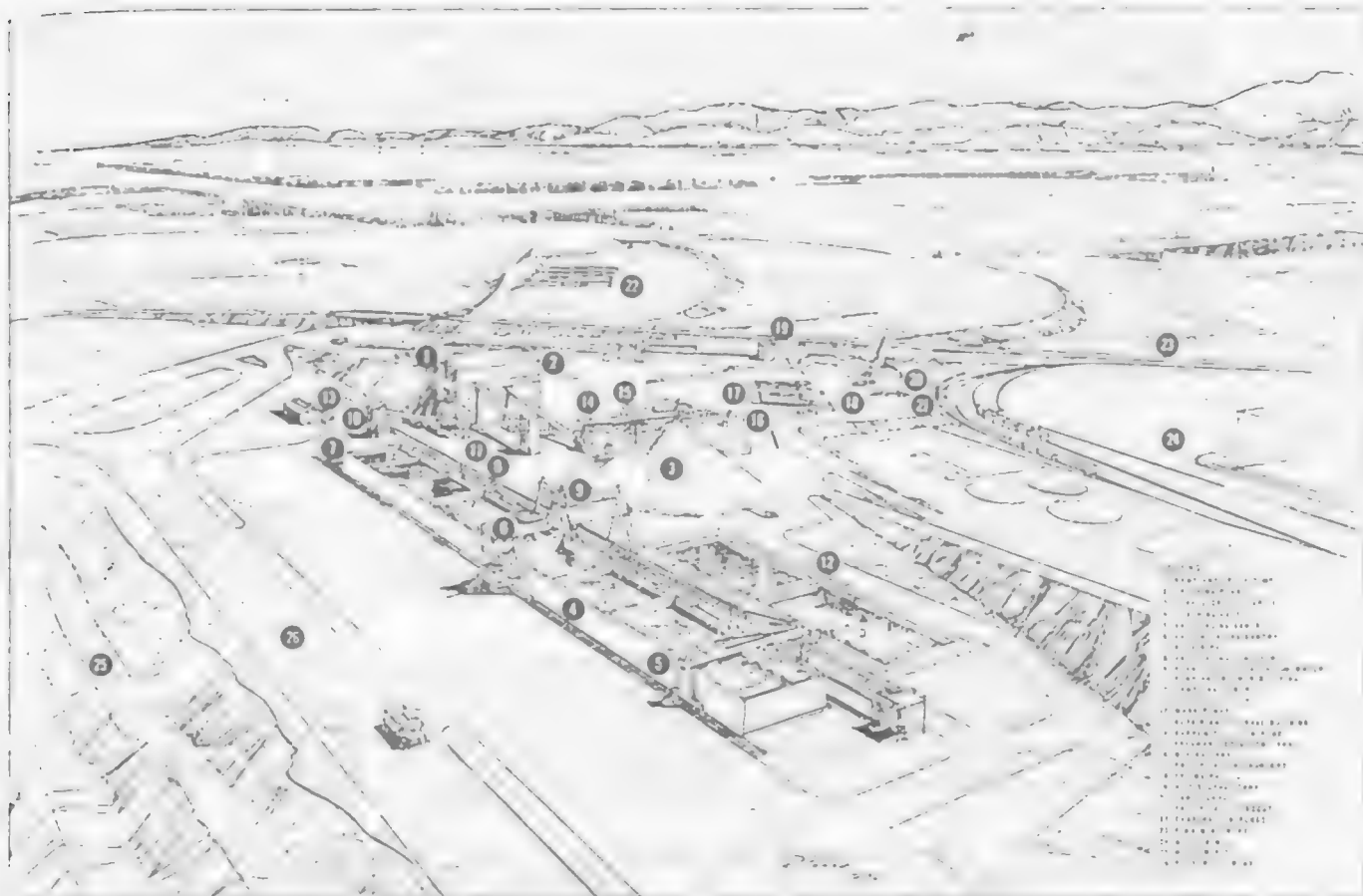
Agitation leaching can be used to recover copper oxide from sulfide flotation tailings^(22,23) and oxide flotation concentrates⁽²⁶⁾ without additional size reduction. Grinding is required for the treatment of oxide ore.⁽²⁹⁾ Examples of agitation leaching in the U. S. are the Morenci Tailing Leach Plant at Morenci and the Anamax Oxide Plant at Twin Butte.

A general flow sheet of the copper tailings leach plant⁽³³⁾ at Morenci, Arizona is shown in figure 5.3.17. At Morenci, the Phelps Dodge Corp. (due to an increase in their sulfuric acid production capacity, e.g., 500 to 2,000 tpd) had the opportunity to recover oxide copper previously discarded in the flotation mill tailings. The tailings contain about 0.1% oxide copper; primarily chrysocolla, brochantite and azurite.

The leaching plant consists of 11 mechanically agitated vessels (each being 34-ft high by 30-ft diameter) in series followed by two stages of counter-current decantation and washing. The plant capacity is 30,000 tpd. The leaching operation is conducted on 42% solids. Concentrated sulfuric acid is added to the slurry in either the first or second tanks. The pH value in each step is controlled at 1.5. The total retention time for leaching is about 200 minutes. After the solid/liquid separation, the pregnant solution contains 0.298 g/l Cu (representing 73.88% copper oxide recovery). The copper in the pregnant solution is recovered by cementation with scrap iron. The operation data of the Morenci Tailing Leach Plant are presented in Table 5.3.6.

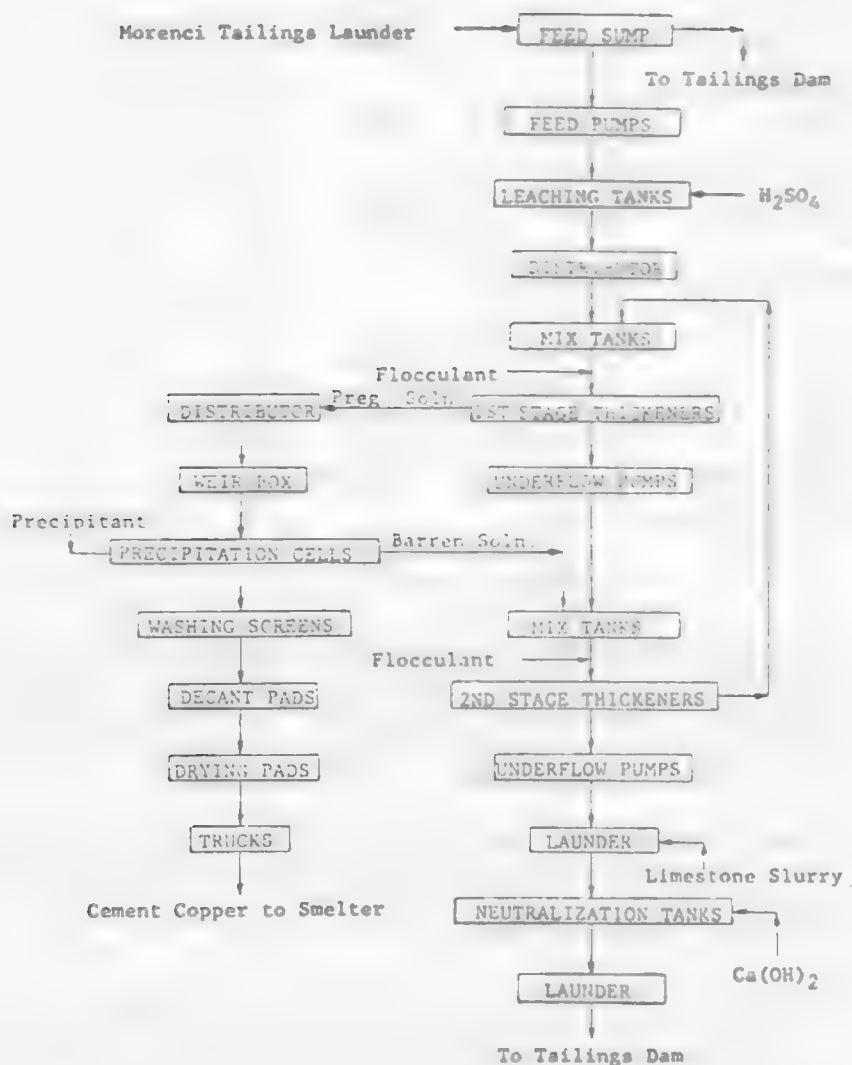
A simplified flowsheet of the Anamax Oxide plant at Twin Buttes is presented in figure 5.3.18. The plant is designed to treat 10,000 tpd of

Figure 5.3.16 ASARCO San Xavier Vat Leaching Plant.



Source: "ASARCO's New Cu Leach-Precipitate Plant for San Xavier North Pit Ore",
World Mining, Oct., 46.

Figure 5.3.17 Flowscheme of One Leaching Module of the Morenci Tailings Leaching Plant.



Source: Kovac-Figueroa, C., "Morenci Tailing Leaching Plant", Trans. SME/AIME, 260, 170.

Table 5.3.6 Morenci Tailings Leaching Plant Operations.

Leach Feed	
% Total Copper	0.209
% Oxide Copper	0.100
Leach Tail	
% Total Copper	0.130
% Oxide Copper	0.020
Pregnant Solution	
gpl Copper	0.298
Indicated Leaching Extraction Based on Copper in Pregnant Solution	92.62
Reagent Consumption--lb/ton of Tailings	
Sulfuric acid	39.3
Lime	15.3
Limestone	7.1
Flocculant	0.024
Precipitant--Iron	2.16 lb/lb Cu
Power--Kw-hr per ton of Leach Feed	2.82

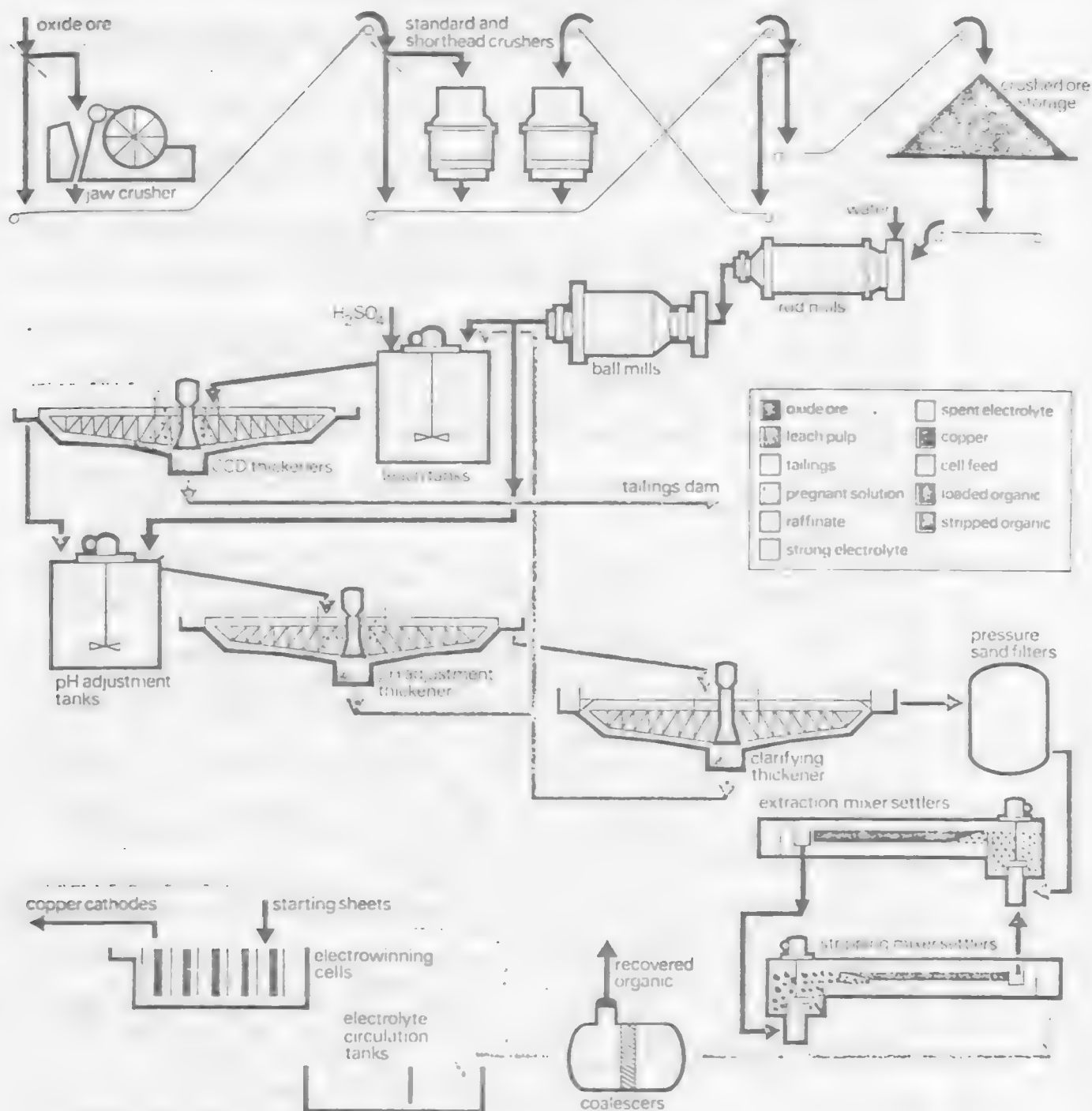
high-lime ore averaging about 1.25% copper. The ore, crushed and ground to 95% minus 48-mesh, with up to 60% solids, is charged to a series of five 30 ft diameter by 31-ft high mechanically agitated vessels. After 5 hours of retention, most of the soluble copper has been leached from the ore. Up to 250 lbs of sulfuric acid is consumed per ton of ore.

The leached slurry is decantated in a series of 4 thickeners. The pH of the slurry is adjusted to from 1.5 to 2.5 by adding unleached oxide ore. The filtered solution contains about 2.5 g/l of copper and is produced at a flow rate of 7120 gallons per minute.

The filtered solution is purified by solvent extraction using LIX 64N. The solution is split into two streams during the purification. Each stream moves through four extraction and two stripping mixer-settlers. Copper is transferred from the pregnant solution to the organic extractant in the extraction stages. The raffinate containing about 0.08 g/l copper is recycled to the leaching step. The loaded organic is then transferred to the stripping stages where the organic solution is contacted counter currently with spent electrolyte from the electrowinning tank house. Copper is transferred from the organic phase to the electrolyte. The fresh organic is recycled to the extraction stages and the loaded electrolyte, containing about 50 g/l copper and 90 g/l sulfuric acid, is pumped back to the tank house.

During the electrowinning, copper is deposited on the cathode, oxygen is liberated at the lead anode, and acid is regenerated. The spent electrolyte contains 25 g/l copper and 130 g/l sulfuric acid.

Figure 5.3.18 Flowsheet of 10,000-tpd Anamax Copper Oxide Plant.



Source: Hopkin, W. R. and A. J. Lynch, "Anamax Oxide Plant: A New U.S. Dimension in Solvent Extraction", EM/J., Feb. 56(1977).

5.3.7 References

1. Merritt, R.C., The Extractive Metallurgy of Uranium, Colorado School of Mines Research Institute, Chap. 5(1970).
2. Hose, H. R., "Bauxite Mineralogy", Extractive Metallurgy of Aluminum, Vol. 1. Alumina, G. Gerard and P. T. Stroup ed., TMS/AIME, Interscience Publishers, 3(1962).
3. Boldt, J. R., Winning of Nickel, van Nostrand, Princeton, New Jersey, 1967.
4. Roorda, H. J. and P. E. Queneau, "Recovery of Nickel and Cobalt from Limonites by Aqueous Chlorination in Sea Water", Trans. IMM, 82, C79-89(1973).
5. Calson, E. T. and C. S. Simons, Extractive Metallurgy of Copper, Nickel and Cobalt, Interscience Publisher, New York, 1961.
6. Canterford, J. H., "The Treatment of Nickeliferous Laterites", Min. Sci. Engl, 7, No. 1, Jan. 3(1975).
7. Chou, E. C., P. B. Queneau, and R. S. Rickard, "Sulfuric Acid Pressure Leaching of Nickeliferous Limonites", Met. Trans. 80, 547(1977).
8. "Nicaro Expands Nickel Capacity", EM/J, 158, No. 9, Sept. 82(1957).
9. Brown, E. L. and V. N. Mackiw, "Process for the Production of Nickel and Cobalt from Nickel- and Cobalt-Bearing Material", U.S. Pat. 3,141,765 (1964).
10. Voltman, H., D. J. I. Evans, and V. N. Mackiw, "Reduction Roasting and Acid Pressure Leaching of Calcined Cobalt Concentrates", CIM Bull. Dec. 1281(1964).
11. Mackiw, V. N., and T. W. Benz, "Application of Pressure Hydrometallurgy to the Production of Metallic Cobalt", Annual Meeting, AIME, Feb. 1960.
12. Seidel, D. C. and E. F. Fitzhugh, "A Hydrothermal Process for Oxidized Nickel Ores", Trans. SME/AIME, 241, 261-268(1968).
13. Bush, P.D., L. F. Engle, E. H. Gates and M. D. Vizayaraphavan, "The Pressure Leaching-Cementation-in-Pulp Process for Nickel Laterites and Sulfides", Internat'l Sympsm. on Hydrometallurgy, Chicago 1973, Evans and Shoemaker eds., New York, AIME 63-91(1973).
14. Drolet, J. P., "Deep Seabed Mining--A Canadian Perspective in Relation to the Nickel Industry", CIM Bull, Jan 113(1979).
15. Agarwal, J. C., N. Beecher, D. S. Davis, G. L. Hubred, V. K. Kakaria, and R. N. Kust, "Processing of Ocean Nodules: A Technical and Economic Review", J. of Metals, 28, April 24-31(1976).
16. Agarwal, J. C., et.al., "Kennecott Process for Recovery of Copper, Nickel, Cobalt and Molybdenum from Ocean Nodules", presented AIME Annual Meeting at Denver 1978, reprint 78-B-89.
17. Hubred, G., "Deep-Sea Manganese Nodules: A Review of the Literature", Mineral Science Eng., 7, No. 1, Jan., 71(1975).
18. Han, K. N. and D. W. Fuerstenau, "Kinetics of the Extraction of Metal from Deep Sea Manganese Nodules", Met. Trans/AIME, 7B, 679-692(1976).
19. "Nicaro Expands Nickel Capacity", EM/J, 158, No. 9, 82(1957).
20. Mero, J. L., The Mineral Resources of the Sea, Amsterdam, Elsevier, 1965.
21. Agarwal, J. C., et.al., "A New Fix on Metal Recovery from Sea Nodules", EM/J, Dec. 74(1976).
22. Kovac-Figueroa, C., "Morenci Tailing Leaching Plant", Trans. SME/AIME, 260, 170(1970).
23. Holmes, J. A., A. D. Deuchar, H. N. Stewart and J. D. Parker, "Design Construction and Commissioning of the Nchanga Tailings Leach Plant", Extractive Metallurgy of Copper, Vol. II, J. C. Yannopoulos and J. C. Agarwal ed., TMS/AIME, New York, 907(1976).

24. Power, K. L., "Operation of the First Commercial Copper Liquid Ion Exchange and Electrowinning Plant", Copper Metallurgy.
25. Power, K. L., "Copper Dump Leaching at Asarco's Silver Bell Unit, Arizona", Unit Processes in Hydrometallurgy, M. E. Wadsworth and F. T. Davis ed., AIME, Gordon and Breach Science, N.Y. 806-823 (1964).
26. They, L., "Forty Years of Progress in the Hydrometallurgy and Electrowinning of Copper--The Experience of Union Minière," CIM Bull., 63, 339-351 (1970).
27. Hopkin, W. R. and A. J. Lynch, "Anamax Oxide Plant: A New U.S. Dimension in Solvent Extraction," EM/J., Feb. 56(1977).
28. Sheffer, H. W. and L. G. Evans, "Copper Leaching Practices in the Western United States", USBM, IC 8341.
29. Fletcher, J. B., "In-Place Leaching at Miami Mine, Miami, Arizona", Trans. SME/AIME, 250, No. 4., Dec. 310-316(1971).
30. "Rancher's Big Blast Shatters Copper Ore Body for In-Situ Leaching", EM/J, 173, No. 4, 98-100(1972).
31. "Ranchers Development Sets off Blast: Will Leach at Big Mike", Mining Engineering, 25, No. 8, 10(1973).
32. Catanach, C. B., "Developments and In-Place Leaching of Mountain City Chalcocite Ore Body", Extractive Metallurgy of Copper, Vo. V, J.C. Yannopoulos and J. C. Agarwal ed., TMS/AIME, 849-872(1976).
33. Rampacek, C., and J. T. Dunham, "Copper Ore Processing--U.S. Practices and Trends", Mining Congress Journal, Feb. 40(1976).
34. Huttle, J. R., "Anaconda Adds 5000-tpd Concentrator to Yerington Enterprise at Weed Heights", EM/J, 165, No. 3, 74-81(1962).
35. Biswas, A. K. and W. G. Davenport, Extractive Metallurgy of Copper, Pergamon International Library, Chap. 13(1976).
36. "ASARCO's New Cu Leach-Precipitate Plant for San Xavier North Pit Ore", World Mining, Oct., 46 (1973).

LEARNING ACTIVITY 5

5.4 Leaching of Sulfides

Learning Activity Objective

After completing your study of this learning activity material you should be able to discuss the thermodynamic and kinetic aspects of sulfide mineral leaching; and be able to describe, in general terms, the leaching processes for nickel and cobalt sulfide minerals.

5.4.1 Introduction

Leaching of sulfide minerals received considerable attention during the past 20 years, e.g., leaching of flotation concentrates and leaching of mine waste dumps. A great deal of research has been conducted in sulfide leaching and several sophisticated processes have been developed and used for commercial recovery of metal values. The most cited reason for the intense interest in sulfide leaching is, perhaps, the comparative absence of pollution, especially air pollution.

One of the factors of concern in the leaching of sulfides is the kinetic aspects of the reaction. Most metal oxides are readily dissolved in acid, but dissolution of sulfide minerals in acids is usually slow. As a result, most of the sulfide leaching processes have to be conducted under elevated temperatures and pressures.

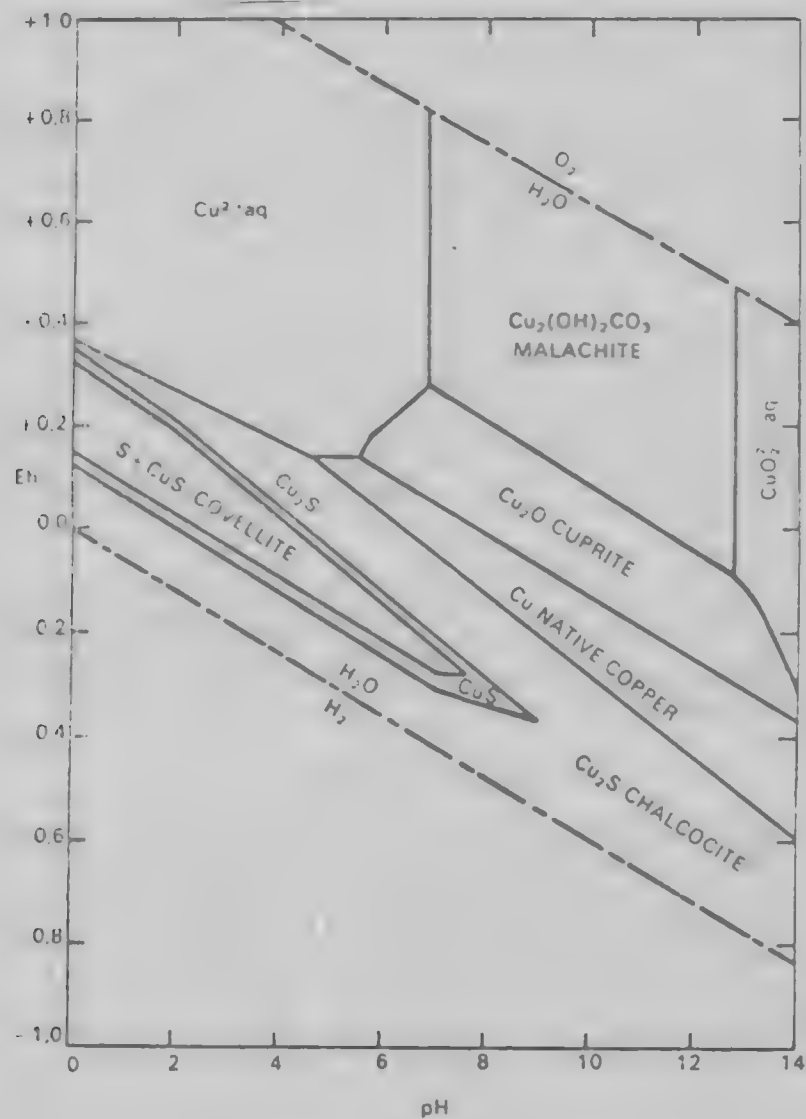
5.4.1.1 Thermodynamics

The thermodynamic relationship of various sulfides in an aqueous environment is best illustrated by use of Pourbaix diagrams (see Module 1). The $\text{Cu-H}_2\text{O-O}_2\text{-S-CO}_2$ system is presented in figure 5.5.1. In acid media, oxidizing potentials between 0.2 and 0.4 volts are required to dissolve the copper sulfides into sulfur species and soluble copper. In alkaline solution, in which insoluble copper oxide products form, the dissolution requires not only an oxidizing agent, but also a complexing agent to stabilize the dissolved copper. Although the Eh-pH diagram for each sulfide assemblage is unique, it can be generally stated that most of the sulfides require a fairly strong oxidizing potential to effect their dissolution. In addition, they require a strong complexing agent when dissolved in alkaline media.

The Eh-pH diagram for Fe-H₂O system at 25° is presented in figure 5.5.2. The potential for the $\text{Fe}^{3+}/\text{Fe}^{2+}$ couple is approximately 0.8 volts. All sulfide minerals exhibiting half cell potentials less than the $\text{Fe}^{3+}/\text{Fe}^{2+}$ couple are favored to react anodically, i.e., they dissolve in the presence of the ferric ion. For example, from the thermodynamic point of view, the ferric ion is important in the dissolution of chalcocite. This is indicated by the following calculation. All solution species are assumed to have unit activity.

Cathodic reaction,

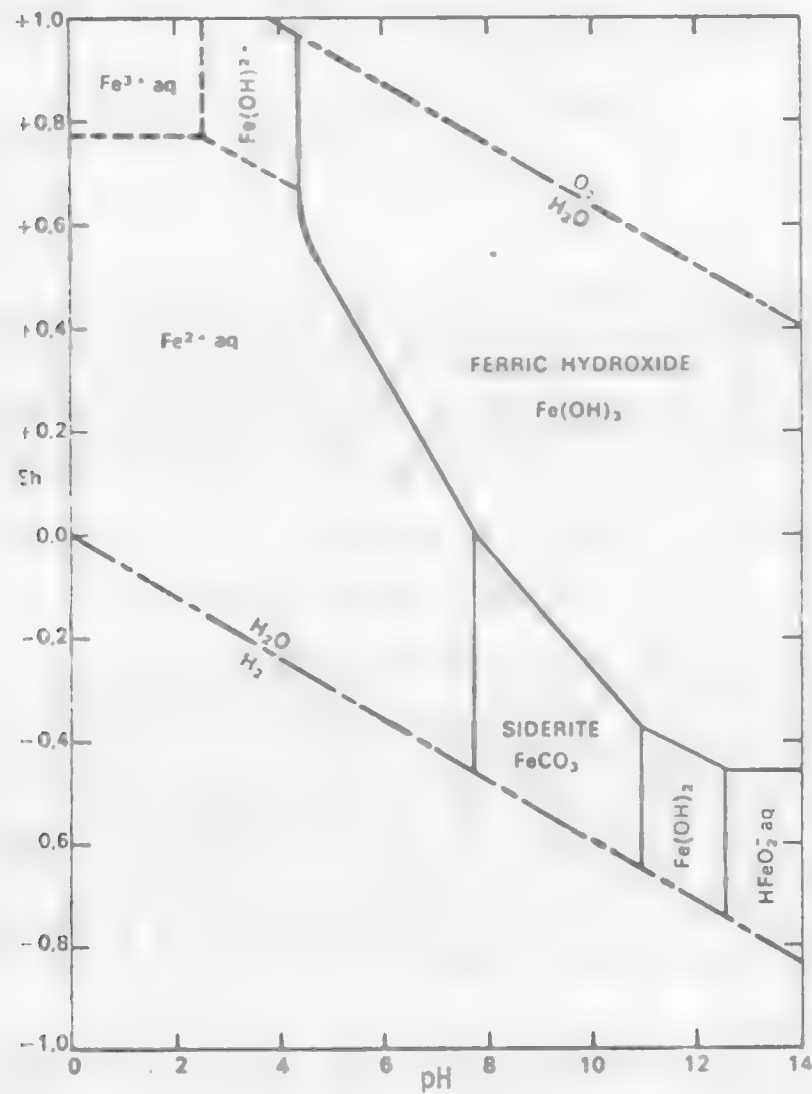


Figure 5.5.1 Eh-pH Diagram for the Cu-H₂O-O₂-S-CO₂ System.

Concentration of dissolved species is 10^{-6} ; P_{CO_2} is $10^{-3.5}$ atm and total dissolved sulphur species is 10^{-1} M; temperature 25°C; pressure 1 atm.

Source: Garrels, R. M. and C. L. Christ⁽¹⁾

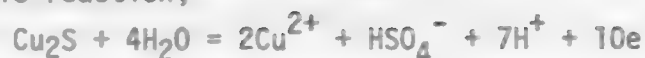
Figure 5.5.2 Eh-pH Diagram Showing the Relationship Among Metastable Iron Hydroxide Species and Siderite at 25°C and 1 atm Total Pressure.



Concentration of dissolved species 10^{-6} M.

Source: Garrel, R. M. and C. L. Christ.⁽¹⁾

Anodic reaction,



$$E_0 = -0.427 \text{ volts} \quad [5.5.2]$$

Overall reaction,



$$\Delta E = 0.344 \text{ volts} \quad [5.5.3]$$

$$\Delta G = -79.33 \text{ kcal}$$

The negative standard free energy (-79.33 kcal) indicates the reaction is thermodynamically favorable. The Eh-pH diagram indicates that the stability region for the ferric ion is limited to a pH < 3. It is, therefore, necessary to perform the leach process in a strong acidic environment when ferric ion is used as an oxidizing agent. Note in figures 5.5.1 and 5.5.2 the benefit of using oxygen gas as the oxidant, i.e., for the O₂/H₂O couple,



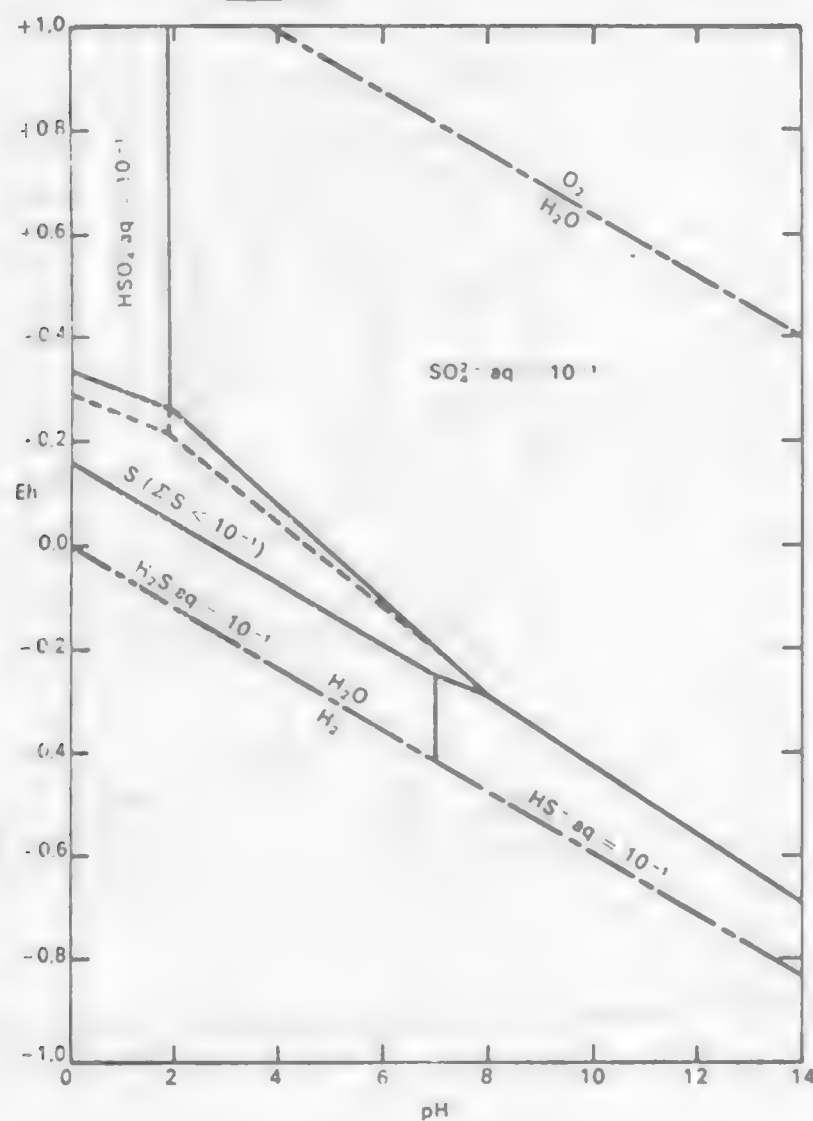
$$E = 1.228 - 0.059/\text{pH} + 0.0147 \log P_{\text{O}_2} \quad [5.5.5]$$

A standard equilibrium potential of about 1.23 volts will be able to dissolve most sulfide minerals. In addition, oxygen can be used in an alkaline media. The Eh-pH diagram for sulfur at 25°C is presented in figure 5.5.3. In an alkaline solution only the sulfate ion is stable in water. In acidic solution, however, elemental sulfur is stable under neutral or slightly oxidizing environments. For oxidizing potential greater than about +0.3 v. elemental sulfur becomes unstable with respect to sulfate or bisulfate formation, depending on the pH of the solution. It is expected from thermodynamic consideration that when a metal sulfide is oxidized in acidic media, the elemental sulfur will only be an intermediate species, i.e., the stable species are soluble metal ions and bisulfate or sulfate ions.

Pourbaix diagrams have several limitations when applied to hydrometallurgy. For example, metal ions shown in the diagrams are usually presented as simple hydrated ions. For alkaline or alkaline earth metals (Na⁺, K⁺, Mg²⁺, etc.) this assumption is usually valid. But for transition metal ions, (Cu²⁺, Fe³⁺, Fe²⁺, Ni²⁺, etc.) stable complex ions tend to form with anions (SO₄²⁻, Cl⁻, etc.) or polar ions (NH₃, H₂O, etc.). And the concentration of simple ions may exist in only a very small concentration. Figure 5.5.4, for example, shows the equilibrium ion species existing in a solution containing 0.1 M Fe³⁺ and 0.5 M total sulfate. The diagram indicates that the predominant ionic species in acid solutions are FeSO₄⁺ and Fe(SO₄)₂⁻. The simple hydrated ferric ion occurs only at the lowest pH values.

Pourbaix diagrams are equilibrium diagrams derived from thermodynamic relationships. They, therefore, have the same limitations in their application. e.g., metastable species may form rather than true equilibrium species. Nor do the diagrams provide information about reaction rates. An example of this is

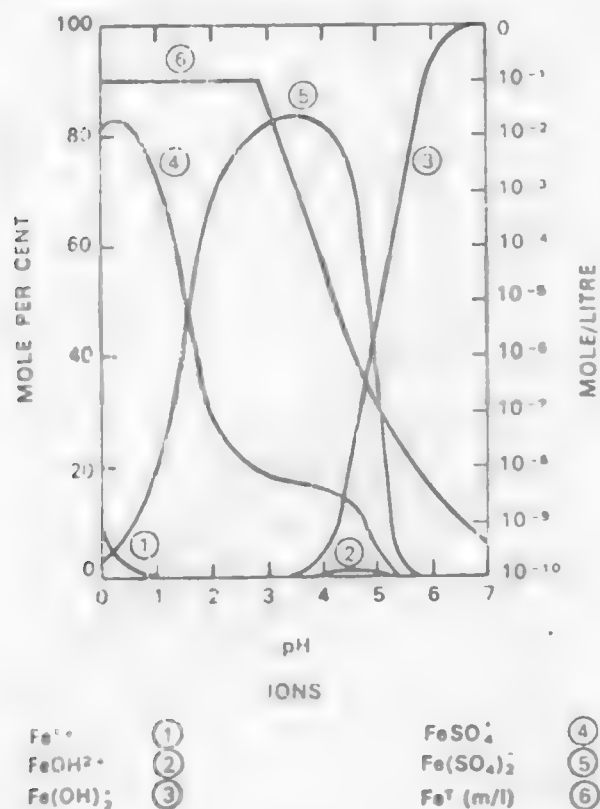
Figure 5.5.3 Eh-pH Diagram for the S-H₂O System at 25°C and 1 atm Total Pressure.



Concentration of dissolved sulphur is 10^{-1} M.

Source: Garrel, R. M. and C. L. Christ.⁽¹⁾

Figure 5.5.4 Equilibrium Iron Species Existing in a Solution Containing 0.1 M Fe^{3+} and 0.5 M Total Sulphate at 25°C.



Source: Bhappu, R. B., Trans. Soc. Mnt. Engre., AIME, V. 244, 1969.⁽²⁾

shown in equations [5.5.6] and [5.5.7]. In the presence of ferric ions chalcocite is thermodynamically favored to dissolve to form Cu^{2+} and HSO_4^- .



$$\Delta G^\circ = -79.32 \text{ kcal}$$

However, a kinetic study⁽⁴⁾ shows that the reaction actually results in covellite at room temperature.



Note, therefore, that one cannot use the magnitude of the free energy to predict whether a reaction will occur or not, i.e., both reactions [5.5.3] and [5.5.4] are thermodynamically possible. The one that occurs depends on kinetic factors and cannot be predicted from thermodynamics.

At high temperature CuS becomes unstable and the dissolution continues to form Cu^{2+} . According to thermodynamics, the favored reaction will be



$$\Delta G^\circ = -68.11^{(5)}$$

The large negative free energy is due to the formation of bisulfate ion. In acidic media it is known, however, that the dissolution of sulfide minerals often produces elemental sulfur and very little bisulfate and sulfate. The leaching reaction that actually occurs is better represented as



This experimental kinetic study⁽⁵⁾ showed that the relative reaction rate of oxidation of elemental sulfur to sulfate or bisulfate is slow at low temperature and elemental sulfur remains as a metastable intermediate specie. The formation of metastable species in hydrometallurgical system is of practical importance since the apparent final product may be metastable, as in the cases of sulfur and covellite, and not the species that are predicted from thermodynamic calculations.

5.4.1.2 Kinetics

As stated previously, thermodynamics predict the possibility of a reaction, but whether or not the reaction does, in fact, proceed is determined by kinetic factors. Leaching reactions are heterogeneous in nature, the rate of a reaction may be either limited by a chemical reaction or controlled by a transport process. For transport control, the effect of temperature is small, activation energies being 5 kcal/mole or less. If controlled by the chemical reaction, the rate of reaction increases rapidly with temperature, having activation energy usually greater than 10 kcal/mole. The chemical reaction involved in the leaching of a sulfide can be a combination of several reactions, e.g., adsorption, heterogeneous reaction, and electrochemical redox reaction, etc. In general, leaching processes involve the following steps:

- (1) dissolution of gaseous reactants;
- (2) transport in liquid phase;
- (3) transport in solid phase; and
- (4) reaction at solid/liquid or solid/solid interfaces.

Pressurized systems are used to increase the solubility of gaseous reactants and to increase the temperature of the system above the normal boiling point of the solution. Good agitation increases the gas dissolution rate by increasing the surface area. It also increases the rate of mass transport within the liquid phase. High temperatures increase the rate of all the steps, especially chemical reactions.

Unlike oxide minerals, most sulfides are semiconductors and their electrical resistivities are sufficiently low (shown in Table 5.5.1)^(3,5) to allow the electron to move relatively freely within the solid. This semi-conducting property may be due to the nature of the sulfide molecular structure or due to the non-stoichiometry between the metal and sulfur elements⁽⁶⁾. This, then, leads us to study the leaching of electron conducting sulfides in hydrometallurgy by directly applying the electrochemical concepts that have been developed in the field of metal corrosion, e.g., polarization measurements, kinetics of corrosion and metal deposition. These techniques are directly applicable to the field of sulfide leaching.

Table 5.5.1 Electronic and Structural Properties of Selected Sulfide Minerals.

Sulfide	Name	Resistivity, Ohm-m	Usual Conductor Type
Cu ₅ FeS ₄	Bornite	10 ⁻³ -10 ⁻⁵	p-type
Cu ₂ S	Chalcocite	4.2x10 ⁻² -8x10 ⁻⁵	p-type
CuFeS ₂	Chalcopyrite	0.2x10 ⁻³ -9x10 ⁻³	n-type
CuS	Covellite	0.8x10 ⁻³ -7x10 ⁻⁷	metallic
PbS	Galena	1x10 ⁻⁵ -6.8x10 ⁻⁵	n-type & p-type
MoS ₂	Molybdenite	7.5-8x10 ⁻³	n-type & p-type
(Fe,Ni) ₉ S ₈	Pentlandite	1-11x10 ⁻⁶	n-type & p-type
FeS ₂	Pyrite	3x10 ⁻² -1.2x10 ⁻⁴	n-type & p-type
ZnS	Sphalerite	2.7x10 ⁻³ -1.2x10 ⁻⁴	n-type
S	Sulfur	2x10 ¹⁵	insulator

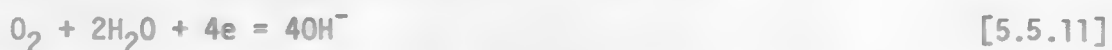
Several sulfide leaching systems have been found to be controlled by electrochemical reactions, and an electrode kinetic model has been used successfully to interpret the rate data and to propose the reaction mechanisms.⁽⁷⁻⁹⁾ Polarization studies on several sulfide minerals have also demonstrated the electrochemical nature of sulfide leaching.⁽¹⁰⁻¹³⁾

As in corrosion processes, two types of redox couples may be operative. One type is a corrosion couple and involves only a single phase. The single phase contains both anodic and cathodic regions on the same surface. Ammonia

and oxygen leaching of chalcopyrite is an example of a corrosion couple, shown in figure 5.5.5.(7) Part of the chalcopyrite surface serves as anodic sites where oxidation occurs,

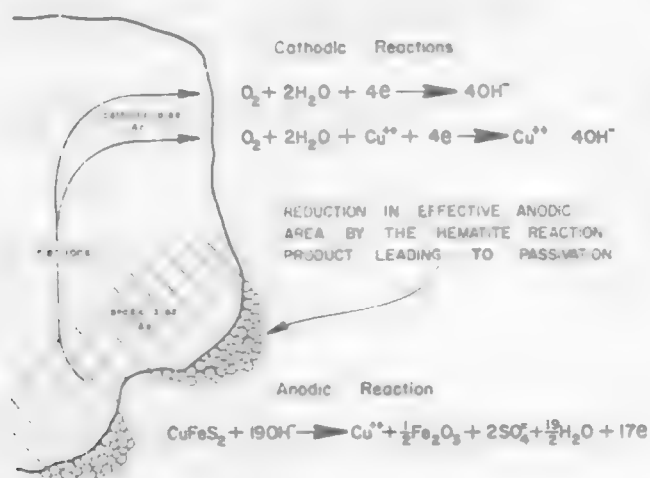


and other parts of the surface serves as cathodic sites where the reduction of oxygen occurs,



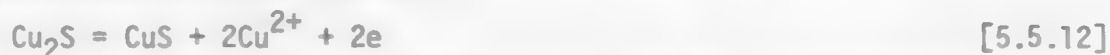
Each part of the chalcopyrite surface can be cathodic or anodic alternatively but not simultaneously. The electrons can transform an area from anodic to cathodic by traveling through the solid chalcopyrite.

Figure 5.5.5 Schematic Representation of the Electrochemical Reaction and the Reduction of the Anodic Area by the Hematite Reaction Product.



Source: Beckstead, L.W. and J. O. Miller, Met. Trans. 13, 8B, 1977.

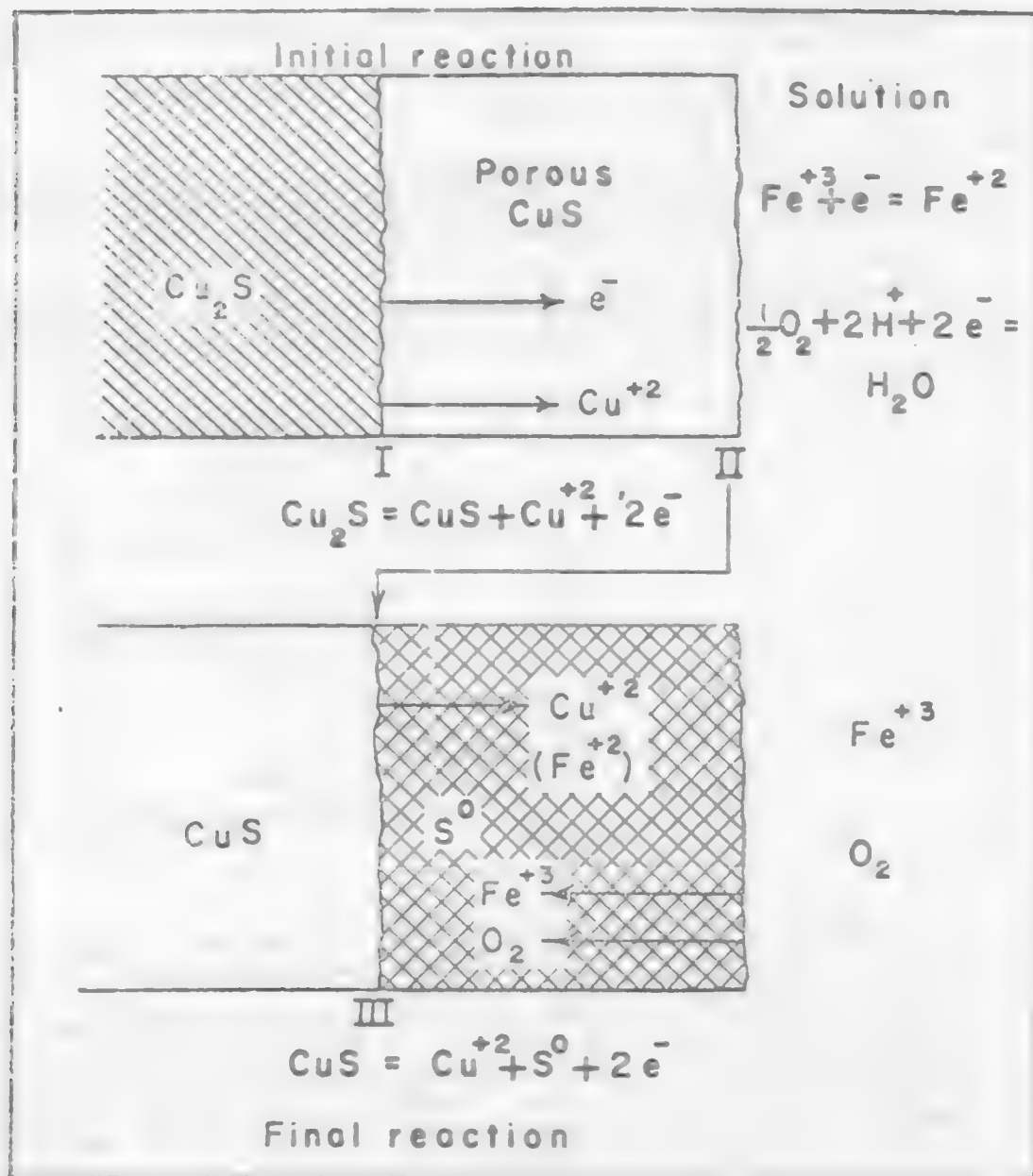
A second type of redox couple is a galvanic couple where two or more solid phases are involved. The cathodic and the anodic reactions occur on their own separate surface. The two surfaces must be in electrical contact by an electrolyte or by a conducting solid. Leaching of chalcocite to covellite is an example. This is shown schematically in figure 5.5.6. The reaction results in the formation of a CuS surface layer on the Cu₂S. The anodic reaction takes place on the Cu₂S/CuS solid interface,



and the coupled cathodic reaction, takes place at the CuS/water interface depending on the type of oxidant used,



Figure 5.5.6 Surface Layers Formed During the Anodic Dissolution of Chalcocite (Cu_2S) and Covellite (CuS).



Source: R. B. Bhappu, et.al., "Theoretical and Practical Studies on Dump Leaching", Trans, SME/AIME, 244, 307-320.



The overall reaction proceeds as the electrons transfer and the Cu^{2+} ions diffuse from the anodic area through the CuS layer to the cathodic area.

Other important concepts involved in the kinetics of sulfide leaching are summarized below:

1. Elemental sulfur that normally forms on the surface of sulfides during the leaching is a nonconductor. This results in a marked retardation of the rate of the reaction, especially for the formation of a non-porous sulfur product.
2. Increases in temperature and pressure in a leaching system are normally made for kinetic purposes rather than thermodynamic reasons. For instance, increasing the oxygen pressure from 1 atm to 10 atm may result in increasing the rate 10 times if the rate is first order with respect to the oxygen pressure. But from a thermodynamic point of view, the temperature increase will only change the oxidizing potential by 0.0147 volts.

Several excellent review and discussion papers on leaching of sulfide are listed below:

1. M. E. Wadsworth, "Advances in the Leaching of Sulfide Minerals", Min. Sci. Eng., vol. 4, no. 4, Oct. 36(1972).
2. M. E. Wadsworth, "Physical Chemistry of Hydrometallurgy Electrochemical Processes", The Darken Conference.
3. R. Derry, "Pressure Hydrometallurgy: A Review", Min. Sci. Eng., vol. 4, no. 3, 3(1972).
4. R. J. Roman and R. B. Benner, "The Dissolution of Copper Concentrates", Min. Sci. Eng., vol. 5, no. 1, Jan. 3(1973).
5. J. E. Dutrizac and R. J. C. MacDonald, "Ferric Ion As A Leaching Medium", Min. Sci. Eng., vol. 6, no. 2, Apr. (1974).
6. E. Peters and H. Veltman, "Theory of Leaching", Hydrometallurgy, First Tutorial Symposium on Hydrometallurgy, 1972.
7. R. E. Doan, "The Treatment of Metal Sulfide Concentrates by Pressure Hydrometallurgy", Colo. Sch. Mines Resch. Inst. Bull., vol. 15, no. 6, Nov. 1972.
8. J. T. Woodcock, "Some Aspects of the Oxidation of Sulfide Minerals in Aqueous Suspension", Proc. Australs. Inst. Mining and Met., no. 198, 47-84(1961).
9. J. C. Paynter, "A Review of Copper Hydrometallurgy", J. of South Africa IMM, Nov., 158(1973).
10. M. E. Wadsworth, "Metallurgical Process: Hydrometallurgy", Annual Review, J. of Metals, March, 4(1976).
11. M. E. Wadsworth, "Metallurgical Process: Hydrometallurgy", Annual Review, J. of Metals, March, 8(1977).
12. M. E. Wadsworth, "Metallurgical Process: Hydrometallurgy", Annual Review, J. of Metals, April, 32(1978).
13. M. E. Wadsworth, "Metallurgical Process: Hydrometallurgy", Annual Review, J. of Metals, April (1979).
14. M. E. Wadsworth, "Metallurgical Process: Hydrometallurgy", Annual Review, J. Of Metals, April (1980).

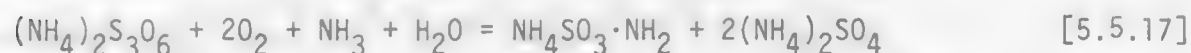
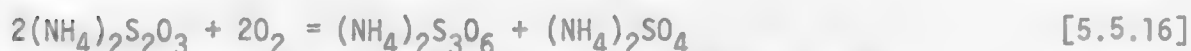
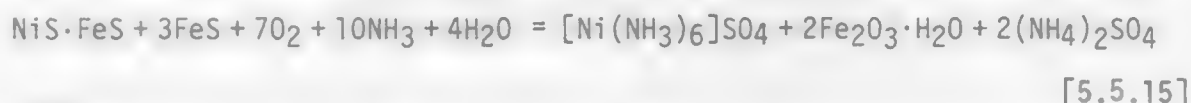
5.4.2 Leaching of Nickel and Cobalt Sulfide Minerals.

Over the last 25 years pressure hydrometallurgical techniques have been increasingly applied in commercial processes to recover nickel, cobalt and copper from Ni-Co concentrates and Ni-Cu mattes. The processes usually consist of leaching, solution purification and metal recovery. The leach process is normally conducted in an ammonia solution or in a dilute sulfuric acid solution at elevated temperatures and pressures. Air is usually the oxidizing agent.

5.4.2.1 Ammonia Oxidation Leaching of Ni-Co Sulfide.

The most widely publicized method for the leaching of Ni-Co sulfide minerals is the use of ammoniacal solutions. Ammonia oxidation pressure leaching of nickel sulfide concentrates combined with hydrogen pressure reduction of the purified leach solution was developed by Sherritt Gordon Ltd. and has been used in operations at Saskatchewan, Alberta since 1954.⁽¹⁵⁾ More recently the same process has been adopted for the treatment of sulfide concentrate at Kwinana in Western Australia.⁽¹⁶⁾ A simplified flowsheet of the process is presented in figure 5.5.7, and a brief description is as follows.

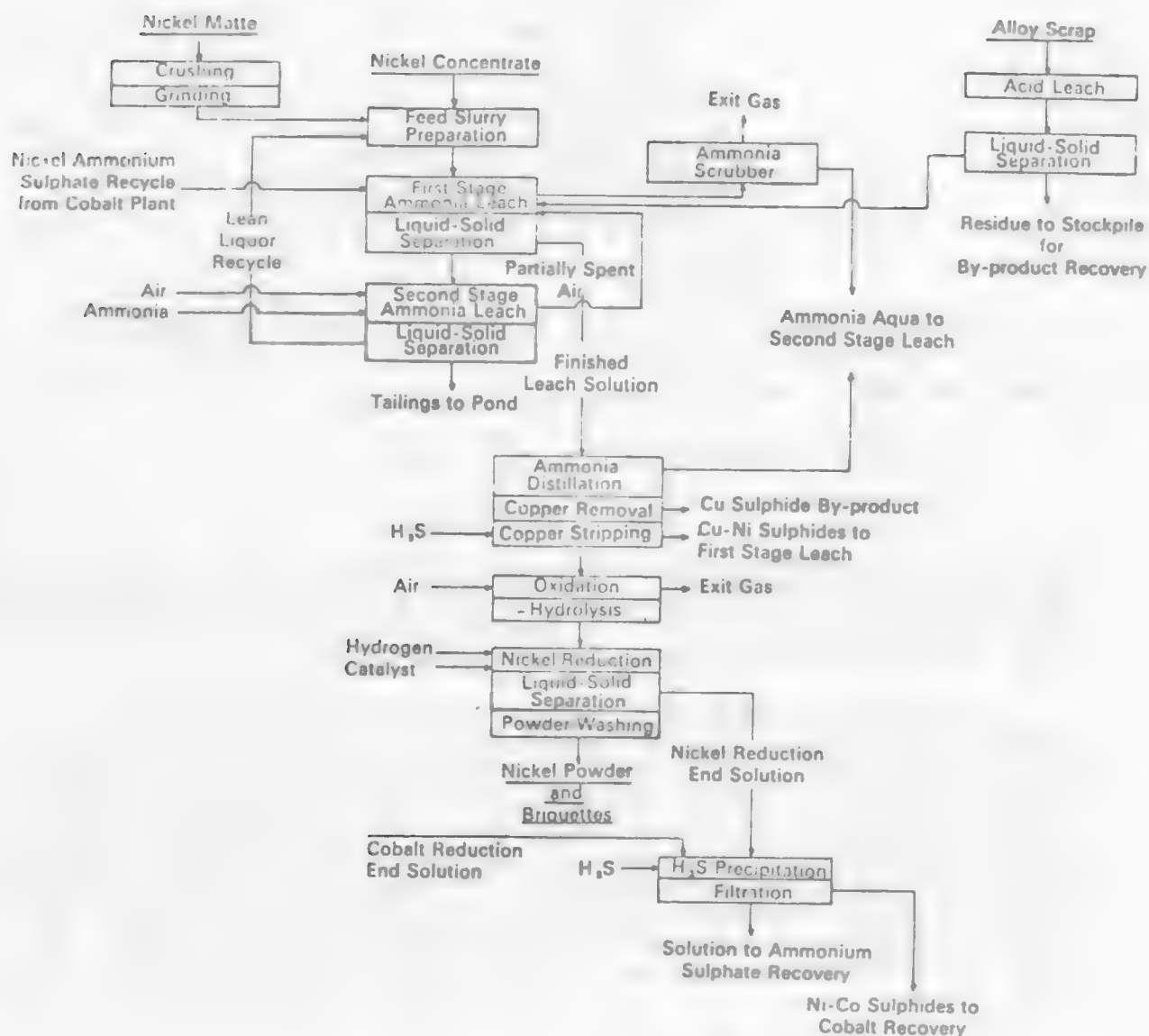
Finely ground nickel sulfide concentrates, containing significant amounts of copper and cobalt, are leached in autoclaves with ammoniacal solutions of ammonium sulfate. Air is the oxidizing agent. The temperature and pressure (air) used in the first stage is 94°C, 165 psig, and in the second stage is 80°C and 128 psig. Total retention time is about 8-1/2 hours. The primary reactions during the leaching are:



Nickel, cobalt and copper are solubilized as ammine complexes, iron is hydrolyzed to an insoluble hydrated iron oxide, and pyrite does not react (it remains in the leach residue). Sulfur passes through a series of oxidation reactions, e.g., thiosulfate, polythionate and then partially to sulfamate and sulfate. A shrinking core model has been proposed for the leaching reaction (figure 5.5.8), i.e., an unreacted sulfide core is surrounded by an iron oxide envelope through which (in the case of pentlandite, NiS·FeS, for example) the nickel and sulfur ions diffuse outward to react with oxygen at the liquid-solid interface, while the oxygen diffuses inward, possibly by a mechanism associated with vacancies in the oxide lattice. The reaction rates have been demonstrated to be influenced by temperature, oxygen pressure, concentration of reactants in the solution, agitation of the pulp, and particle size.

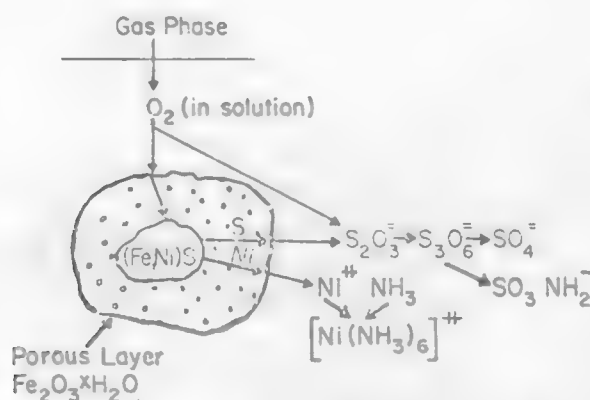
Following a solid-liquid separation, the first step of solution purification is atmospheric pressure distillation of excess ammonia, which is recycled. During the distillation the unsaturated sulfur compounds in the leach liquor

Figure 5.5.7 Sherrit Gordon Mines, Ltd., Simplified Nickel Refinery Flow Diagram.



Source: Advances in Extractive Metallurgy, 1967, I.M.M.

Figure 5.5.8 Diagrammatic Representation of Leaching a Sulphide Particle.



Source: Forward, F. A. and V. N. Mackiw, J. Met., 7, 1955.⁽¹⁵⁾

react with copper, which precipitates as a sulfide,



The remaining copper is later stripped by hydrogen sulfide pressure precipitation. The second step in the solution purification is to remove the remaining unsaturated sulfur compounds by oxidizing them to sulfate. This is accomplished at 250°C and 600 psig air pressure in about a half hour.

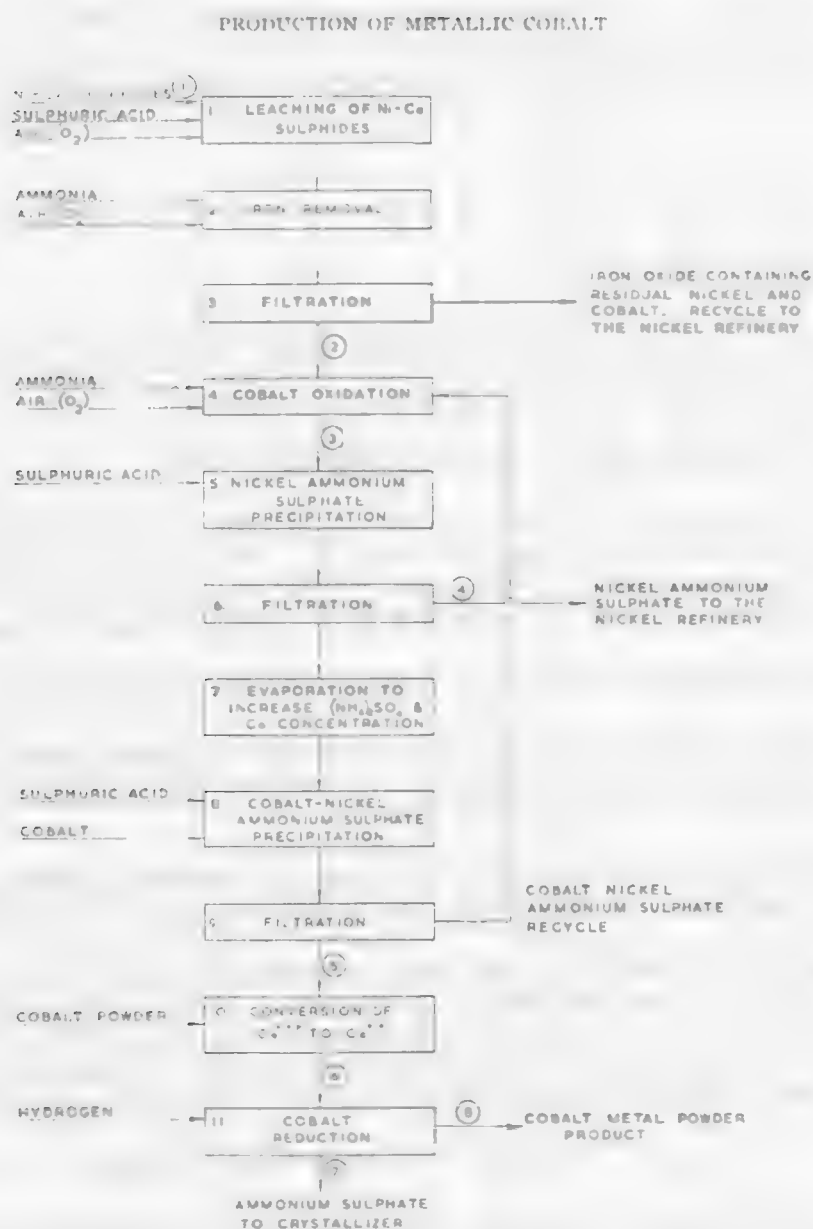
The purified solution from the purification steps contain about 45 g/l nickel, 1 g/l cobalt, 350 g/l ammonium sulfate, and 28 g/l (free) NH₃. This solution is heated at 175 to 200°C in hydrogen at 500 psig. The hydrogen reduction process is carried out batchwise. First, a nucleation reaction is performed to produce very fine nickel seed. This is followed by 40 to 50 nickel reduction batch treatments to build up the nickel particle size before the product nickel powder is discharged. In the successive batch reduction treatments (densification), nickel builds up on the seed particles. The nickel in solution is reduced preferentially with respect to cobalt. The reduction is continued until the nickel concentration has decreased to about 1 g/l.

The solution from the Ni reduction reactor contains about 1 g/l nickel and the same amount of cobalt. Hydrogen sulfide is used to precipitate these metals as mixed Ni-Co sulfides. Cobalt is recovered from the sulfide mixture by a sulfuric acid leach. Acid is used rather than ammonia because the leach rate in acid is faster and better cobalt extraction results.⁽¹⁷⁾

5.4.2.2 Acid Leaching of Nickel and Cobalt Sulfides⁽¹⁷⁾

The Fort Saskatchewan acid process for the recovery of pure metallic cobalt from a mixed nickel-cobalt sulfide consists of the following operations (figure 5.5.9): (1) Leaching of the mixed sulfides, (2) Iron removal,

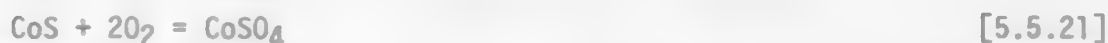
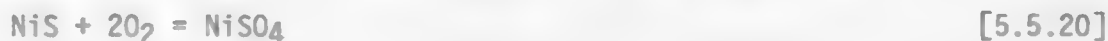
Figure 5.5.9 Cobalt Recovery. Soluble Cobaltic Ammine Process Flowsheet.



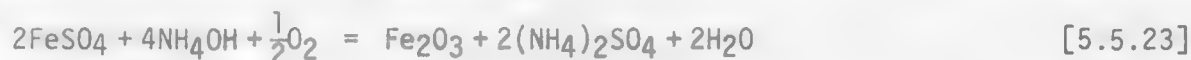
Source: V. N. Mackiw and T. W. Benz, "Application of Pressure Hydrometallurgy to the Production of Metallic Cobalt", Extractive Metallurgy of Copper, Nickel, and Cobalt.

(3) Oxidation of the cobaltous ion to cobaltic ammine complex, (4) Separation of nickel and cobalt by precipitation of nickel ammonium sulfate, (5) Conversion of the cobaltic ammine in the solution to the cobaltous form, and (6) Cobalt recovery.

Acid pressure leaching of nickel and cobalt sulfides is conducted in an autoclave using dilute sulfuric acid (pH 1.5 to 2.5) under 100 psig air pressure at about 120°C. A retention time of 2 to 3 hours is sufficient to dissolve 98% of metal values. The overall leaching reactions are as follows:



Iron in the solution is subsequently treated with ammonia and air at atmospheric pressure to raise the pH to 4.5 and to oxidize the ferrous ions to ferric ions, which then precipitate as hematite.



The purified leach liquor is then prepared for nickel-cobalt separation using the soluble cobaltic ammine process. First, the solution is made strongly ammoniacal and subjected to pressure oxidation using air at 100 psig at about 70°C. Cobaltous sulfate is oxidized to a cobaltic ammine complex,



and the nickel remains unoxidized as a nickelous ammine complex. The nickel can be removed as a nickel ammonium sulfate precipitate by acidifying the solution with sulfuric acid (pH=2.6).

The solution is then treated with cobalt powder to reduce the cobaltic pentammine complex to a cobaltous ammine complex prior to hydrogen reduction.

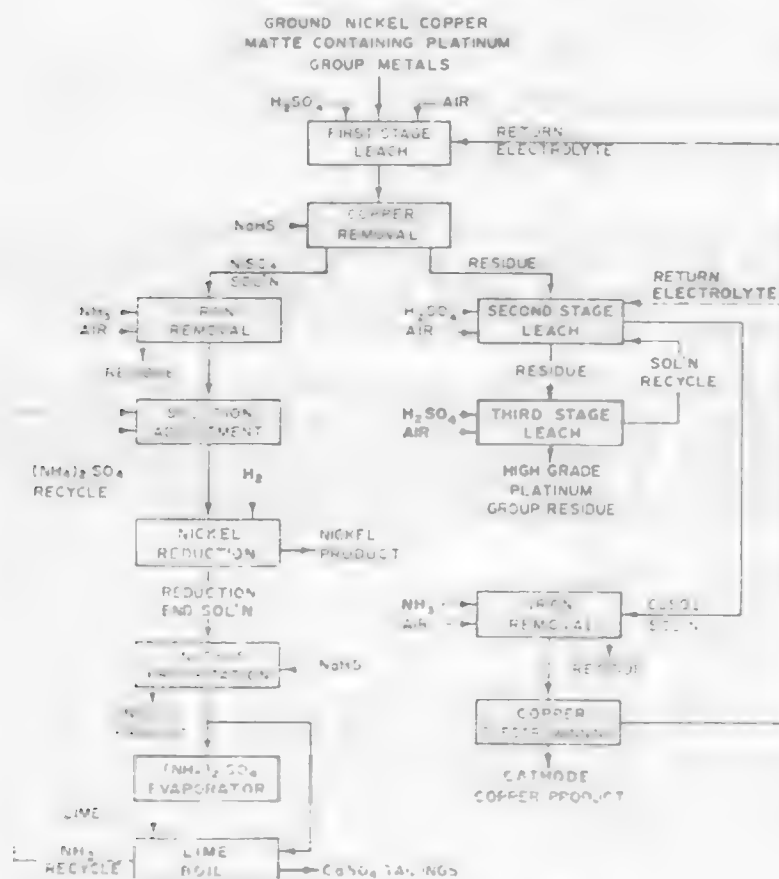
Sulfuric acid leaching was used commercially by Calea Mining Company in Garfield, Utah to process cobalt concentrate,⁽¹⁸⁾ and by National Lead Company at their plant at Fredericktown, Missouri for the recovery of nickel, cobalt, and copper. It is used by INCo at their Coppercliff, Canada plant to recover nickel, cobalt, copper, and elemental sulfur from carboxylation residues.⁽¹⁹⁾

5.4.2.3 Leaching of Copper-Nickel Matte.

Pressure leaching in either sulfuric acid or ammoniacal solution can be used to recover nickel and copper from Ni-Cu matte.^(15,20-22) Currently some companies in South Africa are using a sulfuric acid leach method to recover Cu and Ni from their matte. The matte is a copper nickel sulfide mixture in which platinum and other precious metals are components of major economic value.

A simplified flow sheet to recover nickel and copper from the matte at Impala Platinum⁽²¹⁾ is presented in figure 5.5.10. The process involves a separation leach, i.e., copper and nickel are extracted and the precious metals are left in the residue.

Figure 5.5.10 Simplified Flow Sheet. Recovery of Nickel and Copper from High-Grade Matte.



Source: Plasket, R. and S. Romanchuk, Hydromet., 3, 1978.

Copper is recovered by electrowinning and nickel is recovered by hydrogen reduction. Ammonium sulfate and ammonia are regenerated and recycled.

The leaching sequence involves three stages in series. The first stage yields 80% nickel extraction and a solution low in copper. The second stage leach removes substantially all of the copper and residual nickel value. The third stage leach extracts the remaining small amount of nickel, copper and iron.

In the first stage leach, the ground matte is leached with spent electrolyte containing 80-100 g/l H_2SO_4 and 18-22 g/l Cu. The operation is conducted in an autoclave at 135 psig oxygen pressure and 130-140°C. The reactions involved in this stage are:

(1) Copper cementation by matte



[5.5.25]

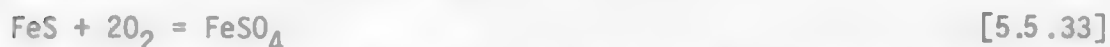
(2) Metal dissolution by H_2SO_4 and Oxygen

(3) Copper replacement by nickel in the leach solution



After a 3 hour retention time, the discharged solution contains 100-110 g/l of nickel, and <10 g/l of copper. The solution is further purified by the addition of NaHS to reduce the excess copper to <0.005 g/l Cu. Nickel metal is then recovered by hydrogen reduction from the purified solution.

The objective of the second stage leach is to extract as much of the soluble Ni, Cu and Co metal values as possible from the first stage leach residue. The process is conducted in an autoclave at 275°F and 20 psig of oxygen pressure. The solution contains a sufficient amount of sulfuric acid for reaction. The reactions occurring during this stage are shown below:



After a 4 hour retention time, a total of 39.9% of the nickel, 99.0% of the cobalt, 98.0% of the copper and 93.0% of the iron from the matte are extracted. At this stage the solution contains about 75 g/l copper, 25 g/l nickel, 2 g/l iron. Iron content is then reduced from 2 g/l to 1 g/l by the addition of ammonia, prior to the recovery of copper by electrowinning.

The solid residue is then subjected to a third stage pressure leach to extract essentially all the remaining nickel, cobalt, copper and iron. The final leach residue is obtained, and fed to the platinum refinery for recovery of the platinum group of metals.

A similar type of acid pressure leach operation for Cu-Ni mattes is operating at Port Nickel Refinery in Braithwaite, Louisiana,⁽²²⁾ and at Spring, Transvaal, South Africa.⁽²⁰⁾

LEARNING ACTIVITY 6

5.4.3 Leaching of Copper Sulfides--Fundamental Studies.

Learning Activity Objective

After completing your study of this learning activity material you should be able to describe the types of leach systems that have been applied to leaching copper sulfides, and be able to list the advantages and disadvantages of each leach system.

Extensive research has been performed on the leaching of copper concentrates in an attempt to provide alternative processes for conventional smelting and refining. Part of the reason is undoubtedly the concern for sulfur oxide emissions, since a typical copper concentrate contains 20-30% sulfur by weight. Roast-leach processes can be used to produce copper while recovering the sulfur dioxide off gas as sulfuric acid. However, if sulfuric acid cannot be marketed, then other approaches must be considered, e.g. leaching processes to produce elemental sulfur, or jarosite type compounds which can be disposed of in an environmentally safe manner.

Some of the important developments in copper sulfide concentrate leaching will be discussed in the following section.

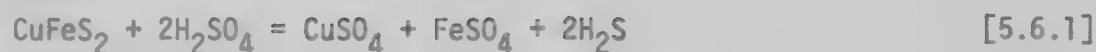
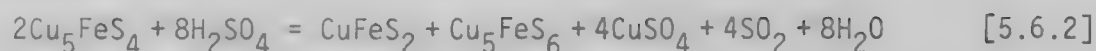
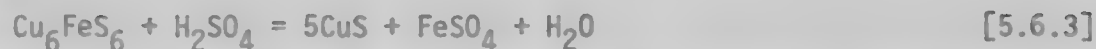
5.4.3.1 Sulfuric Acid Leach.

Sulfuric acid, in combination with various oxidizing agents, has received a great deal of attention for leaching copper sulfides. The process offers several advantages, i.e., low capital cost, acid availability, minimal corrosion problems, recovery of copper by electrowinning, and the regeneration of sulfuric acid during the electrowinning. And under proper conditions the excess sulfur in the concentrate can be removed as elemental sulfur or as the complex basic iron sulfate (jarosite) for easy disposal. The main concern in the sulfuric acid leach is a kinetic problem, i.e., the formation of a compact sulfur layer on the surface of the sulfide. The rate of the leaching reaction is slow due to the solid state diffusion transport through the product layer.

Most studies on leaching in sulfuric acid systems can be divided into three groups: (1) Leaching in concentrated sulfuric acid, (2) Leaching in dilute sulfuric acid with oxygen as the oxidizing agent, and (3) Leaching in sulfuric acid with ferric iron as the oxidizing agent.

Concentrated Sulfuric Acid Leach.⁽²³⁾ The dissolution of copper sulfide in hot concentrated sulfuric acid involves two steps. First, the sulfation of the sulfide in concentrated sulfuric acid, then a water leach of the sulfated concentrate.

In the first step, concentrated sulfuric acid at 200-230°C behaves as the oxidizing agent. Prater⁽²³⁾ has shown that chalcopyrite is the most reactive of the sulfides, and is readily sulfated at 190°C in one hour. Digenite, which is the least reactive, requires two hours retention at 260°C. The chemistry of sulfation reactions are proposed to be as follows:

Chalcopyrite**Bornite****Idaite**

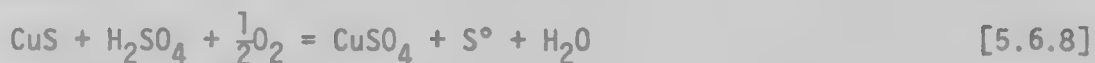
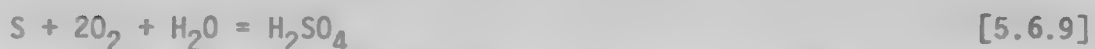
Hydrogen sulfide, H_2S , rapidly reacts with sulfuric acid to form elemental sulfur,



And at 230°C or lower, the formation of sulfur dioxide is as low as 5%. So, the main sulfur product is elemental sulfur.

Copper sulfate and iron sulfate that is produced from the sulfation reaction are insoluble in concentrated sulfuric acid, however, they are readily dissolved in water. After sulfation, the copper must be water leached. The copper can then be recovered by electrowinning.

Dilute Sulfuric Acid Leach--Oxygen. The reactions involved in the dissolution of copper sulfide by sulfuric acid-oxygen leach conditions are

Chalcopyrite**Bornite****Chalcocite****Covellite****Sulfur**

As the acid is consumed, iron can be removed by the precipitation reactions,



and



In addition, iron can be precipitated as hematite or as hydroxide.

Sulfur species produced from the sulfide usually exist as elemental sulfur and can be recovered by flotation. Vizsolyi⁽²⁴⁾ indicated that 85% of elemental sulfur can be recovered at oxygen pressures as high as 500 psi at 240°F.

Several investigators have reported on the kinetics and mechanism of acid dissolution of chalcopyrite under autoclave conditions. Depending on the reaction temperature two distinct controlling steps have been found, figure 5.6.1.⁽²⁵⁾ A high activation energy process occurs at high temperatures, and a low activation energy process at low temperature. The transition temperature between these two processes corresponds to the melting point of elemental sulfur. Warren⁽²⁶⁾ and Yu, et.al.⁽²⁷⁾ suggested a surface reaction mechanism control at high temperatures. Yu⁽²⁷⁾ et.al. have studied the leaching of monosized chalcopyrite. They have shown that the experimental data fits the rate equation for the shrinking core model for the surface reaction control (figure 5.6.2). The rate equation is simplified as,

$$1-(1-\alpha)^{1/3} = \frac{k}{r_0} t \quad [5.6.12]$$

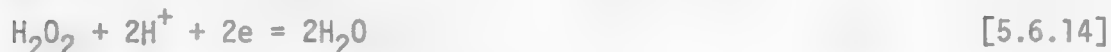
where α = fraction of solid reacted,

k = rate constant for surface reaction, including necessary concentration term,

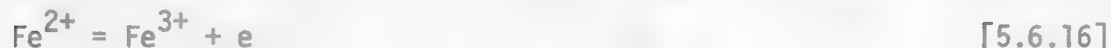
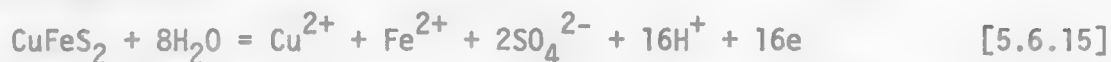
r_0 = radius of original solid particle.

Although the reaction was electrochemical in nature, i.e.,

Cathodic reactions



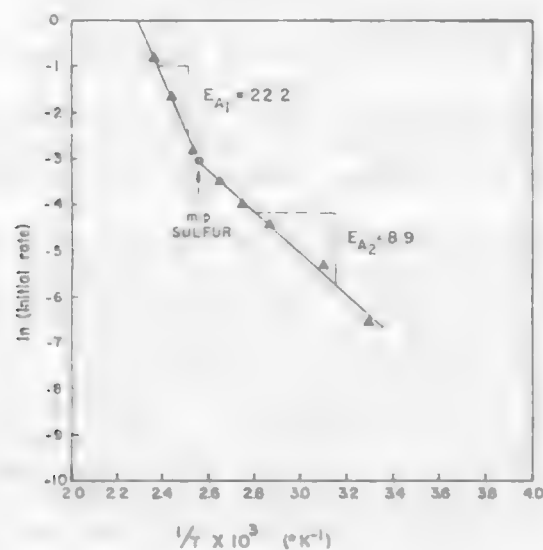
Anodic reactions



the rate data did not reflect voltage dependence. The authors have suggested⁽²⁷⁾ that the reaction rate is not controlled by the charge transfer reaction but rather by a chemical reaction in conjunction with an adsorption reaction.

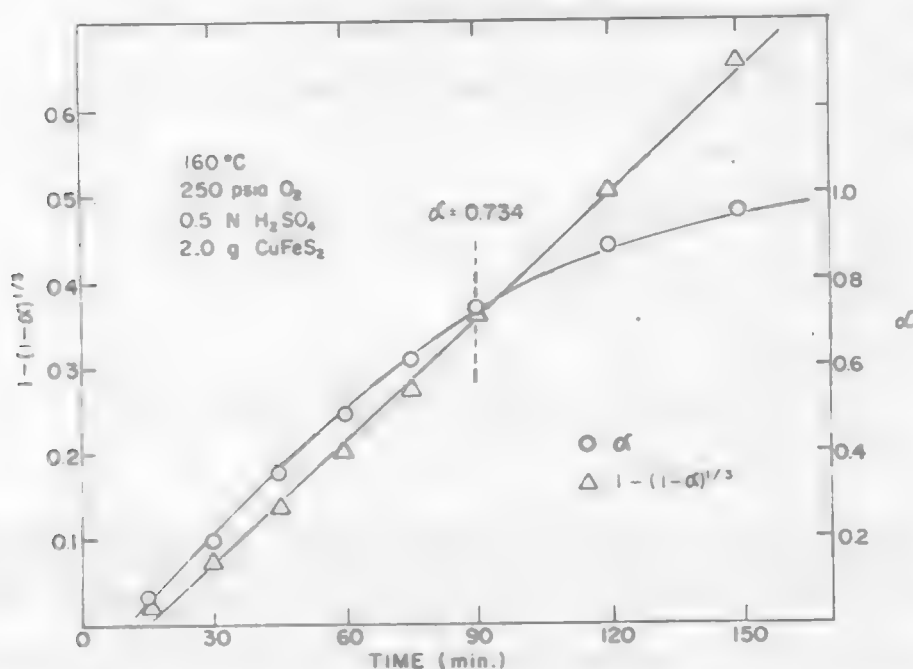
When leaching at a temperature below the melting point of sulfur, Forward⁽²⁸⁾ suggests the rate controlling process is the transport of reactants through the coating of elemental sulfur on the mineral surface. Braithwaite and Wadsworth⁽²⁵⁾ have studied the leaching kinetics under relative low temperature and low acidity

Figure 5.6.1 Arrhenius Plot of Initial Rate Data for the Oxidation of Chalcopyrite (200/270 Mesh) to Determine the Experimental Activation Energy (kcal/mole).



Source: Braithwaite, J. and M. Wadsworth, Ext. Met. Copper, TMS/AIME, V. 2, 1976. (25)

Figure 5.6.2 Comparison of α With $1-(1-\alpha)^{1/3}$ As A Function of Time.

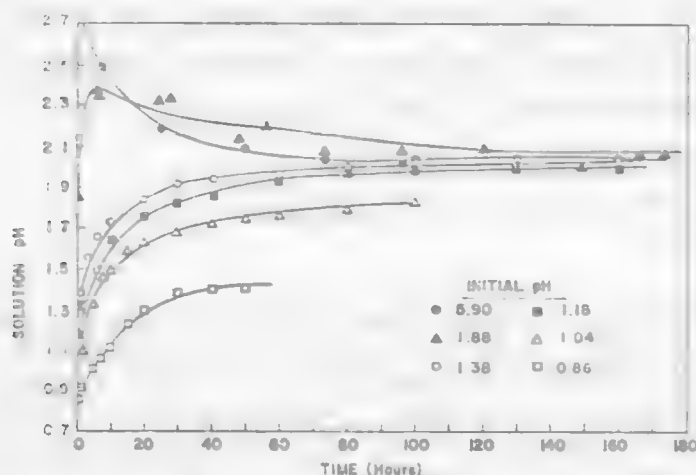


Source: Yu, P., C. Hansen, M. Wadsworth, Int. Sym. Hydromet., AIME, Chap. 15, 1973. (27)

conditions to simulate deep solution mining. Their results indicate that the rate is controlled by the diffusion of H^+ through sulfur layer when leached at high pH, whereas at low pH, the reaction is principally surface reaction controlled.

Braithwaite et.al.(25) have also showed that chalcopyrite is a pH buffering mineral under the condition of their study (figure 5.6.3). The buffering phenomenon is explained as a dynamic equilibrium between the rate of acid consumption, such as the leaching reaction, and the rate of acid generation, such as the iron hydrolysis reaction.

Figure 5.6.3 Plot of Solution pH Versus Time at Various Initial pH Values for the Oxidation of Chalcopyrite (200/270 Mesh) at 90°C and 500 psia Oxygen Pressure.



Source: Braithwaite, J. and M. Wadsworth, Ext. Met. Copper, TMS/AIME, V. 2, 1976(25).

Dilute Sulfuric Acid Leach--Ferric Ion. Ferric ion is a strong oxidizing agent. The associated oxidation potential is about 0.8 v. (SHE). It can, therefore, dissolve copper sulfide minerals at relatively low temperatures and low pressures compared to oxygen leaching. The requirement for using autoclaves for ferric sulfate leaching is, therefore, not necessary. Ferric sulfate has also been recognized to be an important factor in leaching copper from sulfide waste dumps.

The reactions for the dissolution of copper sulfide in the presence of ferric ions are:

Chalcopyrite



Chalcocite



Bornite



Covellite



Dissolution of chalcopyrite by ferric sulfate can be successfully modeled by the product layer diffusion controlled equation for the shrinking core model,

$$1 - \frac{2}{3}\alpha - (1-\alpha)^{2/3} = \frac{b/a}{d_o^2 \rho_\beta} \quad [5.6.21]$$

where α = fraction of CuFeS_2 reacted at time t

b/a = stoichiometry ratio, moles CuFeS_2 per moles of diffusion species

$D_A(\text{eff})$ = effective diffusivity of diffusion species through the product layer

C_A = concentration of diffusion species

d_o = initial partial diameter

ρ_β = molar density of chalcopyrite

t = time

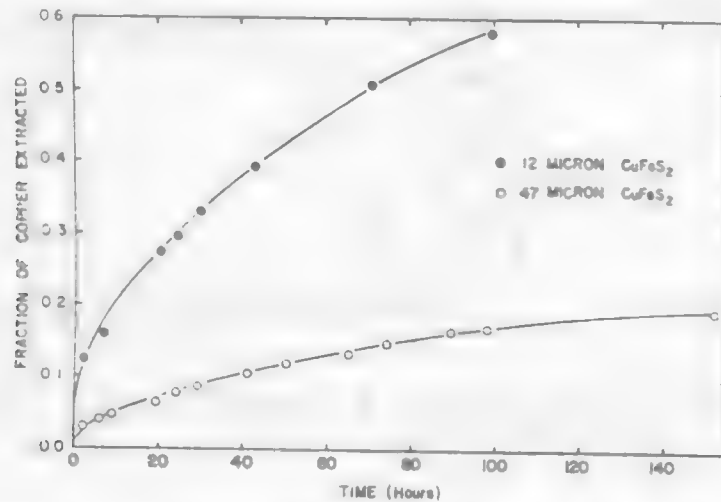
The results of leaching experiments⁽²⁹⁾ on 12 micron and 47 micron monosize samples at 1 M H_2SO_4 , 0.25 M $\text{Fe}_2(\text{SO}_4)_3$, and 93°C show a linear relationship between $1 - \frac{2}{3}\alpha - (1-\alpha)^{2/3}$ and reaction time. This confirms the diffusion controlled kinetic (figure 5.6.4) model. Dutrizac et.al.⁽²⁹⁾ have used a rotating disc technique to study the leaching of synthetic chalcopyrite by ferric sulfate. Parabolic rate dependence was found, indicating that the reaction was also controlled by diffusion transport. Dutrizac et.al.⁽³⁰⁾ also studied the effect of ferric sulfate concentration on the rate of leaching chalcopyrite, figure 5.6.5. Above a ferric ion concentration of 0.01 M, the rate of leaching was insensitive to changes in concentration. In a commercial application the concentration of ferric ion will probably always be above this concentration, and therefore, the process will have a rate independent of the ferric concentration. This result was confirmed by Beckstead.⁽²⁹⁾

In the product layer diffusion controlled model, the rate is inversely proportional to the square of the original particle diameter (Equation [5.6.21]). Particle size is the most important factor in determining the rate of leaching. Beckstead et.al.⁽²⁹⁾ demonstrated this dependence, e.g., excellent copper extraction was obtained after three hours leaching for a median particle size of 0.5 μ whereas, copper extraction from coarser products were substantially less, figure 5.6.6. The schematic diagram of the attritor apparatus used to produce the fine particle size is illustrated in figure 5.6.7.

5.4.3.2 Ammonia-Oxygen Leach.

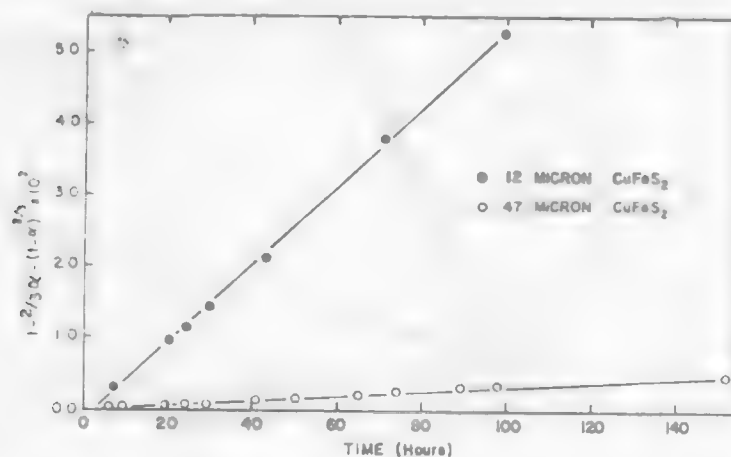
Cupric ion combines with ammonia to form a stable copper-ammine complex of the form $\text{Cu}(\text{NH}_3)_4^{2+}$. The Eh-pH diagram showing the equilibrium conditions

Figure 5.6.4.a A Plot of Fraction of Copper Extracted from Monosize Chalcopyrite Particles as a Function of Time for 1.0 M H_2SO_4 , 1.0 M $\text{Fe}_2(\text{SO}_4)_3$, 93°C, 0.5 Percent Solids and 1200 rpm.



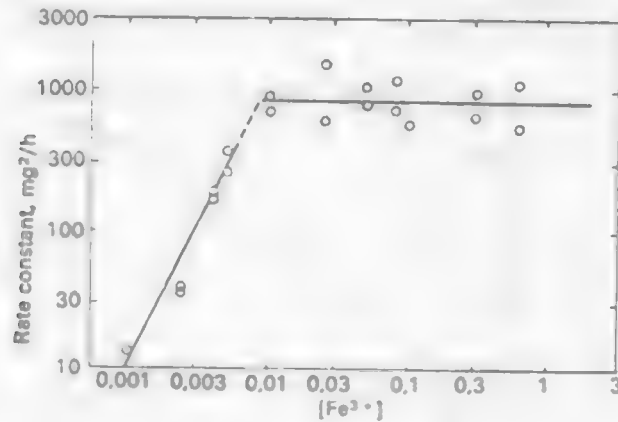
Source: Beckstead, L. W., et.al., Ext. Met. Copper, AIME, V. 2, 1976.⁽²⁹⁾

Figure 5.6.4.b A Plot of $1 - \frac{2}{3}\alpha - (1-\alpha)^{2/3}$ For Monosize Chalcopyrite Particles as a Function of Time for the Data Shown in Figure 5.6.3.



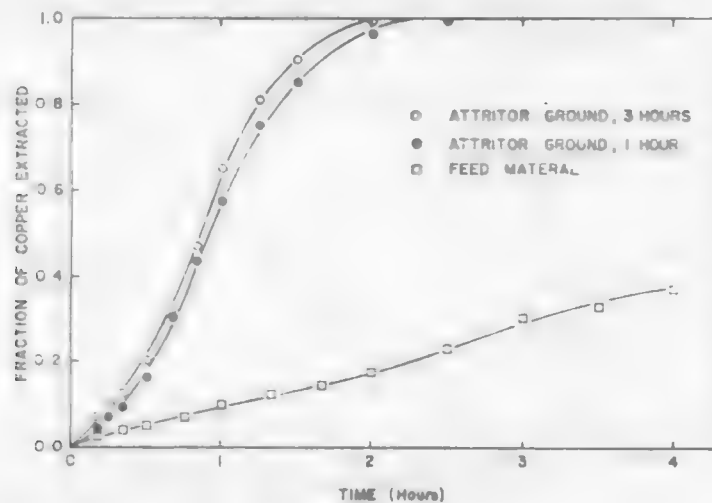
Source: Beckstead, L. W., et.al, Ext. Met. Copper, AIME, V. 2, 1976.⁽²⁹⁾

Figure 5.6.5 Effect of Ferric Ion Concentration on the Rate of Chalcopyrite Leaching.



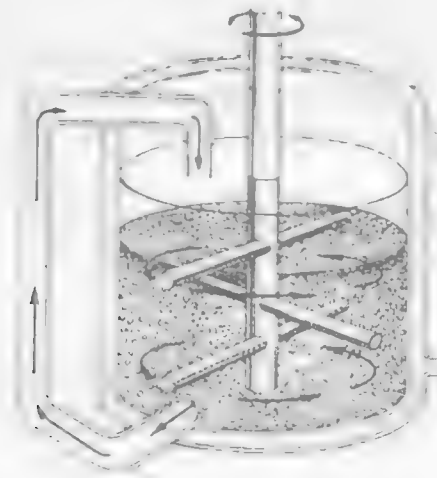
Source: Dutrizac, J. E., R. MacDonald, and T. Ingraham, Trans. AIME, 245, 1969. (30).

Figure 5.6.6 A Plot of Copper Extracted by Ammonia Oxidation Leaching as a Function of Time for Various Chalcopyrite Products at 93°C, 1.0 atmos. O₂, 1.8 M Total Ammonia at pH 10.20, 1.0 Percent Solids and 2000 rpm.

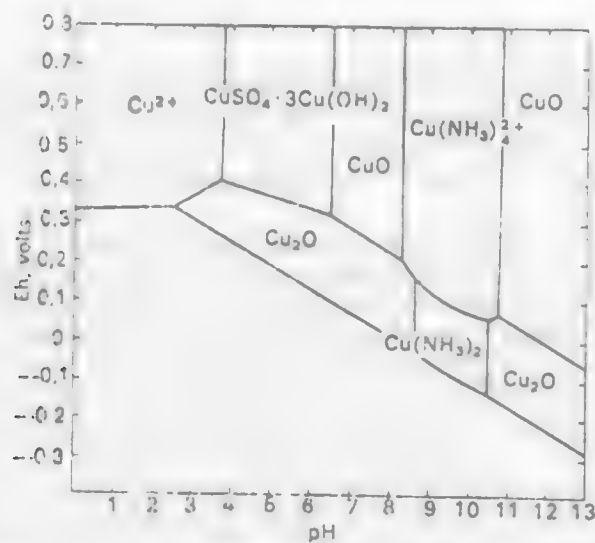


Source: Beckstead, L., et.al., Ext. Met. Copper, AIME, V. 2, 1976. (29)

Figure 5.6.7 Schematic Drawing of Attritor.



Source: Beckstead, L., et.al., Ext. Met. Copper, AIME, V. 2, 1976. (29)

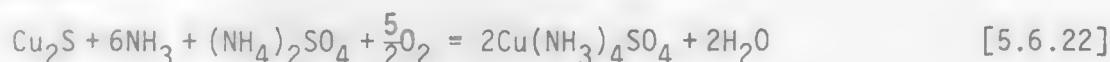
Figure 5.6.8 Eh-pH Diagram for Cu-NH₃ System [Cu] = 0.5 m [NH₃] + [NH₄⁺] + 1.0 m.

Source: Dutrizac, J. E., R. MacDonald, and T. Ingraham, Trans. AIME, 245, 1969. (30)

under which copper-ammine complexes are stable is presented in figure 5.6.8. The ammonia-oxygen leaching method offers several advantages over the acid leach process, e.g., (1) sulfur is converted into sulfate rather than elemental sulfur (recall that sulfur tends to block the surface of the concentrate), (2) the leach reactions are more selective, i.e., the pyrite remains unreacted; iron is oxidized to ferric oxide and will remain in the residue; most of the molybdenum will remain in the residue; arsenic and antimony will be oxidized and will combine with iron to form highly insoluble ferric arsenate and antimonate.

The dissolution reactions for copper sulfides in an ammonia-oxygen environment are,

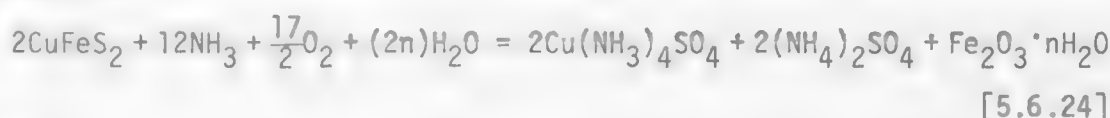
Chalcocite



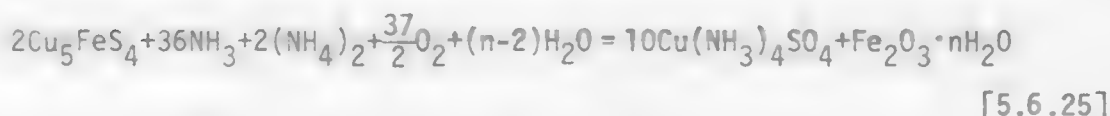
Covellite



Chalcopyrite



Bornite



Stanczyk and Rampacek⁽³¹⁾ have shown that 96% of the copper can be extracted by leaching copper concentrate at 75°C under 100 psig oxygen pressure with ammoniacal solution for 60 minutes. Bornite, chalcocite and covellite dissolve faster than chalcopyrite under the same conditions.

When leaching chalcopyrite, Stanczyk and Rampacek⁽³¹⁾ have found the formation of a ferric oxide product layer on the surface of the sulfide, and suggested that the rate controlling step is diffusion through this layer. However, this oxide layer can be diminished by the use of intense agitation.⁽³²⁾ The Arbiter process has applied intense agitation to abrade the oxide from the surface to expose fresh surface for reaction; also to provide good transport of oxygen. As a result, the Arbiter process is conducted at a relatively low temperature, 70°C, and low oxygen pressure, 5 psig. In contrast the Sherritt-Gordon ammonia-oxygen process does not use internal abrasion but uses autoclave reactors to speed up the transport through the deposited layer, i.e., 85°C and an air pressure of 110 psig.⁽³³⁾

Under the conditions of the Arbiter process, Beckstead et.al.⁽³⁴⁾ have explained the kinetics of the oxidation based on the electrochemical model. This model is shown schematically in figure 5.6.9. The formation of hemite

Figure 5.6.9 Schematic Representation of the Electrochemical Reaction and the Reduction of the Anodic Area by the Hematite Reaction Product.

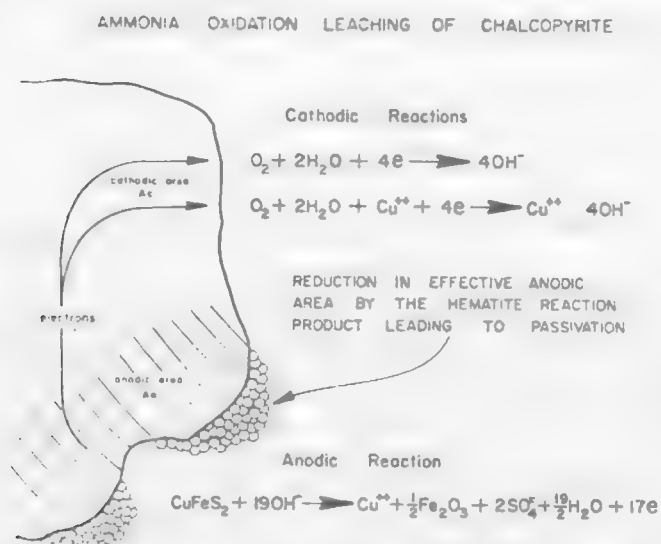
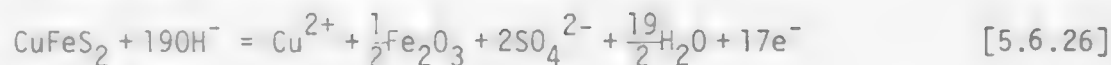


Fig. 8—Schematic representation of the electrochemical reaction and the reduction of the anodic area by the hematite reaction product.

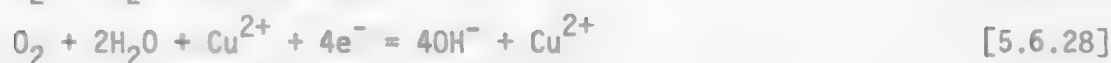
Source: Beckstead, L.W. and J. W. Miller, Met. Trans. 13, 8B, 1977.

passivates the anodic reaction, as seen in figure 5.6.9. The proposed electrochemical reactions are:

Anodic reaction



Cathodic reactions

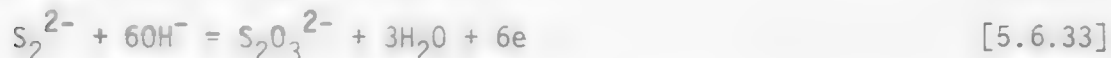
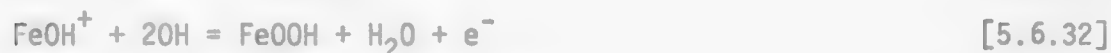
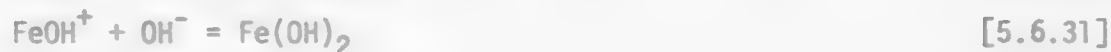


where Cu^{2+} in the cathodic reactions behaves as a catalyst.

Warren and Wadsworth⁽³⁵⁾ have studied the electrochemical behavior of chalcopyrite in ammoniacal solutions. The polarization measurement for chalcopyrite in the anodic direction (Equation [5.6.26]) in the absence of oxygen was performed by a potentiostat. Results, shown in figure 5.6.10, indicate the reaction is charge transfer controlled when the potential is lower than 1.0 volt (SHE). If oxygen gas is used as the oxidizing agent, which has an equilibrium potential less than 1.0 volt in alkaline solutions, the anodic dissolution of chalcopyrite will be controlled by a charge transfer reaction. This result is in agreement with the Beckstead study.⁽³³⁾ The Tafel slope value, 140 mv/decade, was interpreted to be a single electron transfer process, and the reaction order was found to be first order with respect to both $[\text{OH}^-]$ and $[\text{NH}_3]$. The rate controlling step was, then, proposed to be



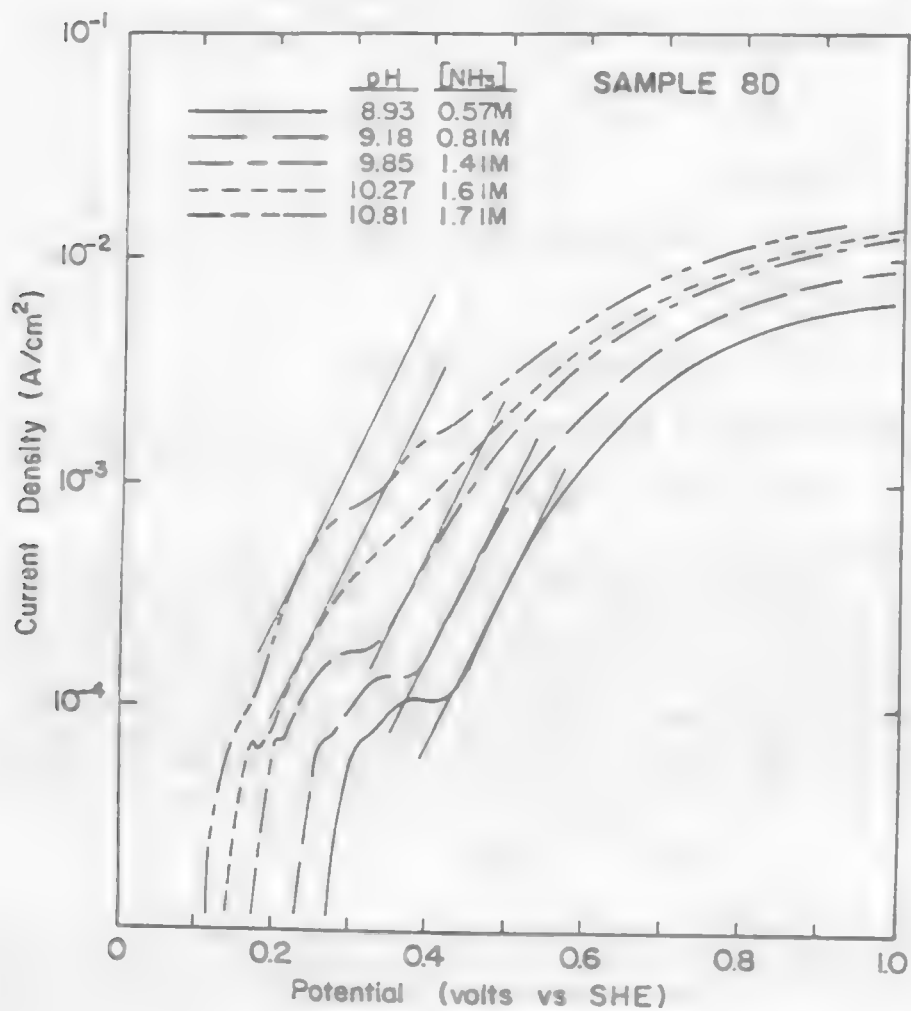
All products represented are intermediate species and would be expected to react further:



5.4.3.3 Ferric Chloride Leach.

Chloride leaching is important because many metal chlorides have a high aqueous solubility, e.g., CuCl_2 readily dissolves in hot water, 107.9 g/l, and even CuCl is a stable species. Use of an acid chloride environment offers other advantages. Such as, the sulfur layer formed during the chloride leach does not passivate the reaction to as great an extent as during the sulfate leach. The recovery of elemental sulfur is usually higher in the chloride system than in the sulfate system. Chloride leach systems also require less oxidant than the sulfate systems because the reaction product can be CuCl rather than Cu(II) ion.

Figure 5.6.10 Polarization Curves at 25°C for Sample 8D in Five Solutions of Different $[\text{OH}^-]$ Concentration. Other Components Remained Essentially Constant: $[\text{Cu}^{II}] = 0.083 \text{ M}$, $[\text{SO}_4^{2-}] = 1.0 \text{ M}$, $\Sigma (\text{NH}_4 + \text{NH}_3) = 1.76 \text{ M}$. Ionic Strength Varied from 2.6 to 2.9.



Source: Warren, G. M. and M. E. Wadsworth, 1978 AIME Annual Meeting, SME/AIME Reprint 78-B-68, 1978.⁽³⁵⁾

Problems generally arising in chloride leach systems are the maintenance of equipment due to the corrosive nature of the liquid environment and the subsequent recovery of copper from the chloride leach solution.

Several chloride-containing reagents, or combinations of reagents, can be used to leach copper sulfide, but the most widely used is ferric chloride because it is relatively inexpensive and can be regenerated. The leach reactions of interest in ferric chloride solutions are,

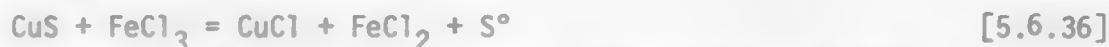
Chalcopyrite



Chalcocite



Covellite



Sometimes, CuCl_2 is involved in the reaction as an oxidizing agent,

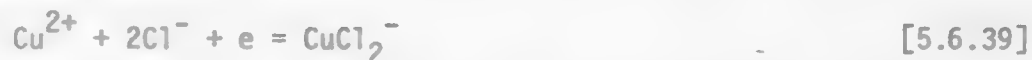


Leaching chalcopyrite with ferric chloride is faster than with ferric sulfate. Haver and Wong^(36,37) reported almost 100% copper extraction from finely ground chalcopyrite using a strong ferric chloride solution at 106°C (figure 5.6.11). They also found that the rate was sensitive to temperature and suggested that the chemical reaction was the rate-controlling step in the reaction sequence. Jones and Peters⁽³⁸⁾ have shown that the dissolution of monosize chalcopyrite by ferric chloride follows the chemical reaction controlled rate equation based on the shrinking core model,

$$1 - (1 - \alpha)^{1/3} = \frac{k}{r_0} t \quad [5.6.38]$$

Results for several sizes are shown in figure 5.6.12. By using mixed potential measurements, Jones and Peters have postulated that the cathodic reaction on chalcopyrite in chloride solution is catalyzed by aqueous copper,

Cathodic reaction:



so that ferric chloride leaching is, in reality, cupric chloride leaching. The ferric ion serves to reoxidize the cuprous ions. Since the measured mixed potential is close to the equilibrium potential for the cathodic reaction, Equation [5.6.39] (i.e., small cathodic polarization), the leaching of chalcopyrite in ferric chloride solution was proposed to be controlled by the anodic reaction,

Anodic reaction:

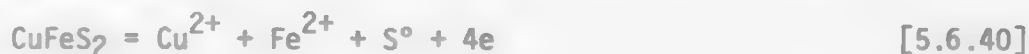
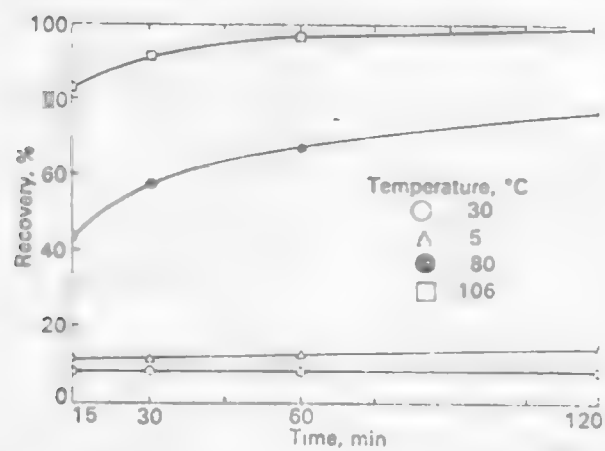
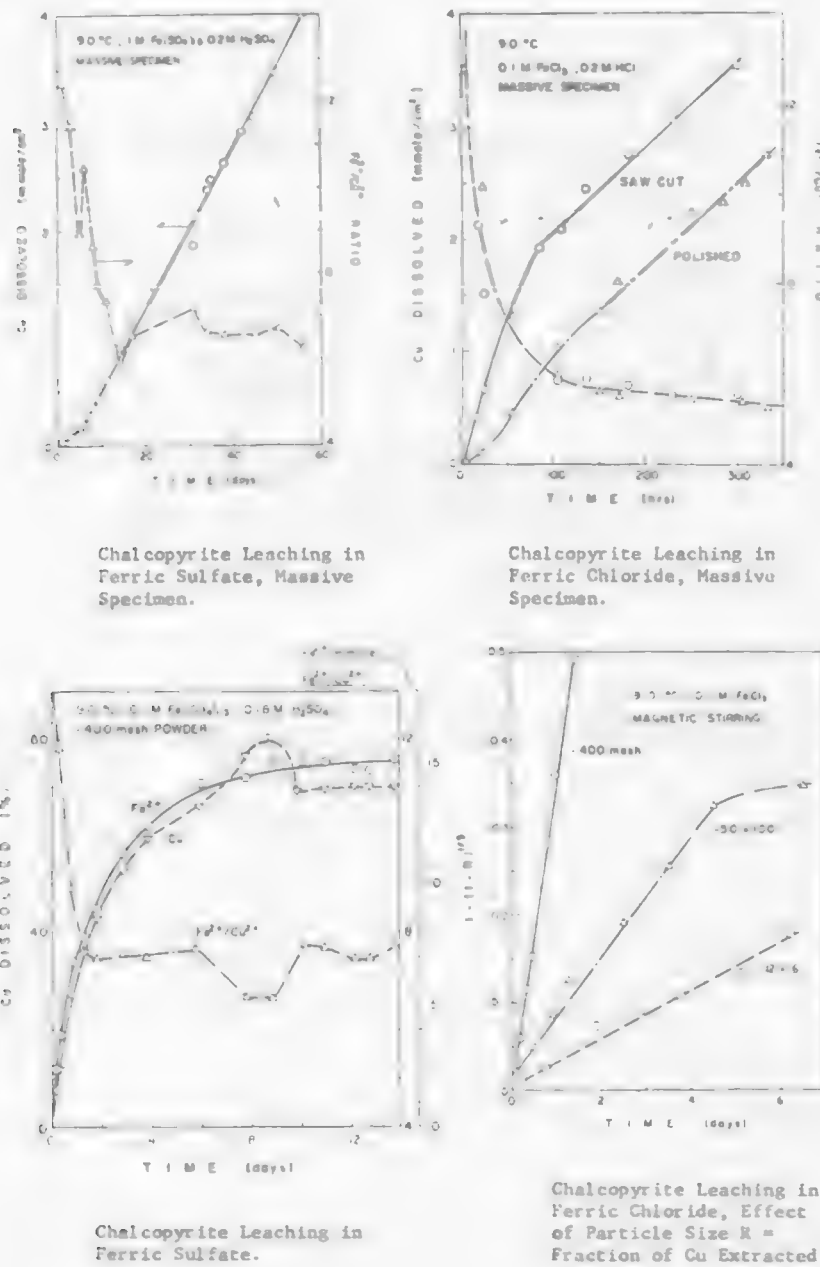


Figure 5.6.11 Effect of Temperature on Recovery from a Chalcopyrite Concentration in a FeCl_3 Solution.



Source: Haver, F. and M. Wong, U. S. B.M., R.I. 7474, 1971. (36)

Figure 5.6.12 Ferric Chloride Leaching of Chalcopyrite.



Source: Jones, D. and E. Peters, Ext. Met. of Copper, V. 11, TMS/AIME, 1976, (38)

5.4.3.4 Nitric Acid Leach.

The powerful oxidizing power of nitric acid is well recognized. Several attempts have been made to use the oxidizing ability to leach copper sulfide. The main concerns of using nitric acid are: The high costs of nitric acid, the difficulties of regenerating nitric acid from off gas nitrogen oxide, the difficulty recovering copper from nitrate solutions, and the corrosive nature of the solution on container vessels.

Bjorling and Kolta⁽³⁹⁾ investigated the oxidation of copper sulfides and other minerals in a sulfuric acid solution containing a low concentration of nitric acid as a catalyst. The chemistry of sulfuric-nitric acid leach process is complex. The following general reactions have been proposed:^(39,40)

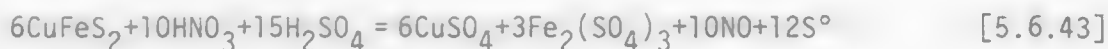
Covellite



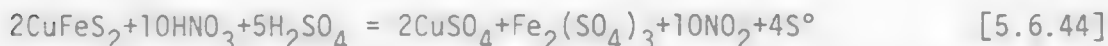
or



Chalcopyrite



or



Whether NO or NO₂ is the reaction product depends greatly on the nitric acid concentration, figure 5.6.13. It is preferable to form nitric oxide rather than nitrogen dioxide because 3/2 moles of nitric acid are required per mole of CuS if nitric oxide is the product, and 2 moles of HNO₃ is required per mole of CuS if nitrogen dioxide is the product.

5.4.3.5 Cyanide Leach.

Cyanide solutions are capable of dissolving copper sulfide in the absence of an oxidizing agent, e.g.,



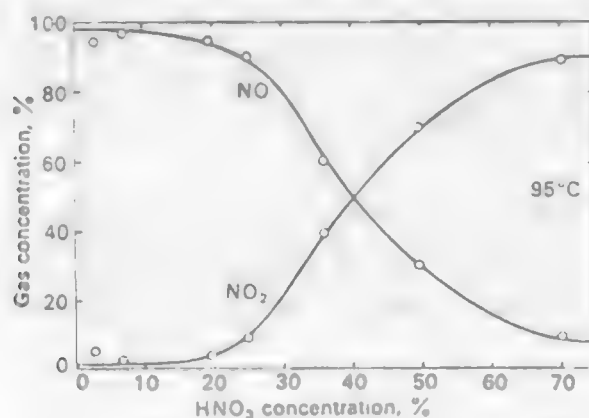
Elemental sulfur does not form in the absence of an oxidizing agent. In the presence of cyanide ion, the cuprous ion will not be oxidized further to cupric because the cyanide ion stabilizes the cuprous state in the solution. Chalcocite is dissolved in the cyanide solution rapidly,⁽⁴¹⁾ but chalcopyrite is not appreciably attacked (figure 5.6.14), nor is pyrite.

In the presence of oxygen the sulfide ion could be expected to oxidize to elemental sulfur,



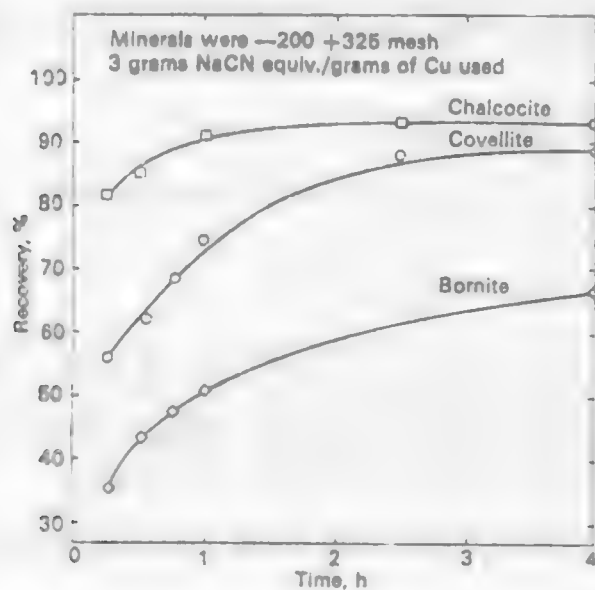
which tends to accumulate on the surface of the mineral. The dissolution rate would be hindered.

Figure 5.6.13 Distribution of NO and NO₂ in the Gas as a Function of HNO₃ Concentration.



Source: Dutrizac, J. E., R. MacDonald, and T. Ingraham, Trans. AIME, 245, 1969. (30)

Figure 5.6.14 Recovery of Copper from Chalcocite, Covellite, and Bornite by Cyanide Leaching as a Function of Time.



Source: Lower, G. and R. Booth, Min. Engr., 1975. (41)

A detailed kinetic study⁽⁴²⁾ indicates that the rate of leaching of Cu_2S with cyanide ion is directly proportional to the free cyanide ion concentration and surface area, and inversely proportional to the sulfide ion concentration to a low power (0.1). The maximum extraction occurs at a pH of 9.9 and CN:Cu ratio greater than about 4:1.

LEARNING ACTIVITY 7

Learning Activity Objective

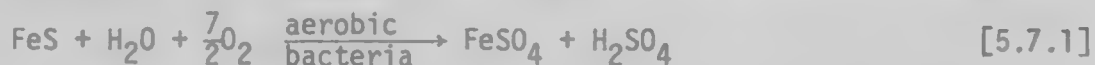
After completing your study of this learning activity material you should be able to list the types of microbial species used in leach systems, and list the systems to which microbial action is of importance.

5.4.3.6 Microbiological Leach. (45)

The oxidative dissolution of sulfide minerals in copper waste dumps account for a large portion of copper recovered by hydrometallurgical techniques. Today more than 10% of the primary copper produced in the United States is from dump leaching. The bacterium activity plays an important role in the oxidative dissolution of the sulfide minerals.

In general, the bacteria that are found in the nature that account for the dissolution of the mineral, and for the formation of the secondary enriched ore deposits by supergene enrichment can be classified into two general categories: Autotrophic and heterotrophic bacteria. Autotrophic bacteria obtain self-nourishment for their energy and reproductive cycles from purely inorganic material, and heterotrophic bacteria require the availability of organic matter to complete their cycle.

Both autotrophic and heterotrophic bacteria can be further classified as aerobic and anaerobic bacteria. The aerobic bacteria operate specifically in the presence of oxygen and perform primarily the oxidation reaction. They are responsible for oxidizing metal sulfides to water soluble sulfates. For instance, bacteria thiobacillus thiooxidans accelerate the oxidation reaction of pyrite to sulfuric acid and ferrous sulfate,



The anaerobic bacteria function in the absence of oxygen and perform the reduction reactions that result in the deposition of secondary enrichment found in nature. The geological alternation is generated by the reduction of the water soluble metal sulfate to an insoluble metal sulfide deposit. For instance, bacteria, desulforibrio sulfuricans, accelerate the reaction of copper sulfate to covellite according to the following reaction,



The oxidation of sulfide, and other reduced inorganic sulfur compounds, to sulfate as an energy-yield process is the ability of a group of bacteria known as thiobacilli. This genus of bacteria are aerobic, motile, rods approximately 0.5 μ in length, and autotrophic. The thiobacilli are widely distributed in soils, muds, mine water, and fresh and marine waters. The members of this genus can function over a significant range of pH and temperature. (45) Two strains of commonly found thiobacilli in waters from copper mine waste are thiobacillus thiooxidans and thiobacillus ferrooxidans. The latter has the ability to oxidize ferrous iron to ferric iron. This last property is also shared by another group of bacteria to which the generic

name of ferrobacillus has been given. Some of the ferrobacilli have also been shown to oxidize sulfur compounds and the validity of these two genera, thio-bacillus and ferrobacillus is open to question.⁽⁴⁴⁾ For the purpose of the present discussion no distinction will be made between these two groups. These microorganisms will be treated as a class of iron-sulfur bacteria. Some of the common iron-sulfur oxidizing bacteria and their occurrence are listed in Table 5.7.1.

Table 5.7.1 The Iron and Sulfur Oxidizing Bacteria.⁽⁴⁵⁾

The members of these genera are non-sporulating rods, 0.5 μ in diameter, aerobic and autotrophic.

Organism

Thiobacillus thiooxidans	Soil	Optimum growth 28-30°C, pH=2; oxidizes sulfur, sulfide but not ferrous iron
Thiobacillus ferrooxidans	Acid mine and soil water containing hydrogen sulfide	Optimum growth pH 2.5-5.8; oxidizes ferrous iron and sulfur compounds; motile
Thiobacillus thioparus	Canal water, mud, soil	Growth pH range 7.8-4.8; generally aerobic and motile; oxidizes sulfur compounds
Ferrobacillus ferrooxidans	Acid, bituminous coal mine effluent	Optimum growth 15-20°C, pH 3.5; oxidizes ferrous iron and sulfur compounds
Ferrobacillus sulfooxidans	Acid coal mine water	Optimum growth 32°C, pH 2.8; oxidizes ferrous iron and sulfur

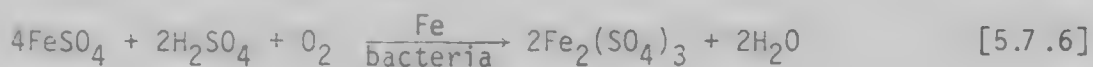
Ferrous iron sulfide such as pyrite and chalcopyrite appear to be oxidized directly by iron-sulfur bacteria with the production of soluble metals and elemental sulfur,



The elemental sulfur may further be oxidized by the bacteria to generate sulfuric acid,



The iron oxidizing bacteria will oxidize the available ferrous iron to ferric iron according to the following reaction,



It has been reported that iron-sulfur bacteria oxidized 200 ppm of ferrous iron in 3 days, otherwise, ferrous iron was chemically stable for more than two years.⁽⁴⁵⁾

Ferric sulfate is a strong oxidizing agent, and readily reacts with pyrite or chalcopyrite resulting in the formation of soluble metals, and sulfur or sulfuric acid,

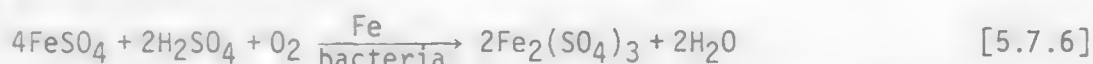


The reaction product, ferrous sulfate, is further oxidized according to equation [5.7.6], and the cycle is repeated.

The oxidation of non-ferrous sulfides such as covellite and sphalerite is more complex, and it would appear that iron stimulates the reaction. Molouf and Prater⁽⁴⁶⁾ have demonstrated that the bacterial release of zinc from sphalerite is stimulated about 10-fold by the presence of pyrite. It is probably due to the contribution of ferric sulfate in the same way as previously stated in Equations [5.7.7] and [5.7.8], e.g., covellite; ferric sulfate oxidizes covellite to cupric sulfate according to the following reaction,

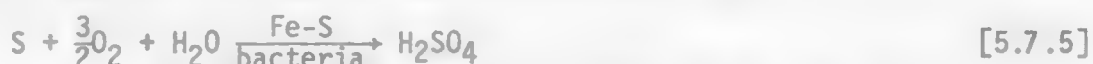


Ferrous ions will be reoxidized with the help of bacteria to form ferric ions according to Equation [5.7.6],



and recycled to Reaction [5.7.9] for further dissolution of covellite. Reactions [5.7.9] and [5.7.6], i.e., the consumption and regeneration of ferric sulfate, show an example of an indirect bacteria leaching mechanism in which bacteria may not be necessarily in contact with the mineral. Several experiments have also indicated that bacteria are able to attack some non-ferrous sulfide minerals directly.⁽⁴⁷⁾ These direct and indirect bacterial leaching mechanisms for non-ferrous sulfide mineral probably occur in parallel. Typical reactions involving microbiological leaching of sulfide minerals by iron-sulfur bacteria are listed in Table 5.7.2.⁽⁴⁸⁾

Acid that is required for the oxidation of ferrous to ferric iron, for the leaching of minerals and for the maintenance of acidity, is generated by the biological oxidation of elemental sulfur to sulfuric acid,



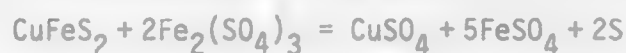
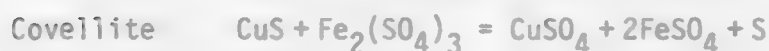
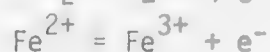
Additional acid may be generated by chemical hydrolysis of ferric ion,



Numerous laboratory studies as well as direct field examination suggest that the optimum temperature for the activity of the iron-sulfur bacteria is

Table 5.7.2 Autotrophic-Aerobic Acid Media Species

Thiobacillus Thiooxidans
Thiobacillus Ferrooxidans

ReactionsArsenicCopperLeadIronMolybdenumNickelAntimonyUranium

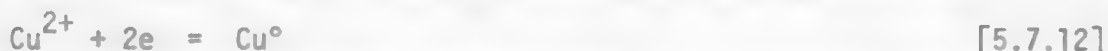
between 25° and 30°C with an upper limit in the region of 40°C. Thiobacillus thiooxidans can tolerate 5% H₂SO₄ and 20 g/l copper, however, the optimum pH is between 2 and 3.5.

5.4.3.6 Electrochemical.

Copper sulfides are semiconductors and will conduct an electric current at room temperature. Because leaching sulfide minerals involve an electrochemical reaction, it is possible to dissolve a sulfide mineral by applying an electric current. The technique for electrochemical leaching is analogous to the conventional electrolytic refinery. If copper sulfide is made the anode in an acidic aqueous electrolyte, an electric current will dissolve copper and leave behind elemental sulfur according to the following reaction,⁽⁵⁰⁾



while at the cathode, cupric ions in the electrolyte will be recovered,



Numerous attempts have been made to apply this technique to the hydrometallurgy of chalcopyrite. Following is an example of a pilot plant tested process, i.e., the Cymet process.⁽⁵¹⁾ The Cymet process combines chemical leaching with electrochemical dissolution to treat chalcopyrite according to the following reactions:

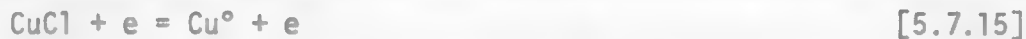
1. Leaching chalcopyrite particles by ferric chloride,



2. Electrochemical dissolution of chalcopyrite electrode at the anode,

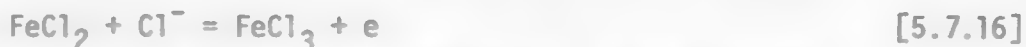


3. Electrochemical deposition of copper from electrolyte at the cathode,

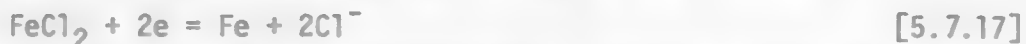


The oxidizing agent, ferric chloride, is regenerated in a separate electrolytic cell. Metallic iron is also produced in this cell, e.g.,

- (1) Electrochemical oxidation of ferrous to ferric iron occurs at the anode,



- (2) Electrochemical deposition of iron occurs at the cathode,



Problems normally involved in electrochemical leaching processes to treat chalcopyrite are (1) the formation of a sulfur layer on the solid particle

surface which requires a higher cell voltage as the reaction proceeds and (2) the impurity level in the cathodic copper deposit is high, and a subsequent refining step is necessary.

LEARNING ACTIVITY 8

Learning Activity Objective

After completing your study of this learning activity material you should be able to list the types of leach environments used for treating copper sulfides in commercial operations. You do not need to memorize flow sheets but you should be able to describe the basic types of process each commercial operation uses.

5.4.4 Leaching of Copper Sulfide - Processes.

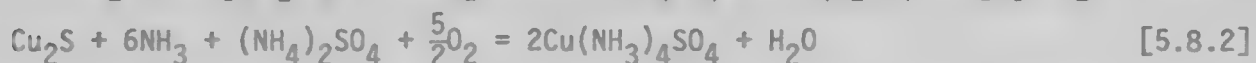
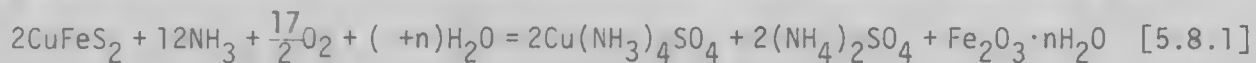
Hydrometallurgical processing of copper concentrates has been developing rapidly. Several processes have been tested on a pilot plant scale, and some have advanced to commercial systems. A brief description of some of these processes is given in the following discussion.

5.4.4.1 Roast--Leach--Electrowin Process. (52)

The roast-leach process combines a pyrometallurgical operation (roasting) with a hydrometallurgical process. This technology has been practiced in Africa for several years and recently Hecla Mining Company installed this process at their Lakeshore Mine in Arizona. The process involves the sulfation roasting of chalcopyrite in a fluidized bed roaster in which the temperature is controlled between 685-700°C. The flue gas, after dust removal and cooling, is converted into concentrated sulfuric acid. The calcine (the solid roasted product) is hot quenched and leached in agitation tanks by spent acidic electrolyte from the electrowinning circuit. The electrolyte contains about 20 g/l H₂SO₄. About 96% of copper is dissolved in a 3 hour retention time. After a solid-liquid separation, copper is recovered from the pregnant liquor by electrowinning. The copper product has a purity of 99.95%. This is comparable to electrolytic refined copper. The spent electrolyte is recycled to the leaching step. The acid generated from the acid plant is used for vat leaching of copper oxide ore. The flow sheet of the R-L-E process at Lakeshore Mine is presented in Figure 5.8.1.

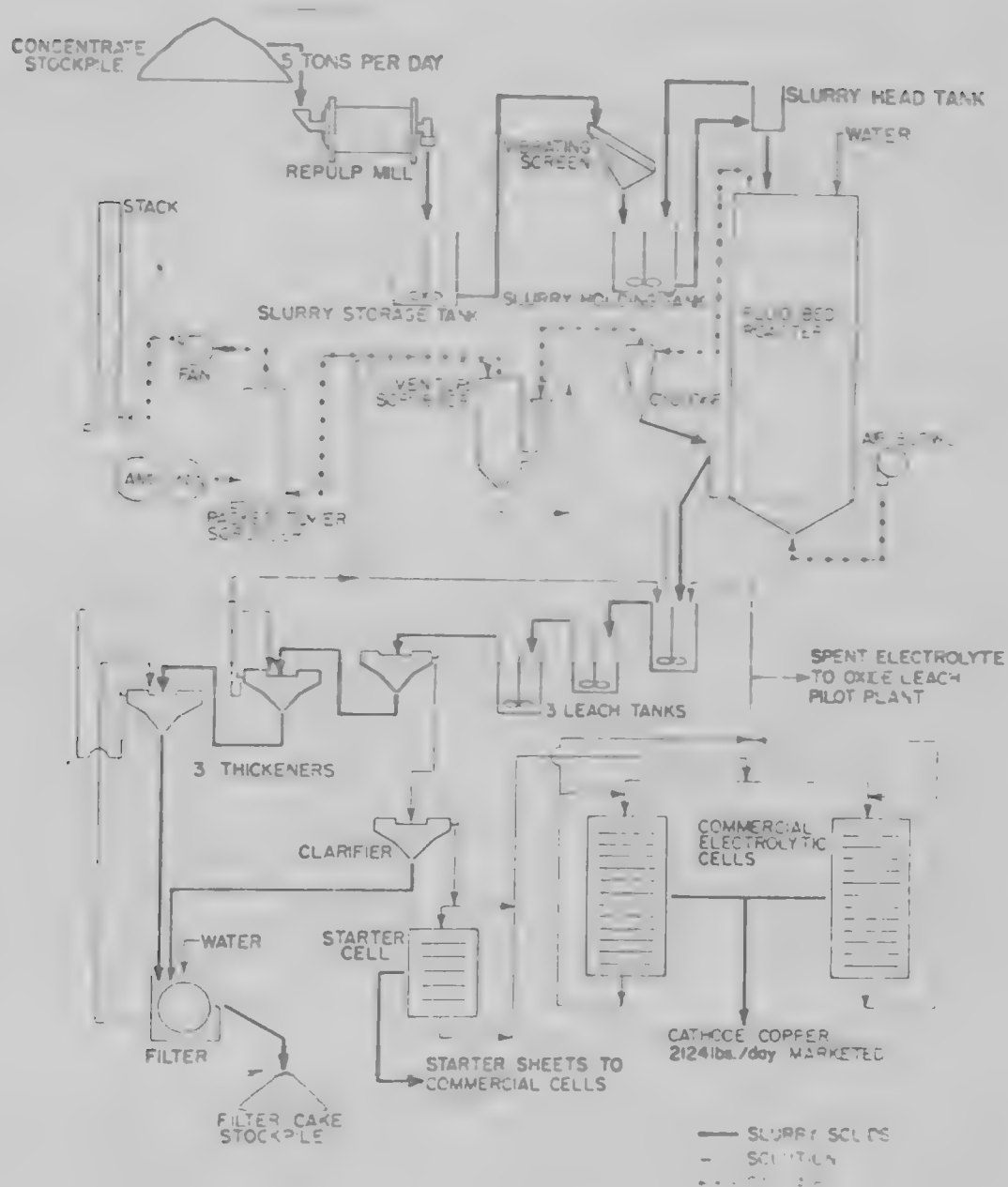
5.4.4.2 Ammonia Leach Processes.

The basis of these processes is the fact that copper is solubilized in an alkaline solution as an ammine complex. Also, iron does not dissolve and complex but rather is oxidized to hematite which can be easily removed as a solid product. So are acid consuming minerals, lime and magnesia. Arsenic and antimony are oxidized and combined with excess ferric iron to form a highly insoluble ferric arsenate and antimonate. The leaching reactions are,



Oxidized sulfur can be in the form of thiosulfate, polythionate, sulfamate and sulfate. The Sherritt-Gordon Copper Process and Arbiter Process are examples of the application of this type process for extracting copper.

Figure 5.8.1 Lakeshore Project-Plant Flowsheet.



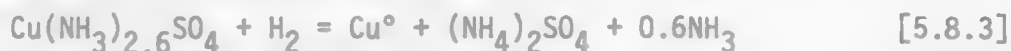
Source: Griffith, W., et.al., J. M., 27, 1975. (52)

Sherritt-Gordon Copper Process.⁽⁵³⁾ This process has been developed in the Sherritt-Gordon Laboratory for the treatment of the copper-zinc concentrates from the Bagacay and Sipalay Mines in the Phillipines. The process is made up of (shown in figure 5.8.2) the following steps:

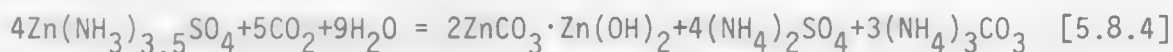
1. The copper-zinc concentrate is leached in autoclaves in air at 85°C, 110 psig. Under these conditions 95.6% Cu, 80.0% Zn and 58% S are dissolved in 9 hours. Iron is oxidized to solid ferric hydroxide; molybdenum remains quantitatively in the residue, so does alumina, silica, lime, magnesia, gold and silver.

2. The unsaturated sulfur compounds, thiosulfate and polythionate are oxidized to sulfate and sulfamate, then precipitated.

3. Copper powder is recovered by hydrogen reduction in autoclaves at 200°C, 500 psig, in the presence of ammonium polyacrylate.



4. Zinc is precipitated as zinc carbonate in an autoclave at a carbon dioxide pressure of 100 psig,



5. Basic zinc carbonate is redissolved by sulfuric acid in spent electrolyte, and then is recovered as metallic zinc by electrowinning.

Arbiter Process.⁽⁵⁴⁾ The process developed by Anaconda was in operation for several years at Arbiter Plant, Anaconda, Montana. The process utilized intense agitation to abrade the hematite product layer from the particle surfaces and to increase the dissolution rate of oxygen gas into the solution. As a result, this process was carried out in a stirred tank reactor at a relatively low temperature, i.e., about 75°C, and low oxygen pressure, i.e., about 5 psig. The process involved four main steps: leaching, solvent extraction, electrowinning and ammonia regeneration (figure 5.8.3). During the leach step iron was precipitated; copper and sulfate dissolved as ammonium sulfate, Equation [5.8.1]. After solid-liquid separation, copper was extracted by an organic solvent LIX 65N. The raffinate was treated with lime to regenerate ammonia and to produce disposable gypsum (CaSO_4).

The loaded organic was stripped with acid electrolyte recycled from electrowinning. Finally, copper was produced by electrowinning practice.

The ammonia oxidation leach, as applied to the Anaconda Weed concentrate was designed to extract only about 80% of copper values. The remaining copper was recovered by flotation and then recycled to their smelting circuit. In the laboratory an average leach time of 1-1/2 hours was required for 80% extraction of the Weed concentrate.

5.4.4.3 Ferric Chloride Leach Processes.

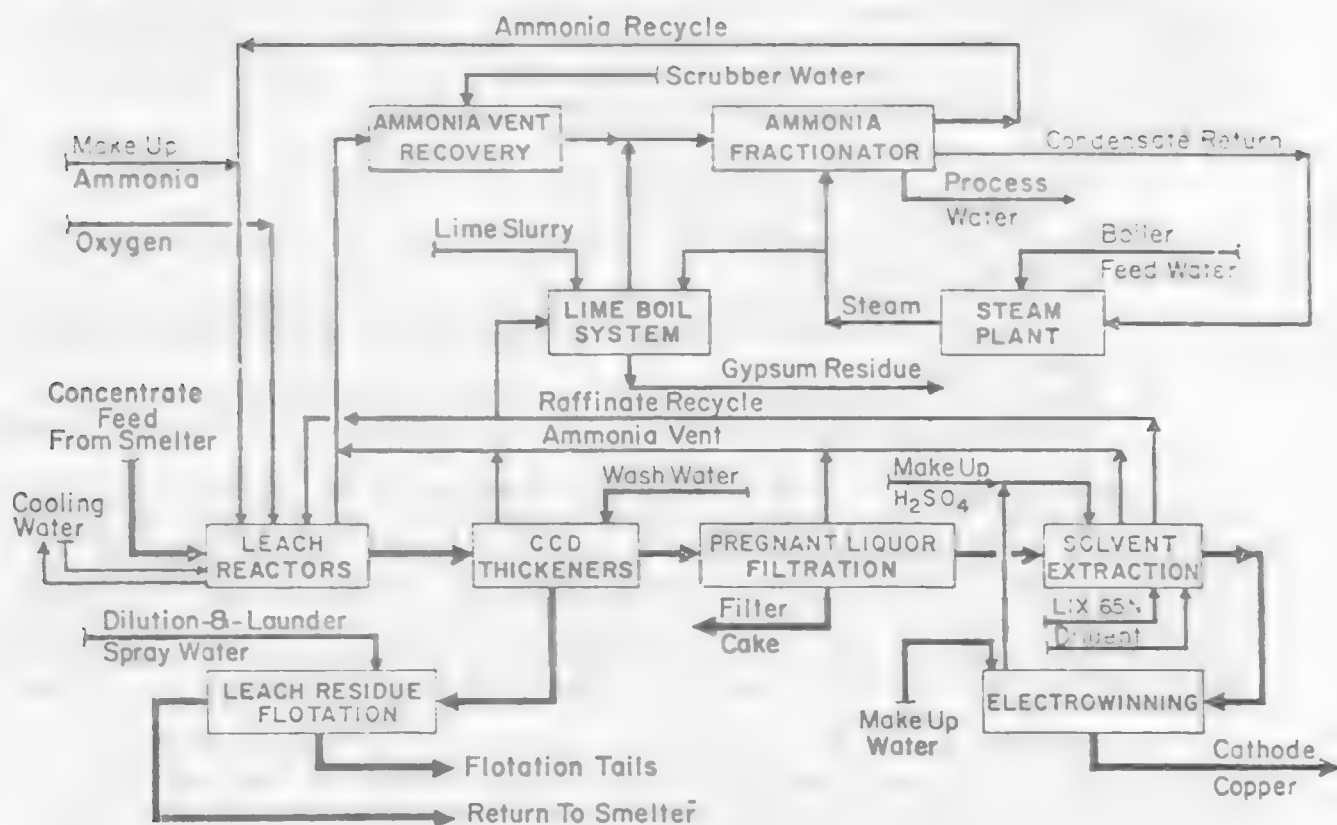
Ferric chloride leach processes offer some advantages, e.g., the sulfur layer which generally forms on the surface of the copper sulfide minerals in

Figure 5.8.2 Flow Diagram for Production of Copper and Zinc from Sulphide Concentrates.



Source: Evan, D., et.al., CIM Bull., 57, 1964.⁽⁵³⁾

Figure 5.8.3 Anaconda Arbiter Plant - Block Flow Diagram.



Source: Kuhn, M., et.al., CIM Bull., 67, No. 742, 1974. (54)

these reactions does not passivate the reaction to the extent encountered in sulfate systems; ferric iron is a stronger oxidizing agent than oxygen so that high temperature, high pressure autoclaves are not necessary. The problems which generally arise in these processes are due to the corrosive nature of the leach solution to the equipment and the difficulty on copper recovery from a chloride leach liquor.

Cyprus Process. ⁽⁵⁵⁾ This process has been developed by Cyprus Mine to replace the Cymet process. The plant envisaged at Bagdad, Arizona has a capacity of 75,000 tpy, and could reportedly be built for less than 50% of the cost of a conventional smelting and refining plant. Basically, the process can be described as four fundamental stages:

1. Leaching of copper concentrate in a ferric-chloride solution to produce cuprous ions in solution.
2. Precipitation of solid cuprous chloride by either vacuum or refrigeration techniques.
3. Reduction of the cuprous chloride crystals with hydrogen in a fluid-bed reactor to metallic copper, in the form of copper pellets mixed with 8% sand.
4. Removal of sand and impurities as slag by conventional smelting of the fluidbed reaction products and the casting of pure copper wirebar.

CLEAR Process. ⁽⁵⁶⁾ This process was developed by the Duval Corporation and is now being scaled up to a 32,500 tpy commercial operation in Arizona. The process recovers metallic copper from chalcopyrite and other copper-containing materials by ferric chloride oxidation to produce cupric chloride. The cupric chloride is reduced to cuprous chloride and copper is recovered by electrolysis. Ferric chloride is regenerated by oxidation, with a concurrent purge of iron, sulfate ions, and other impurities from the process solution.

By combining the ferric chloride oxidation and the ferric chloride regeneration, an advantageous reduction in iron content of the process solution is effected, along with significant retardation of scaling. The desired chloride molal concentration is maintained by the addition to the process solution of sodium chloride, potassium chloride, and/or magnesium chloride. Potassium chloride is a preferred source of chloride ions as a means of purging substantially all sulfate ions from the process solution. The flow sheet of CLEAR process is presented in figure 5.8.4.

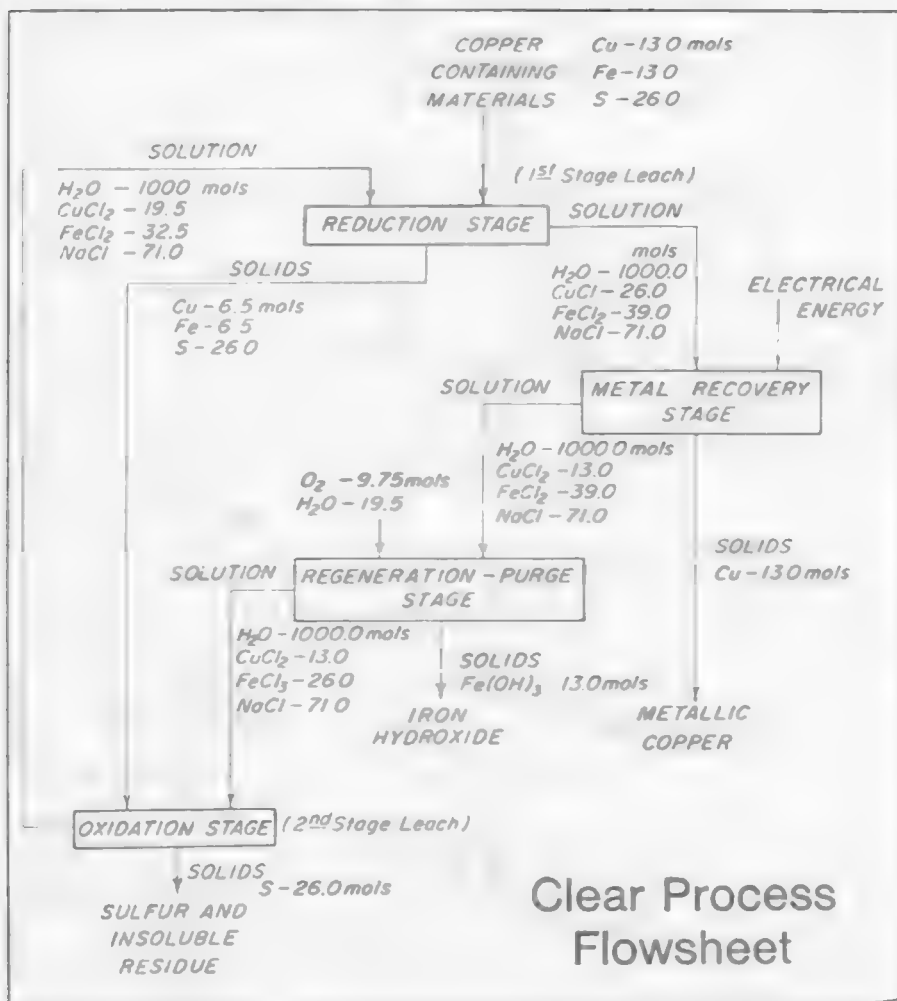
5.4.4.4 Acid Leach Processes.

Sherritt-Cominco Copper Process. ⁽⁵⁷⁾ The process developed by Sherritt-Gordon and Cominco has been pilot plant tested at Fort Saskatchewan in Canada. It is designed to treat copper concentrate with a high content of pyrite, also to recover sulfur in elemental form. The process involves the following steps, see figure 5.8.5.

1. Hydrogen thermal activation: Roasting is performed in hydrogen at 750-780°C to decompose chalcopyrite and pyrite into sulfides more amenable to acid leaching. The reactions are,

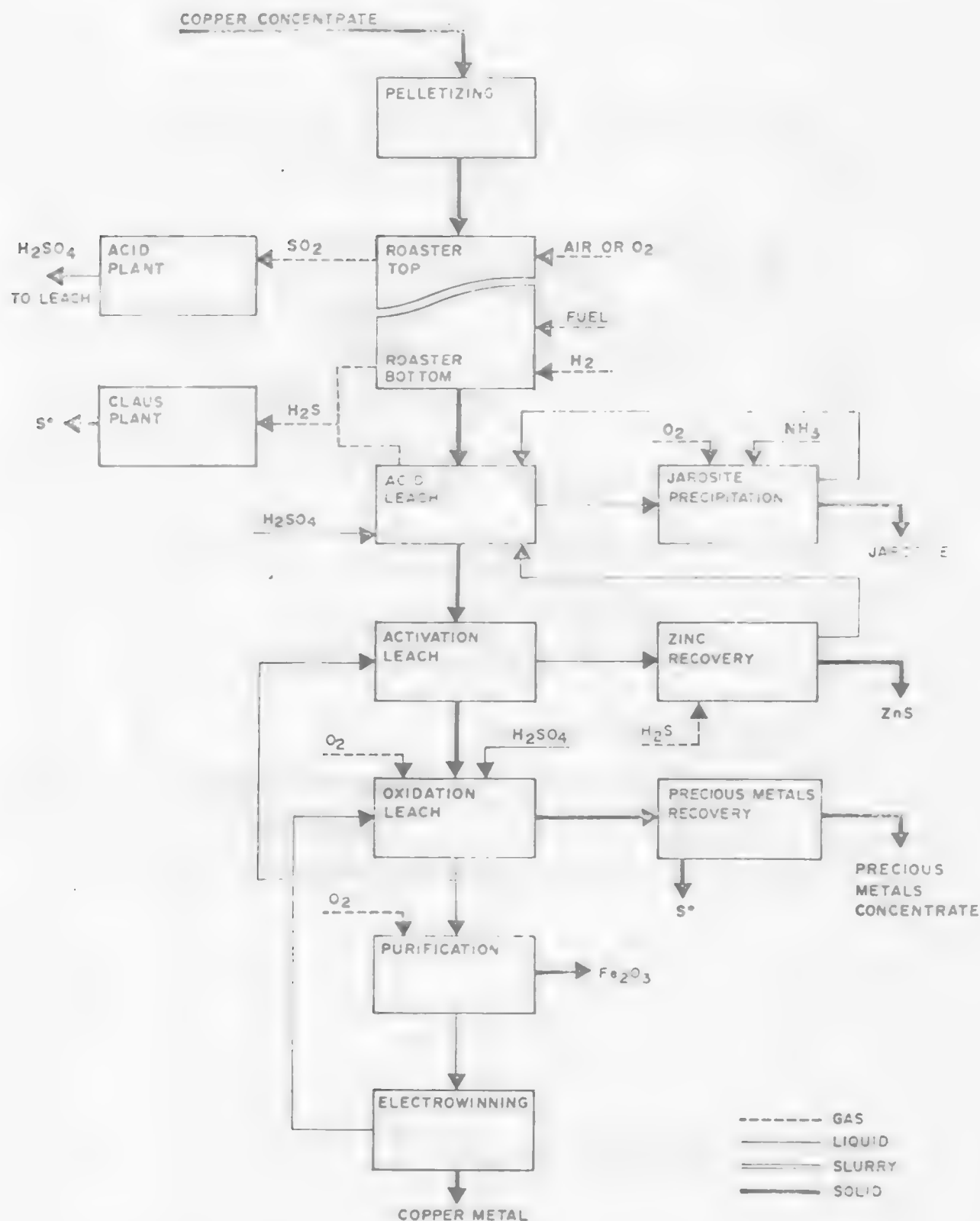


Figure 5.8.4 Clear Process.

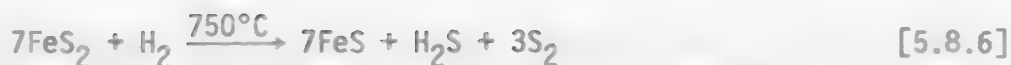


Source: Hydrometallurgy, EMJ, 1976. (56)

Figure 5.8.5. The Sherritt-Cominco Copper Process--Simplified Block Flow Diagram.

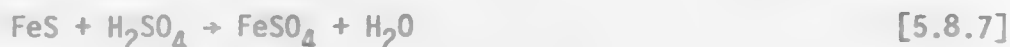


Source: Kawaika, P., et al., CIM Bull., 1978. (57)

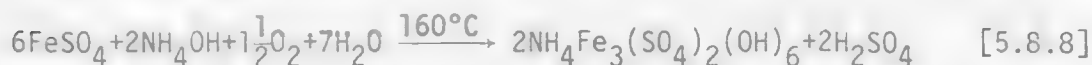


2. Acid leach: Iron is then selectively leached at 60°-85°C with sulfuric acid. It is subsequently rejected as jarosite:

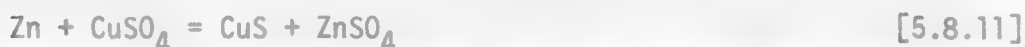
acid leach,



jarosite precipitation,



3. Activation leach: This leach is to ensure removal of the remaining iron and other impurities; also to activate some of the copper sulfides. The leaching is performed on the solid from stage 2 with CuSO_4 from the oxidation leach (stage 4) for one hour at 150°-160°C. The main reactions involved are,



4. Oxidation leach: The solid residue from the activation leach (stage 3) is leached with sulfuric acid at about 95°-110°C under oxygen pressure. About 98-99% of the copper is dissolved, and subsequently recovered by electro-winning or by hydrogen reduction.

The residue from the oxidation leach contains >98% of the silver and virtually all of the gold of the feed concentrate. These precious metals have been upgraded 50 to 100 fold and are recovered by subsequent treatment.

Nitric-Sulfuric Leach Process.⁽⁵⁸⁾ This process has been developed by E. I. DuPont de Nemours and Kennecott. The leaching reactions result in the following overall equation,



The process involves: leaching to dissolve 99% of copper in a 3-stage counter-current system with solid-liquid separation between each stage. The sulfuric acid has about 10% nitric acid added. The temperature is about 90°C. The leach stage is followed by a series of removal steps (nitric removal), iron removal and selenium removal). The copper is recovered by electrowinning.

Ferric Sulfate Leach.⁽⁵⁹⁾ This proposed process involves extensive size reduction of the copper sulfide concentrate by attritor milling. The attrition-ground product (average particle size of 0.5 μ) is leached at ambient pressure with a sulfuric acid-ferric sulfate solution at 90°C,



The copper is then separated from the leach liquor by solvent extraction and recovered from the strip solution by conventional electrolytic deposition. Ferric sulfate is regenerated and excess iron is removed by precipitation.

5.4.5 Leaching of Other Sulfide Minerals.

Hydrometallurgical processes to treat zinc sulfide, lead sulfide, molybdenum sulfide and other sulfide minerals have been studied quite extensively. Processing of zinc sulfide minerals is the most extensively developed and will be discussed here. Two processes are considered, i.e., the roast-leach or direct leach processes.

5.4.5.1 Roast-Leach Process for Zinc Sulfide.

The problem associated with the roast-leach process is that zinc ferrite ($\text{ZnO} \cdot \text{Fe}_2\text{O}_3$) forms during the pyrometallurgical oxidation roasting stage. Zinc ferrite is insoluble in dilute acid or neutral solutions, but dissolves in strong hot acid solutions. However, when hot acid leach is used, a large amount of iron also dissolves and an additional step is required to remove it from solution. The iron removal step is usually accomplished either by the geothite process or by the jarosite⁽⁶⁰⁾ process. The latter is more popular. Today there are more than ten zinc electrolytic plants that have adopted the jarosite process for iron removal.

A simplified roast-leach-jarosite process is presented in figure 5.8.6. Some operation data from Outokumpu Zinc Plant in Kokkola, Finland⁽⁶¹⁾ will be used to describe this process. The process involves the following steps.

1. Oxidation Roasting. Zinc concentrate containing about 50% Zn is roasted in a fluidized bed roaster at about 950°-1000°C. Sulfuric acid is produced from the flue gas.

2. Neutral Leach. The calcine (from step 1) containing 59.2% Zn is neutral leached in two agitation vessels in series. A total retention time of 5 hours is needed at a temperature between 70° to 80°C. The pH of the slurry is regulated, i.e., in the first reactor, the pH is maintained at 4.5. The pregnant solution from this step contains 147 g/l of Zn, 0.49 g/l of Cu, 0.35 g/l of Cd, 0.03 g/l Co and 0.03 g/l of Fe. The solution must be purified before electrolysis.

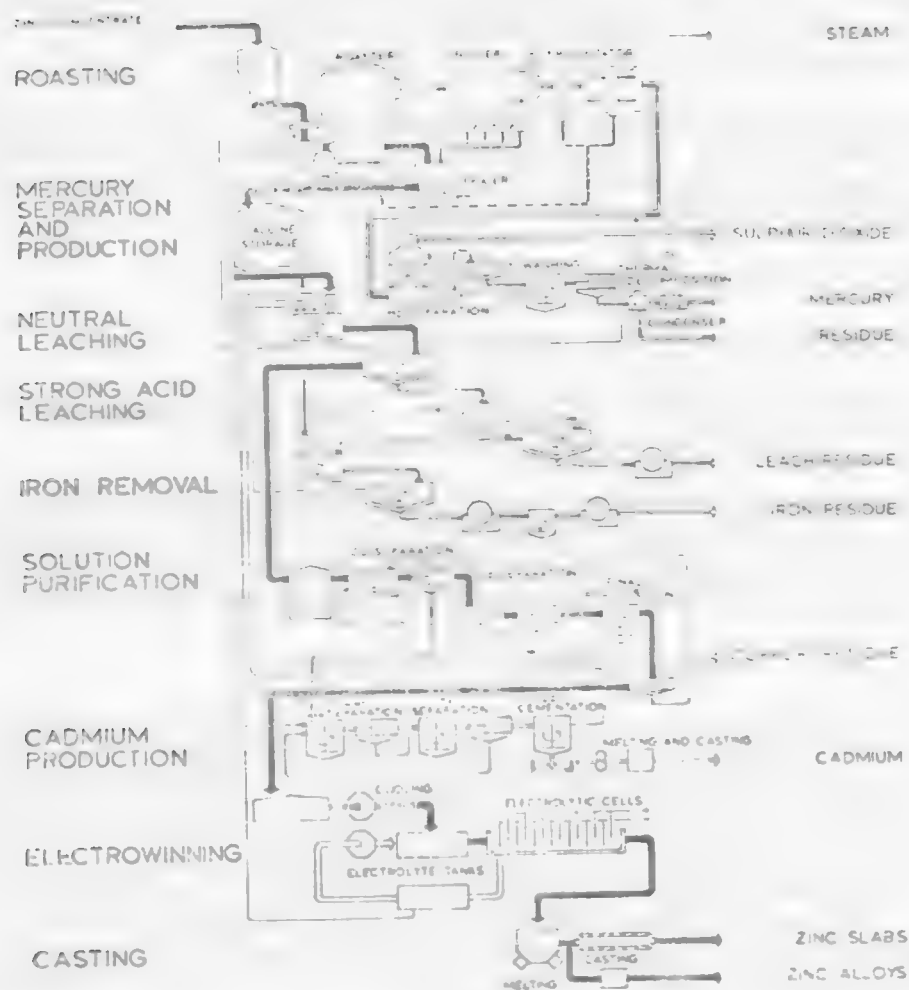
3. Hot Acid Leach. The residue from the neutral leach contains about 27% Zn. It is further treated in four agitation vessels in series at 95°C with spent electrolyte. The final acid concentration is 50 to 60 g/l H_2SO_4 . The reactions involved in this step are,



(Me being Zn, Cd, Cu, etc.)

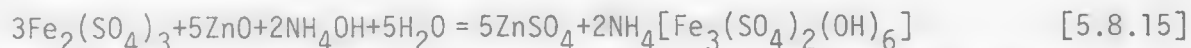
After the hot acid leach, the solution contains about 140 g/l of Zn, and 30 g/l of Fe. Usually, the slurry is charged to the iron precipitation step (Jarosite Process) without solid-liquid separation.

Figure 5.8.6. Acid Leaching of Zinc Calcines with Jarosite Process.



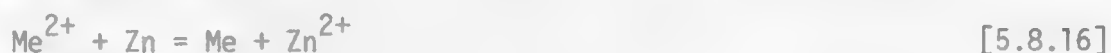
Source: Evans, D. J., International Sympos. on Hydromet., AIME, 1973.

4. **Jarosite Process.** The ferric iron in the hot acid leach solution is precipitated as a readily settling and filterable ammonium jarosite in a series of three reactors. The ammonium ion source is usually ammonium hydroxide. The jarosite reaction is,



The calcine, ZnO, is used as a neutralizing agent. After a total retention time of about 6-7 hours, the concentration of iron in the solution is reduced to 2.2 g/l. After a solid-liquid separation stage the solution is sent to the neutral leach step; the solid is sent to a land disposal area.

5. **Solution Purification.** The pregnant solution from the neutral leach has to be purified prior to electrolysis. The impurities are removed by charging Zn powder to the solution. The impurities are precipitated according to the cementation reaction,



(Me being Cu, Ni, Co, Cd, etc.)

The purified solution contains 152 g/l Zn, and only small amount of impurities: 0.1 mg/l Cu, <1.2 mg/l Cd, 0.028 g/l Fe, and 0.4 mg/l Co.

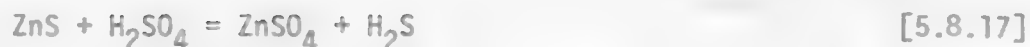
6. **Electrolysis.** The zinc content in the purified solution is electrowon. Inert anodes are made of lead containing 0.75% silver and the cathodes are aluminum. The cell is operated at a maximum current density of 660 amp/m² and current efficiency of 90%. The purity of the zinc cathode is 99.995%.

5.4.5.2 Direct Leaching of Zinc Sulfide.

Sheritt Gordon Ltd. has developed an ammonia oxidation leach to recover zinc metal from copper-zinc concentrates from their Bagacay and Sipalay Mines in the Philippines. A great deal of attention has also been given to the use of an acid pressure leach system which results in a recovery of elemental sulfur rather than sulfuric acid or ammonium sulfate. Elemental sulfur is easier to store, easier to handle and can be readily converted into other compounds. Cominco Ltd. has announced the start of construction of the world's first commercial-scale zinc pressure leach plant at Trail, British Columbia, Canada. Operation will begin in the spring of 1981. The pressure leach plant will produce 70,000 tons of zinc annually.

The pressure leaching technology,⁽⁶¹⁾ as announced, was developed jointly by Cominco and Sheritt-Gordon in 1977 at a pilot-plant project at Fort Saskatchewan, Alberta. Zinc concentrates will be reacted with sulfuric acid and oxygen at high temperature and pressure to dissolve the zinc and produce elemental sulfur. With the sulfur removed, the remaining zinc-rich slurry will be pumped to the sulfide leaching plant, where it will join the main flow from a conventional roast-leaching operation.

Several researchers have studied the fundamental aspect of acid pressure oxidation of zinc sulfide.⁽⁶²⁾ Ferric ions appear to be important as oxygen carriers. The reactions, of interest, are,



The overall leaching reaction is



The ferrous sulfate can be produced by pressure oxidation of iron sulfides present in the zinc concentrates, according to the reaction



and towards the end of the reaction, when nearly all the sulfuric acid has been reacted with zinc sulfide, the iron hydrolyses and precipitates as a mixture of ferric oxide and basic ferric sulfate.

Scott and Dyson⁽⁶³⁾ have studied the influence of catalytic agents on the oxidation of ZnS under pressure leaching conditions at 113°C in dilute sulfuric acid, i.e., 250 psi oxygen. Pronounced catalytic activity was found for copper, bismuth, ruthenium, molybdenum, and iron in order of decreasing effectiveness. To account for the activation effect, it was suggested that catalyst ions displace zinc from the surface layers of the solid, thereby making it electrically conducting. Under such conditions, zinc would be dissolved by a galvanic mechanism.



The authors further suggested that the metals copper, bismuth, and so forth, must also catalyze the cathodic reaction of oxygen (Equation [5.8.22]) at active sites on the crystal surface.

5.8.6 References.

1. R. M. Garrels and C. L. Christ, "Solutions, Minerals and Equilibria", New York, Harper and Row, 1965.
2. R. B. Bhappu, et.al., "Theoretical and Practical Studies on Dump Leaching", Trans, SME/AIME, 244, 307-320 (1969).
3. M. E. Wadsworth, "Physical Chemistry of Hydrometallurgy Electrochemical Processes in Leaching", The Draken Conference.
4. P. Marcantonio, "Chalcocite Dissolution in Acidic Ferric Sulfate Solutions", Ph.D. thesis, Dept. of Mining, Metallurgical and Fuels Engineering, University of Utah, 1976.
5. O. F. A. Koch, "Electrochemistry of Sulfide Minerals, Modern Aspects of Electrochemistry", Plenum Press, New York, No. 10, 211-237 (1975).
6. R. T. Shuey, "Semiconducting Ore Minerals", Elsevier Publishing, N.Y., 1975.
7. L. W. Bectstead and J. D. Miller, "Ammonia, Oxidation Leach of Chalcopyrite--Reaction Kinetics", and "Ammonia, Oxidation Leaching of Chalcopyrite--Surface Deposit Effect", Met. Trans., B, 8B, 19-38 (1977).
8. P. Marcantonio, "Chalcocite Dissolution in Acidic Ferric Sulfate Solution", Ph.D. thesis, Dept. of Mining, Metallurgical and Fuels Engineering, U. of Utah, 1976.
9. J. B. Hiskey and W. E. Wadsworth, "Galvanic Conversion of Chalcopyrite", Met. Trans. B, 6B, 183 (1975).
10. T. Biggler, D. A. Rand and R. Woods, "Oxygen Reduction on Sulfide Minerals, Part I. Kinetics and Mechanisms at Rotated Pyrite Electrodes", Electroanal. Chem. Interfacial. Electrochem. 60, 151 (1975).
11. F. Habash, "The Electro Metallurgy of Sulfides in Aqueous Solution", Min. Sci. Eng., 3, No. 3, 3-11 (1971).
12. E. Peters, et.al., "Theory of Leaching", in Hydrometallurgy: Theory and Practice--First Tutorial Symposium on Hydrometallurgy, the University of Denver, 1972.
13. G. W. Warren and W. E. Wadsworth, "The Electrochemical Oxidation of Chalcopyrite in Ammoniacal Solutions", presented at AIME Annual Meeting at Denver, 1978, reprint 78-B-68.
14. W. E. Wadsworth and E. E. Malout, "Rate Process in Hydrometallurgy", Hydrometallurgy: Theory and Practice--Second Tutorial Symposium on Extractive Metallurgy, U. of Utah and U. of Denver, 1972.
15. F. A. Forward and V. N. Mackiw, "Chemistry of the Ammonia Pressure Process for Leaching Nickel, Copper and Cobalt from Sheritt Gordon Sulfide Concentrates", J. of Metals, 7, 457-462 (1955).

16. D. K. Giles, "Kwinana Nickel Refinery", *Aust. Chem. Eng.*, 10, No. 2, 17-18 (1969).
17. V. N. Mackiw and T. W. Benz, "Application of Pressure Hydrometallurgy to the Production of Metallic Cobalt", *Extractive Metallurgy of Copper, Nickel, and Cobalt*, Interscience Publishers, New York, AIME, 503 (1961).
18. B. Medding and D. J. I. Evans, "The Changing Role of Hydrometallurgy", *CIM Bull.*, Feb., 42 (1971).
19. Anon, "Inco Develops New Route to Pure Nickel", *Can. Chem. Process*, 53, 67-69 (1969).
20. B. Medding and J. D. I. Evans, "The Changing Role of Metallurgy", *CIM Trans.*, 64, No. 706, 48-57 (1971).
21. R. P. Plasket and S. Romanchuk, "Recovery of Nickel and Copper from High-Grade Matte at Impala Platinum by the Sherritt Process", *Hydrometallurgy*, 3, 135-151 (1978).
22. P. B. Queneau, et.al., "Turbine Mixer Fundamentals and Scale-Up Method at the Port Nickel Refinery", *TMS. Trans. B, AIME*, 6B, March, 149 (1975).
23. J. D. Prater, et.al., "The Sulfation of Copper-Iron Sulfides with Concentrated Sulfuric Acid", *J. of Metals*, 22, No. 12, 23-27 (1970).
24. A. Vizsolyi, et.al., "Copper and Elemental Sulfur from Chalcopyrite by Pressure Leaching", *J. of Metals*, 19, No. 11, 52-59 (1967).
25. J. W. Braithwaite and M. E. Wadsworth, "Oxidation of Chalcopyrite Under Simulated Conditions of Deep Solution Mining", *Extractive Metallurgy of Copper, Vol. 2*, TMS/AIME 1976.
26. I. H. Warren, "A Study of the Acid Pressure Leaching of Chalcopyrite, Chalcocite and Covellite", *Aust. J. App. Sci.*, 9, No. 1, 36-51 (1958).
27. P. H. Yu, C. K. Hansen and M. E. Wadsworth, "A Kinetic Study of the Leaching of Chalcopyrite at Elevated Temperature", *Inter. Sym. on Hydromet.*, AIME, Chap. 15, 375 (1973).
28. F. A. Forward and I. H. Warren, "Extraction of Metals from Sulfide Ores by Wet Methods", *Met. Rev.*, 5, 137-164, 1960.
29. L. W. Beckstead, et.al., "Acid Ferric Sulfate Leaching of Attritor-Ground Chalcopyrite Concentrates", *Extractive Metallurgy of Copper*, J. C. Yannopoulos and J. C. Agarnal ed., AIME, Vol. 2, Chap. 31, 611-632 (1976).
30. J. E. Dutrizac, R. J. MacDonald and T. R. Ingraham, "The Kinetics of Dissolution of Synthetic Chalcopyrite in Aqueous Acidic Ferric Sulfate Solutions", *Trans. AIME*, 245, 955-959 (1969).
31. M. H. Stanczyk and C. Rampacek, "Oxidation Leaching of Copper Sulfides in Ammoniacal Pulps at Elevated Temperature and Pressure", USBM RI6808 (1966).

32. M. C. Kuhn, et.al., "Anaconda's Arbiter Process for Copper", CIM Bull., 67, No. 742, 62 (1974).
33. D. J. Evans, "Treatment of Copper-Zinc Concentrates by Pressure Hydro-metallurgy", CIM Bull., August, 857 (1964).
34. L. W. Beckstead and J. D. Miller, "Ammonia, Oxidation Leaching of Chalcopyrite--Reaction Kinetics and --Surface Deposit Effect", Met. Trans., 8B, 19-38 (1977).
35. G. W. Warren and M. E. Wadsworth, "The Electrochemical Oxidation of Chalcopyrite in Ammoniacal Solutions", presented at 1978 AIME Annual Meeting, SME/AIME reprint 78-B-68 (1978).
36. F. P. Haver and M. M. Wong, "Recovery of Elemental Sulfur from Non-ferrous Minerals. Ferric Chloride Leaching of Chalcopyrite Concentrate", USBM, R. I. 7474 (1971).
37. F. P. Haver, et.al., "Improvements in Ferric Chloride Leaching of Chalcopyrite Concentrate", USBM, RI 8007.
38. D. L. Jones and E. Peters, "The Leaching of Chalcopyrite with Ferric Sulfate and Ferric Chloride", Extractive Metall. of Copper, Vol. II, J. C. Yannopoulos and J. C. Agarnal ed., TMS/AIME, N.Y. 1976.
39. G. Bjorling and G. A. Kolta, "Oxidizing Leach of Sulfide Concentrates and Other Minerals Catalyzed by Nitric Acid", 7th Proc. Internat'l. Mineral Processing Congress, New York, N. Arbiter ed., Gordon and Breach, New York, 127-138 (1965).
40. J. D. Prater, et.al., "A Nitric Acid Route to Processing Copper Concentrates", SME/AIME, 254, 117 (1973).
41. G. W. Lower and R. B. Booth, "Recovery of Copper by Cyanidation", Mining Engineering, Nov. 56 (1975).
42. R. Shantz and W. W. Fisner, "Leaching Chalcocite with Cyanide", EM/J, Oct. 72 (1976).
43. E. E. Malouf, "Bioextractive Mining", SME/AIME short course, Bio Extractive Mining, Denver, Colorado, Feb. 1970.
44. A. B. Ray and P. A. Trudinger, The Biochemistry of Inorganic Compounds of Sulfur, London, Cambridge University press (1970).
45. P. A. Trudinger, "Microbes, Metals, and Minerals", Min. Sci. Eng., 3, No. 4, 1-3 (1971).
46. E. E. Malouf and J. D. Prater, "Role of Bacteria in the Alteration of Sulfide Minerals", J. of Metals, 13, 353-356 (1961).
47. J. A. Sutton and J. D. Corrick, "Leaching of Copper Sulfide Minerals with Selected Autotrophic Bacteria", USBM, RI 6423 (1964).

48. E. E. Malouf, "Bacteria Leaching", Hydrometallurgy: Theory and Practice Second Tutorial Symposium on Hydrometallurgy, Denver, Colorado, 1972.
49. E. E. Malouf, "Leaching as a Mining Tool", International Symposium on Hydrometallurgy, D. J. I. Evans and R. S. Shoemaker ed., AIME, New York, 615-626 (1973).
50. F. Habash, "Electrometallurgy of Sulfides in Aqueous Solutions", Mineral Sci. and Eng., 3, No. 3, 3-12 (1971).
51. P. R. Kruesi, "The Cymet Copper Process", Mining Congress Journal, Sept. 22 (1974).
52. W. A. Griffith, et.al., "Development of the Roast-Leach-Electrowin Process for Lakeshore", J. of Metals, 27, Feb., 17 (1975).
53. D. J. I. Evans, et.al., "Treatment of Copper-Zinc Concentrate by Pressure Hydrometallurgy", CIM Bull., 57, 857 (1964).
54. M. C. Kuhn, et.al., "Anaconda's Arbiter Process for Copper", CIM Bull., 67, No. 742, 62 (1974).
55. "New Copper Process from Cyprus is Billed as Technological Breakthrough", E/MJ, Oct., 33 (1977).
56. "Hydrometallurgy: New Processes Move to Commercialization", E/MJ, June, 244 (1976).
57. P. Kawalka, et.al., "The Sherritt-Cominco Copper Process--Part I: The Process, and Part II: Pilot-Plant Operation", CIM Bull., Feb., 105-139 (1978).
58. H. M. Brennecke, et.al., "The Nitric Sulfuric Leach Process for Recovery of Copper from Concentrate", presented at 1978 AIME Annual Meeting, Denver, Colorado, SME/AIME reprinting 78-B-113.
59. L. W. Beckstead, et.al., "Acid Ferric Sulfate Leaching of Attritor-Ground Chalcopyrite Concentrates", Extractive Metallurgy of Copper, J. C. Yano-poulous and J. C. Agarnal ed., AIME, Vol. 2, Chap. 31, 611-632 (1976).
60. A. R. Gordon and R. W. Pickering, "Improved Leaching Technologies in the Electrolytic Zinc Industry", Met. Trans. B, 6B, March, 43-53 (1975).
61. "World's First Zinc Pressure Leach Plant", CIM Bull., 72, May, 122(1979).
62. R. Derry, "Pressure Hydrometallurgy: A Review", Min. Sci. Eng., Vol. 4, No. 1, 3-24 (1972).
63. T. R. Scott and N. F. Dyson, "The Catalyzed Oxidation of Zinc Sulfide Under Acid Pressure Leaching Conditions", TMS/AIME Trans., 242, Sept., 1815-1821 (1968).

UNIT PROCESS IN EXTRACTIVE METALLURGY
HYDROMETALLURGY

Module 8

Solution Concentration and
Purification

FIVE LEARNING
ACTIVITIES

Module 6 Concepts

Extraction, Concentration, and Purification

6.1 Solvent Extraction*

Learning Activity 1

1. Introduction
2. Characterization of Extraction Reaction
3. Extraction Chemistry
4. Solvent Extraction Systems

Learning Activity 2

Learning Activity 3

6.2 Ion Exchange**

Learning Activity 4

1. Introduction
2. General Principles
 1. Chemical Composition and Structure of Resins
 2. Selectivity of Ion Exchanger
 3. Kinetics of Ion Exchange Reaction
3. Hydrometallurgical Applications
 1. Uranium Extraction--Chemistry of Adsorption and Elution
 2. Uranium Ion Exchange--Processes and Equipment
 3. Extraction of Other Metals
 4. Separation of Metal Ions

Learning Activity 5

*Dr. J. D. Miller

Professor of Metallurgical Engineering
Department of Metallurgy and Metallurgical
Engineering
University of Utah

**Dr. H. H. Haung

Assistant Professor of Metallurgical Engineering
Montana College of Mineral Science and Technology

LEARNING ACTIVITY 1

6.1 Solvent Extraction

Learning Activity Objective

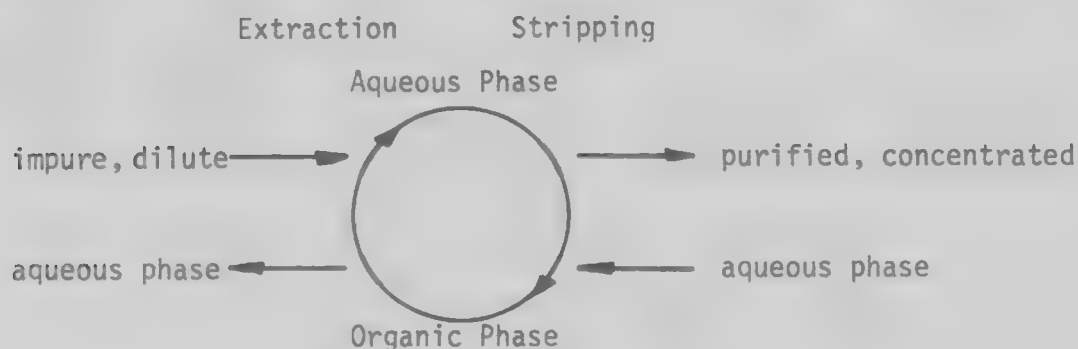
After completing your study of this learning activity material you should be able to describe solvent extraction reaction types and be able to characterize the main features of the extraction process.

6.1.1 Introduction

The phenomenon of the partition of a particular component between an aqueous and organic phase was reported as early as 1842 by Pergot.

Although this technique of concentrating and separating a given component from an aqueous phase has been used extensively by analytical chemists during the early part of the 20th century, it was not until the 1950's that solvent extraction was used on an industrial scale in hydrometallurgy. The large scale development of solvent extraction technology in the processing of natural resources was initiated by the uranium boom for the development of nuclear weapons and as a potential energy source. Since that time the use of S-X has expanded. A large number of hydrometallurgical processes use solvent extraction in processing of natural resources as shown in Table 6.1.1.

The basis for the separation is the use of a recycled organic phase which acts as the exchange media to affect the selective partition of a given component. The component is selectively transferred to the organic phase during extraction and then released in a concentrated, purified solution during stripping.



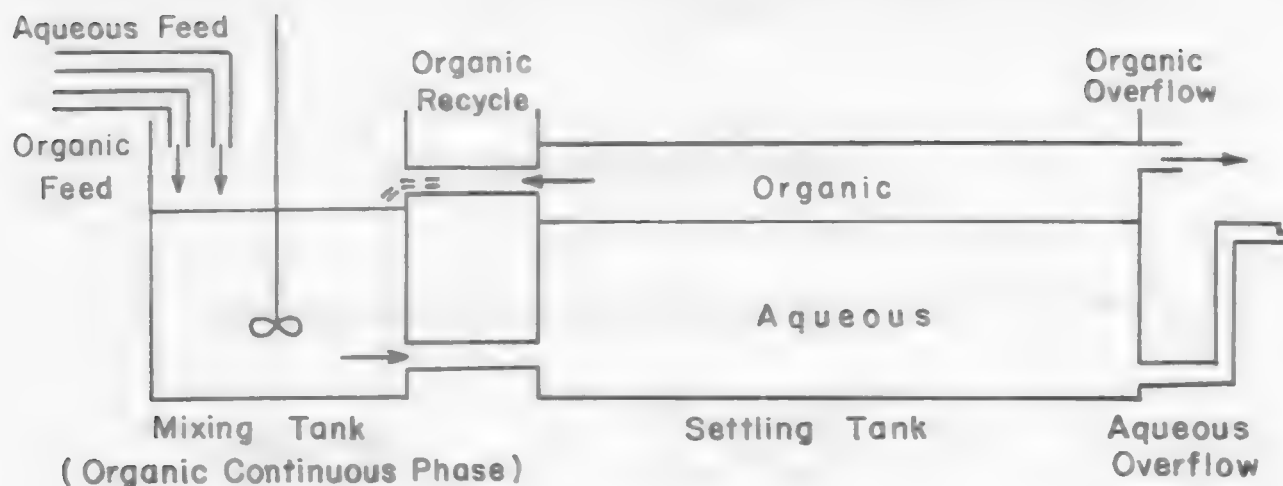
A number of different reactors are available to accomplish the solvent extraction reaction but the most common in the mineral industry is a mixer-settler unit as shown in Figure 6.1.1. In essence the unit consists of a stirred tank reactor coupled to a settling tank to allow for phase disengagement. Generally the reaction rates are rapid and a number of stages of mixer-settler units are used in countercurrent flow to achieve the desired extent of reaction.

6.1.1 Solvent Extraction Applications in the Processing of Mineral Resources.

Element	Extracted Species	Feed Solution	Organic Solution	Strip Solution	Reaction Type
Beryllium	Cation	Acid sulfate	EHPA	$(\text{NH}_4)_2\text{CO}_3$	Ion exchange
Boron	Neutral	Alkaline brine	Phenyl glycol	H_2SO_4	Solvation
Bromine	do	Brine	Tetrabromoethane	C_2H_2	"
Columbium-tantalum	{Neutral columbium} {Neutral tantalum	H_2SO_4 -HF	MIBK	Cb, H_2SO_4 Ta, Kf	"
Copper	Cation	Acid sulfate or $\text{NH}_4\text{OH}-(\text{NH}_4)_2\text{CO}_3$	LIX-64N	H_2SO_4	Chelation
Hafnium-zirconium	{Neutral hafnium} {Neutral zirconium	HCl-HCNS HNO_3	MIBK TBP	H_2SO_4 H_2O	Solvation
Molybdenum	Anion	Acid sulfate	Tertiary amine	NH_4OH	Ion exchange
Phosphorus	Neutral	H_3PO_4 -CaCl ₂	C ₄ -C ₅ alcohol	H_2O	Solvation
Rare earths	Cation	Acid chloride	EHPA	HCl	Ion exchange
Rhenium	Anion	Alkaline sulfate	Quaternary amine	HClO_4 or NH_4SCN	"
Thorium	Cation	Acid Sulfate	HDPA	H_2SO_4	"
Tungsten	Anion	do	Secondary amine	NH_4OH	"
	{Anion {Cation {Neutral	do	Tertiary amine	$\text{NH}_3-(\text{NH}_4)\text{SO}_4$	"
Uranium		Acid sulfate-chloride Acid nitrite	EHPA	Na_2CO_3	Solvation
		Acid chloride Acid sulfate-chloride	TBP	H_2O	
Vanadium	{Anion {Cation		Tertiary amine EHPA	$\text{NH}_3-\text{NH}_4\text{Cl}$ H_2SO_4	Ion exchange

Source: Bureau of Mines Information Circular IC 8502.

Figure 6.1.1 Mixer Settler.



Mixer-Settler Diagram

The key to the success of the separation is the nature of the organic phase and whether a specific selective chemical interaction can be achieved with a particular component in the aqueous phase. Notice, that this must be a reversible reaction; a unique and important feature of solvent extraction systems. Frequently, for a particular S-X system, the following components of the organic phase can be identified:

- a. Carrier, or diluent - inert compound
- | |
|------------------------|
| {aliphatic (kerosene) |
| {aromatic (rykue) |
| {napthenic (naphthene) |

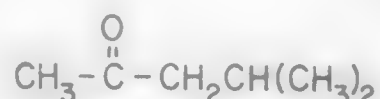
This component of the organic phase can affect the quality of the separation due to chemical effects (activity considerations and solvation) and physical effects (phase disengagement).

- b. Extractant - The reactant, a compound containing a functional group that is capable of chemically reacting with a particular species in the aqueous phase.

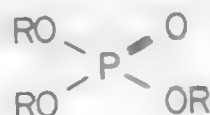
Solvent extraction reaction systems can be conveniently categorized according to three different reaction types based on the type of bonds involved

in the reaction. The first reaction type is solvation which involves transfer of neutral molecular species from the aqueous phase to the organic phase. In this case simple solubility considerations govern the extent of extraction, i.e., displacement of coordinated water molecules by solvent molecule. The following systems would be included in this category; e.g.,

- nobium separation from tantalum and zirconium separation from hafnium by methylisobutylketone (MIBK)

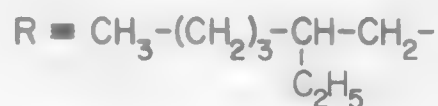


- uranium and thorium extraction by tributyl phosphate (TBP)



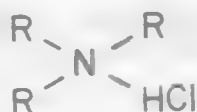
The second reaction type is the exchange reaction which involves the formation of more specific bonds between an extractive and an aqueous species. This chemical reaction can be thought of as simply the formation of an organic salt compound from an acid base or other salt. The extractants encountered in this category will be discussed later. The following systems are representative of the exchange reaction, e.g.,

- beryllium extraction with the cationic extractant di-ethylhexyl phosphoric acid (DEHPA)



The beryllium cation exchanges with the hydrogen atom of the acid to form the organic salt compound which is soluble in the carrier.

- vanadium extraction with an anionic extractant tertiary amine chloride (R_3NCl)



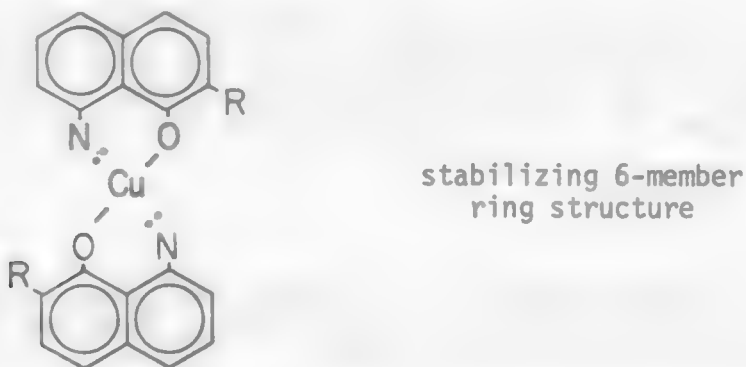
The vanadium anion exchanges with the chloride ion.

The third reaction type, chelation, involves the formation of even stronger and more specific chemical bonds and in essence is an exchange reaction. The term chelation comes from the Greek word for crab's claw which is an accurate description for it is convenient in these reactions to think of the extractant as pinching the extracted aqueous species forming a closed ring structure which lends stability to the extracted species. These extractants have been used by analytical chemists to make specific analytical separations for a number of years and in the 1960's were developed to be used on an industrial scale in hydrometallurgical processes. An excellent example is the use of oxine-type molecules;

--copper extraction with oxine (hydroxyquinoline) - Kelex 100



The exchangeable hydrogen atom of the oxine is released and the copper salt that forms is soluble in the appropriate carrier dilution stabilized by the following 6-membered structure:



6.1.2 Characterization of Extraction Reaction.

The effectiveness of a particular solvent extraction reaction can be described in several different ways. Generally the effectiveness of a particular system is determined from pseudo-equilibrium measurements (shake-out tests) made with a separatory funnel. From these measurements the following parameters and functions are used to characterize the solvent extraction reaction.

1. Distribution Coefficient (D) - sometimes referred to as the partition coefficient. The distribution coefficient is the ratio of the concentration of species i in the organic phase divided by the concentration of species i in the aqueous phase. Sometimes this is distinguished from the extraction coefficient though generally in hydrometallurgy they are used interchangeably.

2. Extraction Coefficient (E) - The extraction coefficient is defined as the total concentration of an element in the organic phase divided by the total concentration of the element in the aqueous phase. In a formal sense the difference between extraction and distribution coefficient would be that the extraction coefficient considers all species in either phase which contain the element in question. Clearly from an engineering standpoint we are most interested in considering all species of a given element whatever the coefficient is called.

As should be expected, this experimentally determined coefficient is related to the equilibrium constant for the extraction reaction. For a simple reaction of a metal ion, M^{++} , with an acid extraction



the mass action expression is

$$K = \frac{(H^+)^2(R_2M)}{(M^{++})(RH)^2} \quad [6.1.2]$$

or assuming no other species in the system the extraction coefficient would be

$$E = \left[\frac{RH}{H^+} \right]^2 K \quad [6.1.3]$$

3. Selectivity Index (S_B^A) - The selectivity index is used to describe the extent to which a favorable extraction can be achieved. The selectivity index is the ratio of extraction coefficients for two different elements achieved in a single shake-out test involving both elements

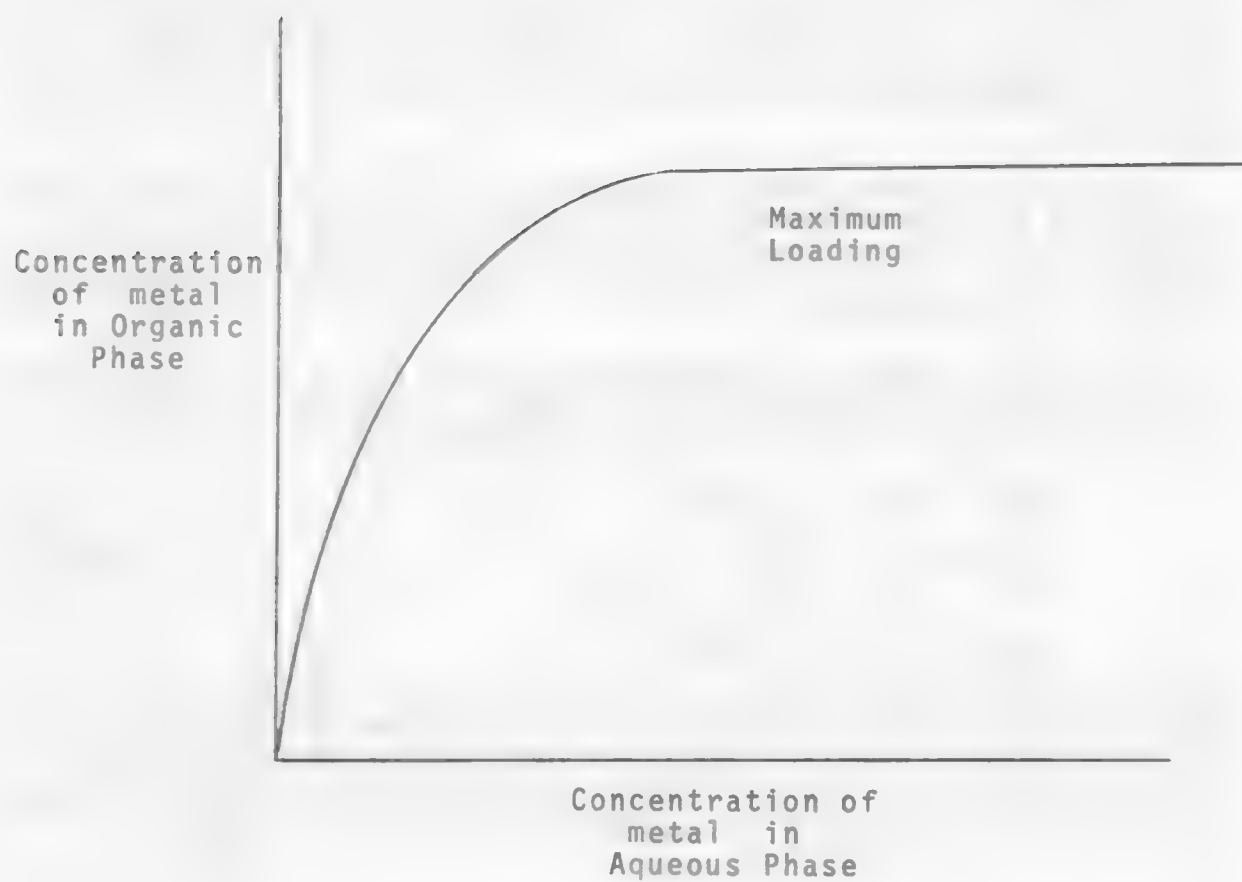
$$S_B^A = \frac{E_B^A}{E_B^B} \quad [6.1.4]$$

4. Percent Extracted - The percent extraction represents the fraction of an element present in the feed solution which has been extracted upon contact with an organic phase.

5. Extraction Isotherm - The extraction isotherm is probably the most significant method of characterizing the solvent extraction system. Basically the extraction isotherm is a plot of the concentration of the specified element in the organic phase vs. the concentration of that element in the aqueous phase, figure 6.1.2. Some aspects of the plot are of importance. First of all, how is the isotherm determined experimentally? Naturally the concentrations in each phase must be measured, typically by atomic absorption. Experimentally, the following techniques are used. Technique (b) is frequently preferred.

- a. vary the concentration of the element in the aqueous feed (this doesn't represent a real system),

Figure 6.1.2 Extraction Isotherm (Schematic).

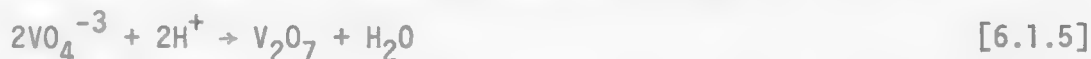


- b. vary the phase ratio (A/O), i.e., a fixed aqueous feed composition is used,
- c. repeated contacts with fresh organic. The aqueous feed composition is fixed.

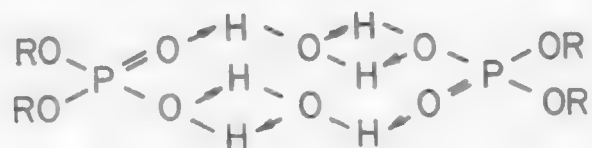
The normal shape of an extraction isotherm is characterized by a rapidly rising curve (the greater the slope, the greater the specificity. The extraction coefficient is the slope at any point on the curve) which reaches a plateau at higher concentrations in the aqueous phase where the capacity of the extractant has been exhausted. This plateau level is referred to as the point of maximum loading where the reaction has essentially been driven to completion.

Deviations from the normal isotherm (such as the S-type isotherm) may result from the fact that sufficient time for equilibration has not been allowed. This situation can arise from slow complexation reactions in the aqueous phase or from slow inter and intra-molecular bonding reactions in the organic phase, figure 6.1.3.

This S-type isotherm is sometimes encountered due to slow complexation reactions, e.g., vanadium extracted by amines. The complex oxyanion that forms and the rate at which it forms is dependent on pH.



Other deviations in the extraction isotherm can be due to interactions in the organic phase. In the case of extraction with concentrated alkyl phosphoric acids, the extent of reaction can be inhibited due to the formation of polynierie species. For example, the dihydrate dimer has been identified and its stability can influence the equilibrium position of the system.



Finally, in principle the isotherm could go through a maximum; an effect which may arise due to an insufficient concentration of liquid to complex a particular metal. This is to say that at higher metal ion concentrations in the aqueous phase and when an anionic complex is extracted, there may not be enough of the anionic liquid to form the appropriate anionic complex and allow complete extraction. The effect is depicted schematically in figure 6.1.4.

Figure 6.1.3 S-Type Isotherm.

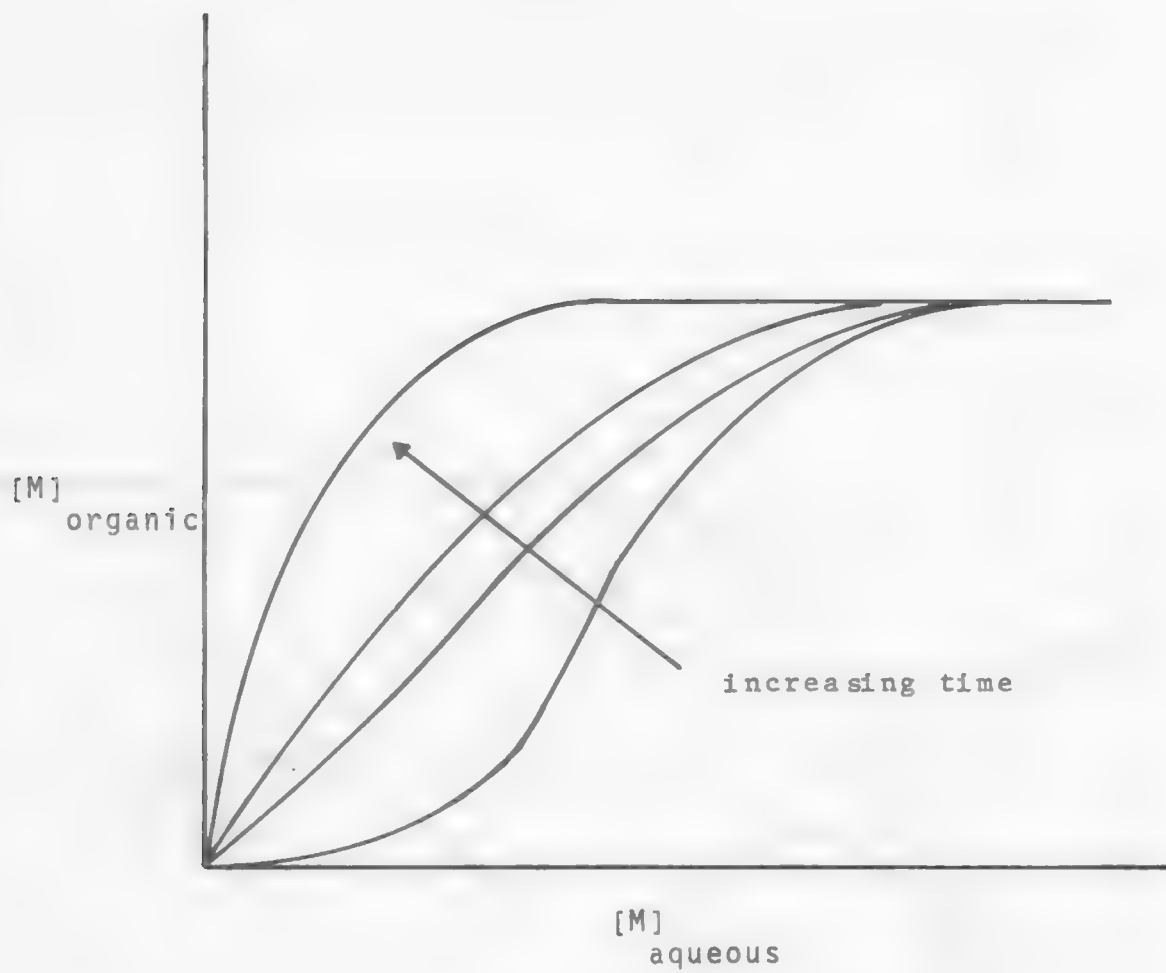
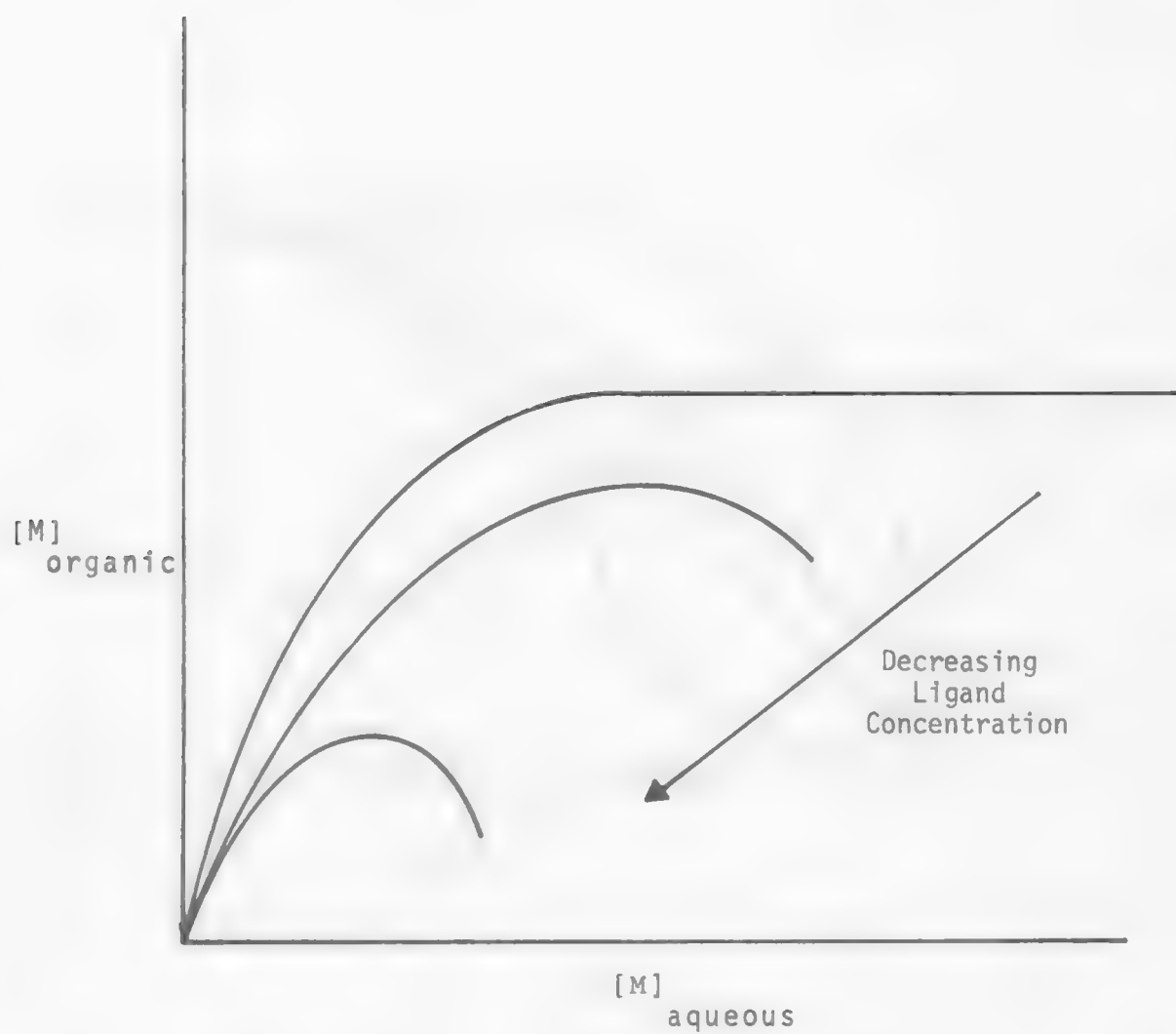


Figure 6.1.4 Influence of Decreasing Ligand Concentration, Schematic.



LEARNING ACTIVITY 2

6.1.3 Extractive ChemistryLearning Activity Objective

After completing this learning activity you should be able to describe the fundamental chemistry about the commonly used solvent extractant.

Organic solutions differ significantly from aqueous solutions in that there is little, if any, ionization and the solute is present as neutral molecular species. Solute-solute and solute-solvent interactions arise primarily due to hydrogen bonds.

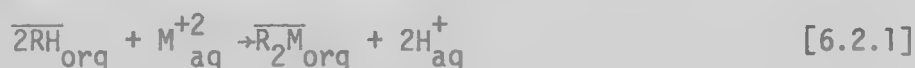
Cationic Extractants

Cationic extractants are generally in the acid form and exchange their hydrogen atom for a particular cation. As would be expected, then, the strength of the acid group is an important consideration in the evaluation of the effectiveness of a particular extractant for a given system.

For simple organic acids, the acidity, or extent of extraction, can be controlled and predicted by substituents on the extractant molecule. As the substituents become more electronegative, the extractant becomes a stronger acid due to electron delocalization. Common cationic extractants are presented in Table 6.2.1.

Carboxylic Acids. Carboxylic acids which are characterized by the carboxylate group (COOH) have limited use as extractants in the hydro-metallurgical processing of natural resources.

The two commercially available extractants are the cyclic naphthenic acid and the branched chain versatic acid. In the simplest case, extraction of a divalent metal ion can be represented by



As seen from this equation the extraction is a function of pH. The pH of effective extractions can be varied by controlling the substitutional group used.

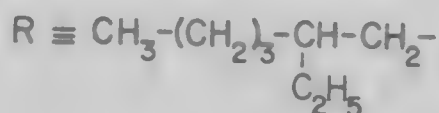
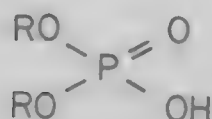
Although carboxylic acids are much less expensive than phosphoric acid extractions (1/5 the cost) and chelating extractants (1/10 the cost), they are of limited use. One reason is that they exhibit a rather high solubility especially at higher pH values. For example the solubility of naphthenic acid at pH 4 is 0.09 gpl and increases to 0.9 gpl at pH 6.5.

The solution of versatic acid varies from 0.07 gpl to 0.25 gpl. Of course this solubility represents lost extractant which is not recycled and adds substantially to the operating cost.

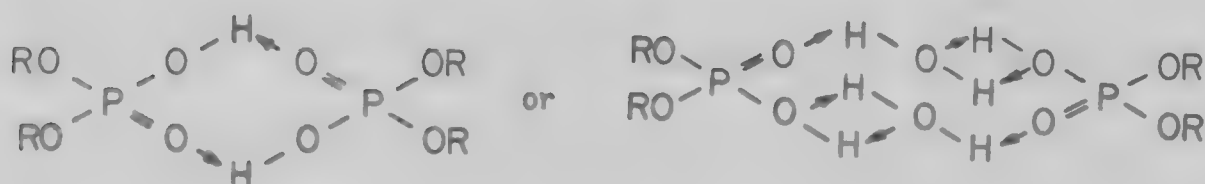
Alkyl Phosphoric Acid Extractants. The monobasic dialkyl phosphoric acid extractants frequently form dimers in the organic phase and the reaction can be written



The most common extractant is DEHPA



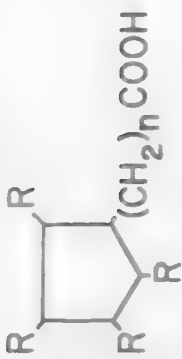


Dimerization is effected via strong intermolecular hydrogen bonding



Undiluted systems frequently exhibit an acid to water molecules of unity and a dimer structure has been proposed which unaffectedly accounts for the means by which water is dissolved in the organic phase.

Polar organic modifier such as alcohols can be added to prevent the formation of the dimer. It appears that with these extractants a pseudo chelate structure may form, however the stability is not as great as would be expected for an 8 member ring.

Table 6.2.1. Common Cationic Extractions.

Reagent	Structure	Availability	Typical Uses
Naphentic acids	 $ \begin{array}{c} R \\ \diagup \quad \diagdown \\ R \quad \quad R \\ \diagdown \quad \diagup \\ R \quad \quad R \\ \diagup \quad \diagdown \\ (CH_2)_n COOH \end{array} $	Commercial (Shell Chemical Co.)	Proposed extractant for dibasic metal ions probably in commercial use in Eastern Europe/Russia.
Versatic acids	 $ \begin{array}{c} CH_3 \\ \diagdown \\ R_2 - C \\ \diagup \\ R_1 \end{array} \begin{array}{c} COOH \end{array} $ <p>$(R_1, R_2 = C_3 - C_4 \text{ chains})$</p>	Commercial (Shell Chemical Co.)	Copper/nickel separation. Treatment of rare earth solution.
Di-2-ethyl hexylphosphoric acid (DEHPA)	 $ (CH_3(CH_2)_3CH(CH_2)_2)_2P(=O)(OH) $	Commercial (Union Carbide)	Rare earth separations. Has been used for uranium recovery from leach liquors. Beryllium extraction.

Chelation Extractants

A number of chelating extractants are now available for use in hydrometallurgical systems. The use of this type of extractant began in the 1960's when the LIX extractants for copper were introduced by General Mills. Since that time many new extractants have been developed. Currently available extractants in the acid form are listed in Table 6.2.2. Basically, the following types of chelating extractants are being used:

hydroxyoximes
oximes (hydroxyquinoline)
 β diketones

In each case the distinguishing feature of the chelating extractants is the high selectivity for a specific ion which arises from the strong stability of the ring structure of the chelate complex.

Commercial hydroxyoximes were first marketed by General Mills in 1965. The first copper extraction plant was the Bluebird plant constructed in 1968. Since that time many plants have been installed. Most recently N'Changa Consolidated Copper Company has built a plant capable of processing 14,000 gpm at Chingola, Zambia. The size of this plant alone represents an area equivalent to three football fields.

The stability of LIX type extractants is dependent on temperature, oxidation potential and acidity. Extended use of these extractants as any other extractant results in their degradation - they wear out. Table 6.2.3 shows the effect of temperature on the half life of both the α -hydroxyoxime and the β hydroxyoxime.

Anionic Extractants

Anion exchange processes are analogous to resin ion exchangers. The extraction process can be described simply as:



where $\overline{B^{n-}}$ is an n - valent anion, $\overline{R_4N^+}$ is an alkyl ammonium cation, and R is alkyl chains or hydrogen. The barred species are present in the organic phase.

This reaction is an oversimplification of the extraction reaction occurring in many systems but actual descriptions are beyond the scope of this course.

The industrially important anionic extractants are limited to the amine extractants as listed in Table 6.2.4. The primary amine which acts as a weak base is rather soluble in the aqueous phase and has limited

Table 6.2.2. Common Chelating Extractants.

Reagent	Structure	Availability	Typical Uses
LIX65N		Commercial (General Mills)	Copper extraction from ammoniacal solution. Also extracts nickel and cobalt.
LIX64N (LIX65N + LIX63)		Commercial (General Mills)	Copper extractant from acidic leach liquors selective for copper over ferric iron.
KELEX 170		Commercial (Ashland Chemical)	Copper extractant from acidic leach liquors selective for copper over ferric iron.
SME 529		Commercial (Shell Chemical Co.)	Copper extractant from acidic leach liquors selective for copper over ferric iron.
polyol		Commercial (Dow Chemical)	Boron extraction from brines.

application, while the tertiary and quaternary amines act as strong bases and are frequently used in solvent extraction systems. Amine extractants are used in the processing of uranium, vanadium, rhenium, cobalt, and nickel. These compounds extract complex metallic anions, i.e.,

- a) Oxyanions:
vanadates
rhenates
- b) Complex anions:
sulfates $\text{UO}_2(\text{SO}_4)_2$
chlorides $\text{CoCl}_4^{=}$

Table 6.2.3. Effect of Temperature on Life Terms.

Organic Phase: 5% LIX 65N, 2% LIX 63, n Napoleon 470
Aqueous Phase: 20 g/l Cu, 150 g/l H_2SO_4

It should be noted that this mixture of LIX 65N and LIX 63 is not meant to be typical of commercial LIX 64N material.

Temperature	Half Life of LIX 63	Half Life of LIX 65N
82°C	78 days (0.87%/day)	280 days (0.25%/day)
55°C	300 days (0.22%/day)	1,000 days (0.064%/day)
30°C	1,100 days (0.06%/day)	Over 4,500 days % too small to measure

Solvating Extractant

The main reaction of extraction by solvation involves the transfer of a neutral metal salt or metal complex from the aqueous to the organic phase by solvation of the metal ion. The reaction can be represented as



where $(\text{MA})(\text{H}_2\text{O})_m$ is the hydrated neutral ion pair and S is the extractant. Such solution agents can be alcohols, ethers, esters, ketones, or phosphorus-containing compounds such as trialkyl phosphates and trialkyl phosphine oxides. The common used solvating extractants are listed in Table 6.2.5.

Table 6.2.4. Anionic Extractants.

Reagent	Structure	Availability	Typical Uses
Primene JMT	$ \begin{array}{c} \text{CH}_3 \qquad \text{CH}_3 \\ \qquad \quad \\ \text{CH}_3 - \text{CH} - (\text{CH}_2 - \text{CH})_4 - \text{NH}_2 \\ \qquad \quad \\ \text{CH}_3 \qquad \text{CH}_3 \end{array} $	Commercial (Rohm and Haas)	No known commercial use. Proposed for iron removal. Generally useful for extraction of metals from acid sulphate solution.
LA-1 and LA-2	$ \begin{array}{c} \text{R}_2\text{NH} \\ \text{N lauryl trialkyl methyl amine} \end{array} $	Commercial (Rohm and Haas)	Uranium extraction from leach liquors.
Alamine 336	$ \begin{array}{c} \text{R}_3\text{N} \\ \text{R} \equiv \text{C}_8 - \text{C}_{10} \end{array} $	Commercial (General Mills Inc.)	Extraction of uranium from leach liquors. Vanadium extraction, tungsten extraction. Proposed for Ni, Co extraction from chloride solution.
Aliquat 336	$ \begin{array}{c} (\text{R}_3\text{N}^+\text{CH}_3)\text{Cl}^- \\ \text{R} \equiv \text{C}_8 - \text{C}_{10} \end{array} $	Commercial (General Mills Inc.)	Vanadium extraction. Chromate extraction.

Table 6.2.5. Solvating Extractants.

<u>Reagent</u>	<u>Structure</u>	<u>Availability</u>	<u>Typical Uses</u>
Tributylphosphate	$(\text{BuO})_3\text{P}=\text{O}$	Commercial (Albright and Wilson)	Refining of U_3O_8 concentrates. Uranium/plutonium separation in nuclear fuel reprocessing, zirconium/hafnium separations. Rare earth separations. Thorium extraction.
Methyl isobutylketone	$\begin{array}{c} \text{CH}_3 \\ \diagup \\ \text{C}=\text{O} \\ \diagdown \\ \text{Bu}^i \end{array}$	Commercial	Niobium/tantalum separation. Zirconium/hafnium separation.
$\text{C}_4 - \text{C}_5$ alcohol	$\text{CH}_3(\text{CH}_2)_3 \text{ or } 4 \text{ OH}$	Commercial	Extraction of H_3PO_4 from acid chloride solutions.

LEARNING ACTIVITY 3

6.3.1 Solvent Extraction Systems

Learning Activity Objectives

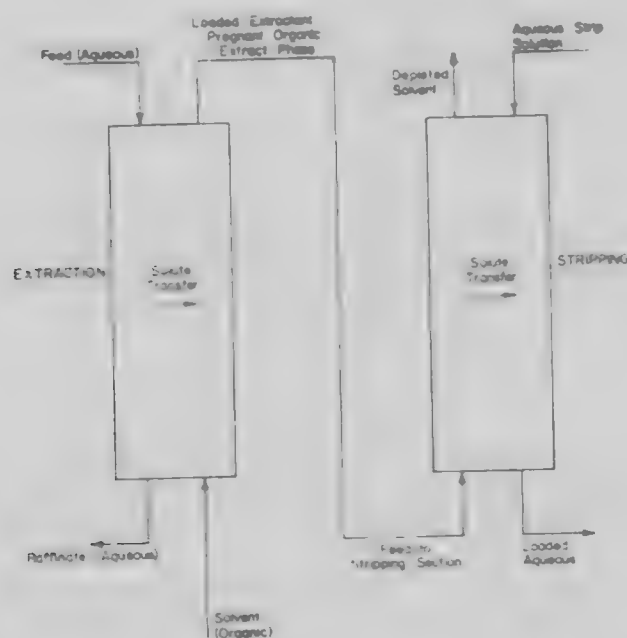
After completing your study of this learning activity material you should be able to discuss the importance of solvent extraction; the important control parameters; the type of equipment used in industrial practice; and be able to describe examples of the application of solvent extraction to commercial processes.

The material in this learning activity is a condensed version of a published article by John O. Golden. It is quoted from the article by written permission.

Essentially, liquid-liquid extraction as usually applied in the minerals industry involves two basic steps (Figure 6.3.1).

- (1) extraction
- (2) stripping

Figure 6.3.1. Extraction-stripping process for mineral separations applications.



In the first step, an aqueous feed solution containing the species of interest (solute) is contacted with a solvent. The solute is transferred to the solvent phase thus effecting a separation from other species left in the raffinate. After the solute is extracted, it must then be recovered from the organic phase by a stripping operation. In the stripping process, the solute is transferred to an aqueous phase after which it can be taken to additional steps for further processing and recovery.

Liquid-liquid extraction analysis techniques have existed for simple systems in the chemical engineering literature for many years. References, such as Treybal (1963), Smith (1963), Brown (1950), and McCabe and Smith (1956), offer good treatments of analysis techniques, types of equipment, and process technology. However, the difficulty in applying much of this information to the mineral industry resides in the fact that usually the liquid-liquid systems found in the mineral industries are very complex, quite often involving reacting systems and a large number of species, rather than the ternary system found in most of the texts. The references, however, do offer excellent treatments and are recommended as starting points in understanding solvent extraction technology.

At this point, it may be well to summarize the process development considerations that may be encountered when evaluating solvent extraction as a potential separation technique. In outline form, the following points should be considered when evaluating a new separations problem:

- (1) solvent selection
- (2) determination of equilibrium data
- (3) simulated column analysis
- (4) process evaluation using analysis techniques
- (5) pilot plant evaluation
- (6) process scale-up
- (7) process economics

The above points are not necessarily in their chronological order of consideration nor would all have to be considered for a particular problem. They are, however, worthy of consideration when laying out a process development schedule for a potential SX application.

SOLVENT SELECTION

Many authors have discussed the problem of solvent selection in liquid-liquid extraction. Treybal (1963) lists the following points for consideration when selecting a solvent for a particular application:

- (1) solvent selectivity: the solvent should have the ability to extract one component of solution in preference to another.
- (2) distribution coefficient: this parameter is related to selectivity and by definition is the ratio of the concentration of one solute in the solvent-rich phase to the concentration in the raffinate-rich phase. The larger the distribution coefficient, the easier the separation.

- (3) **capacity:** the solvent should have the ability to dissolve a large amount of the solute, otherwise large quantities of solvent may be required.
- (4) **solvent solubility:** the solvent, if organic, should have a high degree of insolubility in the aqueous phase.
- (5) **recoverability:** the solvent must be easily recovered from the solute for recycle purposes.
- (6) **density:** the density difference between the contacted phases should be as great as possible for ease of phase separation.
- (7) **interfacial tension:** the interfacial tension between the immiscible phases should be as high as possible for rapid coalescence.
- (8) **chemical reactivity:** this point must be considered in terms of extraneous reactions and also in terms of enhancing the extraction process, particularly in many metals systems.
- (9) **corrosiveness:** ideally, the solvent should cause no serious corrosion with common materials of construction.
- (10) **viscosity:** a low viscosity is desired for ease of solution handling.
- (11) **vapor pressure:** usually, a low vapor pressure is desired so that extraction operations are possible at reasonable pressures, and solvent losses are minimized.
- (12) **flammability and toxicity** should be low.
- (13) **cost:** the solvent should be as inexpensive as possible and readily available.

One rarely encounters an optimum combination of the above properties and usually, particularly in the mineral industries, a compromise among properties is necessary.

Many authors have dealt specifically with the problem of solvent selection for metals applications. Hazen (1963) lists two types of solvent extraction systems. The first is termed "liquid ion exchange" because of its similarity to ion exchange processes using solid resins. In this process a small quantity of an active component is dissolved in a second organic (diluent) which serves as a carrier for the active component. The solute is extracted by reacting chemically with the active organic component. An example of this type of liquid solvent extraction is the extraction of uranium by amines.

The second type of extraction system involves simply solubility considerations. The total organic phase operates as a solvent for the solute with no chemical reaction taking place. This system is commonly found in the petroleum industry and, to a lesser extent, in a number of metallurgical systems.

Additives or modifiers are often added to the solvent system to improve the chemical or physical characteristics. Some of the major purposes of such modifiers are:

- (1) to increase the rate of phase separation;
- (2) to increase the solubility of the loaded organic in the carrier;
- (3) to prevent cation exchanger loss to the aqueous phase during alkaline stripping.

The usual modifiers are neutral materials, such as alcohols (for example, isodecanol), tributyl phosphate, or a phosphonate.

In some cases a synergistic agent may be added; such materials apparently interact with the metallic species to form complexes which are then more readily taken up by the solvent system. These materials are not normally called additives, but are considered an integral part of the extractant combination. The first example of synergism was noted in the extraction of uranium with di-2-ethylhexyl phosphoric acid, when it was found that the extraction was enhanced by addition of a neutral organophosphorus compound, such as a phosphine oxide. Many other examples of synergism have since been reported, such as the combination of a beta-diketone with tributyl phosphate or trioctyl phosphine oxide.

Although the selection of a solvent for a particular application is not simple, the ability to tailor or modify a solvent for a particular application is one of the advantages offered by liquid extraction over other separation techniques. Considerable technical effort has been expended in evaluating solvent systems, and effort will continue in this phase of solvent extraction research for years to come. Substantial advances have been made in understanding solvent systems and solvent chemistry during the last 10 years. However, we cannot as yet predict from theoretical considerations the best solvent for a particular application. Solvent selection usually ends in bench-scale laboratory evaluation. Some of the more widely known solvents and their trade names have been summarized by Zakarias and Cahalan (1966), and are presented in Table 2. Sample SX were shown previously in Table 6.3.1.

ANALYSIS TECHNIQUES

Although the techniques for analyzing extraction problems involving ternary systems are covered in the texts mentioned previously, they have found limited application for metallurgical systems. Usually, a metallurgical separation involves many components and the chemistry of the

Table 6.3.1. Solvents for Liquid-liquid Extraction.

AMINES:

Primary	Primene *
Secondary	Amberlite *
Tertiary	Alamines *
Quaternary ammonium	Aliquats *

ORGANOPHOSPHATES:

Tri-n-butyl phosphate (TBP)
Trioctyl phosphine oxide (TOPO)
Triphenyl phosphate (TPP)
Tetrabutyl ethylenediphosphonate (TBEDP)
Dodecyl phosphoric acid (DDPA)
Dialkyl phosphoric acids (DAPA, D2EHPA)

CARBOXYLIC ACIDS:

Branched chain carboxylic acids Versatic Acids *

OXIMES:

LIX-63 * An alpha-hydroxyoxime
LIX-64 * A substituted 2-hydroxy benzophenoxime

KETONES:

Methyl isobutyl ketone (MIBK)

SULFONIC ACIDS:

Dinonyl naphthalene sulfonic acid

* Names are registered trademarks.

extraction system may be quite complex, thus negating a simple triangular diagram analysis.

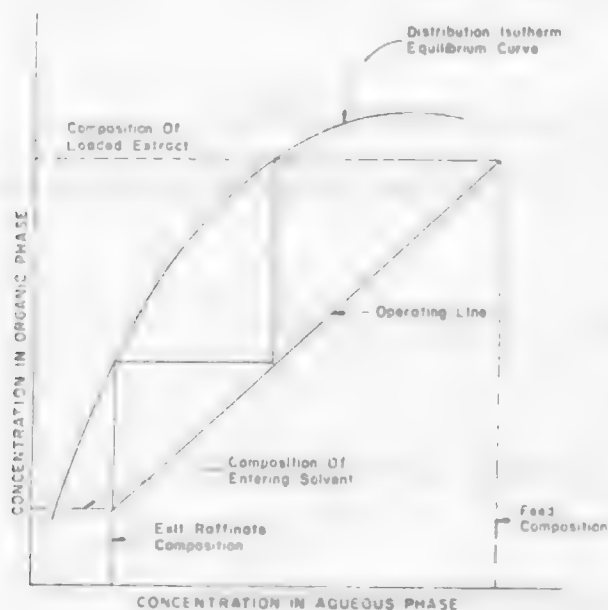
Usually after determining that an extraction system will work for a particular application, the next questions to be answered are:

- (1) How many equilibrium stages or contact units are required to effect the separation?
- (2) What should be the solvent and feed flow rates?
- (3) What should be the process temperature and pressure?

Since the above parameters are interrelated, either an analysis technique or experimental evaluation is necessary to answer the above questions.

The technique that has found the widest use for minerals separations is the McCabe-Thiele procedure. A sample diagram is shown in Figure 6.3.2. If distribution data are available as a function of concentration for a fixed pressure and temperature, the equilibrium curve can be determined. If sufficient information is available concerning feed, solvent and exit stream compositions, and flow rates, the operating line can be fixed on the diagram. By stepping off stages, one can then determine the number of contact units required.

Figure 6.3.2. Sample McCabe-Thiele Diagram for SX Analysis.



Providing the assumptions necessary to apply the technique are approximately satisfied and sufficient equilibrium data are available, one can in principle evaluate the effects of flowrate, feed composition, and number of stages without pilot plant data. However, usually the equilibrium data are not available and this information must be determined from bench-scale equilibrium studies prior to system analysis.

LABORATORY DATA

Perhaps the most powerful tool for evaluation of solvent extraction as a separation technique, and the one that has been used most extensively in industry, is that of laboratory shake-out data. Very simply, a solvent system is added to a separatory funnel along with the appropriate feed solution and the two-phase liquid system is mixed until equilibrium is achieved. After allowing the phases to separate, each phase is then analyzed for solute composition. With this approach, one can determine the potential of the solvent for extracting the desired solute. From these data, the distribution coefficient can be evaluated along with the identification of process problems, such as emulsion formation, interfacial scum formation, and the rate at which the phases coalesce.

After identification of the correct solvent system, continuous counter-current operation can be simulated where the actual feed and solvent flow rates are evaluated along with the specified number of stages. Essentially, this technique involves simulating actual mixer-settler operating conditions with laboratory batch shake-out data. Treybal (1963) gives a rather comprehensive treatment of this technique and the details will not be presented here. This form of analysis has the advantage of yielding process information on continuous countercurrent extraction operation without having to build a pilot plant or develop a bench-scale extraction set-up. Thus, the engineer can explore the effect of process variables with batch extractions in glassware. Quite often, this may be a valuable process development step prior to pilot plant tests.

PROCESS METHODS

Some of the processing methods which may be used for liquid-liquid extraction separation problems are presented in the following discussion.

Batch Contact

Batch contact processing is the simplest form of contact available. Simply, the feed solution and solvent are mixed in a batch operation and the phases allowed to coalesce, after which they are separated. It has the disadvantages inherent in a batch operation as opposed to continuous operation. With this contact, the maximum separation that can be obtained is equilibrium between the feed and solvent streams, thus yielding one equilibrium stage.

Single Contact Continuous

The single contact technique involves one contact unit with continuous feed and solvent flows. In principle, equilibrium is achieved between the feed and solvent streams, thus yielding one equilibrium stage. After mixing, the two phases are allowed to pass to another part of the process unit where they settle and then separate.

Crosscurrent Contact

The crosscurrent contact method is an extension of single contact extraction where the raffinate from the first stage is contacted with fresh solvent, thus removing more and more solute. This processing method has the obvious disadvantages of batch contact and has not received a great deal of attention in the mineral industries.

Continuous Countercurrent Contact

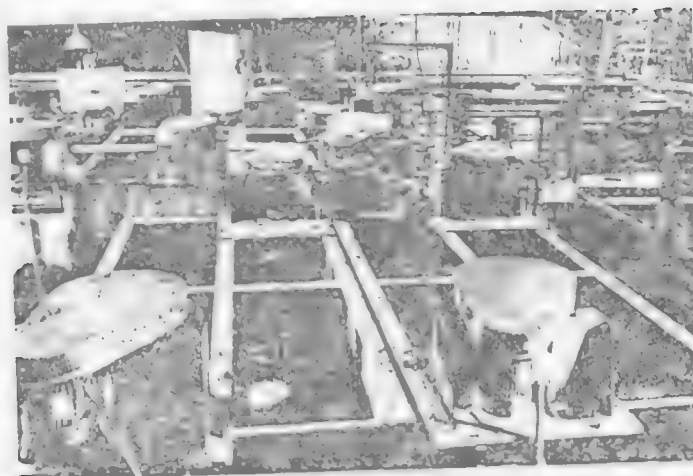
The continuous countercurrent contact method is used for difficult separations where a large number of equilibrium stages are required, or may involve only a few equilibrium stages where the separation is relatively easy. A series of mixer-settler units (single contact) may be placed in series to achieve this method of contact or the solvent and feed may be fed to a single column, such as a pulse or Scheible column. This method of operation has received extensive application in the mineral industries. There are many applications where mixer-settlers in series have been used and a substantial number where column operation has been attempted with varying degrees of success.

PROCESS EQUIPMENT

There are many kinds of process equipment that have been evaluated and used in the mineral industries. Only samples of the more common types will be presented here. A mixer-settler unit, probably the most extensively used piece of equipment in the mineral industries, is shown in Figure 6.3.3.

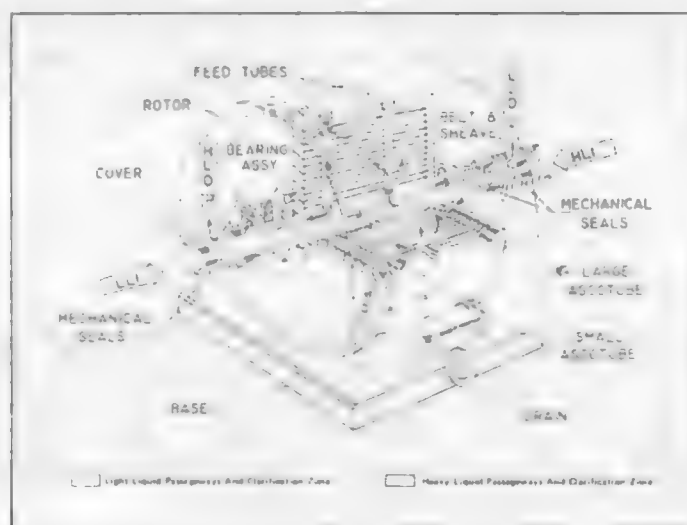
A diagram of a Podbielniak Extractor, a centrifugal contactor which has found application in uranium recovery, is shown in Figure 6.3.4. Traybal (1963) discusses the advantages of this type of extractor. Essentially, this unit has the advantage of permitting high fluid velocities with small extractor volumes. The small extractor volume with high flow rates permits space savings, lower inventories of solvent, and rapid achievement of steady state. An additional advantage of the Podbielniak unit is that the closed system permits the use of a low flash point diluent or solvent without presenting an unusual fire hazard. The major advantage for the unit, however, is that entrainment of one liquid phase within another is minimized. This contactor has the disadvantage of higher initial and maintenance costs when compared to mixer-settler units.

Figure 6.3.3. Mixer-Settler.



—Mixer-settler units for the recovery of europium at the Mountain Pass California plant of Molybdenum Corporation of America (photo courtesy of the Denver Equipment Company).

Figure 6.3.4. Centrifugal Contractor.



—Diagram of a Podbielniak[®] centrifugal contractor (used by permission of Baker Perkins Inc.). Legend: LLI - light liquid in; HLO - heavy liquid out; LLO - light liquid out; HLI - heavy liquid in.

The pulse column has been used successfully for the extraction of metals from the radioactive solutions of atomic energy operations. Van Dijck (1935) developed the general principles involved with this type of extractor. The essential feature is that a hydraulic pulse of short amplitude is applied to the liquids within the column. The essential feature is that a hydraulic pulse of short amplitude is applied to the liquids within the column. The pulsing action results in the dispersion of the two liquid phases through perforated plates within the column, thus providing mixing and agitation. This column has been used for difficult separations where a large number of stages is required within a reasonably short column. The power requirements for this form of operation must be considered when evaluating the potential of a pulse column.

There are many other column types that have been used in the solvent extraction field (particularly in the petroleum, pharmaceutical, and chemical process industries). The reader is referred to reviews by Akell (1966), Hanson (1968), and Treybal (1963) for discussion of other processing equipment.

APPLICATIONS IN THE MINERAL INDUSTRY

In view of the wealth of published information on a number of applications and also the large number of situations where SX has been considered or successfully applied in minerals processing, it will be impossible to discuss all of the available literature. Instead, sample applications will be listed with brief process information and some indication of the degree of success for the commercial processes. A number of the processes and applications are proprietary, and so discussion in these areas will not be current.

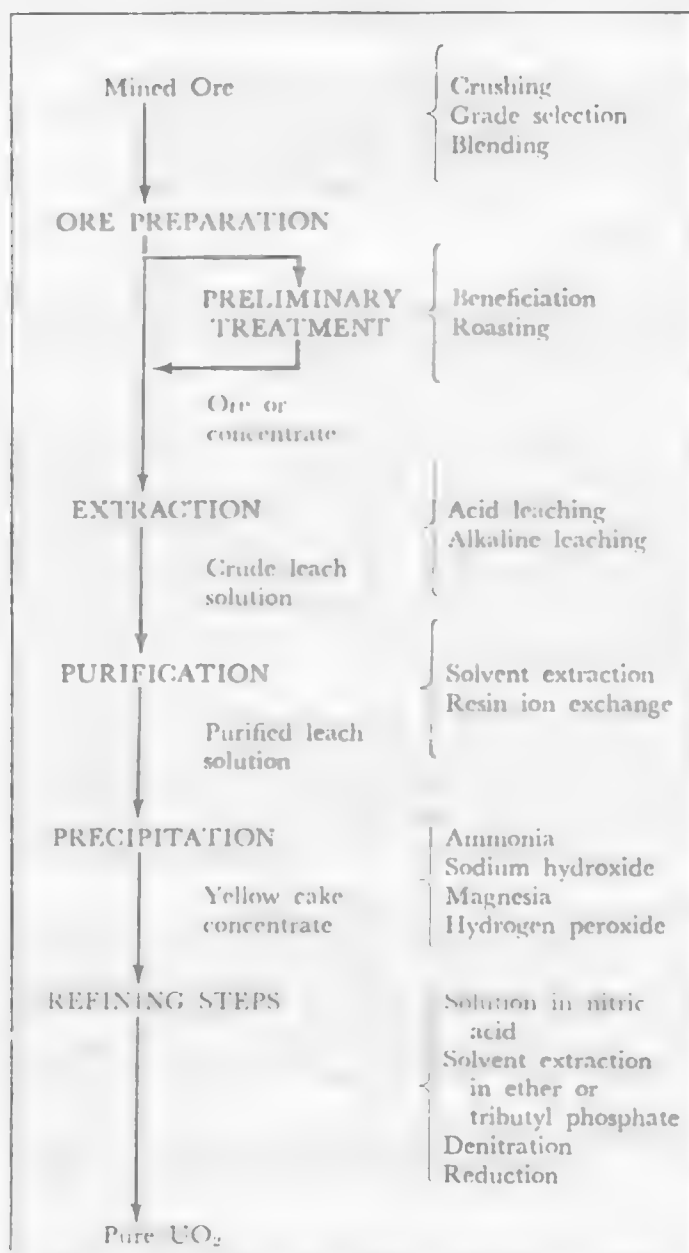
Commercial Applications

Uranium

The processing of uranium with SX pointed the way for other successful commercial applications in the minerals industry and a great deal of information has been published on solvent extraction technology as applied to the processing of uranium. Merritt (1969, 1971) provides an excellent summary of much of the work and these references are recommended for more detailed discussion of processing technology.

Merritt (1969) reported that solvent extraction at present is used in most of the uranium processing plants in the United States and also in a number of acid leaching plants in other countries. In the same reference, a simplified flow sheet was presented for the extraction of uranium from ores (Figure 6.3.5). Not all of the steps will be required for some ores; however, the processing scheme does show the reader where solvent extraction is applied as a purification step after the leaching operation. Up to 1969, SX had not been adapted to the processing of alkaline leach liquors but had been used extensively with acid leach solutions.

Figure 6.3.5. Extraction of Uranium from Ores.



In acid leach solutions, uranium is found both as an anionic complex, chiefly $[\text{UO}_2(\text{SO}_4)_3]^{-4}$, and as a cation, UO_2^{+2} . Consequently, either an anionic or cationic type of liquid ion exchange system may be used to separate uranium from acid leach solutions. Cationic extractants include:

- DDPA -- monododecyl phosphoric acid
- EHPA -- di-2-ethylhexyl phosphoric acid
- HDPa -- heptadecyl phosphoric acid
- OPPA -- dialkyl pyrophosphoric acid

Anionic solvents include:

- secondary amines with aliphatic side chains
- high molecular weight tri-alkyl tertiary amines
- quaternary ammonium compounds

In general, the solvent is dissolved in a low-cost carrier (diluent), such as kerosine containing a TBP modifier or a long chain alcohol to avoid formation of an additional liquid phase and to aid solubility of the extractant. Solvent losses, including diluent and modifier, may occur by entrainment in the aqueous phase, by evaporation, or by chemical breakdown. Merritt (1969) reports that amine and phosphate solvents in commercial use show losses in the range of 0.2 to 0.25 gallon of organic phase per 1000 gallons of solution contacted.

The uranium can be effectively stripped from an amine solvent phase by using a number of stripping agents, such as nitrates, chlorides, sulfates, carbonates, hydroxides, and acids. The chlorides are most frequently selected on the basis of cost and effectiveness. Sodium carbonate is usually used to strip the uranium from phosphoric acid solvents.

Merritt (1969) reported that amine solvent extraction (designated the AMEX process) is being used in seven out of ten operating mills in the United States. Three of the plants used this technique in conjunction with resin ion exchange and this process is called the "Eluex process." The Dapex process (phosphate solvent extraction) is being used in three mills. Usually, kerosine is the diluent and TBP is added as a modifier/

Mixer-settlers have been the primary equipment used in uranium extraction and have the advantage of low cost, ease of operation, and ease of maintenance.

Copper

Another example of the successful application of solvent extraction in metallurgical processing is in the recovery of copper. In 1964, General Mills developed LIX-64 (trade-mark registered) which was a selective reagent for solvent extraction of copper ions from acid solution (Ager 1965). Since then, an improved reagent, LIX-65N, has been developed

which is capable of being used at higher organic phase concentrations owing to improved phase separation characteristics (Flett 1970). Ashland Oil Company has announced the production of other solvents for copper extraction, Kelex 100 and Kelex 120. Kelex 100 extracts copper in preference to ferric iron from acidic leach liquors. The leaching solvent extraction, and electrowinning operations of the Ranchers Bluebird Mine have been described by Power (1970).

McGarr (1970) summarized Bagdad Copper Corporation's solvent extraction process for copper. The feed stream for the plant is leach liquor obtained by percolating weak sulfuric acid solution over heaps of waste material containing low-grade copper. The leach solution (pregnant liquor) goes to the extraction stage where the copper is extracted with LIX-64. The solvent phase is then stripped of copper with a high acid content solution which regenerates the solvent for further copper extraction. The copper (in solution as copper sulfate) is then passed to an electrowinning operation for production of cathode copper. Before this plant went on stream, Bagdad Copper produced copper by a cementation process which involved:

- (1) passing the acid leach solution over scrap iron that caused the copper to precipitate as a fine powder mixed with impurities, and
- (2) returning the solution from the precipitation launder (containing acid iron sulfate) to the heap for further leaching.

The solvent extraction process eliminates the following problems that were encountered with the cementation process:

- (1) materials handling, cost and availability of scrap iron;
- (2) return to the dump of a high level of iron sulfates which would prevent further leaching of copper.

Bagdad can remove all of the copper in the dump that is leachable with the SX process and uses mixer-settlers as the contacting equipment with four parallel trains in the plant, each train consisting of four extracting and three stripping stages.

Capital Wire and Cable Company is treating scrap copper with SX. Flett (1970) reports that the process scheme involves an ammonia leach followed with LIX-64N solvent extraction. In the same paper, Flett also mentions that another plant using LIX-64N extraction to be built by Power Gas Corporation for Anglo American Corporation at Nchanga, Zambia. The Nchanga plant's proposed capacity of 55,000 tons per year--as compared to 5400 tons per year for Ranchers and 6400 tons per year for Bagdad--makes it the largest plant at that time and represents a significant breakthrough by a British firm into an American market.

CITED REFERENCES

- Agers, D. W., and others, 1965, Copper recovery from acid solutions using liquid ion exchange: *Mining Eng.*, v. 17, no. 12, p. 76.
- Akell, R. B., 1966, Extraction equipment in the U.S.: *Chem. Eng. Progress*, V. 62, no. 9, p.50-54, Sept.
- Ashbrook, A. W., 1972, Carboxylic acids as extractants for the separation of metals in commercial solvent extraction operations: presented, Am. Inst. Mining Metall. Petroleum Engineers meeting, San Francisco, Feb. 22.
- Brown, G. G., 1950, *Unit Operations*: New York, John Wiley and Sons.
- Butters, P. A., 1967, The separation of tantalum and niobium by solvent extraction: *Chemistry and Industry*, p. 613-615, Apr.
- Carlson, C. W., and Nielsen, R. H., 1960, Pure columbium and tantalum oxides by liquid-liquid extraction: *Jour. Metals*, p. 472, 475, June.
- Chementator, 1972, *Chem. Eng.*, p. 50, Apr. 17.
- Churchwood, P. E., and Rosenbaum, J. B., 1963, Rhenium recovery by solvent extraction and electrodeposition: *Jour. Metals*, p. 648-650, Sept.
- Deco Trefoil, 1970, v. 34, no. 4, Fall.
- Engineering and Mining Journal, 1969, Engineering and Mining Journal flow-sheet study: p. 172, June.
- _____, 1972, Trends in chemical processing and hydrometallurgy: p. 173-174, June.
- _____, 1972, New recovery process can yield both electrolytic nickel and copper: p. 94-95, Jan.
- Flett, D. S., 1970, Solvent extraction of nonferrous metals: Reprints on the *Progress of Applied Chemistry*, v. 55, p. 365-370.
- George, D. R., and others, 1968, Recovery and production of alumina from waste solutions by solvent extraction: *Jour. Metals*, p. 59-63, Sept.
- Hanson, Carl, 1968, Solvent extraction theory, equipment, commercial operations and economics: *Chem. Eng.* p. 76-97, Aug. 26.
- Harrah, H. W., 1967, Rare earth concentration at Molybdenum Corporation of America: Denver Equipment Company, Bull. M4-B167, Denver, Colo., Nov.-Dec.
- Hazen, W. C., 1963, Solvent extraction techniques: Denver Equipment Company, Publ. T4-B32, p. 11.
- House, J. E., 1967, Industrial application of solvent extraction in solvent extraction chemistry: *Proc. Internat. Conf.*, Gothenburg, Sweden, Aug. 27-Sept. 1, 1966, John Wiley and Sons.
- Jamrack, W. D., 1963, *Rare Metal Extraction*, New York, MacMillan Company.
- Klopfenstein, R. K., and Arnold, D. S., 1966, Recent developments in solvent extraction technology: *Jour. Metals*, p. 1195-1197, Nov.
- Levin, I. S., and others, 1967, The extraction of elements of the gallium and arsenic subgroups with alkylphosphoric acids, The mechanism of extraction: *Solvent Extraction Chemistry*, *Proc. Internat. Conf.*, Gothenburg, Sweden, Aug. 27-Sept. 1, 1966, John Wiley and Sons.
- Lewis, C. J., and House, J. E., 1960, Recovery of molybdenum by liquid-liquid extraction from uranium mill circuits: Presented Am. Inst. Mining, Metall. Engineers meeting, N.Y.
- McCabe, Warren L., and Smith, J. C., 1956, *Unit Operations of Chemical Engineering*, New York, McGraw-Hill, Second Edition.

- McGarr, H. J., 1970, Liquid ion exchange recovers copper from wastes and low grade ores: *Eng. Mining Jour.*, p. 79-81, Oct.
- Merritt, R. C., 1971, The Extractive Metallurgy of Uranium: Colorado School Mines Research Institute, Golden, Colo.
- Merritt, R. C., and Pings, W. B., 1969, Processing of uranium ores, Part II: *Mineral Industries Bulletin*, V. 12, no. 6, p. 20, Nov.
- Orth, D. A., 1965, Performance of 3% and 30% TBP process: *Solvent Extraction Chemistry of Metals*, Cleveland, Ohio, CRC Press, p. 47-79.
- Paist, D. A., and Pings, W. B., 1970, Vanadium-1970: *Mineral Industries Bulletin*, v. 13, no. 4, p. 24.
- Palley, J. N., and Paige, P. M., 1972, Can electrowinning replace cement copper: *Eng. Mining Jour.*, p. 94-96, July.
- Pearce, R. F., 1971, Cobalt: *Eng. Mining Jour.*, p. 113-114, March.
- Pings, W. B., 1972, Titanium, Part I: *Mineral Industries Bulletin*, v. 15, no. 4, July, p. 13.
- Power, K. L., 1970, Operation of the first commercial copper liquid ion exchange and electrowinning plant: Paper presented Am. Inst. Mining, Metall. and Petroleum Engineers, Denver, Feb.
- Smith, B. D., 1963, Design of Equilibrium Stage Processes, New York, McGraw-Hill.
- Solvent Extraction Chemistry of Metals*, 1965, Cleveland, Ohio, CRC Press, 456 p. (ed. by H. A. C. McKay, and others).
- Teybal, R. E., 1963, Liquid Extraction: New York, McGraw-Hill, Second Edition.
- Van Dijck, W. J. D., 1935, Process and apparatus for intimately contacting fluids: U. S. Patent no. 2,001, 186.
- Vermeulen, L. W., 1966, Recovery of throrium from uranium solutions: *Jour. Metals*, p. 22-25, Jan.
- Wiyotol, E., and Froyland, K., 1972, Solvent extraction in nickel metallurgy: The Falconbridge matte leach process: *Proc. Internat. Symposium on Solvent Extraction in Metallurgical Processes*, Antwerp, p. 71-81, May 4-5.
- Zakarias, M. J., and Cahalan, M. H., 1966, Solvent extraction for metal recovery: *Inst. Mining and Metall. Trans.*, Section C, v. 75, Bull. 718, Sept.

UNCITED REFERENCES

- Agers, D. W., and others, 1965, Copper recovery from acid solutions using liquid ion exchange: paper presented, Section meeting of the Am. Inst. Mining, Metall. and Petroleum Engineers, Phoenix, Arizona, Oct. 7-9.
- Akell, R. B., 1966, Extraction equipment available in the U. S.: Chem. Eng. Progress, v. 62, no. 9, p. 50-55, Sept.
- Arnold, D. S., Ryle, B. G., and Davis, J. O., 1958, Metal refining by solvent extraction of leach slurries: Chem. Eng. Progress, v. 54, no. 10, p. 90-95, Oct.
- Bridges, D. W., and Rosenbaum, J. B., 1962, Metallurgical application of solvent extraction: U. S. Bur. Mines Inf. Circ. 8139.
- Brooks, P. T., and Potter, G. M., 1970, Electrochemical recovery of high-purity nickel and cobalt from crude nickel and ferronickel: U. S. Bur. Mines Rept. Inv. 7402, June.
- Coleman, C. F., and Roddy, J. W., 1971, Kinetics of metal extraction by organo phosphorus acids: Solvent Extraction Reviews, v. 1, no. 1, p. 63-91.
- Connolly, J. R., and Winter, R. L., 1969, Approaches to mixing operation scale-up: Chem. Eng. Progress, v. 65, no. 8, p. 70-78, Aug.
- Cooper, F. D., 1968, Copper hydrometallurgy: U. S. Bur. Mines Inf. Circ. 8394, Sept.
- Crabtree, E. H., and Lewis, C. J., 1958, Liquid-liquid extraction of uranium from aqueous solutions: Eng. and Mining Jour., Sept.
- Deco Trefoil, 1969, Hydrometallurgy applied to copper ores: Bull. G3-B-146, p. 9-16, Fall.
- Drobnick, J. L., and Lewis, C. J., 1966, Recovery of vanadium: U. S. Patent no. 3,257,164, June 21.
- Duckworth, J. P., and Michels, L. R., 1964, New neptunium recovery facility at the Hanford Purex plant: Industrial and Engineering Chemistry, Process Design and Development, v. 3, no. 4, p. 302-305, Oct.
- Fletcher, A. W., and Flett, D. S., 1965, Carboxylic acids as reagents for the solvent extraction of metals: paper, Internat. Conf. on the Chemistry of the Solvent Extraction of Metals, A.E.R.E., Harwell, Sept. 27-29.
- Gardner, S. A., and Warwick, G. C. I., 1971, Pollution-free metallurgy-copper via solvent extraction: Eng. and Mining Jour., p. 108-110, April.
- Graef, E. F., and Foster, S. P., 1956, Design of box-type, counter-current mixer-settler units-factors affecting capacity: Chem. Eng. Progress, v. 52, no. 7, p. 293-298, July.
- Gregory, J. G., Evans, B., and Weston, P. C., 1971, Solvent extraction: Proc. Internat. Solvent Extraction Conference, The Hague, April 19-23, Academic Press.
- Hanson, Carl, 1968, Solvent extraction: Chem. Eng., p. 76-97, Aug.
- _____, 1968, Recent research in solvent extraction: Chem. Eng., p. 135-142, Sept. 9.
- Healy, T. V., 1961, Synergism in the solvent extraction of di-, tri-, and tetravalent metal ions-II. Synergic effects in so-called inert diluents: Jour. Inorg. Nuclear Chemistry, v. 19, p. 328-339.

- _____, 1961, Synergism in the solvent extraction of di-, tri-, and tetra-valent metal ions-I. Synergic effects of different phosphate esters: *Jour. Inorg. Nuclear Chemistry*, v. 19, p. 314-327.
- Ingham, J., 1967, Solvent extraction in Israel: *Chemistry and Industry*, p. 1863-1967, Nov. 4.
- Kindig, J. K., and Hazen, W. C., 1970, Cyclone separators for solvent extraction in metallurgy: presented Am. Inst. Mining, Metall. and Petroleum Engineers, meeting, Denver, Colo., Feb.
- Lewis, C. J., and Drobnick, J. L., 1963, Liquid-liquid extraction recovery of vanadium and molybdenum values using a quaternary ammonium extractant: U. S. Patent no. 3,083,085, Mar. 26.
- _____, 1958, Solvent extraction in the mining industry: *Ind. and Eng. Chem.*, v. 50, no. 12, Dec.
- McKay, H. A. C., 1970, Selectivity of extractants for metals: *Chemistry and Industry*, p. 610-615, May 9.
- Millsap, W. A., and Peterson, H. D., 1966, Process for treating rare earths: *Canadian Patent no. 828,085*, Jan. 10.
- Moore, James D., 1957, Uranium recovery by the solvent extraction process: *Jour. Metals*, p. 757-761, June.
- Olson, R. S., 1958, Optimum economic extraction: *Chem. Eng.*, p. 143-145, Oct. 6.
- Remun, G. H., 1966, Extraction equipment outside the U. S.: *Chem. Eng. Progress*, v. 62, no. 9, p. 56-61, Sept.
- Ross, A. M., 1957, Solvent extraction newcomer to the Colorado Plateau: *Mining Eng.*, p. 997-1000, Sept.
- Ryon, A. D., Dalley, F. L., and Lowrie, R. S., 1959, Scale-up of mixer-settlers: *Chem. Eng. Progress*, v. 55, no. 10, p. 70-75, Oct.
- Swanson, R. R., Dunning, H. N., and House, J. E., 1961, Commercial recovery of vanadium by the liquid ion exchange process: *Eng. and Mining Jour.*, Oct.
- Todd, D. B., 1966, Liquid extractor performance: *Chem. Eng. Progress*, v. 62, no. 9, p. 67-75, Sept.
- _____, 1958, Estimation of the stage efficiency of simple, agitated vessels used in mixer-settler extractors: *Am. Inst. Chem. Engineers Jour.*, v. 4, no. 2, p. 202-207, June.
- _____, 1956, Liquid extraction: *Ind. and Eng. Chem.*, v. 48, no. 3, p. 510-519.
- Vashist, P. N., and Bechman, R. B., 1968, Liquid-liquid extraction: *Ind. and Eng. Chem.*, v. 60, no. 11, p. 43-49, Nov.
- Warwick, G. C. I., Schuffham, J. B., and Lott, J. B., 1970, Solvent extraction—today's exciting process for copper and other metals: *World Mining*, p. 38-44, Oct.

LEARNING ACTIVITY 4

Learning Activity Objective

After completing your study of this learning activity material you should be able to list the types and describe the chemistry of ion exchange process; be able to give examples of the application of IX to hydrometallurgical processes, and be able to describe the methods used in the industry.

6.4 Ion Exchange**6.4.1 Introduction**

Ion exchange reactions involve the interchange of ions between an aqueous solution and insoluble solid resin. It is one of the unit operations used in hydrometallurgy to purify and concentrate the metal values from leach liquors. The use of ion exchange is especially prevalent in the uranium and other rare earth industries. Although solvent extraction is used now more than ever, there are problems in its use, e.g., emulsion formation, and solvent loss in the operation circuit can be costly and troublesome. The ion exchange technique has been proven to be an economic process for recovering low concentrations of uranium from mine waste streams. Also, the resin-in-pump process can be used to recover metal ions from uranium containing slimy pulp (from which the separation of clear liquor is difficult). Ion exchange technology is seen as a complementing technology, and sometimes a substitute technology, for solvent extraction.

Ion exchange technology that has been adapted to hydrometallurgical processes can be described by a two stage sequence:

a. **adsorption:** utilization of an anionic or cationic organic resin to remove metal ions from an aqueous solution when that solution is passed through a bed of resin.

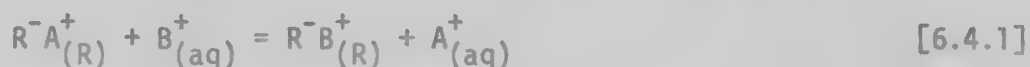
b. **elution:** the recovery of metal ions in a concentrated and purified form (aqueous solution) by passing a small volume of suitable solution (eluent) through the loaded bed.

The reactions can be performed in fixed bed, moving bed or resin-in-pulp reactors.

6.4.2 General Principles

Chemical Composition and Structure of Resins. Modern ion exchange resins are synthetic polymers in which hydrocarbon groups make up a three dimensional network and hold stable, reactive ionic groups. These ionic functional groups may be a strong acid, e.g., $-\text{SO}_3\text{H}$; or a weak acid, e.g., $-\text{COOH}$; or a strong base, e.g., a quaternary ammonium group.

$-\text{NR}_3\text{Cl}$; a weak base, e.g., secondary or tertiary amine groups, $-\text{NH}_2\text{RCl}$, or $-\text{NH}_3\text{Cl}$ where anions such as chloride ions are capable of exchange with other anions. The resins containing acid groups are called cation-exchanger. The reversible reaction for cation exchangers can be written



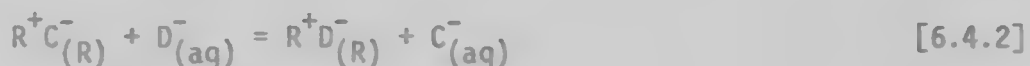
where R^-A^+ = functional group in a cationic exchanger

R^- = fixed ion in the functional group

A^+ = exchangeable cation ion in the resin

B^+ = exchangeable cation ion in the solution

The resins with basic groups are called anion-exchangers. The exchange reaction can be written as



where R^+C^- = functional group in an anionic exchanger

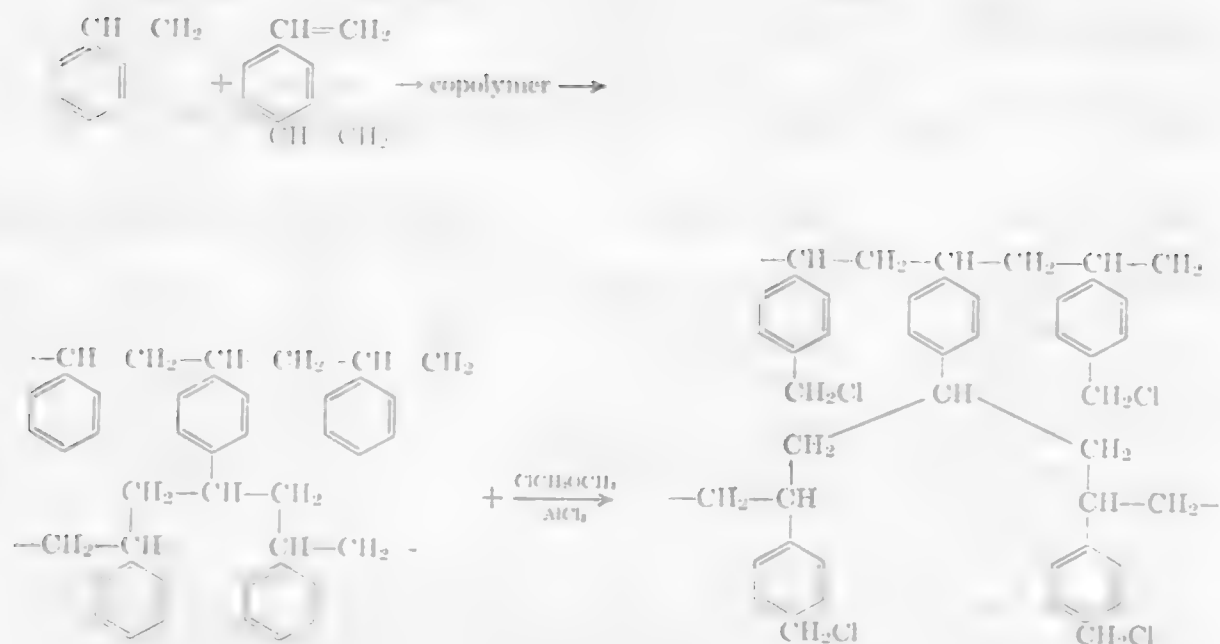
R^+ = fixed ion in the functional group

C^- = exchangeable anion ion in the resin

D^- = exchangeable anion ion in the solution

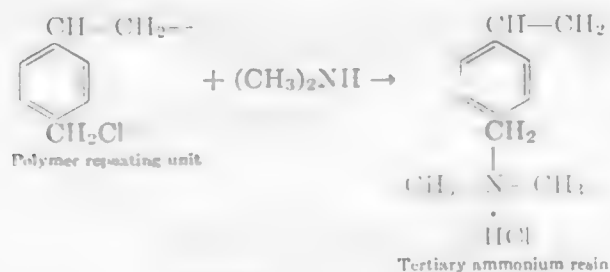
The normal procedure¹ used to synthesize the resin is to first form a cross-linked polymer unit and then to subsequently introduce the functional groups into the hard polymer structure. The degree of crosslinking in these polymers is of importance because the crosslinkage influences the chemical and mechanical characteristics of the resin. Linear, non-crosslinking, polymers are relative soluble in aqueous solutions. However, polymers too highly crosslinked cannot swell to allow the counter ions to enter the resin, i.e., the porosity is too low.

Most of the modern ion-exchange resins are addition copolymers prepared from vinyl monomers. These polymers have a high chemical and thermal stability, and they can be prepared with a wide choice in the degree of crosslinking and particle size. The most important resins of this type are crosslinked polystyrenes with sulfonic acid cation exchange and quaternary ammonium anion exchange resins. For the latter resins, styrene is first polymerized with divinylbenzene in suspension and cured. The copolymer is chloromethylated with chloromethyl ether using a Friedel-Crafts catalyst (ZnCl_2 , AlCl_3 , SnCl_4) according to the reaction.



[6.4.3]

This chloromethylated copolymer can be used to prepare quaternary ammonium exchange resins by amination with $(\text{CH}_3)_3\text{N}$ as shown below:



[6.4.4]

There are two commonly accepted ways to characterize the capacity of an ion exchanger: weight capacity and volume capacity. The weight capacity is defined as the number of ionogenic groups contained in the "specific amount" of the resin, usually given in milliequivalents per gram. The specific amount is defined as the amount of resin which weighs one gram when the material is completely converted to the H^+ or Cl^- form. The volume capacity, for technical applications and design purposes, is defined as the number of ionogenic groups per unit volume of packed bed of resin, usually given in equivalents per liter of (fully swollen) bed.

Some types and properties of commercially available ion exchanger polystyrene resins are listed in Table 6.4.1.

Table 6.4.1. Typical Properties of Polystyrene Ion Exchanger Resin.

Ionic Group	Trade Name	Capacity		pH Range	Temp. °C
		meq/g	meq/ml		
Cationic -SO ₃ H	Amberlite IR/20	4.3-5	1.9	0-14	120
-PO ₃ H ₂	Duolite C63	6.6	3.2	4-14	120
-COOH	Amberlite IRC 50	9.5	3.5	5-14	120
Anionic -N(Alkyl) ₃ ⁺	Amberlite IRA 425		1.3	0-12	60
-weak base amino group	Amberlite IR 45	5	2	0-9	100

Beside the type of functional group and the capacity of a particular resin, the durability is also an important factor for consideration. For many applications, the resins must be resistant to physical breakdown, chemical degradation, and solubility. Other important factors are density, resin size, moisture, hydraulic expansion, etc. The moisture specification is essentially a measure of the degree of cross-linking. Cross-linking controls such factors as reaction rate, selectivity and swelling of exchanger. Some physical and chemical properties of a commercial ion exchanger, sulfonated styrene-divinylbenzene, are listed in Table 6.4.2.

Table 6.4.2. Specification for a Typical Commercial Ion Exchange Resin (Sulfonated Styrene-Divinylbenzene).

Property	Specification
Moisture	44-48%
Volume Capacity	1.90 meq/ml (minimum)
Weight Capacity	4.5 meq/gram (minimum)
Color Throw	25 APHA
Order and Taste	None
pH	6.0-7.0
Hydraulic Expansion	37-75%
Density	48-54 lb/cu. ft.
Compressibility	5.0 gal/sq.ft./min. - 0.6 lb/sq.ft./ft. (max.)
Effective Size	0.4-0.6 mm
Uniformity Coefficient	1.7 (maximum)

Selectivity of Ion Exchanger. The affinity of an ion exchanger for various ions present in the solution differs, i.e., some ions are held more strongly than others. The affinity is usually represented by the ion exchange equilibrium for a particular condition such as constant pH, and a given temperature. Ion exchange equilibrium can be described in terms of a quantity called the selectivity coefficient or distribution coefficient.

The preference of the ion exchanger for one of the two counter ions is often expressed as the selectivity coefficient which is derived from the equilibrium constant of the exchange reaction, e.g.,



The counter-ions A^+ and B^+ are competing for the reactive sites of the ion exchanger. The selectivity coefficient, K_c , is defined as,

$$K_c = \frac{(RB)(A^+)}{(RA)(B^+)} \quad [6.4.5]$$

where brackets represent the concentration of various species. If the ion B is associated with R, the factor K_c is larger than unity. If we arbitrarily assign values of $(A^+)/ (RA)$ to be equal to 1.0, then for Li^+ (representing symbol A^+), the relative selectivity coefficient for other species (from experimental data) can be tabulated as shown in Table 6.4.3.

Table 6.4.3.² Relative Selectivity Coefficients for the Exchange of Various Cations for Li^+ on Sulfonated Polystyrene with 4% DBV.

Counter Ion	Selectivity Coeff.	Counter Ion	Selectivity Coeff.
Li^+	1.0	UO_2^+	2.36
H^+	1.32	Mg^{2+}	2.95
Na^+	1.58	Zn^{2+}	3.13
K^+	2.27	Co^{2+}	3.29
Rb^+	2.46	Cd^{2+}	3.37
Cs^+	2.67	Ni^{2+}	3.45
Ag^+	4.73	Ca^{2+}	4.15
Tl^+	6.70	Sr^{2+}	4.70
		Pb^{2+}	6.56
		Ba^{2+}	7.47

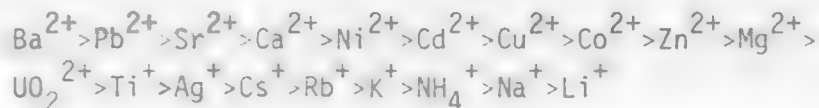
As can be seen from the above table, the affinity of this particular resin for many ions is larger than that for the Li^+ ion.

In certain practical applications, equilibrium is most conveniently expressed in terms of the distribution coefficients of the counter ions. The distribution coefficient is defined as

$$D = \frac{(RB)}{(B^+)} \quad [6.4.6]$$

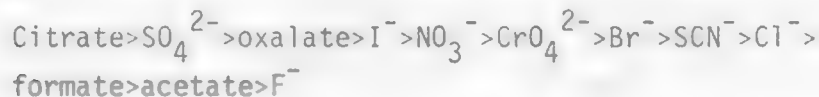
For specified conditions, the distribution coefficient can be calculated from the selectivity coefficient.¹ However, there is no simple explicit relationship between these two. The use of the distribution coefficient is particularly advantageous if the species of interest is present only in trace amounts (for example $RA \gg RB$, $A^+ \gg B^+$). Usually for this condition, the distribution coefficient is a constant. Again the ion exchanger will prefer the ions that have a large distribution coefficient.

Relative affinities of ions have often been arranged in series to indicate whether one ion will replace another or not under comparable conditions of concentration, etc. For the usual general-purpose cation exchangers the selectivity sequence of the most common cations is (also shown in Table 6.4.3)



For strong acid resins, the selectivity of H^+ usually falls between Na^+ and Li^+ . For weak acid resins, the position of H^+ depends on the acid strength of the fixed anionic group.

The selectivity sequence of the usual general purpose anion-exchanger is



For strong-base resins, the selectivity of OH^- usually falls between acetate and fluoride. For weak-base resins, the position of OH^- is farther to the left and depends on the base strength of the fixed inorganic groups.

In general, the ion exchanger tends to prefer:

the counter ion of high valence,

the counter ion with the smaller (hydrated) equivalent volume,

- the counter ion with the greater polarizability,
- the counter ion which interacts more strongly with the fixed ionic groups or with the matrix,
- the counter ion which participates least in complex formation with the co-ion.

6.4.3 Kinetics of Ion Exchange Reaction

Ion exchange reactions are heterogeneous and involve five steps in series; the slowest still determines the overall rate of the reaction. Consider the following ion exchange reaction,



The five steps are:

1. Film diffusion of counter ion B^+ across a stagnant film to the surface of the resin particle,
2. Particle diffusion of counter ion B^+ within the resin particle,
3. Exchange reaction between counter ions A^+ and B^+ at the fixed ionic group,
4. Particle diffusion of exchanged counter ion A^+ from the interior to the surface of the particle, and
5. Film diffusion of counter ion A^+ across the stagnant film to the bulk solution phase.

The chemical reaction (step 3) seldom controls the rate. Thus, the rates are normally dependent on diffusion phenomena.

Because of the principle of electroneutrality, the flux (in equivalents) of B^+ to the particle (Step 1) should be equal but in an opposite direction to the film diffusion of A^+ away from the particle (Step 5). These two steps can be regarded as inter-diffusion of co-center ions across the stagnant film. The term inter-diffusion can be replaced by binary diffusion when the diffusion process involves only two species. Therefore, steps 2 and 4 can be regarded to be binary diffusion of counter ions within the particle.

It is important to grasp the mechanism that produces the equivalence of fluxes. The faster ion, of course, tends to diffuse at the higher rate. However, any excess flux of an ion is equivalent to a net transfer of electric charge and thus produces an electric field. This hinders

the movement of the faster ion and enhances the movement of the slower ion until the fluxes become equal. The rate equations that describe ordinary self diffusion, e.g., Fick's Law, can also be applied to the binary diffusion system. However, the diffusion coefficient used in the equations has to be modified. The diffusion coefficient for a binary system can be derived. The equation for a system where the charges of species A and B are Z_A and Z_B respectively is,

$$D_{AB} = \frac{D_A D_B (Z_A^2 C_A + Z_B^2 C_B)}{Z_A^2 C_A D_A + Z_B^2 C_B D_B} \quad [6.4.8]$$

where D_{AB} = binary diffusion coefficients for species A or B in a binary system,

D_A, D_B = ordinary self diffusion coefficient of A and B, respectively,

C_A, C_B = concentration of species A and B, respectively.

This binary diffusion coefficient, however, is by no means constant. Its value depends on the relative concentration of A and B. For $C_A \gg C_B$ the coefficient is approximately equal to D_B ; and for $C_A \ll C_B$, the coefficient is approximately equal to D_A . In other words, the ion present in smaller concentration will determine the diffusion coefficient in a binary diffusion process.

Of the two steps, film diffusion and particle diffusion, particle diffusion is normally the slower, e.g., particle diffusion coefficients are about 10^{-7} , while the film diffusion coefficients are about 10^{-5} . However, film diffusion control may prevail in systems with ion exchangers of high concentration of fixed ionic groups, low degree of crosslinking, and small particle size, with dilute solutions, and with inefficient agitation.

The rate equations for particle diffusion for various conditions can be found in Reference 3.

References

1. R. Kunin, Ion Exchange Resins, John Wiley & Son, Chap. 5, (1958).
2. F. Helfferich, Ion Exchange, McGraw-Hill, Chap. 5 (1962).
3. Ibid., Chap. 6.

LEARNING ACTIVITY 5

Learning Activity Objective

After completing your study of this learning activity material you should be able to illustrate and discuss exchange applications of ion exchange in industry.

6.5 Hydrometallurgical Applications

Ion exchange techniques may be used in hydrometallurgical operations in one of several ways. First, the resins are used to concentrate and purify the metal values contained in the leach liquors. Second, ion exchange resins are used to recover metal values from mine waters or tailing streams. Third, ion exchange resins are used to separate chemically similar metals from a leach solution, e.g., rare earths.

6.5.1 Uranium Extraction--Chemistry of Adsorption and Elution

Cation exchangers do not show a strong affinity for uranyl cation, UO_2^{2+} . This is shown in previous activity Table 6.4.3. However, due to the formation of uranyl sulfate anions in an acid leach system, and of uranyl carbonate anions in an alkaline leach system, uranium can be selectively adsorbed by a strong base anion-exchange resin such as polystyrene with quaternary ammonium groups attached. Typical commercial resins used in uranium processing in the United States and their rated total capacities are given in Table 6.5.1. Typical reactions between the mobile ion adsorbed on the resin and uranium anion in solution (R designating the fixed ion group and X the mobile ion) will proceed as follows:

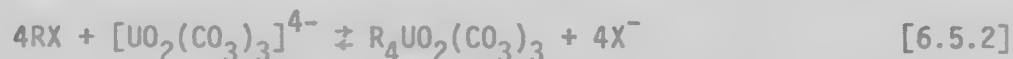
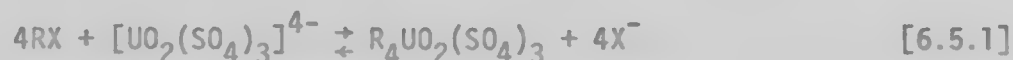


Table 6.5.1. Anion Exchange Resins Used for Uranium.

<u>Resin</u>	<u>Capacity, meq/g</u>	<u>meq/ml</u>
Amberlite IRA 425	---	1.3
Amberlite IRA 430 (for RIP)	---	1.1
Dowex 11	4.0	1.24
Dowex 21 K	4.5	1.25
Ionac A-580 (same as Permatite SK)	---	1.30
Ionac A-590 (same as Permatite SKB)	---	1.30

Acid leaching of uranium ores and the subsequent purification by ion exchange is used commercially. The treatment steps for recovering uranium is described below.

1. The clarified sulfuric acid leach liquor is passed through a column of the resin until the presence of uranium is detected in the barren effluent.
2. The column is rinsed and backwashed with water.
3. The uranium is eluted with a chloride or nitrate salt solution.
4. The uranium is precipitated from the eluate with ammonia or some other alkaline agent and the precipitate is filtered, dried, and calcined.

In practice, during the adsorption, the pH value of the solution is controlled at 1.5. At lower pH, the solution generates strongly adsorbed bisulfate ions, and at high pH, the precipitation of uranium ion occurs. Chloride and nitrate ions are also strongly adsorbed; it is desirable to maintain these ions below 2 g/l. Anionic ferric sulfate complexes, VO_4^{3-} and VO_3^- will also influence the adsorption of uranium. It is usual practice to add metallic iron to reduce ferric ions to ferrous iron which in turn will reduce pentavalent vanadium to the tetravalent state.

In the elution circuit, the eluent is usually a nitrate or chloride solution. In either case the eluting reagent is slightly acidified with dilute acid to prevent the precipitation of uranium ions. When the chloride eluent is used, the most effective solution in practice contains 0.9 M NH_4Cl or NaCl and 0.1 M HCl or H_2SO_4 .

Before recycling the stripped resin to the adsorption circuit, it is desirable to convert the resin from the nitrate or chloride form to the sulfate form by treating with 5 to 10% sulfuric acid solution.

Solvent extraction has been successfully applied as a second stage of uranium purification following ion exchange. This combination is referred as the "Eluex" process in the United States or the "Bufflex" process in South Africa. A high-grade product is produced. One molar solution of sulfuric acid is used as the eluent instead of a nitrate or chloride solution. This technique permits the user to treat the acidic eluate by solvent extraction without the need for neutralizing excess acid, and to recycle the resin directly to the adsorption circuits without further treatment. For these reasons and the relative low cost and availability of sulfuric acid, this technique is the favored process.

Certain impurity ions are so strongly adsorbed by the resin that they resist normal elution and gradually reduce the capacity of the resin. These ions are usually called resin "poisons." Examples of

resin poisons are: silica, molybdenum, polythionates, sulfur, and titanium. Poisoning is not always attributable to ionic adsorption but may be the result of materials mechanically blocking the pore openings in the resin. This, of course, inhibits the rate of transport of material in and out of the resin. Ions that are known to act as mechanical poisons include silica, titanium, zirconium, hafnium, niobium, antimony, and arsenate or phosphate complexes.

The "regeneration" of resins is possibly by a special elution stage for the removal of the impurities. The common resin poisons are usually removed first by an alkaline treatment. This is followed by a strong acid treatment. Other regeneration techniques include the use of a mixture of H_2SO_4 and ammonium bifluoride to remove silica and titanium and the use of dilute alkaline cyanide to elute polythionates, sulfur and silica.

Alkaline leach liquor can be purified and upgraded by a similar ion exchange process. However, the alkaline leach is usually more selective. This simplifies the ion exchange operation since there are usually less impurities present in solution to compete for resin sites. Several companies precipitate the uranium directly without going through either the ion exchange or solvent extraction procedure.

6.5.2 Uranium Ion Exchange--Processes and Equipment

The ion exchange process for uranium can be used on clarified solutions and slime slurries. Clarified solutions can be treated with a fixed bed or moving bed ion exchange column, and slime slurries can be handled by basket or a continuous Resin-In-Pump (RIP) process.

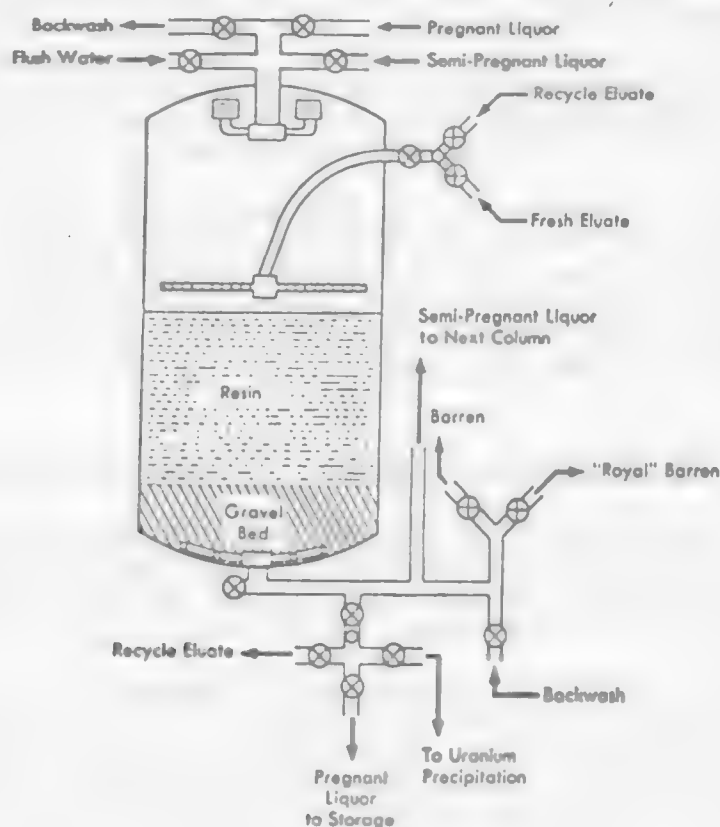
Fixed bed ion exchange columns are cylindrical pressure vessels, usually about one ft. high by 7 ft. diameter. They are constructed of steel. An example of a fixed bed reactor is shown in Figure 6.5.1. The reactors are vertically mounted and suitably connected through valves and pipe manifolds for control of the passage of the various solutions. The resin bed normally occupies about half of the total column height. It rests on a perforated plate or sized rock. Typical pressure drops for each column is in the range of 5 to 10 psi. Figure 6.5.1 also indicates the locations for entrance and exit of pregnant solution, eluent and backwash water.

Fixed bed ion exchange plants are usually operated with a 3- or 4-column system (see Figure 6.5.2). At least two columns are always operated in series in the adsorption circuit. When the leading column is saturated with uranium, it will be removed from the series, washed and placed on elution. Meanwhile a freshly eluted column is added as the trailing column on adsorption.

A typical flowsheet for a moving bed column is presented in Figure 6.5.2. The adsorption, backwashing, and elution processes are carried out in separated columns, so that each column can be designed specifically for a particular purpose. Adsorption and elution columns are about 8 ft.

by 14 ft. The separate backwash column is approximately 16 ft. high. The resin is transferred from one column to the other by hydraulic pressure to minimize the attrition of resins.

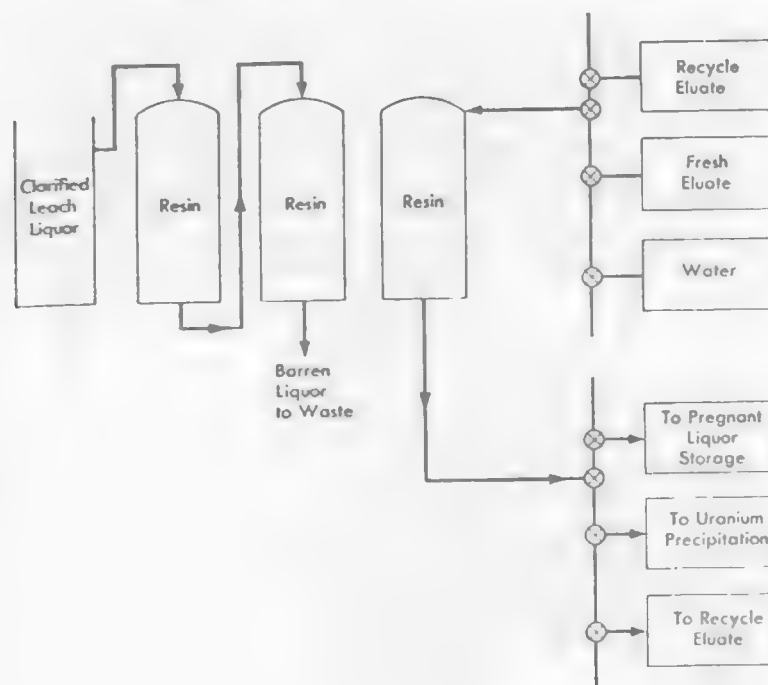
Figure 6.5.1. Fixed Bed Ion Exchange Reactor¹



In operation (see Figure 6.5.3), the pregnant solution is split between two sets of adsorption columns, with the cycles arranged so that the leading column in each set becomes saturated alternately. Three columns are used in series for each set of adsorption. When the leading column is fully loaded, its resin is transferred into the empty backwash tank, after that a charge of completely stripped resin from the elution section is transferred into the empty adsorption vessel. This then becomes the third line. After backwashing, the loaded resin becomes third in the line in the elution series.

The Resin-In-Pulp methods were developed to recover uranium from the pregnant solution without a filtration step. Commercial operations

Figure 6.5.2. Solution Flow Through a Three-Column Ion-Exchange Fixed Bed Circuit.(1)



are carried out either by a semi-continuous basket process or by a continuous countercurrent mix and screen process. For the basket ion exchange process, the resins, (at least 90% between 10- and 20-mesh size) are retained in cubic-shaped baskets. The basket size varies from 4 to 6 feet on a side, and holds 15 to 40 cubic feet of resins. The baskets are moved up and down (shown in Figure 6.5.4) at a rate of between 6 and 12 strokes per minute in rectangular banks containing flowing slurry or elution solutions. The baskets are arranged in 14 banks, usually there are two baskets in each bank, seven banks in series for adsorption, one for wash, four for elution and one on standby (as shown in Figure 6.5.5). The flow of slurry or solution from bank to bank may be accomplished either by an air lift or by gravitation flow. This process can handle a slurry containing up to 7% solids.

When a bank of baskets is saturated, it is drained and rinsed. The feed is then switched to the next bank. At the same time a new bank, containing eluted resin, is added at the end of the series. The loaded bank is then added to the end of the series in the elution section.

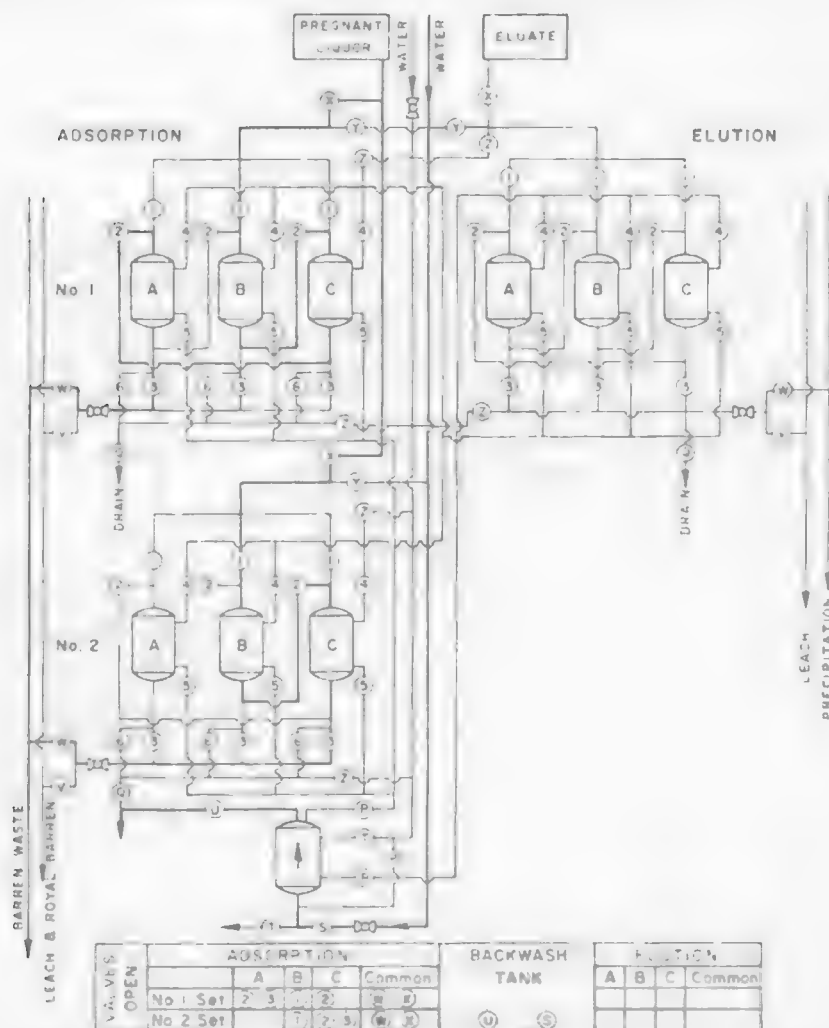
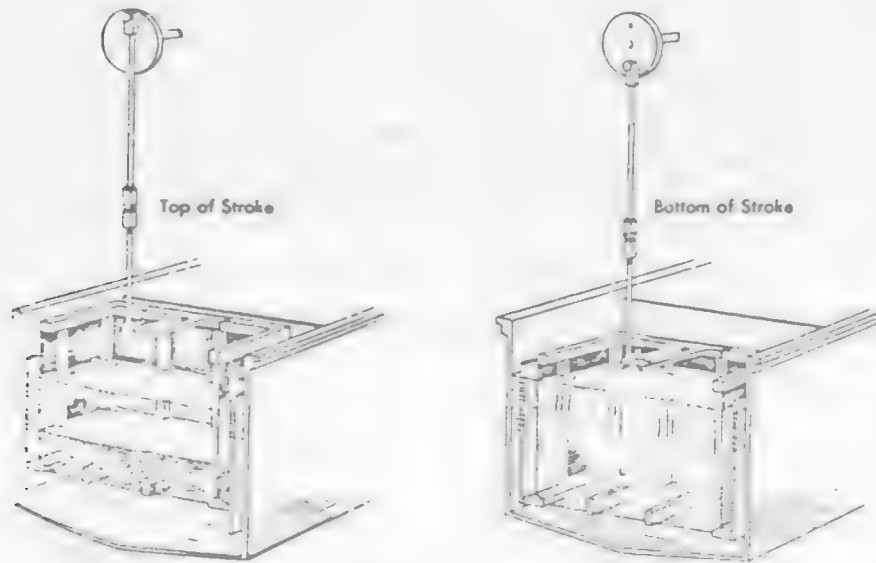
Figure 6.5.3. Flowsheet for Moving Bed Column Ion Exchange Process.²

FIGURE 6-14.—Flow diagram of plant showing no. 1 set on three-column adsorption, no. 2 set on two-column adsorption, one loaded column being back-washed prior to elution.

Figure 6.5.4. Cross Section of RIP Basket.³Figure 6.5.5. Basket RIP Circuit.³

The mix and screen ion exchange process is a continuous counter-current system in which resin and slurry or resin and eluent are moved in an opposite direction through a series of stirred tanks with air lifts and screens between them. A schematic diagram is shown in Figure 6.5.6, and the operation circuit is shown in Figure 6.5.7. The agitation is provided by air or mechanical mixers. The discharge from each tank is pumped to a vibrating 60 mesh screen located above the following tank; the slurry falls directly into this tank by gravity while the resins are captured and sent to a following tank. This method can be used on uranium slurries containing up to 15% solid (with resin size ranged 20-50 mesh).

Figure 6.5.6. Schematic Diagram of Mix and Screen RIP Contractor.⁴

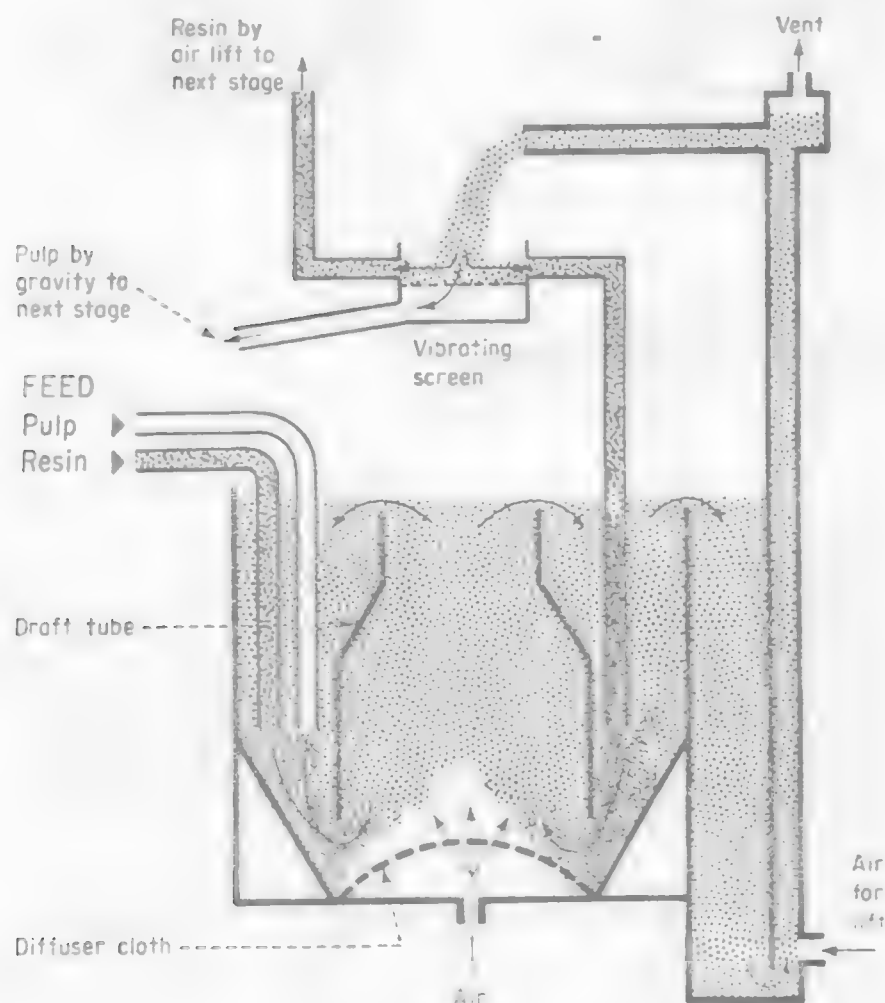
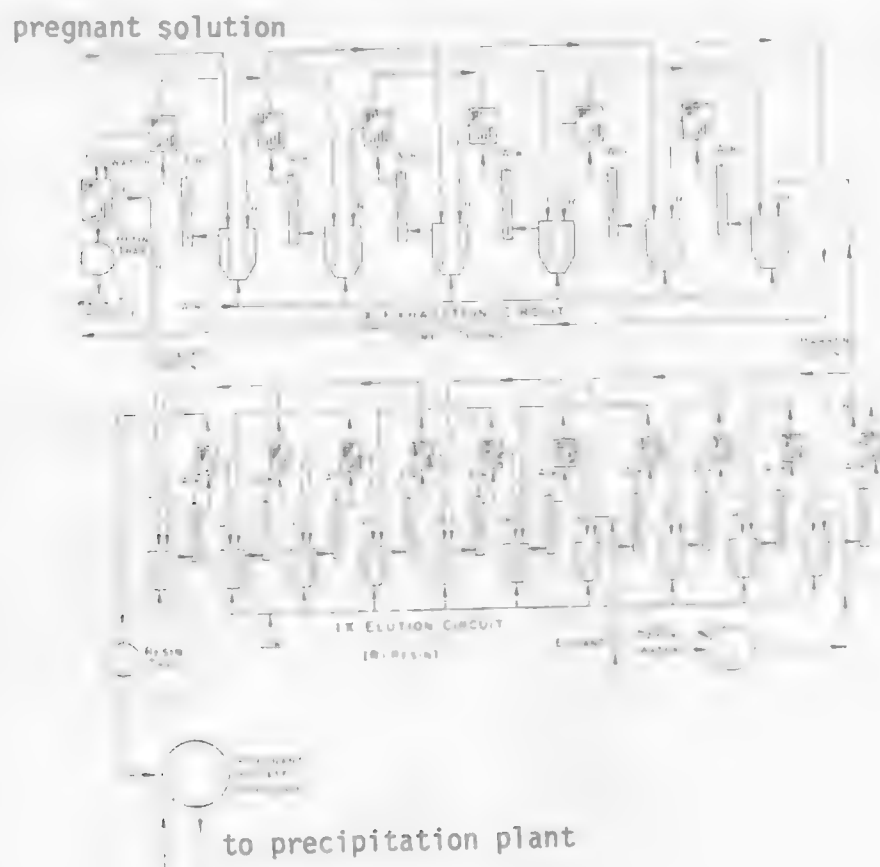


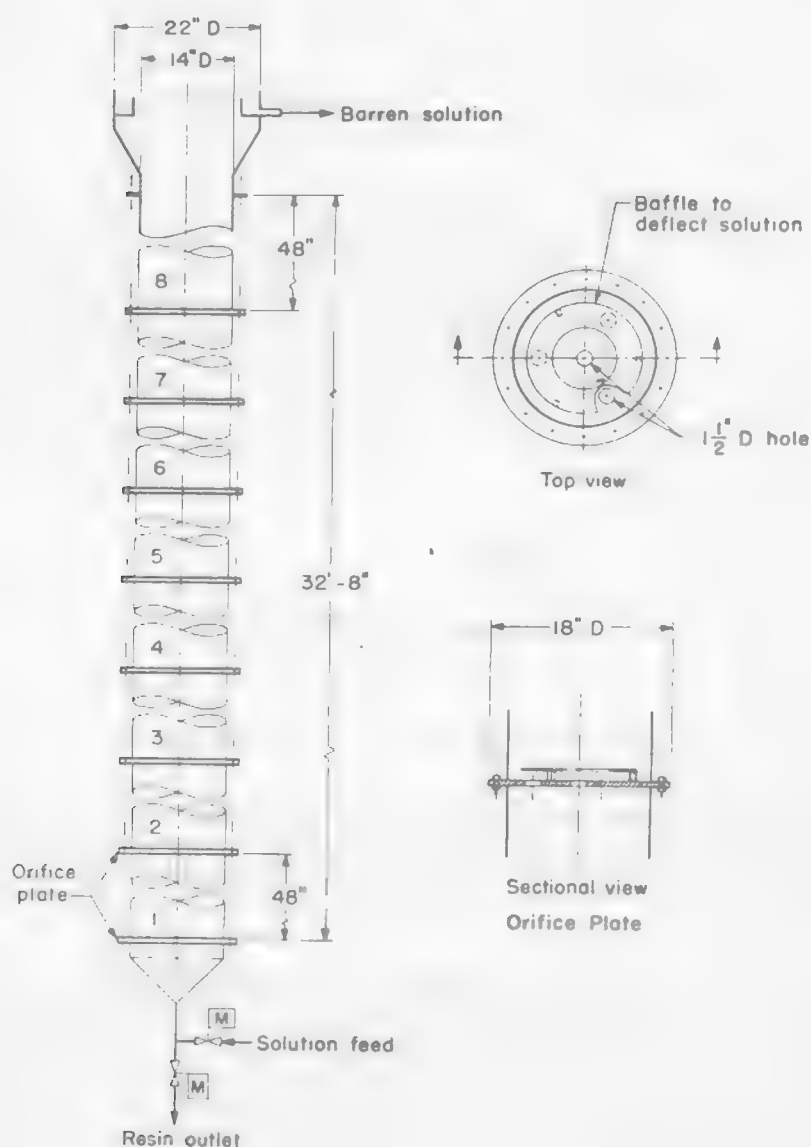
Figure 6.5.7. Flowsheet of Mix and Screen RIP Operation.²

Loaded resin moves continuously from the adsorption stages to the elution stages and barren resin from elution back to adsorption. Normally, from 6 to 8 stages are employed in adsorption and from 7 to 14 for elution.

These two RIP processes (basket and mix and screen) share the same disadvantage, i.e., each unit represents only one theoretical stage. Therefore, a large number of cells, consequently a large area of space, are required for a full adsorption and elution operation. A multiple-component ion exchange circuit has been proposed by U. S. Bureau of Mines. The feature of the column is the use of orifice plates to divide a resin column into separate compartments so that each compartment serves as a unit in a countercurrent multiple-stage system. By regulating the flow of solution, the slurry flows upward through the column, the sized resin falls downward through the column, while maintains each compartment as a fluidized bed. The effect of this design is to provide a number of separate batch contact stages in one column, instead of several columns in series.

A schematic diagram of a pilot plant operation is shown in Figure 6.5.8. It consists of an extraction column built of 7 compartments, a regeneration column and a wash section. Test results have shown 99% uranium extraction can be achieved.

Figure 6.5.8. U. S. Bureau of Mines Multiple-Compartment Ion Exchange Column.⁵



6.5.3 Extraction of Other Metals

Ion exchange technique can also be used to recover gold, copper, nickel, cobalt, chromium, rare earths, and rare metals, etc.

6.5.4 Separation of Metal Ions

The separation of metal ions by ion exchange was developed originally for analytic and research purposes. The technique has become an important procedure for the separation of metals with similar valence, e.g., the separation of rare earths. The separation can be carried out either by the separation of metal ions of opposite charge or by ion exchange chromatography.

The separation of metal ions of opposite charge can be achieved by adjusting the aqueous environment so that one particular metal ion will be transformed into a stable anionic complex. This ion is then subsequently removed by a single cation-anion ion exchange separation. The environment adjustment can be accomplished by selecting the proper pH; addition of complex reagent; or by changing the oxidation state of one particular ion, etc. The technique of changing pH to reverse the charge of a metal ion is demonstrated by the following example. Ethylenediaminetetraacetic acid (EDTA), which is known as a complexing reagent, binds different metal cations selectively (depending on the pH) to form anionic complexes. These complexes of course are not retained in a cation exchange column. It is, therefore, possible to separate lanthanum from thorium at a pH of 2.2, samarium from iron at a pH of 1.8, yttrium from scandium at a pH of 1.35, and magnesium from aluminum at pH 4.0.

The same principle can be used for the separation of metal ions by adding the complexing reagents into the solution in which a certain metal cation will form a negative charge complex with the reagent. This complex can be adsorbed by an anion exchanger and be selectively separated from uncomplexed cations when the solution passes through an anion exchanger. A classic example of this type is the separation of uranium ion from other metal cations by complexing the uranyl cations with sulfate, chloride or carbonate ions to form complexed uranyl anions.

However, there are many instances in which the differences between ionic species are not sufficiently great to permit separating. Separations of such ionic mixture may be accomplished by applying the ion exchange chromatographic technique. The technique may be resolved into two classes, those that may be separated on the adsorption cycle--adsorption chromatography, and those that may be separated on the elution cycle--elution chromatography.

The basic principle of adsorption chromatographic technique is that two different ions may be adsorbed by the exchanger at different rates. Therefore, one type of ion will stay on the top part of the exchange column, and the other type stays on the bottom part. When eluted with suitable eluant, one type of the ion will be in the first fraction of the eluate, and the other type in a later fraction.

The basic principle of elution chromatographic technique is that both ions may be adsorbed at about the same rates, but desorbed by the eluent at different rates. When eluting the loaded column, one type of ion may be in the first portion of the eluate, and the other type of ion in the later portion. Depending on the type of eluent used, the elution chromatographic technique is further classified into displacement chromatography, elution chromatography, and chromatography with complex reagent. More detailed discussion on this topic can be found in Reference 6.

Adsorption chromatography is generally applied to the separation of ions which exhibit reasonably different selectivities for an exchanger. Examples of this type include the separation of sodium from calcium and the separation of chloride from sulfate.

6.5.5 References

1. J. W. Clegg, D. D. Foley, Uranium Ore Processing, Addison-Wesley Publication, Chap. 9, 1957.
2. R. C. Merritt, Extractive Metallurgy of Uranium, Colorado School of Mines Research Institute, Chap. 6 (1971).
3. T. V. Arden, "Ion Exchange Processes in the Atomic Industry," Austria Inst. Mining and Met., Proceedings, No. 198, p. 153 (1961).
4. Editorial: New Contractor Unravels Difficult Ore, Chem. Eng., May, 52 (1959).
5. D. R. George, J. R. Ross, New Developments in the Recovery of Uranium by Ion Exchange, presented at the Uranium Symposium, AIME, June 15-19, 1959.
6. K. Dorfmer, Ion Exchangers Properties and Applications, Ann Arbor Science, Ann Arbor, Michigan, Chap. 4 (1962).

UNIT PROCESSES IN EXTRACTIVE METALLURGY
HYDROMETALLURGY

Module 7

Module Recovery

FIVE LEARNING
ACTIVITIES

Module 7 Contents

Module 8 Contents

7.1 Gaseous Reduction in Aqueous Solutions

1. Hydrogen Gas Reduction
2. Other Gases

Learning Activity 1

7.2 Cementation

1. Introduction
2. Theory
3. Initial Concentration
4. Temperature
5. Summary

Learning Activity 2

7.3 Electrolysis

1. Introduction
2. Sample Calculations
3. Electroplating of Copper
 1. Electroplating reactions
 2. Cell Voltage and energy consumption
 3. Cathode Current Efficiency: Interfering Ion Reactions
 4. Quality of Cathode: Behavior of Electrolyte Impurities
 5. Electroplating Tankhouse Practice
 6. Special Problems of Solvent Extraction Electrolytes
 7. Recent Improvements in Electroplating Procedure
 8. Summary

Learning Activity 3

Learning Activity 4

7.4 Electrowinning Plant Practice

1. Purpose of Process
2. The Leach Process
3. The Refining Process
4. Solution Mining
5. Control of Acid Mist
6. Role and of Heat Generation
7. Heat Recovery and Size of Operations
8. Chemistry and Electrochemistry of the Zinc Cell
9. Cathode Materials
10. Anode Materials
11. Cell Design Considerations

Learning Activity 5

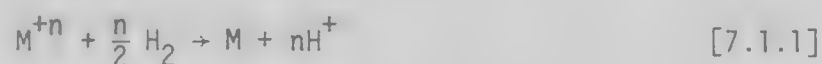
LEARNING ACTIVITY 1

7.1 Gaseous Reduction in Aqueous SolutionsLearning Activity Objective

After completing your study of this learning activity material you should be able to describe the reduction of metal ions from aqueous solutions by the use of gaseous reducing agents, particularly hydrogen.

7.1.1 Hydrogen Gas Reduction

One means of recovering a metal from aqueous solution is by metal ion reduction by a reducing gas such as hydrogen, carbon monoxide or sulfur dioxide. By far the most widely used reducing gas for precipitating metals from solutions is hydrogen. This reaction is illustrated by the following equation.



The equilibrium position of this reaction can be calculated from the standard free energy function.

Example:

The hydrogen reduction of Ni from solution by far exceeds any other metal recovered by this technique.

If we consider reaction 7.1.1 applied to nickel:



$$\Delta G^\circ = -RT \ln K \quad [7.1.3]$$

$$= \Delta G^\circ_{\text{Formation of Products}} - \Delta G^\circ_{\text{Formation of Reactants}} \quad [7.1.4]$$

$$= 0 - (-11,530 \text{ calories})$$

$$= +11,530_{@ 298^\circ K} \quad [7.1.5]$$

Therefore,

$$K_{@298^\circ K} = 3.4 \times 10^{-9} \quad [7.1.6]$$

$$= \frac{(a_{H^+})^2}{P_{H_2} \cdot a_{Ni^{++}}} \quad [7.1.7]$$

The reaction is certainly unfavorable at 298°K. Its extent is also (besides being temperature dependent) dependent on hydrogen pressure and pH.

The deposition of Ni from solution is commercially accomplished in autoclaves, i.e., at elevated temperature and pressure in the presence of ammonia (see reference 4, pp. 310-312).

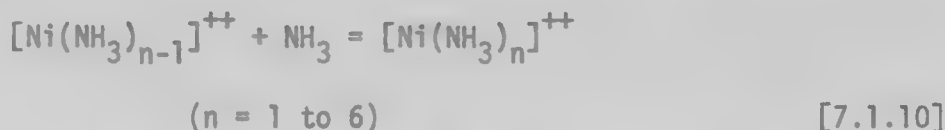
Let's look at the reduction reaction again.



In an ammoniacal solution reactions are occurring in addition to [7.1.8]. Hydrogen ions combine with ammonia to form ammonium ions.

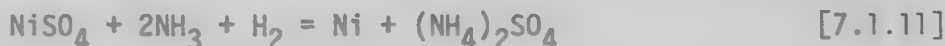


Therefore, increasing the free ammonia concentration reduces the concentration of hydrogen ion and thus promotes reaction [7.1.8]. But nickel ions are complexed:



This tends to reduce the Ni^{++} availability for reduction. In practice it has been found that nickel can be almost completely reduced if two moles of NH_3 per mole of Ni^{++} is present, when less NH_3 is present the reaction stops with some nickel unreduced from lack of NH_3 to neutralize the H^+ resulting from the reduction. If more than two moles/mole Ni^{++} is present the ratio of concentration of ammonia to concentration of nickel increases as the reduction proceeds, resulting in Ni^{++} complexing until the Ni^{++} concentration is so low that reaction stops. Care is taken in commercial operations to maintain the NH_3/Ni^{++} ratio between 1.9 and 2.1.

The actual mechanism of reaction is much more complex than is described above but is beyond the scope of this course. The overall reaction is summarized by the following equation.



The commercial operating conditions quoted by the Freeport Nickel Company for their process at Port Nickel, Louisiana are pH = 1.8,

temperature = 375°F, hydrogen pressure = 700psi.

As a student exercise, calculate the free energy change for these conditions.

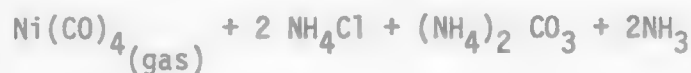
Metals that are commercially produced by hydrogen reduction are nickel and cobalt. Metals that can theoretically be reduced from solution are copper, silver, gold, platinum and palladium.

7.1.2 Other Gases (2)

Hydrogen is by far the most used reducing gas for depositing metals from aqueous solutions. The reasons for this are hydrogen is a simple gas and relatively cheap to produce on a large scale. The reaction products in an aqueous solution are simple, i.e., either hydrogen ions or hydroxyl ions. Neither of these ions create other solution by-products that would be a disposal problem. Other reducing gases such as carbon monoxide and sulfur dioxide do produce either a gas product or solution reaction product that must be recovered or further treated for disposal.

Although carbon monoxide, CO, is used extensively by INCO as a reactant to pyrometallurgically purify nickel, it is not used commercially as a reducing agent in aqueous solutions. Studies have been made that demonstrate the technical possibility of its use, e.g.,

Nickel (3) via the reaction

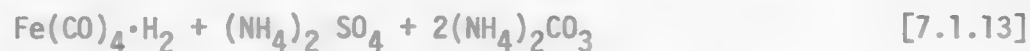


$$T = 150^\circ\text{C}$$

$$P_{\text{CO}} = 100 \text{ atm.}$$

The nickel carbonyl could be decomposed and the CO recovered and recycled for further reduction.

Iron and cobalt (4) via the reaction



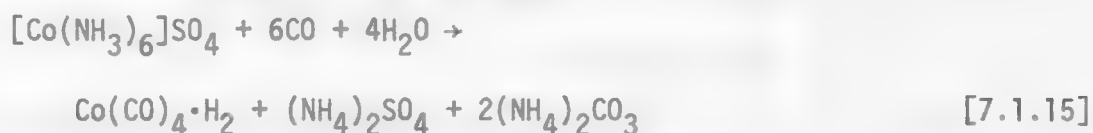
$$T = 80^\circ\text{C}$$

$$P_{\text{CO}} = 100 \text{ atm.}$$

The iron carbonyl hydride decomposes in the presence of excess CO to yield iron pentacarbonyl gas.



Cobalt may be recovered by the reaction



The cobalt hydride is stable in basic solutions but if the solution is acidified, it can be evolved in a vacuum as $\text{Co(CO)}_4 \cdot \text{H}_2$. This compound decomposes to yield the tetracarbonyl.



Sulfur dioxide has been studied over the years as a reducing agent in laboratory and pilot scale operations but has not been utilized commercially.

References

1. Boldt, J. R. and P. Queneau, The Winning of Nickel, Van Nostrand Co., New York, 1967, 487 p.
2. Meddings, B. and V. Mackiu, The Gaseous Reduction of Metals from Aqueous Solutions, Unit Processes in Hydrometallurgy, AIME, Dallas, 1963, pp. 345-384.
3. Reppe, W., Experienta, 5, 1949, p. 93.
4. Reppe, W., Experienta, 6, 1950, p. 68.

LEARNING ACTIVITY 2*

Dr. Jan Miller
 Professor of Metallurgical Engineering
 Department of Metallurgy and Metallurgical Engineering
 University of Utah

7.2 CementationLearning Activity Objective

After completing your study of this learning activity material you should be able to describe metal value recovery by cementation processes; be able to predict the theoretical possibility of a cementation reaction; list the experimental process parameters of importance in cementation; and be able to discuss the kinetic aspects of cementation processes.

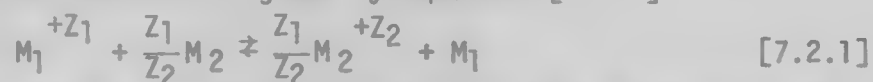
7.2.1 Introduction

One of the most ancient, yet most effective, hydrometallurgical processes for the recovery of dissolved metal values from aqueous solution is cementation, a process that was first reported in the 16th century.⁽¹⁾ In principle, the electrochemical cementation reaction, or contact reduction, is relatively simple, involving the discharge of a noble metal ion (i.e., the ion to be cemented) at the expense of a more reactive metal. In modern times it has been used extensively for the recovery of metals and the purification of electrolytes. Classic examples of industrial importance include: copper cementation with iron, gold cementation from cyanide solutions with zinc dust, and cadmium cementation from electrolytic zinc sulphate solutions with metallic zinc.

In the past decade a significant research effort has been expended to better understand the ancient art of cementation. A few practical, as well as many theoretical studies, have been reported in the literature. The most significant development from an industrial point of view has been the development of copper cementation cones, designed to replace launders--so common to the extractive metallurgist in years past.⁽²⁾ The success that these cones have achieved, as compared with the more traditional launders, can well be realized from a basic understanding of the principles that govern the copper cementation reaction.^(3,4,5) Further realization of their success comes from their acceptance and use by industry. A recent installation of three cones by Nchanga Consolidated Copper Company at Chingola, Zambia, is illustrated by the photograph in Figure 7.2.1.

7.2.2 Theory

The basic cementation reaction is given by equation [7.2.1].



and the overall reaction is the sum of numerous microcells, one of which is depicted schematically in Figure 7.2.2. Essentially, the system is a set of shortcircuited electrolytic microcells and the cementation reaction can be considered in terms of the respective half cells:

* The material presented as Learning Activity 2 is a condensation of a publication by Dr. Miller in Minerals Science and Engineering, Vol. 5, No. 3, pp. 242-254, July 1973.

Figure 7.2.1. Cementation Cones Recently Installed at Chingola, Zambia.

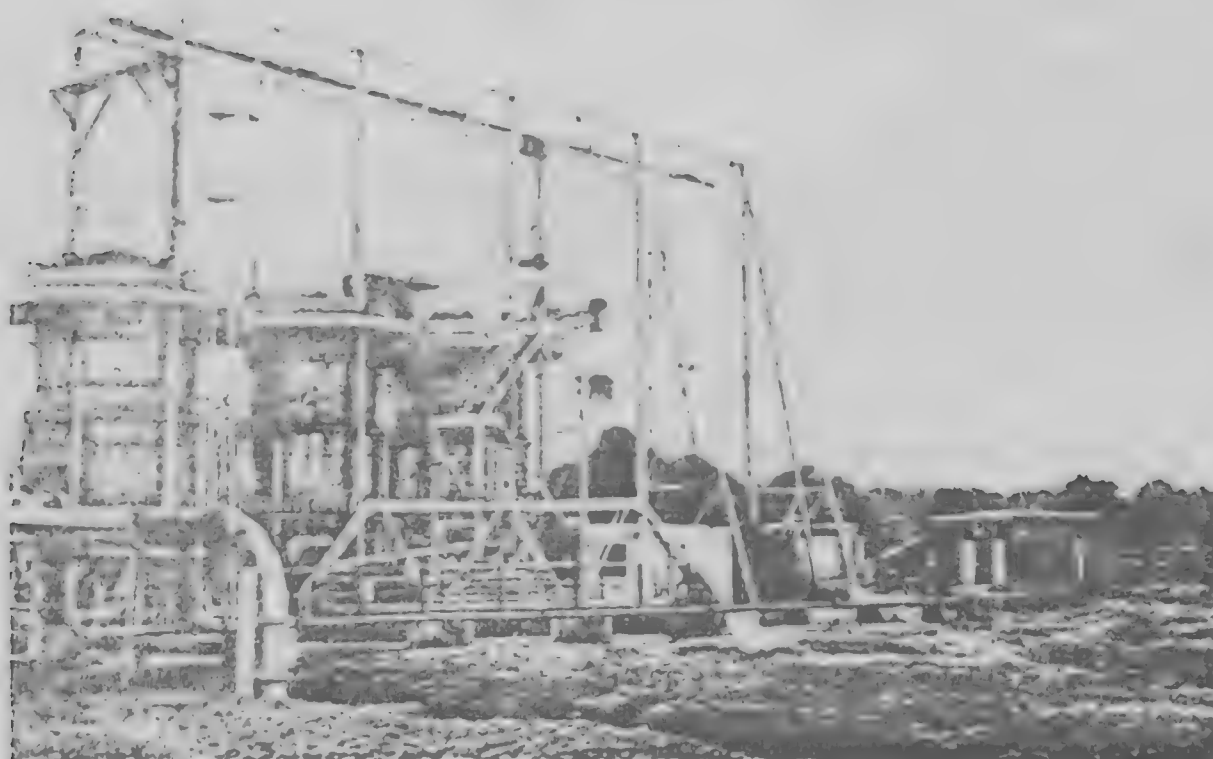
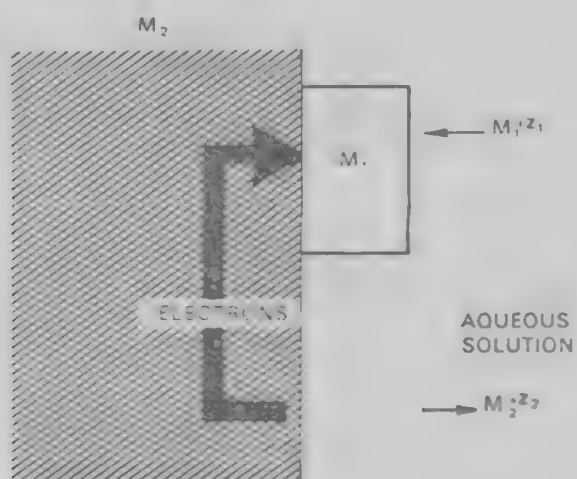
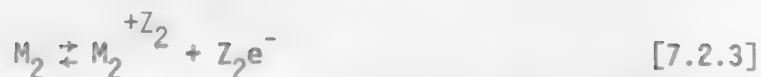
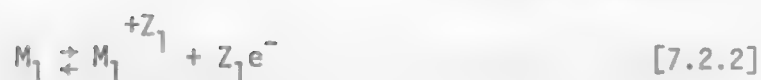


Figure 7.2.2. Schematic Representation of an Electrochemical Microcell Operative in Cementation Systems.





The reaction is termed electrochemical, as opposed to a chemical redox reaction, in the sense that the electrons are not exchanged at the same site, but rather the half-cell reactions are separated by an arbitrary, finite distance which necessitates that the solid phase be a conductor or semiconductor. Also, cementation should be distinguished from electrolytic deposition in which the source of electrons is from a generator rather than a less noble metal.

Most of the common cementation reactions exhibit large negative free energy changes, and generally the reactions can be considered to go to completion in a thermodynamic sense. The standard free energy change for any given couple can be calculated from the half cell potentials given in Table 7.2.1.⁽¹³⁾ For example, in the case of cadmium cementation on zinc the reaction would be:



The standard free energy change is:

$$\Delta G^\circ = -nFE^\circ \quad [7.2.5]$$

$$\Delta G^\circ = 2 \frac{\text{equiv}}{\text{mol}} \times 23.06 \frac{\text{kcal}}{\text{volt equiv}} \times 0.36 \text{ volt} \quad [7.2.6]$$

$$\Delta G^\circ = -16.6 \text{ kcal/mol} \quad [7.2.7]$$

Thus, at 25°C the net reaction would stop when:

$$\frac{a_{Zn^{2+}}}{a_{Cd^{2+}}} > 10^{12.2} \quad [7.2.8]$$

As in all hydrometallurgical systems, a good understanding of solution chemistry is necessary in order to characterize the cementation reaction. In particular, it is important to note that the ionic activities are controlled both by complexation reactions and by the ionic strength of the solution.

As might be expected, in some respects, cementation is analogous to electrolytic deposition. In cementation systems the anode and cathode are short-circuited and the current density is most frequently controlled by the concentration of the discharging metal ions at cathodic sites, due to diffusional processes, whereas in electrolysis such is not

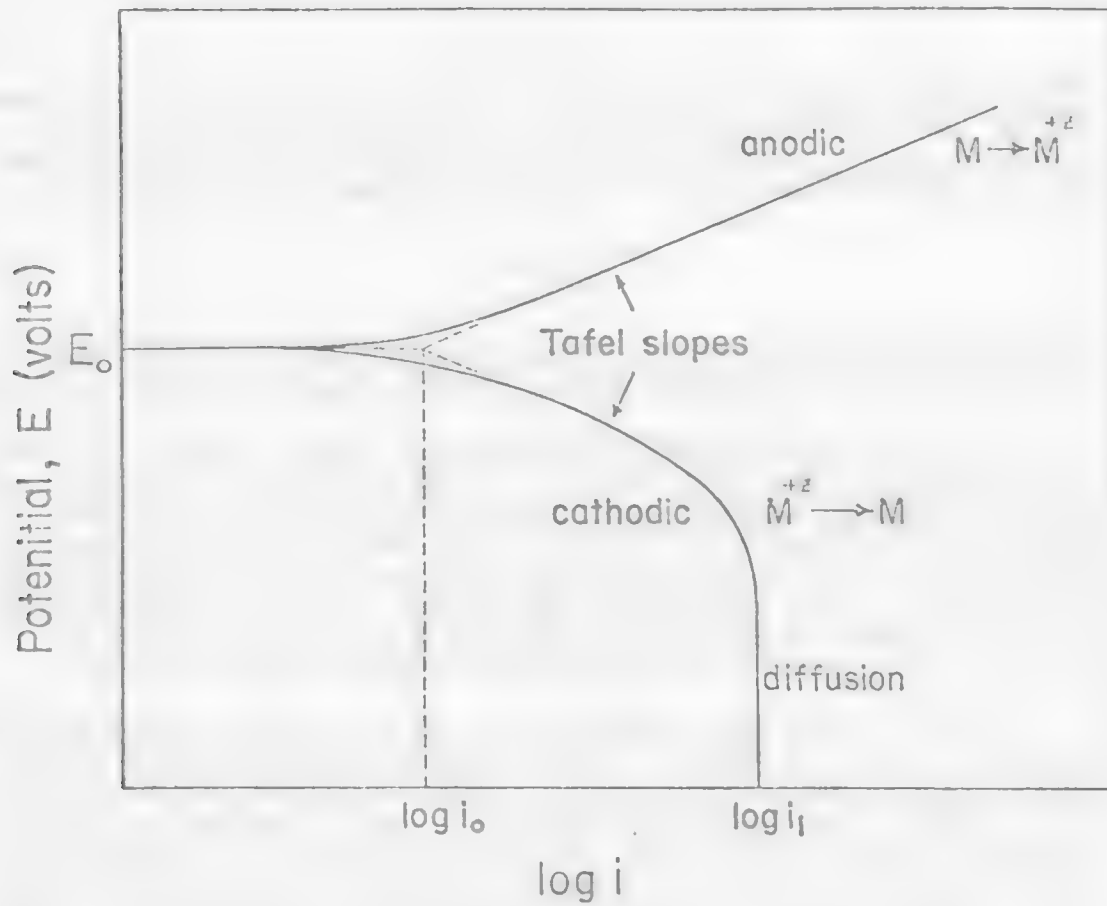
necessarily the case. The reaction rate, which is equivalent to the current density, is the response most frequently used by researchers to characterize a given cementation system. A detailed analysis of cementation reactions in terms of electrochemical theory has been given by Wadsworth.⁽¹²⁾

TABLE 7.2.1. Standard Half-Cell Potentials at 25°C.

Half cell	E°, volts	Half cell	E°, volts
$\text{Zn} \rightarrow \text{Zn}^{2+} + 2\text{e}^-$	+0.763	$\text{H}_2 \rightarrow 2\text{H}^+ + 2\text{e}^-$	0.000
$\text{Fe} \rightarrow \text{Fe}^{2+} + 2\text{e}^-$	+0.440	$\text{Bi} \rightarrow \text{Bi}^{3+} + 3\text{e}^-$	-0.32
$\text{Cd} \rightarrow \text{Cd}^{2+} + 2\text{e}^-$	+0.403	$\text{Cu} \rightarrow \text{Cu}^{2+} + 2\text{e}^-$	-0.337
$\text{In} \rightarrow \text{In}^{3+} + 3\text{e}^-$	+0.342	$\text{Co} \rightarrow \text{Co}^{3+} + 3\text{e}^-$	-0.400
$\text{Co} \rightarrow \text{Co}^{2+} + 2\text{e}^-$	+0.277	$\text{Cu} \rightarrow \text{Cu}^+ + \text{e}^-$	-0.521
$\text{Ni} \rightarrow \text{Ni}^{2+} + 2\text{e}^-$	+0.250	$\text{Ag} \rightarrow \text{Ag}^+ + \text{e}^-$	-0.799
$\text{Pb} \rightarrow \text{Pb}^{2+} + 2\text{e}^-$	+0.126	$\text{Pd} \rightarrow \text{Pd}^{2+} + 2\text{e}^-$	-0.987
$\text{Fe} \rightarrow \text{Fe}^{3+} + 3\text{e}^-$	+0.036	$\text{Pt} \rightarrow \text{Pt}^{2+} + 2\text{e}^-$	-1.200

A convenient way to think about cementation reaction kinetics is to plot the current-potential curves for the respective half cells involved in the cementation reaction, as done by Power.⁽³¹⁾ These diagrams are referred to as Evans diagrams and have been used in the analysis of corrosion reactions. In essence, the diagrams are simply the superposition of two current-potential (polarization) curves. A typical polarization curve for an arbitrary metal is shown in Figure 7.2.3. At very low currents the potential, E_0 , is equivalent to the reversible electrode potential. As E is made more negative (cathodic) than E_0 , the metal ions begin to be reduced. At some point the potential begins to vary linearly with $\log i$. This region of the polarization curve is known as the Tafel region and the slope of the linear portion of the polarization curve is known as the Tafel slope. For large negative values of potential, the current density reaches a maximum value, the limiting current density. Under these conditions the current is

Figure 7.2.3. Polarization Curve for an Arbitrary Metal Showing Cathodic and Anodic Reaction.(31)



determined by the rate of transport of metal ions to the surface. Similar regions can be identified for the anodic behavior of the system when the potential is made more positive than E_0 . In this case, however, the limiting current density is reached only when the metal surface becomes saturated with respect to a salt of the metal. From the linear region of polarization curves, the Tafel equation is defined,

$$\eta = a \pm b \log i \quad [7.2.9]$$

where: a and b are constants and η is the overpotential (the difference between the potential at some current i and the reversible electrode potential, $E_0 - E$). Alternately, the Tafel equation can be written from the Butler-Volmer equation in terms of the exchange current density,

$$\eta = b \log \frac{i}{i_0} \quad [7.2.10]$$

The polarization curves can be determined experimentally or calculated provided the exchange current density and transfer coefficients are known.

The use of Evans diagrams in cementation systems is best illustrated by some examples taken from Power.⁽⁴⁾ In these systems it will be assumed that the polarization curves are independent, that the cathodic and anodic areas are equal and that there is no ohmic resistance between cathode and anode. Further, the diagrams are constructed for mass transfer rates calculated for a rotating disc at 100 rad/sec. The most important feature of these diagrams is that they demonstrate quite clearly whether the reaction will be controlled by an electrochemical surface reaction.

For the first example, consider the (Cu^{++}/Fe) Evans diagram presented in Figure 7.2.4. The point of intersection of the polarization curves determines the mixed potential for the reaction and the rate controlling step. Because the polarization curves intersect the cathodic copper curve in the diffusion limited region, the reaction would be expected to be controlled by mass transfer of cupric to the reaction surface. Many investigators have found this to be true from experimental cementation studies.

As the other example, consider the (Fe^{++}/Zn) system shown in Figure 7.2.5 for which a different conclusion would be reached. In this case the point of intersection occurs in the Tafel region of the polarization curve and one would expect the reaction to be electrochemically controlled.

The criterion for chemical control is that the anodic curve intersect the cathodic curve in the Tafel region. An idealized Evans diagram can be constructed as shown in Figure 7.2.6 and the point at which rate control switches from mass transfer to chemical reaction can be evaluated. Solution of the respective Tafel equations for cathodic and anodic half cells at the transition mixed potential results in;

Figure 7.2.4. Evans Diagram for the Cu^{++}/Fe System - Mass Transfer Controlled. (31)

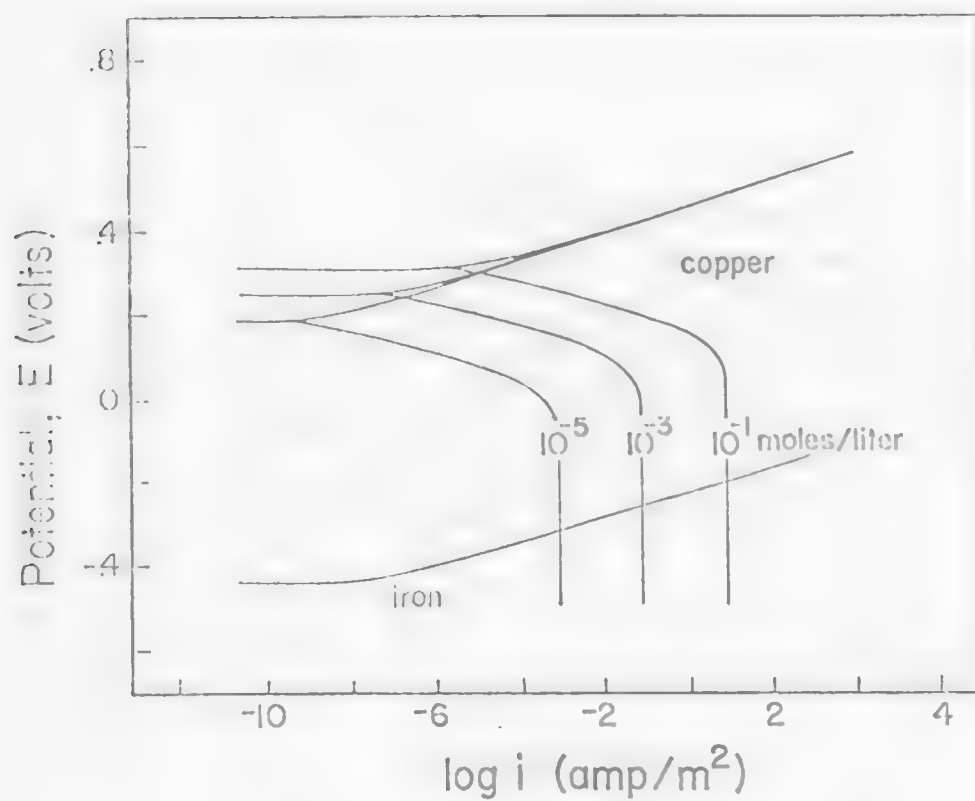


Figure 7.2.5. Evans Diagram for the Fe^{++}/Zn System - Electrochemical Reaction Controlled.(31)

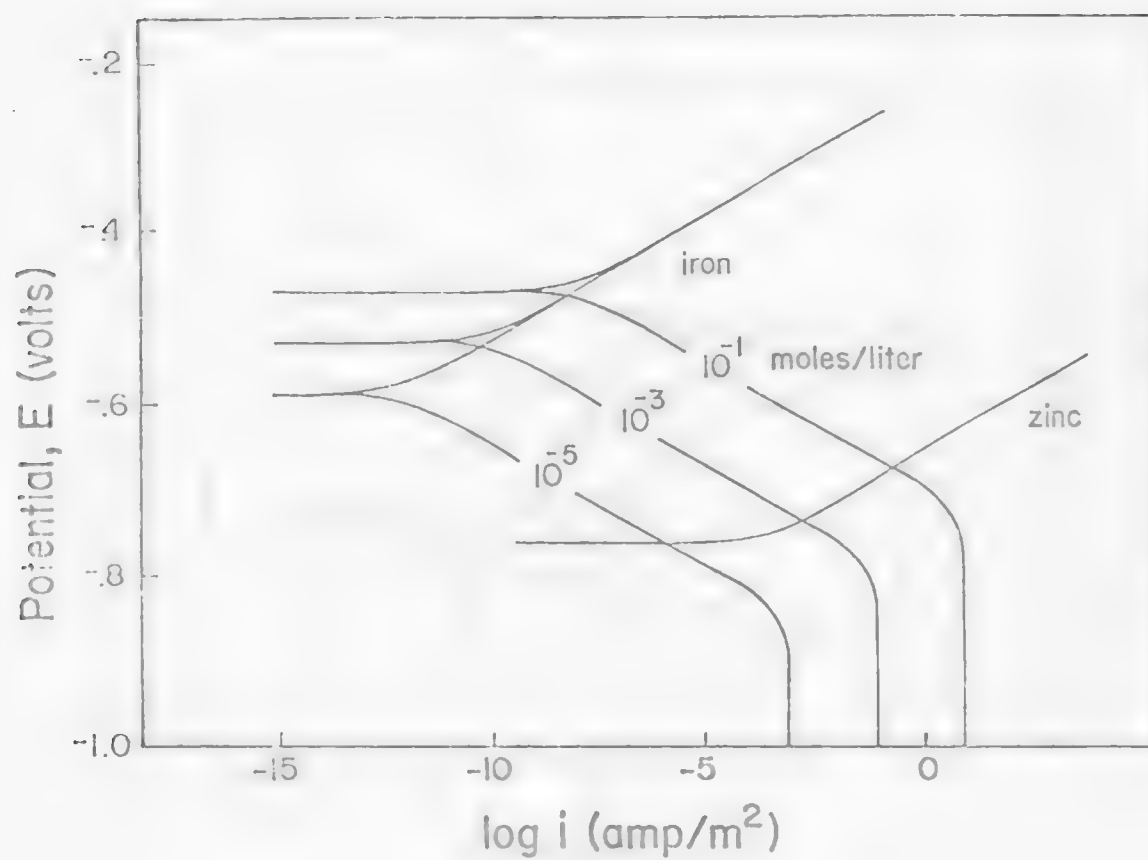
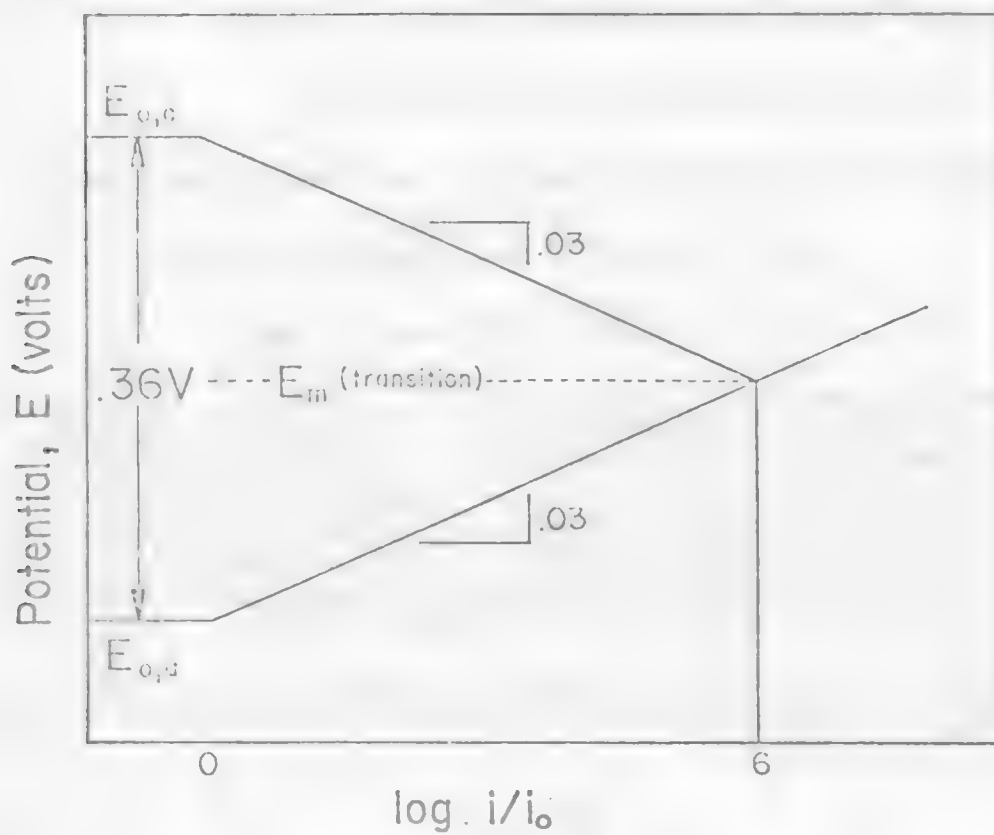


Figure 7.2.6. Idealized Evans Diagram which Represents the Transition from Mass Transfer Control to Electrochemical Reaction Control. (31)



$$\Delta E_0 = b \left[\log\left(\frac{i_l}{i_0}\right)_c + \log\left(\frac{i_l}{i_0}\right)_a \right] \quad [7.2.11]$$

The variables in equation [7.2.11] take on the following values

$b \approx 0.03$ volts/decade current density for many metals (Cu, Fe, Zn)

$i_l \approx 10^2 \text{ amp/m}^2$ (0.1M solution)

$i_0 \approx 10^1 \text{ amp/m}^2$ (Cu) $\rightarrow 10^{-4} \text{ amp/m}^2$ (Fe)

Consequently, for cementation reactions a good rule-of-thumb would be:

$$\Delta E_0 < 0.06 \text{ volt} - \text{electrochemical control} \quad [7.2.12]$$

$$\Delta E_0 > 0.36 \text{ volt} - \text{mass transfer control} \quad [7.2.13]$$

Between these values, the exchange current densities must be known in order to predict the rate limiting step. As a further approximation, the standard electrode potentials ΔE_0^0 of the respective half cells can be used to approximate ΔE_0 . When these values are calculated, it is found that most cementation systems have a difference in standard electrode potential of greater than 0.36 volts. Further, experimental investigations indicate that most cementation reactions are controlled by mass transfer processes as indicated by the results presented in Table 7.2.2.

Almost without exception cementation reactions appear to be first-order processes with respect to $M_1^{+Z_1}$ and can be represented by the first-order rate equation:

$$\frac{dC_1}{dt} = \frac{kA}{V} C_1 \quad [7.2.14]$$

As can be seen from equation [7.2.14], the rate of cementation, as in most heterogeneous reactions, is determined by the labile area on which the noble metal ion is to be reduced. However, this area parameter is much more complex than one would initially suspect. In fact, the area that controls experimentally observed reaction rates is determined by the nature of the surface deposit. Accordingly, then it would not be unreasonable to suspect that the reaction rate constant for a given system would be a function of the variables that affect the structure of the surface deposit. For electrolytic processes these variables are well recognized to be: (15,16)

temperature
concentration of metal ion
agitation

concentration of ligands
current density
addition agents

Generally, these variables affect the surface deposit in the following way. Coarse-grained, loose and/or spongy deposits, i.e., deposits with a large effective surface area, are favored at elevated temperatures, high current densities, and high metal ion concentrations, whereas organic addition agents (glue, dextrine, and gelatine), low metal ion concentrations (which can be achieved by the addition of complexing ligands), and low temperatures favor bright, coherent, fine-grained deposits with a relatively smaller effective surface area. As an example, silver deposition from a nitrate solution by electrolysis tends to be coarse grained, but deposition from a cyanide solution results in a surface that is fine-grained, lustrous, and compact.

The supposition that the structure of the surface deposit in cementation reactions also changes with these variables has been confirmed, both qualitatively and quantitatively, in a number of systems. Drozdov⁽¹⁷⁾ has made the statement that porous deposits, those with a large effective area, result if the process takes place at a high rate, i.e., when concentrated solutions and active metals are used. Conversely, fine-grained coherent deposits are obtained from dilute solutions of inactive metals. In cementation systems the influence of these variables on the surface deposit would be reflected in the reaction rate constant. Two of these variables, concentration of the noble metal ion and temperature, will be considered in further detail later.

Another generalization, which may be more far-reaching than suspected, is that cementation reactions are diffusion controlled, especially at high temperatures. Frequently, activation energies in these systems range from 2 kcal/mol to 6 kcal/mol, which is to be expected for diffusion control in an aqueous system. Recent evidence in one system,⁽²³⁾ suggests that diffusion is rate controlling even at low temperatures, where previously it was thought that a surface reaction controlled the kinetic response. In any event as a consequence, the cementation rate constant, k , may be determined in most instances by the diffusion coefficient, D , and the diffusion layer thickness ΔX :

$$k = \frac{D}{\Delta X} \quad [7.2.15]$$

We have in effect, for cementation systems, the analogue of concentration polarization for electrolytic deposition.

In most heterogeneous solid-liquid systems, with increased mechanical agitation, or stirring, ΔX can be reduced to a constant thickness of about 10^{-3} cm and under such conditions is referred to as the Nernst limiting-boundary layer. For diffusion-controlled cementation reactions then, the rate constant is very sensitive to the hydrodynamics of the system (the relative velocity between solid and liquid phases) up to the condition where the limiting-boundary layer is reached, after which the rate constant is independent of stirring rate.

TABLE 7.2.2. Data for Selected Cementation Systems at 25°C. (3,5)

Systems	ΔE_0^0 volts	Activation Energy kcal/mole	Rate Constant cm/sec
Ag^+/Cu	0.46	2.0-5.0(12)	$2.5-6.0 \times 10^{-2}$
$\text{Ag}^+/\text{Cu}(\text{CN}^-)$	1.83	3.7-5.8	1.5×10^{-2}
$\text{Ag}^+/\text{Fe}(\text{Cl}^-)$	1.29	3.0	2.2×10^{-2}
$\text{Ag}^+/\text{Zn}(\text{CN}^-)$	0.95	5.5	5.5×10^{-2}
Ag^+/Zn	1.56	2.0-6.0(12)	$2.6-5.2 \times 10^{-2}$
Bi^{+3}/Fe	0.76	4.5-7.6	2.9×10^{-2}
Cd^{++}/Zn	0.36	4.0-4.7	$0.54-1.1 \times 10^{-2}$
Cu^{++}/Fe	0.75	3.1-5.1	$0.6-0.9 \times 10^{-2}$
Cu^{++}/In	0.83	2.3	5.9×10^{-2}
Cu^{++}/Ni	0.57	2.7-3.7(14.2-19.0)	$0.25-1.0 \times 10^{-2}$
Cu^{++}/Zn	1.10	3.1	$1.6-2.1 \times 10^{-2}$
Ni^{++}/Fe	0.21	-7.0	-1×10^{-4}
Pb^{++}/Fe	0.31	12.0	-
Pb^{++}/Zn	0.64	-	0.64×10^{-2}
Pd^{++}/Cu	0.49	9.5-7.4	$0.36-2.3 \times 10^{-2}$

7.2.3 Initial Concentration

To begin with, one can see from the empirical first-order rate equation [7.2.14] that ideally the rate constant should be independent of the initial concentration of the noble metal ion. Very few systems reported in the literature exhibit this independence. Only in the work of Episkoposyan,⁽²¹⁾ Cu²⁺/Fe system, was the rate constant found to be independent of the initial copper concentration and that being over a rather limited range of concentration. The effect the initial concentration has on the reaction rate constant is variable and rather interesting. The results from a number of systems are presented in Table 7.2.3.

Table 7.2.3 Summary of the Effect Increased Initial Noble Metal Ion Concentration Has on the Experimentally Observed Rate Constant.

System	Ref	Apparent rate constant	Concentration range, g/l
Cu ²⁺ /Al (SO ₄ ²⁻)	9	decreased	0.0635–0.635
Cu ²⁺ /Fe (Cl ⁻)	21	no change	0.245 –2.667
Cu ²⁺ /Fe (SO ₄ ²⁻)	4	decreased	0.508 –1.585
Cu ²⁺ /Fe (SO ₄ ²⁻)	23	increased	0.01 –0.2
		decreased	0.2 –2.0
Cu ²⁺ /Ni (SO ₄ ²⁻)	11	decreased	0.53 –2.9
Cu ²⁺ /Zn (SO ₄ ²⁻)	22	increased	0.005 –0.1
Cd ²⁺ /Zn (SO ₄ ²⁻)	14	decreased	50.0 –100.0
Cd ²⁺ /Zn (SO ₄ ²⁻)	24	increased	0.005 –0.1
Ag ⁺ /Cu (NO ₃ ⁻)	25	increased	0.0027–4.28
Ag ⁺ /Cu (SO ₄ ²⁻)	24	increased	<0.1
Ag ⁺ /Zn (NO ₃ ⁻)	25	increased	0.0028–3.21
Ag ⁺ /Zn (SO ₄ ²⁻)	24	increased	<0.1

7.2.4 Temperature

From the temperature dependence of the reaction rate constant, the apparent activation energy, E_a , can be calculated, as was first proposed by Arrhenius at the turn of the century. The familiar relationship is:

$$k = A \exp (-E_a/RT) \quad [7.2.16]$$

A plot of $\log k$ versus $1/T$ frequently results in a straight line from which E_a is determined. For reactions controlled by diffusion in a liquid

phase, E_a is generally between 2 and 6 kcal/mol; whereas for a process controlled by a chemical reaction E_a is greater than 10 kcal/mol.

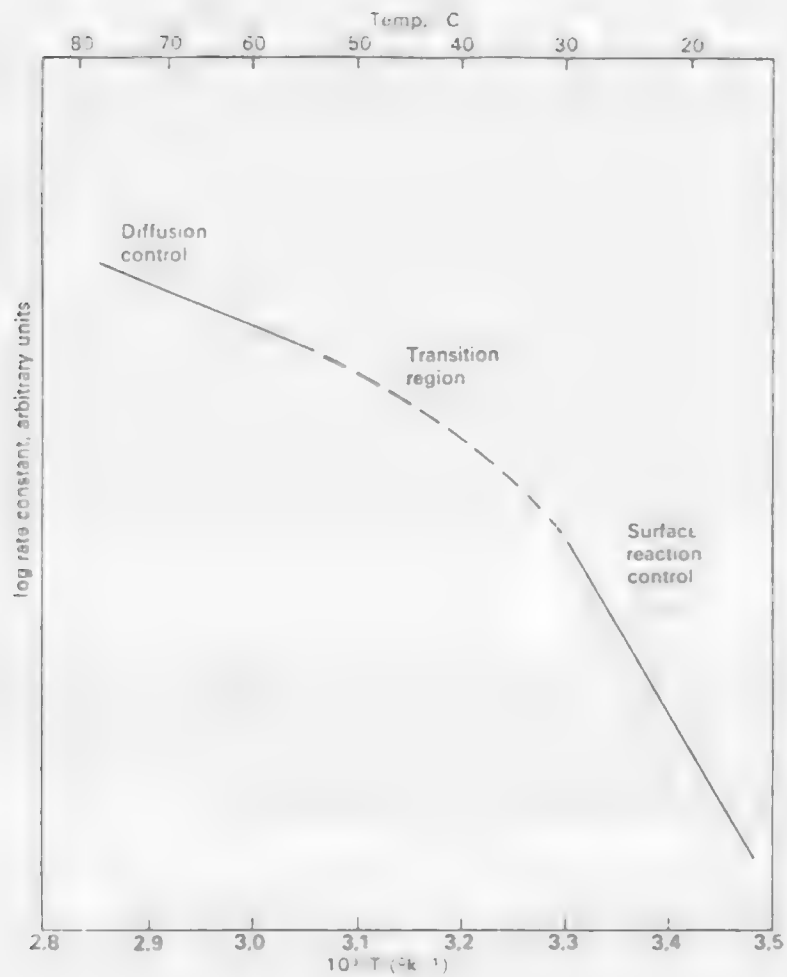
Most cementation systems at high temperatures have activation energies between 2 and 6 kcal/mol and are diffusion-controlled reactions. See Table 7.2.4 taken from Wadsworth.

Table 7.2.4 Activation Energies from Selected Cementation Systems.
After Wadsworth.¹²

System	Activation energy, kcal/mol	Ref.
Cu^{2+}/Zn	3.0	22
	3.12	29
Cu^{2+}/IA	5-16	9
Cu^{2+}/In	2.28	28
Cu^{2+}/Fe	3.08	21
	5.08	3,4
	5.06	5
Cu^{2+}/Cd	2.02	29
Cu^{2+}/Ni	2.7 to 19	11
	7.0 to 45	10
Ag^+/Zn	6.0	30
Ag^+/Fe	2.99	21
Ag^+/Cu	5.0	7
Pd^{2+}/Cu	2.0 to 9.5	6
Cd^{2+}/Zn	4.0 to 4.7	8

A few systems, however, exhibit rather large energies of activation at low temperatures, which has been interpreted as being a change from a diffusion-controlled process at high temperature to a surface reaction-controlled process, or a pore diffusion process at low temperature. This phenomenon has been observed in the Cu^{2+}/Ni system, Pd^{2+}/Cu system, and the Cu^{2+}/Fe system. The characteristic shape of Arrhenius plots for these systems are presented in Figure 7.2.7. In each system, the critical temperature is about 35°C. Below this temperature it appears that the reaction is controlled by nondiffusional processes in that apparent activation energies from 10 to 45 kcal/mol have been observed.

Figure 7.2.7. Arrhenius Plot for a Cementation System that Appears to Exhibit a Change in Reaction Mechanism.



Recent cementation experiments (Cu^{2+}/Fe system) in an ultrasonic field by Beckstead suggest that these results are a consequence of the temperature sensitivity of the surface deposit, i.e., the observed activation energies at low temperatures are much too high, either because the nature of the surface deposit inhibits the anodic reaction or because of a change in the effective cathodic area. The ultrasonic system provides an efficient way of maintaining a clean surface so that the surface deposit does not interfere with the interpretation of the kinetic data. As can be seen in Figure 7.2.8, when a clean surface was maintained by studying the reaction in an ultrasonic bath, an activation energy of 4.55 kcal/mol was obtained at all temperatures indicating that the reaction is boundary-layer diffusion-controlled over this range of temperatures. However, in the absence of the ultrasonic field there appears to be a critical temperature below which the reaction is not boundary-layer diffusion-controlled. This may be attributed to a tight, coherent deposit whose formation is enhanced at lower temperatures and as a consequence appears to change the rate-controlling mechanism from cupric ion diffusion through the boundary layer to pore diffusion of ferrous ion from anodic sites. At low temperatures, when a tight, coherent deposit is formed the anodic area is greatly reduced and contact with the electrolyte may be minimal. In this case the rate should be independent of the cupric ion concentration, which is difficult to confirm because of the small fraction reacted. Alternately, *and more probably*, the observed phenomenon may simply be a continual decrease in the cathodic surface area with a decrease in temperature, as is suggested by the photographs in Figure 7.2.9.

7.2.5 Summary

In conclusion, kinetic data from most cementation reactions support a diffusion-controlled, first-order reaction model. The anomalous effects of the initial concentration of the noble ion and the temperature dependence of some systems, which indicates a change in mechanism, may be interpreted in terms of the nature of the surface deposit and/or the concentration dependence of self-diffusion coefficients.

Practical application of these concepts suggest that concentration systems should be operated above the critical temperature in order to maintain either a clean surface or a porous surface deposit with a large effective surface area. Unfortunately, the critical temperature may well be a function of the concentration of the noble metal ion. However, in practice the effect of initial concentration and temperature may be trivial when typical plant results are considered. A comparison of the operations of two plants using cementation cones is given in Table 7.2.5. Notice that, to a good approximation, the production rate is directly proportional to the copper concentration as would be expected from a simple, pseudo first-order reaction. These results may indicate that the surface deposit is being effectively removed by the jets of the cone, a condition that most probably was not achieved by cementation in launders. The effects discussed in this review are difficult to see in a comparison of plant data that reflects variation and fluctuations in many of the parameters that control the reaction, and that may compensate for each other.

Figure 7.2.8. Arrhenius Plot for the Cementation of Copper (Initial Concentration 2 g/l) by Iron in the Presence and Absence of an Ultrasonic Field.

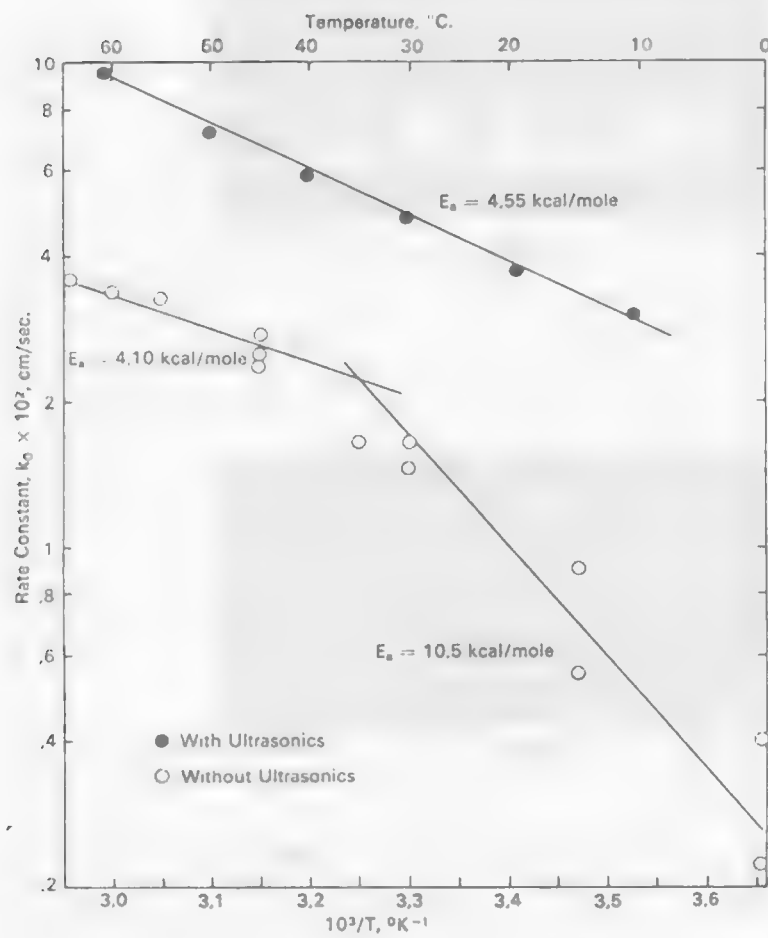
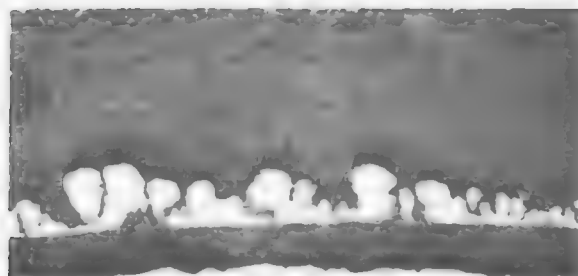
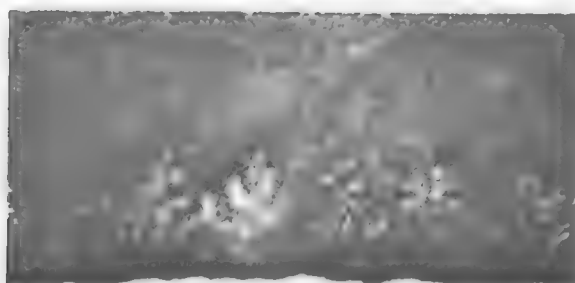


Figure 7.2.9. Photograph of Surface Deposit for the Cu^{2+}/Fe System at 15 and 45°C.



IRON

15°C



IRON

45°C

Table 7.2.5 Typical Plant Data for Copper Cementation on Iron Using Cementation Cones.

<u>Plant</u>	<u>Number of cones</u>	<u>Copper production rate t/d/cone</u>	<u>Copper concentration g/l, in feed</u>
#1	26	5.8	0.7 (30°C)
#2	3	25	2.5 (30°C)

REFERENCES

1. Agricola, G., *De re metallica*, New York, Dover, 1950.
2. Spedden, H. R., Malouf, E. E., and Prater, J. D., Cone-type precipitators for improved copper recovery, *J. Metals*, N. Y., vol. 18, 1966, pp. 1137-1141.
3. Nadkarni, R. M., et al., A kinetic study of copper precipitation on iron - Part I, *Trans. Metal Soc., AIME*, vol. 239, 1967, pp. 581-585.
- 4a. Nadkarni, R. M., and Wadsworth, M. E., A kinetic study of copper precipitation on iron - Part II, *Trans. Metal Soc., AIME*, vol. 239, 1967, pp. 1066-1074.
- 4b. Nadkarni, R. M., A kinetic study of the cementation of copper with iron, Ph.D. thesis, University of Utah, 1967.
5. Rickard, R. S., and Fuerstenau, M. C., An electrochemical investigation of copper cementation by iron, *Trans. Metal Soc., AIME*, vol. 242, 1968, pp. 1487-1493.
6. Von Hahn, E. A., and Ingraham, T. R., Kinetics of Pd¹¹ cementation on sheet copper in perchlorate solutions, *Trans. Metal Soc., AIME*, vol. 236, 1966, pp. 1098-1103.
7. Idem. Kinetics of silver cementation on copper in perchloric acid and alkaline cyanide solutions, *Trans. Metal Soc. AIME*, vol. 239, 1967, pp. 1895-1900.
8. Ingraham, T. R., and Kerby, R., Kinetics of cadmium cementation on zinc in buffered sulfate solutions, *Trans. Metal Soc. AIME*, vol. 245, 1969, pp. 17-21.
9. Mackinnon, D. J., and Ingraham, T. R., Copper cementation on aluminum canning sheet, *Can. metall. Q.*, vol. 10, 1971, pp. 197-201.
10. Mackinnon, D. J., Ingraham, T. R., and Kerby, R., Copper cementation on nickel discs, *Can. metall. Q.*, vol. 10, 1971, pp. 165-169.
- 11a. Miller, R. L., and Wadsworth, M. E., Kinetics of copper cementation on nickel, *AIME Ann. meeting*, 1968, Paper A68-21.
- 11b. Miller, R. L., A kinetic study of the cementation of copper with nickel, Ph.D. thesis, University of Utah, 1968.
12. Wadsworth, M. E., Reduction of metals in solution, *Trans. metal Soc. AIME*, vol. 245, 1969, pp. 1381-1394.
13. Latimer, W. M., *Oxidation potentials*, Englewood Cliffs, N.J., Prentice Hall, 1952.

14. Chizhikov, D. M. Cadmium, Oxford, Pergamon, 1966.
15. Mantell, C. L., Electrochemical engineering, 4th Ed., New York, McGraw-Hill, 1960.
16. Potter, E. C., Electrochemistry, London, Cleaver-Hume, 1961.
17. Drozdov, B. V., Conditions of contact reduction of a metal from its solution, Zhur. Priklad. Khim., vol. 31, 1958, pp. 1048-1054.
18. Harned, H. S., and Owen, B. B., The physical chemistry of electrolytic solutions, 3rd Ed., New York, Reinhold, 1958.
19. Chapman, T. W., Transport properties of concentrated electrolytic solutions, Ph.D. thesis, Berkeley University, California, Lawrence Radiation Laboratory, 1967, UCRL 17768.
20. Bockris, J. O'M., and Reddy, A. K. N., Modern electrochemistry, New York, Plenus, 1970.
21. Episkoposyan, M. L., and Kakovskii, I. A., Kinetics of cementation of copper and silver from chloride solutions with metallic iron, Tsvetn. Metal, vol. 38, no. 10, 1965, pp. 15-19.
22. Strickland, P. H., and Lawson, F., Cementation of copper with zinc from dilute aqueous solutions, Proc. Australas. Inst. Min. Metall., no. 236, Dec. 1970, pp. 25-34.
23. Beckstead, L., Surface deposit effects in the kinetics of copper cementation by iron, M. Sc. thesis, Salt Lake City, University of Utah, 1972, Submitted for publication in Trans. AIME Met. Soc.
24. Strickland, P. H., and Lawson, F., The cementation of metals from dilute aqueous solution, Proc. Australas. Inst. Min. Metall., no. 237, Mar. 1971, pp. 71-79.
25. Glicksman, R., Mouquin, H., and King, C. V., Rate of displacement of silver from aqueous silver nitrate by zinc and copper, J. Electrochem. Soc., vol. 100, 1953, pp. 580-585.
26. Cornet, I., Lewis, W. N., and Kappessner, R., Effect of surface roughness on mass transfer to a rotating disc, Trans. Instn. Chem. Engng., vol. 47, 1969, pp. T222-T226.
27. Calara, J., Kinetics of copper cementation on a rotating iron disc, M. Sc. thesis, Manila, University of the Phillipines, 1969.
28. Bashkova, L. F., and Kovalenko, P. N., Cementation of small amounts of copper from solutions of indium sulfate by metallic indium. Zh. Prikl. Khim., vol. 35, 1962, pp. 1797-1801.
29. King, C. V., and Burger, M. M., The rate of displacement of copper from solutions of its sulfate by cadmium and zinc, Trans. Electrochem. Soc., vol. 65, 1934, pp. 403-411.

30. Von Hahn, H. E. A., and Ingraham, T. R., Kinetics of silver cementation of zinc in alkaline cyanide and perchloric acid solutions, Can. metall. Q., vol. 7, 1968, pp. 15-26.
31. Power, G., Cementation Reactions, Ph.D. thesis, University of W. Australia, Nedlands W. Australia, 1975.

LEARNING ACTIVITY 3

Dr. T. J. O'Keefe
Professor of Metallurgical Engineering
University of Missouri - Rolla

7.3 ElectrolysisLearning Activity Objective

After completing your study of this material you should be able to describe the important features of an electrowinning cell and be able to use Faraday's laws for electrodeposition.

7.3.1 Introduction

On a production tonnage basis, the most widely used metal recovery technique (from aqueous solutions) is electrolysis.

Electrolysis is the recovery of a metal from a solution by the use of electrical current. Schematically this is shown in Figure 7.3.1.

An electrolytic cell must contain four essential components, i.e.,

- a) an anode surface where oxidation occurs,
- b) a cathode surface where reduction occurs,
- c) an electrical conductor to carry current, and
- d) an electrolyte (an ionic conductor).

A source of electrical power must be available in order to force reactions to occur that are not themselves spontaneous.

In the mid-1800's, Faraday established the relationship between the quantity of electricity flowing and the amount of material liberated. His investigations led to the formulation of the two laws of electrolysis.

1. The amount of electrochemical decomposition produced at an electrode is proportional to the quantity of electricity (coulombs) passing through the circuit.
2. The amounts of different substances produced by the same quantity of electricity will be proportional to their equivalent weights.

One equivalent of any substance will be liberated (oxidized or reduced) by a Faraday, F, which is equal to about 96,500 coulombs.

$$w = \frac{EIt}{96,500}$$

[7.3.1]

w = wt. in grams

$$E = \text{equivalent wt.}, \frac{\text{atomic wt.}}{\text{valence}}$$

$$I = \text{current, amps}$$

$$t = \text{time, sec.}$$

Another term sometimes used is the electrochemical equivalent - the amount of material liberated by one coulomb, i.e., $E/96,500$.

7.3.2 Sample Calculations

1. Metallic silver is deposited from a nitrate solution for 40 minutes by a current of 1.65 amps. Calculate the weight of silver collected.

Solution

The atomic weight of Ag is 107.87 g/mole. Silver is univalent, thus, the reaction is



The weight deposited can be calculated from 7.3.1,

$$w = \frac{EIt}{96,500} \quad [7.3.3]$$

$$w = \frac{(107.87 \text{ g/eq.wt.})(1.65 \text{ amps})(40 \text{ min.})(60 \text{ sec/min.})}{96,500 \frac{\text{amp}\cdot\text{sec}}{\text{eq. wt.}}} \quad [7.3.4]$$

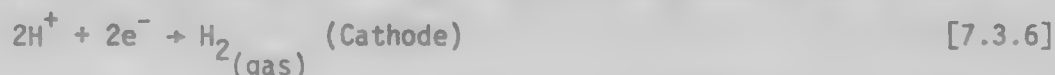
$$w = 4.42\text{g} \quad [7.3.5]$$

2. One molar sulfuric acid (H_2SO_4) is electrolyzed between two platinum electrodes. Determine the quantities of products obtained at each electrode if two Faradays of current pass through the circuit.

Solution

Any Faraday calculation must be proceeded by a correct evaluation of the reactions that will occur. Techniques for predicting the reactions occurring will be demonstrated in following learning exercises and will be shown to depend on the thermodynamic stability of the system.

In this case, the Pt will not react to any extent at either electrode and the SO_4^{2-} ion will also be stable. The reactions occurring are thus:



Hydrometallurgy

Electrolysis

$$E_H = \frac{1 \text{ g/mole}}{1 \text{ eq.wt./mole}} = 1 \text{ g/eq.wt.} \quad [7.3.8]$$

$$w_H = \frac{(1 \text{ g/eq.wt.})(2 \text{ Faradays})(96,500 \text{ amp.sec/F})}{96,500 \text{ amp.sec/eq.wt.}} \quad [7.3.9]$$

$$= 2\text{g} \quad [7.3.10]$$

$$E_O = \frac{16\text{g/mole}}{2 \text{ eq.wt./mole}} = 8 \text{ g/eq.wt.} \quad [7.3.11]$$

$$w_O = \frac{8(\text{g/eq.wt.})(2F)(96,500 \text{ amp.sec.})}{(96,500 \text{ amp.sec/eq.wt.})} \quad [7.3.12]$$

$$w_O = 16\text{g} \quad [7.3.13]$$

The gas volumes can be calculated from the ideal gas law, i.e.,

Hydrogen

$$\begin{aligned} 2 \text{ g H} &\times \frac{\text{mole H}}{1 \text{ gH}} \times \frac{1 \text{ mole H}_2}{2 \text{ mole H}} \times \frac{22.4 \text{ liters}}{\text{mole H}_2} \\ &= 22.4 \text{ liters H}_2 \text{ (at S.T.P.)} \end{aligned} \quad [7.3.14]$$

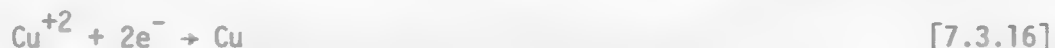
Oxygen

$$\begin{aligned} 16 \text{ g O} &\times \frac{\text{mole O}}{16\text{g O}} \times \frac{\text{mole O}_2}{2 \text{ moles O}} \times \frac{22.4 \text{ l}}{\text{mole O}_2} \\ &= 11.2 \text{ liters of O}_2 \text{ (at S.T.P.)} \end{aligned} \quad [7.3.15]$$

3. Calculate the amount of Cu deposited from a solution at 90% current efficiency at a cathode current density of 20 amps per square foot for 1 hour. The cathode is 2 feet by 3 feet.

Solution

First the cathode reaction must be determined. In many electrolytes the Cu valence is (+2), however, it can be (+1) in some plating solutions or in the presence of certain organic compounds. If we assume the (+2) state for copper, then,



$$E = \frac{63.5}{2} = 31.75 \text{ g/eq.wt.} \quad [7.3.17]$$

$$I = \frac{20 \text{ amps}}{\frac{\text{ft}^2}{\text{side}}} \times 2 \text{ ft.} \times 3 \text{ ft.} \times \frac{2 \text{ sides}}{\text{cathode}} = 240 \text{ amps} \quad [7.3.18]$$

$$w = \frac{(31.75 \text{ g/eq.wt.})(240 \text{ amps})(1 \text{ hr.})(3600 \text{ sec./hr.})}{96,500 \text{ amp.sec./eq.wt.}} \quad [7.3.19]$$

$$= 284.3 \text{ g at 100\% C.F.}$$

If only 90% of the current gives Cu,

$$w_{\text{Cu}} = 284.3 \times .90 = 255 \text{ g} \quad [7.3.20]$$

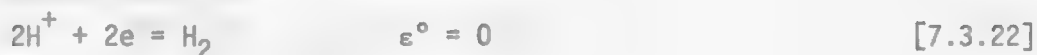
These same conditions for a Cu^{+1} solution would yield twice this weight since

$$E = \frac{63.5}{1} = 63.5 \text{ g/equivalent} \quad [7.3.21]$$

This points out the importance of the valence of the ion undergoing the electrochemical change.

Theoretically, water will electrolysis at a potential of 1.23 volts, i.e., the following half cell reactions when summed give the cell potential as 1.23 volts.

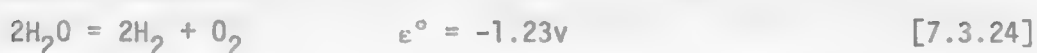
Cathode Reaction



Anode Reaction



Overall Reaction



The sign of the cell potential is negative, therefore, the reaction is theoretically non-spontaneous as written, i.e., 1.23 volts are required to force the reaction to occur. In actual practice a higher voltage is required than 1.23 volts because of polarization and resistance efforts in the system.

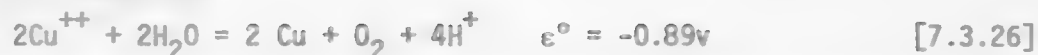
In electrolyzing copper bearing solutions,



Figure 7.3.1. Electrowinning Cell.



Cell Reaction



Theoretically, 0.89 volts will be required to deposit copper from a solution of Cu^{++} at a concentration of 1 mole/liter. In actual practice the voltage requirement is a function of pH, temperature and copper ion concentration, i.e.,

$$\epsilon = \epsilon^\circ - \frac{RT}{nF} \ln \frac{(a_{\text{H}^+})^4 p_{\text{O}_2}}{(a_{\text{Cu}^{++}})^2} \quad [7.3.27]$$

The actual cell voltage required in plant practice is also a function of electrolyte resistance, electrical connection resistance, electrode polarization effects. Copper electrowinning is discussed in learning activity 4.

In electrolyzing zinc bearing solutions the theoretical cell potential is -1.99v. As a student exercise, show how this value is calculated. (Assume $a_{\text{Zn}^{++}} = 1$ and temperature is 298°K.)

The cell potential required is about 2 volts. Why doesn't the solution decompose to H_2 and O_2 gas rather than depositing Zn?

LEARNING ACTIVITY 4

7.3.3 Electrowinning of CopperLearning Activity Objective

After completing your study of the material in this learning activity you should be able to describe copper electrowinning processes; its features, and its problems.

The material in this learning activity is from the text "Extractive Metallurgy of Copper" by A. K. Biswas and W. G. Davenport. It is reproduced here by written permission.

"Leaching operations and leaching plus solvent extraction operations produce solutions containing 30-60 kg m⁻³ of dissolved copper. The copper in these solutions is recovered in the form of copper cathodes, by electrowinning. The electrowinning process entails the application of an electrical potential between an inert anode (usually antimonial lead) and a copper cathode, both immersed in the copper-bearing solution. Approximately 550,000 tonnes of electrowon cathodes are produced per year.

The cells and electrical circuitry are similar (Table 7.4.1) to those employed in electrorefining. The essential difference between the processes is that;

- (a) electrorefining uses copper anodes, from which copper enters the electrolyte during the process;
- (b) electrowinning uses inert (non-dissolving) anodes.

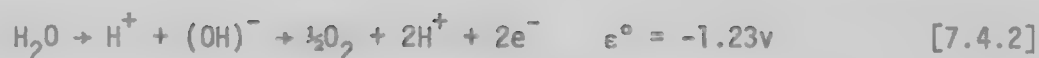
All the copper plated into cathodes during the electrowinning originates in the leach solutions.

ELECTROWINNING REACTIONS

The electrowinning cathode reaction is identical to that in refining, i.e.,



but the anode reaction is completely different. Since the anode is inert there is no copper to dissolve and some other reaction must occur. This reaction is the formation of oxygen gas which may be represented (Andersen, *et al.*, 1973) as:



The net electrowinning reaction (including sulphate ions) is:



for which the standard cell potential is:

$$\epsilon^\circ = -0.89\text{v}$$

It can be seen from equation [7.4.3] that the products of electrowinning are copper metal at the cathode, oxygen gas at the anode, and a net re-generation of sulphuric acid which is recycled to the leaching or solvent extraction stripping circuits.

CELL VOLTAGE AND ENERGY CONSUMPTION

The overall electrowinning process involves changing ionic species to atomic species so that a definite energy and decomposition voltage are required. The theoretical voltage requirement may be calculated from the standard potential of reaction [7.4.3] and the activities of the ions in solution, i.e.,

$$\epsilon = \epsilon^\circ - \frac{RT}{2F} \ln \frac{(a_{\text{H}^+})^2}{a_{\text{Cu}^{2+}}} \quad [7.4.4]$$

(assuming the electrode products are pure Cu° and O_2).

The value of $a_{\text{Cu}^{2+}}$ is approximately 0.1 (0.5 molar solution; activity coefficient 0.2; Weast, 1974) while a_{H^+} is approximately 1 in the strongly acidic solution, from which:

$$\epsilon^\circ = -0.92\text{v} \quad (318^\circ\text{K}).$$

In addition to this theoretical decomposition potential, the production of gaseous oxygen at the anode requires a significant "overvoltage" in the order of $\frac{1}{2}$ V. This overvoltage must be applied to provide the activation energy for combining absorbed oxygen atoms (at the anode) into oxygen gas (O_2). Thus the actual decomposition potential is approximately 1.5V and the total cell potential (operating at a current density of 180 Am^{-2}) is the sum of the voltages in Table 7.4.2.

The total cell voltage for electrowinning is in the range of 2-2.5 V as compared to only 0.2-0.25 V for copper refining. As the list below shows, most of this extra potential is due to the 1.5 V decomposition potential, but in addition, the IR voltage drop through the electrowinning solutions is high due to their relatively low H_2SO_4 concentration. The conductivity of leach electrolytes is in the order of $0.2 \Omega^{-1} \text{ cm}^{-1}$ (Weast, 1974), solvent extraction electrolytes $0.6 \Omega^{-1} \text{ cm}^{-1}$, and refinery electrolytes $0.7 \Omega^{-1} \text{ cm}^{-1}$.

TABLE 7.4.2

Decomposition potential to produce Cu°	0.9
Anode overvoltage	0.6
Voltage drop in the electrolyte ($V = I \times R$)	0.5
Cathode potential due to organic and polarization	0.05
Anode and cathode connections, busbar and lead losses	0.05
Total cell voltage	2.1 V

Since the electrical energy per ton of cathode copper is directly proportional to cell voltage, i.e.,

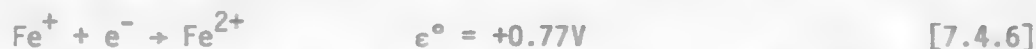
$$(\text{kWh/tonne of cathode}) = \frac{V \times 8.4 \times 10^5 (\text{ampere hours tonne}^{-1})}{1000 \times \text{CE}/100}$$

it can be seen that the energy consumed in electrowinning is approximately 10 times that of electrefining, i.e., 2000 - 2500 kWh/tonne⁻¹ DC energy (2100-2700 kWh AC accounting for rectification). This energy consumption can be lowered slightly by lowering the current density (which lowers the IR voltage drops throughout the electrical system) but this step has the negative effect of lowering the production rate of cathode copper.

CATHODE CURRENT EFFICIENCY: INTERFERING IRON REACTIONS

Cathode current efficiencies in electrowinning plants vary from 77 to 92% (Table 7.4.1). These rather low values are indicative of high energy consumptions (per tonne cathode) and low production rates.

The low current efficiencies are inevitably the result of high ferric ion concentrations in the electrolyte, which consume part of the cathode current by the reaction:



Furthermore, the resulting Fe²⁺ ions may be reoxidized by dissolved ³⁺ oxygen (from air or from the oxygen evolving at the anode) so that Fe³⁺ ions may be regenerated. The results are that the iron reduction/oxidation reactions become cyclic and that, as a consequence, significant quantities of cathode current are consumed. Thus, the Chambishi electrolyte (Fe³⁺, 6 kg m⁻³) results in a 77% current efficiency while the Nchanga electrolyte (Fe³⁺, 0.3 kg m⁻³; Fe²⁺, 0.9 kg m⁻³) gives a current efficiency of over 90% (Table 7.4.1). An important method of lowering energy cost and raising production rates is, therefore, the removal of iron from the electrolyte.

7.4.3

Table 7.4.1 Details of Electrowinning Tankhouses. (The 1975 Nchanga data were supplied by Nchanga Consolidated Copper Mines Limited, Chingola Division).

	Chimbalaba (Zambia) (Verney <i>et al.</i> , 1969)	Nchanga (Zambia) agitation leach tankhouse (1975)	Shituru (Zaire) (Theys, 1970)	Chingolomunda (Zaire) (McArthur and Leleham, 1961)	Bluebird Mama Arizona (Power, 1970) solvent extraction	Bagdad Arizona (Hughes, 1971) solvent extraction	Nchanga (Zambia) New (1975) solvent extraction tankhouse (1975)
Production rate (tonnes year ⁻¹)	20,000	110,000	125,000 ^a	1 M (100)	5000	6540	100,000
Electrolytic cell							
Cu kg m ⁻²	4 ⁵	45	55	22	36	50	55
Free H ₂ SO ₄ (kg m ⁻²)	30	29	—	54	146	150	150
Fe ²⁺ (kg m ⁻²)	4	2.1	1.8	3.4	6.2	—	0.1
Fe ³⁺ (kg m ⁻²)	6	0.5	1.0	1.4	1.1	—	0.6
Impurities (kg m ⁻²)	(Co 1, Mn 2, Ni 0.6, Bi 0.04)	Co 0.4, Mn 1.5, Mg 4.5, P 1.5, Al 1.4	—	As 0.15, Sb 0.04, Mo 0.45, Cr 0.11, HNO ₃ 0.7	—	—	—
Solids (kg m ⁻²)	0.1	0.2	0.13	30	25	27	41
Temperature, °C	—	55	62	—	—	—	—
Electrolytic form cells							
Cu kg m ⁻²	25	28	30	8	33	25	30
Free H ₂ SO ₄ (kg m ⁻²)	70	59	62	60	151	185	185
Anodes							
Material	Antimonial lead	Sb 6%, Pb 94%	Sb 6%, Pb 94%	Sb 14.5%, Ag 0.6%	Sb 6%, Pb 94%	—	Sb 6%, Pb 94%
L x W x T (cm)	—	110 x 85 x 1.2	115 x 75 x 1.1	140 x 85 x 1.0	—	—	108 x 85 x 1.5
Spacing (cm)	10	10	9	8	11	—	10
Life (years)	—	2.5	2-3	6-7	—	—	2
Cathodes							
Substrate	—	—	—	—	—	—	—
L x W (cm)	—	95 x 95	105 x 85	120 x 90	90 x 90	Electrowinning starting sheets	Refinery starting sheets
Wt. of substrate (kg)	4.5	5	5	5	5	95 x 95	95 x 95
Deposition time (days)	5	4.5	5	5	8	—	3
Final weight (kg)	40	40-50	45	70	60	—	80
Analysis (g t ⁻¹)	—	99.54	99.75	99.9	99.9	99.9	99.5
Impurities (ppm)	Ph 15, Se 5, Bi 1, Fe 2, Ni 1, As 0.5	Se 1.4, Ni 1.1, Bi 0.4, As 0.2	—	Cr 65, Fe 31, Pb 29, Sb 4, Ag 1	—	—	—
Electrowinning cells							
Number	200	800	160	682	48	48	130
L x W x D (m)	—	4.5 x 1.2 x 1	20 x 1.2 x 1.3	5.8 x 1.1 x 1.5	—	48 x 6 starting sheet 42 production	6.6 x 1.1 x 1.1
Anodes, cathodes	—	—	—	71, 72	41, 40	49, 48	—
Concrete construction	—	—	—	—	—	—	—
Lining	—	—	—	—	—	—	—
Circulation (m ³ min ⁻¹)	—	0.015	0.02	—	—	0.3	—
Electrical conditions							
Rectification	—	—	—	—	—	—	—
Cell current (A)	—	16,000 (max.)	26,000	—	—	—	—
Current density (A m ⁻²)	—	2.35	2.35	—	—	—	—
Cathode efficiency	—	77	85	76	80	—	—
Applied voltage	—	2.5	2.25	2.05	2.0	—	—
Energy per tonne of cathode (kWh)	—	2700 (1.8 x calculated)	2000 (DC)	2200 (DC)	2600 (AC)	2200 (1.8 x ^a)	2200 (AC)

^a A similar plant of 90,000 tonnes per year (Luilu) is also operated by Gecamines (Zaire).

One further problem caused by ferric ions is that they tend to cause corrosion of the cathode loops at the solution line by the reaction (Andersen, *et al.*, 1973):



This limits the time which a cathode can be left in the cell. For this reason, electrowon cathodes are somewhat lighter (40-70 kg) than refining cathodes (100-150 kg). This problem can be alleviated to some extent by varying the level of the electrolyte and by operating at a lower temperature, 30-35°C (McArthur and Ledebor, 1961).

Iron is always present in the minerals which enter the leach plant and it always dissolves to some extent in the electrolyte. It must, therefore, be removed to prevent it from building up during the cyclic use of the electrolyte as the leaching agent. This removal is performed by:

- (a) decopperizing and discarding a portion of the leach solution (a method which is of decreasing importance due to pollution problems and acid wastage);
- (b) oxidizing the solution with MnO_2 and neutralizing it with burnt lime to pH 2 or 2.5. This procedure causes the precipitation of iron hydroxides or Na or NH_3 iron jarosites, which are settled using organic flocculating agents.

This latter method is the most common, and it is often modified to suit local conditions. For example, the phosphates of the Zaire ores are used (Theys, 1970) to precipitate hydrolysed ferric phosphate, which requires less neutralization (i.e., lower burnt lime additions) than the normal $\text{Fe}(\text{OH})_3$ type of precipitation.

A novel development in the Chambishi leach plant circuit (Verney, *et al.*, 1969) is the diversion of some of the pregnant leach liquor into the fluid bed roaster of the sulphide-roast-leach plant. This has three beneficial effects: the roaster is kept cool; the water balance in the plant is maintained by evaporation; and about half the iron in the leach liquor is rendered insoluble (as Fe_2O_3), thus effectively removing it from the electrolyte circuit.

PURITY OF CATHODE: BEHAVIOR OF ELECTROLYTE IMPURITIES

The purity of electrowon cathodes (99.75-99.9% Cu, Table 7.4.1) is inferior to that of electrefined cathodes (99.99% Cu less than 0.005% metallic impurities). Electrowon cathodes are, however, suitable for all non-electrical uses. Only in the Chambishi operation (Verney, *et al.*, 1969) has an attempt been made to attain refinery grade cathode purity but as of yet the bismuth, selenium and lead contents are all at excessive levels. Lead is an especially difficult impurity to avoid because it originates with the anodes. Lead adversely affects the annealing properties of copper wire and hence it represents a serious quality problem for electrowon cathodes.

Most of the cathode impurities are caused by the occlusion of solid material arising from: (a) incomplete clarification of the leach solution, and (b) the corrosion products (solid lead sulphate or lead oxide) from the lead anodes. The evolution of oxygen gas at the anodes created turbulent conditions in the electrowinning cells and this causes the particulate solids to reach the cathode surface where there is a high probability that occlusion will occur. It is important, therefore, to remove as much as possible of the particulate solids from the leach solutions (by clarification and filtration).

The most important source of impurities is the lead anode. The surface is oxidized to form an almost insoluble oxide (PbO_2) layer but this layer tends to flake to a slight extent and these flakes tend to be carried over into the cathode deposit. Flaking and corrosion of the anode are minimized by alloying the lead with Sb (6-15%) with or without Ag (0.15-0.5%).

A possible answer to the lead carryover problem is the use of truly noncorroding anode materials (Hopkins, 1973). The most extensively studied materials are refractory metals (specifically titanium) plated with a very thin layer of noble metal. This latter layer is necessary because in anodic service, the refractory metals form a completely non-conductive oxide surface layer, i.e., they anodize. Gold, platinum, iridium, rhodium and ruthenium are the suggested coatings and it may also be possible to make the refractory metal oxide sufficiently conductive by doping it with other metal cations to form a semiconductor layer. All of these electrodes are expensive, however, and to date their use is restricted to the test stage.

The principal organic additions to electrowinning solutions are flocculents which aid in the settling of solids thereby minimizing occlusion at the cathode. The types in common use are colloidal polysaccharides (Guartec Jaguar), polyacrylonitriles or polyacrylamides (Separan, Aerofloes). Organic oil mist inhibitors are often floated on the electrolyte to minimize the quantity of sulphuric acid mist generated by oxygen bubbles bursting at the anode-electrolyte surface.

ELECTROWINNING TANKHOUSE PRACTICE

The use of inert anodes and the application of high voltages in electrowinning are the only significant differences from electrorefining operations. The cells are concrete, lined with lead (often protected with wooden slats), and they have the same range of dimensions as in electrorefining. The substrates for the cathodes are most commonly starting sheets obtained from copper refineries but in one case electrowon starting sheets are employed. The latter tend, however, to be somewhat brittle (McArthur and Ledebor, 1961).

The lead anodes are cast around copper support bars. They weigh in the order of 100 kg and, since they corrode very slowly, they remain permanently in the cells (i.e., they last 2-7 years).

The anodes and cathodes are interleaved as in refining and they are connected electrically in parallel. Cells and sections are connected in series. Completed cathodes are "pulled" every 5-8 days (depending on the current density) after which time they weigh 40-70 kg. Only half the cathodes are pulled from the cell at one time (to be replaced by new starting sheets) in order that electrical current flow and copper deposition are not interrupted. There is very little residue or sludge formed in the cell or on the anode faces and cleaning need only be carried out every 6 months to a year.

Since the anode material tends to contaminate the cathode product the electrodes are often held apart by porcelain, rubber or plastic spacer knobs or bars affixed to the anodes.

The electrolyte becomes depleted in copper during its passage through the deposition cells and it becomes more acidic (equation 7.4.3) as it does so. This "spent" electrolyte is recycled to the leaching circuit or, in the case of solvent extraction plants, to the stripping mixer/settlers.

The final cathodes are sold directly, melted into ingots for mechanical and alloying use or melted and blended with refined copper for all-purpose use.

SPECIAL PROBLEMS OF SOLVENT EXTRACTION ELECTROLYTES

Solvent extraction electrolytes differ from direct leach electrolytes in that they are high in sulphuric acid (150 kgm), they are very low in impurities, and they are contaminated with the extraction solvent.

The high sulphuric acid level is an advantage from the point of view of providing a high conductivity electrolyte but it does lead to an increased rate of corrosion and PbO_2 flaking at the anode (Hopkins, *et al.*, 1973). The cathode deposit occludes some of this lead-bearing solid and the cathode always contains more than 15 ppm of lead. In practice this means that whereas the cathode copper is perfectly suitable for mechanical and alloying usage it cannot be used for electrical engineering purposes.

Improvement of cathode purity from solvent extraction electrolytes will require an insoluble anode.

The presence of small amounts of the organic phase from the solvent-extraction process causes discoloration of the cathode deposits particularly at the top of the cathode and at the side edge (Hopkins, 1973). This dark chocolate-colored portion of the deposit is referred to as "organic burn." The deposits in the "organic burn" area are soft and powdery and it is likely that a high entrainment of impurity solids occurs on the burn areas.

Hopkins, *et al.* (1973) have shown that this "organic burn" is a direct consequence of the carry-over of entrained solvent (e.g., LIX 64N) into the electrolysis cells. The solvent extraction diluents (e.g., kerosene) and the small amount of dissolved solvent alone do not create this condition. Good mixer-settler design will minimize the amount of solvent carry-over and it will prevent any serious organic burn condition.

In summary, it can be seen that unless truly inert anodes are employed the cathode product from solvent extraction will be less pure than refinery copper. There is a large market for non-electrical grade copper, however, and solvent extraction cathodes are suitable for it.

RECENT IMPROVEMENTS IN ELECTROWINNING PRACTICE

Improvements in electrowinning practice have in general followed a similar pattern to those of electrorefining. High current density electrowinning with periodic current reversal is being developed (Lickens and Charles, 1973) and it is being incorporated in the Zaire electrowinning plants. The pilot tests reported by Lickens indicated that doubling the current density from 240 A m^{-2} DC to 480 A m^{-2} with periodic current reversal (9 sec. forward, 0.5 sec. reverse always at 250 A m^{-2}) causes no deterioration in cathode appearance or increase in modular growth. Unfortunately the test data are limited and no figures on cathode purity or production rate are available. The energy consumed per ton of cathodes is reported to increase by 20% with the doubling of current density.

Other improvements have largely followed the mechanical and control improvements incorporated in modern electrorefining plants. These have been:

- (a) improved filtering and settling facilities in the leach plant to minimize impurity solids in the electrolyte;
- (b) the use of mechanical starting sheet straightening and mechanical cell loading devices to optimize labour utilization and cell efficiency; and
- (c) the use of solid-state rectifiers which are efficient in energy conversion, and which will be necessary for any current reversal system.

These improvements have all served to improve cathode quality, production rate, energy efficiency and labour utilization.

SUMMARY

This chapter has shown that the electrowinning of copper from leach and solvent extraction electrolytes results in the plating of copper at a cathode and oxygen at an (inert) anode. The process requires 2000-2500 kWh of electrical energy per ton of cathode copper at an applied potential of 2-2.5 V, both of which are ten times the equivalent requirements for copper refining.

Electrowon cathodes are inferior in purity to electrorefined cathodes but they are perfectly suitable for all but electrical uses. A major source of impurities is the solid corrosion products of the antimonial lead anodes which tend to become occluded in the cathode deposit. The use of truly non-corroding anodes (such as titanium, plated with platinum) may improve cathode purities. Efficient clarification of leach solutions is also important in obtaining high-purity cathodes.

Periodic current reversal is being tested with the view of increasing production rates but its implementation is considerably behind that in the electrorefining industry.

SUGGESTED READING

Mantell, C. L., (1960), *Electrochemical Engineering*, McGraw-Hill, New York (Chap. 10, "Electrowinning").

Theys, L., (1970), Forty years of progress in the hydrometallurgy and electrowinning of copper--the experience of Union Miniere, C.I.M. Bull., 63, 339-351.

Verney, L. R., Harper, J. E., and Vernon, P. N., (1969), Development and operation of the Chambishi Process for the roasting, leaching and electrowinning of copper, in *Electrometallurgy*, Henrie, T. A., and Baker, D. H., Editors, A.I.M.E., New York, pp. 272-305.

REFERENCES

Andersen, T. N., Wright, C. N., and Richards, K. J., (1973), Important electrochemical aspects of electrowinning copper from acid leach solutions, in *International Symposium on Hydrometallurgy 1973*, Evans, D. J. I., and Shoemaker, R. S., Editors, A.I.M.E., New York, pp. 171-202.

Bagdad, (1971), How Bagdad uses LIX to recover copper from dump leach solutions, *World Mining*, 24(4), 46-48.

Hopkins, W. R., Eggett, G., and Scuffham, J. B., (1973), Electrowinning of copper from solvent extraction electrolytes--problems and possibilities, in *International Symposium on Hydrometallurgy, 1973*, Evans, D. J. I., and Shoemaker, R. S., Editors, A.I.M.E., New York, pp. 127-154.

Liekens, H. A., and Charles, P. D., (1973), High current density electrowinning by periodic cell short circuiting, *World Mining*, 26(4), 40-43.

McArthur, J. A., and Ledebor, B. J., (1961), The electrolytic tankhouse operation and cell room practice at Chuquicamata, Chile, in *Extractive Metallurgy of Copper, Nickel and Cobalt*, Queneau, P., Editor, A.I.M.E., Interscience Publishers, New York, pp. 449-468.

Power, K. L., (1970), Operation of the first commercial copper liquid ion exchange and electrowinning plant, in *Copper Metallurgy*, Ehrlich, R. P., Editor, A.I.M.E., New York, pp. 1-26.

Theys, L., (1970), Forty years of progress in the hydrometallurgy and electrowinning of copper--the experience of Union Miniere, C.I.M. Bull., 63, 339-351.

Verney, L. R., Harper, J. E., and Vernon, P. N., (1969), Development and operation of the Chambishi Process for the roasting, leaching and electrowinning of copper, in *Electrometallurgy*, Henrie, T. A., and Baker, D. H., Editors, A.I.M.E., New York, pp. 272-305.

Weast, R. C., (1974), *Handbook of Chemistry and Physics*, CRC Press, Cleveland, Ohio, Section D.

LEARNING ACTIVITY 5

Dr. D. Robinson
University of Arizona
Tucson, Arizona

7.4 Electrowinning Plant Practice

Learning Activity Objective

Following your study of this learning activity you should be able to describe the electrowinning process and to describe some of the industrial problems encountered in the process.

7.4.1 Purpose of the Process

One way to produce a high purity metal is to smelt a concentrate to a crude bullion (pyrometallurgy) and then electrorefine that product. This was discussed in the previous learning activities. Another way is to dissolve the concentrate values in a solution (hydrometallurgy) and then recover the metal electrolytically from solution. In this latter approach, the electrodeposition operation has been termed electrowinning. The metal is "won" from the solution by deposition. The electrowinning process is run in conjunction with a leaching process. The solution produced in the leaching plant must be suitable for use in the electrolysis plant, and the depleted solution from the electrowinning plant must be suitable to be returned for further use in the leaching plant.

In a typical zinc leaching plant, zinc oxide concentrate is dissolved in sulphuric acid. The solution rich in zinc and oxygen is sent to a tankroom where the zinc is deposited on the cathode. The oxygen is evolved from the solution and sulphuric acid is regenerated for further leaching. The process is depicted in Figure 7.5.1. Three functions are accomplished, i.e., metal is recovered from solution, oxygen is driven off, and acid is regenerated.

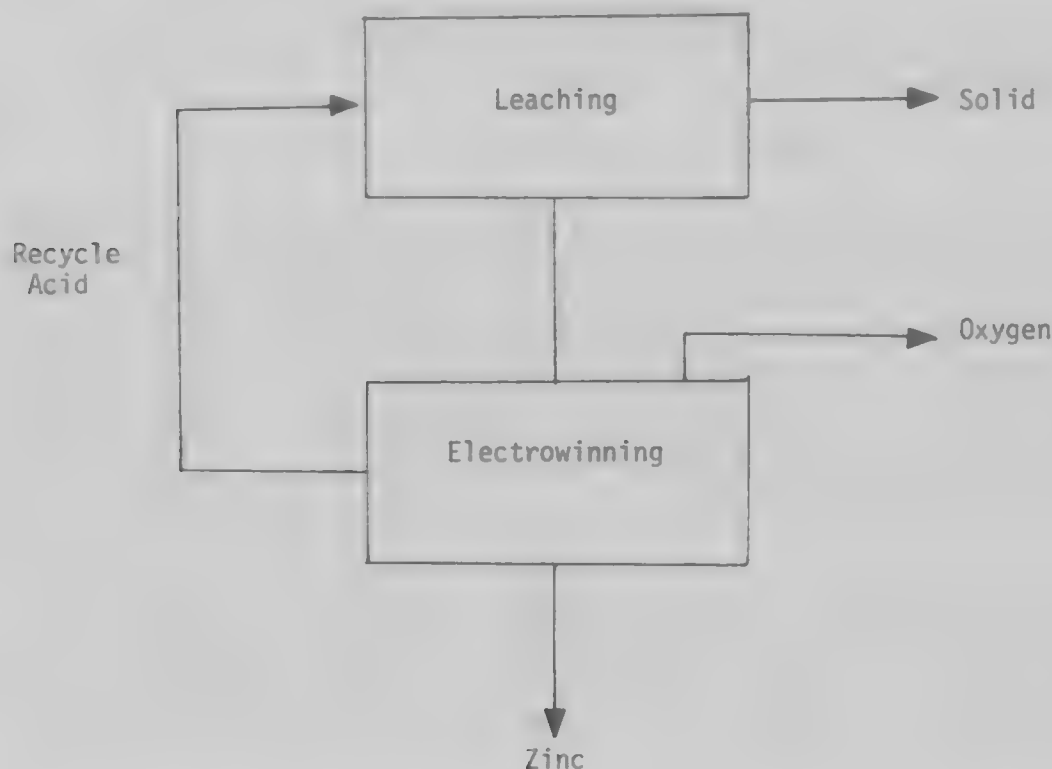
7.4.2 The Cathodic Process

Since the metal values are already in solution, there is no chance to recover impurities more noble than the major metal in an anode slime, i.e., there is no anode dissolving in the solution. However, the more noble impurities will deposit at the growing cathode along with the major metal. Some selectivity is achieved, i.e., the less noble impurities present in the electrolyte are rejected and not deposited at the cathode. If the more noble impurities are to be kept out of the cathode, they have to be removed from the solution in a previous purification step.

Almost every metal can theoretically be recovered in an electrowinning type of process. However, the deposition will not take place properly unless the more noble impurities are removed almost completely from the solution. In copper or silver electrowinning, noble impurities deposit at the cathode. However, when the less noble metals like zinc, nickel, iron, and manganese are to be deposited, the more noble impurities

depositing at the cathode form galvanic cells with the major metal and cause the latter to re-dissolve after being initially plated. This effect is so important that in a zinc plant, if the antimony concentration is greater than 0.2 mg per litre, virtually no zinc will be deposited.

Figure 7.5.1. Simplified Zinc Leaching Electrowinning Circuit.



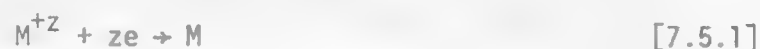
The fact that less noble metals react in solution with the more noble impurities, however, is the basis for a purification process. In a zinc powder mixed into the leach solution causes the more noble impurities in solution to precipitate as a sponge or slime. This is called cementation. The process can yield a solution free of impurities so that very pure (99.99-99.999%) metal can be deposited.

7.4.3 The Anodic Process

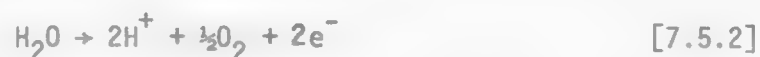
In electrowinning, the anode does not serve as the source of the metal ions as it did in electrefining. It serves only as the positive electrode in the cell. Thus it must be made of a material which will not dissolve in the solution.

Most leaching - electrowinning is accomplished in sulphuric acid solutions. Lead or lead alloys are not readily soluble in sulfuric acid and they are extensively used as anodes.

In electrowinning the cathodic process has the same chemical reaction as in electrorefining, i.e.,



The anode reaction, however, is different. In sulphuric acid it is the decomposition of water.



Oxygen is evolved from the cell. Hydrogen ions combine with sulphate ions, to form sulphuric acid:



The anode forms a coating on the surface of lead dioxide, PbO₂. It is actually on the oxide surface that the oxygen evolution reaction occurs. It cannot occur on pure lead. During electrolysis, some of the oxygen diffuses into the lead oxide coating. It reacts with fresh lead at the lead - lead oxide interface. This leads to a thickening of the film. At the same time, the portion of the coating that is exposed to the solution dissolves very slowly to yield lead ions in the solution. The lead solubility is very low, about 10 mg/l, but it is still slightly soluble. The lead ions that go into solution are incorporated into the growing cathode. Cathodes with 1-10 ppm of lead are commonly obtained.

Various lead alloys have been found to dissolve slowly in particular solution, e.g., Pb - 0.75% Ag in zinc solutions, while Pb - 0.05% Ca in some copper sulphate solutions.

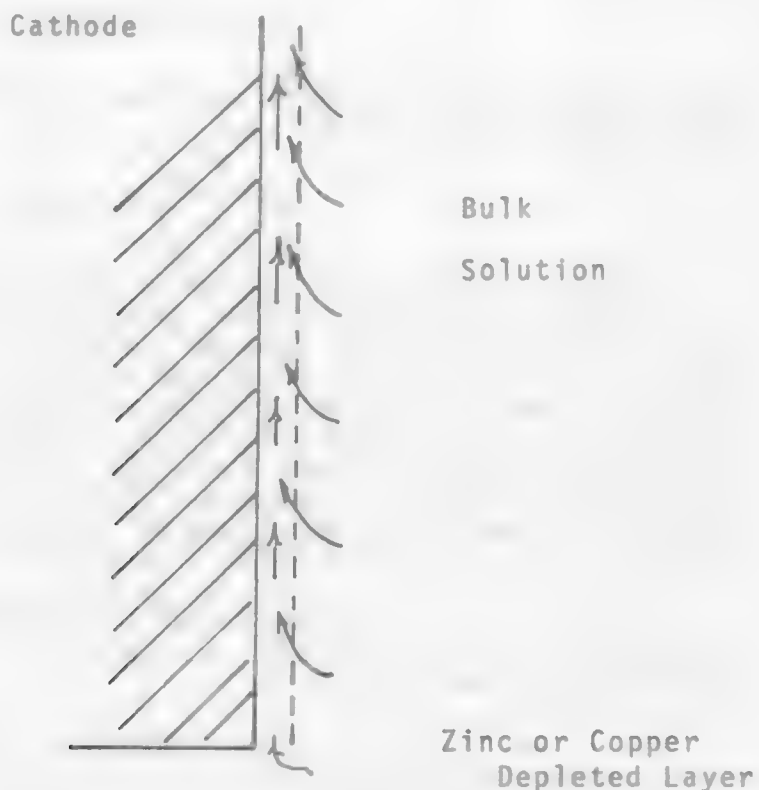
To overcome this slow rate of corrosion and totally prevent lead from entering the cathodes, anodes of titanium with conductive coatings of precious metal oxides have been used. General acceptance of this technique has not yet been achieved.

The anodic process of evolving oxygen leads to the formation of very fine bubbles of oxygen. They originate at many points on the anode and then rise to leave the cell solution. As the bubbles form and rise to the surface of the solution, they pick up and carry small quantities of the cell solution. When the bubble reaches the surface, it breaks and causes a mist to be sprayed up from the cell. The mist will often be present in the entire plant atmosphere, and can be objectionable to work in, as well as being corrosive to plant equipment. The problem is intensified at higher operating current densities.

7.4.4 Solution Mixing

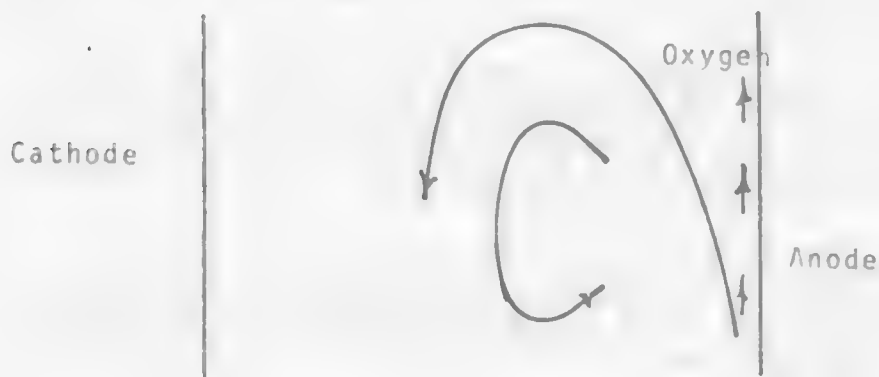
Solution movement is generated in several ways. As the metal deposits at the cathode, a very thin layer of solution depleted in metal ions exists at the cathode surface. This layer has a lower density than the rest of the solution, hence it tends to rise and be replaced by fresh solution rich in the metal ions. This creates a slow upward natural convective motion at the cathode, Figure 7.5.2.

Figure 7.5.2. Natural Convection at Cathode.



The anode generated oxygen bubbles produce an upward motion at the face of the anode. The movement becomes more intense as the current density is increased. As seen in Figure 7.5.3, the solution rises up the anode and descends in front of the cathode. Most of the motion actually occurs as eddies of solution circulating at the top half of the electrodes. Little motion is generated near the bottom.

Figure 7.5.3. Anode Induced Convection.



New solution entering (rich in metal ions) and leaving (depleted in the metal) causes a general movement of solution in the cell. It does not contribute greatly to the solution movement between electrodes because of the baffling effect of the plates.

When metals such as nickel, zinc and manganese, all of which are less noble than hydrogen, are deposited, there is a natural tendency to reduce some hydrogen ions to hydrogen atoms. These react to form gas bubbles. These bubbles (generally small in number) move very quickly up the cathode face. This motion occurs immediately adjacent to the cathode and creates local intense mixing to the solution.

Solution mixing allows the cells to run at higher currents than if the solution were stagnant.

7.4.5 Control of Acid Mist

Several methods have been devised to eliminate acid mist from the tankroom atmosphere. These can be divided into two general types: a) scrubbing the acid mist at the vessel surface, and b) moving air above the cells to prevent buildup of objectional concentrations of acid mist in the surroundings.

An effective method for mist depression can be achieved by forming a blanket of foam on the surface of the cell solution. A proprietary solution of Dowfax 2A-1 added as a few drops to each cell spreads out like an

oil slick and is frothed into a blanket by the rising anode bubbles. This has been used extensively in copper electrowinning plants and to a lesser extent in zinc plants. The organic frothing solution reacts unfavorably with some solutions such as copper solvent extraction solutions and most zinc electrolytes, rendering it unuseable. The foam blanket is very effective at depressing the acid mist, and preventing it from leaving the cell, Figure 7.5.4.

When the foam type scrubber cannot be used, a blanket of hollow or solid polypropylene balls 2-3 layers deep has been successfully used. It also depresses the acid mist and retains the acid in the cell. The small balls, usually $\frac{1}{8}$ to $\frac{1}{2}$ inch in diameter may enter pumps, tanks, filters, etc. throughout the plant, Figure 7.5.5.

A third shrouding method is to simply cover the cells with a plastic box, Figure 7.5.6. This does prevent acid mist from getting into the plant atmosphere, but it allows the condensed acid solution to fall onto the leader bars, bus bars, and contacts. Corrosion normally is, therefore, very rapid.

The second conceptual method is to allow the acid to enter the plant atmosphere. Air is moved horizontally along the tops of the cells and is expelled from the plant through a scrubbing tower, Figure 7.5.7.

A modification of the laminar air flow method is to place cover plates 6 to 12 inches above the cells. Then a current of air is directed between the cells and the cell cover.

7.5.6 Problems of Heat Generation

The resistance of the electrolyte causes heating in the cell. Heat is also generated at electrical contact, and other electrode resistances. Some of this heat is lost from the cell by vaporization processes. The electrolyte rises to some stable temperature.

In most electrowinning plants there is an optimum solution temperature, 30-45°C. If the temperature is too high, the anode corrosion rate increases, leading to a higher lead content in the cathode, and a shorter anode life. The cathode deposit can be deleteriously effected by temperatures both above and below the optimum level.

If solution heating is required, in excess of that generated in the cell, shell and tube heat exchangers are generally used. If cooling is required, cooling coils placed in each cell or an external atmospheric cooling tower can be used.

7.4.7 Metal Recovery and Size of Operations

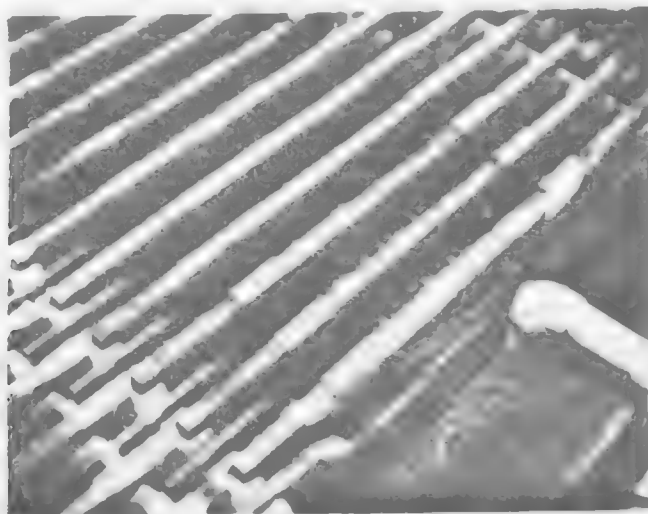
The metals that are electrowon on a commercial scale include zinc, cadmium, copper, nickel, cobalt, and manganese. The plants range in size from 200 to about 800 tpd. Cadmium is recovered solely as a by-product of zinc processing. A typical zinc plant size will produce 1000-3000 pounds of Cd per day.

Figure 7.5.4. View of a Cell with a Foam Blanket on the Solution.



Photograph of an operating electrowinning cell at the Ray Mines Division plant. The cell as viewed from 5-10 feet away to show the cell walls and the electrode header bars as well as the foam blanket used to suppress the acid mist. (Photo Courtesy of Kennecott Copper Corporation)

Figure 7.5.5. Supression of Mist by Polypropylene Spheres.



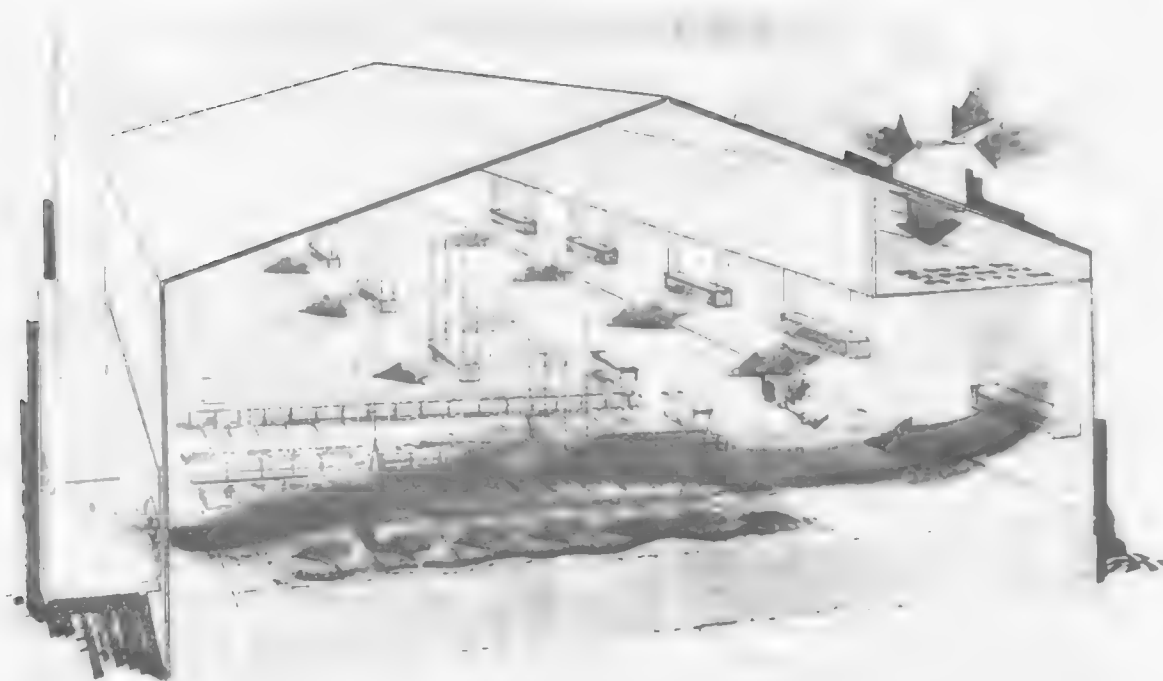
(Photo Courtesy of Bagdad Copper Company)

Figure 7.5.6. Supression of Mist by Shrouding the Cell with Polythene Sheets.



(Photo Courtesy of Bagdad Copper Company)

Figure 7.5.7. Control of Mist by Use of Moving Air Over the Tank Surface.



(Courtesy of Powesland Engineering, Toronto, Canada)

Copper is produced in leach - electrowinning plants ranging in size from 1 or 2 tpd up to 150-200 tpd. Nickel is processed in only a few plants in the world by electrowinning. The production rate is about 20-100 tpd. Cobalt, like cadmium is exclusively a byproduct metal occurring with nickel and sometimes copper ore. Quantities in the hundreds of pounds per day are treated. Pure manganese metal is produced solely in electrolytic plants.

7.4.8 Chemistry and Electrochemistry of the Zinc Cell

Zinc is the highest tonnage metal processed by electrowinning. It is also one of the most technically difficult metals to recover. A study of the various features of the zinc cell will be used to provide an understanding of electrowinning in general.

Contents of the Solution

The purified solution from the zinc leach plant will contain 150-200 gpl of zinc as zinc sulphate, up to 10 gpl of magnesium and lesser quantities of calcium, chromium, manganese and aluminum as less noble impurities. Noble impurities, 0.01 to 10 mg/l, such as antimony, arsenic, cadmium, cobalt, iron nickel, selenium copper and lead will also be present. Some non-metallic impurities will also be present, such as chloride and fluoride ions. Some organic materials, gum arabic or animal glue, may also be present.

Each of the above species may have an important effect on the winning process. The less noble elements will generally increase the solution resistance and hence increase the cell heating. The more noble impurities will be removed from solution during purification, so the remaining quantities are often not harmful. Their general role, though, is to deposit at the cathode and decrease the metal purity. Manganese will be discussed later.

Reactions in the Solution

The most prominent feature of an operating zinc cell is that the solution is red tinted. This color is due to the presence of manganese, as the permanganate ion. The red color is usually an indication that most of the harmful chemicals are under control.

If one of the more noble impurities is present in a higher than normal concentration, e.g., antimony at 0.1 mg/l instead of 0.01 mg/l, it would have an adverse effect on the cathode. It would deposit with the zinc. A galvanic cell with zinc would be formed and zinc would dissolve. Also, it would cause hydrogen to be evolved at a higher rate than normal. The hydrogen would reduce the permanganate ions to the colorless manganous ion. The solution would become more acid due to the increased hydrogen ion concentration. The increased acidity would increase the rate at which the zinc was dissolved. Therefore, the color of the solution can be an indication of how well the cathode process is operating.

Reactions at the Anode

As indicated in the previous session, the anode is a silver-lead alloy that forms an oxide (PbO_2) coating. The principal reaction is the decomposition of water to form oxygen gas and hydrogen ions. The zinc solution contains some manganese as manganous ions. This reacts at the anode to form a MnO_2 coating over the PbO_2 coating. The MnO_2 coating helps by decreasing the corrosion rate of the lead. The MnO_2 layer thickness increases. After 30-60 days the anodes have to be scraped to remove the thick coating.

Reactions at the Cathode

The more noble impurities deposit slowly at the cathode. They have the effect of both decreasing the purity of the zinc, and of causing it to redissolve. The fluorides present in the cell, even though present as anions with a negative charge can still be present near the negatively charged cathode. The adverse effect of this will be discussed under cathode materials.

7.4.9 Cathode Materials

In zinc electrowinning, aluminum and its alloys are used exclusively as the cathode material. Aluminum forms a thin and somewhat porous oxide film in air. This film is quite important to the electrowinning process. If the film were totally absent, zinc would attach itself very tightly to the cathode blank and it would be difficult to remove the zinc from the blank. If the surface were completely covered with a fairly thick oxide film, the cathode blank would not conduct electricity and hence no zinc would be deposited.

Fluoride ions in solution are attracted by the aluminum oxide film, and dissolve it quite quickly leading at times to an undesirable tendency of the zinc to stick to the aluminum.

In copper electrowinning, several materials have been used as blanks. The most successful has been titanium, stainless steel and copper plates precoated with an oil or emulsion. In some manganese electrowinning plants, nickel copper plates precoated with an oil or emulsion are used. In manganese, nickel and cobalt electrowinning plants, stainless steel and titanium are in use. Cadmium electrowinning plants normally use aluminum as the cathode material.

Pretreatments are sometimes employed to control the adhesion of the depositing metal to the blank. Wire brushing abrasion has been useful for controlling adhesion to aluminum and stainless steels. Anodic etching or mechanical abrasion are another possible surface treatment, e.g., used on Ti starter sheets.

7.4.10 Anode Materials

As mentioned previously, Pb-0.75\% Ag is widely used in zinc plants as the anode material. Alloys of lead with calcium or antimony are

used in copper plants. The most widely used alloy in copper plants has been the Pb-6% Sb alloy. The corrosion rate of this alloy is often reported to be greater than other lead alloys but it is a very hard alloy with good structural strength.

In zinc plants, the anodes are often pretreated in a fluoride - sulphate solution to form a stable lead oxide coating. In copper plants, the presence of 50-100 mg/l of cobalt in the electrolyte has a similar effect of forming a stable oxide film.

7.4.11 Cell Design Considerations

To avoid contamination problems, resulting from electrode short circuiting, electrode spacers are installed. Some of the spacers in use include: slotted boards in the bottom of the cell; plastic insulators affixed near the bottom of the anodes; and plastic or wooden spacers mounted along the top of cells. These are shown in Figure 7.5.8, 7.5.9, and 7.5.10.

A sludge of lead sulphate, lead dioxide and manganese dioxide generally forms in the cells and cleaning is necessary every 30-60 days. The sludge is vacuumed out of the cells in some plants and flushed out through bottom drains in others. In most cases the sludge is treated for the recovery of lead. In zinc plants the slimes are treated for silver and manganese recovery.

Figure 7.5.8. Use of a Spacer Board Fixed to the Bottoms of the Electrodes to Provide Spacing.

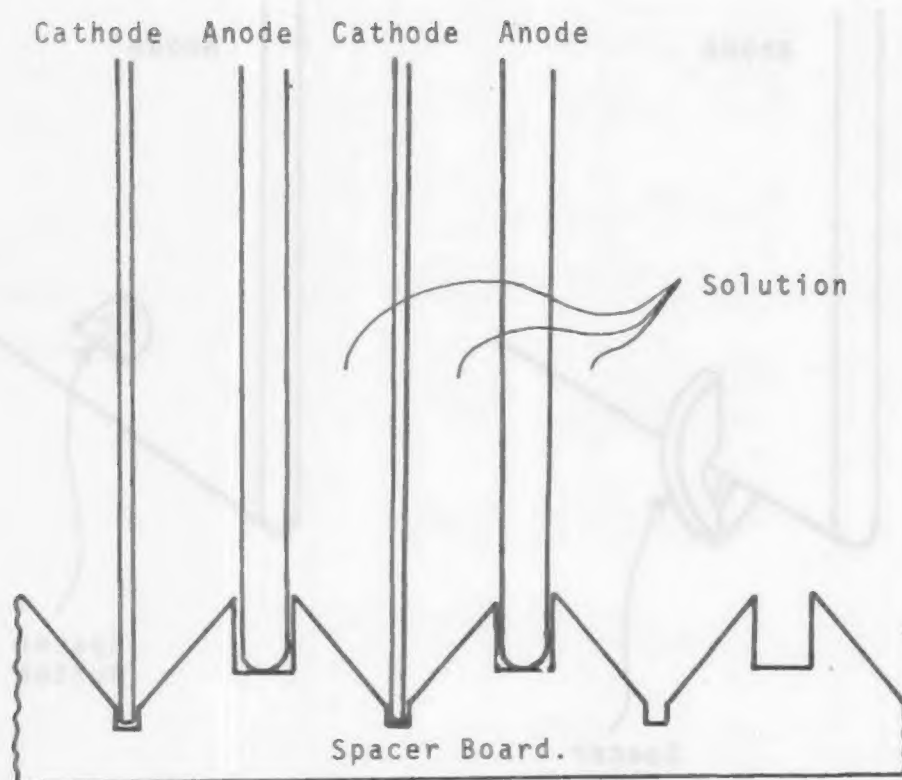


Figure 7.5.9. Use of Plastic Insulators Fixed to the Bottom of Individual Anodes to Space the Electrodes.

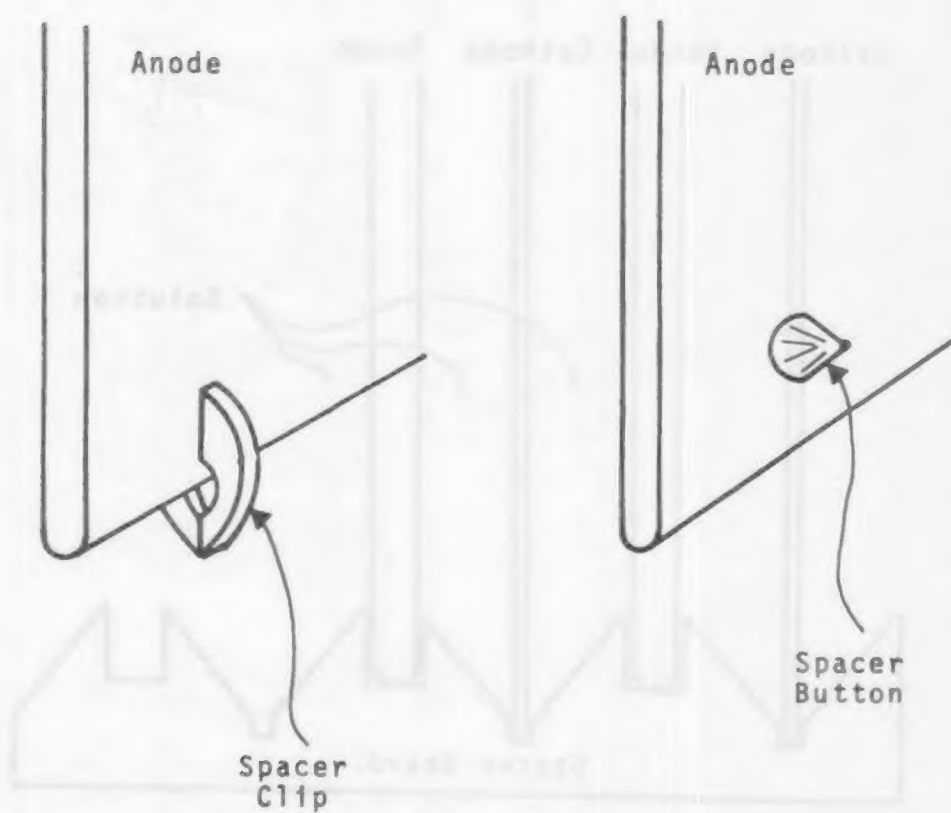


Figure 7.5.10. Use of Plastic Insulator on the Cell Top Bus Bar to Provide Electrode Spacing.

